Regional Symposium on Electrochemistry

RSE-SEE

South-East Europe

# Abstract Collection

**of the contributions presented at the**

**First Regional Symposium on Electrochemistry of South-East Europe**

Crveni Otok (St. Andrew's Island), Rovinj, Croatia, May 4-8, 2008.



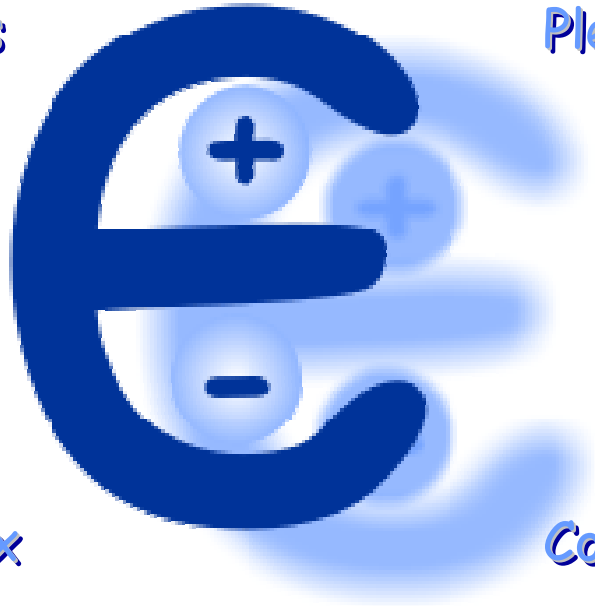

**This Abstract Collection is not an official Book of Abstracts of the Symposium, and should not be cited as a bibliographic reference. For this purpose, please refer to the printed Book of Abstracts.**


Prepared by Višnja Horvat-Radošević & Aleksandar Dekanski

# Contents

First Regional Symposium on Electrochemistry of South-East Europe, Rovinj, Croatia, May 4-8, 2008.

# PLENARY LECTURES

PI-1-1

## ELECTROCATALYSIS IN WATER ELECTROLYSIS

**S. Trasatti**

*Department of Physical Chemistry and Electrochemistry*
*University of Milan, Via Venezian 21, 20133 Milan, Italy*

Water electrolysis is the oldest process of conversion of electrical energy into chemical energy. It was the first application of the availability of electric power allowed by Volta's invention of the electric pile. Traditionally, water electrolysis has been conducted in alkaline solution. Typical practical electrode materials have long been steel or nickel for the cathode, and nickel for the anode. These materials are however relatively unstable during $O_2$ or $H_2$ evolution, with an unfavorable drift of the overpotential with time due to surface oxidation and hydrogen absorption, respectively. The activity of Ni can be improved by forming Ni-Raney, but the basic instability is not eliminated.

The origin of the overpotential is dealt with in the field of *electrocatalysis*, which is not the acceleration due to the application of an electrode potential, but the effect on the electrochemical reaction rate of the chemical interaction of reactants, intermediates and/or products with the electrode surface. If concepts of catalysis are applied to electrode reactions, a dependence of activity on adsorption energy is found, which shows up as a so-called "volcano" curve. Thus, it is possible to make predictions on the activity of metals for hydrogen evolution, and of oxides for oxygen evolution.

Further improvement in activity has called for the introduction of "activated" electrodes, consisting of a conducting, inert support coated with a thin layer of electrocatalyst. In this way, not only the chemical nature of the electrode can be modified, but also its morphology and structure in dependence on the procedure of preparation.

Environmental constraints may require that water electrolysis is carried out using electric power generated via solar energy conversion. In these conditions *intermittent* electrolysis may result due to the alternate periods of sun light. Intermittent electrolysis leads to more severe conditions for electrode materials, so that research has to be carried out to develop specific materials for these conditions.

More recently, with the advent of membrane cell technology, water electrolysis in solid polymer electrolyte (SPE) cells, where the medium is strongly acidic, has been developed. In these electroyzers the use of compounds of Pt group metals is at the moment unavoidable. Further improvement is expected from the exploitation of strong metal/support interaction (SMSI) effects.

The high overpotential for $O_2$ evolution could be avoided if the reaction were replaced by a different anodic reaction. This replacement could in turn reduce $\Delta E$,

the minimum cell potential difference that depends on the nature of the electrode reactions. Such a strategy has already been applied with success in the chlor-alkali industry where the couple $Cl_2$-$H_2$ ($\Delta E$ = 1,35 V) has been replaced with the couple $Cl_2$-$O_2$ ($\Delta E \approx 0.90$ V) ($O_2$ is reduced at the so-called air cathode).
A few attempts to apply the same strategy have been carried out quite recently. In one case, anodic $O_2$ evolution is replaced with oxidation of carbonaceous materials dispersed in the solution (slurry). This would correspond to an average practical $\Delta V$ = 0.5 V. However, in a scenario of $H_2$ economy to reduce the production of greenhouse gases, an anode where C is oxidized to $CO_2$ would constitute a striking contradiction.
In another case the electrolysis of an aqueous solution of $NH_3$ is proposed. The net reaction would be:

$$2NH_3 \rightarrow N_2 + 3\ H_2$$

with oxidation of $NH_3$ at the anode. The theoretical $\Delta$E would be 0.06 V with a decrease of almost 1.2 V with respect to conventional electrolysis. The amount of energy consumption is impressively small, only ca. 30% of that conventional. However, also the production rate is strikingly small (ca. 1/100 of that conventional). This is certainly in relation with the fact that $NH_3$ is a solute and as such its oxidation at the phase boundary is subject to mass transfer limitations. Moreover, $NH_3$ oxidation calls for very sophisticated electrocatalysts (precious metals) that are subject to poisoning phenomena. In the end, such a proposed change in technology of $H_2$ production does not appear so close to implementation.
Further examples of recent attempts to reduce the consumption of electrical energy are the electrolysis of aqueous solutions of methanol (but $CO_2$ is still produced at the anode), and water electrolysis using ionic liquids as electrolytes. In the latter case the authors claimed the possibility of obtaining high hydrogen production efficiencies using an inexpensive material such as low carbon steel.

***Acknowledgements.*** *Financial support of MIUR (PRIN) is gratefully acknowledged.*

## References

1. S. Trasatti in *Electrochemical Hydrogen Technologies*, H. Wendt Ed., Elsevier, Amsterdam (1990), p. 1-14; 104-135.
2. E. Guerrini, S. Trasatti in *Catalysis for Sustainable Energy Production*,
3. C. Bianchini, P. Barbaro (Eds.), Wiley-VCH (2008), in the press.

First Regional Symposium on Electrochemistry of South-East Europe, Rovinj, Croatia, May 4-8, 2008.

PI-1-2

# FUEL CELLS: SCIENCE, ENGINEERING AND APPLICATIONS

**F. Barbir**

*Faculty of Electrical Engineering, Mechanical Engineering and Naval Architecture, Uuniversity of Split, R. Boskovica bb, 21000 Split, Croatia*
*Frano.Barbir@fesb.hr*

Fuel cells are an emerging technology with applications in transportation, stationary and portable power generation, with outputs ranging from mW to MW. The most promising and most widely researched, developed and demonstrated type of fuel cells is Proton Exchange Membrane or PEM Fuel Cell (PEMFC). State-of-the-art in PEM fuel cell technology and challenges for their development and widespread applications are discussed.

PEM fuel cells have been demonstrated in almost any imaginable power generation application, yet their commercial availability seems to be elusive. This paper presents an overview of the status of PEMFC stack and system development for various applications, and it discusses the possible reasons for continuous postponement of their commercialization with the emphasis on the technical challenges such as increase in power density, obtaining uniformity of cells in a multi-cell stack configuration, optimal flow field design, operation with low stoichiometric ratios and low humidity gases, understanding and increasing durability, reducing size and weight and most importantly reducing the manufacturing cost. The system issues such as operation at higher temperature, sensitivity to sub-freezing temperature and related engineering solutions, choice of fuel, system complexity and cost will also be discussed.

PEM fuel cells have achieved >1 W $cm^{-2}$ peak power, but in normal operation (Vcell $\geq$ 0.6 V) achievable power density is 0.6-0.7 W $cm^{-2}$ and 0.3-0.4 W $cm^{-2}$ in high efficiency operation (Vcell $\geq$ 0.7 V). The goal of fuel cell development is to keep increasing power density. This is possible through improvements in key materials, such as catalyst and electrolyte, as well as through improvements in fuel cell design.

Performance of a stack of cells is limited by performance of the weakest cell in stack. It is therefore important to achieve high uniformity in performance of the individual cells in the stack, through stack design, mass production techniques, quality control and automated stack assembly process. Optimum flow field design, which is one of the critical parameters in achieving cell performance uniformity, may be obtained by careful Computational Fluid Dynamic techniques and experimental validation including flow visualization techniques.

Water plays a crucial role in operation of a fuel cell stack. The membrane's ionic conductivity is a strong function of its hydration state. Although water is produced in the cathode some water still has to be brought in the fuel cell to prevent the

membrane from drying. Too little water may cause polymer drying and too much water may cause electrode flooding. The form of water depends on local conditions, primarily gas flow rate, pressure and temperature. The stack design, selection and control of operating conditions affect water management and therefore the stack performance.

Operation with low relative humidity of the gases at the stack inlet is preferred because it simplifies the system (humidification of reactant gases and water recovery). PEM fuel cells are operational even at room temperature, but the typical operating temperature is between 60°C and 80°C. In order to reduce the size of the heat rejection equipment there is a lot of R&D on high temperature membranes that would allow operation at 130°C to 140°C.

For most mobile applications size and weight of the fuel cell is very important. Automotive fuel cell stacks have gravimetric and volumetric power density >1 kW/kg and >1 kW/l, respectively. For smaller stacks <10 kW, power density is significantly lower.

Although PEM fuel cells exhibited several thousand hours of either continuous or intermittent operation, this may not be sufficient for most of the potential applications. It has been found that the operating conditions have a strong effect on durability decay rates. This has been utilized to develop the accelerated life tests. Long life times (in excess of 10,000 hours) have been achieved with good diligence in cell design and control of operating conditions, but durability continues to be one of the most critical challenges for fuel cell commercialization. The exact mechanism(s) of PEM fuel cell low durability or failure is(are) not yet well understood. The researchers often chase the symptoms of performance degradation, such as hydrogen crossover, fluoride emissions rate or Pt particle size distribution, instead of addressing the causes. There are several possible PEM fuel cell failure mechanisms, such as manufacturing defects, unwanted chemical reactions, caused by either contaminants or by-products, polymer/catalyst stability, mechanical forces, thermal effects (insufficient local heat removal rate) and combination of two or more mechanisms from the above list.

The fuel cells are still too expensive for most applications (several thousand U.S. dollars per kilowatt). This is due to the amount and kind of materials, manufacturing processes and manufacturing volumes. The most critical components are the catalyst and the membrane materials. Pt loading in today's fuel cells are typically around 0.3 mg $cm^{-2}$ of electrode active area, which corresponds to 0.6 mg per peak Watt (or 0.6 g $kW^{-1}$). The cost of the membrane material is expected to decrease by half with every two orders of magnitude increase in manufacturing volume.

For many potential applications a fuel cell system must be capable of surviving and operating in extreme conditions. Presence of water in the membrane and fuel cell requires special attention to fuel cell stack and system design to allow system survival and start-up in extremely cold conditions. Most automotive systems have already demonstrated this capability.

Fuel for fuel cells is hydrogen. Hydrogen is being considered as future replacement for fossil fuels. Commercial hydrogen is today primarily being used as industrial gas and it is very expensive. Most of hydrogen is today produced from natural gas. However, as a replacement for fossil fuels, hydrogen from natural gas does not make much sense - it may be justified only in a transition period to allow commercialization of promising hydrogen technologies such as fuel cells. Fuel cells with their numerous possible applications may actually be the main driver for "hydrogen economy". It can be envisioned that in "hydrogen economy", hydrogen, together with electricity, will be produced from clean renewable energy sources and will be used instead of fossil fuels to satisfy all the energy needs. Of course, changing of the entire energy system is a gigantic endeavor on global scale, which may have already started, but which may take several decades to complete.

First Regional Symposium on Electrochemistry of South-East Europe, Rovinj, Croatia, May 4-8, 2008.

PI-1-3

# ADVANCES IN ELECTROCHEMICAL IMPEDANCE SPECTROSCOPY

**Z. Stoynov**

*Bulgarian Academy of Sciences, Institute of Electrochemistry and Energy Systems*
stoynov@bas.bg

The Electrochemical Impedance Spectroscopy (EIS) is the most powerful method for the analysis of electrochemical systems. With unbeatable sensitivity and auto ranging the state of the art measuring instruments cover 7 to 11 frequency decades and supports the observation of a large variety of phenomena which take place from nanoseconds to several hours – fast charge transfer, adsorption and intercalation, diffusion and transport processes, formation and growth of new phases or energetic structures, corrosion and degradation. In addition the instruments are able to measure impedances from $10^{-9}$ to $10^{13}$ ohms and capacitance from 10 pF to $10^{5}$ F.

These huge information capabilities are however very often explored inefficiently. With carefully engineered experimental set-up and optimally designed programs for data acquisition and analysis, the obtained results can be much more informative about the complex nature of the objects under study.

From system analysis point of view the electrochemical systems are large integrated, non -linear and quasi -irreversible statistical systems with elements of memory. Processes of charge transfer and mass transport are taking place – they lead to accumulation and reorganization and often to a formation/growth of a new phase(s), changing the total behaviour of the system under study. By following this approach, the classical notion of the impedance as a transfer function should be enlarged drastically.

From this general point of view, the electrochemical impedance is an observation and partial description of a complex system then a full description (transfer function) of a linear, causal and stationary system.

Important possibilities for enrichment of the obtained experimental information are lying in the exploration of the full capabilities of the measurement programs. The selection of the optimal mode of regulation, the amplitude of the measuring signal and the frequency scanning programme can provide for acquisition of precise information concerning the studied processes, but frequently elucidates interesting unexpected phenomena, taking place in the object.

The information capabilities of the sweep down-up are illustrated with experimental measurements of the impedance of a single dislocation compared with that of five dislocations. The results show an well pronounced phenomenon of memory of the perturbation history. The observed hysteresis between the sweep down and sweep up is always an evidence for a formation of a new phase or of a new energetic structure in the object under study.

The importance of the adequate amplitude of the sinusoidal signal is illustrated with impedance measurements of an quasi-perfect, atomic flat, dislocation free single crystal phase Ag [100]. With a carefully designed measurements at amplitude of 50 micro-volts the dependence of the double-layer capacity from small variations (several mV) of the DC- bias voltage is shown. These results show the CPE-like behaviour of the atomic flat surface populated with clusters of different sizes as well as the correlation of the CPE-parameters with the DC bias voltage.

From the system analysis point of view, the electrochemical objects are large integrated systems with spatially distributed local parameters, for which the effective resistances and capacitances are typically frequency dependent. The application of the classical analysis with lumped models in these cases is inadequate.

The application of the soft-computing tools of the Differential Impedance Analysis is a solution of this problem. The produced as a result parametric spectra ensure the interpretation of the results and can serve as efficient tools for elucidating and understanding the observed phenomena.

The power of the Differential Impedance Analysis will be demonstrated with the processing of the experimental data of lubricating oils impedance. The frequency dependence of the effective resistance and capacitance is the primary result of the analysis. The resulting time-constant is strongly correlated with the oil viscosity.

The analysis of the frequency dependent capacity shows unexpected interesting phenomenon of immense increasing of the capacity with decrease of the frequency down to millicycles. Obviously this phenomenon is related with a formation of internal structure of dipole molecules. This process is slow and needs time, which is however closely related with the viscosity of the oil. With the time of the oil operation this process is initially accelerated but later the oil properties degradation is observed.

First Regional Symposium on Electrochemistry of South-East Europe, Rovinj, Croatia, May 4-8, 2008.

PI-2-4

# VOLTAMMETRY AT THREE-PHASE ELECTRODES INVOLVING ION TRANSFER AT THE WATER|IONIC LIQUID INTERFACE

**F. Scholz[1]*, F. Quentel[2], C. Elleouet[2], M. L'Her[2], V. Mirčeski[3], V.A. Hernández[1], M. Lovrić[4], Š. Komorsky-Lovrić[4]**

*[1]Institut für Biochemie, Universität Greifswald, Greifswald, Germany;*
*[2]Laboratoire de Chimie Analytique, UMR-CNRS 6521, Université de Bretagne Occidentale, Brest, France;*
*[3]Institute of Chemistry, Faculty of Natural Sciences and Mathematic, „Ss Cyril and Methodius" University, Skopje, Republic of Macedonia;*
*[4]Department for Marine and Environmental Research, "Rudjer Bošković" Institute, Croatia;*
*fscholz@uni-greifswald.de

Three-phase electrodes provide excellent possibilities to study the ion transfer across liquid|liquid interfaces. The use of electrodes with immobilized droplets of water immiscible solutions of a suitable redox probe allows the determination of the free energy of ion transfer [1-4]. This methodology has been further developed for the study of ion transfer reactions at water|ionic liquid interfaces [5-7]. Ionic liquids possess unique properties that lead to very surprising results, especially because a number of new pathways of ion transfer reactions are possible. Because of the steadily increasing importance of ionic liquids in many chemical and electrochemical applications, it is important to know what ions transfers occur under what conditions.

**References:**

[1] F. Scholz, Š. Komorsky-Lovrić, M. Lovrić : *Electrochem. Commun.* 2 (2000) 112-118
[2] F. Scholz, R. Gulaboski: *ChemPhysChem* 6 (2005) 16-28
[3] F. Scholz: *Annu. Rep. Progr. Chem., Section C* 102 (2006) 43-70
[4] F. Scholz, U. Schröder, R. Gulaboski: Electrochemistry of Immobilized Particles and Droplets, Springer, Heidelberg, Berlin 2005
[5] V. A. Hernández, F. Scholz : *Electrochem. Commun.* 8 (2006) 967-972
[6] F. Quentel, C. Elleouet, V. Mirčeski, V. Agmo Hernández, M. L'Her, M. Lovrić, Š. Komorski-Lovrić, F. Scholz : J. Electroanal. Chem. 611 (2007) 192-200
[7] M. Lovric, Š. Komorsky-Lovric, F. Scholz : *J. Solid State Electrochem.* 12 (2008) 41-45

First Regional Symposium on Electrochemistry of South-East Europe, Rovinj, Croatia, May 4-8, 2008.

PI-2-5

# NEW APPROACH TO THE IMPEDANCE OF ANION ADSORPTION ONTO SINGLE CRYSTAL SURFACES

**V.D. Jović**

*Institute for Multidisciplinary Research, 11030 Belgrade, P.O.Box 33, Serbia*
vladajovic@ibiss.bg.ac.yu

After in situ STM technique had been introduced in the processes of anion adsorption investigation onto single crystal surfaces, it was obvious that even single crystal surfaces are not perfectly flat, but contrary, it is shown that they consist preferentially of significant number of atomically flat terraces separated by monoatomic steps [1,2]. It is also shown that during the process of anion adsorption first step is adsorption of anions at the monoatomic steps accompanied by the dynamic change of the STM image and movement of monoatomic steps and terraces along the electrode surface [3], indicating the presence of heterogeneous charge distribution over the single crystal surface. Simultaneously with adsorption of anions at the monoatomic steps, adsorption of anions occurs at the flat terraces with a formation of 2D islands of adsorbed structures (homogeneous charge transfer distribution over the terrace), while the movement of monoatomic steps and terraces along the electrode surface still occurs [3]. After reaching the potentials of the sharp peaks on the CVs, in all cases ordered adsorbed structures were detected all over the electrode surface and the movement of monoatomic steps and terraces stopped [1-4]. Hence, in such a case it would be reasonable to assume that these two processes, adsorption on the heterogeneous and the homogeneous part of the electrode surface, occur simultaneously during the anion adsorption.

## Model and equivalent circuit for anion adsorption onto real single crystal surfaces

It was shown for Ag(111) in 0.01 M NaCl [5] that $C_{\text{diff}}$ vs. $E$ curves are very sensitive to the frequency although the process of anion adsorption is not controlled by anion diffusion, indicating that even single crystal surfaces cannot be treated as being homogeneous and that, instead of $C_{\text{dl}}$, a constant phase element (*CPE*) ($Z_{CPE} = Y_0(j\omega)^{\alpha}$)[6] should be introduced in the analysis of $C_{\text{diff}}$ vs. $f$ curves. The impedance of an equivalent circuit for parallel connection of *CPE* and *R* can be expressed by two different equations [7];

$$Z_{\text{CPE}}(\omega) = \frac{R}{1+(j\omega CR)^{\alpha}} \qquad (1)$$

and

$$Z_{\text{CPE}}(\omega) = \frac{R}{1+(j\omega)^{\alpha} CR} \qquad (2)$$

Eqn. (2) is used in all commercially available software for fitting impedance spectra, with *CPE* being considered as an independent parameter ($Y_0$ having dimension $\Omega^{-1}cm^{-2}s^{\alpha}$). Eqn. (1) seems to be correct one, since in this equation the frequency dispersion of the capacity as a consequence of the surface heterogeneity is closely related to the charge transfer distribution over the same surface and these two parameters are mutually dependent. Hence, considering all above mentioned it could be concluded that the equivalent circuit for anion adsorption onto real single crystal surfaces should be represented by two impedances, one corresponding to the process of anion adsorption onto heterogeneous part of the surface (monoatomic steps), $Z_{ad}^{he}$, and another one corresponding to the process of anion adsorption (formation of ordered structures) onto homogeneous part of the surface (flat terraces), $Z_{ad}^{ho}$. Such an equivalent circuit is presented in Fig. 1 with $R_{ad}^{he}$ and $CPE_{dl}^{he}$ corresponding to the adsorption resistance and constant phase element on the heterogeneous part of the surface respectively and $R_{ad}^{ho}$ and $C_{ad}$ corresponding to the adsorption resistance and capacity on the homogeneous part of the surface respectively.

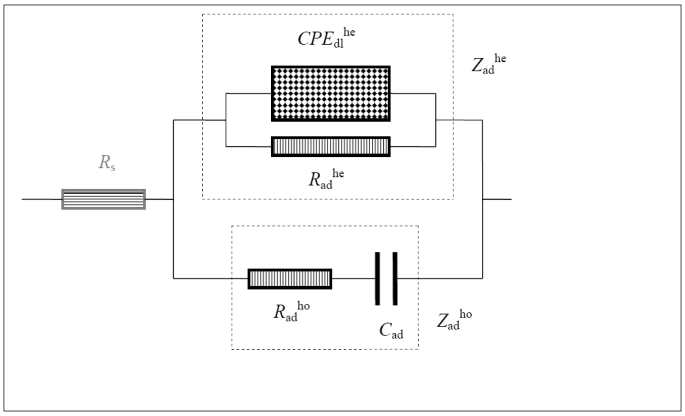


*Fig. 1. Equivalent circuit for anion adsorption onto real single crystal surfaces.*

Following equation (after subtraction of the solution resistance, $R_s$) for the imaginary ($C_{Im}$) capacitance is obtained.

$$C_{Im} \equiv C_{diff} = (C_{dl})^{\alpha}(\omega R_{ad}^{he})^{\alpha-1}\sin(\frac{\alpha\pi}{2}) + \frac{C_{ad}}{1+\omega^2 C_{ad}{}^2 R_{ad}^{ho\,2}} \qquad (3)$$

$C_{Im} \equiv (C_{diff})$ vs. $f$ dependence (Fig. 2) is seen to be very sensitive to the value of $\alpha$ in a whole range of frequencies, being characterized by two inflection points. In the range of high frequencies ($f > 10^2$ Hz for given equivalent circuit parameters) $C_{Im} \equiv (C_{diff})$ slightly changes with $f$ down to the inflection point. Between two inflection points sharp, non-linear increase of $C_{diff}$ with $f$ occurs, while with further decrease of frequency $C_{diff}$ exponentially increases, with this increase being more pronounced at lower values of $\alpha$. The values of $C_{diff}$ at inflection points are defined by the values of $C_{dl}$ and $C_{ad} + C_{dl}$.

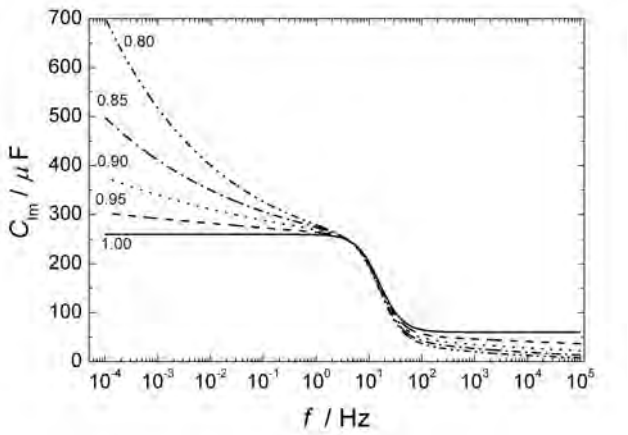


*Fig. 2. Calculated $C_{im}$ vs. f dependences for different α values (marked in the figure) for the para-meters of the equivalent circuit shown in Fig. 1: $C_{ad}$=200 μF, $C_{dl}$=60 μF, $R_{ad}^{he}$=50 Ω, $R_{ad}^{ho}$=5 kΩ.*

## Real system investigations

Two systems were investigated: Ag(111)/0.01M NaCl and Ag(100)/0.01M KBr. CVs recorded at the sweep rate of $v$ = 20 mV $s^{-1}$ are presented in Fig. 3, while corresponding $C_{diff}$ vs. $E$ curves, recorded for different frequencies are presented in Fig. 4. As can be seen excellent agreemnet between the CV's and the $C_{diff}$ vs. $E$ curves is obtained for frequencies lower than 10 Hz.

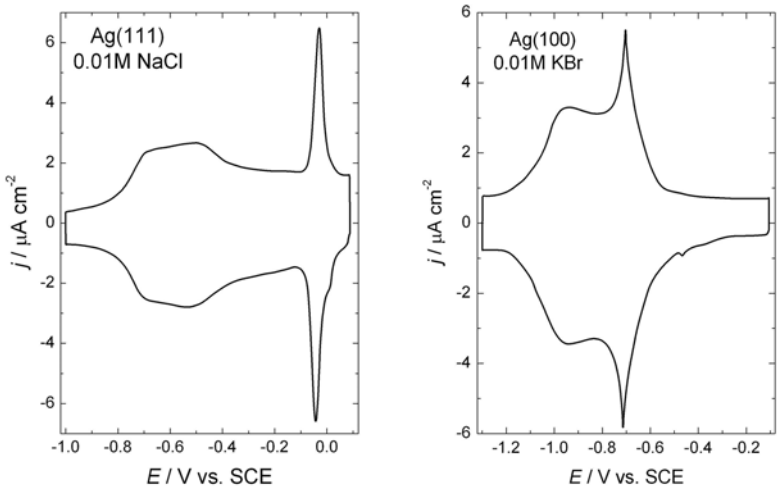


*Fig. 3. Cyclic voltammograms for the investigated systems.*

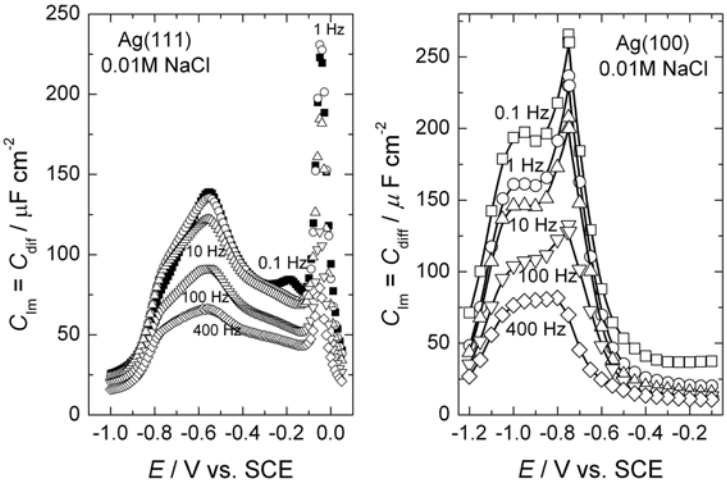


*Fig. 4. $C_{diff}$ vs. E curves for the investigated systems (frequencies marked in the figure).*

By the analysis of the $C_{diff}$ vs. $E$ curves, $C_{diff}$ vs. $\omega$ dependences were obtained for each potential applied. These dependences were of the shape presented in Fig. 2. By fitting them with the equation (3) parameters of the proposed equivalent circuit were obtained and plotted as a function of potential. Obtained results are presented in Figs. 5 and 6. Chloride and bromide anions are known as strongly adsorbing species characterized by the formation of ordered adsorbate structures on all investigated single crystal faces [3-5,8-15]. Generally accepted explanation for the frequency dependence of the interfacial - differential capacity ("capacity dispersion") could be given as: this phenomenon is a consequence of either adsorption of organic [10] or inorganic [12] molecules, or surface roughness and heterogeneity [5,12,13], or specific adsorption of anions [5,7,14]. It should be emphasized here that except in our previous paper [5] "capacity dispersion" as a consequence of both, anion adsorption and surface heterogeneity, has not been considered in the literature. Considering results presented in Figs. 5 and 6 it could be concluded that these two systems are significantly different, i.e. the processes of chloride and bromide anions adsorption are different. The first difference is expressed in the shape of ($C_{dl}$+$C_{ad}$) vs. $E$, $C_{dl}$ vs. $E$ and $C_{ad}$ vs. $E$ curves. For the system Ag(111)/0.01 M NaCl all three curves follow the shape of the CV, whereas for the system Ag(100)/0.01 M KBr the shapes of these curves are different, with $C_{ad}$ vs. $E$ curve only being similar to the CV. As can be seen in Fig. 6a $C_{dl}$ increases with potential up to -0.75 V and then sharply decreases to a very small values of about 3-5 $\mu$F cm$^{-2}$. At the position of a maximum on the $C_{ad}$ vs. $E$ curve, $C_{dl}$ is practically neglecting and at potentials more positive than -0.60 V a total capacity ($C_{dl}$+$C_{ad}$) is practically determined by the value of $C_{ad}$. A second difference is expressed in the shape of $\alpha$ vs. $E$ curves. For the system Ag(111)/0.01 M NaCl the value of $\alpha$ is slightly dependent on potential (Fig. 5a), whereas for the system Ag(100)/0.01 M KBr the value of $\alpha$ sharply decreases from about 0.95 at -0.70 V to about 0.45 at -0.10 V. This is in accordance with the findings that after the formation of an ordered $c$(2x2) structure (sharp peak on

both, the CV and $C_{diff}$ vs. $E$ curves), incommensurate adsorbed structures, compressing uniformly with increasing potential, have been detected [15]. The third difference is demonstrated in $R_{ad}^{ho}$ vs. $E$ and $R_{ad}^{he}$ vs. $E$ curves (Figs. 5b and 6b). Finally, considering charges under $C_{ad}$ vs. $E$ curves for the system Ag(111)/0.01 M NaCl (29 $\mu$C cm$^{-2}$) and Ag(100)/0.01 M KBr (31 $\mu$C cm$^{-2}$) and assuming that the electrosorption valence corresponds to the formation of ordered adsorbed structures, it appears that $\gamma(Cl^-) = -0.4$ and $\gamma(Br^-) = -0.3$ respectively, i.e. adsorbed anions are partially discharged. Hence, this analysis clearly indicates that neither the charge under the CV, nor that under the $C_{diff}$ vs. $E$ curve recorded at a single frequency, can be considered as relevant for determining either the structure of adsorbed anions or the value of $\gamma$.

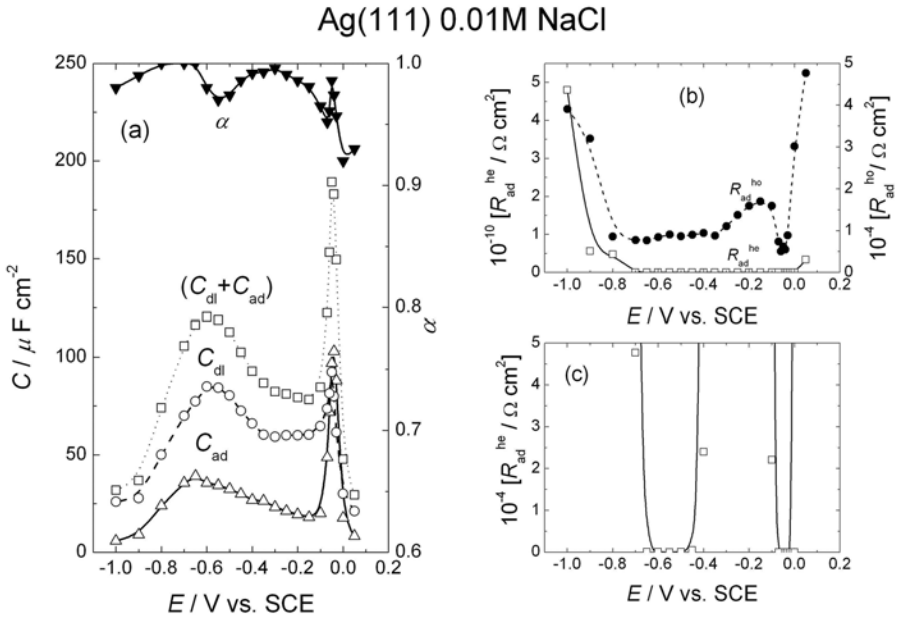


*Fig. 5. (a) ($C_{dl}$+$C_{ad}$) vs. E, $C_{dl}$ vs. E, $C_{ad}$ vs. E and $\alpha$ vs. E curves. (b,c) $R_{ad}^{ho}$ vs. E and $R_{ad}^{he}$ vs. E curves.*

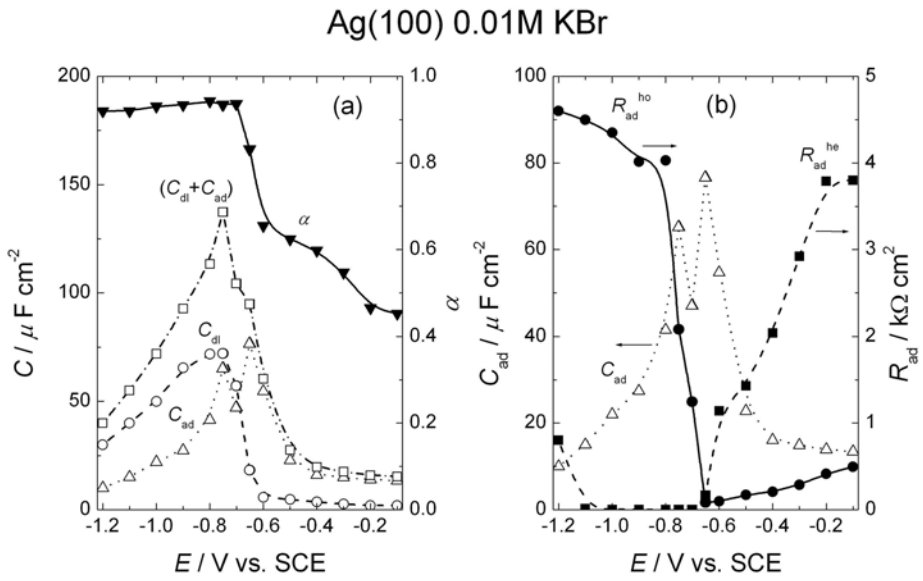


*Fig. 6. (a) $(C_{dl}+C_{ad})$ vs. E, $C_{dl}$ vs. E, $C_{ad}$ vs. E and $\alpha$ vs. E curves. (b) $C_{ad}$ vs. E, $R_{ad}^{ho}$ vs. E and $R_{ad}^{he}$ vs. E curves.*

**References**

1. T.P. Moffat, in: A.J. Bard and I. Rubinstein (Eds.), *Electroanalytical Chemistry: a Series of Advances*, vol. 21, Marcel Dekker Inc., New York, Basel, 1999, pp. 211-316.
2. M. Schweizer, D.M. Kolb, *Surf. Sci*. **544** (2003) 93.
3. H.-H. Streblow, V. Maurice, P. Marcus, *Electrochim. Acta* **46**(2001)3755.
4. A. Cuesta, D.M. Kolb, Surf. Sci. 465(2000)310.
5. V.D. Jović, B.M. Jović, J.*Electroanal.Chem.* **541**(2003)1.
6. J.R. Macdonald, I*mpedance Spectroscopy Emphasizing Solid Materials and Systems*, Wiley, New York, Chichester, Brisbane, Toronto, Singapore, 1987.
7. M.E. Orazem, P.Shukla, M.A. Membrino, *Electrochim. Acta* **47**(2002)2027.
8. M.S. Zei, *J.Electroanal.Chem.* **308**(1991)295.
9. G. Aloisi, A.M. Funtikov, T. Will, *J.Electroanal.Chem.* **370**(1994)297.
10. W. Lorenz, F. Möckel, *Z. Elektrochem.* **60**(1994)507.
11. C.N. van Houng, C. Hinnen, J.P. Dalbera, R. Parsons, *J.Electroanal. Chem*. **125**(1981)177.
12. M. Sluyters-Rehbach, *Pure & Appl. Chem.* **66**(1994)1831.
13. Z. Kerner, T. Pajkossy, E*lectrochim. Acta* **46**(2000)207.
14. V.D. Jović, R. Parsons, B.M. Jović, *J.Electroanal.Chem.* 339(1992)327.
15. J.X. Wang, R.R. Adžić, B.M. Ocko, In Situ X-ray Scattering Studies of Electrosorption, in: A. Wieckowski (Ed.), *Interfacial Electrochemistry: Accomplishments and Challenges*, Marcel Dekker Inc., New York, 1999, pp. 175-185.

First Regional Symposium on Electrochemistry of South-East Europe, Rovinj, Croatia, May 4-8, 2008.

# CONTRIBUTIONS - ORAL

O-1-01 Keynote lecture

## AN EVALUATION OF FACTORS THAT DETERMINE THE PERFORMANCE OF A MICROBIAL FUEL CELL USING DIFFERENT ELECTROCHEMICAL TECHNIQUES

**A.K. Manohar[1], O. Bretschger[1], K.H. Nealson[2], D.A. Harrington[3], F. Mansfeld[1,*]**

*[1]Corrosion and Environmental Effects Laboratory (CEEL), The Mork Family Department of Chemical Engineering and Materials Science, E-mail: mansfeld@usc.edu*
*[2]Department of Earth Sciences, University of Southern California, Los Angeles, CA 90089-0241, USA,*
*[3]Department of Chemistry, University of Victoria, Victoria, BC, V8W 3V6, Canada.*

The properties of the anode and the cathode of a mediator-less microbial fuel cell (MFC) and the power output of the MFC have been evaluated using different electrochemical techniques. In the MFC under investigation the biocatalyst - *Shewanella oneidensis MR-1* oxidizes the fuel – lactate – and transfers the electrons directly to the anode which consists of graphite felt. Oxygen is reduced at the cathode which consists of Pt-plated graphite felt. A proton exchange membrane separates the anode and the cathode compartments. Ag/AgCl reference electrodes have been placed into both compartments [1, 2].
Electrochemical impedance spectroscopy (EIS) carried out at the open-circuit potential (OCP) has been used to determine the electrochemical properties of the anode and the cathode as a function of time and experimental conditions [1, 2]. Potential sweeps have been employed to record the cell voltage (V) – current (I) curves for the MFC. From these V – I curves the cell voltage $V_{max}$ at which the power output of the MFC has a maximum value $P_{max}$ has been determined. Power (P) – time (t) curves have been measured at $V_{max}$ for 12 h periods. Cyclic voltammetry (CV) and potentiodynamic polarization curves have been used to evaluate the anodic and cathodic reaction kinetics in a wide potential range.
The internal resistance ($R_{int}$) of the MFC has been determined as a function of V using EIS for the MFC described above and a MFC in which, stainless steel balls have been added to the anode compartment. The $R_{int}$ of the MFCs studied here is calculated as the sum of the polarization resistance of the anode ($R^a_p$) and the cathode ($R^c_p$), and therefore $R_{int}$ depends on V (Fig.1). Additions of MR-1 or SS balls to the buffer and lactate solution produced a very large decrease of $R_{int}$. For all cases studied, $R_{int} = R_{ext}$ at $V_{max}$, where $R_{ext}$ is the load that has to be placed between the anode and the cathode to obtain $V_{max}$. Additionally, it has been experimentally shown that $R_{int}$ equals the slope of the V- I curve. A comparison of the results of theoretical calculations and the experimental data shows very good agreement for these two sets of data.

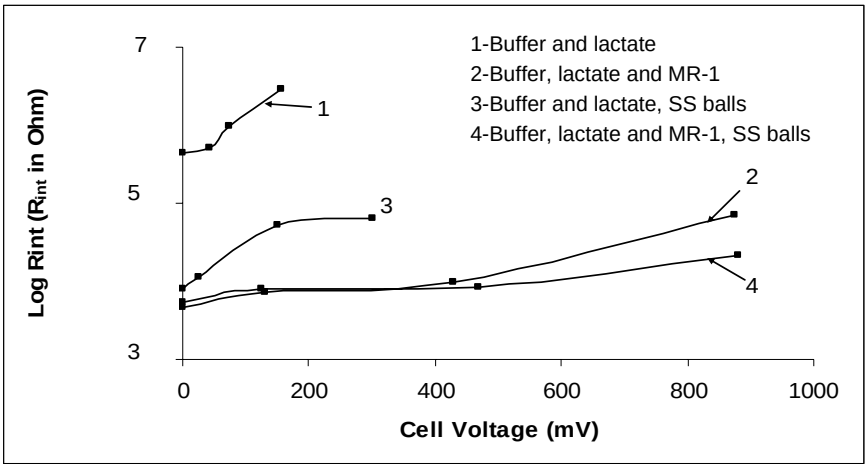


*Fig 1: $R_{int}$ vs cell voltage.*

***Acknowledgment****. This project is supported by the AFOSR MURI program, Award No. FA9550-06-1-0292, Maj. Jennifer Gresham, contract monitor.*

**References:**

1. A. K. Manohar, O. Bretschger, K. H. Nealson and F. Mansfeld, *The Use of Electrochemical Impedance Spectroscopy (EIS) in the Evaluation of the Electrochemical Properties of a Microbial Fuel Cell.* Bioelectrochemistry. (in press)**.**
2. A. K. Manohar, O. Bretschger, K. H. Nealson and F. Mansfeld, *The Polarization Behavior of the Anode in a Microbial Fuel Cell.* Electrochimica Acta. (in press).

First Regional Symposium on Electrochemistry of South-East Europe, Rovinj, Croatia, May 4-8, 2008.

O-1-02

# GLUCOSE ELECTROOXIDATION FOR BIOFUEL CELL APPLICATIONS

**I. Ivanov[1], T. Vidaković[2], K. Sundmacher[1,2]**

*[1]Max Planck Institute for Dynamics of Complex Technical Systems, Sandtorstr. 1, D-39106 Magdeburg, Germany*
*[2]Otto-von-Guericke-University Magdeburg, Process Systems Engineering, Universitätsplatz 2, D-39106 Magdeburg, Germany, vidakovi@mpi-magdeburg.mpg.de*

Biofuel cells are a fuel cell type which employs biocatalysts (whole living cells – microbial or complex protein structures (enzymes) - enzymatic). Currently, enzymatic biofuel cells are considered more beneficial due to higher power density. This fuel cell type is prone to miniaturisation and is often considered as a candidate to replace lithium batteries as power sources for implantable medical devices. Additionally, due to the high catalyst specificity a membraneless fuel cell design is possible. However, the state-of-the-art enzymatic fuel cell has very low performance. The main reasons are kinetic limitations and the stability. The kinetic limitations are mainly imposed by difficulties to achieve efficient electron transfer between the redox active center of the enzyme and the electron conducting surface. In this communication we report new insights into glucose oxidase (GOx) redox activity on gold electrode and implications regarding the glucose oxidation, especially in the context of the electroactivity of gold itself (Fig. 1. A and B).

All experiments were performed in a three-electrode electrochemical cell using gold electrodes. For the enzyme immobilisation procedure developed in [1] was used. The GOx redox active center (flavin adenine dinucleotide (FAD)) was modified following the procedure described in [2] and Apo-GOx was obtained according to [3].

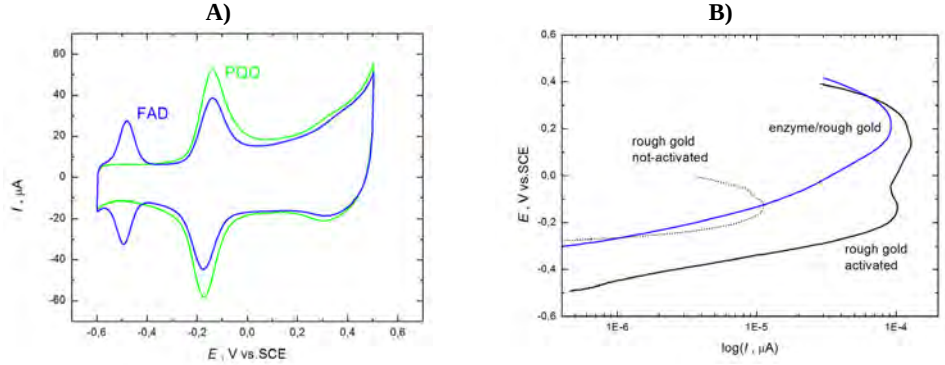


*Fig. 1. A) Redox peaks of FAD and pyrroloquinoline quinone (PQQ) on gold surface at sweep rate of 50 mV $s^{-1}$; B) Glucose oxidation on rough gold surface and gold surface modified by GOx at sweep rate of 5 mV $s^{-1}$ and at 5 mM glucose concentration. Conditions: 0.1 M phosphate buffer solution at 22 $^{o}$C (A) and 37$^{o}$C (B).*

**References:**

1. I. Willner, V. Heleg-Shabtai, R. Blonder, E. Katz, G. Tao, *J. Am. Chem. Soc.*, **118** (1996) 10321.
2. A.F. Bückmann, V. Wray, A. Stocker, *Methods in Enzymology - Flavins and derivatives*, **280** (1997) 360.
3. B.E.P Swoboda, *Biochim. Biophys. Acta*, **175** (1969) 365.

First Regional Symposium on Electrochemistry of South-East Europe, Rovinj, Croatia, May 4-8, 2008.

O-1-03

# TESTING AND OPTIMIZATION OF HYDROGEN ELECTRODES FOR THE ELECTROCHEMICAL HYDROGEN ENERGY CONVERTERS WITH POLYMER ELECTROLYTE

**I. Radev[1], P. Paunović[2], O. Popovski[2], A. Dimitrov[2], E. Slavcheva[1], E. Budevski[1]**

*[1]Institute of Electrochemisty and Energy Systems, 1113 Sofia, Acad. G. Bonchev Str., bl. 10, ivan.radev@gmail.com*
*[2]Faculty of Technology and Metallurgy, 1000 Skopje, Ruger Boshkovik 16*

In the context of the promising already advancing hydrogen economy, the polymer membrane (PEM) electrochemical hydrogen energy converters (EHECs) comprising fuel cells, water electrolyzers and bifunctional cells undoubtedly will play a major role. Due to the high current densities, absence of liquid electrolyte, compact design and easy production, they are considered to possess the highest potential for automotive, emergency, and remote applications. Although these devices are in a rather advanced stage of development, an essential price reduction is required for their wide commercialization. The amount and utilization of the Pt incorporated in the main active PEM EHEC element – the membrane electrode assembly (MEA) is one of the most price determienative parameters. In the state-of-the-art EHEC two main approaches for reduction of Pt loadings are applied: (i) increase of Pt active surface by deposition on proper supports with extended surface area and (ii) usage of composite catalysts containing Pt and a second non noble metal. In the present work the non-aqueous sol-gel method was applied to synthesise PtCo catalysts with varying ratios aiming to reduce Pt loading in the hydrogen electrode without decrease in MEA performance. The influence of the 2 catalyst supports – carbon nanotubes and Vulcan XC-72 on the catalyst activity are studied and discussed. The results obtained in a recently deveoped EasyTest Cell regarding hydrogen partial reaction in fuel cell and electrolyzer mode are compared to commercially available ELAT electrode (E-TEK). The long term tests carried out at intensive hydrogen evolution show a stable electrode performance.

First Regional Symposium on Electrochemistry of South-East Europe, Rovinj, Croatia, May 4-8, 2008.

O-1-04

# MODELING OF PERVOSKITE-TYPE PROTON CONDUCTOR FOR INTERMEDIATE TEMPERATURE ELECTROLYSER

**C. Deslouis[1], M. Keddam[1], K. Rahmouni[1], H. Takenouti[1], O. Lacroix[2], B. Sala[2], S. Willemin[2]**

*[1]UPR 15 du CNRS - LISE, UPMC Univ Paris 06, 3 rue Galilée, 94200 Ivry sur Seine, France*
*[2]Areva NP, IEM, Place Eugène Bataillon, 34095 Montpellier, France*

The increase in the operating temperature of hydrogen production by vapour electrolyser allows the improvement of energy efficiency and the increase of ionic conduction. The solid oxide fuel cell (SOFC) with yttrium stabilized zirconia (YSZ) is often working at temperature ranging between 800 – 1000 °C. However, it is interesting from technological point of view to decrease the operating temperature such that more common alloys to be used for structures (cell, connectors, valves, thermal exchangers, and so on). One of the problems that occur for decreasing operating temperature is the loss of the solid electrolyte conductivity. The use of proton conducting ceramic allows a lowering of operating temperature. A target temperature range is 400 to 600 °C. However, for development of new proton conducting materials, it is crucial to characterize separately their conducting and dielectric properties at bulk and grain boundaries.

The experimental electrochemical impedance spectra in the frequency domain spreading between 10 MHz to 1 Hz on perovskite type proton conducting ceramics were interpreted by the series connexion of bulk, grain boundaries and the interface behaviour between Pt electrode and the solid electrolyte. The electrical response of grain and grain boundaries is described by conductivity and the dielectric constant with relaxation time constant obeying Cole-Cole type relaxation. The platinum – electrolyte interface exhibits below ca. 100 Hz the charge transfer resistance, the interface capacitance and the Warburg type impedance. No electronic conduction was detected except for a temperature above 750 °C for certain ceramic synthesized.

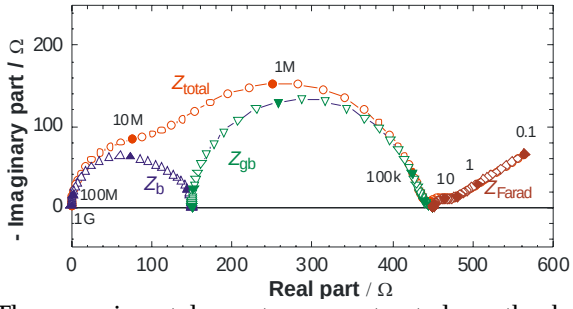


*Impedance spectrum of perovskite type ceramics (model).*
*$Z_b$: Impedance relatvie to grain*
*$Z_{gb}$: that of grain boundary*
*$Z_{Farad}$: Faradic impedance at Pt – solid electrolyte interface*
*$Z_{total}$: overall impedance*
*The dissimetry observed in $Z_b$ and $Z_{gb}$ is due to the Cole-Cole type relaxation of dielectric constant.*

The experimental spectra were treated on the basis of the brick layer model. As measured, the condcutance (S) of grain boundary and that of bulk are similar whereas when expressed as the conductiviy (S $cm^{-1}$), the bulk showed a much higher value as expected.

*This work was carried out in the framework of PAN'H project, ANR-06-PANH-05 « Celeva ».*

**Key words:** Ceramic, Dielectric relaxation, Electrolyser, Grain boundary, Hydrogen

First Regional Symposium on Electrochemistry of South-East Europe, Rovinj, Croatia, May 4-8, 2008.

O-1-05

# ELECTRODE IMPEDANCE AND BULK CONDUCTIVITY IN TERMS OF REACTION LIMITED DIFFUSION

**G. Nagy, J. Balog, Z. Kerner, R. Schiller**

*Central Research Institute for Physics, Atomic Energy Research Institute*
*P.O.B. 49 Budapest H-1525 Hungary, E-mail: schiller@aeki.kfki.hu*

Spatial motion of reactants, i.e. their diffusion and/or migration, influences the rate of chemical transformation. The simplest of the cases is when diffusion and reaction are independent of each other; here the rate of concentration change is equal with the algebraic sum of the rates of diffusion and chemical transformation. This process is called *diffusion controlled reaction.*
The rate of the encounter of reaction partners is determined by diffusion; hence, if the reaction is very fast the rate of diffusion sets an upper limit of the reaction rate. Such processes can be denoted as *diffusion limited reactions*.
The third possible scenario is when the random walk of reacting particles is interfered by a chemical reaction: for this case we propose the name *reaction limited diffusion.* This third type is the subject of the present paper. The theoretical treatment is based on the ideas of continuous time random walk by Scher and Lax[1].
By considering the effect of a pseudo-first order chemical reaction on the random walk of the reactant, a dispersive diffusivity (mobility) is found with two time constants: one for the random walk, the other for the reaction. The theory is applied to the problems of (*1*) charge carrier diffusion in and electrode admittance, $Y_{dr}$, of thick metal oxide layers[2], (*2*) charge carrier mobility in and electrode admittance, $Y_{mr}$, of thin metal oxide layers[3], and (*3*) mobility and reaction rate coefficient as determined by the time-of-flight of the charge carriers, $t_f$ , in the bulk of a reacting system[4].

Impedance determinations are usually performed in the frequency domain, hence the relevant theoretical expressions are formulated in terms of dependencies on angular frequency, ω. The frequency dependent terms for the cases (*1*) and (*2*), respectively, are given as

$$Y_{dr} \propto \left( i\omega\tau \frac{1+i\omega\tau_D}{1+i\omega\tau} \right)^{1/2} \qquad \text{and} \qquad Y_{mr} \propto \left( \frac{1+i\omega\tau_D}{1+i\omega\tau} \right),$$

where $\tau_D$ and $\tau_C$ are the characteristic time constants for diffusive displacement and chemical reaction, respectively, and $1/\tau = 1/\tau_D + 1/\tau_C$ holds.
The kinetics of bulk reactions is usually described in the time domain. Using the notation $\eta = \tau_C/(\tau_C + \tau_D)$ one finds an expression for the time-of-flight, in terms of $\tau_D$ and $\tau_C$ as parameters,

$$l^2 = \mu_0 U\left[\eta t_f + (1-\eta)\tau\left(1-e^{-t_f/\tau}\right)\right].$$

Here $U$ is the applied potential, $l$ the electrode distance, and $\mu_0$ the charge carrier mobility. For a number of practical cases the above expression can be simplified as

$$\mu_0 \eta \cong \frac{l^2}{U t_f}.$$

By recalling that $\tau_C^{-1} = k_s' c_s$ holds, a linear relationship between $t_f$ and $c_s$ is obtained,

$$\frac{U}{l^2} t_f = \frac{1}{\mu_0} + \frac{\tau_D}{\mu_0} k_s' c_s.$$

Thus if one determines $t_f$ as a function of $c_s$, both mobility and rate coefficient can be determined.

**References**

1. H. Scher and M. Lax, *Phys. Rev. B* **7**, 4491, 4502 (1973)
2. R. Schiller, J. Balog and G. Nagy, *J. Chem. Phys.* **123**, 094704 (2005)
3. G. Nagy, Zs. Kerner and R. Schiller, *Electrochimica Acta*, **53**, 1737 (2007)
4. R. Schiller and G. Nagy, *Rad. Phys. Chem.* **76**, 1248 (2007)

First Regional Symposium on Electrochemistry of South-East Europe, Rovinj, Croatia, May 4-8, 2008.

O-1-06

# APPLICATION OF ELECTROCHEMICAL IMPEDANCE SPECTROSCOPY FOR FUEL CELL CHARACTERIZATION

**N. Wagner**

*German Aerospace Center, Institute for Technical Thermodynamics,*
*Pfaffenwaldring 38-40, D-70569 Stuttgart, Germany, Norbert.Wagner@dlr.de*

The most common method used to characterize the electrochemical performance of a fuel cell is recording of current/voltage U(i) curves. Separation of electrochemical and ohmic contributions to the U(i) characteristics requires additional experimental techniques like Electrochemical Impedance Spectroscopy (EIS). The application of EIS is an approach to determine parameters which have proved to be indispensable for the characterization and development of fuel cell electrodes and electrolyte electrode assemblies [1].

By varying the operating conditions of the fuel cell and by simulation of the measured EIS with an appropriate equivalent circuit, it is possible to split the cell impedance into electrode impedances and electrolyte resistance. Integration in the current density domain of the individual impedance elements enables the calculation of the individual overpotentials in the fuel cell and the determination of the voltage loss fraction.

Examples of EIS measured at different fuel cell systems and operating conditions will be shown, like:

- Polymer Electrolyte Fuel Cells (PEFC) with symmetrical gas supply, with hydrogen and oxygen at different cell potentials
- Solid Oxide Fuel Cells (SOFC) supplied with hydrogen with different water partial pressures and operated at different temperatures
- Alkaline Fuel Cells, oxygen reduction at porous Silver Gas Diffusion Electrodes (GDE) at 80°C in 10 N NaOH

Furthermore, in the presentation the theory of impedance spectra measured at fuel cells with electrodes changing their state with time e.g. anode surface changing during CO poisoning of PEFC anodes and water flooding of the cathode during “dead end” operation mode of the PEFC. Also experimental results of EIS measured on different electrodes e.g. Pt/C and PtRu/C will be presented and discussed.

For the evaluation of the measured impedance spectra a porous electrode model was used. After a brief overview of different porous electrode models used in literature for fitting experimental date the porous electrode model of Göhr [2] will be discussed in detail. This porous electrode model includes different impedance contributions like impedance of the interface porous layer/pore, interface porous layer/electrolyte, interface porous layer/bulk, impedance of the porous layer and impedance of the pores filled by electrolyte.

[1] N. Wagner, “Electrochemical power sources – Fuel cells” in *Impedance Spectroscopy: Theory, Experiment, and Applications*, 2nd Edition, Edited by Evgenij Barsoukov and J. Ross Macdonald, John Wiley&Sons, Inc., ISBN: 0-471-64749-7, pp. 497-537, 2005

[2] H. Göhr, *Electrochemical Applications*, **1** (1997) 2 (http://www.zahner.de)

First Regional Symposium on Electrochemistry of South-East Europe, Rovinj, Croatia, May 4-8, 2008.

O-1-07 Keynote lecture

# MAGNETRON SPUTTERING AS A FEASIBLE TECHNIQUE FOR CATALYST DEPOSITION AND FABRICATION OF MEA

**E. Slavcheva**

*Institute of Electrochemistry and Energy Systems – Bulgarian Academy of Sciences, Akad. G. Bonchev Str. 10, 1113 Sofia, Bulgaria, slavcheva@bas.bg*

Deposition of thin catalytic films by the physical vapour deposition method of magnetron sputtering is a comparatively new and promising approach. This technique allows deposition of thin compact films upon a selected substrate material and ensures simplicity of the catalysts preparation as well as improved stability, durability, and utilisation. The method is particularly favourable for applications in hydrogen energy converting electrochemical cells with polymer electrolyte membrane The energy transfer in these devices proceeds in the so called membrane electrode assembly (MEA) which has a rather complex architecture and consists of at least 5 different layers – a polymer electrolyte membrane on whose sides the anode and cathode are attached each consisting of catalytic and gas diffusion layers. The usage of the conventional powder catalysts requires a number of consecutive processes to fabricate the catalytic layer on each electrode before attaching it to the membrane. In contrast, the sputtered catalysts can be deposited directly on the gas diffusion layer or even on the polymer electrolyte membrane. In this way, the preparation steps can be essentially reduced, simplifying the whole MEA fabrication. The technique offers deposition of various single and composite materials. It is easily controlled in obtaining homogeneous, well dispersed reproducible thin films with a very low catalyst loading and is open for large scale and practical employment.

In this work the influence of sputtering parameters (dc power, argon pressure) and film thickness/metal loading on the surface structure and morphology of thin sputtered films of noble metals (Pt, Ir and their combinations) and the resulting effect on the catalytic activity toward the partial reactions proceeding in the hydrogen energy converters (fuel cells and water electrolysers) is investigated using variety of experimental techniques. It is demonstrated that by simple variations in the sputter regime it is possible to tailor the catalysts morphology and to guide the catalytic activity toward the electrochemical reaction of interest.

First Regional Symposium on Electrochemistry of South-East Europe, Rovinj, Croatia, May 4-8, 2008.

O-1-08

# SYNTHESIS AND CHARACTERIZATION OF PROTONIC CONDUCTING MEMBRANES INCORPORATING AN IONIC LIQUID FOR FUEL CELL APPLICATION PEMFC

**M. Hanna, J.C. Lepretre, J.Y. Sanchez**

*LEPMI –1130, rue de la Piscine, 38402 Saint Martin d'Hères – France,*
maha.hanna@lepmi.inpg.fr

The PEMFC (proton exchange membrane fuel cell) technology seems today a promising source of energy because of its high energetic efficiency and its simple, not polluting operating system, which exploits an electrochemical reaction between a fuel ($H_2$) and carburant ($O_2$ or air) with production of water, the only product generated during the reaction. For the application for clean vehicle, the fuel cell with solid polymeric electrolyte (PEMFC) is largely studied. Even if this technology is currently available, its production cost remains high (cost of the catalyst (platinum), the bipolar plates, the membrane) and slow down its use. This is why of many research are invested in the study of the PEMFC, by accentuating their efforts on the development of a new family of protonic conducting membranes in which the conduction of ions $H_3O^+$ would be ensured by the incorporation of a protonic ionic liquid. The membranes usually used in technology PEMFC are perfluorinated polymers with sulphonic groups, such as Nafion®, producted by Dupont de Nemours.
In spite of its interesting properties (conductivity, mechanical resistance), the instability of its conduction beyond 80°C makes difficult the use of Nafion® in fuel cells at high temperature what would however make it possible to increase energy efficiency appreciably [1,2]. This is why various alternate membranes were tested with higher temperatures with 100°C. Especially membranes containing protonic ionic liquids can be developed because of the great thermal and chemical stability of this type of compounds. The choice of the protonic ionic liquids (choice of the cation and the against-ion) is determining to ensure a high conductivity and a thermal stability in a broad range of temperature, while the redox reactions with the electrodes should not be slowed down in the presence of the PIL [3]. Moreover these materials or PILs (Proton Ionic Liquids) must make it possible, when they are incorprated in a suitable polymeric membrane [5], to reach performances higher or equal to those of Nafion® (about 600 mA/cm$^2$ to 0.6 V to 80°C) with a satisfactory durability. Thus, although impregnated membranes by a salt of triflate or tetrafluorofluoroborate of ethyl 3-methylimidazolium have a conductivity higher than 100 mS/cm towards 180°C [3], their test in cell shows that these compounds are not usable for this technology. This is why, we chose our interest in ionic liquids of acid-bases of Brönsted type, which are obtained by transfer of protons, by combining an organic amine and a mineral acid [4]. Ionic salts thus synthesized are characterized and thereafter, these compounds are incorporated into sulfonic polymer membranes. The protonic conducting membrane is obtained by impregnation of dry polymer by the protonic ionic liquid. The elaborate films are characterized by measurements of conductivity by complex impedance and thermal (DSC) and mechanical (DMA) analyses. The results obtained are compared with those of the free ionic liquids in order to understand the mechanism of conduction of these conducting membranes and optimizing their composition.

Nafion®-$H^+$'s glass transition temperature is estimated to be about 150°C. We have noticed that this value decreases once Nafion® membranes are neutralised by alkylamins and than swollen with ILs because of the very weak associations between ion pairs, the efficiency of the physical cross-links to locally restrict the mobility of chains decreases, yielding a relatively larger population of chains in a more mobile state [6].

As mentioned before, ILs present relative high conductivities (30 $mS.cm^{-1}$ at 130°C, Figure 1), which decrease strongly once IL is incorporated in Nafion membrane (6 $mS.cm^{-1}$ at 130°C, Figure 1.). The mechanism for protonic conduction in these ILs is under studies. Although the conductivity of the Nafion® -$H^+$ membrane swollen with EMATf or $CH_3CH_2(CH_3)NH_2^+$, $CF_3SO_3^-$ ($7.10^{-3}$ $S.cm^{-1}$) is appreciable at 130°C, fuel cell applications would generally prefer conductivities in the 0.1 $S.cm^{-1}$ range to improve the power density. Assuming that much of the ionic conductivity is due to mobile protons, this implies that the higher absorption of ionic liquid solvent brings about a greater dissociation of protons from the ionomer [3].

In the other hand, the neutralisation of Nafion® by alkylamin dosen't affect a lot Nafion®'s mechanical properties, but once swollen by the corresponding IL (Figure 2: MBATf or $CH_3(CH_2)_2(CH_3)CHNH_2^+$, $CF_3SO_3^-$), it loses strongly its mechanical properties: Nafion®-$H^+$ = 230 MPa, Nafion®-$H^+$-MBA = 140 MPa, Nafion®- $H^+$-MBA $_{\text{swollen with MBATf}}$ = 7 MPa at 80°C (Figure 2.).

In correlation with Moore and al [6], our study with different alkylamins showed that the Nafion®'s physical properties are related to the counterion size, and are affected by two contributing factors. As the size of the counterion increases, (1) the larger counterions significantly decrease the strength of the electrostatic interactions (i.e., weaken the electrostatic network) and (2) the bulky, organic counterions can effectively plasticize the material, thus decreasing the relaxation temperatures.

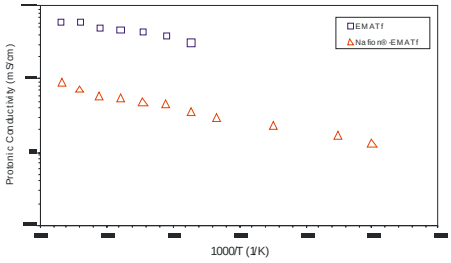


*Figure : Ionic conductivity vs. Temperature for EMATf neat IL and imbibed into Nafion® membrane.*

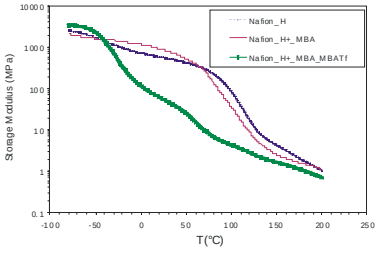


*Figure : Storage modulus vs. Temperature for protonic form, neutralised form, and swollen form for Nafion® membranes.*

References:

1. E. Chalkova, X. Zhou, C. Ambler, M.A. Hofmann, J.A. Weston, H.R. Allcock et S.N. Lvov. *Electrochemical and Solid-State Letters*. A221-A222, **5(10)** (2002)
2. P. Jannasch. C*urrent Opinion in Colloid and Interface Science*. 96-102, **8** (2003)
3. M. Doyle, S.-K. Choi, G. Proulx. *Journal of The Electrochemical Society*. 34-37, **147** (1) (2000)
4. J-H. Chang, J. H. Park, Gu-Gon Park, C-S. Kim, O. O.Park. *Journal of Power Sources*, 18-25, **124** (2003)
5. C. Chiappe, D. Pieraccini. *Journal of Physical Organic Chemistry*. 275-297, **18** (2005)
6. K. A. Page, K. M. Cable, R. B. Moore, *Macromolecules*, 2005, **38**, 6472-6484

First Regional Symposium on Electrochemistry of South-East Europe, Rovinj, Croatia, May 4-8, 2008.

O-1-09

# METHANOL OXIDATION AT ELEVATED TEMPERATURE AND PRESSURE –A DIFFERENTIAL ELECTROCHEMICAL MASS SPECTROMETRY STUDY

**M. Chojak, Z. Jusys, J.R. Behm**

*Institute of Surface Chemistry and Catalysis, Ulm University, D-89069 Ulm, Germany*
malgorzata.chojak@uni-ulm.de

Direct methanol fuel cell (DMFC) related processes have been extensively studied during the last decades. Model studies of fuel cell related electrocatalytic reactions can offer deeper insight into the kinetics and mechanism of these processes. These model studies should be performed under conditions as close as possible to realistic situation, since DMFCs are mostly operated at elevated temperatures (~100°C) and pressures (3 bar). However, because of the associated experimental problems, elevated temperature measurements of the methanol oxidation reaction were reported only by few groups, rarely reaching the fuel cell operation relevant temperatures [1-4].

Because of different products formed during methanol oxidation ($CO_2$, formic acid and formaldehyde [5,6]), the quantitative determination of the product distribution is highly desirable. This is possible by on-line mass spectrometry (*Differential Electrochemical Mass Spectrometry*, DEMS), and a previous study revealed a distinct relation between catalyst loading and efficiency for complete oxidation to $CO_2$ [7]. Elevated temperature (100°C) DEMS model studies, however, were not available so far due to the severe technical problems related to interfacing the high temperature/high pressure cell to the vacuum system.

In this contribution we report on a novel thin-layer flow cell developed for reaction studies at elevated temperatures (up to 100°C) and pressures (4 bar). It is coupled via a thin Teflon membrane to a DEMS system, which allows to quantitatively analyze the $CO_2$ production rate under these conditions. We present first results on the methanol oxidation reaction activity and selectivity obtained with this set-up. These measurements were performed under realistic, fuel cell relevant conditions, including continuous electrolyte flow, elevated temperatures and carbon-supported Pt catalyst (both potentiodynamic and potentiostatic measurements). Activation energies for the overall methanol oxidation process and for the specific pathway leading to $CO_2$ formation, the current efficiency for $CO_2$ production as a function of temperature will be derived. It is shown that even for the low catalyst loading applied in these experiments, thermal activation leads to complete conversion of methanol to $CO_2$ when approaching 100°C reaction temperature.

## References:

[1] J.L. Cohen, D.J. Volpe, H.D. Abruna, *Phys. Chem. Chem. Phys.*, **9** (2007) 49
[2] T.H. Madden, N. Arvindan, EM. Stuve, *J. Electrochem. Soc*, **150** (2003) E1
[3] T.H. Madden, E.M. Stuve, *J. Electrochem. Soc.*, **150** (2003) E574
[4] N. Wakabayashi, H. Uchida, M. Watanabe, *Electrochem. Solid State Lett*, **5** (2002) E62
[5] V.S. Bagotzky, Y.B. Vassiliev, O.A. Khazova, *J. Electroanal. Chem.*, **81** (1977) 229
[6] T. Iwasita, *Electrochim. Acta*, **47** (2002) 3663
[7] Z. Jusys, J. Kaiser, R.J. Behm, *Langmuir*, **19** (2003) 6759

First Regional Symposium on Electrochemistry of South-East Europe, Rovinj, Croatia, May 4-8, 2008.

O-1-10

# SYNTHESIS AND PROPERTIES OF OXIDE-MODIFIED Pt AND Pt –ALLOY ELECTROCATALYSTS FOR ETHANOL OXIDATION

**A. Kowal[a, b], K.S. Lee[b], S.J. Yoo[b], P. Olszewski[a], Y.E. Sung[b], R. Adžić[c]**

[a]*Institute of Catalysis and Surface Chemistry, Polish Academy of Sciences, Krakow, Poland*
[b]*School of Chemical & Biological Engineering and Research Center for Energy Conversion & Storage, Seoul National University, Seoul, S. Korea*
[c]*Department of Chemistry, Brookhaven National Laboratory, Upton, USA*

We studied Pt, Pt-Rh nanoclasters without and with $SnO_2$ cluster modification as electrocatalysts for anodic oxidation of ethanol in Direct Ethanol Fuel Cells (DEFC). Stable Pt, Pt-Rh and $SnO_2$ clusters were produced in the absence of any usual capping agents by heating corresponding metal hydroxide colloids in ethylene glycol solution. The particle size distribution was determined using STM and TEM techniques.

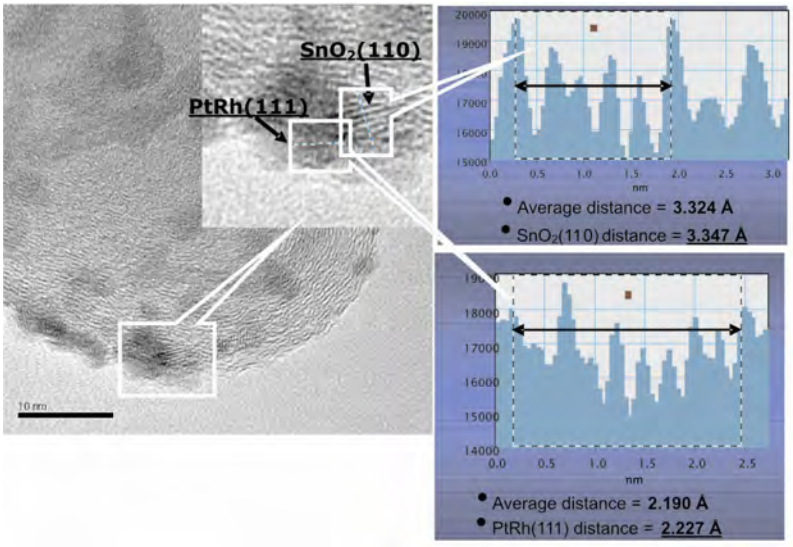


*Fig.1. TEM images of Pt-Rh/$SnO_2$ nanoparticles prepared from $H_2PtCl_6$, $RhCl_3$, and $SnCl_4$ precursors with polyol [2-4] method.*

TEM micrographs show that the obtained materials were spherical nanoparticles. It was found that average diameters of the Pt and Pt-Rh nanoclasters were in the range from 1 to 3 nm. The sizes of $SnO_2$ clusters deposited with Pt-Rh nanoclasters (Pt-Rh/$SnO_2$) were in the range 3-5 nm.
The size of Pt, Pt-Rh and $SnO_2$ nanoclasters determined by XRD method correlates well with TEM data. Rietveld analysis for Pt-Rh/$SnO_2$ catalyst gave the

average crystallite size 1.8 nm and 1,3 nm for Pt-Rh and $SnO_2$ respectively. The composition of Pt-Rh/$SnO_2$ catalyst was 28% of Pt-Rh and 72% of $SnO_2$ .
Cyclic voltammetry was used to evaluate and compare the electrocatalytic activities to ethanol oxidation over prepared catalyst deposited on Vulcan 72 support. Ethanol oxidation surface specific activity currents, registered at a potential equal to 0.6 V vs. NHE in 0.5 M $H_2SO_4$ + 1 M ethanol solution, were equal: 168, 193, 340, 629 microamper/$cm^2$ for the Pt-Rh, Pt, Pt/$SnO_2$ and Pt-Rh/$SnO_2$ respectively (Fig. 2).

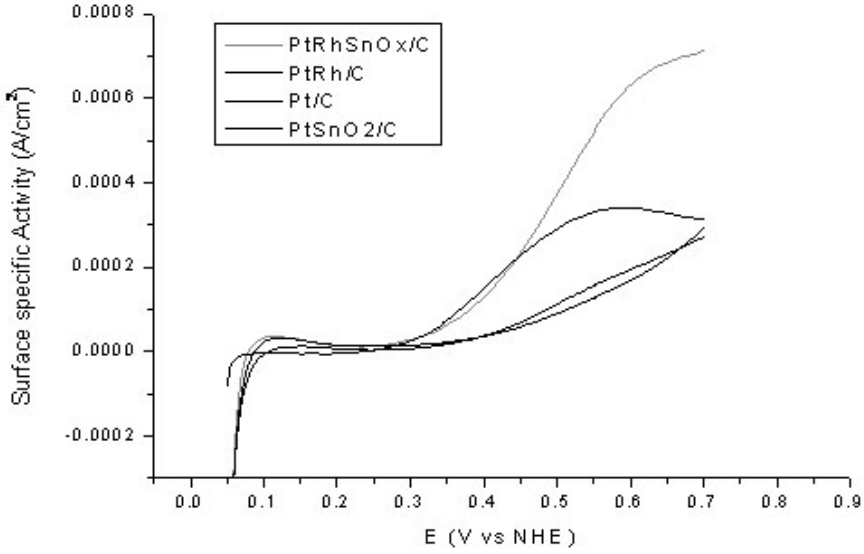


*Fig. 2. Anodic scan in 1M ethanol + 0,5 $H_2SO_4$, scan rate 50 mV/s , temp 20$^o$ C.*

$SnO_2$ and Rh have a synergetic effect on the process of electrochemical oxidation of ethanol. $SnO_2$ and Rh causes also splitting of the C-C bond as verified by detection of $CO_2$ in IRRAS spectra [1].
It can be concluded that addition $SnO_2$ and Rh on Pt surface significantly improves the process of electrochemical oxidation of ethanol and that Pt-Rh/$SnO_2$ catalyst is promising material for further investigations.

**References:**

1. Y. Wang, J. Ren, K. Deng, L. Gui, Y. Tang, *Chem. Mater.* **12** (2000) 1622.
2. Y. Wang, J. Zhang, X. Wang, J. Ren, B. Zuo, Y. Tang, *Top. Catal.* **35** (2005) 35.
3. L. Jiang, G. Sun, Z. Zhou, S. Sun, at all., J. Phys. Chem. B **109** (2005) 8774.
4. A. Kowal, J. Zhang, M. Shao, R. Adzic,"Oxidation of Etanol on Metal Oxide- Modified Pt Electrodes", Book of Abstracts, *Intern. Symposium on Surface Imaging/Spectroscopy at the Solid/Liquid Interface*, Kraków, 2006, page 85, ISBN 83-60514-02-X.

First Regional Symposium on Electrochemistry of South-East Europe, Rovinj, Croatia, May 4-8, 2008.

O-1-11

# INFLUENCE OF MORPHOLOGY OF Pt ELECTRODEPOSITED ON GLASSY CARBON SUPPORT ON FORMIC ACID OXIDATION

**D. Tripković[a] , S. Stevanović[a], A. Tripković[a], A. Kowal[b], V. M. Jovanović[a]**

[a]*University of Belgrade, ICTM – Institute of Electrochemistry, Njegoševa 12, P.O.Box 473, 11000 Belgrade, Serbia, E-mail: vlad@tmf.bg.ac.yu*
[b]*Institute of Catalysis and Surface Chemistry, Polish Academy of Science, Krakow, Niezapominajek 8, 30-239, Poland*

Formic acid oxidation on Pt electrodes follows the dual path mechanism[1] involving a reactive intermediate (main path – dehydrogenation) and adsorbed CO as a poisoning species (parallel path – dehydration). Examining of this reaction on low and high index single crystals of Pt clearly revealed its structural dependence[2] which is in fact based on the influence of surface structure on poisoning capabilities. The most active plane (111) is characterized by HCOOH oxidation to $CO_2$ through the direct path on Pt sites free of adsorbed poisoning species (CO) generated by dehydration of HCOOH molecules[3]. Pt (111) is also the least poisoned surface. The activity decreases on stepped or high index single crystals due to increaing of $CO_{ad}$ coverage mostly on the step sites. Consequently, the surfaces with the highest step densities, i.e. with the smallest terrace length have the lowest activity[4].

Formic acid oxidation has been studied on high surface area Pt catalysts as well[5-8] . In this case the catalyst activity has been mostly related to the lower poisoning rate[6] and smaller number of defects[7-8] as a consequence of particle size effect.

We studied structural effect of Pt nanoparticles on formic acid oxidation using Pt electrochemically deposited on glassy carbon (GC) as a model system. The electrodes were prepared by potentiostatic deposition of Pt onto the polished glassy carbon support (GC/Pt, different loadings) as well as on differently pretreated support (polarized in acid $GC_{OX\text{-}AC}$/Pt or alkali $GC_{OX\text{-}AL}$/Pt; similar loading). Morphology of Pt deposited on GC is defined by agglomerates whose number, size and distribution depend on Pt loading and support pretreatment as revealed by AFM characterization. Increase in Pt loading leads to more closely crowd and coalescence agglomerates. Pt deposited on $GC_{OX\text{-}AC}$ is uniformly distributed in a form of small mostly separated spherical agglomerates. When the support is $GC_{OX\text{-}AL}$ than Pt is deposited in agglomerates coalesced in complex forms mostly like rings (Fig. 1).

STM analysis of the electrodes shows that increase of Pt loading leads to increase of Pt particles size and their coalescences. Electrochemical treatment of the support prior to Pt deposition results in decrease of particle size on $GC_{OX\text{-}AC}$ and in their negligible change on $GC_{OX\text{-}AL}$ support (Fig. 1). The coalescences of the particles detected cause the formation of different defects. The number of defects grows with the increase of the loading and particle coalescence and the ratio between the facets and defect sites on the grain boundaries changes in favor of defects.

Voltammograms of formic acid oxidation on these electrodes clearly exhibited the influence of Pt particle structure on the reaction (Fig. 1). The most active are the electrodes GC/Pt with low loading and $GC_{OX\text{-}AC}$/Pt consisting of the smallest particles arranged in small mostly separated agglomerates, thus the least coalesced and defected. The onset potential is shifted for some 200 mV more negatively and the

current maximum is achieved at the lowest potential (~ 0.45 V). The increase in particle size i.e. the number of defects decreases the activity at low potentials. The onset potential is shifted more positively and simultaneously the peak at 0.7 V is appeared. The lowest activities have the GC/Pt electrode with highest loading and $GC_{OX\text{-}AL}$/Pt with the support treated in alkali. This electrode is even less active than the one with similar Pt loading and similar particle size on polished support, due to more coalesced agglomerates and more defected surface.

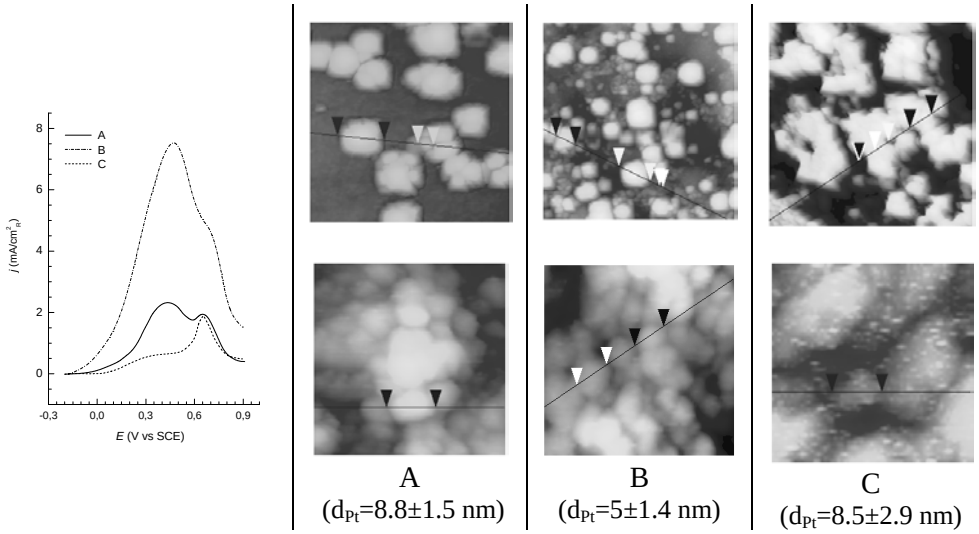


*Fig. 1: Cyclic voltammograms in 0.5 M $H_2SO_4$ + o.5 M HCOOH and AFM(↑) and STM(↓) images of A – GC/Pt, B - $GC_{OX\text{-}AC}$/Pt and C - $GC_{OX\text{-}AL}$/Pt electrodes (20.3±0.8 μg Pt/cm$^2$)*

The results presented here lead to the conclusion that particle structure i.e. morphology rather than particle size plays predominant role in the activity of Pt catalysts for formic acid oxidation. The particle structure is directed by particle growth which is influenced by the support morphology and saturation of active centers of the support by metal precursor.

**References:**

1. A. Capon and R. Parsons, *J. Electroanal. Chem.*, **45,** 205 (1973.)
2. R. Adžić, A.V. Tripković and W. O'Grady, *Nature* **296**, 137 (1982).
3. R. Adžić, A.V. Tripković and N.M. Marković, *J. Electroanal. Chem.*, **150**, 79 (1983).
4. A. Tripković, K. Popović and R. Adzić, *J. Chim. Phys.*, **88**, 1635 (1991).
5. J.D. Lović, A.V. Tripković, S.Lj. Gojković, K.Đ. Popović, D.V. Tripković, P. Olsyewski and A. Kowal, *J. Electroanal. Chem.*, **581**, 294 (2005).
6. S. Park, Y. Xie and M. Weaver, *Langmuir*, **18**, 5792 (2002).
7. K. Yahikozawa, Y. Fujii, Y. Matsuda, K. Nishimura and Y. Takasu, *Electrochim. Acta*, **36**, 973 (1991).
8. F.J.E Scheijen, G.L. Beltramo, S. Hoeppener, T.H.M. Housmans and M.T.M. Koper, *J. Solid State Electrochem.*, DOI 10.1007/s10008-007-0343-z

First Regional Symposium on Electrochemistry of South-East Europe, Rovinj, Croatia, May 4-8, 2008.

O-1-12

# FORMALDEHYDE ANODIC OXIDATION KINETICS ON Au AND ITS ALLOYS WITH Ag AND Cu IN ALKALINE MEDIUM

**A. Vvedenskii, L. Kirilova, N. Morozova**

*Voronezh State University, Russia, 394006. Voronezh, Universitetskaya pl.1*
*E-mail: alvved@chem.vsu.ru*

Formaldehyde exists in an alkaline water solution mainly as methylene glycol anion $H_2C(OH)O^-$. In the present work anodic oxidation of $H_2C(OH)O^-$ on polycrystalline gold and its homogeneous binary alloys with silver and copper is investigated.

To research applied by methods no-current potentiometry, chronovoltamperometry, multipulse chronoamperometry, and also reflective IR-spectroscopy.

It is established, that adsorption of anion methylene glycol on gold is dissociative and leads to replacement of two molecules water to a surface of a gold electrode, and products of dissociation - atomic hydrogen $H^*$ and anion-radical $H\dot{C}(OH)O^-$.

Anodic oxidation of formaldehyde on gold is realized in the wide area of potentials including area of specific adsorption $OH^-$. Up to potentials ~ 1.3 V process of electrooxidation is "soft" and comes to the end with formation of electrochemical stability (in this area of potentials) a formate-ion. The current efficiency of process of electrooxidation thus is close to 100 %.

In the area of potentials from –0,2 up to 0,6 V kinetic of process electrooxidation is it volumetric - diffusion. At removal diffusion restrictions the process is controlled by a stage of dissociative chemical adsorption of anion methylene glycol and submits to laws of typical CE-process.

Hard braking of process of electrooxidation at E> 0.6 V is connected to formation of phase gold oxide that proves to be true data of reflective IR-spectroscopy. So, since potentials ≥ -0.4 V in a spectrum the band concerning to formation Au - $OH_{(ads)}$ are registered, and at E ≥ 0,4 V - band typical to formation of oxide phase $Au_2O_3$. Thus intensity of the given bands increases with growth of anodic potential. About formation of oxide testifies, besides characteristic "plateau" with the subsequent clear maximum of a current on anodic branch of voltamperogramms on Au - electrode, received in background solution NaOH. On a site "plateau" currents increase linearly grow with growth of scan rate of potential v, that it to point out from an adsorbed condition specifies oxidation. While the anodic limit of scanning ($E_{scan}$) does not exceed 0.6 V, and values v are great, the degree of covering of a surface gold of oxygen $\Theta_O$ is less than one. With growth $E_{scan}$ and at v < 0.1 V/s, $\Theta_O$ appreciablly exceeds one because of process oxide formation.

On the currents corrected on a limiting current of heterogeneous chemical reaction, are received values of seeming kinetic orders of reaction (n) on $H_2C(OH)O^-$ (n = 0,30 ÷0,55) and $OH^-$ (n = 0,61¸0,86) in the area of potentials up

-0,5 to -0,1 V, that it is typical of the processes proceeding on energetically non-uniform surface.
Kinetic laws of process of electrooxidation of formaldehyde on Ag-Au and Cu-Au alloys ($X_{Au}$> 50 at. %) as a whole same, as on pure gold. Preliminary surface anodic modification of Ag,Au-alloys, resulting to formation of a superficial layer of gold with the increased concentration of vacancies, also does not affect values of kinetic parameters and speed of electrooxidation. It allows to conclude, that the general kinetic scheme of process of anodic oxidation of formaldehyde does not vary at transition from gold to its homogeneous alloys with copper and silver with $X_{Au}$> 50 ат. %.

*The work was supported by CRDF (USA), project VZ-010 and Ministry of Education of Russia (Program "Basic researches and Higher education").*

First Regional Symposium on Electrochemistry of South-East Europe, Rovinj, Croatia, May 4-8, 2008.

O-1-13

# INVESTIGATION OF OXYGEN REDUCTION ON SPUTTERED PLATINUM CATALYSTS USING ROTATING DISC ELECTRODE

**G. Topalov[1], G. Ganske[2], E. Slavcheva[1], U. Schnakenberg[2]**

*[1]Institute of Electrochemistry and Energy Systems – Bulgarian Academy of Sciences Acad. G. Bonchev bl.10, 1113 Sofia, Bulgaria, E-mail: gtopalov@mail.bg*
*[2]Institut für Werkstoffe der Elektrotechnik-I, RWTH-Aachen Sommerfeldstraße 24 52074 Aachen, Germany*

The present work concerns the electrochemical behaviour of low Pt loaded electrodes during oxygen reduction in sulphuric acid solution. The Pt films with equal loading of 0.15 mg.cm$^{-2}$ are deposited on a thin Ti-adhesion layer upon a hydrophobic carbon paper substartes by magnetron sputtering at dc power 100W. The sputtering pressure is varied in the range 15 – 68 mTorr to study the influence of film morphology changes on the catlalytic activity. The surface structure and morphology are analysed with scanning electron microscopy (SEM) and X-ray diffraction (XRD). The kinetics of the oxygen reductio reaction (ORR) is investigated on a rotating disk electrode (RDE) in 0.5M $H_2SO_4$ applying low sweep voltammetry (LSV). The experiments are performed by varying the rotating speed of the RDE from 400 to 2000 rpm. Fig.1 presents the polarisation curves of a catalyst deposited at sputtering pressure of 50mTorr. Koutecky-Levich plots (Fig.2) are used to obtain information on ORR mechanism. The method of Allen-Hickling is applied to catlculate the charge transfer kinetic parameters α and $i_0$. In virtue of these parameters an assessment of the catalytic activity is made.

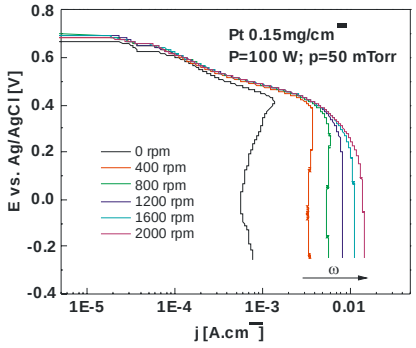


*Fig.1 Low sweep polarisation curves at scan rate 5 mV/s of sputtered Pt thin film by various rotation rates.*

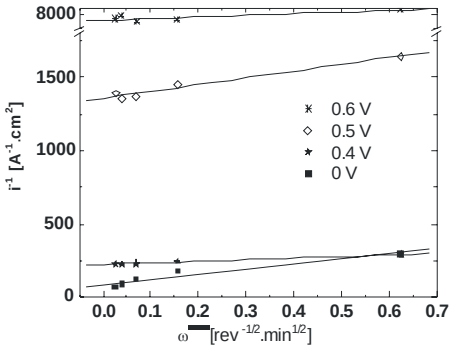


*Fig.2 Koutecky-Levich plots of sputtered Pt at plasma power 100W and pressure 50 mTorr.*

The SEM alalysis proved that the Pt particles are very evenly distributed on the substrate surface. The layers deposited at high sputtering pressure (above 30mTorr) possess an increased porousity and a higly developed surface, resulting in essential improvement of their catalytic activity toward oxygen reduction.

First Regional Symposium on Electrochemistry of South-East Europe, Rovinj, Croatia, May 4-8, 2008.

O-1-14 Keynote Lecture

# THE PROPERTIES OF SOL-GEL PROCESSED NOBLE METAL OXIDES SUPPORTED ON CARBON-BASED MATERIALS FOR SUPERCAPACITIVE APPLICATIONS

**V.V. Panić, A.B. Dekanski, B.Ž. Nikolić***

*ICTM – Department for Electrochemistry, University of Belgrade, Njegoševa 12, Belgrade, Serbia*
**Faculty of Technology and Metallurgy, University of Belgrade, Karnegijeva 4, Belgrade, Serbia, panic@ihtm.bg.ac.yu*

Metallic conductivity and good electrocatalytic properties enabled the use of noble metal oxides, such as $RuO_2$ and $IrO_2$, as an electrode material for a number of applications, which resulted in commercial fabrication of so-called dimensionally stable anodes for chlorine generation in chlor-alkali industry[1]. In addition, these oxides exhibit almost pure-capacitor behavior with extremely high capacitance value during charging/discharging process in acid solutions[2]. This is due to oxide pseudocapacitive behavior related to the surface solid-state redox transitions of metal, assisted by proton injection/ejection into the hydrous oxide. The capacitive properties of ruthenium oxide depend on the degree of hydration and crystallinity, which varies with the calcination temperature[3]. For the practical purposes, the expensive noble metal oxide is usually combined with the cheap carbon blacks of highly developed surface area, to prepare the composite materials of large specific capacitance, actually comprising oxide pseudocapacitance and double layer capacitance of carbon black[2]. The capacitance values of up to 700 F per gram of the composite can be achieved in slow charging/discharging process of $RuO_2 \cdot H_2O$/C composite[3]. The usual preparation procedures of these supercapacitive composite materials involve the oxide precipitation from the solution of salts containing suspended carbon black particles. In the previous work[3], the $RuO_xH_y$/C composite was obtained from oxide sol prepared by forced hydrolysis of $RuCl_3$. The impregnation of carbon black was done by mixing the water suspension of carbon black and the oxide sol. The capacitive properties of oxide-impregnated high surface area carbon black were found to depend on concentration of the oxide in the impregnating medium and the ageing time of oxide sol. Due to the extremely high surface area of carbon black (above 1000 $m^2\ g^{-1}$), the available active surface of the composite is considerably reduced at fast charging/discharging process.

This work reports the recent results related to the investigation of supercapacitive composite materials based on different noble metal oxides, such as $RuO_2$ and $IrO_2$, which physico-chemical properties are controlled by defined conditions of sol-gel synthesis, while the properties of composite material are investigated in the function of different impregnation procedures. Different carbon-based materials, such as carbon blacks and fibers, as well as carbides, are tested as supporting materials.

1. S. Trasatti, in: *Interfacial Electrochemistry – Theory, Experiment and Applications*, A. Wieckowski, Ed., Marcel Dekker Inc., New York, USA, 1999, p. 769.
2. B. Conway, *Electrochemical Supercapacitors – Scientific Fundamentals and Technological Applications*, Plenum Publishers, New York, USA, 1999.
3. V. Panić, T. Vidaković, S. Gojković, A. Dekanski, B. Nikolić, *Electrochim. Acta* **48** (2003) 3805.

First Regional Symposium on Electrochemistry of South-East Europe, Rovinj, Croatia, May 4-8, 2008.

O-1-15

# ADVANCED COMPOSITE MATERIALS FOR ENERGY STORAGE DEVICES

**V. Barsukov, V. Khomenko, K. Lykhnytsky, E. Illin**

*Department of Electrochemical Power Engineering & Chemistry, Kiev National University of Technologies & Design, 2, Nemirovich-Danchenko str., Kiev 02011 Ukraine*
*E-mail: chemi@mail.kar.net; chemi@mail.vtv.kiev.ua*

## Aim

Developing inexpensive and quite effective composite materials for lithium-ion batteries (1), air-metal batteries (2), fuel cells (3) and electrochemical capacitors (4).

## Materials, Methods, Equipments

The following composite materials were tested and developed: different types of graphite, modified by Si, Sn, Al, etc. [1,2] for negative electrodes of application (1); $LiFePO_4$, $LiCoO_2$, $LiMn_2O_4$ in combination with different types of carbon materials (like graphitized carbon black, known as PUREBLACK® 205-110 Carbon, thermally expanded graphite (TEG), hard carbons, etc. [3]) for positive electrodes of application (1); some conducting polymers (CPs) and their composites with above-mentioned carbon materials as air/oxygen gas-diffusion electrodes for applications (2), (3), as well as electrodes with super high capacity (ca 1000 mA·h/g) for supercapacitor (SC) application (4). A series of full lithium-ion batteries (LIB) and SC were developed in the 2016 coin cell configuration. CPs/TEG gas-diffusion electrodes where developed and tested in two types of with. The main available equipments of Kiev's team are as following: SOLAAR S4 Double Beam Automatic Atomic Absorption Spectrometer (from ThermoElectron Co., USA); Argon Glove box UNILAB (from MBraun Inc., USA); Automatic battery ARBIN 32-channel battery test systems (from Arbin Instruments Co., Texas, USA); VMP3 automatic multi-channel potentio-stat/galvanostat with electrochemical impedance spectroscopy (from Princeton Applied Research, UK) and rotating disc electrode; Different technological equipment for coin batteries producing (sizes of 2016, 2325, etc.).

## Summary & Conclusion:

(1). Modification of graphite with silicon and carbon appears to be a promising approach for increasing the specific capacity of negative electrodes (Table 1). It has been shown that usage of anodes based on the graphite/Si/C composites gives possibility to ensure the stable prolonged cycling with the specific capacity of about 600 mA·h/g.

The achieved specific energy of LIB model is ca 200 W·h/kg only due to increasing the capacity of negative electrode (Table 1). Further improvement of LIB energy and reduction of costs could be achieved also by using $LiFePO_4$ based composites, which have demonstrated the capacity ca 150 mA·h/g instead of 130 mA·h/g for $LiCoO_2$ in combination with optimal carbon additives.

*Table 1. The parameters of 2016 coin lithium-ion batteries* based on the $LiCoO_2$ positive electrode, standard and modified graphite negative electrode*

| Type of graphite in the negative electrode | Specific capacity of electrode | | Specific energy of cell | |
|---|---|---|---|---|
| | positive mA·h/g | negative mA·h/g | per mass** W·h/kg | per volume W·h/L |
| Standard graphite | 132 | 341 | 162 | 512 |
| Graphite/Si/C composite | 136 | 598 | 204 | 626 |

**Electrolyte 1M $LiPF_6$ in EC:DEC:DMC=1:1:1 w/w*
**Without the mass of 2016 cell body*

(2). The polyaniline (PANI)/thermally expanded graphite (TEG) compositions are developed for realization of air gas-diffusion electrodes. Principally new concept for creation of metal-air batteries with such type of catalysts is proposed. The main characteristics of cylindrical AAA size metal-air batteries with PANI/TEG catalysts, as well as standard Zn-$MnO_2$ battery have gathered in the Table 2. Realization of all types of batteries in the same AAA size gives the possibilities for comparison of above electrochemical systems for some applications.

*Table 2. Characteristics of cylindrical AAA size metal-air batteries with PANI/TEG catalysts, as well as $MnO_2$-Zn battery*

| Characteristics of cells | (PANI) $O_2$\|Zn | (PANI) $O_2$\|Mg | $MnO_2$\|Zn |
|---|---|---|---|
| Discharge capacity, mA·h | 420 | 340 | 380 |
| Specific energy, W·h/kg | 140 | 200 | 45 |
| Weight of the cells, g | 3 | 2.7 | 11 |
| Dimensions (H / d), cm | 4.5 / 1.0 | 4.5 /1.0 | 4.5/1.0 |
| Open circuit voltage, V | 1.2 | 1.8 | 1.5 |
| Average discharge voltage, V (at $R_{DISCH}$ = 200 Ohm) | 1.0 | 1.6 | 1.1-1.3 |
| Short - circuit current, A | 1.0 | 1.2 | 1.4 |
| Self - discharge, % per month | 1.5 - 2.0 | 2.0 - 4.0 | 1.0 - 3.0 |
| Service life, years | ~ 5 | < 1 | < 2 |

The average weight for the experimental Air-Zn and Air-Mg batteries of AAA size is 3 g and 2.7 g correspondingly against of 11 g for traditional $MnO_2$-Zn battery in the same size. It is a main reason of sharp increasing the specific energy of Air-Zn (140 W·h/kg) and Air-Mg (200 W·h/kg) batteries against of traditional one (45 W·h/kg).

We believe that new type of CPs composite electrodes will find a practical application also for some types of fuel cells (3). These aspects, as well as a possibility of creation of hybrid SCs with such electrodes (4), we plan to discuss during the paper presentation.

***Acknowledgements***

*Authors acknowledge financial support by the IPP and STCU (project P-154) as well as Superior Graphite. Co. (Chicago, IL, USA) and Sud-Chemie (Germany) for providing the samples of advanced initial materials.*

**References:**

1. V. Khomenko, V. Barsukov, *Electrochim. Acta*, **52(8)**, 2829 (2007).
2. V. Khomenko, V. Barsukov, J. Doninger, I. Barsukov, *J. Power Sources*, 165(2), 598 (2007).
3. New Carbon Based Materials for Electrochemical Energy Storage Systems/ Eds: I.V. Barsukov, C.S. Johnson, J.E. Doninger and V.Z. Barsukov, Springer (2006).

First Regional Symposium on Electrochemistry of South-East Europe, Rovinj, Croatia, May 4-8, 2008.

O-1-16

# SAXS/DSC/IS STUDY OF $Zn^{2+}$- ION NANOPOLYMER ELECTROLYTE

**A.Turković[a], M. Lučić-Lavčević[b], P. Dubček[a], M. Pavlović[a], B. Etlinger[a], S. Bernstorff[c]**

*[a]Institute "Ruđer Bošković", P.O. Box 180, HR-10002 Zagreb, Croatia*
*[b]Department of Physics, Faculty of Chemical Technology, University of Split, Teslina 10/V, 21000 Split, Croatia*
*[c]Sincrotrone Trieste, ss. 14, km 163,5 Basovizza, 34012 Trieste, Italy*

The preparation of $(PEO)_8ZnCl_2$ polymer electrolytes and nanocomposites was performed by using PEO γ-irradiated by a selected dose of 309 kGy and $TiO_2$ nanograins. We have studied the influence of the added nanosize $TiO_2$ grains on the polymer electrolytes and the effect of γ-radiation from a Co-60 source. For this purpose we have utilized synchrotron technique small-angle X-ray scattering (SAXS) simultaneously recorded with differential scanning calorimetry (DSC). These measurements were performed at SAXS beamline of the synchrotron ELETTRA. Impedance spectroscopy (IS) was also performed and compared with SAXS/DSC results. The conductivity of the polymer electrolyte was greatly enhanced by the above-mentioned treatments. An increase up to two orders of magnitude was achieved for the room temperature conductivity. The conductivity increased by addition of nanograins more than can be ascribed to the changes in crystallinity. Nanograins interacted with anions in all samples increasing conductivity and additionally reduced the brittleness of the γ-irradiated electrolyte.

First Regional Symposium on Electrochemistry of South-East Europe, Rovinj, Croatia, May 4-8, 2008.

O-1-17

# POLYMERIC ELECTROLYTES. HOW THE CHARGED AND HYDROPHOBIC GROUPS SHAPE THEIR SOLUTION PROPERTIES

**V. Vlachy**

*Faculty of Chemistry and Chemical Engineering, University of Ljubljana*
*Aškerčeva 5, 1000 Ljubljana, Slovenia, vojko.vlachy@fkkt.uni-lj.si*

Macromolecules with covalently bound charges possess properties that distinguish them from low−molecular weight electrolytes. Due to the strong electrostatic field around the polyion, in which low−molecular weight ions of the opposite sign charge (counterions) are trapped, the osmotic and activity coefficients of these solutions are very low. Experimental results indicate that in addition to the long−range Coulomb interaction ion−specific effects play a significant role. So not only the charge, but also the chemical nature of the counterion and charged and uncharged groups on the polyion seem to be important.

The presence of ion−specific effects is clearly reflected in the enthalpy of dilution measurements. The effects mediated by solvent are observable even with strong polyelectrolytes [1,2]; ΔH, of ionene solutions was found to be positive for bromine and chlorine counterions, while theories treating the solvent as a dielectric continuum predict ΔH to be negative in all cases. Deviations from the continuum−solvent calculations are significant for weakly hydrated counterions, ΔH results for strongly hydrated counterions are often in quantitative agreement with the continuum−solvent theories. In the present contribution we review our recent theoretical and experimental studies, some yet unpublished, of the ionene polyelectrolyte with various ($F^-$, $Cl^-$, $Br^-$, and $I^-$) counterions in solution.

*Fig. 1: Schematic representation of the portion of 3−3 ionene polymer; dark circles – N atoms, grey – C atoms, white – H atoms.*

The ionenes with various numbers of hydrophobic groups between N−atoms (3−3, 4−5, 6−6, and 6−9 ionenes) were studied using the experimental techniques such as: osmometry, enthalpy of dilution measurements, conductometry, and the dielectric relaxation spectrum measurements. The experimental results were complemented with the explicit water Molecular Dynamics [3] calculations and integral–equation theory named PROZA [4], to better understand the combined effect of charged and hydrophobic groups on polyelectrolyte properties.

## References:

1. K. Arh, C. Pohar, and V. Vlachy, *J. Phys. Chem. B*, **106**, 9967−9973 (2002).
2. I. Lipar, P. Zalar, C. Pohar, V. Vlachy, *J. Phys. Chem. B*, **111**, 10030−10136 (2007).
3. M. Druchok, B. Hribar–Lee, H. Krienke, V. Vlachy, *Chem. Phys. Lett.*, **450**, 81–285 (2008).
4. Yu.V. Kalyuzhnyi, V. Vlachy, P.T. Cummings, *Chem. Phys. Lett.*, **438**, 38–243 (2007).

First Regional Symposium on Electrochemistry of South-East Europe, Rovinj, Croatia, May 4-8, 2008.

O-2-18

# VOLTAMMETRIC STUDIES ON AZO-AZULENE COMPOUNDS

**E.M. Ungureanu[1], A. Razus[2], L. Birzan[2], E. Diacu[1]**

*[1]Faculty of Applied Chemistry and Material Science, University "Politehnica" of Bucharest, Splaiul Independentei 313, 060042, Romani, aem_ungureanu2000@yahoo.com*
*[2]Institute of Organic Chemistry "C. D. Nenitzescu" of Romanian Academy, Spl. Independentei 202B, PO Box 15-258, 71141-Bucharest, Romania*

The azo-azulenes are interesting compounds as they are molecules with unique properties and potentially enhanced NLO coefficients[1] and electrochromic behaviour[2]. This work presents voltammetric studies on some azo-azulene compounds (Az-N=N-Y, where Az = Azulene, Y = substituted phenyl, pyridine, thiazole) performed by cyclic voltammetry (CV), differential pulse voltammetry (DPV), and rotating disk electrode (RDE) methods in organic solvents.
Complementary results have been obtained by these techniques in the study of the oxidation and reduction processes characteristic for this type of organic compounds. The oxidation and reduction potentials vary according to the electronegativity of the aryl moieties or their substituents. Comparison with benzene azo derivatives leads to conclusions regarding the enhanced azulene electro-reactivity in respect with aromatic structures. Experiments regarding the influence of donor and acceptor substituents on the behaviour of azulene and azo groups[3] have been also performed.
By electrochemistry the azulene derivatives under present study could generate polymers which have similar properties as the other reported azulene polymers which have high electrical conductivity,[4] being attractive as cathode active materials for performing rechargeable batteries.[5]
Calculations were performed by a MOPAC program using both AM1[6] and PM6 methods (MOPAC 2007).[7] We observed a better fit between the ionization potentials calculated with AM1 method with the oxidation potentials of azoazulenes while the reduction potentials are better correlated with the LUMO calculated using PM6 method.[8]
The present work established the correlations between electrochemical properties of the azo-1-azulene compounds under study and their structure revealing the influence of donor and withdrawing substituents Y upon the electrochemical behaviour of the azulene and the azo groups.

***Acknowledgments:*** *Financial support from CNCSIS 87 and CNMP REMORESE 71-067 is gratefully acknowledged.*

**References:**

1. X.-J. Liu, W.-N. Leng, J.-K. Feng, A.-M. Ren and X. Zhou, *Chin. J.Chem.*, **21**(2003), 9.
2. S. Ito, T. Kubo, N. Morita, T. Ikoma, S. Tero-Kubota, J. Kawakami and A. Tajiri, *J. Org. Chem.*, **70**(2005), 2285.
3. E. M. Ungureanu, A. C. Razus, L. Birzan, G. Buica, M. Cretu and C. Enache, *Electrochim. Acta.*, **52**(2006), 794-803.

4. R. J. Waltman and J. Bargon, *Can. J. Chem.*, **64**(1986), 76.
   G. Tourillon, F. J. Garnier, *J. Electroanal. Chem.*, **135**(1982), 173.
   J. Bargon, S. Mohmand and R. Waltman, *J., Mol. Cryst.*, **93**(1983), p. 279.
5. T. Osaka,K. Naoi and T. Hirabayashi, *J. Electroanal. Chem.*, **134**(1987), p. 2645. K. Naoi, K. Ueyama and T. Osaka, *J. Electroanal. Chem.*, **136**(1989), 2444.
6. F. De Jong, and M. J. Ianssen, *J. Org. Chem.*, **36**(1971), 1645.
7. J. J. J. Stewart *J. Comp. Chem.* **10(2)**(1989), 209-21; 221-64.
8. J. J. P. Stewart *J. Mol. Model.* **13**(2007), 1173-1213.

First Regional Symposium on Electrochemistry of South-East Europe, Rovinj, Croatia, May 4-8, 2008.

O-2-19

# ELECTROCHEMICAL PROPERTIES OF MANGANESE PORPHYRIN (MnTE-2-PyP$^{5+}$) IN AQUEOUS MEDIA

**T. Weitner[1], M. Biruš[1], Z. Mandić[2]**

[1]*Faculty of Pharmacy and Biochemistry, University of Zagre, E-mail: tweitner@pharma.hr*
[2]*Faculty of Chemical Engineering and Technology, University of Zagreb*

In recent years there has been a considerable interest in manganese porphyrins due to their unique electronic properties which allow them to function as sodium dismutase (SOD) mimetics. Accessibility of several oxidation states of manganese enables removal of reactive oxygen and nitrogen species, such as superoxide and peroxynitrite, and consequently facilitates relief of oxidative stress. Investigated manganese tetra(ortho-ethylpyridyl) porphyrin Mn$^{III}$TE-2-PyP$^{5+}$ (Figure 1.) has the formal reduction potential close to the potential of the SOD enzyme itself and excellent *in vitro* and *in vivo* SOD-like activity.[1] In aqueous solution, manganoporphyrins coordinate two axial water molecules that depending on pH can be possible deprotonation sites.[2]

Several redox and protonation states of manganoporphyrins give rise to complex electrochemical equilibria in aqueous solutions which could be described by a "square scheme" (Figure 2., axial water molecules and actual charges of manganese porphyrin species have been omitted for simplicity).

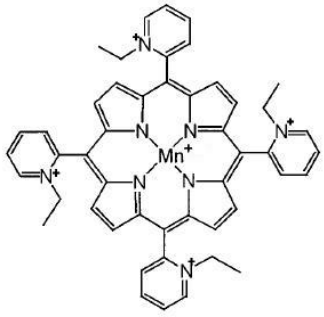


*Figure 1. Structure of Mn$^{III}$TE-2-PyP$^{5+}$*

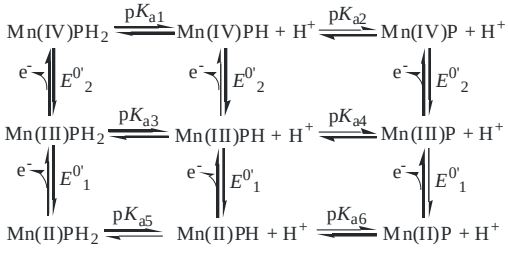


*Figure 2. "Square scheme" of reactivity of Mn$^{III}$TE-2-PyP$^{5+}$ in aqueous solutions.*

In order to investigate the redox and optical properties of Mn$^{III}$TE-2-PyP$^{5+}$, cyclic voltammetry (CV) and UV/vis spectroelectrochemical measurements were carried out. CV measurements were performed using a three-electrode cell with glassy carbon working electrode (0.037 cm$^2$ area) Spectroelectrochemical measurements were performed in a custom built optically transparent thin-layer electrochemical cell with Pt-mesh working electrode. Investigated compound Mn$^{III}$TE-2-PyPCl$_5$ was synthesized and kindly donated by Ines Batinić-Haberle and coworkers.[3] Measurements were performed under the $N_2$ atmosphere in pH range from 7.5 to 13.0.

At pH values below 10 only one pH independent electron transition has been observed and has been attributed to $Mn(III)PH_2/Mn(II)PH_2$ redox couple (Figure 3, trace a.). Current peaks are well defined with linear dependence of peak current on scan rate indicative of a reversible single electron transfer. Value of the determined reduction formal potential of $Mn(III)PH_2/Mn(II)PH_2$ redox couple is $E_1^{0'}$ = 11 mV vs. Ag/AgCl.

At pH = 10.6 an additional redox process appears which can be attributed to Mn(IV)P/Mn(III)P redox couple (Figure 3, trace b). The current peak potentials of both current peaks are pH dependent and the values of their determined apparent reduction formal potentials at pH=10.6 are $E_1^{0'}$ = -6 mV and $E_2^{0'}$ = 365 mV vs. Ag/AgCl

Finally, at pH = 13.0 spectral changes of $Mn^{III}TE\text{-}2\text{-}PyP^{5+}$ were recorded. The cell potential was varied from 550 to -450 mV in steps of 10 mV vs. Ag/AgCl electrode in both directions. Principal factor analysis of resulting UV/vis spectra predicted at least three spectrally different species which were attributed to Mn(II)P, Mn(III)P and Mn(IV)P (Figure 4.). Values of the calculated apparent formal potentials were $E_1^{0'}$ = -199 mV and $E_2^{0'}$ = 276 mV vs. Ag/AgCl.

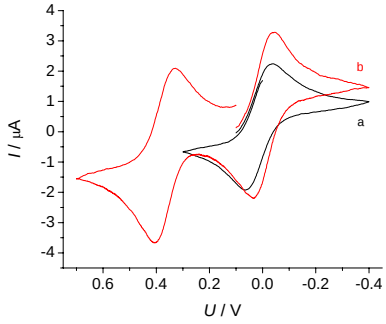


*Figure 3. Cyclic voltammograms of $Mn^{III}TE\text{-}2\text{-}PyP^{5+}$, a. $[Mn^{III}TE\text{-}2\text{-}PyP^{5+}]$ = 0.5 mM, pH = 7.5, $[NaH_2PO_4]$ = 0.05 M, [NaCl] = 0.1 M, v = 0.2 V/s, t = 25ºC, b. $[Mn^{III}TE\text{-}2\text{-}PyP^{5+}]$ = 0.5 mM, pH =10.6, $[Na_2B_4O_7]$ = 0.05 M, [NaCl] = 0.1 M, v = 0.2 V/s, t = 25ºC*

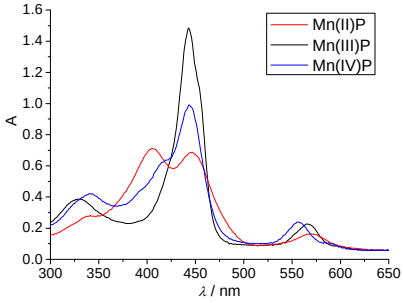


*Figure 4. Spectral species of $Mn^{X}TE\text{-}2\text{-}PyP^{5+}$, ($[Mn^{III}TE\text{-}2\text{-}PyP^{5+}]$ = 0.14 mM, pH = 13, $[Na_2HPO_4]$ = 0.05 M [NaCl] = 0.1 M, t = 25ºC, l = 0.07 cm*

Presented results indicate that $Mn^{III}TE\text{-}2\text{-}PyP^{5+}$ as a model SOD mimetic compound has a fairly complex redox properties. Further investigation of these properties and construction of a complete reaction scheme is necessary for complete understanding of its behavior in aqueous media.

**References:**

1 I. Batinić-Haberle, I. Spasojević, P. Hambright, L. Benov, A.L. Crumbliss, I. Fridowich, *Inorg. Chem.* 1999, **38**, 4011-4022
2 A. Harriman, *J. Chem. Soc. Dalton Trans.* 1984, 141-146
3 R. Kachadourian, I. Batinić-Haberle, I. Fridovich, *Inorg. Chem.* 1999, **38**, 391-392

First Regional Symposium on Electrochemistry of South-East Europe, Rovinj, Croatia, May 4-8, 2008.

O-2-20

# ELECTROCHEMICAL DETERMINATION OF GLYCEROL AND ACETALDEHYDE USING A BIENZYMATIC STRATEGY AT POLY(NEUTRAL RED) MODIFIED CARBON FILM ELECTRODES

**M.E. Ghica, R. Pauliukaite, C.M.A. Brett**

*Departamento de Química, Universidade de Coimbra, 3004-535 Coimbra, Portugal*
*E-mail: brett@ci.uc.pt*

Chemical analysis of wine is of great interest in achieving an adequate quality of production. Glycerol is the most important secondary product of alcoholic fermentation, contributing to its sensory properties, with final concentrations varying from 1 to 10 g $L^{-1}$ - deviations indicate technological alterations during the process or deterioration of the harvested grapes. Acetaldehyde is found in fruits and vegetables, in dairy food and in cooked meat. In alcoholic beverages it occurs mainly as a result of enzymatic oxidation of ethanol, and plays an important role in the manifestation of alcoholic intoxication, usual concentrations being between 31 and 79 mg $L^{-1}$. Official methods for the determination of glycerol or acetaldehyde, such as chromatography, are time consuming, expensive and unsuitable for routine analysis.

Electrochemical bienzymatic biosensors prepared by immobilisation on poly(neutral red) (PNR)-modified carbon film electrodes have been investigated. PNR films, prepared by electropolymerisation, have been electrochemically characterised [1] and used as a redox mediator in biosensors [2].

The enzymes were immobilised by glutaraldehyde cross-linking. The glycerol biosensor was prepared by co-immobilisation of glycerol-3-phosphate oxidase and ATP-dependent glycerol kinase [3] whilst for the acetaldehyde biosensor FMN-dependent NADH oxidase- and $NAD^+$-dependent aldehyde dehydrogenase were immobilized together [4].

The biosensors and their components were characterised voltammetrically and optimised for use in fixed potential amperometric mode, by studying the influence of pH and applied potential, the concentration of cofactors and ratio of the immobilised enzymes. The optimised biosensors showed linear responses between 10 and 147 µM for glycerol and between 3 and 100 µM for acetaldehyde with detection limits of 5 µM and 3 µM, respectively. The selectivity of both biosensors was studied with respect to other compounds usually present in wines; none of them led to significant interferences.

The developed biosensors were used to measure glycerol and acetaldehyde in wine samples in good agreement with reference methods.

[1] R. Pauliukaite, M.E. Ghica, M.M. Barsan, C.M.A. Brett, *J. Solid State Electrochem.* **11** (2007) 899.
[2] M.E. Ghica, C.M.A. Brett, *Electroanalysis* **18** (2006) 748.
[3] M.E. Ghica, C.M.A. Brett, *Anal. Lett.* **39** (2006) 1527.
[4] M.E. Ghica, R. Pauliukaite, N. Marchand, E. Devic, C.M.A. Brett, *Anal. Chim. Acta* **591** (2007) 80.

First Regional Symposium on Electrochemistry of South-East Europe, Rovinj, Croatia, May 4-8, 2008.

O-2-21

# VOLTAMMETRIC SENSORS BASED ON COMPOSITE NANOTUBES AND DOUBLE DECKER LANTHANIDE BISPHTHALOCYANINES

**C. Apetrei[a], I. Apetrei[a], G. Cârâc[a], M. Nieto[b], M.L. Rodríguez-Méndez[b], J.A. de Saja[c]**

*[a]Dpt Chemistry, Faculty of Sciences, E-mail: capetrei@yahoo.com*
*[b]Dpt. Of Inorganic Chemistry, E.T.S. Ingenieros Industriales, University of Valladolid, Spain*
*[c]Dpt Condensed Matter Physic, Faculty of Sciences, University of Valladolid, Spain*

Electrodes modified with phthalocyanines have shown great promise for the determination of many important inorganic, organic or biological compounds[1,2,]. Voltammetric sensors based on phthalocyanines show particular responses when immersed in different solutions. This behaviour has opened the possibility of using such electrodes as the sensing units of an "electronic tongue" [3-5].

In previous works carbon paste electrodes were prepared by mixing the corresponding phthalocyanine with carbon. A conglomerant substance such as Nujol was used to form a paste that can be deposited onto the electrode surface. The development of new sensors with an enhanced selectivity and stability is crucial to obtain arrays of sensors with improved characteristics.

In this work, new sensors based on phthalocyanines with improved properties have been developed. The rich electrochemical properties of the lanthanide double decker phthalocyanine derivatives have been improved by forming a composite material with carbon nanotubes. Sensors with enhanced cross selectivity have been prepared by using bisphthalocyanine molecules with different central metal ions or having substituents in the benzene groups. The phthalocyanine-nanotube paste has been deposited onto gold substrates (1 mm diameter) previously lithographied in an alumina card.

The sensors have been used to evaluate a range of liquids including solutions of basic tastes and antioxidants. It has been observed that the presence of carbon nanotubes modifies the response of the electrodes, facilitating the oxidation of the phthalocyanines forming the electrode. Nanotubes also favour the oxidation of the molecules with redox activity present in the studied solution. The stability of the sensors could be greatly improved by covering the mixed phthalocyanine-nanotube film with Nafion membranes.

The Principal Component Analysis (PCA) of the obtained signals has allowed the discrimination of the studied solutions.

***Acknowledgments:*** *Financial support provided by the Junta de Castilla y León. ITA CyL (VA-16/2005-02-08) and FILFLOSEC (71/125/62D7/07) are gratefully acknowledged.*

**References:**

1. R.W. Cattrall, Chemical sensors, Oxford University Press, U.K, 1997.

2. A.B.P. Lever, *J. Porph. Phthaloc*. **3**, 488 (1999)
3. Y. Vlasov, A. Leguin and A. Rudnitskaya, *Sensors Update*, **10**, 143 (2002)
4. A. Arrieta, M. L. Rodriguez-Mendez and J. A. de Saja, *Sens. Actuators B* **95**, 357 (2003)
5. C. Apetrei, S. Cassili, M.A de Lucca, L. Valli. J. Jiang, M.L. Rodríguez-Méndez, J. A. de Saja. *Appl. Surf. Sci.* **246**, 304 (2005)

First Regional Symposium on Electrochemistry of South-East Europe, Rovinj, Croatia, May 4-8, 2008.

O-2-22

# A SIMPLE BUT HIGHLY SELECTIVE ELECTROCHEMICAL SENSOR FOR DOPAMINE

**R.L. Doyle, C.C. Harley, J. Colleran, A.D. Rooney, C.B. Breslin**

*Department of Chemistry, National University of Ireland Maynooth, Maynooth, Co. Kildare, Ireland.* RICHARD.L.DOYLE@nuim.ie

This novel sensor is based on the incorporation of macrocyclic cages, cyclodextrins (Figure 1a) and calixarenes (Figure 1b), into a conducting polymer. Calixarenes are cyclic oligomers of phenol units while cyclodextrins are made up of glucose units. Although they have similar cylindrical structures and both posses a hydrophobic cavity they differ in their rigidity. In cyclodextrins the cavity has been fixed whereas in calixarenes the cavity is flexible and can change its dimensions leading to more versatile host-guest interactions. While cyclodextrins are naturally soluble in water calixarenes require functionalisation, the sulphonated calixarenes introduced by Shinkai and co-workers are particularly soluble[1-2]. Both calixarenes and cyclodextrins have been shown to form inclusion complexes with a wide variety of ionic and neutral guest molecules [3-4].

Sulphonated calixarenes and cyclodextrins are anionic in aqueous media and so can be electrochemically incorporated into a polymer matrix during an oxidation process. Moreover, they can retain their recognition properties within the matrix [5].

In this work sulphonated calix[n=4,6,8]arenes and sulphonated β-cyclodextrin have been permanently incorporated into a polypyrrole matrix during electropolymerisation and shown to be highly selective and sensitive sensors for the neurotransmitter dopamine (DA) which has been implicated in neurological disorders such as Parkinson's and Alzheimer's.

Electrochemical methods are particularly attractive for the detection of DA due to its electrochemical activity. However, complications can arise with these sensors due to the presence of interferents, the major one being ascorbic acid (AA) [6-7]. AA can hinder the detection of DA in two ways. Firstly, it is oxidised at a potential close to that of DA and, secondly, it can reduce dopamine-quinone (the oxidised form of DA) back to DA. These problems are increased due to the fact that AA is present in the body in significantly higher concentrations than DA. Modifying electrodes in the way described here significantly helps overcome these problems.

DA was detected at the modified electrodes using a range of electrochemical techniques giving peak currents at approximately 500 mV (SCE) and 300 mV (SCE) respectively. Using simple cyclic voltammetry the detection limit is 0.1 mM. AA had little effect on the sensors performance even at relatively high concentrations of 0.001 mol $dm^{-3}$ giving a highly selective sensor for the detection of DA.

The supramolecular chemistry of the macrocycles with DA was studied using several methods including NMR, cyclic voltammetry and RDE. There is evidence to suggest the inclusion of DA into the cavity.

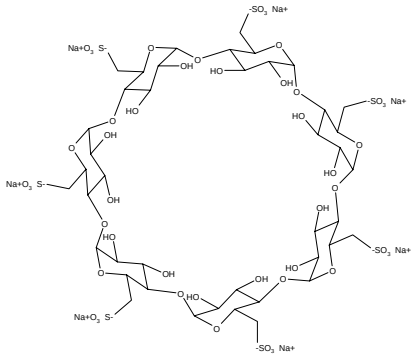

*Figure 1a: sulphonated β-cyclodextrin*

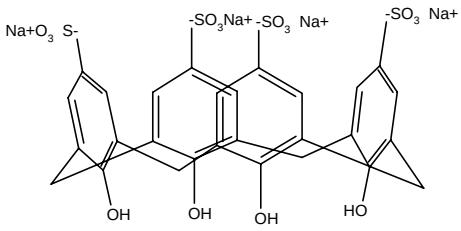


*Figure 1b: p-sulphonatocalix[4]arene*

## References:

1. S. Shinkai, S. Mori, T. Tsubaki, T. Sone, and 0. Manabe, *Tetrahedron Lett.*, 1984, **25,** 5315.
2. S. Shinkai, S. Mori, H. Koreishi, T. Tsubaki, and O. Manabe, *J. Am. Chem. Soc.*, 1986, **108**, 2409-2416.
3. S. Shinkai, *Tetrahedron*, 1993, **49**, 8933-8968.
4. E. M. Martin Del Valle, *Process Biochemistry*, 2004, **39**, 1033-1046.
5. G. Bidan and M.A. Niel, *Synthetic Metals*, 1997, **84**, 255-256.
6. S. Alpat, S.K. Alpat and A. Telefoncu, *Analytical and Bioanalytical Chemistry*, 2005, **383**, 695-700.
7. J.B. Raoof, R. Ojani and S. Rashid-Nadimi, *Electrochimica Acta*, 2005, **50**, 4694-4698.

First Regional Symposium on Electrochemistry of South-East Europe, Rovinj, Croatia, May 4-8, 2008.

O-2-23

# THE INTERFACIAL CAPACITANCE OF THE PLATINUM GROUP METALS IN AQUEOUS SOLUTIONS

**T. Pajkossy, D.M. Kolb**

*Institute of Materials and Environmental Chemistry, Hungarian Academy of Sciences, Budapest, Pusztaszeri út 59-67, H 1025 Hungary, pajkossy@chemres.hu*
*Institute of Electrochemistry, University of Ulm, D-89069 Ulm, Germany*

Consider a "classical" electrochemical system: a metal electrode in an aqueous soulution. In the absence of Faradaic reactions, the interfacial impedance is usually regarded to be capacitive, due to the charging of the double layer and to adsorption of some solute species. Accordingly, the voltammograms of platinum group metals are usually dominated by peaks and humps due to adsorption processes of various origins, with a "double layer region" in between them. An example is shown in Fig.1a: on the voltammogram of a single crystalline Rh(111) in 0.1M HCl the peak marks the potential at which adsorbed hydrogen is replaced by adsorbed chloride during the positive scan. In the double layer region (at E>-0.2V) the surface is covered by adsorbed chloride. Impedance spectroscopy gives information about the rate of these processes. As shown in Fig. 1b, the interfacial capacitance, calculated from the interfacial admittance, $Y(\omega)$, as $C(\omega)=Y(\omega)/i\omega$ - is not a frequency-independent, single value, but on the complex plane has a characteristic shape of an arc or arcs. Such a capacitance behaviour implies *slow* ion adsorption, and corresponds to an equivalent circuit with one or two adsorption branches, as it is shown in the inset of the Fig.1b.

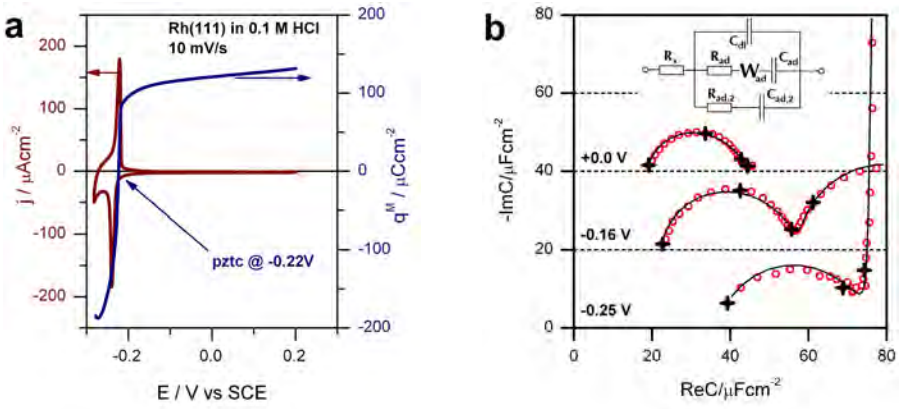


For the Rh(111)/HCl system one obtains arcs as capacitance spectra in the full potential range of the voltammogram; other platinum group metals behave similarly in certain solutions. These measurements indicate that the dynamic behaviour of the double layer of reactive metals is mainly determined by the adsorption-desorption rates of ions.

First Regional Symposium on Electrochemistry of South-East Europe, Rovinj, Croatia, May 4-8, 2008.

O-2-24

# ADSORPTION OF IODIDE AND CAESIUM ON ZIRCONIUM AND STAINLESS STEEL

**R. Répánszki, Z. Kerner*, G. Nagy**

*MTA KFKI Atomic Energy Research Institute, H-1525 Budapest, P.O.B. 49, Hungary*
*kerner@aeki.kfki.hu

In a nuclear reactor the contamination of structural materials is an important question. Normally the cooling water does not contain any fission products, but due to a leakage they can appear. In this study the sorption properties of the fission products were investigated by electrochemical quartz crystal microbalance on stainless steel surface created by sputter technique and on zirconium surface deposited in vacuum onto a 1 inch diameter AT-cut 5MHz quartz crystal. The EQCM head was installed into a thermostated glass was a saturated calomel electrode using a Luggin-capillary. The solution contained proper amount of boric acid and KOH modelled the primary circuit water chemistry of a VVER nuclear power plant. The measurements were carried out at the open circuit potential; during the measurement the solution of the investigated adsorbing ions was injected into the cell in several steps. The mass, pH and potential changes were recorded. After the maximal coverage was reached a cyclic voltammogram was recorded. Using a flow cell the kinetics of adsorption and desorption were studied.

Caesium adsorbed on both surface the mass of the adsorbed ions was 0.72 μg/cm$^2$ on stainless steel and it was 0.82 μg/cm$^2$ on zirconium. On the CV in case of both metals some adsorption peak appeared on the CV but no sign of corrosion was found.

On stainless steel more iodide adsorbed than on zirconium surface, however both of them can be described with a Langmuir equation. The mass of the adsorbed iodide was 1.42 μg/cm$^2$ on stainless steel, in case of zirconium it was 0.97 μg/cm$^2$. On the cyclic voltammogram noise of the corrosion appeared in case of stainless steel and zirconium also; but on the steel surface the mass increased with the corrosion and the steel dissolved from 454 mV to cathodic potentials, while on zirconium the mass hardly changed, only 0.08 μg/cm$^2$ during the cyclic voltammogram. The sorption on zirconium is a simpler process. No dissolution was observed on higher anodic potential and maximum monolayer coverage were found with little change in the electrode potential.

It is an important to examine the iodide contamination because iodide can easily indicate corrosion on steel surface and causes pits on the heat exchanger pipes.

First Regional Symposium on Electrochemistry of South-East Europe, Rovinj, Croatia, May 4-8, 2008.

O-2-25

# THE ROLE OF SILVER CRYSTALLOGRAPHIC ORIENTATION AND Ag-Au ALLOYS COMPOSITION IN STRUCTURE-SENSITIVE PARAMETERS OF ANODIC Ag(I) OXIDE

**S. Grushevskaya*, A. Vvedenskii, D. Kudryashov**

*Voronezh State University, Department of Physical Chemistry,*
*Universitetskaya pl. 1, 394006 Voronezh, Russia*
**E-mail: sg@chem.vsu.ru*

The anodic dissolution or corrosion of metals and alloys is usually accompanied by the film formation. The appearance even of a thin oxide film can sufficiently vary the nature and kinetics of the anodic reaction. The structural features of anodic oxide determine the character of the influence. In order to get the *in situ* information about the film structure we used structural-sensitive photopotential and photocurrent measurements.

Thin Ag(I) oxide formed in 0.1M KOH by potentiostatic polarization at E = 0.52_0.56 V (s.h.e.) on polycrystalline $Ag_{poly}$, single crystalline $Ag_{100}$, $Ag_{110}$, $Ag_{111}$ and polycrystalline Ag-Au alloys (with gold concentration 1; 4 and 15 at.%) were the object of investigation.

Photoelectrical measurements were performed by means of the set of light-emitting diodes. Photopotential $E_{ph}$ was measured in the open circuit after the polarization switching off. Photocurrent $i_{ph}$ was measured under potentiostatic polarization at the potentials of oxide Ag(I) formation. The role of potential of oxide Ag(I) formation (0.52-0.56 V s.h.e.), film thickness L (6-22 nm), light intensity (0.8-3.0 mW $cm^{-2}$) and wavelength $\lambda$ (385-875 nm) was examined.

It was found that $E_{ph} < 0$ and $i_{ph} > 0$ independent of potential of $Ag_2O$ formation and film thickness. It proves the n-type conductivity connected with the excess of metal in oxide structure.

After the polarization switching off, photopotential decays in time in exponential manner. The decay is caused by the film dissolution. Photopotential and photocurrent increase with the film thickening. $E_{ph}$ and $i_{ph}$ dependence on film thickness L points that:

- the anodic film is thin (its thickness is less than the space charge region);
- the photopotential and photocurrent arise in oxide volume but not in the surface electronic states.

The same conclusion results from the difference in $E_{ph}$ and $i_{ph}$ for oxides grown on $Ag_{poly}$, single crystals $Ag_{hkl}$ and alloys (Table).

The concentration of donor defects decreases in the row $Ag_{poly} > Ag_{hkl} >$ Ag-Au. Hence, more stoichiometric oxide is formed on alloys. As a result the photoconductivity drops in the same order. The shape of $i_{ph}$ - $\lambda$ dependences, hence, the band gap slightly changes at transition from $Ag_{poly}$ to $Ag_{hkl}$ and Ag-Au alloys.

*Table. Coefficient of light absorption $\alpha$ (at $\lambda$ = 470 nm), space charge region W, donor defect concentration $N_D$, band gap for direct transition $E_{bg}^{dir}$ and photoconductivity $\sigma$ in $Ag_2O$*

| Parameter | | Electrode system | | |
|---|---|---|---|---|
| | | $Ag_2O\|Ag_{poly}$ | $Ag_2O\|Ag_{hkl}$ | $Ag_2O\|Ag$-Au |
| $\alpha$, $cm^{-1}$ | | 2.3 | 0.7÷1.4 | 0.001÷0.1 |
| W, nm | | 100 | 164÷330 | 767÷2300 |
| $N_D \cdot 10^{-15}$, $cm^{-3}$ | | 22.4 | 2.1÷8.3 | 0.05÷0.4 |
| $E_{bg}^{dir}$, eV | by $i_{ph}$ | 2.32 | 2.23 | 2.19 |
| | by $E_{ph}$ | 2.09 | - | - |
| $\sigma \cdot 10^5$, $Ohm^{-1} \cdot cm^{-1}$ | | 9.8 | 4.8÷8.0 | 0.4÷2.2 |

The concentration of donor defects decreases in the row $Ag_{poly}$ > $Ag_{hkl}$ > Ag-Au. Hence, more stoichiometric oxide is formed on alloys. As a result the photoconductivity drops in the same order. The shape of $i_{ph}$ - $\lambda$ dependences, hence, the band gap slightly changes at transition from $Ag_{poly}$ to $Ag_{hkl}$ and Ag-Au alloys.

The dependence of structure-sensitive parameters on the state of the electrode surface (different crystallographic orientation and different Au concentration) proves, in our opinion, that the oxide film is formed in the course of direct anodic oxidation but not in the course of dissolution-precipitation.

*This work is supported by CRDF (RUXO-000010-VZ-06) and RFBR (06-03-32274-a).*

First Regional Symposium on Electrochemistry of South-East Europe, Rovinj, Croatia, May 4-8, 2008.

O-2-26

# EXPERIMENTAL DETERMINATION OF SURFACE STRESS CHANGES IN ELECTROCHEMICAL SYSTEMS – POSSIBILITIES AND PITFALLS

**G. G. Láng*, N. S. Sas, S. Vesztergom**

[1] *Eötvös Loránd University, Institute of Chemistry, Laboratory of Electrochemistry and Electroanalytical Chemistry, H-1117 Budapest, Pázmány P. s. 1/A*
**E-mail: langgyg@chem.elte.hu*

The surface stress or specific surface energy of solid electrodes is an important physical quantity, since most electrochemical systems involving solids are, in fact, capillary systems, because any interaction between the bulk solid and the remainder of the system takes place via the surface region. Since thermodynamic properties of the surface region directly influence the electrochemical processes, an understanding of the thermodynamics of solid surfaces is of importance to all surface scientists and electrochemists. It is not surprising therefore, that during the past decades several attempts have been made to derive thermodynamic equations for the solid/liquid interface, and several methods were suggested for measurements of changes of the specific surface energy of solid electrodes. Unfortunately, for solid electrodes the thermodynamic interpretation of the results from various methods in terms of physicochemical properties of the system is not quite clear.

In principle, the results of the theoretical work can be checked experimentally. Unfortunately, specific surface energies of solid electrodes are very difficult to measure owing to the lack of reliable and sensitive methods. In a few specific situations, the surface tensions of some solid surfaces have been determined experimentally. These experimental methods are designed for the solid/gas interface, and are mostly incompatible for use at room temperature or in the presence of an electrolyte solution. Consequently, they cannot be applied to study the surface energy of solid electrodes.

The methods suggested for measurement of the surface energy of solid electrodes only yield changes of surface stress as a function of various physicochemical parameters e.g. as a function of electrode potential [1-5]. Variation in surface stress may either be obtained indirectly by measuring the potential dependence of the strain (i.e. electrode deformation) and then obtaining the variation in stress from the appropriate form of Hooke's law, or it may be measured "directly" e.g. with a piezoelectric element. (In principle, if there are both "plastic" and "elastic" contributions to the total strain, the "generalized surface parameter" [6] can be determined.)

Unfortunately, the determination of surface stress changes is difficult. Most methods have some drawbacks; i.e., they are technically demanding, they cannot be used to monitor changes of the surface stress, they are semiempirical and depend on further assumptions, or they are not generally applicable.

In the present lecture, the different techniques used for the determination of changes of surface stress of electrodes (bending beam (or "bending cantilever", "laser beam deflection","wafer curvature", etc.) method (Fig.1) [5,7,8,9], interferometry [5,7], piezoelectric method [10,11], extensometer method [12], contact-angle methods [1], etc.), as well as the kind and quality of information that can be achieved using these methods will be discussed. Several illustrative examples will be presented and advantages/drawbacks highlighted.

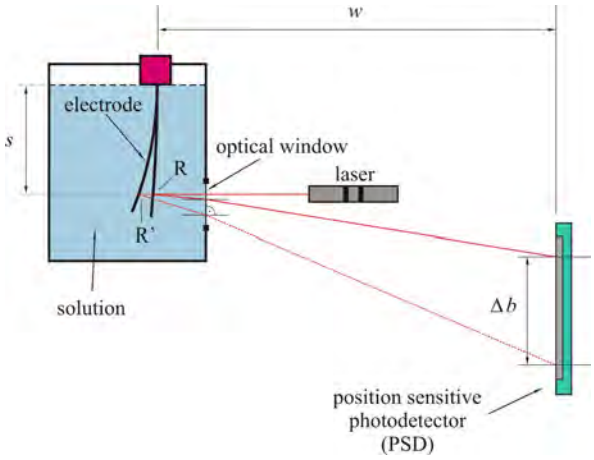


*Fig.1. Scheme of the electrochemical (optical) bending beam setup.*

*Financial support by the Hungarian Scientific Research Fund (OTKA K045888, OTKA K67994) is gratefully acknowledged.*

**References:**

[1] Morcos I ''*Specialist Periodical Reports Electrochemistry*'', Vol 6. In: Thirsk HR (ed) The Chemical Society, Burlington House, London, pp. 65-97 (1978).
[2] Jaeckel L, Láng G, Heusler KE, *Electrochim. Acta* **39** (1994) 1031.
[3] Ibach H, Bach CE, Giesen M, Grossmann A, *Surf. Sci.* **375** (1997) 107.
[4] Haiss W, *Rep. Prog. Phys.* **64** (2001) 591.
[5] Láng GG, Seo M, Heusler KE, *J. Solid State Electrochem.* **9** (2005) 347.
[6] Trasatti S, Parsons R, *Pure&Appl Chem* **58** (1986) 437.
[7] Jaeckel L, Láng G, Heusler KE, *Electrochim. Acta* **39** (1994) 1031.
[8] Láng GG., Ueno K., Ujvári M., Seo M., *J. Phys. Chem. B.* **104** (2000) 2785.
[9] Rokob TA, Láng GG, *Electrochim. Acta* **51** (2005) 93.
[10] Gokhshtein A. Ya. "*Poverkhnostnoe natyazhenie tverdykh tel i adsorbtsiya*" *(Surface Tension of Solids and Adsorption)*, Nauka, Moscow (1976).
[11] Ueno K. Seo M, *J. Electrochem. Soc.* **146** (1999) 1496.
[12] Beck TR, *J. Phys. Chem.* **73** (1969) 466;

First Regional Symposium on Electrochemistry of South-East Europe, Rovinj, Croatia, May 4-8, 2008.

O-2-27 Keynote lecture

# CORROSION BEHAVIOR OF COMPOSITE COATINGS OBTAINED BY ELECTROLYTIC CODEPOSITION OF COPPER WITH $Al_2O_3$ NANOPARTICLES

**I. Zamblau[1], S. Varvara[2], L.M. Mureşan[1]***

[1]*Department of Physical Chemistry,"Babes-Bolyai" University, 400028 Cluj-Napoca, ROMANIA,*
[2]*Department of Topography, "1 Decembrie 1918" University Alba-Iulia, Romania*
*limur@chem.ubbcluj.ro

One of the ways used to obtain metallic coatings with improved corrosion resistance consists in the incorporation of inert micro- and nanoparticles (ex. $TiO_2$, $SiO_2$, $Al_2O_3$) in the metallic matrix by using the co-electrodeposition method [1-3]. This method to obtain composite materials has some interesting advantages: (i) possibility of rigorous control of the deposited layer thickness; (ii) control of deposition speed; (iii) work at room temperature and (iv) use of accessible equipments. Moreover, the electrodeposition is suitable for obtaining non-uniform films on substrates with complex shapes (*e.g.* deposition only on some surfaces of the substrate, deposition on porous profiles etc.) [4].

The present work aims to obtain and to characterize a model composite system consisting of copper incorporating $Al_2O_3$ nanoparticles, electrodeposited on carbon steel (OL37).

By using electrochemical investigation methods such as open circuit potential measurements, hydrodynamic voltammetry and electrochemical impedance method, the corrosion behavior of the two different types of $Al_2O_3$-copper nanocomposite coatings was examined.

The corrosion parameters determined from Tafel interpretation of polarization curves recorded in $Na_2SO_4$ solution (pH 3) indicate that the corrosion process on copper-alumina composite surface is slower than on pure copper surface.

On the other hand, the impedance spectra recorded in the absence and in the presence of $Al_2O_3$ nanoparticles in the copper coatings show an increase of the polarisation resistance in time, which can be explained by the development of corrosion products on the electrode surface. Using a 3RC equivalent electrical circuit, the process parameters were obtained by non-linear regression calculations with a simplex method. From these parameters it can be seen that the aluminium oxide particles embedded in electroplated copper increase the polarisation resistance and decrease the corrosion rates with 1.32 times as compared with electrodeposited pure copper.

The electrochemical results were corroborated with those obtained by SEM and EDX investigations.

## References:

[1] J. Fransaer, J.P. Celis, *Galvanotechnik*, **92** (2001) 1544.
[2] A. Hovestad, L.J.J. Jansen, *J. Appl. Electrochem.*, **25** (1995) 519.
[3] M. Musiani, *Electrochim. Acta*, **45** (2000) 3397.
[4] K. I. Popov, S. S. Djokic, B. N. Grgur, *Fundamental Aspects of Electrometallurgy*, Kluwer Academic/Plenum Publ. NY, (2002).

First Regional Symposium on Electrochemistry of South-East Europe, Rovinj, Croatia, May 4-8, 2008.

O-2-28

# INFLUENCES OF pH AND COMPONENTS OF SOLUTION ON ANODIC BEHAVIOUR OF COPPER IN ACETATE -BORATE -PHOSPHATE ELECTROLYTE

**I.V. Protasova, S.N. Belova**

*Voronezh State University, Universitetskaya sq., 1, Voronezh, Russia, 394006*
prot@l47.chem.vsu.ru

Examination of anodic behavior of copper at potentials of its passivity caused by formation of film of insoluble products its anode oxidation, Cu (I) and Cu (II) with oxygen and anions of a solution, is actual scientific problem.

Anode dissolution of copper was studied at 298 K in air-free solutions containing acetate, borate, and phosphate ions with concentration of each anion 0,02 M and pH 1,8 ÷ 11,9 and also in the solutions containing one type of anion with concentration from 0,01 M up to 2 M at pH 4.1 and 12.5. Stationary and rotating disk copper (Cu ≥ 99.99 %) electrodes were used.

It is shown, that anode process on copper in these solutions combine electron transfer stage with diffusion of products of copper oxidation in the electrolyte and solid - phase diffusion in surface oxide layer not depending on pH and type of anions. It could be recognized that value of pH and complex anion composition of electrolyte assign a character of rate-controlling stage.

In all solutions with pH < 4.1 kinetic stage is anode oxidation of copper with hydroxyl-ions up to Cu(II), rate-controlling stage at active dissolution potentials – diffusion transfer of soluble complexes of copper with components of the solution. At the further increase of potential effects of salt passivity take place.

In solutions with pH ≥ 4.1 adsorption of $OH^-$ or water leads to formation of adsorptive Cu(I) hydroxides which then are hydrolyzed and break up in the solution. There dehydratation at more positive potentials with formation of phase $Cu_2O$ causes a passivity of copper.

In neutral and alkaline solutions with acetate, borate and phosphate ions, as far as in cleanly alkaline, increasing of anode process speed in the active dissolution field with increase pH takes place. However at passivity potentials, decreasing of an anode current with growth of $OH^-$ concentration is observed.

An influence of nature of anion on anode processes on copper is not simple. In acetate or borate alkaline solutions anode process on copper in all researched potential areas runs with higher speed in comparison with cleanly alkaline and acetate – borate - phosphate solutions. However, anode currents in phosphate alkaline solutions essentially low in comparison with all other solutions in all potential areas.

It can be suppose, that such complicated character of anions influence on kinetic of anode process can be caused by possible embedding of solution anions in adsorptive hydroxo - complexes. Probably, formed intermediate acetate- and borate-containing adsorptive hydroxy-compounds is soluble and so activate anode process. On the contrary phosphate-containing adsorptive compounds with intermediate of copper are insoluble and their stability increases with increasing of $OH^-$ - ion concentration.

*Research is supported by RFBR, project 06-03-32274a.*

First Regional Symposium on Electrochemistry of South-East Europe, Rovinj, Croatia, May 4-8, 2008.

O-2-29

# STUDY OF SOME COMPOSITES CORROSION

**A. Bărbulescu, D.C. Toncu**

*Ovidius University of Constanța, Romania*
*E-mail: abarbulescu@univ-ovidius.ro*

The authors studied special composites obtained by copper powder sintering with carbon concrete. The resulted material is a porous structured alloy able to adsorb bearing oils. The sintering temperature is about 66.6 % of alloy melting point, which is enough to create chemical bond between atoms.
The base material is made out of 7 % Sn, 4 % Zn, 2 % Pb, 87 % Cu. There were three kinds of composites, the first consisted only from the base material, the second had a 1.5 %wt. carbon addition, and the third contained 2.5 %wt. carbon addition (graphite allotropic form). The performed study also aimed to compare and characterize the response of these composites under the working conditions inside ship engine, especially by mass loss, microscopy and Brinell hardness.
The three composites, immersed in water and bearing oil, had a different corrosion rate, and, furthermore, a very specific chemical behaviour in the stationary medium. The mass loss determined lead to the creation of a mathematical model, able to describe the corrosion process and, in the same time, to offer a comparative analysis of different material mass loss. This model, made with the help of the SPSS programme, takes into accounts the corrosion factors (porosity and carbon content), calculating corrosion effects.

First Regional Symposium on Electrochemistry of South-East Europe, Rovinj, Croatia, May 4-8, 2008.

O-2-30

# ELECTROCHEMICAL OXIDATION OF Ti-6Al-7Nb ORTHOPAEDIC ALLOY STUDIED BY XPS AND EIS TECHNIQUES IN SIMULATED PHYSIOLOGICAL SOLUTION

**I. Milošev[a,b], T. Kosec[a], H.H. Strehblow[c]**

[a]*Jožef Stefan Institute, Department for Physical and Organic Chemistry, Jamova 39, SI-1000 Ljubljana, Slovenia, E-mail: ingrid.milosev@ijs.si*
[b]*Orthopaedic Hospital Valdoltra, Jadranska c. 31, 6280 Ankaran, Slovenia*
[c]*Heinrich-Heine University, Institute of Physical Chemistry, of Düsseldorf, Germany*

The composition and structure of the passive film formed on Ti-6Al-7Nb alloy by electrochemical oxidation in Hank's physiological solution were studied using X-ray photoelectron spectroscopy (XPS) and electrochemical impedance spectroscopy (EIS). The oxide layer was predominantly $TiO_2$, but contained small amounts of sub-oxides TiO and $Ti_2O_3$ at potentials more negative than 0.75 V. At more positive potentials, $TiO_2$ was the only oxide formed. The formation of sub-oxides in the lower potential range is less pronounced than in Ti-6Al-4V alloy. The passive range in Hank's physiological solution is broad and extends up to 6.0 V. Aluminium oxide $Al_2O_3$, and niobium oxides, $Nb_2O_5$, and NbO and/or $NbO_2$, are incorporated in the passive layer. Angular resolved XPS analysis confirmed that the oxides of minor elements are located mainly at the outer oxide/solution interface of the $TiO_2$ matrix. After oxidation at most positive potential, the thickness of the oxide layers reached approximately 9 nm. EIS measurements correlate well with the XPS data. The incorporation of the oxides of alloying elements into the $TiO_2$ layer is beneficial for the overall stability and high corrosion resistance of Ti-6Al-7Nb alloy under physiological conditions.

*Keywords:* Ti alloys; electrochemical oxidation; Hank's physiological solution; XPS; EIS

First Regional Symposium on Electrochemistry of South-East Europe, Rovinj, Croatia, May 4-8, 2008.

O-2-31

# EFFECT OF HEAT TREATMENT ON ANODIC BEHAVIOUR OF Ti-Al-Si LAYERS IN PHYSIOLOGICAL SOLUTION WITH FLUORIDE ADDITIONS

**T. Kubatík[1], D. Vojtěch[2], E. Kalabisová[1], V. Číhal[1]**

*[1]SVÚOM Ltd., Prague, kubatik@svuom.cz*
*[2]Institute of Chemical Technology, Prague*

## Introduction

Ternary aluminide-silicide layers, capable of protecting titanium surfaces, are interesting because of their easy preparation. Ternary layers created on titanium and on TiAl6V4 alloy exhibit excellent protection against atmospheric oxygen, however, their resistance in aqueous media has not yet been extensively described in commercial publications. The layers are porous and it is probable that their protective effect may decline because of the fact that the positive effect of low surface oxidation of the most frequently present phase of $Ti_{30}Al_{25}Si_{43}$ under formation of $SiO_2$ and consequent sealing of pores may not occurs. Annealing of prepared layers promotes sealing of pores as well as hinders migration of ions to interface layer/substrate. At high temperatures superficial oxidation of ternary layers occurs accompanied by formation of $SiO_2$ and $Al_2O_3$.

## Experimental

For the preparation of aluminide-silicide layers on TiAl6V4 melt AlSi20 was used. Samples were placed on the bottom of crucible containing melt maintained at 800°C and left there at that temperature for 10 minutes.. Stuck solidified melt was removed by etching in 10-15% HCl. After that samples were annealed at temperatures 800-1000°C for 1 hour. Potentiodynamic measurements were performed in physiological solutions (9 g NaCl per 1 litre) containing different fluoride concentrations 2,500 and 5,000 ppm (NaF), at a temperature of 37°C. Saturated calomel electrode was used as reference electrode

## Results

It can be seen, that in absence of fluoride is anodic behaviour of sample with layer annealed at 800°C significantly better in comparison to sample with layer annealed at 1000°C only at potentials lower than 0V. At higher potentials are differences in values of anodic current densities both samples rather small. In opposite to it however in solution with fluoride content 5000ppm is anodic behaviour of sample with layer annealed at 1000°C best of all tested samples, i. e. even better in the case of bare alloy and layer without heat treatment.

## Conclusions

- Prepared layers are porous and that is why its application is unsuitable for environment containing fluorides. This disadvantage can be solved by annealing of prepared layers supporting sealing of pores by oxidation accompanied by formation of $SiO_2$ a $Al_2O_3$.
- In solution with high fluoride content this protective effect has been observed for layer annealed at 1000°C.

First Regional Symposium on Electrochemistry of South-East Europe, Rovinj, Croatia, May 4-8, 2008.

O-2-32

# INFLUENCE OF FLUORIDE AND pH ON CORROSION BEHAVIOR OF BIOMATERIALS

**M. Poddaná, E. Kalabisová, V. Číhal**

*SVÚOM Ltd.,U Měšťanského pivovaru 934/4, 17000 Prague 6*
*E-mail: poddana@svuom.cz*

*Introduction:* Application of alloys in dentistry encounters problems relating to the stability of material in the mouth cavity environment, which keeps changing due to intake of food. The agents of oral hygiene containing high concentrations of fluorides also influence composition of oral environment. This circumstance may exert negative effects with some materials.
*Methods:* Six types of materials were used in the measurements (ISO 5832-1, ISO 5832-9, ISO 5832-12, Osteofix, Ti grade 2 and Ti6Al4V). Measurements were performed in saline solution with various concentrations of fluoride and pH. The free corrosion potential, polarization resistance, potentiodynamic curves and the susceptibility of materials to non-uniform corrosion were measured.
*Results:* The results, observed from measurement of potentiodynamic dependences of three types of stainless steels (ISO 5832-1, ISO 5832-9 and Osteofix) and Co-Cr alloy (ISO 5832-12),demonstrate, that the effect of pH and fluoride concentration on shape of potentiodynamic curves are not very striking. The effect of pH and fluoride on polarization resistance is the same. The polarization resistance values decrease moderately as the pH is lowered. The same also applies to the Rp values obtained at increasing fluoride concentrations in the electrolyte.

**Polarization resistance** [Ω. $m^2$]

| pH | Fluoride [ppm] | ISO 5832-12 | Osteofix | ISO 5832-1 | ISO 5832-9 | Ti6Al4V | Tigr2 |
|---|---|---|---|---|---|---|---|
| unadjusted | ***0*** | 307 | 462 | 263 | 148 | 18.3 | 39.5 |
| | ***5000*** | 314 | 419 | 102 | 105 | 1.3 | 3.7 |
| **5.8** | ***1000*** | 225 | 311 | 90.5 | 92.1 | 0.1 | 0.6 |
| **4.2** | ***100*** | 188 | 347 | 89.2 | 71.9 | 0.1 | 0.5 |

Different results were observed from experiments with titanium materials. The addition of fluoride to the solution and decrease of pH had a negative effect on corrosion behavior of titanium materials. The addition of fluoride to the solution caused decrease of polarization resistance about order. The reducing of electrolyte pH lead to other decrease of polarization resistance. On potentiodynamic curves was possible to observe their shift to higher current densities and lower value of corrosion potential with fluoride and more acidic environment.

Non-uniform corrosion was observed on the stainless steels and Ti6Al4V alloy.Ti grade 2 and Co-Cr alloy were susceptible to localized corrosion under experimental conditions.

*Conclusions:* The results demonstrate that the effects of pH and of the fluoride on the corrosion behavior of stainless steels and Co-Cr alloy are not very striking. In the case of titanium materials, the more acidic is the corrosion environment, the more sensitive the materials become to the presence of fluorides. Even small shifts in the fluoride concentration can provoke marked changes in corrosion behavior of them.

First Regional Symposium on Electrochemistry of South-East Europe, Rovinj, Croatia, May 4-8, 2008.

O-2-33

# ELECTROCHEMICAL AND AFM STUDY OF CORROSION INHIBITION WITH RESPECT TO APPLICATION METHOD

**H. Otmačić Ćurković, K. Marušić, E. Stupnišek-Lisac, J. Telegdi***

*Faculty of Chemical Engineering and Technology, Zagreb, Croatia, helena.otmacic@fkit.hr*
**Institute of Chemistry, Hungarian Academy of Science, Budapest, Hungary*

One of the most important methods for the corrosion protection of metals is the use of organic inhibitors. It is common to apply corrosion inhibitor either by adding it directly to the corrosive media or form protective inhibitor film prior to exposing the metal to the corrosive environment. The choice between these two methods usually depends on the properties of the inhibitor and on the type of the corrosion media.

Imidazole derivatives were found to be efficient copper corrosion inhibitors in various corrosive environments [1-3]. Previous research has shown that their inhibiting action depends on the anion and the pH value of the solution [4]. The aim of this work was to study if it is possible to obtain higher efficiency of the inhibitor by varying the method of its application.

Two imidazole compounds were studied 4-methyl-1-phenyl imidazole and 4-methyl-1-(*p*-tolyl) imidazole. Their efficiency as copper corrosion inhibitors was examined in chloride and sulphate media. Inhibitors were either added to corrosive solution or the inhibitor film was formed prior to immersion in the corrosive solution. Investigations were performed by the means of electrochemical methods (polarization measurements and EIS) and atomic force microscopy.

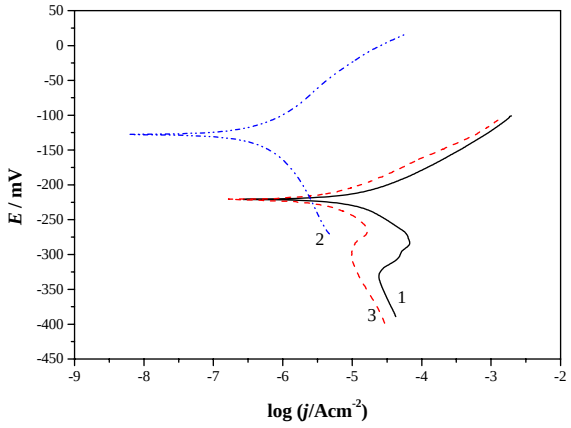


*Figure 1. Polarization curves of copper in 0.5 M NaCl (1), with 5 mM 4-methyl-1-phenyl imidazole added (2) and after formation of inhibitor layer during 60 min in THF (3)*

Figure 1 shows polarization curves of copper in 0.5 M NaCl solution with and without the addition of 4-methyl-1-phenyl imidazole and the polarization curve of

copper electrode covered by 4-methyl-1-phenyl imidazole film formed in organic solvent. It can be readily seen that for both manners of inhibitor application decrease of corrosion rate was observed. In the case when inhibitor had adsorbed on metal surface in organic solvent, polarization curve obtained was in shape very similar to that for unprotected electrode and the corrosion potential was almost the same. On the contrary polarization curve measured in 0.5 M NaCl containing inhibitor differs in the shape and the corrosion potential is shifted towards nobler values. From these observations it can be concluded that there are differences in inhibiting mechanism of two differently formed inhibitor layers. These differences were also observed with AFM study of metal surface (Fig.2)

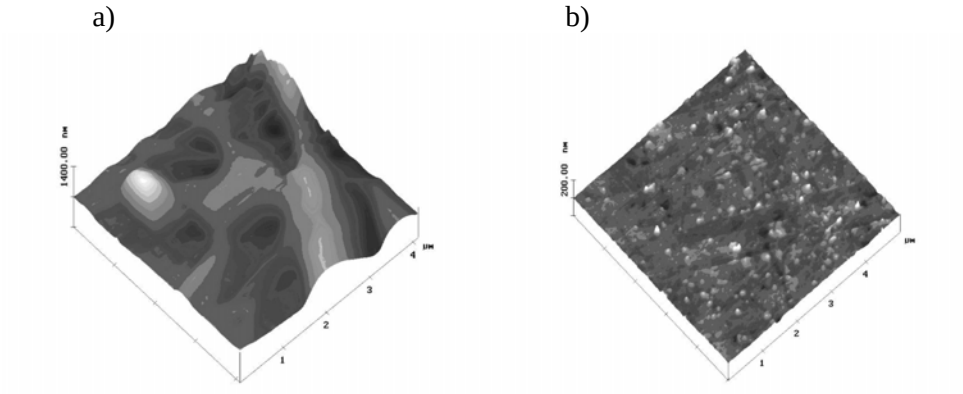


*Figure 2. AFM images of copper electrode after 60 min immersion in 0.5 M NaCl containing inhibitor (a), and after 60 min of inhibitor formation in THF followed by 60 min immersion in 0.5 M NaCl (b).*

The differences in morphology of samples prepared by two techniques (i.e. in the first case the inhibitor was dissolved in the NaCl solution, in the second one the experiment was carried out by copper with previously developed inhibitor layer) is demonstrated in Figure 2a and b. Formation of polymer-like structures was observed in the case when inhibitor was directly added to chloride solution but not when the inhibitor film was separately preformed.

Investigations performed in sulfate media with the other inhibitor (4-methyl-1-(*p*-tolyl) imidazole) have also shown that protection mechanism and inhibitor efficiency significantly depend on the application method of inhibitor.

## Literature

1. H. Otmačić and E. Stupnišek-Lisac, *Electrochim. Acta*, **48** (2003) 985-991
2. R. Gašparac, C. R. Martin, E. Stupnišek-Lisac, *J. Electrochem. Soc.* **147** (2000) 548
3. R. Gašparac, E. Stupnišek-Lisac, *Corrosion*, **55** (1999) 1031
4. H. Otmačić, E. Stupnišek-Lisac, H. Takenouti, *4th Croatian Symposium on Electrochemistry*, Primošten, 2006. 118-123

First Regional Symposium on Electrochemistry of South-East Europe, Rovinj, Croatia, May 4-8, 2008.

O-2-34

# THE MECHANISM OF BENZOTRIAZOLE INHIBITION OF COPPER, ITS ALLOYS WITH ZINC AND ZINC IN CHLORIDE SOLUTION

**T. Kosec[a], I. Milošev[a,b]**

[a]*Jožef Stefan Institute, Department for Physical and Organic Chemistry, Jamova 39, SI-1000 Ljubljana, Slovenia, e- mail: tadeja.kosec@ijs.si*
[b]*Orthopaedic Hospital Valdoltra, Jadranska c. 31, 6280 Ankaran, Slovenia*

The research is aimed to study the mechanism of formation of protective layers on copper, zinc and copper-zinc (Cu-10Zn and Cu-40Zn) alloys in chloride solution containing benzotriazole, by use of different electrochemical techniques, atomic force microscopy (AFM) and X-ray photoelectron spectroscopy (XPS). Electrochemical reactions and surface products formed at the open circuit potential and as a function of externally applied potential are discussed. The addition of benzotriazole to aerated, near neutral 0.5 M NaCl solution affects the dissolution of copper, zinc, Cu-10Zn and Cu-40Zn alloys. The inhibition efficiency and Gibbs adsorption energies of the investigated process are compared. Gibbs adsorption energies prove the BTAH inhibitor to chemisorb onto investigated materials, for being the energies in the range around -40 kJ/mol.

Benzotriazole, generally known as an inhibitor of copper corrosion is also shown to be an efficient inhibitor for copper-zinc alloys and zinc metal. Impedance measurements showed that copper and both alloys are efficiently inhibited at different immersion times. Protective layer on zinc exhibits some sort of protection but to a lesser extent than on copper and the alloys. Results were fitted using equivalent circuit that mimics the physical chemical properities in a system investigated.

XPS results showed that the surface layer formed on alloys in BTA-inhibited solution comprised both oxide and polymer components, namely $Cu_2O$ and ZnO oxides, and Cu(I)-BTA and Zn(II)-BTA polymers. The formation of $Cu_2O$/Cu(I)-BTA on copper, ZnO/Zn(II)-BTA and Cu(I)-BTA on copper-zinc alloys ZnO/Zn(II)-BTA polymer surface film provides an effective barrier against corrosion on materials investigated in chloride solution.

*Keywords:* copper; brass; benzotriazole; inhibition, electrochemical techniques, XPS

First Regional Symposium on Electrochemistry of South-East Europe, Rovinj, Croatia, May 4-8, 2008.

O-2-35

# INHIBITION OF STEEL CORROSION BY ELECTROSYNTHESIZED POLY(o-ANISIDINE)-DODECYLBENZENESULFONATE COATINGS

**P.P. Patil*, S. Chaudhari**

*Department of Physics, North Maharashtra University, Jalgaon 425 001 Maharashtra, INDIA, E-mail: pnmu@yahoo.co.in*

Poly(o-anisidine)-Dodecylbenzenesulfonate (POA-DBSA) was investigated for corrosion protection of stainless steel. Uniform and strongly adherent POA-DBSA was electropolymerized on stainless steel from aqueous dodecylbenzene sulfonic acid solution by using cyclic vltammetry. The structure and properties of these coatings were characterized by Fourier transform infrared spectroscopy, UV-visible absorption spectroscopy, scanning electron microscopy and cyclic voltammetry. Corrosion tests were carried out in aqueous 3% NaCl solution for POA-DBSA coated steel using open circuit potential (OCP) measurements, potentiodynamic polarization technique and electrochemical impedance spectroscopy (EIS). Results of this study reveal that POA-DBSA has a corrosion protection effect for stainless steel in aqueous 3% NaCl. The corrosion protection efficiency of the poly(o-anisidine) coatings against 304-stainless steel corrosion is found to be ~ 96%.

First Regional Symposium on Electrochemistry of South-East Europe, Rovinj, Croatia, May 4-8, 2008.

O-2-36

# POLY(o-TOLUIDINE)/$ZrO_2$ NANOCOMPOSITE COATINGS ON COPPER: SYNTHESIS, CHARACTERIZATION AND CORROSION PROTECTION PROPERTIES

**S. Chaudhari*, P.P. Patil**

*Department of Physics, North Maharashtra University, Jalgaon 425 001, INDIA*
*sudeshna6480@yahoo.co.in

This study explores the possibility of using poly(o-toluidine)/$ZrO_2$ (POT-$ZrO_2$) nano-particle composite coatings for corrosion protection of copper (Cu) in chloride environment. In this work, POT-$ZrO_2$ nanocomposite coatings were synthesized on Cu through an electrochemical route. These coatings were characterized by cyclic voltammetry, UV-visible absorption spectroscopy, Fourier transform infrared spectroscopy, scanning electron microscopy and x-ray photoelectron spectroscopy. The performance of POT-$ZrO_2$ nanocomposite as protective coating against corrosion of Cu in aqueous 3% NaCl was evaluated by the potentiodynamic polarization technique and electrochemical impedance spectroscopy. The results of this study demonstrate that the POT-$ZrO_2$ nanocomposite coating provides better protection to Cu against corrosion as compared to that offered by the pure POT coating. The corrosion potential was about 0.150 V versus SCE more positive in 3% NaCl for the nanocomposite coated Cu than that of uncoated Cu (*cf.* Fig.1) and reduces the corrosion rate of Cu almost by a factor of 538.

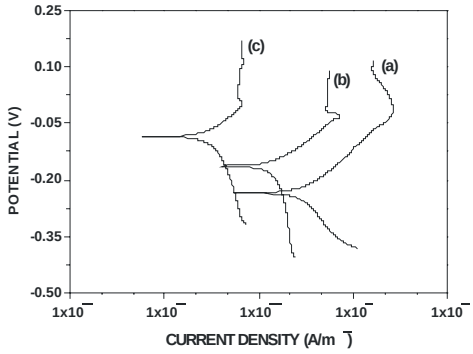


*Fig.1 : Potentiodynamic polarization curves for (a) uncoated Cu, (b) POT coated Cu and (c) POT-$ZrO_2$ coated Cu recorded in 3% NaCl.*

First Regional Symposium on Electrochemistry of South-East Europe, Rovinj, Croatia, May 4-8, 2008.

O-2-37

# INVESTIGATION OF AMINATED X-RESIN ON BASIS OF POD-OILS AS CORROSION INHIBITOR

**G. Ostapenko[1], P. Gloukhov[1], S. Sadivskiy[2], V. Pisareva[1], S. Sabitov[2]**

[1]*Department of Chemistry, Togliatti State University,*
*14, Belorusskaya St., Togliatti, 445667, Russia; gostap@tltsu.ru*
[2]*Joint-Stock Company KuibyshevAzot,*
*6, Novozavodskaya St., Togliatti, 445652, Russia*

The technological waste at caprolactam production is a multicomponent mixture of products of cyclohexanol dehydrogenation and cyclohexane oxidizing. This mixture is defined as POD-oil (Product of Oxidizing and Dehydrogenation). The inhibiting composition (aminated X-resin) is synthesized by means of POD-oil condensation with formalin at the presence of the alkaline catalytic agent and at amination of the product. The special investigations have shown that the surface-active component in aminated X-resin is cyclohexylidenecyclohexanon.

Corrosion of carbon steel in 20 % hydrochloric acid at various inhibiting composition concentrations is investigated. The corrosion potential is displaced to the anodic direction with increasing of inhibitor concentration. Hence the investigated inhibitor retards mainly anodic reaction.

The impedance hodographs are shown in Fig.1 at various concentrations C (numbers on the curves, per cent by mass). The equivalent circuit is simulated by a parallel connection Constant Phase Element (CPE) and corrosion resistance R.

Fig. 2 shows that the inhibitor efficienties z rather high (92 – 93 %). Hence aminated X-resin is the high effective inhibitor of carbon steel in hydrochloric acid.

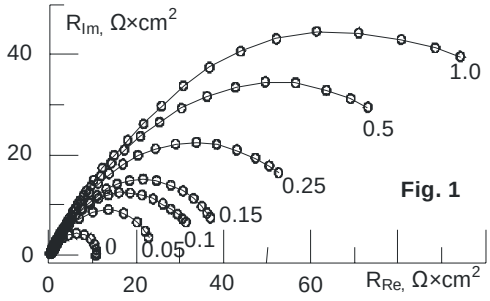


Fig. 1

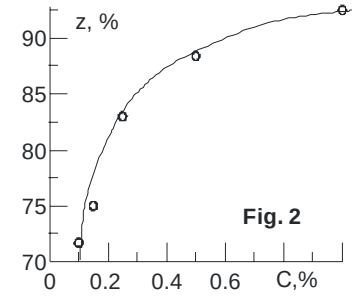


Fig. 2

First Regional Symposium on Electrochemistry of South-East Europe, Rovinj, Croatia, May 4-8, 2008.

O-2-38

# ELECTROCHEMICAL METHODS TO INVESTIGATE LOCAL CORROSION BEHAVIOUR OF Zr-1%Nb

**A. Somogyi, Z. Kerner, J. Balog, G. Nagy, Á. Horváth**

*MTA KFKI Atomic Energy Research Institute, H-1525 Budapest 114, P.O.B. 49. Hungary,*
somogyi@aeki.kfki.hu

Structural materials under conditions which prevail in a VVER primary circuit can be sensitive to local corrosion damage. Our aim was to determine the local corrosion behaviour of the Zr-1%Nb alloy, used in VVER type nuclear reactors as cladding of the fuel rods, especially at high temperatures. Several electrochemical techniques like cyclic voltammetry, chronoamperometry, potential noise measurements were applied to detect and describe pitting corrosion. The studies were performed at ambient and elevated temperatures in electrolytes containing aggressive ions.

The measurements on room temperature were made in a conventional three-electrode electrochemical cell in boric acid solution using calomel reference electrode and a Pt counter electrode. Chemically polished and pre-oxidized samples were used. Polishing were carried out in mixture of $HF:H_2SO_4:HNO_3$, oxidizing had been in autoclave for 3 months before the measurements. The measurements on high temperature (300 °C) were carried out in autoclave, using both yttria-stabilized zirconia ceramic membrane electrode filled with Ni/NiO and external Ag/AgCl reference electrodes. A Pt plate was used as counter electrode. An AUTOLAB PGSTAT30 potentiostat was used for the work. To initiate localized corrosion aggressive ions ($Cl^-$, $I^-$) were injected stepwisely to the base solution (8 g/l boric-acid + 5 mg/l potassium-hydroxide in twice distilled water). Surface morphology was characterised by ex situ optical methods.

The critical pitting potential could be determined from cyclic voltammograms for all ion concentrations. On room temperature pitting was not observable in the base solution at OCP. It was found that to initiate the pitting process the solution must contain a limiting value of aggressive ions and the metals must be polarized until a certain value. On the polished samples pits can stabilize and grow, while on oxidized surfaces pits often heals and the corrosion process stops, i.e. only unstable pitting was observed. Chronoamperometric measurements resulted in the same conclusion. It was obvious that chloride ions are more aggressive than iodine ions. When the solution contained oxygen and high concentration of chloride we observed pitting also at OCP. At 300 °C we got similar results, although pitting was observed even if the concentration of $Cl^-$ and $I^-$ was two orders of magnitude smaller than at room temperature.

First Regional Symposium on Electrochemistry of South-East Europe, Rovinj, Croatia, May 4-8, 2008.

O-2-39

# THE USE OF ELECTROCHEMICAL NOISE FOR DETECTION OF STRESS-CORROSION CRACKING IN AUSTENITIC STAINLESS STEEL

**J. Kovač[1], E. Govekar[2], Ž. Bajt[1], M. Leban[1], A. Legat[1]**

*[1]Slovenian National Building and Civil Engineering Institute, Dimičeva 12, 1000 Ljubljana, Slovenia, jaka.kovac@zag.si*
*[2]Faculty of Mechanical engineering University of Ljubljana, Aškerčeva 6, 1000 Ljubljana, Slovenia.*

This work presents and discusses the potential use of electrochemical noise (EN) for the detection and characterization of different types of stress-corrosion cracking (SCC) in austenitic stainless steels. It is known that stress-corrosion cracking is a complex process, because it causes the initiation and propagation of cracks by the synergistic action of mechanical stress and corrosion reactions. Three main conditions should be satisfied for development of SCC: a material sensitive to SCC, a corrosion solution that causes localized corrosion and a large enough tensile load. Stress-corrosion cracking as a process is non-stationary. The process consists of alternating steps of mechanical events - fractures and electrochemical events - dissolutions. Regarding crack propagation, SCC processes could be divided into transgranular SCC (TGSCC) and intergranular SCC (IGSCC) modes. It is known that the TGSCC process advances with bigger discontinuous steps, while there is no complete agreement among researchers about the discontinuity of IGSCC.

Several different mechanisms describing transgranular and intergranular stress-corrosion cracking processes have been proposed in the past, but there is no general, widely accepted model that can describe SCC processes. One important reason for the insufficient knowledge about SCC processes are the measuring techniques for their detection and monitoring. Conventional electrochemical methods for monitoring corrosion processes (different types of potentiodynamic polarization, impedance spectroscopy, etc.) are due to stationarity not suitable for the detection and monitoring of SCC processes. These techniques can only estimate the susceptibility of the investigated system metal/corrosion solution to a certain type of corrosion. On the other hand electrochemical noise (EN) is a promising technique, which has been developed for the monitoring and characterization of non-stationary SCC processes. Electrochemical noise is an electrochemical method and it measures only electrochemical process. Since SCC is also a mechanical process some other methods (acoustic emission and elongation measurements) that detect physical changes were additionally applied during experiments.

Electrochemical noise (EN) is a method that uses three electrodes: a working electrode and two reference electrodes. Potential is measured between the working electrode and one of the reference electrodes, whereas current is measured between the working electrode and the other reference electrode. Corrosion events

on a single electrode are reflected in the measured fluctuations in current and voltage. The main advantage of the EN method in comparison with the other electrochemical methods is its ability to monitor corrosion in a freely corroding system without any external excitation signals. This feature makes it possible to measure the development of the natural corrosion process.

During past years different experiments using electrochemical noise for detection of SCC were performed. Important achievement in understanding, detection and technique development, which were accomplished during our research, are presented. Three different sets of experiments performed in our investigations are shown in this work. The selected experiments follow from the easiest system to detect SCC to the hardest system to detect SCC regarding material SCC susceptibility.

The first example shows measurement that was made during SLRT tests on stainless steel 304, where specimens were taken from an old boiler. This material was chosen, because the boiler failed during operation due to SCC. The material in received condition was found to be very susceptible for SCC due to non-homogeneousness and presence of defects. Experiments on that material were performed in different solutions. The process of SCC was clearly detected by spikes in EN. Elongation of specimen was measured as an additional technique and a clear relationship between specimen elongation rate, which is related to crack growth and electrochemical noise signal, was found.

On the basis of clear detection of SCC processes another set of measurements was performed on stainless steel 304 exposed to constant load test at room temperatures. In this case, material with better quality - more homogeneous with no large defects, was used. Material was additionally heat treated in order to increase susceptibility to intergranular SCC. Both transgranular and intergranular SCC modes were investigated separately by using different corrosion solutions. Results of measured electrochemical noise, elongation of specimen and acoustic emission showed a successful detection of SCC event during transgranular stress-corrosion cracking propagation by simultaneous use of all three methods. In the case of intergranular SCC propagation on the same type of steel, no such events were detected, but it was observed that the process could be detected as an accumulation of several small steps. This could be observed as an increase of direct current component of measured electrochemical current noise signal.

After positive results from previous tests, further set of experiments was performed on highly SCC sustainable stainless steel (AISI 304L). Measurements were realized during SLRT tests. In results a clear differentiation between active corrosion processes during steel exposure to aqueous solution of ammonium thiocyanate was compared to low corrosive action in steel exposed to aqueous solution of sodium thiosulphate. The difference in intensity of corrosion processes could be clearly seen from electrochemical noise measurements. The experiments also showed the effect of pitting on EN signals and the potential problem of distinguishing between those two sources of EN signal.

On the basis of our research, it can be concluded that EN is promising method that can be use for detection of SCC processes on different quality stainless steels. In case of a highly SCC susceptible material the detection was clear and even relation

between measured EN spikes and displacement rate was observed. The method in combination with acoustic emission technique and elongation measurement also showed its ability to detect individual SCC event in case of discontinuous transgranular SCC process on specimens made from high quality stainless steel AISI 304. On the other hand in case of smoother intergranular SCC propagation, observed on the same kind of stainless steel, only an accumulation of SCC processes was detected. The experiments performed on low SCC susceptible stainless steel 304L also showed that the detection of corrosion processes are possible with EN method, but the main difficulty concerning detection of SCC by EN signals was distinguishing between different corrosion processes, especially pitting processes and crack propagation processes. However, the use of additional techniques, as acoustic emission and elongation measurement, was found to be useful for distinguishing of those two processes.

First Regional Symposium on Electrochemistry of South-East Europe, Rovinj, Croatia, May 4-8, 2008.

O-2-40

# ELECTROCHEMICAL METHOD FOR THE DETERMINATION OF MAXIMUM RATE OF PIT PROPAGATION IN HIGH – ALLOYED STAINLESS STEELS AND CORROSION RESISTANT ALLOYS IN THE ENVIRONMENT MODELLING WASTE WATER TREATMENT OF FLUE GAS DESULPHURIZATION PLANTS

**B. Eremias, V. Janik, V. Cihal, E. Kalabisová**

*SVUOM Ltd., U Měšťanského pivovaru 934/4, 170 00 Prague, Czech Republic*
*eremias@svuom.cz*

Results are presented for potentiostatic current versus time transients during pitting attack in surface layer of two different high alloyed materials in 6,22 $CaCl_2$ solution at 115°C. In dependence on the chemical composition of studied materials the values of polarization potential $E_{app}$ for the materials concerned were such as to guarantee that the condition of nucleation of pits is satisfied. Electrochemical method in combination with post-exposure metallographic examination of the specimen surfaces is proposed for calculation of maximum rate of pit propagation for two different materials tested at different potentials in 6,22 $CaCl_2$ solution at 115°C.

First Regional Symposium on Electrochemistry of South-East Europe, Rovinj, Croatia, May 4-8, 2008.

O-2-41

# ELECTROCHEMICAL METHODS TO STUDY THE TRIBOCORROSION PROCESSES

**L. Benea**

*Dunărea de Jos University of Galati, Competences Center Interfaces –Tribocorrosion and Electrochemical Systems (CC-ITES), 47 Domneasca St., 800008 Galati, Romania*
*E-mail: Lidia.Benea@ugal.ro*

Tribocorrosion is defined as the chemical-electrochemical-mechanical process leading to a degradation of materials in sliding, rolling or erosion contacts immersed in a corrosive environment. That degradation results from the combined action of corrosion and wear. The mechanism of tribocorrosion is not yet fully understood due to the complexity of the chemical, electrochemical, physical, and mechanical processes involved. Examples of the occurrence of tribocorrosion in service are the accelerated corrosion of steel conveyors exposed to ambient air of high relative humidity, the fall out of electrical connectors in the automotive industry, the degradation of hip prosthesis and dental fillers, the erosion wear of turbine blades, etc. The combined corrosion-wear degradation of materials in sliding contacts immersed in electrically conductive solutions is investigated in-situ by electrochemical methods. Such techniques are the open circuit potential measurements, $E_{OC}$, the potentiodynamic polarization measurements, PD, and the electrochemical impedance spectroscopy. Capabilities and present limitations of these techniques are discussed based on a tribocorrosion study of a cobalt chromium alloy hard coating (Stellite6) immersed in water-based electrolytes, namely aerated 0.5 M sulphuric acid, or cooling water reactor (12 ppm Li as LiOH+1000 ppm Boric Acid) and sliding against a corundum counterbody. Uni-directional pin-on-disk contact geometry has been used in this investigation. Pin-on-disk materials were immersed in the electrolyte and placed in an electrochemical cell containing a counter electrode and a reference electrode. The disks were made of cobalt chromium alloy (Stellite6). Cobalt - Chromium alloy was selected for their good corrosion resistance that results from the formation of a nanometer thick protective oxide layer (passive film) at its surface in contact with air and or with many oxidizing electrolytes in open circuit potential conditions.

All sliding tests were carried out at a constant rotation speed between 30 and 120 rpm. Applying a load on the rotating disk facing downwards, against the fixed corundum ball generated friction. Such uni-directional sliding conditions lead to a steady electrochemical condition all over the wear track area on the disk material. That steady state is however quite complex since between the successive passes of the pin or ball, each point on the wear track reacts with the surrounding liquid. Notwithstanding that time-related evolution of the material in the wear track, the achievement of a steady state is revealed by the fact that, if a constant potential value is applied to the metal under friction in the potential range where passivation or dissolution occurs, a steady-state current is obtained. Such a condition is required for the implementation of electrochemical techniques (polarization curves, impedance measurements, etc.).

**The variation of the open circuit potential** with contact frequency is linked to the time interval between two successive contact events during which material in the wear track may repassivate. At higher contact frequency, the amount of active material in the wear track area thus increases. This results in a cathodic shift of the open circuit potential due to an increased ratio of active-to-passive area. Variations of the open circuit potential of materials subjected to sliding conditions can thus be correlated with variations in the surface conditions of the material under investigation.

**Potentiodynamic polarization measurements** can be used to derive the dependence of anodic or cathodic current, I, on the electrode potential, V, measured *vs.* a reference electrode. This method is useful in determining the active/passive behaviour of materials at different potentials. Such potentiodynamic polarization curves obtained at increasing potential dV/dt (direct scan) on cobalt chromium alloy (Stellite6) immersed in 0.5 M sulphuric acid is shown in Fig. 1. Two cases are shown, namely one (1) without any external loading and (2) in contact with a sliding corundum ball loaded at 15 N. Both curves were recorded after the open circuit potential of the alloy has reached the passive value.

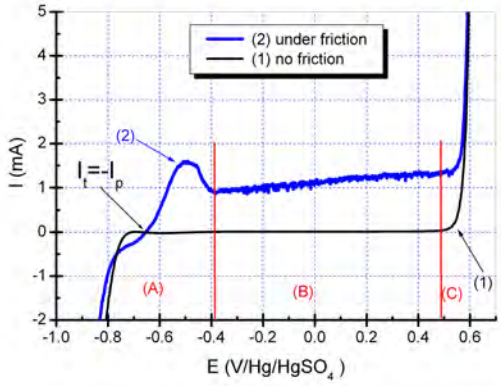


*Fig. 1. Potentiodynamic polarization curves of Stellite6 in H2SO4 0.5M recorded by direct potential scan, from −1.0 to +0.6 V/SSE, at 0.1 V/min. Curve (1): no friction applied. Curve (2): continuous friction (10 N; 120 rpm).*

If the stellite surface of the sample is not subjected to rubbing (curve 1), hydrogen evolution and oxygen reduction are the only reactions detected in the potential domain A. In domain B, the alloy was passivated, and the current remained very small (<10μA). The zero-current potential lay between −0.3 and −0.5 V/SSE. In domain C (potential >0.4V/SSE), the anodic current increases with the applied potential, revealing the dissolution of the alloy, induced by oxidation of the $Cr^{3+}$ cations of the passive film, giving soluble $Cr^{6+}$. When friction is applied (curve 2), the shape of the polarization curve changes: hydrogen evolution on Stellite6 is not modified in domain A, but an anodic current of about 0.5–1.0mA appears in the potential range from [−0.75; +0.5] V/SSE, indicating dissolution of the alloy. A first approach for interpreting the polarisation curve under friction can be developed from the following considerations, based on a concept of "**active wear track**":

The measured current, I can be considered as the sumof two partial currents $I_t$ and $I_p$:

$$(I = I_t + I_p)$$

Where: $I_t$ is the current originated from the wear track areas where thepassive film is destroyed and metal is active, and $I_p$ the current linked to the surface not subjected to friction and that remains in passive state.

Some novel insights into the tribocorrosion mechanism of active and passive materials are discussed. These in-situ electrochemical data provide insights into a possible synergism between corrosion and wear processes in sliding contacts. This paper concludes on the benefit of using different electrochemical analyzing techniques when investigating the behaviour of materials under corrosion-wear test conditions.

First Regional Symposium on Electrochemistry of South-East Europe, Rovinj, Croatia, May 4-8, 2008.

O-2-42

# THE POTENTIOMETRIC PERFORMANCE OF TERBIUM (III) SELECTIVE MEMBRANE ELECTRODE BASED ON NEUTRAL IONOPHORE

**V.K. Gupta*, A.K. Singh, B. Gupta**

*Department of Chemistry, Indian Institute of Technology-Roorkee, Roorkee- 247667, India. *E-mail: vinodfcy@iitr.ernet.in*

A new highly selective terbium (III) electrode was prepared with a polymeric film doped with using S-2-Benzothiazolyl-2-amino-α-(methoxyimino)-4-thiazolethiol acetate as an electroactive material, benzyl acetate (BA) as a plasticizer and potassium tetrakis (4-chlorophenyl) borate (KTpClPB) as an anionic site in the percentage ratio of 3.17:1.58: 63.4:31.7 (Ionophore: KTpClPB: BA: PVC w/w). The electrode exhibited linear response with a near Nernstian slope of 19.5 mV/decade within the concentration range of $1.5 \times 10^{-7}$ -$1.0 \times 10^{-2}$ M terbium ions, with a working pH range from 2.0 - 8.0, and a fast response time of 10 s and presented satisfactory reproducibility. The limit of detection was $9.3 \times 10^{-8}$ M. The results show that this electrode can be used in ethanol media until 30% (v/v) concentration without interference. It can be used for 3 months without any considerable divergence in the potentials. Selectivity coefficients for terbium (III) with respect to many cations were investigated. The electrode is highly selective for terbium (III) ions over a large number of monovalent, bivalent and trivalent cations. This shows the valuable property of the proposed electrode. The stability constant (*β*IL*n)* of ionophore towards $Tb^{3+}$ ions was determined with sandwich membrane method. It was successfully used as an indicator electrode in potentiometric determination of terbium (III) ions with EDTA and in direct determination in tap water and binary mixtures with quantitative results. The utility of the proposed electrode was also determined in the presence of ionic and non-ionic surfactants and determination of fluoride ions in four pharmaceutical (mouthwash) preparations.

*Keywords:* Terbium, neutral ionophore, potentiometry and Ion- selective electrodes.

First Regional Symposium on Electrochemistry of South-East Europe, Rovinj, Croatia, May 4-8, 2008.

O-2-43

# ELECTROCHEMICAL CHARACTERIZATION OF IRON(III) COMPLEXES WITH CITRIC, MALIC AND SUCCINIC ACID

**P. Cmuk, M. Mlakar**

*Ruđer Bošković Institute, Zagreb, Croatia, E-mail: pcmuk@irb.hr*

Dissolved iron(III) in form of organic complex is very important for a large variety of biological and chemical processes in natural waters [Martin, J. H. and Fitzwater, S. E., 1988; Timmermans, K. R., et al., 1998], especially for phytoplankton growth. According to numerous researches, iron is an element that regulates ecosystem structure and the rate of primary production in large areas of oceans. Since naturally present in seawater [Puskaric, S. and Mortain-Bertrand, A., 2003], citric, malic and succinic acids are possible candidates for solubilization of iron(III). Binding of dissolved iron(III) during phytoplankton bloom shows enhancement by the factor 3 compared to non-productive seawater [Hiemstra et al., 2006].

Electrochemical characterization of iron(III) complexes with citric, malic and succinic acid in aqueous solution (0.55 mol $dm^{-3}$ NaCl) using square wave and cyclic voltammetry, was preformed. Working electrode was static mercury drop electrode (SMDE) and Ag/AgCl(NaCl, sat.) a reference electrode. Iron(III) concentration was varied from $5x10^{-6}$ to $4x10^{-5}$ mol $dm^{-3}$, and concentration of these organic acids from $2x10^{-2}$ to 0.15 mol $dm^{-3}$. A square-wave voltamograms of these three iron(III)-complexes are shown in Figure 1 (curves 1-3).

By pH titration of these iron(III)-complexes, their reduction peak potentials shifted towards negative values in investigated pH range: from pH = 4.9 to 7.0 from -90mV to -270 mV vs. Ag/AgCl for succinate, from pH = 4.9 to 6.3 from -30mV to -190 mV for malate and from pH = 4.0 to 7.3 from -30 mV to -290 mV for citrate ligand). Reduction peak current also depended on pH and maximum reduction current for iron(III)-succinate was at pH =6.0, -malate at pH =5.5, and -citrate at pH =6.2 were recorded.

The formation/dissociation kinetic rates of investigated iron(III)-organic acid complexes with various ligand concentrations was examined as well. Results showed that iron(III)-organic complexes stabilities decrease in order Fe(III)- citrate, -malate, -succinate due to formation of insoluble iron(III)-hydroxo complexes as cited in numerous publications [Liu, X. and Millero, F.,1999; Byrne, R. H. and Kester, D.R. 1976]. Stability of iron(III)-complexes varied with ligand concentrations, as well.

These preliminary results showed that iron(III) in 0.55 mol $dm^{-3}$ NaCl aqueous solutions is complexed with all examined organic acids, and since algae are capable of assimilating organic acids [Puskaric, S. and Mortain-Bertrand, A., 2003], one can assume that these dissolved iron(III) organic complexes are possible iron supply for phytoplankton during its grow in seawater.

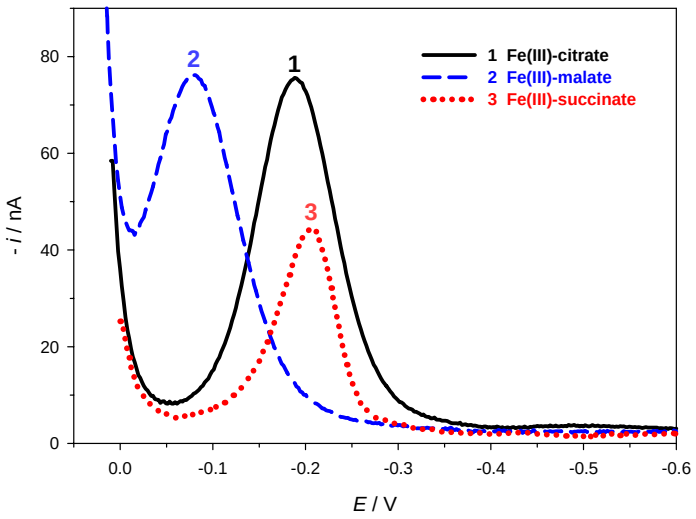


*Figure 1. SW voltamograms of iron(III) complexes (ligand: citric, malic and succinic acid) in 0.55 mol dm$^{-3}$ NaCl. Total iron(III) concentration in each solution was 4x10$^{-5}$ mol dm$^{-3}$ and ligands 0.1 mol dm$^{-3}$. Curve 1 represents reduction of iron(III)-citrate at pH = 6.25; curve 2 iron(III)-malate at pH = 5.53 and curve 3 iron(III)-succinate complex at pH = 6.00. SW parameters: frequency, f = 50 Hz; amplitude, a = 25 mV; potential step increment, $E_{inc}$ = 2 mV; equlibration time, t = 5s.*

## References:

1. Martin, J. H. and Fitzwater, S. E., 1988, Iron deficiency limits phytoplankton growth in the north-east Pacific subarctic, *Nature*, **331**, 341-343.
2. Timmermans, K. R., Gledhill, M., Nolting, R. F., Veldhuis, M. J. W., de Baar, H. J. W. and van den Berg, C. M. G., 1998, Responses of marine phytoplankton in iron enrichment experiments in the northern North Sea and northeast Atlantic, *Ocean. Mar. Chem.*, **61**, 229-242.
3. Puskaric, S. and Mortain-Bertrand, A., 2003, Physiology of diatom Skeletonema costatum (Grev.) Cleve photosynthetic extracellular release: evidence for a novel coupling between bacteria and phytoplankton, *Journal of Plankton Research*, **25**, 1227-1235.
4. Hiemstra, T. and van Riemsdijk, W. H., 2006, Biogeochemical speciation of Fe in ocean water, *Mar.Chem.* **102**, 181-197.
5. Liu, X. and Millero, F., 1999, The solubility of iron hydroxide in sodium chloride solution, *Geochim.Cosmochim Acta*, **63**, 3487-3497.
6. Byrne, R. H. and Kester, D. R., 1976, Solubilty of hydrous ferric oxide and iron speciation in seawater, *Mar. Chemistry*, **4**, 255-274.

First Regional Symposium on Electrochemistry of South-East Europe, Rovinj, Croatia, May 4-8, 2008.

O-2-44

# ELECTROCHEMICAL DETERMINATION OF METAL SULFIDE SPECIES: DISCRIMINATION BETWEEN COLLOIDAL AND "TRULY DISSOLVED" PHASES

**E. Bura-Nakić[1], I. Ciglenečki[1], G.R.. Helz[2], G. Inzelt[3]**

[1]*Center for Marine and Environmental Research, Ruđer Bošković Institute, Bijenička 54, 10 000 Zagreb, Croatia, ebnakic@irb.hr*
[2]*Department of Chemistry and Biochemistry and Department of Geology, University of Maryland, College Park MD 20742, USA*
[3]*Department of Physical Chemistry, Eötvös Loránd University, P.O.Box 32, 1518 Budapest 112, Hungary*

In this work, the electrochemical behaviour of different metal-sulfide particles and nanoparticles (CuS, HgS, PbS, FeS, MnS and ZnS) at the HMDE (hanging mercury drop electrode) and PIGE (paraffin-impregnated graphite electrode) in 0.55 M NaCl + 0.03 M $NaHCO_3$ electrolyte, pH = 8.5. was studied. The aim was to investigate the possibility of using voltammetry in the detection of metal-sulfide nanoparticles in natural waters. The proposed electrochemical approach was applied to the detection of metal sulfide particles in natural samples.

The results of this work surprisingly demonstrate that cathodic curves obtained in suspensions of different metal-sulfide species at the HMDE were characterized by well pronounced reduction peaks situated between -0.9 and -1.8 V (vs. Ag/AgCl electrode) (1,2). Our results also demonstrate that positions and charges of observed peaks will depend on experimental conditions, i.e. ageing of the particles, deposition potential, accumulation time as well as mineral phases formed in the solution (Fig. 1A) (1,3). In some metal-sulfide suspensions (FeS, HgS) more than one reduction wave can be observed (situated at -1.1 and -1.65 V vs. Ag/AgCl, (Fig 1B); these can be assigned to the reduction of different metal-sulfide phases or to some more complex voltammetric processes. Similar reduction peaks to those observed in the model solutions, were observed in natural samples from the anoxic, sulfidic environment (crater Pavin Lake, France) which can be assigned to the reduction of FeS dissolved and/or colloidal species (Fig. 1B).

Experiments done with abrasively stripping voltammetry showed that anodic stripping peaks recorded in abrasively transferred solid state phases of synthetic zinc, ferrous, manganese and copper sulfides at the PIGE after a prior electrogeneration step are essentially almost identical for all investigated phases (4). After a preelectrolysis at potentials ranging from -1.0 to -1.5 V (vs. SCE) a well-defined anodic stripping peak corresponding to the oxidation of metal deposits generated at deposition potentials is obtained around -0.74 V (vs. SCE). Consistent with our work on CuS, FeS, PbS and HgS nanoparticles and powders at the Hg electrode (1-3), observed peaks can be assigned to the oxidation of metal deposits (Cu, Fe, Zn, Mn) formed during the reductive accumulation which with

the presence of traces of sulfide in the diffusion layer form metal sulfide species retained to the electrode surface according to the following reaction:

a) reduction: $MS + 2e^- + H^+ \rightarrow M^o + HS^-$

b) oxidation (stripping scan): $M^o(PIGE) + HS^- \rightarrow MS\downarrow + H^+ + 2e^-$

Preliminary results obtained by the electrochemical quartz crystal microbalance (EQCM) technique, which was performed to follow the mass changes during the electrochemical transformations of different metal sulfide phases in electrolyte solutions, will be presented and discussed.

The key finding of this work is that analytes: FeS, $Cu_2S$, CuS, PbS, HgS, CdS, $Ag_2S$ nanoparticles, metal sulfide powders and sulfur powder produce similar reduction peaks. Therefore, here, we propose an experimental procedure that can clarify the origin of voltammetric peak around -1.1 V in anoxic natural waters.

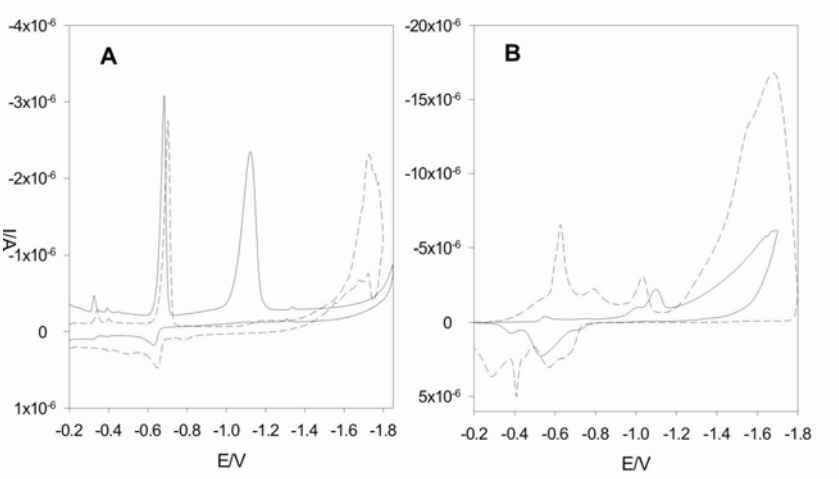


*Fig. 1(A) metacinnabar (solid line) and cinnabar (dash line) HgS powder suspensions ($t_d$=120s, $E_d$=-0.2 V) and (B) FeS suspension prepared by mixing $4\times10^{-5}$ $Fe^{2+}$ and $2\times10^{-5}$ $HS^-$ (solid line, $t_d$=30 s, $E_d$=-0.2 V) and Pavin Lake sample at 68 m depth (solid line, $t_d$=120 s, $E_d$=-0.2 V) at HMDE.*

**References:**

1. Bura-Nakić, E., Krznarić, D., Jurašin, D., Helz, G.R., Ciglenečki, I., 2007. Voltammetric characterization of metal sulfide particles and nanoparticles in model solutions and natural waters. *Anal. Chim. Acta* **1**, 45-51.
2. Ciglenečki, I., Krznarić, D., Helz, G.R., 2005. Voltammetry of copper sulfide particles and nanoparticles: Investigation of the cluster hypothesis. *Environmental Science & Technology* **39(19)**, 7492-7498.
3. Krznarić, D., Helz, G.R., Ciglenečki I., 2006. Prospect of determining copper sulfide nanoparticles by voltammetry: A potential artifact in supersaturated solutions. *Journal of Electroanalytical Chemistry* **590**, 207-214.
4. Ciglenečki, I., Bura-Nakić, E., Inzelt, G., 2007. Voltammetry as an alternative tool for trace metal detection in peloid marine sediments. *Electroanalysis* **19(13)**, 1437-1445.

First Regional Symposium on Electrochemistry of South-East Europe, Rovinj, Croatia, May 4-8, 2008.

O-2-45

# SULFUR SPECIATION IN TWO CONTRASTING ANOXIC ENVIRONMENTS

**E. Bura-Nakić[1], I. Ciglenečki[1], E. Viollier[2], D. Jèzèquel[2], G. R. Helz[3]**

*[1]Center for Marine and Environmental Research, Ruđer Bošković Institute, Bijenička 54, 10 000 Zagreb, Croata, ebnakic@irb.hr*
*[2]Laboratoire de Gèochimie des Eaux, Universitè Paris 7 – Denis Diderot et I.P.G. Paris, URA CNRS 1762, Tour 53/54, 2, place Jussieu 75251 Paris cedex 05, France*
*[3]Department of Chemistry and Biochemistry and Department of Geology, University of Maryland, College Park MD 20742, USA*

Using different electrochemical methods it is possible to measure a variety of soluble sulfur compounds (1). In this work we used a HMDE electrode to measure different dissolved and particulate sulfur species, including $\sum S^{2-}$, $\sum S^0$ and metal sulfide species in two contrasting anoxic environments: seawater lake, Rogoznica Lake (Croatia) and crater lake, Pavin Lake (France). In the Pavin Lake samples, sulfide concentrations were determined in parallel by using a second analytical technique: spectrophotometric methylene-blue and results were compared to ones obtained by electrochemical measurements. Obtained electrochemical measurements of $\sum S^{2-}$ and $\sum S^0$ were used for mathematical calculations of sulfur speciation ($S_8$, polysulfides) in the water column of both lakes. Calculations were made on the basis of voltammetric measurements for $\sum S^{2-}$ and $\sum S^0$ and by using equilibrium constants for polysulfide disproportionation [$(n-1)/8S_8(s) + HS = S_n^{2-} + H^+$] reported by Giggenbach and Kamyshny (2-3).

The anoxic layer in Rogoznica Lake (usually situated from 10 to the 15 m depth) is characterized by relatively high free $S^{2-}$ concentrations (up to the $10^{-2}$ M) which completely binds and precipitates almost completely metals from the water phase (4). Our calculations showed that during the stratification period the anoxic part of the Rogoznica Lake water column is saturated with respect to the rhombic and/or colloidal form of $S_8$ and at the same time $S_8$ concentrations in the oxic part are low (up to the $4.12 \times 10^{-9}$ M, Fig. 1A). Major polysulfide species concentrations ($S_5^{2-}$, $S_4^{2-}$, $HS_4^-$) in anoxic water column are relatively high (up to the $2 \times 10^{-4}$) implying that polysulfides are contributing the most to the $\sum S^0$ (up to the $1.40 \times 10^{-4}$ M) found and measured by voltammetric methods. Electrochemical sulfur speciation in the anoxic part of the Pavin Lake water column (usually situated from 62 to the 92 m depth) is completely different than in Rogoznica Lake. $\sum S^0$ concentrations determined by voltammetry in Pavin Lake were lower (up to the $3.40 \times 10^{-6}$ M). $\sum S^{2-}$ concentrations determined with methylene-blue technique were in the range from $6 \times 10^{-7}$ to $1.67 \times 10^{-5}$ M and are substantially higher than $\sum S^{2-}$ concentrations determined by voltammetric measurements which ranged from $1 \times 10^{-7}$ to $3.7 \times 10^{-6}$ M. The difference in the RSS concentrations between the two methods can be assigned to the presence of FeS dissolved and/or colloidal species, the presence of which is confirmed electrochemicaly by the appearance of voltammetric peaks

typical for FeS species, situated at -1.1 V (Fig. 1B) in the anoxic part of the Pavin Lake samples (5). Consequently, in the anoxic deep layer of Pavin Lake free $S^{2-}$ was relatively low (up to the 3.7 x $10^{-6}$ M); and about 80 % of total sulfide detected (<0.2 μm) was in the $FeS_{aq}$ and/or $FeS_{am}$ colloidal form. Obtained results are supported as well by high concentrations (>1 x $10^{-3}$ M) of dissolved Fe (<0.2 μm) determined in the anoxic water column of Pavin Lake, which indicate that Fe is dominant metal involved in sulfur redox cycling and precipitation (6).

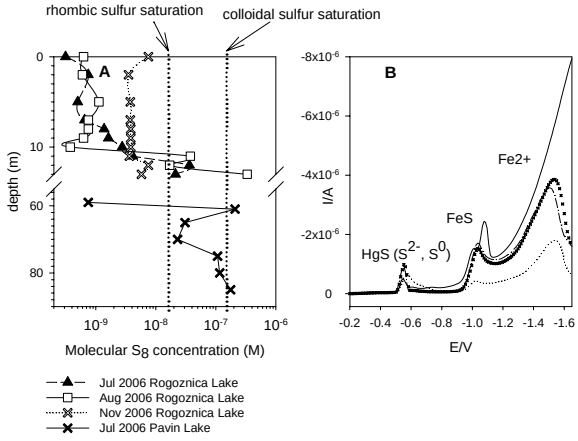


*Fig. 1(A) Vertical profile of molecular $S_8$ concentration in the water column of Rogoznica and Pavin Lake; 1(B) LSV curves ($E_d$=-0.2 V, $t_d$=30 s) for Pavin Lake samples at 62.5 m (dotted line), 80 m (solid line), 87 m (x symbols) and 91 m depth (dash-dot line).*

**References:**

1. Ciglenečki, I., Ćosović, B., 1997. Electrochemical determination of thiosulfate in seawater in the presence of elemental sulfur and sulfude. *Electroanalysis* **9(10)**, 1-7.
2. Kamyshny, A., Goifman, A., Gun, J., Rizkov, D., Lev, O., 2004. Equilibrium distribution of polysulfide ions in aqueous solutions at $25^0$C: A new approach for the study of polysulfide's equilibria. *Environ. Sci. Technol.* **38**, 6633-6644.
3. Giggenbach, W., 1972. Optical spectra and equilibrium distribution of polysulfide ions in aqueous solutions at $20^0$C. *Inorg. Chem.* **11**, 1201-1207.
4. Ciglenečki, I., Carić, M., Kršinić, F., Viličić, D., Ćosović., B., 2005. The extinction by sulfide–turnover and recovery of an naturally eutrophic, meromictic seawater lake. *J. Mar. Systems* **56**, 29-44.
5. Bura-Nakić, E., Krznarić, D., Jurašin, D., Helz, G.R., Ciglenečki, I., 2007. Voltammetric characterization of metal sulfide particles and nanoparticles in model solutions and natural waters. *Anal. Chim. Acta* **1**, 45-51.
6. Viollier, E., Michard, G., Jézéquel D., Pèpe, M., Sarazin, G., 1997. Geochemical study of a crater lake: Lake Pavin, Puy de Dome, France. Constraints afforded by the particulate matter distribution in the element cycling within the lake. *Chem. Geology* **142**, 225-241.

First Regional Symposium on Electrochemistry of South-East Europe, Rovinj, Croatia, May 4-8, 2008.

O-2-46

# HOST-GUEST INTERACTION OF METHYL VIOLOGEN WITH MODIFIED POLYPYRROLE FILMS

**S.M. McDermott, C.B. Breslin, D.A. Rooney**

*Department of Chemistry, National University of Ireland Maynooth, Maynooth, Co. Kildare, Ireland, sinead_maynooth@hotmail.com*

There is an increasing demand for environmental remediation technologies due to the level of persistent pollutants in the environment. The range of toxic substances within soil and water, resistant to chemical degradation include herbicides, pesticides and nitrates. In this study, the electrochemistry of paraquat is investigated in order to establish the properties of this harmful molecule.

Methyl viologen, or Paraquat, as it is more commonly known, is a toxic herbicide composed of a bipyridilium ion with a methyl group attached to each ring. Paraquat is used mainly in weed control. Its appeal is due to its high solubility in water and affinity for soil, but also its ability to resist microbial and photolytic degradation [1]. However due to its high toxicity, concentration limits have been set by the Environmental Protection Agency (EPA) and the European Community [2]. Electrochemically, it exhibits two redox states within a potential window from -1.4 → -0.1 V (Fig. 1).

In this paper, results are presented on the sensing performance of polypyrrole films, doped with sulfated β-cyclodextrin for paraquat. These electropolymerised films are formed by applying an oxidative potential of 0.65 V (Fig. 2). Cyclodextrins are cyclic oligosaccharides composed of glycopyranoside units. They have a hydrophilic exterior and a hydrophobic cavity, which can be used to complex persistent pollutants like paraquat. Although the interaction using sulfated β-cyclodextrin as a dopant is predominantly electrostatic, there is also the possibility for the formation of an inclusion complex. Using cyclic voltammetry, a decrease in peak current with respect to increasing sulfated β-cyclodextrin concentration, showed that at a three fold excess of sulfated β-cyclodextrin all paraquat in solution had been complexed. In order to confirm inclusion within the polymer matrix of polymerised pyrrole and sulfated β-cyclodextrin, differential scanning calorimetry (DSC) was carried out. This method of trapping the pesticide within the cavity of the cyclodextrin is effective in the process of environmental remediation and also as a means of extracting the pollutant.

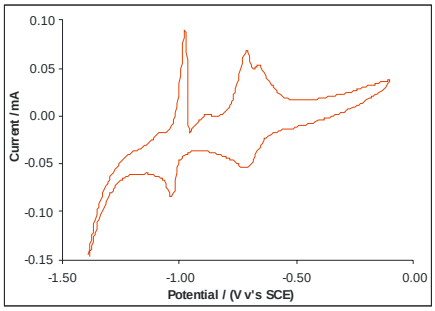


*Fig. 1: Cyclic Voltammagram of 2.5 mM Paraquat showing two oxidative states (positive currents) and two reductive states (negative currents)*

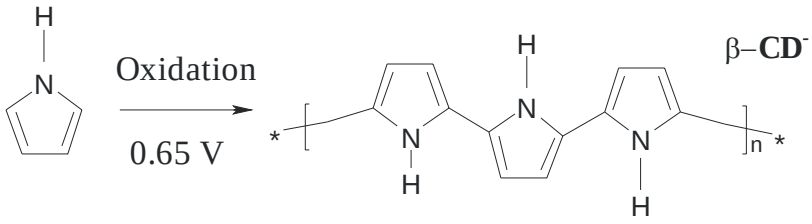


*Fig. 2: Electropolymerisation of pyrrole to polypyrrole by applying an oxidative potential of 0.65 V*

**References**

1. Y.Q. Yang *et al.*, *Int. J. Biological Macromolecules*, **41**, 243 (2007).
2. U.M.F. de Oliveira *et al.*, *J. Braz. Chem. Soc.*, **15**, 735 (2004).

First Regional Symposium on Electrochemistry of South-East Europe, Rovinj, Croatia, May 4-8, 2008.

O-2-47

# SPECTROELECTROCHEMICAL STUDY OF THE P-DOPING OF POLY(2-(3-THIENYL)ETHYL ACETATE) AND ITS DERIVATIVES

**A. Kellenberger[1], N. Vaszilcsin[1], L. Dunsch[2], E. Jähne[3], H.J. Adler[3],**

*[1]University „Politehnica" of Timisoara, Faculty of Industrial Chemistry and Environmental Engineering, Piata Victoriei 2, RO-300006 Timisoara, Romania*
*[2]Leibniz-Institute of Solid State and Materials Research, Department of Electrochemistry and Conducting Polymers, Helmholtzstrasse 20, D-01069 Dresden, Germany*
*[3]Technical University Dresden, Institute of Macromolecular Chemistry and Textile Chemistry, Mommsenstrasse 4, D-01069 Dresden, Germany*
*Corresponding author: Andrea.Kellenberger@chim.upt.ro*

The aim of this study was to investigate the doping behaviour of some chemically synthesized polyalkylthiophenes functionalized with acetoxy and hydroxyl groups attached to the alkyl side chain. Three different polythiophenes were analyzed using cyclic voltammetry and in situ FTIR spectroelectrochemistry.The struc6tures of poly [2_(3-thienyl)ethyl acetate] (PTEtAc), partially hydrolyzed PTEtAc (PTEtAcOH) and poly[2-(3-thienyl)ethanol] (PTEtOH) are given in Figure 1.

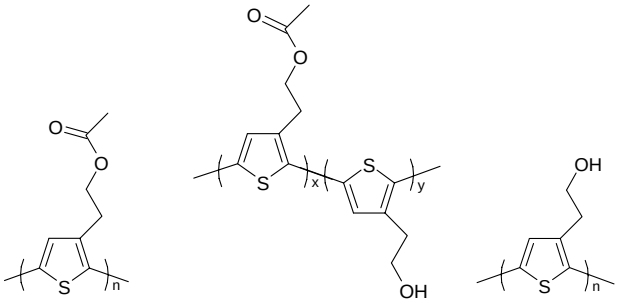


(1) (2) (3)

*Figure 1. Chemical structure of the polymers: (1)PTEtAc; (2) PTEtAcOH; (3) PTEtOH*

The cyclic voltammograms indicate a similar behaviour for PTEtAc and PTEtAcOH, characterized by a reversible charging/discharging process. In contrast, PTEtOH loses its redox activity during consecutive potential scans. This was explained in terms of intermolecular hydrogen bonds. The flexible structure of the PTEtAc allows to accommodate/release a larger amount of dopants, whereas in PTEtOH the access/outlet of the dopant is hindered because the chains are fixed by hydrogen bonds.

The in situ ATR-FTIR spectra recorded for different electrode potentials during one cyclovoltammetric scan are given in Figure 2 for PTEtAc.

In all cases the shape of the FTIR spectra is characterized by the development of two distinct vibrational patterns: the IRAV region at 1600 – 650 $cm^{-1}$ and the region at higher wavenumbers, corresponding to the electronic absorption of free charge carriers. This behavior has been reported for electrochemically and photo-induced doping of different

polythiophenes [1-5] and was explained in terms of a local breaking of the symmetry around the injected charge carrier. The IRAV bands are related to the charge transport along the polymer chain and do not depend on the type of doping and on the nature of the dopant anion.

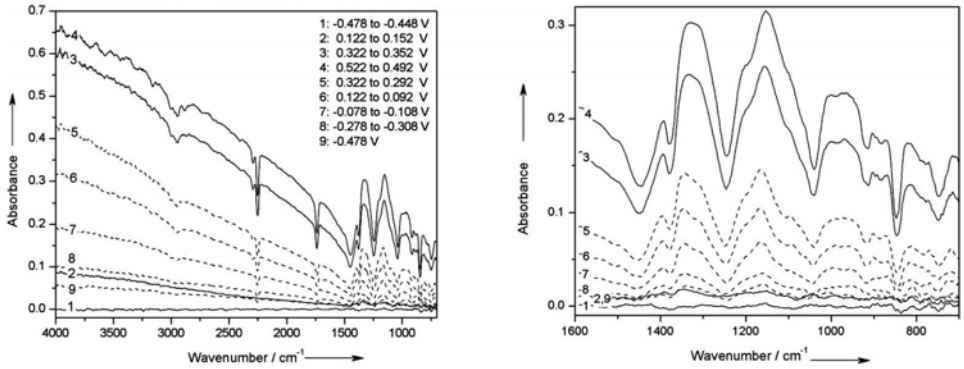


*Figure 2. In situ ATR-FTIR difference spectra of PTEtAc film in $TBAPF_6$ (0.1M) – acetonitrile solution during p-doping; solid lines (——) represent the forward scan and dashed lines (- - - -) the backward scan; (a) full spectral region, (b) enlargement in the region 1600-650 $cm^{-1}$.*

The first changes in the IR spectra of PTEtAc and PTEtAcOH appear at a potential value equal to the onset of the oxidation process observed in the cyclic voltammograms. During the oxidation of both polymer films the bleaching of the bands corresponding to the neutral state can be seen, accompanied by the appearance of some new IR bands with intensities increasing in dependence of the applied electrode potential. The absorption pattern observed for PTEtAc and PTEtAcOH is characterized by three main absorptions centred at 1320, 1150 and 975 $cm^{-1}$ with bandwidth larger than 100 $cm^{-1}$ (the so-called T-modes) which very similar to those observed for the doping of polythiophene [6,7] and poly(3-methylthiophene [1-4]. The appearance of doping induced modes similar to those for other substituted polythiophenes indicates the presence of delocalized charge carriers.

The lower intensity of the electronic absorption of free charge carriers and that of the IRAV bands for PTEtOH indicate a lower charge density and delocalization of the charged states created upon electrochemical doping and a smaller effective conjugation length in the polymer backbone.

1. H. Neugebauer, G. Nauer, A. Neckel, G. Tourillon, F. Garnier, P. Lang, *J. Phys. Chem.*, **1984**, *88*, 652-654.
2. Y. H. Kim, S. Hotta, A. J. Heeger, *Phys. Rev. B*, **1987**, *36*, 7486-7490.
3. V. Hernandez, F. J. Ramirez, T. F. Otero, J. T. Lopez Navarrete, *J. Chem. Phys.*, **1994**, *100*, 114-129.
4. S. Hotta, M. Soga, N. Sonoda, *J. Phys. Chem.*, **1989**, *93*, 4994-4998.
5. A. Cravino, H. Neugebauer, S. Luzzati, M. Catellani, A. Petr, L. Dunsch, N. S. Sariciftci, *J. Phys. Chem. B*, **2002**, *106*, 3583-3591.
6. H. E. Schaffer, A. J. Heeger, *Solid State Commun.*, **1986**, *59*, 415-421.
7. A. J. Heeger, S. Kivelson, J. R. Schrieffer, W.-P. Su, *Rev. Mod. Phys.*, **1988**, 60, 781-850.

First Regional Symposium on Electrochemistry of South-East Europe, Rovinj, Croatia, May 4-8, 2008.

O-2-48

# THE FABRICATION OF CYCLODEXTRIN DOPED POLY-3,4-ETHYLENEDIOXYTHIOPHENE (PEDOT) MODIFIED GOLD ELECTRODES FROM AQUEOUS SOLUTIONS. THEIR APPLICATION IN THE SIMULTANEOUS ELECTROCHEMICAL DETECTION OF DOPAMINE AND ASCORBIC ACID

**J. Colleran, B. Alcock, C.B. Breslin**

*Department of Chemistry, National University of Ireland Maynooth, Co. Kildare, Ireland, John.Colleran@nuim.ie*

Poly-3,4-ethylenedioxythiophene (PEDOT) has good electrochemical stability and a small electronic bandgap, thus enabling efficient electrical conductivity. These properties make PEDOT an ideal candidate for sensor applications [1]. The majority of literature to date reports on the electropolymerisation of EDOT performed in the presence of dopant surfactant anions. Generally, a dopant-related critical micellar concentration is required [2] for EDOT to electropolymerise. Numerous authors have reported on the electropolymerisation of EDOT from organic media, but electro-polymerisation is possible from aqueous solutions using β-Cyclodextrins (β-CD) as the dopant anions [3]. The β-CD forms a host-guest complex with the EDOT monomer, generating micelles, thus promoting polymerisation.

The simultaneous electrochemical detection of the biologically important molecules dopamine (DA) and ascorbic acid (AA) can be difficult, as both oxidise at similar potentials. PEDOT and PEDOT blends have been used to modify electrodes for the simultaneous detection of DA and AA due to the cationic properties of the film [4,5]. The anionic ascorbic acid AA can interact with the polymer matrix, facilitating pre-concentration of AA in the film, and promoting lower AA oxidation potentials. The cationic dopamine is attracted to the hydrophobic regions of the PEDOT film *via* hydrophobic-hydrophobic interaction. In our research, we favoured the use of anionic β-CD as the dopant for PEDOT film formation due to the high affinity β-CD exhibits towards DA inclusion in the cavity.

In this paper, we report on the simultaneous detection (Figure 1) of AA and DA using CV, DVP and RDE voltammetry. Preliminary results with the PEDOT/β-CD/Au sensor exhibit DA detection limits below 5 x $10^{-6}$ M using CV.

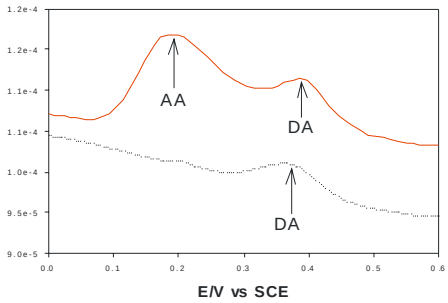


*Figure 1; Typical cyclic voltammograms showing the simultaneous detection of (solid trace, —) $5x10^{-4}$ M AA and $5x10^{6}$ M DA. The dotted trace (···) represents the voltammetric response of the sensor t o a $5x10^{6}$ M DA solution. We observe that DA peak definition and magnitude is adversely not affected by the presence of the 100 fold excess of AA.*

[1] L. Groenendaal, G. Zotti, P.H. Aubert, S.M. Waybright, J.R. Reynolds, *Adv. Mater.*, **15**, 200,3 855.

[2] R. Schweiss, J. F. Lubben,1, D. Johannsmann, W. Knoll, *Electrochimica Acta*, **50,** 2005, 2849.

[3] C. Lagrost, J. C. Lacroix, S. Aeiyach, M. Jouini, K. Chane-Ching, P. C. Lacaze, *Chem. Comm.*, 1998, 489.

[4] S. Kumar, J. Mathiyarasu, K. L. N. Phani, V. Yegnaraman, *J. Solid State Electrochem*, **10,** 2006, 905.

[5] A. Balamurugan, S.-M. Chen, *Analytica Chimica Acta*, **596,** 2007, 92.

First Regional Symposium on Electrochemistry of South-East Europe, Rovinj, Croatia, May 4-8, 2008.

O-2-49

# POLY(o-ANISIDINE)/$SnO_2$ NANOCOMPOSITE: PREPARATION, CHARACTERIZATION AND HUMIDITY SENSING CHARACTERISTICS

**D. Patil, P. Patil**

*Department of Physics, North Maharashtra University, Jalgaon 425 001, India,*
*E-mail: pdew7@yahoo.co.in*

Humidity sensing characteristics such as relative humidity (RH)-resistance property, humidity hysteresis, response time and repeatability of hybrid poly(o-anisidine)/$SnO_2$ (POA/$SnO_2$) have been investigated. The POA/$SnO_2$ hybrid exhibits better humidity sensing properties than pure POA, such as fast response time (humidification : 16 s and desiccation : 39 s), hysteresis within 5% and excellent repeatability. Plausible humidity sensing mechanism of POA/$SnO_2$ hybrid is discussed.

First Regional Symposium on Electrochemistry of South-East Europe, Rovinj, Croatia, May 4-8, 2008.

O-3-50 KEYNOTE LECTURE

# LOCAL ELECTROLESS DEPOSITION OF NANOPARTICLES BY SCANNING ELECTROCHEMICAL MICROSCOPY

**Y. Yerucham, E. Malel, E. Mekahel, D. Mandler***

*Department of Inorganic and Analytical Chemistry, The Hebrew University of Jerusalem, Jerusalem 91904, Israel, E-mail: mandler@vms.huji.ac.il*

Electroless deposition (ED) of metals has enormous importance in modern plating technologies and has widely been used in the printed circuit board industry and manufacturing microelectronic devices and structures. ED and electroless displacement (DD) reactions comprise the reduction of metal ions and metal deposition by a reducing agent and not by an external current source. While in ED the reducing agent is in the solution and the surface catalyzes the process, in DD the source of electrons comes from the surface itself which is oxidized. ED offers several advantages depending on the plating metal; however, two major general benefits are its applicability to non-conducting substrates, such as glass and organic polymers, and the uniformity of the deposits, even on complex shapes.

In spite of the fact that ED is well established and widely used, there are only a limited number of successful reports on the ED of metals **locally** on surfaces. Localization of ED has been achieved by either applying lithographic means or by locally activating the surface using mostly laser irradiation or scanning probe microscopy (SPM) techniques.

The scanning electrochemical microscopy (SECM) is probably the most suitable SPM technique for the local ED of metals. We have developed different approaches for the local ED and DD by the SECM (Figure 1). The approaches are based on generating a flux of metal ions, e.g., $Ag^+$ and $AuCl_4^-$, at the tip, which is held close to a surface. At least four different systems will be presented and discussed: the ED of gold and copper, the DD of silver and the ED of silver by the potential assisted ion-transfer across two immiscible liquids.

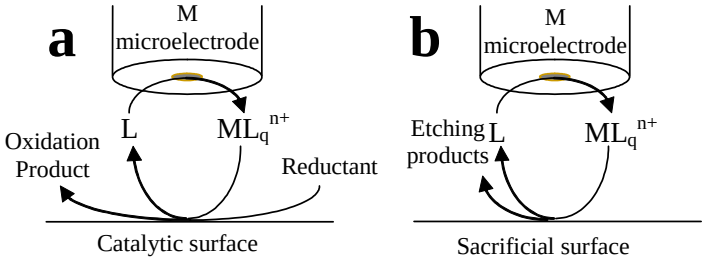


*Figure 1: Local electroless deposition (a) and electroless displacement (b) by SECM*

Local ED of gold was accomplished by the generation of gold ions in the presence of hydroquinone (Figure 2). The surface was either a Pd thin film or Pd nanoparticles. The different parameters that controlled deposition were studied and

optimized. ED of copper was achieved by the generation of copper ions in the presence of tartaric acid, and formaldehyde. This was a particularly challenging system as the dissolution of the copper microelectrode was carried out in strong basic solutions.

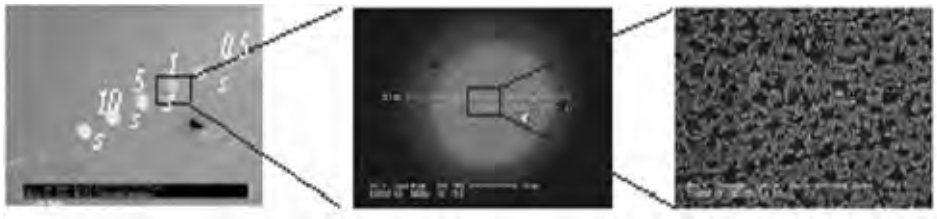

*Figure 2: Locally ED deposition of gold nanoparticles*

On the other hand, the local DD of silver was observed when silver ions electrogenerated at an Ag tip reacted with a copper surface. The structure and distribution of the nanocrystals depend on many parameters, such as the length of the pulse applied to the tip, the surface and the nature of the electrolyte. Moreover, we found that there was a significant effect on the morphology of the deposit as a result of adsorbing a self-assembled monolayer prior to deposition of the silver. The effect of three different short chain thiols was investigated: 2-mercpatopropanoic acid, 2-mercaptoethanesulfonic acid and 2-mercaptoetheneamine (Figure 3).

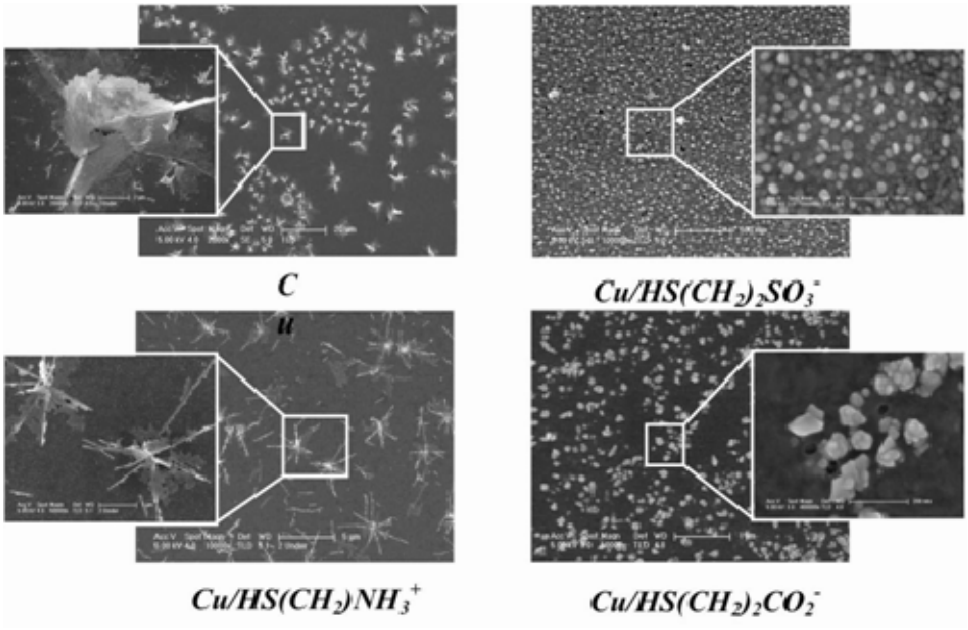


*Figure 3: SEM images showing the effect of a self-assembled monolayer on the DD of silver*

First Regional Symposium on Electrochemistry of South-East Europe, Rovinj, Croatia, May 4-8, 2008.

O-3-51

# SYNTHESIS, SURFACE MODIFICATIONS AND ELECTROCHEMICAL BEHAVIOR OF MIXED, NICKEL-ZINC FERRITE COLLOIDAL MAGNETIC NANOPARTICLES

**P. Krysinski, P. Majewski**

*Departmen. of Chemistry, University of Warsaw, 02-093 Warsaw, Pasteur 1, Poland*
*E-mail: pakrys@chem.uw.edu.pl*

The magnetic ferrite nanoparticles are recently in focus of modern science and biotechnology due to their unique properties, giving them a variety of possible applications. These include both technological[1-3], biological and medical applications, such as contrast increase of MRI and targeted drug delivery[4-9]. Our previous work on the covalent attachment of molecular adlayers to a variety of surfaces has shown that simple displacement reaction can be used on essentially any surface where hydroxyl groups are present. We have attached molecular layers covalently to silica, ITO, boron doped diamond and electrochemically generated gold oxide surfaces by reacting the surface hydroxyl groups with an acid chloride[10-12].

We report here on the covalent attachment of monomolecular adlayers to mixed nickel-zinc nanoferrite surface. Synthesized nanoparticles were subjected to surface modification by means of acid chloride chemistry leading to the formation of covalent bond between the hydroxyl groups at the nanoparticle surface and acid chloride molecules. In this paper we used adipoyl and sebacoyl chlorides to functionalize the surface of nanoferrites. This procedure can be easily tailored to allow for the formation of adlayers containing both hydrophobic and hydrophilic regions stacked at predetermined distance from the magnetic core, providing also the colloidal nanoferrites with functional carboxyl groups capable of further modifications with, e.g. drug molecules. Here, the fluorophore molecules of aminopyrene were bound via the amide bond to such modified nanoferrites and the steady-state fluorescence spectra were recorded proving the fluorophore attachment.

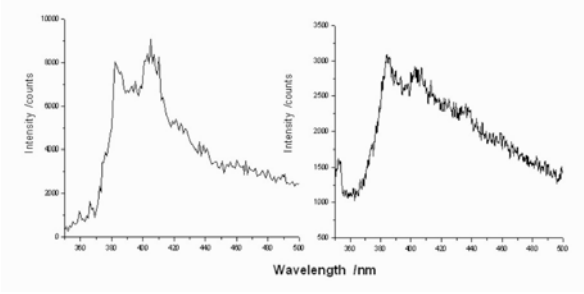


We also used the same chemistry to modify the surface with covalently bound long chain palmitoyl moieties and, for comparison, we also modified the

nanoferrite surface by simple adsorption of oleic acid. Both procedures rendered the surface highly hydrophobic. These hydrophobic, sterically stabilized colloids were subsequently spread on an aqueous surface to form Langmuir monolayers of totally different characteristics. These layers were subsequently transfered onto the gold substrates via the Langmuir-Blodgett technique and electrochemical behaviour was studied.

Colloidal ferrites are usually synthesized in a relatively simple aqueous precipitation reaction[13,14], which can be easily adapted for large-scale preparations. However, the main disadvantage of this route is relatively high polydispersity of the resultant product, unsatisfactory for a number of practical applications, particularly where high electromagnetic permeability and low energy losses are required. Therefore, in this work we propose also an efficient way of sorting nanoferrite particles by size. The colloidal suspension of nanoparticles is centrifuged at increasing rotational speed and the fraction sedimented on the bottom of the centrifuge tube is collected after each run. Quantitatively, the mean size of nanoferrites in each fraction is measured by powder X-ray diffraction (PXRD) technique.

1. Tsutaoka, T. *J. Appl. Phys.* **2003**, *93*, 2789.
2. Leslie-Pelecky, D.I.; Rieke, R.D. *Chem. Mater*. **1996**, *8*, 1770
3. Hartshorne, H.; Backhouse, C.J.; Lee, W.E. *Sens. Actuators B*, **2004**, *99*, 592.
4. Shipway, A.N.; Willner, I. *Chem. Commun*., **2001**, 2035.
5. Schneider, G.; Decher, G. *Nano Letters* **2004**, *4*, 1833
6. Jun, Y.; Huh, Y-M.; Choi, J.; Lee, J-H.; Song, H-T.; Kim, S.; Yoon, S.; Kim, K-S.; Shin, J-S.; Suh, J.S.; Cheon, J. *J. Am. Chem. Soc.* **2005**, *127*, 5732.
7. Kim, J.S.; Rieter, W.J.; Taylor, K.M.L.; An, H.; Lin, W.L.; Lin, W.B. *J. Am. Chem. Soc.* **2007**, *129*, 8962.
8. Grüttner, C.; Müller, K.; Teller, J.; Westphal, F.; Foreman A.; Ivkov, R. *J. Magnet. Magnet, Mat.* **2007**, *311*, 181.
9. Neuberger, T.; Schöpf, B.; Hofmann, H.; Hofmann, M.; von Rechenberg, B. *J. Magnet. Magnet, Mat.* **2005**, *293*, 483.
10. Kelopouris, L.; Krysiński, P.; Blanchard, G.J. *J. Phys. Chem. B*, **2003**, *107*, 4100
11. Krysinski, P.; Blanchard, G.; *Langmuir*, **2003**, *19*, 3875
12. Krysiński, P.; Show Y.; Stotter J.; Blanchard G.J. *J. Am.Chem. Soc.* **2003**, *125*, 12726.
13. Machala, L.; Zboril, R.; Gedanken, A. *J. Phys. Chem. B* **2007**, *111*, 4003.
14. Reddy, K.R.; Lee, K-P.; Iyengar, A.-G. *J. Appl. Polym. Sci.* **2007**, *104*, 4127.

First Regional Symposium on Electrochemistry of South-East Europe, Rovinj, Croatia, May 4-8, 2008.

O-3-52

# ELECTROCHEMICAL SYNTHESIS OF COPPER NANOSTRUCTURES ON POLYPYRROLE-POLYSTYRENE SULFONATE CONDUCTIVE FILMS

**E. Andreoli, C.B. Breslin, D.A. Rooney**

*Department of Chemistry, National University of Ireland, Maynooth*
*Maynooth, Co. Kildare, Ireland, Enrico.Andreoli@nuim.ie*

The ion-exchange properties of polypyrrole-polystyrene sulfonate films (PPy-PSS) have been already used for several technological applications [1-3]. In this work the same properties are exploited to electrosynthesize copper nanostructures through a novel method called Forced Capture Method (FCM).
The FCM consists of two main steps: (1) a selected reductive potential is applied to the PPy-PSS composite to perform a potential-controlled capture of copper ions from a Cu(II) solution, (2) the copper ions are then reduced to nanostructured metallic copper giving the new composite PPy-PSS-Cu.
CV, EQCM, EIS and SEM techniques have been used both to describe and model the way the FCM works and to characterize the composites.
The FCM has been developed as a new synthetic tool that could be applied to any other metal with significant catalytic properties useful for technological applications.

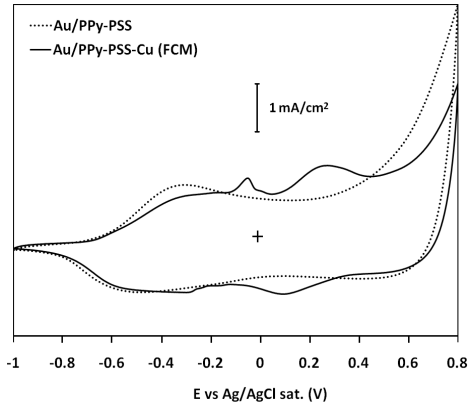


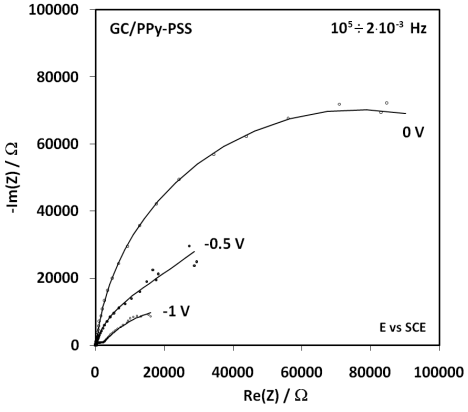


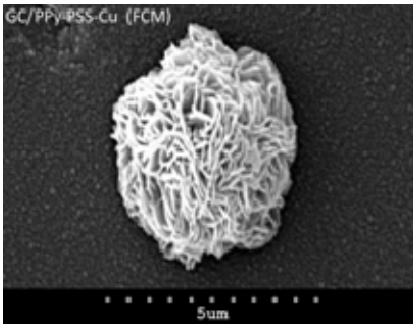

**References:**

[1] C. Weidlich, K.M. Mangold and K. Jüttner, *Electrochimica Acta*, **47**, 741(2001)
[2] J. Wang, C.O. Too and G.G. Wallace, *Journal of Power Sources*, **150**, 223(2005)
[3] M. Hepel, L. Adams and C. Rice-Belrose, *Materials Research Society Symposium* Proceedings, 451(Electrochemical Synthesis and Modification of Materials), 507(1997)

First Regional Symposium on Electrochemistry of South-East Europe, Rovinj, Croatia, May 4-8, 2008.

O-3-53

# ELECTROCHEMICAL AND STRUCTURAL STUDIES OF NANO- AND MICRO – STRUCTURED SiC-Ni COMPOSITE COATINGS

**L. Benea[1], G. Cârâc[2]**

*[1]Dunarea de Jos University of Galati, Competences Center Interfaces –Tribocorrosion and Electrochemical Systems (CC-ITES), 47 Domneasca St., 800008 Galati, Romania, E-mail: Lidia.Benea@ugal.ro*

*[2]Dunarea de Jos University of Galati, Department of Science – Chemistry, 800008 Galati, Romania*

At present the research and development of composite coatings of various types is of great interest. This is explained by their excellent combination of physical-chemical properties, such as low friction coefficient, wear resistance, corrosion resistance and chemical stability, otical properties, etc. This work is focused on: 1) Electrochemical methods (cathodic polarisation and electrochemical impedance spectroscopy diagrams performed at cathodic potential) to study the influence of dispersed nanosized and microsised dispersed phases on the mechanism of nickel reduction; 2) Surface characterisation of composite coatings obtained by SEM and TEM. The composite coatings have been obtained by electrodeposition using a nickel Watts baths and two types of dispersed phases: nanosized SiC (20 nm mean diameter) and microsized SiC (20 μm mean diameter). Influence of nano- and micro- sized SiC particles on nickel electrodeposition was observed by potentiodynamic diagrams and electrochemical impedance spectroscopy measurements performed with and without dispersed particles. The charge transfer resistance calculated from impedance diagrams. The addition of silicon carbide particles displaces the nickel reduction curve to more positive potentials. The shift in reduction potential were attributed to an increase in the active surface area due to the adsorbed particles on the cathode and to a possible increase in ionic transport by dispersed particles with their ionic layers adsorbed. It is supposed that the dispersed particles are surrounded by a thin layer of ($Ni^{2+}$) and ($H_3O^+$) ions adsorbed after the particles were introduced in the electrolyte. These positively charged particles could reach the cathode surface. The negatively charged particles will be rejected to the bulk of the solution. The EDS analysis show the presence of nanosized silicon particles in the composite layer by content of carbon and silicon founded. The SEM investigations shows that the composite coatings with nanosized dispersed particles develop in a nodular disturbed surface structure. The EDS spectra of composite coating obtained by codeposition of microsized SiC with nickel show a higher content of dispersed phase. The highest content of silicon carbide is due to bigger SiC particles (20 μm mean diameter). The structure of nickel matrix is also perturbed but seems to have a more regular grain size than that in the case of SiC nanoparticles codeposition. We suppose that the higher density of nucleation sites due to nanosized silicon carbide particles perturb the

growth of nickel matrix resulting in smaller grain size and random orientation of nanostructured composite coating.

***Acknowledgements*** *to ESF - COST (STSM D19-00391) and CNCSIS (Grant A No. 1347/2005-2006).*

**References:**

1. Benea L., Bonora P. L., Borello A., Martelli S., Wenger F., Ponthiaux., Galland J.; *Solid state ionics*, **151(1-4)**, 89-95, 2002
2. Benea L., Bonora P.L., Borello A., Martelli S.; *Materials and Corrosion*, **53**, 23-29, 2002.
3. G. Cârâc; L. Benea; C. Iticescu; T. Lampke; S. Steinhäuser; B. Wielage; *Surface Engineering*, **20(5)**, 353-359, 2004.

First Regional Symposium on Electrochemistry of South-East Europe, Rovinj, Croatia, May 4-8, 2008.

O-3-54

# THE EFFECT OF NANO $Al_2O_3$ ON THE ELECTRODEPOSITION OF Ni COMPOSITE COATINGS: AN ELECTROCHEMICAL STUDY

**G. Cârâc[a], L. Benea[a], D. Thiemig, A. Ispas[b], A. Bund[b], T. Lampke[c]**

[a]*Department of Chemistry, Faculty of Sciences, "Dunarea de Jos" University, Galați Romania*
[b]*Physical Chemistry and Electrochemistry, Dresden University of Technology, Germany*
[c]*Institute of Composite Materials and Surface Technology, Chemnity University of Technology, Germany*

Electrolytic co-deposition is a successfully used method for obtaining composite coatings. The properties of the coatings depend on the working parameters of the electrodeposition processes. Composite coatings in the nickel matrix were obtained from a Watts-type electrolyte containing nano-$Al_2O_3$ particles (13 nm primary diameter) at the different cathodic potentials. The concentration of $Al_2O_3$ particles in the plating bath was between 5 and 10 g/L. A Princeton Potentiostat/Galvanostat Model 273 coupled with a Solartron Frequency Response Analyzer was used for these experiments.

The potentiodynamic diagrams obtained showed that the current is different at lower potential values applied. Electrodeposited layers obtained were very uniform and homogeneous.

Electrochemical Impedance Spectroscopy (EIS) data were acquired using the same equipment in the frequency range from 100 kHz to 1 mHz using a sinusoidal signal with a 5 mV a.c. amplitude. The resulting impedance spectra for the nickel composite coatings were strongly influenced by the parameters chosen for electrodeposition, which induced specific morphology of the deposit. Differences between the nickel deposits with and without $Al_2O_3$ nanoparticles could be noticed. The incorporation of nano-$Al_2O_3$ into nickel matrix affected the structure of the coatings and induced a decrease of the grain size. Furthermore, the electric potential proved to influence strongly the morphology and the grain size of the deposits. The present study demonstrated the relationship between the electrolyte parameters, the concentration of the nanoparticles in the electrolyte and the quality of the deposits. Surface morphology and microstructure of Ni-$Al_2O_3$ coatings were determined by means of scanning electron microscopy, atomic force microscopy and X-ray diffraction. It was found that the phase structure of matrix cannot be varied by co-deposition of $Al_2O_3$ particles in the Ni matrix but it only influences the growth process and the preferred orientation of the crystal planes.

***ACKNOWLEDGMENTS:*** *Financial support provided by COST Action D19 (STSM D19-00392) and COST Action D33 are gratefully acknowledged.*

**References:**

1. 3. A. Bund, D. Thiemig, *Surface and Coatings Technology*, **201**,.7092-7099 (2007).
2. C. Gheorghies, G. Cârâc, I. V. Stasi , *J. of Optoelectronics and Advanced Materials*, **8(3)**, 1234-1237 (2006).
3. F. Erler; C. Jakob; H. Romanus; L. Spiess; B. Wielage; Th. Lampke and S. Steinhäuser, *Electrochimica Acta*, **48**, 3063-3070 (2003).

First Regional Symposium on Electrochemistry of South-East Europe, Rovinj, Croatia, May 4-8, 2008.

O-3-55

# ION FLUXES THROUGH ASYMMETRIC NANOSTRUCTURES WITH CHARGED SURFACES - EXPERIMENTS AND NUMERICS

**A. Bund[1], A. Ispas[1], H.S. White[2], C. Kubeil[1]**

*[1]TU Dresden, Physical Chemistry and Electrochemistry, Dresden, Germany*
*[2]University of Utah, Chemistry Department, Salt Lake City, Utah, USA*
andreas.bund@chemie.tu-dresden.de

The group of White recently described a bench top method for the fabrication of conical nanopores in glass membranes [1]. These pores have orifice radii in the order of some ten nanometers, lengths of some ten micrometers, and half cone angles of ca. 10 degrees. They are very useful as model systems for biological pores, or they can be used as platforms to support lipid bilayers with inserted porins [2].

In aqueous solutions under most conditions native glass surfaces are negatively charged. Therefore for low ionic strengths the electric double layer near the pore mouth covers a large part of the pore volume. As a consequence the pore mouth becomes perm-selective for cations. In connection with the asymmetric shape of the pore this leads to a rectification of the ionic fluxes (ion current rectification, ICR). ICR manifests itself as an asymmetric current voltage curve of of the pore [3]. Experimental results will be discussed which show a clear correlation of ICR and the Debye length. The experimental results are supported by numerical solutions of the Poisson-Nernst-Planck-equations [4]. A model for ICR will be discussed according to which ICR is a direct consequence of the asymmetric fluxes of $K_+$ and $Cl_-$ at the pore mouth (Fig. 1) which in turn leads to conductivity changes in the lumen of the pore.

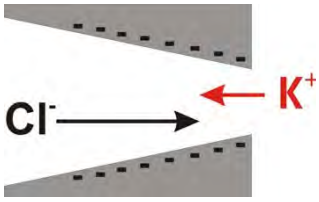


*Fig. 1. Schematic representation of the mechanism of ion current rectification at a conical nanopore. The surface charge leads to a perm-selectivity of the pore mouth which in turn causes an accumulation of neutral salt in the lumen of the pore and thus a conductivity increase*

**References:**

[1] B. Zhang, J. Galusha, P.G. Shiozawa, G. Wang, A.J. Bergren, R.M. Jones, R.J. White, E.N. Ervin, C.C. Cauley, H.S. White: *Anal. Chem.* **79** (2007) 4778.
[2] R.J. White, E.N. Ervin, T. Yang, X. Chen, S. Daniel, P.S. Cremer, H.S. White: *J. Am. Chem. Soc.* **129** (2007) 11766.
[3] Z.S. Siwy: *Adv. Funct. Mater.* **16** (2006) 735.
[4] A. Bund, H.S. White: *Langmuir* (in press)

First Regional Symposium on Electrochemistry of South-East Europe, Rovinj, Croatia, May 4-8, 2008.

O-3-56

# WHY TO USE PIEZOELECTRIC NANOGRAVIMETRY FOR THE STUDY OF ELECTROCHEMICAL TRANSFORMATIONS OF IMMOBILIZED MICROPARTICLES?

**G. Inzelt, A. Róka**

*Eötvös Loránd University, Institute of Chemistry, Budapest, Pázmány Péter sétány 1/a, H-1117, Hungary, E-MAIL: inzeltgy@chem.elte.hu*

The method of voltammetry of immobilized microparticles in combination of electrochemical nanogravimetry by using quartz crystal microbalance (EQCM) is especially useful for the characterization of microcrystals attached to an electrode surface [1]. Although the cyclic voltammetry supplies information regarding the redox reactions occurring in these systems, the elucidation of the voltammograms is a very difficult, often impossible task without additional data concerning the sorption/desorption of ionic species and neutral molecules.

In order to demonstrate the importance of the application of this combined technique the results obtained for α-$RuCl_3$ microcrystals will be presented.

$RuCl_3$ is insoluble in water and organic solvents which is connected with its polymeric structure in solid state. $RuCl_3$ microcrystals can be reduced and reoxidized in several steps in the presence of acidic and neutral aqueous solutions of different electrolytes. The results can be explained by the formation of complexes and intercalation compounds which contain mixed valence $Ru^{III}$ / $Ru^{II}$-centers, $Cl^-$ ions, metals or $H^+$ ions, and solvent molecules, the ratio of which depends on the potential and the solution composition. The redox transformations also involve solid-state phase transitions [2,3]. The insertion of organic molecules (e.g., aniline or pyrrole) is also possible, and it results in polyaniline or polypyrrole – $RuCl_3$ nanocomposites [4,5].

Usually the 'stabilized responses' are studied, e.g., in the case of metal hexacyanometalates, however, in many cases the parent microcrystals undergo irreversible transformations during the first reduction-oxidation cycle. Therefore, it is of importance to investigate also this break-in process which differs from that characteristic of conducting polymer films where usually only morphological changes occur. This effect is illustrated in Fig.1.

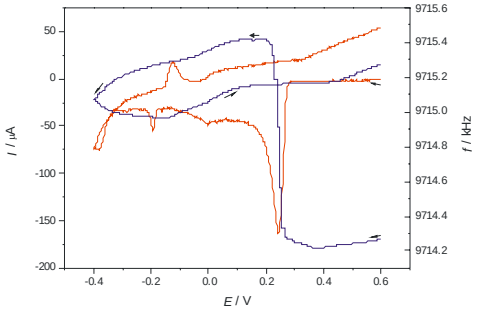


*Fig.1. The first voltammetric cycle of a freshly deposited $RuCl_3$ layer and the corresponding EQCM response. Electrolyte: 0.5 M NaCl. Scan rate: 20 mV $s^{-1}$.*

Another interesting feature that will be discussed is shown in Figures 2 and 3. As seen the cyclic voltammetric responses are rather similar and characteristic of that can be detected in contact with aqueous solutions of KCl. However, the mass changes shown are very different and depend on the prehistory of the $RuCl_3$ layer.

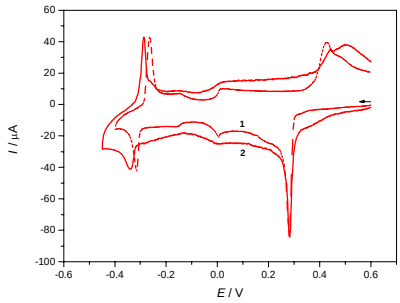


*Fig.2. Cyclic voltammetric curves of $RuCl_3$ layer in contact with 0.5 M KCl. Scan rate: 5 mV $s^{-1}$. (1) $10^{th}$ cycle in KCl after investigation in contact with NaCl solutions; (2) $10^{th}$ cycle after investigation in contact with LiCl and HCl solutions, $10^{th}$ cycle.*

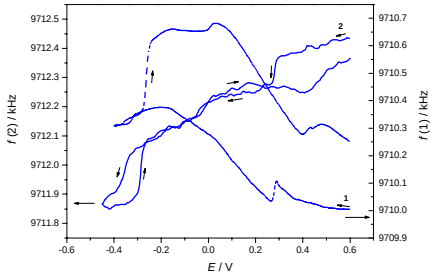


*Fig.3. EQCM responses obtained simultaneously with the cyclic voltammetric curves shown in Fig.2.*

**References:**

[1] F. Scholz, U. Schröder, R. Gulaboski (2005) *Electrochemistry of Immobilized Particles and Droplets*, Springer
[2] G. Inzelt, Z. Puskás, *Electrochem. Commun.* **6** (2004) 805.
[3] G. Inzelt, Z. Puskás, K. Németh, I. Varga, *J. Solid State Electrochem.* **9** (2005) 823.
[4] G. Inzelt, Z. Puskás, *J. Solid State Electrochem.* **10** (2006) 125.
[5] G. Inzelt, A. Róka, *Electrochim. Acta* (2008) doi: 10.1016/j.electacta.2007.06.014

First Regional Symposium on Electrochemistry of South-East Europe, Rovinj, Croatia, May 4-8, 2008.

O-3-57 Keynote Lecture

# BIOLOGICAL ACTIVITY OF SELF ASSEMBLING PEPTIDES RELATED TO THEIR FUNCTIONALITY

**A. Nelson*, E. Protopapa, A. Aggeli**

*Centre for Self Organising Molecular Systems, School of Chemistry, Leeds, LS2 9JT, UK, *andrewn@chem.leeds.ac.uk*

Self assembling peptides are a unique group of peptides which self assemble in aqueous solution to form higher order structures such as fibrils. Because of their unique properties, they have increasing application in uses such as tissue engineering, wound healing and dentistry. However if such materials are not biocompatible their function in this respect is not suitable since they will damage the tissue which they are intended to support. One way of screening their biocompatibility is to examine their interaction with a biologically relevant model phospholipid membrane. The results tell us whether the individual peptides are biomembrane active in which case the peptides will destroy membranes with which they are in contact. This study looks at the interaction of self assembled peptides with a supported model membrane system using in the main electrochemical techniques of interrogation. We show that the activity of the peptides to the model membrane depends on both the peptide's functionality and charge. We also show that an electric field can be used to facilitate phospholipid-peptide interaction. We clarify the actual species or form of the peptide which interacts with the membrane system. We show whether peptides self assemble inside the membrane to form channels. The study concludes with recommendations on which peptides are safe to use for tissue engineering studies.

First Regional Symposium on Electrochemistry of South-East Europe, Rovinj, Croatia, May 4-8, 2008.

O-3-58

# ELECTROCHEMISTRY OF NUCLEIC ACIDS AND PROTEINS. NEW TRENDS IN PROTEIN ANALYSIS

**E. Palecek, V. Ostatna, V. Dorcak, M. Trefulka, H. Cernocka, M. Zivanovic, M. Bartosik**

*Institute of Biophysics, Academy of Sciences of the Czech Republic, Kralovopolska 135, 612 65 Brno, Czech Republic, palecek@ibp.cz*

Electroactivity of nucleic acids was discovered fifty years ago (1,2). At present electrochemistry of nucleic acids is a mature well-established field, involving a number of applications in biotechologies, such as sensors for DNA hybridization (DNA sequencing), sensors fro DNA damage, etc. (3). Faradaic signals of DNA and RNA are electrochemically irreversible, occurring at highly positive or negative potentials. Electroactive labels, including nanocrystals and nanoparticles, were introduced into DNA to obtain signals closer to the potential of zero charge and/or to increase the sensitivity and specificity of the analysis (3-5). Osmium (VIII) and Os(VI) complexes can be used for end-labeling of DNA and RNA. Ss oligodeoxynucleotides (ODN) probes immobilized on solid surfaces are commonly used in DNA hybridization sensors. Direct linkage of thiol-end-labeled ODNs (HS-ODNs) at gold surfaces, facilitating formation of DNA self-assembled monolayer (SAM), is one of the most frequently used ways of DNA immobilization in these sensors. Such monolayers resemble the well-known self-assembly of alkanethiols on gold surfaces (3). Recently we have shown that HS_ODNs form self-assembled monolayers (SAMs) at mercury electrodes providing signals due to (a) reduction of bases and (b) reduction of the Hg-S bond (6). Changes in voltammetric signals due to cytosine and Hg-S bond reduction indicated changes in positioning of the HS-$(TTC)_7$ molecules at the electrode with increasing HS-$(TTC)_7$ concentration from lying flat with respect to SAMs, to upright-standing molecules. Densely packed SAM behaved as an insulator not allowing electron transfer between $[Ru(NH_3)_6]^{3+}$ and the electrode. Different adsorption modes of thiolated and thiol-free DNAs were observed.

In the last decades electrochemistry of proteins focused on some enzymes and a relatively small group of small conjugated proteins (such as metalloproteins) containing non-protein redox centers yielding fast reversible electrochemistry (7,8). Electrochemistry of a vast majority of proteins important in biomedicine and in proteomics was, however neglected. We show that electroactivity of some amino acid residues at carbon and mercury electrodes as well as the electrocatalysis can be utilized in the analysis of proteins important in biomedicine (8). Constant current chronopotentiometry (CPS) with bare and chemically modified electrodes is particularly useful for recognition of changes in protein structures induced by denaturing reducing and oxidizing agents as well as by single amino acid exchange in proteins important in cancer (9-11). Using CPS and other methods, aggregation of amyloidogenic proteins can be traced. Recently pre-

aggregation changes have been discovered by these methods in proteins important in Parkinson's and Alzheimer's diseases (12).

***Acknowledgements:*** *This work was supported by grants from Grant Agency of the Academy of Sciences of the Czech Republic IAA50040513 and from the Grant Agency of the Czech Republic 301/07/0490 to EP and 202/07/P497 to VO and AVOZ50040507 and Ministry of Education, Youth and Sports, CR, LC06035.*

**References:**

**1.** Palecek, E. (1958). Oszillographische Polarographie der Nucleinsäuren und ihrer Bestandteile. *Naturwiss.* **45**, 186-187.

**2.** Palecek, E. (1960). Oscillographic polarography of highly polymerized deoxyribonucleic acid. *Nature* **188**, 656-657.

**3.** Palecek E. and Jelen F. (2005): In: Palecek E., Scheller F. and Wang J. (eds.) (2005): Electrochemistry of nucleic acids and proteins. Towards electrochemical sensors for genomics and proteomics. Elsevier, Amsterdam.74-174.
Palecek, E. and Fojta, M. (2007): Paramagnetic beads as versatile tools for electrochemical DNA and protein biosensing. (Review) *Talanta* 74/3, 246-290.
Palecek E. (2004): Nucleic acids. (a) Electrochemical methods. In: Encyclopedia of Analytical Science 2e. (Poole, C.F. Ed.) Elsevier, London, 399-408.
Palecek E., Fojta M., Jelen F. and Vetterl V. (2002): Electrochemical analysis of nucleic acids. In A. J. Bard and M. Stratsmann (Eds.) The encyclopedia of electrochemistry, Vol. 9, G. Wilson (Ed.) Wiley-VCH, 365-430.

**4.** Trefulka, M., Ostatna, V., Havran, L., Fojta, M. and Palecek, E. (2007): Covalent labeling nucleosides, RNA and DNA with VIII- and VI-valent osmium complexes. *Electroanalysis* **19/12**, 1281-1287

**5.** Trefulka, M., Ferreyra, M., Ostatna, V., Fojta, M., Rivas, G. and Palecek, E. (2007): Voltammetry of osmium end-labeled oligodeoxynucleotides at carbon, mercury and gold electrodes *Electroanalysis* **19/12**, 1334-1338
Fojta, M., Kostecka, P., Trefulka, M., Havran, L. and Palecek, E. **(**2007): „Multicolor" electrochemical labeling of DNA hybridization probes with osmium tetroxide complexes**.** *Anal. Chem.* **79**, 1022-1029.

**6.** Ostatna V. and Palecek E. (2006), *Langmuir* **22**, 6481-6484.

**7.** Palecek, E. In *Electrochemistry of Nucleic Acids and Proteins: Towards Sensors for Genomics and Proteomics*; Palecek, E., Scheller, W., Wang, J., Eds.; Elsevier: Amsterdam, 2005; pp 689-754.

**8.** Palecek E., Ostatna V. (2007): Electroactivity of non-conjugated proteins and peptides. Towards electroanalysis of all proteins. *Electroanalysis* **19/23**, 2383-2403.

**9.** Ostatna V., et al. (2006), *J. Electroanal. Chem.* **593**, 172-178.

**10.** Ostatna V., Palecek E.: Native, denatured and reduced BSA. Enhancement of chronopotentiometric peak H by guanidinium chloride. *Electrochim. Acta*, *in press*

**11.** Dorcak V., Palecek E. (2007): Electrochemical discrimination of reduced and oxidized peptides. *Electroanalysis* **19 /23**, 2405-2412.

**12.** Palecek, E., Ostatna, V., Masarik, M., Bertoncini, C.W. and Jovin, T. M. (2008): Changes in interfacial properties of α-synuclein preceding its aggregation. *Analyst* **133**, 76-84.

First Regional Symposium on Electrochemistry of South-East Europe, Rovinj, Croatia, May 4-8, 2008.

O-3-59

# AMPEROMETRIC ADHESION SIGNALS OF VESICLES, CELLS AND DROPLETS

**N. Ivošević DeNardis, V. Žutić, V. Svetličić, R. Frkanec[a]**

*Ruđer Bošković Institute, POB 180, Zagreb, Croatia, ivosevic@irb.hr*
*[a]Institute of Immunology, Inc., POB 266, Zagreb, Croatia*

The signifficance of adhesion phenomema in single particle/electrode interaction became apparent for more than two decades since the discovery of adhesion signals of vesicles in seawater using a dropping mercury electrode [1]. Electrochemical adhesion imaging presents unique approach for *in situ* characterization of fragile structures in marine systems [2] and in biological fluids [3]. By potential control of the electrode surface charge and interfacial tension, adhesion forces can be fine-tuned in studying interplay of complex processes involved in fluid microparticles/electrode interaction. During their attachment and spreading at the electrode, individual vesicles, cells and microdroplets displace the double-layer charge from the inner Helmholz plane, and the transient flow of compensating current can be recorded as well-defined adhesion signal. Liposomes present classical model in studying physical mechanism of cell adhesion [4]. Incidents and shape of adhesion signals recorded in liposome suspensions in PBS reflect their polydispersity, surface charge density and properties of phospholipid head group. Potential range of adhesion and the shape of adhesion signals of liposomes are compared with those of organic droplets and living cells recorded under the same experimental conditions. We confirmed that general mechanism established for adhesion of hydrocarbon droplets and cells [5] is valid as well for the liposome adhesion within wide range of surface charge densities. Major distinction for the case of liposomes was identified as: (1) different values of critical interfacial tensions of adhesion at the positively and negatively charged electrode, and (2) appearance of adhesion signals even at the lowest surface charge densities of the electrode, revealing the specific interactions of liposome polar head groups and molecular orientation at the electrode [6,7].

## References

[1] V. Žutić, T. Pleše, J. Tomaić, T. Legović, *Mol. Cryst. Liq. Cryst.* **113** (1984) 131.
[2] V. Svetliičić, V. Žutić, A. Hozić Zimmermann, T. Mišić, *Biophys. J.*, Abstract Issue (2008) 655a.
[3] N. Ivošević DeNardis, V. Žutić, V. Svetličić, R. Frkanec, J. Tomašić, *Electroanal.* **19** (2007) 244
[4] R. Lipowsky, E. Sackmann (Eds.) *Structure and Dynamics of Membranes*, Elsevier, Amsterdam, 1995.
[5] V. Svetličić, N. Ivošević, S. Kovač, V. Žutić, *Langmuir*, **16** (2000) 8217.
[6] X. Bin, I. Zawisza, J. Goddard, J. Lipkowski, *Langmuir*, **21** (2005) 330.
[7] V. Žutić, V. Svetličić, A. Hozić Zimmermann, N. Ivošević, DeNardis, R. Frkanec, *Langmuir*, **23** (2007) 8647.

First Regional Symposium on Electrochemistry of South-East Europe, Rovinj, Croatia, May 4-8, 2008.

O-3-60

# ELECTROCHEMICAL AND STM STUDY OF α,ω-ALKANEDITHIOLS SELF-ASSEMBLED MONOLAYERS

**V.C. Ferreira[1,2*], A.F. Silva[2], L.M. Abrantes[1]**

[1]*CQB, Departamento de Química e Bioquímica, Faculdade de Ciências da Universidade de Lisboa, Campo Grande, 1749-016 Lisboa, Portugal, E-mail: vcferreira@fc.ul.pt*
[2]*CIQ-UP, Departamento de Química, Faculdade de Ciências da Universidade do Porto,*

Self-assembled monolayers (SAMs) have been under intense research activity in the last decades owing to their ease of preparation, stability and potential applicability in a wide variety of fields such as catalysis, corrosion and sensors [1]. SAMs of alkanethiols onto gold, which enable the modification of chemical and physical properties of metal surface, have also been relevant in the gold nanoparticles synthesis and surface modification [2]. α,ω-Alkanedithiols play an important role in the development of nanodevices due to the availability of thiol functionalities at the SAM/solution interface which enable the connection to other functional units [3].

The aim of the present work was the preparation of α,ω-alkanedithiols SAMs (with 6, 9 and 10 atoms of carbon atoms in the alkane chain) and mixed thiol/dithiol monolayers, from ethanolic solution. The amount of adsorbate and the SAM stability in alkaline medium was evaluated by reductive desorption of the prepared monolayers by cyclic voltammetry. An upright orientation of the dithiol self-assembled molecules and disulfide bonding at the SAM/solution interface were suggested by the higher reductive desorption charge of the dithiol monolayers (relative to thiol SAMs) for n = 6 and 9. The results show that an improvement on the stability of these dithiol SAMs is obtained by the presence of monothiols, resulting in mixed monolayers. Mixed SAMs prepared from longer alkane chain thiols, n = 10, allowed to overcome the increased possibility of loops formation and therefore lower surface coverage obtained for the 1,10-decanedithiol monolayers.

Morphological characterisation of the modified electrodes was performed by scanning tunnelling microscopy (STM) in air. Typical one atom deep thiol induced depressions are observed in the STM images of the dithiol SAMs.

***Acknowledgments:***
*V.C. Ferreira grateful acknowledges the financial support from Fundação para a Ciência e a Tecnologia, scholarship SFRH/BD/30585/2006.*

**References:**

[1] Love, J.C., Estroff, L.A., Kriebel, J.K., Nuzzo, R.G., Whitesides, G.M., *Chem. Rev.* **105** (2005) 1103.
[2] Daniel, M.-C., Astruc, D., *Chem. Rev.* **104** (2004) 293.
[3] Liang, J., Rosa, L.G., Scoles, G., *J. Phys. Chem. C* **111** (2007) 17275.

First Regional Symposium on Electrochemistry of South-East Europe, Rovinj, Croatia, May 4-8, 2008.

O-3-61 Keynote Lecture

# CATHODIC DEPOSITION OF COMPONENTS IN BiSbTe, ZnSb AND CoSb THERMOELECTRIC FILMS USING VARIOUS ELECTROLYTE MEDIA

**M. Nedelcu[1], A. C. Manea[1], A. Cojocaru[1], S. Bogdan[2], S. Stanciu[2], T. Visan[1]**

*[1]Department of Applied Physical Chemistry and Electrochemistry, University POLITEHNICA Bucharest, Calea Grivitei 132, 010737-Bucharest, Romania, E-mail: t_visan@chim.upb.ro*
*[2]Department of Physics, University POLITEHNICA Bucharest, Splaiul Independentei 313, 060042-Bucharest, Romania*

BiSbTe semiconductor represents a very promising material for thermoelectric refrigeration at low temperature, because of increase Seebeck coefficient and low thermal conduction. Literature shows that BiSbTe ternary system is sometimes prepared as $Bi_2Te_3$-$Sb_2Te_3$ mixture. ZnSb and CoSb are new thermoelectric materials to work in the middle-lower range of temperature. These compounds are relatively low cost and can potentially substitute for high-performance lead tellurides. Boulanger [1] shows that BiSb alloys can be obtained only in the presence of complexing agents. Electrodeposition of BiSbTe ternary system was performed by Fleurial [2] by control of current or electrode potential with EDTA and citric acid as complexants. In previous work [3] we reported the codeposition of Bi, Sb and Te ionic species in very acidic media (6M HCl, 1M $HClO_4$, 4.6M $HBF_4$ solutions). The aim of this work is to study the electrodeposition of BiSb and BiSbTe films in a moderate acid aqueous medium (5M NaCl + 1M HCl mixture). We also report here an investigation of cathodic process during obtaining ZnSb and CoSb films in a nonaqueous medium (ethylene glycol) with advantage of a high-electrochemical window.

Cyclic voltammetry and electrochemical impedance spectroscopy investigations were conducted at room temperature in both aqueous and ethylene glycol baths. The electrodeposition of singular Bi, Sb and Te, as well as binary (BiSb, BiTe and SbTe) and ternary ($Bi_xSb_{2-x}Te_3$) alloys was studied on Pt (0.5 $cm^2$). The electrolyte was a aqueous mixture of 5 M NaCl + 1 M HCl based solution containing $Bi^{3+}$, $Sb^{3+}$, $Te^{4+}$. The deposition of Zn, Co and Sb in bath containing ethylene glycol as solvent was also investigated. In the experiments a computer driven Zahner IM 6e potentiostat was used.

By recording cyclovoltammograms (Figs.1-3) the underpotential deposition (UPD) of Bi, Sb or Te was evidenced, a phenomenon which is involved in simultaneous co-deposition of components of films. Figures 3-6 show examples of voltammograms for SbTe, ZnSb and CoSb. Some data about the cathodic process and properties of films were obtained by electrochemical impedance spectroscopy. Analyzing Nyquist and Bode spectra differences between impedance of various films were observed.

For instance, spectra show very conductive Te and BiSbTe films. Equivalent electrical circuit was depicted in Fig. 7. It was noticed the presence of two constant phase elements (CPE) in the modified Randles scheme. EIS spectra for ZnSb and CoSb were also obtained and interpreted.

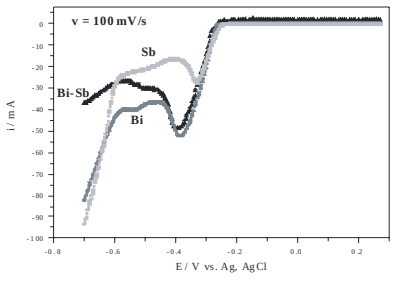


*Fig. 1 Cathodic branches of voltammograms for Bi, Sb and BiSb deposition; $c_{Bi}$ = 0.09 M, $c_{Sb}$ = 0.01 M*

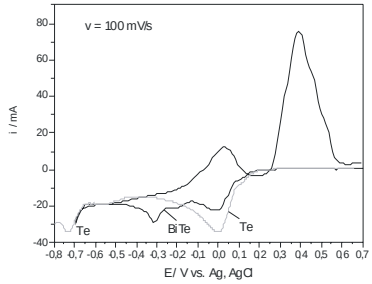


*Fig. 2 Cyclic voltammograms for Te and BiTe deposition, $c_{Bi}$ = 0.025 M, $c_{Te}$ = 0.075 M*

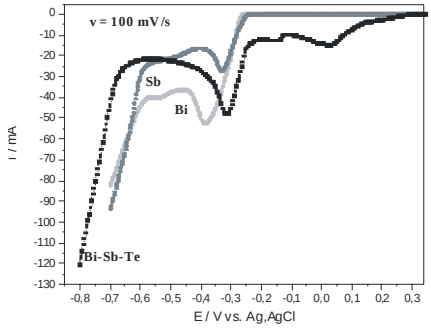


*Fig. 3 Cathodic branches of voltammograms for Bi, Sb, BiSbTe deposition; $c_{Bi}$ = 0.05 M, $c_{Sb}$ = 0.01 M, $c_{Te}$ = 0.05 M*

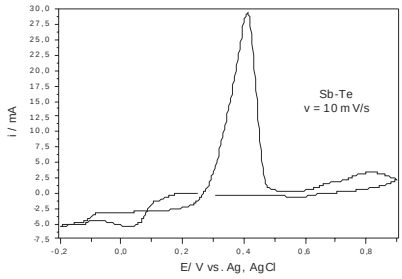


*Fig. 4 Cyclic voltammograms for SbTe; $c_{Sb}$ = 0.05 M, $c_{Te}$ = 0.05 M*

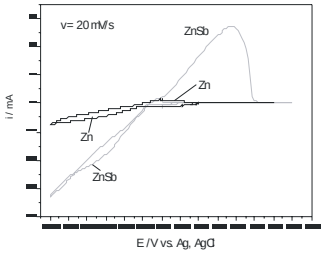


*Fig. 5 Cyclic voltammograms for Zn and ZnSb; $c_{Zn}$ = 0.072M, $c_{Sb}$ = 0.045 M*

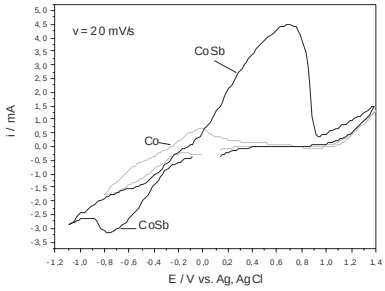


*Fig. 6 Cyclic voltammograms for CoSb; $c_{Co}$ = 0.05M, $c_{Sb}$ = 0.01 M*

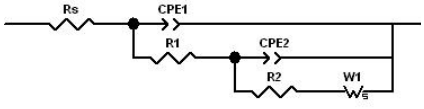


*Fig. 7 Equivalent circuit established using ZView 2.9 soft for single, binary and ternary containing Bi, Sb, Te*

## References:

[1] F. Besse, C. Boulanger, J.M. Lecuire, *J. Appl. Electrochem.* **30** (2000) 585

[2] C.K. Huang, J.A. Herman, N. Myung, J.R. Lim, J.P. Fleurial, *Mat. Res. Soc. Symp. Proceedings*, Vol.793, Materials Research Society, 2004, S8.33

[3] M.Nedelcu, M.Sima, T.Visan, T.Pascu, I.Franga, F.Craciunoiu, *20-th Int. Conf. on Thermoelectrics-Proceedings ICT'01*, IEEE Inc., Piscataway, NJ, 2001, 32

First Regional Symposium on Electrochemistry of South-East Europe, Rovinj, Croatia, May 4-8, 2008.

O-3-62

# CONTROLLING MORPHOLOGY AND COMPOSITION OF TERNARY SEMICONDUCTOR OXIDES GROWN BY ELECTRODEPOSITION

**B. Marí**

*Departament de Física Aplicada- IDF. Universitat Politècnica de València, Camí de Vera s/n, 46022 València, Spain, bmari@fis.upv.es*

Control of morphology, orientation and assembly properties of oxide nanostructures are key parameters for their implementation onto technological devices. Electrochemical procedures are well suited for this purpose since they allow the synthesis of oxide films under different morphologies depending on both the solvent and the substrate used.

In the case of zinc based oxides, electrodeposition in aqueous media produces discontinuous structures under the form of nanocolumns while

when using a non-aqueous solvent, like dimethylsulfoxide (DMSO), extremely smooth and continuous films are mainly obtained. Further when an appropriate substrate is used, the discontinuous structures can be grown in a unique direction and become ordered (Fig 1).

Obviously, both morphologies exhibit different properties. Continuous films are highly transparent due to the flatness of the surface which results in low diffusivities. In contrast nanocolumnar ZnO structures obtained from aqueous solutions exhibit high diffusivity and intense photoluminescence [1]. The results point out the advantage of using dimethylsulfoxide when uniform, oriented and highly transparent films are required while using aqueous bathes produce perfectly defined hexagonal ZnO columns which can be fully oriented by chosen a suitable substrate.

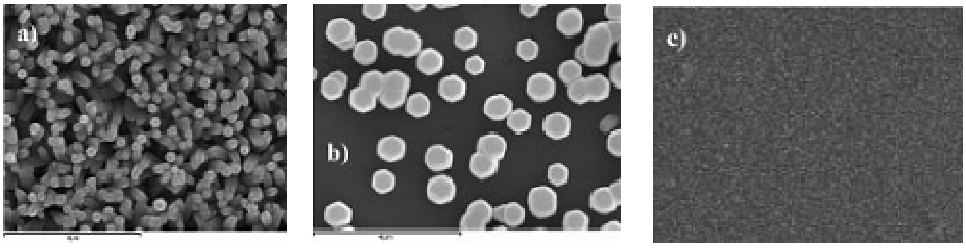


*Fig. 1 Morphologies of ZnO using different solvents and substrates, a) water and ITO, b) water and GaN, c) DMSO and ITO*

Crystal structures are in agreement with morphologies made evident by SEM micrographs. Columnar structures obtained onto polycrystalline ITO substrates in water (Fig.1a) exhibit a preferred orientation following the 002 direction of the hexagonal wurtzite ZnO structure but the rest of crystal orientations are also

present (Fig 2). On contrary films grown on hexagonal GaN in water or on ITO in DMSO (Fig.1 b, c) only show the 002 direction (Fig. 2).

The synthesis of ternary ZnMO semiconductor compounds (certainly difficult using water) can be easily prepared when an organic solvent is used. In our case several ternary compounds like ZnCdO, ZnCoO and ZnMnO have been successfully synthesized by using DMSO as solvent [2].

Ternary ZnMO (M=Cd, Co, Mn) compounds can be electrodeposited using a bath that contain dissolved Zn and M anions from suitable precursors. In this case chlorides were used as precursors and $KClO_4$ as supporting electrolyte. Independent of the third element used (Cd, Co or Mn) very flat films are obtained as long as the wurtzite structure corresponding to ZnO is preserved. The M/Zn ratio in the final film is achieved by choosing the suitable M/Zn ion concentration ratio in the starting solution. In some cases the final concentration of the third element tends to saturate when attaining the solubility limit of the M element in the ZnO lattice.

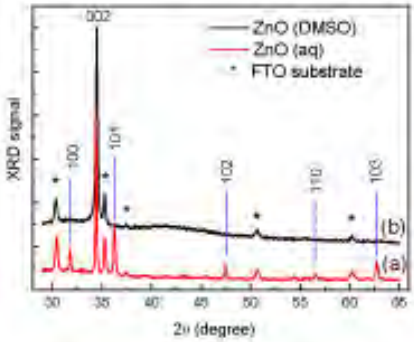


*Fig. 2 XRD diagram of two ZnO layers deposed on FTO covered glass from aqueous (a) and DMSO (b) solvents.*

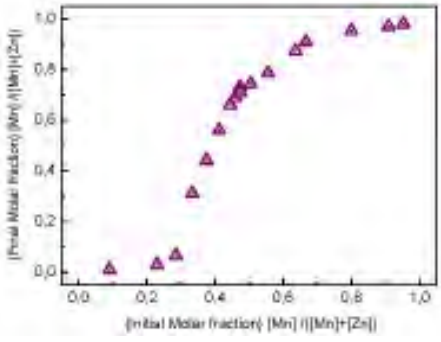


*Fig 3. Mn molar fraction present in the solid film as a function of the Mn molar fraction in the startin solution for Zn1 -xMnO films*

On the contrary electrodeposited $Zn_{1-x}Mn_xO$ films cover the overall x range between 0 and 1. Final composition for $Zn_{1-x}Mn_xO$ films obtained from Energy Dispersive Spectroscopy (EDS) versus the initial molar fraction appears in Fig. 3. $Zn_{1-x}Mn_xO$ films with low Mn concentration exhibit hexagonal wurtzite. Increasing the Mn amount results in a continuous deformation of the crystal structure and the film become amorphous. Further increase of Mn in the starting blend produces films with the structure of manganese oxide.

Magnetic measurements performed on both ZnCoO and ZnMnO compounds point out that ZnCoO films exhibit a paramagnetic behaviour while ZnMnO are ferromagnetic.

**References:**

[1] J. Cembrero, A. Elmanouni, B. Hartiti, M. Mollar and B. Marí; Nanocolumnar ZnO films for photovoltaic applications. *Thin Solid Films* 451-452, **198** (2004)

[2] M. Tortosa, M. Mollar and B. Marí; Synthesis of ZnCdO thin films by electrodeposition, *Journal of Crystal Growth* 304, **97** (2007)

First Regional Symposium on Electrochemistry of South-East Europe, Rovinj, Croatia, May 4-8, 2008.

O-3-63

# OPTICAL PROPERTIES OF ELECTROCHEMICALLY POLISHED AND ANODIZED NIOBIUM SURFACES

**I. Mickova**

*Faculty of Technology and Metallurgy, University "Ss Cyril and Methodius", Skopje, Macedonia E-mail: mickova@tmf.ukim.edu.mk*

Optical properties of electropolished and anodized Nb surface has been studied using ellipsometric method. The working electrodes were cut from massive cylindrical rod with purity 99.8 % (Alfa Aesar). The discs of Nb with 20 mm in dia and height of 10 mm have been embedded in epoxy resin (Struers), leaving the front area in contact with solution. Prior to each measurement the Nb surfaces were abraded using silicon carbide paper (600 grade) and then electropolished in electrolytic bath consisting: 170 ml $HNO_3$ (64%) + 50 ml HF (40%) + 510 ml $CH_3OH$ + 5 g citric acid. As a counter electrode was used a Pt grid with large surface. The best electrochemical polishing was obtained for the bath tempera-ture of t = $-5^O$ C at voltage of 21 V during 1 min for turbulent stirring of the bath. The cell current was raised with steering speed. The quality of electrochemical polishing was tested ellipsometrically through the reflectivity at normal incidence. The electrochemically poli-shed simples had visually homogeneous mirror brightness over all the surface area. After the electrochemical polishing the Nb surfaces were cleaned in an ultrasonic bath and rinsed with ethanol. The ellipsometric measurements were performed with a "thin film ellipsome-ter Rudolph Research, type 43602-200" at wavelength of λ = 546.1 nm. The incidence angle was determined by searching of principal angle. At this angle the sensitivity of measurements are the highest and for the majority of metal surface moves from 60 to $80^O$.

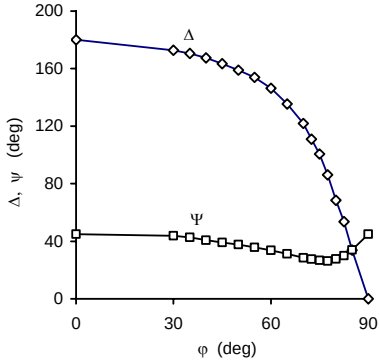


*Fig.1. Dependence of elipsometrical parameters Δ and Ψ from angle of incidence*

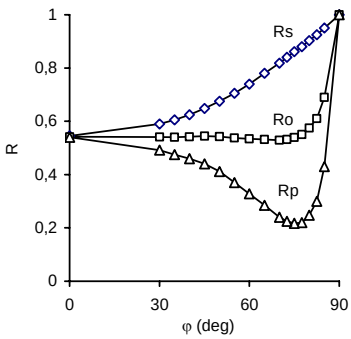


*Fig.2. Dependence of reflectivity from angle of incidence: Rs – perpendicular, Ro - normal and Rp parallel to plane incidence*

On fig.1. the dependence of ellipsometric parameters Δ and Ψ from the incidence angle in limits from $30^O$ to $87^O$ is given. For less values than $30^O$ it is technically impossible to perform measurements, so values of Δ and Ψ for φ = $0^O$ are extrapolated to their

theoretical values of $180^O$ and $45^O$, respectively. As could be seen from fig.1., for $\Delta = 90^O$ the corresponding principal angle is $76^O$ and at this angle there is coincidence between point of inflexion of curve for $\Delta$ and the minimum of curve for $\Psi$. On fig.2., Rs increase monotonically from its minimum value at $\varphi = 0$ to 1 when $\varphi = 90^O$, whereas Rp exhibits a minimum at the pseudo-Brewster angle of $74^O$. Taking into consideration the time between electrochemical polishing and performed measurements, on Nb surface it should be built the natural surface layer of about 2 nm, that moves the Brewster angle several degree to higher value. This is the reason why Smith recommends that the measurements should be always taken at the incidence angle which is for several degrees less than the principle angle [1]. All our future measurements were performed at $70^O$; several degrees less than the determined pseudo-Brewster angle.

The complex refractive index of metal substrate and anodic oxide films in the potential/voltage region from 0–100 V have been determined by in-situ ellipsometric measure-ments in 1 M $H_2SO_4$. For these measurements the special optical electrolytic cell was adopted, presented previously [2]. The anodization was firstly performed potentiosta-tically using HEKA potentiostat/galvanostat. The potential was increased stepwise every 30 s by 0.5 V from 0 to 10 V. For potential up to 10 V, a three electrode system was used. For voltage over the 10 V, a two-electrode system was used and the applied voltage was increased in step every 30 s by 2.5 V from 10 to 100 V, using the high-stabilized supplier.

For three component system: medium (1 M $H_2SO_4$), anodic oxide film ($Nb_2O_5$) and metals substrate (Nb), the complex refractive index of medium $\bar{n}_m = n_m(1 - i\,\kappa_m)$ was determined by Abbe's refractometer. The complex refractive index of metal substrate $\bar{n}_s = n_s(1 - i\,\kappa_s)$ was determined separately [3], and complex index of anodic oxide films $\bar{n}_f = n_f(1 - i\,\kappa_f)$ was calculated from the ellipsometric measured parameters $\Delta$ and $\Psi$.

*Table 1. measured and calculated complex refractive indices.*

| | $\bar{n}_m$ | $\bar{n}_s$ | $\bar{n}_f$ |
|---|---|---|---|
| 1 M $H_2SO_4$ | 1.342(1 – i 0) | | |
| Nb | | 3.62(1 – i 0.993 | |
| $Nb_2O_5$ (1-10 V) | | | 2.347(1 – i 0) |
| $Nb_2O_5$ (10-100 V) | | | 2.345(1 – 1 0.005) |

In the potential range from 0 to 10 V the real part of film refractive index has a little higher value $n_f = 2.347$ than in the voltage region of 10 to 100 V, $n_f = 2.345$. Oppositely the value of imaginary part in the potential region from 0 to 10 V is $\kappa_f = 0$, indicating that the film is transparent and homogeneous. For voltage from 10 to 100 V, the imaginary part is $\kappa_f = 0.0005$, indicating that the oxide film is less transparent as a result of film breakdown. During the breakdown process the various defects are generated in the film and it begins to lost in its homogeneity.

[1] T.Smith, *J.Opt. Soc.Am.* **62**, 774 (1974)
[2] Lj.Arsov, *Electrochim. Acta* **30(12)**, 1645 (1985)
[3] I.Arsova, A.Prusi and Lj.Arsov, *J. Solid State Electrochem.* **7**, 217 (2003)

First Regional Symposium on Electrochemistry of South-East Europe, Rovinj, Croatia, May 4-8, 2008.

O-3-64

# PASSIVATION TREATMENTS OF Sb-BASED PHOTODETECTORS USING ELECTROCHEMICAL PROCESSES

**R. Chaghi, Y. Cuminal, P. Grech, J.B. Rodriguez, P. Christol**

*Institut d'Electronique du Sud (IES), UMR CNRS 5214, Université Montpellier-2, 34 095 Montpellier Cedex 05 France. E-mail: christol@ies.univ-montp2.fr*

Antimonide (Sb) based InAs/GaSb superlattice (SL) is a new material system for the fabrication of high performance infrared (IR) photodetectors suitable for thermal imaging camera [1]. But the Sb-based structures generally exhibit undesirable surface leakage currents, which seriously limit the device performances [2]. Consequently surface passivation of antimonides is a crucial step for achieving improved photodetectors with high $R_0A$ product and high detectivity D*.

Leakage currents are mainly due to the presence at the semiconductor surface of elementary antimony Sb. Indeed, when a GaSb surface is exposed to air, it gives rise to $Sb_2O_3$ and $Ga_2O_3$ native oxide layers. Then, some $Sb_2O_3$ reacts with GaSb to produce $Ga_2O_3$ and a conductive layer of free Sb. The reactions illustrating these processes are:

$$2\ GaSb + 3\ O_2 \rightarrow Ga_2O_3 + Sb_2O_3$$

$$Sb_2O_3 + 2\ GaSb \rightarrow Ga_2O_3 + 4\ Sb$$

In order to suppress this degradation mechanism, sulfur passivation with ammonium sulfide $(NH_4)_2S$ treatment is widely used to produce passivated Sb-based surfaces [3].

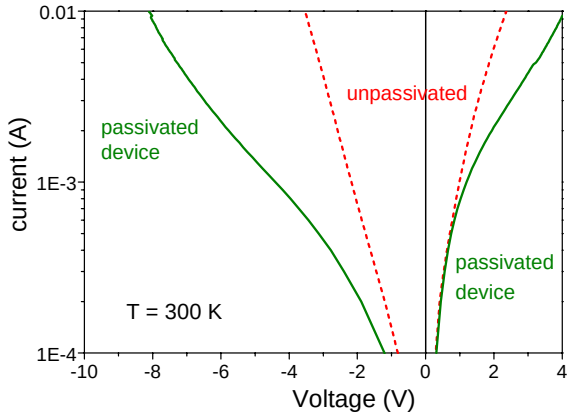


*Room temperature I-V curves of the Sb-based photodiode with and without passivation process.*

In this communication we present our results concerning the use of $(Na)_2S$ and $(NH_4)_2S$ for the passivation of Sb-based structures. The experiments were

performed with potentiostat for routine use of cyclic voltammetry in quantitative analysis. Various ammonium sulfide solutions have been investigated on SL mesa detectors grown by Molecular Beam Epitaxy (MBE) on GaSb substrate [2].
Compared to unpassivated detectors, the devices processed with ammonium sulfide showed superior characteristics. The surface leakage currents were strongly reduced and reverse-bias dark current density was reduced by approximately one order of magnitude at -2V.
A model for explaining improvements with passivation treatments will be proposed.

**References:**

[1] A. Rogalski and P. Martyniuk, *Infrared Phys. Technol.* **48**, 39 (2006)
[2] P. Christol et al., *Phys. Stat. Sol C* **4,** 1494 (2007)
[3] Z. Li et al. *J. Appl. Phys* **94**, 1295 (2003)

First Regional Symposium on Electrochemistry of South-East Europe, Rovinj, Croatia, May 4-8, 2008.

O-3-65

# THE ELECTROCHEMICAL SINTERING OF COPPER POWDER

**Z.D. Stanković, Z. Damnjanović**

*University of Belgrade, Technical Faculty at Bor*
zstankovic@tf.bor.ac.yu

The possibility of copper sintering by electrochemical method has been investigated. The copper powder placed in sulfate copper solution has been used as a model system. The copper powder was kept on cathodic potential using specially, for tjis purpose designed, cathodic current supplier made of titanim plate. The wire of electrchemically refined copper served as counter electrode.
The process of electrochemical sintering has been invastigated at different initial current densities and different shape of curent pulses. The obtained sintered samples have been matter of further investigation of mechanical strain, electroconductibility and porosity.

First Regional Symposium on Electrochemistry of South-East Europe, Rovinj, Croatia, May 4-8, 2008.

O-3-66

# DIRECT ELECTROWINNING OF COPPER FROM MINE WATERS

**V. Stanković, D. Božić, I. Manasijević, G. Bogdanović**

*Technical Faculty BorUniversity of Belgrade, Serbia, vstankovic@tf.bor.ac.yu*

Mine waters originating from active or closed copper mines contain copper ions sometimes in a considerable concentration ($\leq$ 1gdm$^{-3}$) usually associated with an equivalent or even twice higher concentration of $Fe^{2+}/Fe^{3+}$ ions as a consequence of bacterial degradation of sulphide copper and iron minerals. The presence of other heavy metals (Mn, Bi, Cd, Zn, ....) in these waters depends on the ore body mineralization and their concentration is less than the concentration of copper or iron ions and does not exceed few ppms. Mine waters are as a rule acidic having a pH value mainly between 3 and 4. Yealdness of the mine water springs varies in a wide interval: from few liters per minute to several cubic meters per minute and changes very much with season. Anyway, mine waters make serious problem to environment bringing out metal ions and acid to surroundings dammaging heavily ground waters and soil. Copper is usually removed from mine waters by cementation onto iron scrap or, not very often, by some of separation/concentration technologies, such as: solvent extraction followed by the electrowinning, column adsorption or ion exchange, or using membrane techniques. So far no attempt has been made to treat mine waters by means of direct electrowinning method using a reticulated cathode material as it is metal foam, or carbon cloth, or some disperse conductive material as copper grains, filings or some others arising from metal working factories. The main reason for no consideration of direct electrowinning technique for mine waters treatment is a high concentration of $Fe^{2+}/Fe^{3+}$ ions present in such sources, which greatly influence in decrease of current efficiency disabling an efficient copper removal to a desired final concentration.

In this study the results on the electrowinning of copper from mine waters originating from the open pit „Cerovo“ will be presented. There are two springs flowing out from the outer lateral slope of the pit dump. Both sources are characterized with a reasonably high copper concentration ($\approx$ 1gdm$^{-3}$) and with a very low iron ions content allowing to consider a direct electrowinning as a method for the copper recovery from these sources. Zinc ions also exist in an unexpected amount of about 25mgdm$^{-3}$ but they do not affect the electrowinning process. Data about the considered mine waters are presented in the following table.

*Table Some characteristics of the mine waters*

| Source | Colour | Total Fe mg dm$^{-3}$ | $Cu^{2+}$ Mg dm$^{-3}$ | pH | Conductivity mS cm$^{-1}$ |
|---|---|---|---|---|---|
| Spring 1 | blue | <10 | 1050 | 3.38 | 10.74 |
| Spring 2 | blue | <10 | 875 | 3.63 | 7.13 |

Mine waters now flow directly to Cerova river having a quality between 1st and 2nd category before mine waters inflow, making it out of any category downstream of the springs.
Experiments were carried out with an aim to provide data which would be needed in designing the mine waters treatment process by direct electrowinning.
Copper removal from mine waters was performed using two types of electrochemical cells: a cell with inert turbulence promoters and a cell with copper foam both operating in galvanostatic mode at different current densities and at different hydrodynamic conditions. No any pre-treatment of the mine waters were performed prior the electrowinning.
Copper concentration was monitored periodically assaying the samples. Cell voltage was recorded enabling us to derive data about energy consumption in the process.
Obtained results clearly show that it is possible to remove copper successfully from the considered mine waters by means of direct electrowinning achieving high electrowinning degree and satisfactorily well current efficiency. Dense metal deposit was obtained in both cases. Cell voltage was considerably high in both cells an even higher in the cell with inert turbulent promoters achieving at the very beginning 12 to 14 V falling down due to lowering of pH with time as a consequence of oxygen evolution as an anode reaction that increases acid content in the water. Both used cells were compared in a view of their applicability for treatment of mine water. Copper foam allows to apply higher geometrical current densities because of its developed internal surface allowing to apply higher operating currents than those in the cell with inert turbulence promoters and achieving lower final copper concentrations in the outlet stream. A comparison between the direct electrowinning and the cementation on iron has also been drawn.

First Regional Symposium on Electrochemistry of South-East Europe, Rovinj, Croatia, May 4-8, 2008.

O-3-67

# EXCHANGE EQUILIBRIUM PROPERTIES OF CATION EXCHANGE MEMBRANES USED FOR THE TREATMENT OF NICKEL PLATING WATER BY ELECTRODIALYSIS

**T.X. Le[1], C. Buess-Herman**

*Service de Chimie Analytique et Chimie des Interfaces (CHANI) – CP 255, Université Libre de Bruxelles (ULB), Bd. du Triomphe, 1050- Bruxelles (Belgium)*
*[1]Present address: Chemistry of Surfaces and Interfaces, CEA Saclay, DSM/DRECAM/SPCSI, F-91191, Gif-sur-Yvette Cedex, France*

It is reported that the CMV membrane which is not selective toward the monovalent cations was used to reconcentrate both nickel sulfate and sulfuric acid for treatment of nickel plating water while the CMS membrane was used to separate the hydrogen ion from multivalent cation because of its high monovalent permselectivity [1,2]. In the present work, the transport of hydrogen ion and nickel ion through the CMV and CMS membranes was studied when the membranes are in contact with 0.5 N sulfuric acid containing nickel sulfate at different concentrations. We have determined the amounts of $H^+$ and $Ni^{2+}$ in the membrane and measured the membrane conductivity. The mobilities ratios of hydrogen ion by nickel ion in the CMV and CMS membranes respectively equal to 7.4 and 39.8 were obtained from membrane conductivity and ion exchange isotherm data. The CMV and CMS cation exchange membranes are copolymers of styrene and divinylbenzene. Usually, the CMS membrane presents a high degree of cross-linking and is prepared by surface modification in order to improve the permselectivity for the monovalent cations. It is observed that the surface modification does not influence significantly the transport of $H^+$ ion. This observation was confirmed by the similitude of $H^+$ mobilities in the CMV and CMS membranes ($2.02\ 10^{-10}$ $m^2/s$ and $2.15\ 10^{-10}$ $m^2/s$ respectively for CMV and CMS). According to the polyelectrolyte conformation in the CMV and CMS membranes in sulfuric acid media published in previous papers [3,4], we can suppose, at first approximation, that the difference between the nickel ion mobilities in the membranes is mainly linked to the presence of the layer of positively charged ionic groups on the surface of the CMS membrane [5].

**References:**

1. S. Itoi. *Desalination*, **28(3)** (1979) 193-205.
2. B.V. Bruggen, A. Koninckx, C. Vandecasteele. *Wat. Res.*, 38 (2004) 1347-1353.
3. Le Xuan Tuan, M. Verbanck, C. Buess-Herman, H. D. Hurwitz. *J. Membrane Sci.*, **284** (2006) 67-78.
4. Le Xuan Tuan, C. Buess-Herman. *Chem. Phys. Lett.*, **434** (2007) 49-55.
5. Le Xuan Tuan. C. Buess-Herman, H.D. Hurwitz. *J. Phys. Chem. B*, submitted for publication.

First Regional Symposium on Electrochemistry of South-East Europe, Rovinj, Croatia, May 4-8, 2008.

O-3-68

# MICROBIAL DENITRIFICATION BY THE BACTERIA *Pseudomonas denitrificans* STIMULATED BY CONSTANT ELECTRIC FIELD

**T. Parvanova-Mancheva, V. Beschkov**

*Institute of Chemical Engineering, Bulgarian Academy of Sciences, 1113 Sofia, Bulgaria*
*E-mail: bioreac@bas.bg*

Nitrate and nitrite ions occur widely in a variety of process streams, such as those coming from the extensive use of fertilizers. There is a large number of mesophilic bacteria capable of utilizing nitrate as an electron acceptor instead of free oxygen under anoxic conditions converting it to nitrogen [1], following a reaction described by the consecutive steps of nitrate-to-nitrite conversion and nitrite reduction to gaseous nitrogen, as follows:

$$NO_3^- \rightarrow NO_2^- \rightarrow NO\ (g) \rightarrow N_2O\ (g) \rightarrow N_2\ (g) \qquad (1)$$

There are some efforts to use immobilized microbial cells for denitrification in waste water treatment [2,3] because of their longer operational stability and multiple use, particularly in continuous bioreactors.

There is another wide area of research dedicated to the bioelectrochemical reduction of nitrate [4-6]. There are several approaches in this direction. The presumption of one of them is to facilitate the microbial activity by cathode production of hydrogen, which is itself a strong nitrate reducer [5].

These studies deal with the galvanostatic performance with relatively high electric currents, i.e. up to 20 mA.

It is shown [4] that at potentiostatic regime and at very low electric currents (micro-ampers in order of magnitude) bacterial denitrification takes place with satisfactory rate and efficiency. The bio-electrochemical process was sensitive to the cathode potential and its optimum value was close to the standard potential of nitrate-to-nitrite reduction, i.e. 0.01 V *vs.* SHE.

A drawback of this approach is the sensitive balance between the microbial cell proliferation and nitrate reduction in continuous flow. The lack of such a balance (i.e. if the microbial growth is not high enough to maintain the constant cell concentration) may disturb irreversibly the bioreactor operation at shorter hydraulic retention times. Therefore it seems interesting to test the capacity for electrically stimulated nitrate biodegradation of microbial cells immobilized on solid support. We demonstrate such a denitrification potential for the cells of *Pseudomonas denitrificans* covalently bound to solid support operating in continuous stirred tank bioreactor at constant electric field at a potentiostatic regime. The experimental results for microbial nitrate reduction by covalently bound cells in continuous culture are shown in Fig. 2. Higher loading with nitrate solution is possible at lower initial concentrations, whereas at concentrations higher than 200 mg/l there is almost no difference.

Some results of the experiments for denitrification by immobilized cells with application of constant electric field are shown in Fig. 3. The comparison of the outlet nitrate concentrations observed in runs without and with electric field application shows that the wash-out dilution rates at electric field application are much higher compared to the referent ones. This trend is most visible for the highest initial nitrate concentration,300 mg/l, where equal denitrifications can be attained at three times higher dilution rates, i.e. three times higher feeding flow rates.

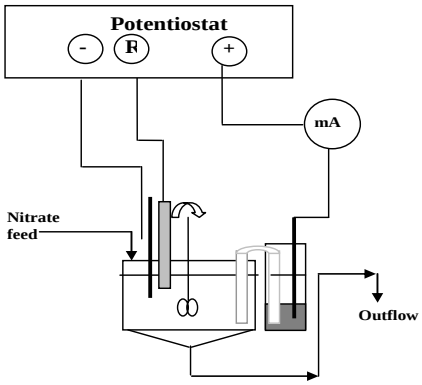


*Fig.1. Sketch of the experimental set-up.*

There are different possible explanations of this effect. Some authors explain it by reduction of hydrogen released on the cathode, or by pure electro-chemical reduction of nitrate. However, the current yield based on the measured electric current was about 0.01 C, whereas the expected stoichiometric yield is higher than 180 C.

We expect that the constant electric field stimulate the living cells, whereas this effect is maximal at certain value of the cathode potential.

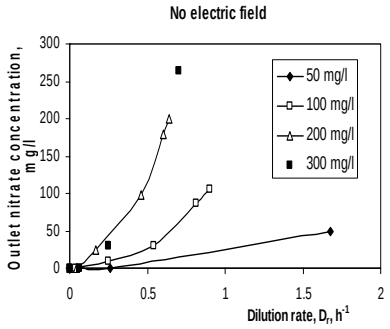


*Fig. 2. Nitrate reduction by immobilized cells in a continuous stirred tank bioreactor at without electric field.*

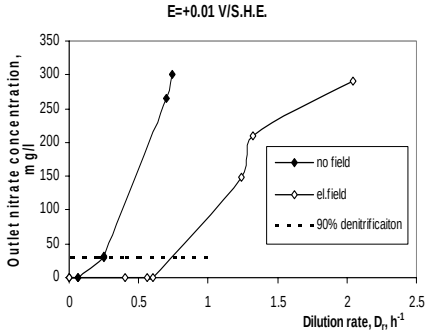


*Fig. 3. Comparison of the outlet nitrate concentrations for runs with and without application of electric field at different inlet concentrations.*

## Conclusion

The obtained experimental results lead us to the conclusion that the use of immobilized cells in continuous bioreactor for water denitrification leads to stable process without wash-out. When coupled with application of constant electric field, the denitrification process becomes more efficient since much higher flow rates are attainable. The effect of electric field becomes more significant at higher initial nitrate concentrations.

## References:

1. L. Foglar, F. Briski, L. Sipos, M. Vukovic, *Bioresource Technology* , **96** (2005) 879.

2. I. Garbayo, R. León, A.J. Vigara, C. Vílchez, *Bioresource Technol.* **81** (2002) 207.
3. I. Nilsson, S. Ohlson, *Appl. Microbiol.& Biotechnol.*, **14** (1982) 86.
4. V. Beschkov, S. Velizarov, S.N. Agathos, V. Lukova, *Biochem. Eng. J.* **17** (2004)141.
5. Z. Feleke, K. Araki,Y. Sakakibara, T. Watanabe, M. Kuroda, *Water Res.* **32** (1998) 2728.
6. A.M. Hayes, J.R.V. Flora, J. Khan, *Water Res.* **32** (1998) 2830.

First Regional Symposium on Electrochemistry of South-East Europe, Rovinj, Croatia, May 4-8, 2008.

O-3-69

# ELECTRO-SWITCHABLE SURFACES FOR HEAVY METAL WASTE TREATMENT: STUDY OF POLYACRYLIC ACID FILMS GRAFTED ON GOLD SURFACES

**T.X. Le, P. Viel, S. Palacin**

*Chemistry of Surfaces and Interfaces, CEA Saclay, DSM/DRECAM/SPCSI, F-91191, Gifsur-Yvette Cedex, France*

Application of electrode coated polymer on the basis of electrochemical switchable method for removal of heavy metal ions from wastewater has been described in the previous works [1-3]. Electro-switchable polymer films have numerous advantages over conventional ion exchange processes. It allows reaching very low concentrations and, more importantly, an easy release of heavy metal ions by simple application of potential. So far, promising results were only obtained in organic phase conditions [2] or with grafted polymer films that were initially prepared by cathodic electro-polymerisation in the highly stringent conditions (using distillated monomers, glove-box condition, highly cathodic potentials …) [1]. Real industrial applications require simple and low cost preparation methods. It is thus interesting to test our recently published Diazonium Induced Anchoring Process (DIAP), that provides grafted polymer films on any surface through a simple chemical process, in that context [4].

The principle of heavy metal ion treatment by polymer films relies on the intrinsic chelating or ion exchange properties of the chosen polymers towards the heavy metals ions. Polyvinylpyridine, polyvinylpyrrolidone, polyacrylic acid… can be considered as representative examples. In particular, polyacrylic acid (PAA) has been reported to be applicable to the treatment of several metals [5-7].The purpose of this work is to investigate PAA films chemically grafted on gold substrates as a pH-switchable chelating medium for capture and electro-induced release of several heavy metal ions. The grafted PAA film will be first characterized by IR, XPS and AFM in order to confirm the grafting on the gold surface by DIAP. Then we will study the electrochemical behaviour of the PAA-coated gold electrodes by impedance spectroscopy and cyclic voltammetry transition techniques in order to estimate their ability to be used in an electro-induced releasing process in contact with sodium sulfate electrolyte. As a broad-range chelating material, PAA is able to capture several heavy metal ions such as $Zn^{2+}$, $Cu^{2+}$, $Co^{2+}$ and $Ni^{2+}$ at low concentration. The release of those metal ions from the grafted PAA film was obtained under electro-induced-acidification by applying an anodic potential at the electrode to promote a localized water electrolysis. Such electrochemical pH-switchable films can be part of a secondary step-treatment after conventional ion exchange process or precipitation for treatment of aqueous effluents in order to reach very low concentration in heavy metal ions.

**References:**

1. P. Viel, S. Palacin, F. Descours, C. Bureau, F. Le Derf, J. Lyskawa, M. Sallé. *App. Surf. Sci.*, **212** (2003) 792-797.

2. J. Lyskawa, F. Le Derf, E. Levillain, M. Mazari, M. Sallé, L. Dubois, P. Viel, C. Bureau, S. Palacin. *J. Am. Chem. Soc.*, **126** (2004) 12194-12195.
3. P. Viel, L. Dubois, J. Lyskawa, M. Sallé, S. Palacin. *App. Surf. Sci.*, **253** (2007) 3263-3269.
4. V. Mevellec, S. Roussel, L. Tessier, G. Denieau, P. Viel, S. Palacin. *Chem. Mater.*, **19** (2007) 6323-6330.
5. R. D. Porasso, J. C. Benegas, M. A. G. T. van den Hoop. *J. Phys. Chem. B*, **103** (1999) 2361-2365.
6. A. El-Hag Ali, H. A. Shawky, H. A. Abd El Rehim, E. A. Hegazy. *Eur. Polym. J.*, **39** (2003) 2337-2344.
7. C. O. M'Bareck, Q. T. Nguyen, S. Alexandre, I. Zimmerlin. *J. Membr. Sci.*, **278** (2006) 10-18.

First Regional Symposium on Electrochemistry of South-East Europe, Rovinj, Croatia, May 4-8, 2008.

O-3-70

# SOLVENT EXTRACTION OF METALS AND THE ELECTROCHEMICAL BEHAVIOUR OF SUCH FORMED ORGANOMETALLIC COMPLEXES IN THE LOADED ORGANIC PHASE

**V. Stanković*, V. Fajnišević**

*Technical Faculty Bor, University of Belgrade; VJ 12; 19210 Bor, Serbia*
*E-mail: vstankovic@tf.bor.ac.yu*

Calixarenes are a class of oligo-molecules that are able to complex heavy- and precious metals but also some alkali and alkali-earth metals from water solutions [1,3]. Beside this, calixarenes are studied to be used for direct electrochemical detection of metal ions [2].

This work presents some results about the electrochemical behaviour of silver(I), lead(II) and palladium(II) complexes, formed in the solvent extraction with amide derivatives of calix[4]arene, when exposed to an electrode potential.

Solvent extraction of silver(I), lead(II) and palladium(II) nitrate from nitric acid solution was used as a model-system in the experiments. Dichloromethane solutions of calix[4]arene tetramide and calix[4]arene thiotetramide were used as extractants. In order to get an insight in the electrochemical behaviour of organo-metal complexes, experiments were carried out by using cyclic voltammetry and chronoamperometry, as well as the electrowinning of these metals from the loaded organic phase. To prevent the anodic oxidation of calixarenes at the electrowinning experiments were performed by two-phase electrolysis using the organic phase as a catholyte, while the aqueous phase served as an anolyte.

Experimental results showed a very high extraction degree of the targeted ions from the aqueous phase as well as a reasonably high electrowinning degree of metal from the organic phase during two-phase electrolysis. High current efficiency and low specific energy consumption were achieved, as well. The most important fact is the possibility to deposit metal without damaging the extractant, making it able to be recycled in the extraction step many times.

**References:**

1. A. F. Danil de Namur, M.T.Goitia, A.R.Casal, J.A.Villanueva-Salas; *PCCP*; (2001), **3**, 5242
2. R.Vataj, H. Ridaoui, A. Louati, V.Gabelica, S.Steyer and D. Matt; *J. Electroanal. Chem.*, **519** (2002) p. 12
3. V. Stankovic, I. Duo, C. Comninellis and F. Zonnevijlle; *J. Applied Electrochemistry*, **37** (2007) 1279

First Regional Symposium on Electrochemistry of South-East Europe, Rovinj, Croatia, May 4-8, 2008.

# CONTRIBUTIONS - POSTERS

P-1-001

## ELECTROCATALYSIS OF HYDROGEN EVOLUTION VIA IRIDIUM ELECTROLESS DEPOSITION ON NICKEL

**E. Guerrini, A. Colombo, M. Duca, S. Trasatti**

*Department of Physical Chemistry and Electrochemistry, University of Milan, Italy*
alessandra.colombo@unimi.it

Activation of cathodes is the key for less expensive hydrogen production.
A number of technologies have been proposed in the past decades, from alloy-based electrodes to thin layers of a different material (electrocatalyst) deposited on top of a conducting substrate. The consequence has been a dramatic decrease in overpotentials for the hydrogen evolution reaction (HER).
Since electrocatalysts are usually noble metals, or a mix of them with less precious components, thin-layer deposition is nowadays the most widely used technique. The most popular methods for thin-layer production involve consumption of energy:

i) Thermal decomposition: suitable precursors are decomposed at high temperatures to obtain kinetically stable electrocatalytic oxides;
ii) Electrodeposition: metals (or a mix of metal and metal-oxides) are deposited from an electroplating bath.

A third way for thin-layer formation is electroless deposition. In this method no external energy is provided to the system in order to deposit the noble metal onto the substrate. The wanted reaction is as follows:

$$M^{n+} + ne^- \rightarrow M^0 \qquad (1)$$

Electrons needed to drive this reaction are provided by a coupled oxidation reaction. In electroless deposition onto such supports as noble metals, the oxidation reaction occurs by means of a reducing agent pre-adsorbed on the surface, or by successive voltammetric treatments [1].
A different approach can be used if the supporting electronic conductor is a non-noble metal. As a prototype, in this study the substrate was Nickel. The corresponding oxidation reaction is:

$$Ni^0 \rightarrow Ni^{2+} + 2e^- \qquad (2)$$

A different approach can be used if the supporting electronic conductor is a non-noble metal. As a prototype, in this study the substrate was Nickel. The corresponding oxidation reaction is:

$$Ni^0 \rightarrow Ni^{2+} + 2e^- \qquad (2)$$

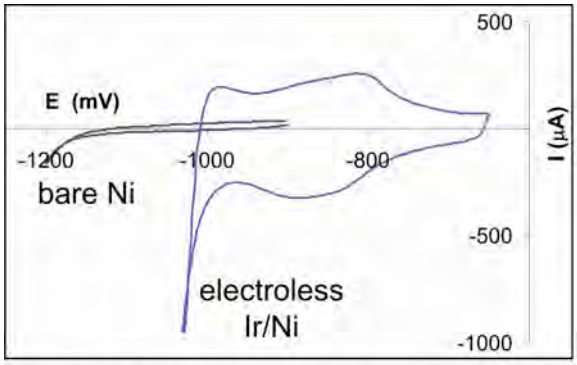


*Fig.1: Cyclic voltammetry of bare Nickel in comparison with electroless deposited Ir on Nickel*

A different approach can be used if the supporting electronic conductor is a non-noble metal. As a prototype, in this study the substrate was Nickel. The corresponding oxidation reaction is:

$$Ni^0 \rightarrow Ni^{2+} + 2e^- \qquad (2)$$

In a previous work [2], we demonstrated the effective possibility of Ruthenium spontaneous deposition onto Nickel electrodes. In the present work Iridium has been tested.

The deposition bath was prepared by dilution of a concentrated mother solution of Iridium(III) chloride and hydrochloric acid.

The factors explored in the experiments were:

a) method of preparation of the depositing solution;
b) Ageing of the solution;
c) Temperature of the deposition bath.

Evidence of Ir deposition was obtained by means of electrochemical and non-electrochemical techniques. The former includes cyclic voltammetry (Fig. 1), OCP measurements and polarization curves. The latter were UV-Vis spectra of the depositing solution, and SEM micrographs.

Unlike Ruthenium, Iridium deposition entails control of bath acidity. The reaction of Ni oxidation in hydrochloric acid solution provides electrons to both Iridium and proton reduction. Strong acidity promotes $H_2$ evolution and thwarts Ir discharge. Low acidity inhibits Ni dissolution. Intermediate acidity gives rise to electrodes active towards the reaction of hydrogen evolution (Fig. 2).

Cyclic voltammetry revealed the presence of different Ir species, in different oxidation states (metal, oxide, hydroxide). Despite the mixed chemical composition, only electrodes with metallic Iridium were stable in time.

The electrocatalytic activity of the electrodes, if correlated with UV-Vis spectra of the corresponding deposition solutions, showed a definite decrease as the depositon bath became older (> 3-4 days). This suggests that the species of ridium complex present in the hydrochloric acid solution are a crucial factor for the course of the reaction.

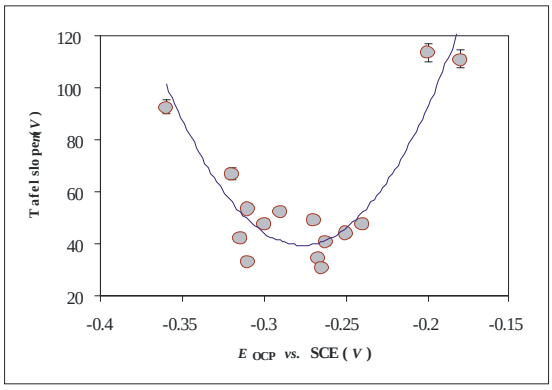


*Fig.2: Open circuit potential of the deposition processes vs. Tafel slope for $H_2$ evolution reaction.*

**References:**

[1] A. Crown, A. Wieckowski, *Phys. Chem. Chem. Phys*. **3** (2001), 3290
[2] I. Bianchi, E. Guerrini, S. Trasatti, *Chem. Phys*., **319** (2005), 192-199.

First Regional Symposium on Electrochemistry of South-East Europe, Rovinj, Croatia, May 4-8, 2008.

P-1-002

# INVESTIGATION OF HYDROGEN EVOLUTION REACTION IN SEAWATER ELECTROLYTE ON VARIOUS NiW AND NiFe ALLOYS DEPOSITIONS

**L. Anicai[1], A. Florea[1], M. Buda[2], T. Visan[2]**

*[1]Div.of Ecological Technologies Development, PETROMSERVICE SA, Calea Grivitei 8-10, 010772, Bucharest, Romania, E-mail: lanicai@itcnet.ro*
*[2]Department of Physical Chemistry and Applied Electrochemistry, POLITEHNICA University of Bucharest, Calea Grivitei 132, 010737, Bucharest, Romania*

In the last years the confidence in the potential use of hydrogen as a significant energy and fuel source considerably increased, a main target being its application in the operation of fuel cells. In a future hydrogen based economy with no $CO_2$ emissions, the water electrolysis should be taken into consideration to be applied on a larger scale. With this in view, the use of seawater, a strongly conductive electrolyte, attracted a sustained attention.

In the case of hydrogen production through seawater electrolysis one of the main targets is to develop more active cathodic materials as compared with black platinum, involving electrodeposition. In order to optimize the cathodic efficiency of hydrogen evolution reaction there are sustained preoccupations to obtain and characterize various cathodic materials involving different formation procedure including electrodeposition, taking into account the incorporation of electrocatalytic elements, as volcano curve described by Norskov et al.[1] suggests. The most of the cahodic materials used as hydrogen electrodes during water electrolysis are based on Ni, including binary and ternary alloys that offer superior performances as compared with pure nickel.

With this in view, the paper presents some preliminary experimental results on the investigation of some Ni alloys electrodepositions, respectively NiW and NiFe ones, as potential cathodic materials suitable for hydrogen evolution reaction during seawater electrolysis. They have been evaluated taking into account the obtained Tafel slopes values and hydrogen production rate *vs.* the applied current, the constructive type and shape.

To investigate the hydrogen electrochemical reduction reaction there have been recorded potentiodynamic polarization curves at a sweep rate of 10 mV/s as well as galvanostatic and potentiostatic transients in natural seawater, involving a Zahner IM6e electrochemical equipment. As working electrodes, NiW (7-20% W) and NiFe (20-25%) electrodeposited alloys applied onto brass substrates as metallic strips and sieves have been investigated, with a constant geometrical surface of 0.64 $cm^2$. For comparison the same experimental sequence has been applied on pure Ni and Pt electrodes. An Ag/AgCl reference electrode and a Pt counterelectrode have been also involved.

To evaluate the produced hydrogen amount through seawater electrolysis as a function of the applied current and cathodic metallic material, an experimental

electrochemical cell was used, with a volume of 150 $cm^3$ for each cathodic and anodic space separated by a PTFE or nylon filter membrane with pore sizes of 0.2-0.45 μm to avoid the mixture of reaction products and to allow the measurement of the evolved hydrogen through an eudiometer.
Based on cathodic polarization curves processing, Tafel slopes between 100-200 mV/decade have been determined, with lower values in the case of alloys electrodeposition onto the sieve type substrate as well as in the case of NiW alloy as compared with NiFe one. Figure 1 shows an example of the recorded cathodic polarization curves in semilogarithmic coordinates for NiW alloy electrodeposition onto various metallic substrate types in seawater electrolyte.

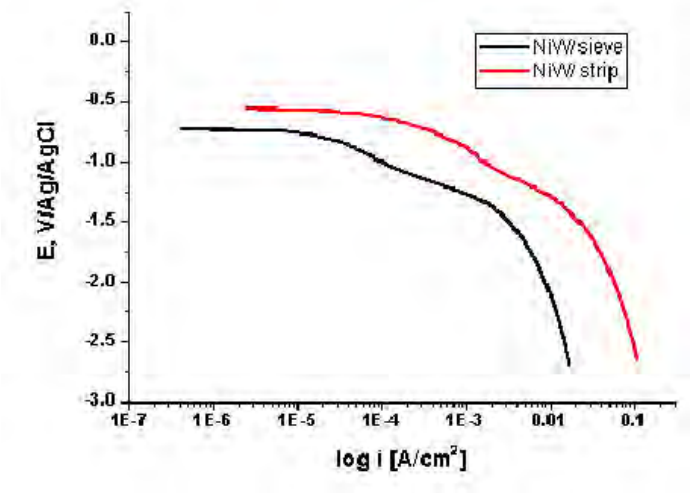


*Figure 1 – Tafel representations (E-log i) for NiW alloy (18%W) electrodeposition onto various metallic substrates types at t=25°C (10 mV/s)*

The investigated cathodic materials have proved the possibility to operate seawater electrolysis at current densities of 5-15 $A/dm^2$ even in stationary conditions, with hydrogen production efficiency of minimum 95%. For current densities of minimum 5-7 $A/dm^2$ hydrogen flows of about 600 $cm^3$ have been determined.
Additional considerations regarding the optimization of hydrogen production through various technological conditions will be also discussed.

***Acknowledgements:*** *Part of this work was supported by the Romanian Ministry of Education and Research, CEEX Program, under Research Contract No. 103/P8/2005.*

**References:**

1. J.K. Norskov, T. Bligaard, A. Logadottir, J.R.Kitchin, J.G. Chen, S. Pandelov, si U.Stimming, *J.Electrochem.Soc.*, **152(3)**, J23, 2005.

First Regional Symposium on Electrochemistry of South-East Europe, Rovinj, Croatia, May 4-8, 2008.

P-1-003

# EFFECT OF PURIFICATION OF MULTIWALLED CARBON NANOTUBES (MWCNTs) ON ELECTROCATALYTIC ACTIVITY OF CATALYSTS FOR HYDROGEN EVOLUTION BASED ON Me-$TiO_2$-MWCNTs

**P. Paunović, A.T. Dimitrov, O. Popovski, E. Lefterova[1], A. Grozdanov, Đ. Petruševski[2], A. Tomova, D. Slavkov, S. Hadži Jordanov**

*Faculty of Technology and Metallurgy, University „Sts. Cyril and Methodius", Skopje, pericap@tmf.ukim.edu.mk*
*[1]Institute of Electrochemistry and EnergySystems, Bulgarian Academy of Sciences, Sofia*
*[2]Faculty of Natural Sciences and Mathematics, University „Sts. Cyril and Methodius", Skopje*

As a catalyst support of mixed hypo-hyper *d*-electrocatalysts based on non-platinum metals or reduced platinum loading multiwalled carbon nanotubes (MWCNTsTs) were used. MWCNTs prepared by electrolysis in molten Li salts [1] and similar comercial MWCNTs (*Guangzhou Yorkpoint Energy Company, China*) were used. Their physical characteristics were investigated by means of DTA/TGA analysis, Raman spectroscopy, SEM and TEM analysis [2]. Their application as a support of electrocatalysts for hydrogen evolution was shown as a superior related to the traditional carbon support materials – carbon black (Vulcan XC-72) [3]. Electrocatalysts consisted of 10% Me + 18 $TiO_2$ + carbon support (Me = Co, Ni,) [4,5]. In order to improve performances of these catalysts, purification and activation of MWCNTs in acid medium was carried out.

Physical and structural changes of MWCNTs and electrocatalysts were observed by the above mentioned techniqes including and infrared spectroscopy. As a result of both shortening and opening of carbon nanotubes, better dispersion of metallic particles as an active catalytic centers, was achieved. With other words trans-particle and inter-particle porosity of the electrocatalytic material was improved. This implies increase of catalytic activity for hydrogen evolution. Electrocatalysts having the same composition as above, with different hyper *d*-metallic phase were investigated, such as: Co, Pt, CoPt with mass ratio 1:4 and 1:1. The best performances has shown electrocatalyst containing 10% CoPt(1:1) + 18% $TiO_2$ + acivated MWCNTs.

## References:

[1] A. T. Dimitrov, G.Z. Chen, I.A. Kinloch, D.J. Fray, *Electrochim.Acta*, **48** (2002) 91-102
[2] P. Paunović, A. T. Dimitrov, Physical Characterization of Carbon Nanotubes Produced by Electrolysis in Lithium Molten Salts, NATO Advanced Study Institute, *Book of Abstracts*, Sinaia, Romania, June 4-15, (2007) p. 47
[3] P. Paunović, A.T. Dimitrov, O. Popovski, D. Slavkov, S. Hadži Jordanov, *Maced. J. Chem. Chem. Eng.*, **26** (2) 87– 93 (2007)
[4] P. Paunović, O. Popovski, A. T. Dimitrov, D. Slavkov, E. Lefterova and S. Hadži Jordanov, *Electrochimica Acta*, **52**, 1610-1618 (2006)
[5] P. Paunović, O. Popovski, A. T. Dimitrov, D. Slavkov, E. Lefterova and S. Hadži Jordanov, *Electrochimica Acta*, **52**, 4640-4648 (2007)

First Regional Symposium on Electrochemistry of South-East Europe, Rovinj, Croatia, May 4-8, 2008.

P-1-004

# THE INFLUENCE OF WATER SOLUBLE POLYMERES ON THE HYDROGEN EVOLUTION REACTION ON Ni – ELECTRODE

**N.V. Sotskaya , Yu.G. Kravtsova*, Yu.V. Hohlov**

*Voronezh State University,Voronezh, Russia, *ushka2004@list.ru*

The ion-exchange materials are having been used successfully for a long time as the membranes, sorbents, catalysts and ets. in the different science and industry branches. For the last years the interest to the water soluble polymers (polyelectrolytes) was increasing, because of the fortunate combination of the high-molecular compounds and electrolytes physico-chemical properties. So, the polyelectrolytes have achieved the resistant position in the wide industrial spectra.
As for the electrochemistry, the water soluble polymers ability to complexation with the heavy and transition metals ions is applied in the membrane segregation methods and in the inversion voltammetric determination of the metals low quantities. Some researchers represent data on the cation-exchange polymeric additive Nafion effecting the electrodeposition of lead dioxide. It has been shown there, that the polymers adsorption on the electrode plays the significant role in the reaction kinetics.
On the present moment the question of great importance is the elucidating of the functional groups of water soluble polymers influence on the electrode reaction kinetics, that has become the aim of our work.
The derivatives of cation exchanger CB-4 and anion exchanger AN-251: polymethacrylic acid (PMA, M ~ 10.000 g/mol) and polyvinyl-imidazole (PVI, M ~ 14.000 g/mol), correspondingly, were chosen as the polyelectrolytes additives. The carboxyl groups are the ionized groups in the PMA molecule, and PVI is the polyelectrolyte, because of the azole cycle presence, where the ionized group is the nitrogen atom in the imidazole ring. The investigating model reaction is the cathodic hydrogen evolution reaction (HER) on Ni – electrode with well known kinetic mechanism.

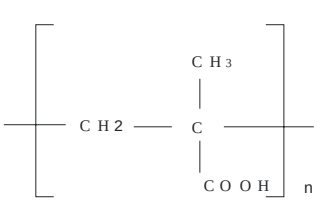


*The PMA elementary unit*

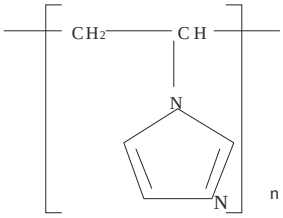


*The PVI elementary unit*

According to the contemporary electrochemical conception the hydrogen evolution reaction in acid media ($2H_3O^+ + 2e \leftrightarrow H_2 + 2H_2O$) on the metal electrode M proceeds via the following mechanism (Eq. 1 – 3):

$$M + H_3O^+ + e^- \rightarrow M - H_{ads} + H_2O, \quad (1)$$

$$M - H_{ads} + H_3O^+ e^- \leftrightarrow H_2 \uparrow + M + H_2O, \quad (2)$$

$$2M - H_{ads} \leftrightarrow H_2 \uparrow + 2M. \quad (3)$$

Here M – is the free metal surface (in this case, Ni), $M - H_{ads}$ – is the adsorbed atomic hydrogen. For the metals, being the good catalysts of HER, reaction (3) – is the rate determining stage at the low overpotentials $\eta_H$. Some authors suggest, that HER on Ni and its alloys occurs via the Volmer-Heyrovskii mechanism (when the stage (1) - is the limiting one and the hydrogen reducing takes place according the reaction (2)). In any case, the reaction kinetics satisfiers the Tafel equation (Eq. 4):

$$\eta = \text{const} + RT/\alpha F \cdot \ln i, \quad (4)$$

or, simply: $$\eta = a + b \lg i, \quad (5)$$

where $\eta$ is HER overpotential, a and b (kinetic parameters) are the constants for this system. The b value is one of the reaction mechanism criteria. When $\eta_H$ increases, the Heyrovskii reaction (Eq. 2) becomes the limiting stage.

The investigations of the polyelectrolytes catalytic influence on the hydrogen evolution reaction kinetics Žwere carried out with voltameter method in the conventional three-electrode cell with $V_w$ = 100 ml. The working electrode was the compact Ni (99,99), armed into the epoxy resin. The copper-sulfate reference electrode was connected with Luggin capillary via the electrolytic key. The Pt served as the counter electrode.

The polymeric additives (the precise volume of saturated PMA solution and the weighted quantity of PVI) were dissolved preliminary in distilled water, and then the required volume of new solution was introduced into the cell for the polyelectrolyte necessary concentration achievement. The PMA and PVI concentrations in the working solutions were $10^{-8} \div 0{,}75$ g/l.

In sake for the HER kinetic parameters elucidating, the potentiodinamic curves were rebuilt in tafel coordinates.

It has been shown, that water soluble complexating polymers introducing into 0,05 M $H_2SO_4$ solution decreased effectively the HER overpotential and enhanced significantly this process rate because of the polyelectrolytes specific adsorption and «bridge» effect on the electrode surface. The maximal catalytic influence is observed at the minima polymethacrylic acid concentration, that is explained by its small molecular weight and by the phenomena of the Ni – surface blocking at the sufficiently high PMA consumptions in the electrolyte. The polyvinylimidazole concentration changes don′t influence the hydrogen evolution reaction rate because of the PVI great molecular weight and its moluculars selfassociation, resulting in the Ni – electrode surface blocking at low quantities in the electrolyte.

First Regional Symposium on Electrochemistry of South-East Europe, Rovinj, Croatia, May 4-8, 2008.

P-1-005

# ELECTROCHEMICAL CHARACTERISATION OF SUBSTITUTED $ABO_3$ PEROVSKITES USED AS SOLID ELECTROLYTE FOR WATER VAPOUR ELECTROLYSIS

**C. Deslouis, M. Keddam, K. Rahmouni*, H. Takenouti, O. Lacroix, B. Sala, S. Willemin**

*UPR 15 du CNRS LISE, UPMC Univ Paris 06, 3 rue Galilée, 94200 Ivry sur Seine, France, E-mail: Rahmouni@courriel.upmc.fr*
*Areva NP, IEM, Place Eugène Bataillon, 34095 Montpellier, France;*

Intermediate temperature proton conducting ceramics have wide applications in the areas of fuel cells, electrolysers, and hydrogen separation. The perovkite materials are of interest due to their good stability and high proton conductivity [1,2]. The conductivity of those ceramic reported in the literature is generally less than 10 mS/cm, even at high temperatures.
In this work the electrochemical behaviour of two proton conducting ceramics $BaZrO_3$ and $CaZrO_3$ [3] was investigate by impedance spectroscopy, and the structural characterisation was realised bay TEM (Transmission Electron Microscopy) and EBSD (Electron Back Scattering Diffraction).
TEM and EBSD analyses show crystalline structure and the grain size of $CaZrO_3$ is larger than $BaZrO_3$.
In impedance spectra, the high frequency loops are allocated to the response of grain and grain boundaries; their contribution was separated by means of equivalent circuit modelling including the dielectric relaxation. The results show a higher conductivity with increasing of temperature. $BaZrO_3$ exhibited a better conducting property.

**Key words:** EIS, EBSD, Proton conducting ceramics, Intermediate temperature

**References:**

[1] B. Sala, S. Willemin, O. Lacroix, Ph .Colomban, K. Rahmouni, A. Julbe, H. Takenouti, "*Characterisation of proton incorporation in perovskite-type structure"*16th World Hydrogen Energy Conference, June 2006, Lyon (France).
[2] S. Willemin, O. Lacroix, B. Sala, Ph. Colomban, A. Julbe, A. Ayral, H. Takenouti, J-P. Py, "*Synthesis and characterisation of proton conducting ceramic membranes*", Desalination, 200 (2006) 92-94
[3] O. Lacroix, Dissertation thesis, "*Etude électrochimiques des électrolytes à conduction protonique de type perovskite destines à l'électrolyseur de la vapeur entre 400 °C et 600 °C*", Université de Montpellier II, Décembre 2007.

First Regional Symposium on Electrochemistry of South-East Europe, Rovinj, Croatia, May 4-8, 2008.

P-1-006

# DIFFERENTIAL IMPEDANCE ANALYSIS FOR CHARACTERIZATION OF LSM-YSZ COMPOSITE ELECTRODES AT DIFFERENT CELL GEOMETRY

**D. Vladikova[1], Z. Stoynov[1], P. Carpanese[2] A. Barbucci[2], M. Viviani[3]**

*[1]Institute of Electrochemistry and Energy – BAS, 10 Acad. G. Bonchev, 1113 Sofia, Bulgaria, d.vladikova@bas.bg*
*[2]DIChePUniversità di Genova, P.le Kennedy 1, 16129 Genova, Italy*
*[3]CNR, IENI, V. De Marini 6, 16149 Genova, Italy*

## 1. Introduction

A basic direction in the attempts for advancement in solid oxide fuel cells (SOFC) is the improvement of the oxygen reduction reaction. Composite structures based on a combination of Sr-doped $LaMnO_3$ (LSM) and yttria stabilized zirconia (YSZ), which have excellent compatibility, are used for enhancement of the cathode behaviour. It is supposed that the addition of an electrolyte to the cathode material increases the number of triple phase boundary (tpb) points and thus the ion conductivity of the electrode. In addition to the complex chemistry and electrochemistry, composite LSM-YSZ cathodes have more complicated multiphase porous microstructure. Despite a wealth of impedance studies, there is a big variety in the reported results for the polarization resistance. One possible explanation is the strong dependence of this parameter on the microstructure which is governed by the sintering conditions. Recently the influence of the measurement cell geometry became an active subject of debate [1,2]. Theoretical calculations of Adler for three-electrode configuration predict a big distortion of the Nyquist plots due to small misalignment of the cathode and anode and difference in their kinetics [1]. This talk presents results obtained from comparative studies of LSM-YSZ cathode materials on symmetric cell and three-electrode electrolyte supported cell with Pt reference electrode, applying the technique of the Differential Impedance Analysis (DIA) [3,4]. The advantage of this approach for data analysis is that it does not use a preliminary working hypothesis for model recognition.

## 2. Experimental

The following cell configurations were used: LSM-YSZ|YSZ|LSM|YSZ and LSM-YSZ|YSZ|Pt + Pt reference electrode. The impedance measurements were performed in the temperature range 650-850$^{o}$C at OVC (to avoid the activation observed after polarization [2]) and different oxygen partial pressure. The quality of the measured data was improved by applying a procedure for elimination of the errors coming from the parasitic inductance [4].

## 3. Results and Discussion

The complicated shape of the obtained Nyquist plots suggests a multi-step process. The results from the DIA analysis are similar for the two cell configurations. A two step reaction is recognized. The high frequency part of the impedance describes a time-constant process, corresponding to the charge transfer. For the low frequency zone, Bounded Constant Phase Element (BCP) is recognized. This element describes the impedance of a bounded homogeneous layer with CPE type conductivity in the elementary volume and a finite conductivity at DC [4]. The recognition of BCP behaviour is an experimental evidence for transport of oxygen ions through the bulk of the LSM phase, as it is accepted to be in mixed conductors with high ionic conductivity. This step is the rate-limiting one.

DIA ensures also parametric identification of the effective resistance for the 2 main steps and calculation of their activation energies. The temperature dependence of the resistivity has similar behaviour for the two configurations (Fig. 1). The activation energy of the charge transfer $E_a$ increases with the temperature(Fig. 1a). This result is in agreement with the hypothesis of Maning et all [5] for impediments in the charge transfer at higher temperatures. The activation energy for Step II is frequency invariant (Fig. 1b). The differences in the resistivity (much smaller that the reported in the literature results) and the activation energy for the two configurations can be attributed to some variations in the technological procedure which cause microstructural changes, as well as to the different anode.

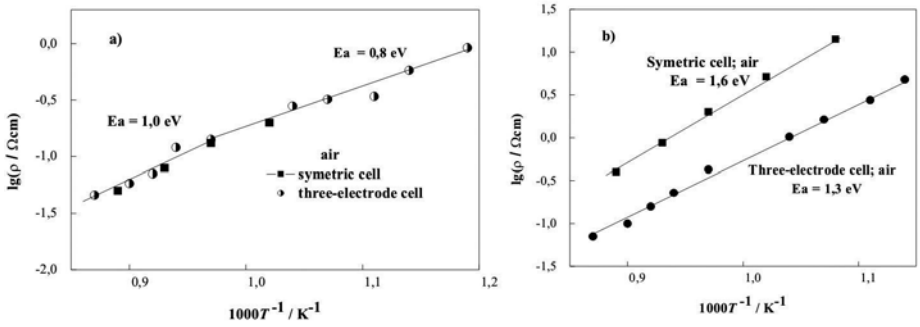


*Fig.1. Arrhenius plots for symmetric (•) and three- electrode (▲) measurements: (a) for step I; (b) for step II.*

The oxygen partial pressure influences only the rate limiting step II. Neighther the electrolyte behaviour, nor the charge transfer process are dependent on this parameter. The results show that the best performance of the electrode material is obtained at 1 atm, which is the highest pressure applied in this study. Since its increase above 0,5 atm has less pronounced effect, this value could be proposed as an optimal one.

The obtained results show that the two configurations - symetric and three-electrode cell, give reliable data. The application of electrolyte supported cell with reference electrode avoids possible distortions in the Nyquist plot, which confirms obsevations of other authors [2]. The study of the composite LSM-YSZ cathode

material will be continued in a complete cell at different oxygen partial pressure by performance of a comparative analysis with a symetric cell.

**References**

1. S.B. Adler, L. *Electrochem. Soc.* **149** (2002) E166.
2. S. McIntosh,S.B. Adler, J.M. Vohs, R.J. Gorte, Electrochem. *Nd Solid State Letters*, **7** (2004) A111.
3. D. Vladikova, Z. Stoynov, *J. Electroanal. Chem.* **572** (2004) 377.
4. Z. Stoynov, D. Vladkova, Differential Impedance Analysis, Marin Drinov Academic Publishig House, 2005, Sofia.
5. P.S. Maning, J.D. Sirman, J.A. Kilner, *Solid State Ionics* **93** (1997) 125.

First Regional Symposium on Electrochemistry of South-East Europe, Rovinj, Croatia, May 4-8, 2008.

P-1-007

# ELECTROCHEMICAL BEHAVIOUR OF TIN SPECIES AND TIN OXIDE-BASED CERAMICS IN HIGH TEMPERATURE IONIC LIQUIDS FOR ALUMINIUM ELECTROLYSIS

**A.M. Popescu, V. Constantin**

*Romanian Academy, „Ilie Murgulescu" Institute of Physical Chemistry,Splaiul Independentei 202, Bucharest-006021,Romania, virgilconstantin@yahoo.com*

Oxygen evolving, non-consumable anodes are being developed for use in industrial aluminium production. Oxide ceramics have been studied as inert anodes for aluminium electrowinning by the Hall-Heroult process because of their stability in the presence of oxygen. However, most of the examined candidate materials exhibit a finite solubility in the cryolite melt, which leads to unacceptably high metal contamination levels in the electrowon aluminium. Of the oxides considered, $SnO_2$ has received the most attention because of low solubility 2 and high electrical conductivity achieved by doping.

The material chosen for this study consisted of $SnO_2$ doped with $Sb_2O_3$ (to achieve electrical conductivity) and CuO (added as sintering aid) and also with $La_2O_3$, ZnO, $Ce_2O_3$.

Steady state current-voltage measurements at galvanostatic conditions and cyclic voltametric experiments were performed in a cryolite base melt of CR=molNaF/$AlF_3$=2.7 with 5wt%$CaF_2$ and 5wt%$Al_2O_3$; liquid Al cathode and $Al/Al^{3+}$ or Pt reference/or quasi reference electrode were used. The samples were tested in a vertical electrode arrangement.

Comparative measurements of anodic polarization were performed with those tin oxide-based anodes, classical carbon anodes (of different types) and platinum anodes. The overvoltages obtained were 3-4 times lower on the tin oxide-based anodes than on carbon anodes and closely to data on Pt. Tafel coefficients and derived kinetic parameters were calculated. Polarization measurements show high ohmic drops that can be generated by the contact between the ceramic and metallic wire.

Starting from literature data and taking in account all our previous researches on tin-dioxide based inert anodes [1-5], we choose for the cyclic voltammetry (CV) measurements only two compositions: (S1) 98%$SnO_2$ + 1%$Sb_2O_3$ + 1%CuO and (S2) 96%$SnO_2$ + 2%$Sb_2O_3$ + 2%CuO.

The oxygen discharge occurs via two electrons exchange step with no secondary reactions (as proved by Figure 1 and 2) and the process is also reversible.

The corrosion behaviour of S1 and S2 was studied and it was found that those tin oxide-based anodes exhibit very low corrosion rates in electrolytes with high alumina content and current densities. Lowering anode-cathode distance may not result in the corrosion of the anode. We proposed also a mechanism of corrosion for those tin oxide-based anodes correlated with the structure and microstructure of those materials. Over the range studied no apparent disintegration of the anode occurred provided that the bath was saturated with alumina.

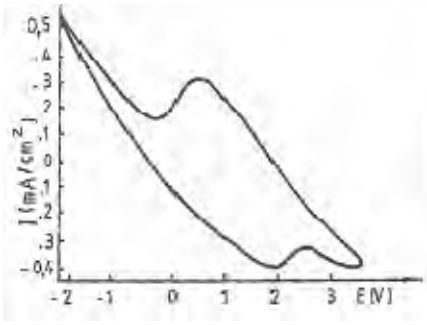


*Fig 1. CV curve using RE=Al/Al³⁺*

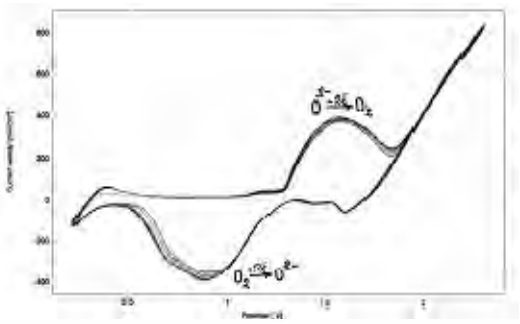

*Fig 2. CV curve using QRE =Pt*

However since all the oxide materials tested exhibit certain solubility in the electrolyte a systematic study of the solubility of the $SnO_2$ and different $SnO_2$-based anodes was undertaken.

In order to determine the solubility CV measurements were performed on platinum and glassy carbon electrode in molten cryolite and cryolite-alumina melts containing additions of $SnO_2$ and $SnF_2$. The experiments were made varying $Al_2O_3$ concentrations, CR and temperature.
Those voltammograms (e.g. Figure 3 and 4) showed peaks which were attributed to the presence of oxidation states of tin in the melt. Some other peaks were only oscillations due to the formation of volatile species, such as $SnF_2$ and $SnF_4$, especially in the melts containing dissolved alumina. The reactions involving dissolved tin species were found to behave reversible.

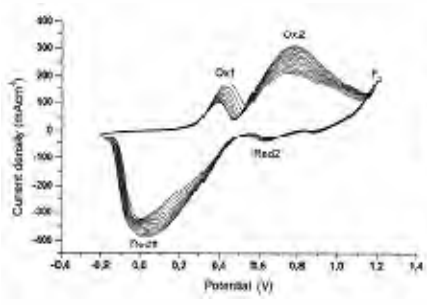


*Fig. 3 CV of dissolution of $SnO_2$ in cryolite-alumina on a Pt electrode*

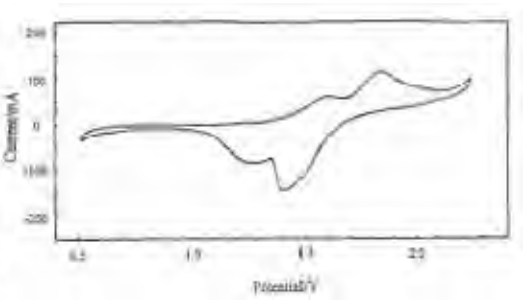


*Fig. 4. CV of dissolution of $SnF_2$ in cryolite on a Pt electrode*

Also by this study (where 2Ox peaks and corresponding 2Red peaks were observed) we conclude that chemical dissolution of $SnO_2$ can be expressed by:

$$SnO_{2(diss)} + 4/3\ AlF_3 = SnF_{4(diss)} + 2/3\ Al_2O_3$$

$$SnF_{4(diss)} + 4/3\ Al = Sn + 4/3\ AlF_{3(diss)}$$

The absence of ripples in Figure 4 indicates that a stable Sn(IV) species is formed in this case. This is due to the presence of $SnO_2$ included in the system because of the boron nitride tube used for the reference electrode. It was found that small amount of $SnO_2$ stabilized dissolved tin species.
So most likely dissolved ion of $SnO_2$ in cryolite-alumina melts is $SnO_2AlF_6^{3-}$ at all $Al_2O_3$ concentrations, while below 1wt%$Al_2O_3$ the oxyfluorides $SnOF_4^{4-}$ are predominant. The presence of $Al_2O_3$ was found to stabilize the dissolved tin species. Also anodic precipitation of $SnO_2$ on platinum was observed.
Unfortunately for the practical point of view, unacceptably high levels of Sn in the electrowon aluminum have been repeatedly observed. Finnaly it has been proposed that the corrosion of the $Sn0_2$ is through chemical attack by dissolved aluminum, which is present at a level of several tenths of a percent.

## References:

[1] A.M. Popescu, S. Zuca, S. Mihaiu, V. Constantin, Progress in Molten salts Chemistry 1, Eds.R.W.Berg & R.H. Hjuler, Elsevier, ISBN:2-84299-249-0, 2000, p.417.
[2] A.M. Popescu, S. Mihaiu, S. Zuca, *Z.Naturforsch.*, **57a**, 2002, p.71.
[3] A.M. Popescu, S. Zuca, M. Gaune-Escard, *Proceed.Intern. Symp.on Ionic Liquids*, France, 2003,491.
[4] A.M. Popescu, M.Gaune-Escard, S. Zuca, S. Mihaiu, V. Constantin, S.Malyovanyi, Proceed. *EUCHEM-Molten Salts Conference*, Poland, ISSN 0239-6661, 2004, p.287.
[5] A.M. Popescu, S. Mihaiu, V. Constantin, *Intern. Rom. Conf. Phys. Chem* -12 (ROMPHYSCHEM), BA-p110.

First Regional Symposium on Electrochemistry of South-East Europe, Rovinj, Croatia, May 4-8, 2008.

P-1-008

# THE FUEL CELL INDUSTRIAL APPLICATION: ENERGY SAVING AND ENVIRONMENTAL PROTECTION IN ELECTROCHEMICAL CHLOR-ALKALI PLANTS USING PEMFC

**I. Iordache[1,4], A. Schervan[2], A. Delfrate[2], M. Iordache[3]**

*1. ICSI, 4 Uzinei Str., 240050 RM. Valcea, Romania*
*2. UHDENORA SpA, Via Bistolfi 35, 20123 Milano, Italy*
*3. INCD-ECOIND, 1 Uzinei Str., 240050 RM. Valcea, Romania*
*4. OLTCHIM, 1 Uzinei Str., 240050 RM. Valcea, Romania*
*Corresponding author E-mail: iordacheioan@k.ro*

The aim of this presentation is to point out some ideas about fuel cell and chlor-alkali state of the art and the possibility to use both electrochemical applications in the energy saving and environmental protection.
A fuel cell produces a DC (direct current) voltage that can be used to power motors, lights or any number of electrical appliances. Fuel cells have many uses, the following are all already in use today. Until at this moment, solid oxide fuel cells (SOFCs) have demonstrated very good performance in combined-cycle applications. SOFCs are a promising option for high-powered applications, such as industrial uses or central electricity-generating stations. Proton Exchange Membrane Fuel Cells (PEMFC) appears as one of the most promising energy conversion technologies presently under development. They are suitable for decentralized combined heat and power production as well as for mobile applications, especially in road vehicles. Today's PEMFCs need pure and clean hydrogen as fuel which may come from chemical processes, from fossil energy resources and finally from renewable energy sources. Suitable fuel supply, conversion and conditioning concepts and technologies are necessary in each case [1].
One of the earliest markets applications are using of fuel cells for recovering hydrogen from industrial chlor-alkali processes (electrolysis process) [2].
UHDENORA and OLTCHIM SA have contacts for the installation of the first industrial fuel cell plant, 2 MW, at the OLTCHIM's chlor-alkali production site at Ramnicu Valcea, Romania. One similar application, 120 kW, was installed at a sodium chlorate production plant, Caffaro Chimica, Brescia, Italy.
The goal of those kinds of approaches is to produce clean electricity by using the hydrogen co-generated in the electrolytic process [3].
Premises of energy save and environmental protection in chlor-alkali industry using PEMFC:
1. Fuel cell reality [4, 5],

- more than 2500 stationary fuel cell systems have been installed all over the world,
- around 55 stationary PMEFC applications over the world. Some of them have an high installed power, 125 or 250 kW, but the biggest majority provide power between 1 and 5 kW,

- Nuvera, Uhdenora and Caffaro have installed and started up of the first industrial fuel cell system for electricity production and savings in the electrochemical industry, Caffaro Chimica, Brescia, Italy.

2. Chlor-alkali reality [6, 7],

- the recycled or re-used hydrogen produced by the chlor-alkali plants was less than 90% in 2006 and the target will not exceed 95% in 2010,
- at each tone of chloride is produced 28 kg (310 $Nm^3$) of hydrogen,
- the world chloride capacity was estimated to approximate 60 million metric tons (18.6 billions $Nm^3$) .

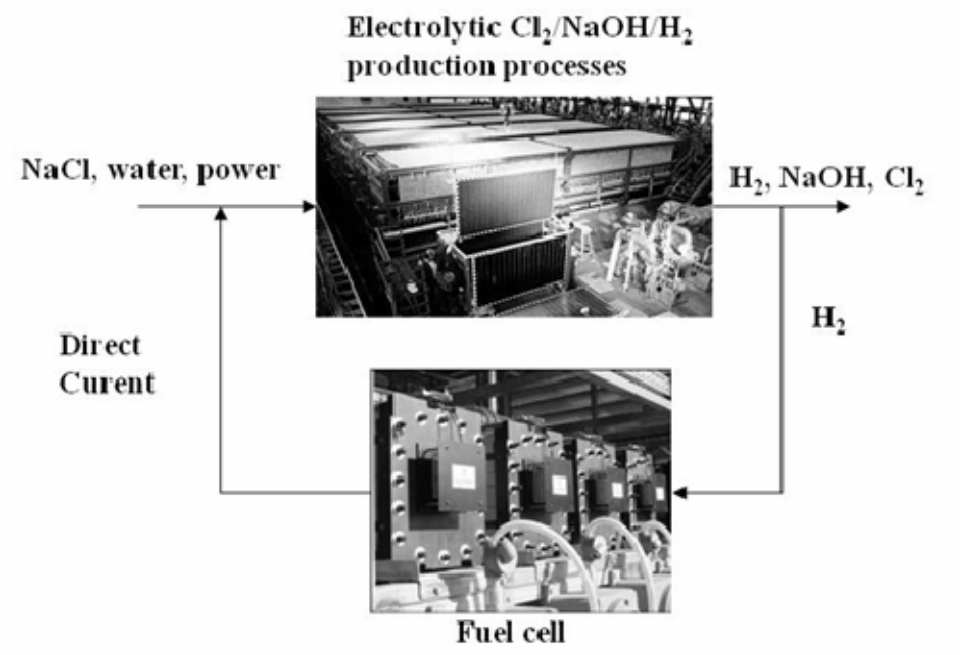


*Fig. 1. Integration of fuel cells in the DC circuit of a chlor alkali plant* [3]

**Reference:**

1. Electric and Lighting Industry Biennial, September 29th, Buenos Aires,
2. Faita et al., U.S. Patent 6 423 203,
3. $H_2$_Fuel_Cells_Millenium Convergence, September 21st, 2007, Bucharest,
4. www.fuelcells.org,
5. www.nuvera.com,
6. www.pvcinsight.com,
7. www.eurochlor.org Chlor-Alkali Market Report, no. 152, 2007.

First Regional Symposium on Electrochemistry of South-East Europe, Rovinj, Croatia, May 4-8, 2008.

P-1-009

# ACTIVITY AND STABILITY OF TERNARY $RuO_2$–$TiO_2$–$IrO_2$ COATINGS ON TITANIUM IN CHLORINE EVOLUTION REACTION

**V.V. Panić[1], V.B. Mišković-Stanković[2], R. Ristić[3], B.Ž. Nikolić[2]**

[1]*ICTM – Center for Electrochemistry, Njegoševa 12,11000 Belgrade, Serbia,*
*panic@ihtm.bg.ac.yu*
[2]*Faculty of Technology and Metallurgy, University of Belgrade,*
*Karnegijeva 4, 11000 Belgrade, Serbia*
[3]*HIP "Petrohemija", Spoljnostarčevačka 82, Pančevo, Serbia*

Due to good activity of $RuO_2$-based anodes for the chlorine evolution and oxygen reaction [1,2], they are commercially wide-spread applied in the various electrochemical processes. However, activated titanium anodes are of limited stability in chlorine evolution processes, since they undergo the degradation due to the electrochemical oxidation of Ru species. The products of oxidation are soluble, hence the anode coating is becoming rich in insulating $TiO_2$, which leads to the anode passivation [3]. The anode activity for oxygen evolution reaction, however, appears to play an important role in the anode degradation process [4]. It is known that activated titanium anodes which contain iridium oxide are more stable against passivation in the electrolysis of NaCl solutions than binary $RuO_2$–$TiO_2$ coating [5]. This is due to slower corrosion rate of $IrO_2$ with respect to $RuO_2$, especially when considerable portion of the current is related to the oxygen evolution reaction. For this reason, commercially available activated titanium anodes contain iridium oxide in small amounts, besides $RuO_2$ and $TiO_2$. Previous works [3,6] reported higher activity for chlorine and oxygen evolution reaction, as well as stability to passivation of $Ti_{0.6}Ru_{0.4}O_2$ coatings on titanium prepared by the sol-gel (sg) procedure, compared to the coatings prepared by thermal decomposition (td) of metal chlorides. This issue is mostly due to the larger real surface area of sol-gel prepared coating. The addition of small amount of td-prepared $IrO_2$ considerably improves the stability of sol–gel prepared $Ti_{0.6}Ru_{0.3}Ir_{0.1}^{(td)}O_2$ anodes [7]. The aim of this work is to investigate the activity and stability of ternary, sg-prepared, $Ti_{0.6}Ru_{0.3}Ir_{0.1}O_2$ coating on titanium in the conditions of chlorine evolution reaction. The anode characteristics are investigated in NaCl solution, and compared to the characteristics of ternary $Ti_{0.6}Ru_{0.3}Ir_{0.1}^{(td)}O_2$ and binary, sg-prepared, $Ti_{0.6}Ru_{0.4}O_2$ coating.

Colloidal mono-dispersions of $RuO_2$, $IrO_2$ and $TiO_2$ are obtained by forced hydrolysis of metal chlorides in boiling HCl [3]. The dispersions of $RuO_2$, $IrO_2$ and $TiO_2$ (oxide sols) were formed during 46, 20 and 10 h (ageing times), respectively. Prepared oxide sols were mixed to form ternary dispersion for the preparation of the coating with desired composition of $Ti_{0.6}Ru_{0.3}Ir_{0.1}O_2$. The dispersions were painted over Ti plates. The coatings were applied in two layers, each converted into the gel phase at 90 °C and annealed at 450 °C, the first layer for 10 min and the second for 20 min, which

developed oxide crystal structure and provided good coating adhesion. The total coating mass was 1.0 mg cm$^{-2}$. The details of the preparation of $Ti_{0.6}Ru_{0.3}Ir_{0.1}^{(td)}O_2$ and $Ti_{0.6}Ru_{0.4}O_2$ coating can be found in previous paper [7]. The physico-chemical properties of pre-pared sols and coatings were investigeted by usual techniques (XRD, TEM, SEM and determination of particle size distribution).

Electrochemical measurements were done in 0.50 and 5.0 mol dm$^{-3}$ NaCl, pH 2, using the methods of cyclic voltammetry, polarization measurements and electrochemical impedance spectroscopy. Anode stability was checked by accelerated stability test. The end of anode service life is seen as sudden increase in potential, which is the measure of the anode stability to passivation under given conditions.

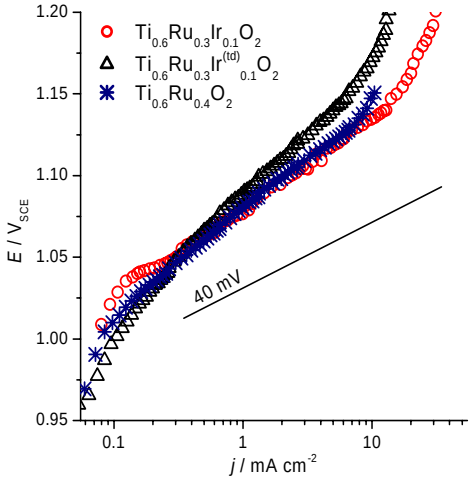


*Fig. 1. The polarization curves of ternary and binary oxide coating on titanium registered in 0.50 mol dm$^{-3}$ NaCl, pH 2. Ternary coatings are obtained from $IrO_2$ component prepared by sol-gel procedure or thermal decomposition (td) of $IrCl_3$.*

The activity of sg-prepared ternary coating for chlorine evolution reaction is illustrated by the polarization curve given in Fig. 1. For the sake of comparison, polarization curves of $Ti_{0.6}Ru_{0.3}Ir_{0.1}^{(td)}O_2$ and $Ti_{0.6}Ru_{0.4}O_2$ coated anodes are shown on the same graph. Tafel slopes of all three curves are close to the value of 40 mV, which is the usual value for $RuO_2$-based titanium anodes [1]. However, the differences in activity are observable, especially in the region of higher current densities. Ternary coating which contains td-prepared $IrO_2$ is of lowest activity at the potentials more positive than 1.07 V. This was explained by the real surface area effect in comparison to the binary coating [7]. Td-prepared $IrO_2$ is of rather large particles, making the real surface area of ternary coating smaller with respect to binary coating. If sg-prepared $IrO_2$ is introduced in the coating, the activity of ternary coating above 1.10 V becomes higher (smaller Tafel slope) than the activitry of binary coating. This could be the indication of an increase in real surface area of sg-prepared ternary coating with respect to the $Ti_{0.6}Ru_{0.3}Ir_{0.1}^{(td)}O_2$ coating, due to the presence of small, uniformly distributed $IrO_2$ particles. This observation should be of importance with respect to the anode stability in NaCl electrolysis, since finely dispersed $IrO_2$ should take over the activity of ternary coating for oxygen evolution reaction, thus additionally increasing anode stability.

**Reference:**

[1] S. Trasatti, in: *Interfacial Electrochemistry of Conductive Oxides for Electrocatalysis, in Interfacial Electrochemistry – Theory, Experiment and Applications*, A. Wieckowski, Ed., Marcel Dekker Inc., New York, 1999, p. 769

[2] A. Cornell and F. Herlitz, *Proceedings*, in *Proceedings of 4th Kurt Schwabe Corrosion Symposium*, Helsinki, Finland, 2004, p. 326

[3] V. Panić, A. Dekanski, V.B. Mišković Stanković, S. Milonjić, B. Nikolić, *J. Electroanal. Chem.* **579** (2005) 67

[4] V. Jovanović, A. Dekanski, P. Despotov, B. Nikolić, R. Atanasoski, *J. Electroanal. Chem*. **339** (1992) 147

[5] V. V. Gorodetskii, V. A. Neburchilov and V. I. Alyab'eva, *Russ. J. Electrochem.* **41** (2005) 1111

[6] V. Panić, A. Dekanski, S. Milonjić, V.B. Mišković-Stanković, B. Nikolić, *J. Serb. Chem. Soc*. **71** (2006) 1173

[7] V. V. Panić, B. Ž. Nikolić, *J. Serb. Chem. Soc*. **72** (2007) 1393

First Regional Symposium on Electrochemistry of South-East Europe, Rovinj, Croatia, May 4-8, 2008.

P-1-010

# PARAMETRIC STUDY OF DIRECT BOROHYDRIDE FUEL CELLS

**N. Duțeanu*, K. Scott**, N. Vaszilcsin*, A. Kellenberger*, M. Dan***

** University "POLITEHNICA" Timisoara, Faculty of Industrial Chemistry, 2 Piața Victoriei, 300006 Timișoara Romania, narcis.duteanu@chim.upt.ro*
*** School of Chemical Engineering and Advanced Materials, Merz Court, University of Newcastle upon Tyne, NE1 7RU, United Kingdom.*

The bigger energy requirements from the last years affect the planet and the human life on earth and in the same time caused the recent climatic changes. Therefore, the research around the world is focused on developing sustainable and environmental friendly power supply [1-3]. Considering the recent climatic changes, the high energy demands and in same times the oil depletions, it is expected to produce some energy converting devices with high efficiency and zero emission. The most promising device in this field is represented by Polymer Electrolyte Membrane Fuel Cell (PEMFC). Most of the studies performed in the last decade are focused to find a safe, cheap and efficient fuel. Sodium borohydride is complying with all these requirements and it is safe to transport and store. Moreover, sodium borohydride can be used directly in PEMFC eliminating in this way the presence of any reformer [5].
The aim of this paper is to present the results obtained during the parametric studies of direct borohydride fuel cell (DBFC). The fuel cell used in our studies was fitted with a membrane electrode assembly (MEA, S=9 $cm^2$) sandwiched between two graphite blocks which had flow fields in form of parallel channels, for methanol or oxygen/air flow [7].
MEA tested in our work was constructed as follows: both anode and cathode consisted of commercial carbon paper support (TGP 090 – E-TEK, USA) upon which was sprayed the microporous layer (MPL – ketjenblack carbon powder with PTFE) and after the catalyst layer, with the same (active) metal loading (1 mg $cm^{-2}$). For the preparation of the anode a 60 wt% Pt-Ru/C catalyst was used and for the cathode a 60 wt% Pt/C [4,6,7]. The electrodes obtained according to the method described above were placed either side of a pre-treated anion exchange membrane.

## Experimental results

The results obtained have shown that the performance of DBFC is strongly influenced by the cell temperature, borohydride concentration and oxidant type. In order to study the temperature influence, anodic, global and power density curves have been drawn. The figure 1 presents anodic polarization curves obtained at different temperatures, from which one can observe that the increasing of temperature has as a result a significant increase of the anodic performances. This

can be explained by the improving of the anodic catalytic activity as well as the intensification of the fuel diffusion through MPL.

Considering the anode behavior one can expect the same influence of the temperature upon the cell performances (figure 2). Based on the global polarization curves, the power density curves have been drawn (figure 3). Highest power densities of about 75 mW $cm^{-2}$ were achieved at 100°C, using 2 M $NaBH_4$ solution and oxygen as oxidant.

Long-term durability tests showed that, after ~ 50 h a steady-state is reached and the cell maintain its characteristics over a period of 300 h (figure 4).

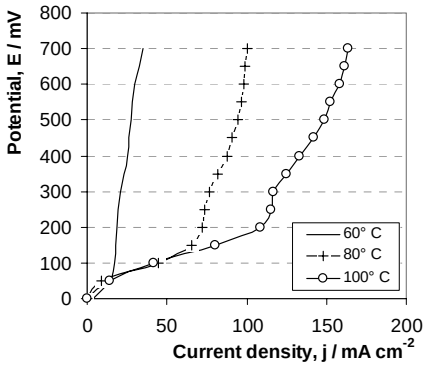


*Fig. 1 Anodic polarization curves*

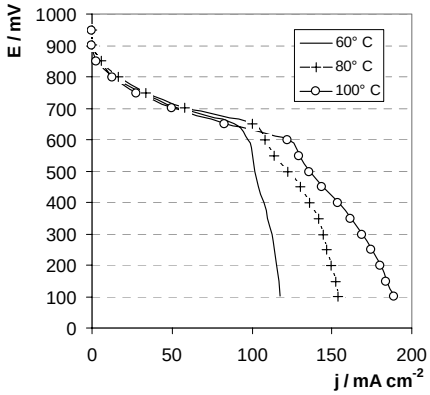


*Fig. 2 Global Polarization curves*

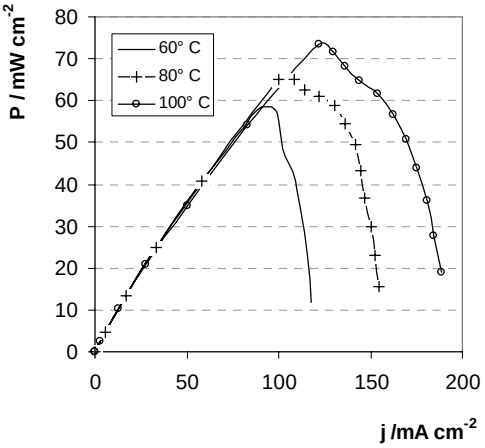


*Fig. 3 Power density's curves*

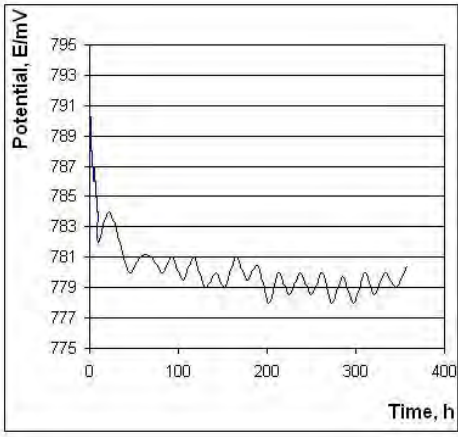


*Fig. 4 Stability curve*

**Reference:**

[1] Fuel Cell Handbook, EG&G Technical Services, *Inc. Science Applications International Corporation*, November, 2002.

[2] R.Dillon, S. Srinivasan, A.S. Aricò, V. Antonucci, *Journal of Power Sources*, **127**, 112 (2004).

[3] T. Schultz, K. Sundmacher, *Chemical Engineering Technology*, **24**, 1223 (2001).

[4] N.M. Duțeanu, M.R. Shivhare, C.L. Jackson, K. Scott, E.B. Martin, *Nordic PEMFC 06*, Stockholm, September 25 – 27 2006.
[5] C. Ponce de Leon, F.C. Walsh, D. Pletcher, D.J. Browning, J.B. Lakeman, *Journal of power Sources*, **172**, 155 (2006).
[6] J.H. Kim, H.S. Kim, Y.M. Kang, M.S. Song, S. Rajendran, S.C. Han, D.H. Jung, J.Y. Lee, *Journal of The Electrochemical Society*, **A1039**, 151-7 (2004).
[7] K. Scott, W.M. Taama, P. Argyropoulos, K. Sundmacher, *Journal of Power Sources*, **83,** 204 (1999).

First Regional Symposium on Electrochemistry of South-East Europe, Rovinj, Croatia, May 4-8, 2008.

P-1-011

# MECHANISM OF BOROHYDRIDE ELECTROOXIDATION ON METAL HYDRIDE TYPE ELECTRODES

**M. Mitov[1,3], G. Hristov[1], R. Rashkov[2], S. Hristov[3], Y. Hubenova[4]**

*[1]Department of Chemistry, South-West University "Neofit Rilsky", Blagoevgrad, Bulgaria, mitovmario@mail.bg*
*[2]Institute of Physical Chemistry – Bulgarian Academy of Sciences, Sofia, Bulgaria*
*[3]Institute of Electrochemistry and Energy Systems – Bulgarian Academy of Sciences, Sofia, Bulgaria*
*[4]Department of Biochemistry and Microbiology, "Paisii Hilendarski" University, Plovdiv, Bulgaria*

Recently, complex $M^{I}M^{III}H_4$ hydrides ($M^{I}$ – Li, Na, K; $M^{III}$ – B, Al) have attracted attention as a perspective alternative for safety hydrogen storage, transportation and generation on demand. Optionally, stabilized aqueous solution of alkaline borohydrides can directly serve as a liquid fuel in the so-called Direct Borohydride Fuel Cells, based on the following reactions:

$$BH^-_4 + 8OH^- \rightarrow BO^-_2 + 6H_2O + 8E^-$$

or

$$BH^-_4 + 4OH^- \rightarrow BO^-_2 + 2H_2O + 2H_2 + 4e^- .$$

Besides the participation of big number of electrons, the electrode potentials of above reactions are more negative than that of hydrogen electrooxidation in alkaline electrolytes. In addition, the formed borates are non-hazardous and can be regenerated. However, most of the appropriate electrodes materials also catalyze the borohydride hydrolysis reaction:

$$BH^-_4 + 2H_2O \rightarrow BO^-_2 + 4H_2,$$

which lowers the efficiency of a fuel use.

A possible way to decrease the hydrolysis effect is the use of metal hydride alloys as anode materials. In this manner, a part of generated hydrogen may be absorbed and stored into the electrode as a "secondary" fuel.

The present work is aimed at evaluating the efficiency of a fuel use at different stages of the discharge process running in the system base-stabilized $NaBH_4$ solution - metal hydride type anode by estimation of the relative part of borohydride electrooxidation and hydrolysis reactions.

Two types of hydrogen-absorbing materials – commercial $AB_5$ hydride-forming alloy and CoNiMnB electrodeposits, which had exhibited quite differing performance in regards to borohydride electrooxidation and hydrolysis in our previous studies, were used as electrode materials.

The tested electrodes were anodically polarized at galvanostatic conditions in 1M $NaBH_4$ / 6M KOH electrolyte. At stated intervals during discharge, the borohydride concentration was analyzed by means of linear voltammetry method. At the same time, the rate of hydrogen generation due to borohydride hydrolysis was determined by water

displacement method. The hydrogen storage capacity was determined from discharge curves, obtained in 6M KOH.

The used $AB_5$ electrodes showed two-three times higher discharge capacity values in comparison with the electrodeposited ones at equal discharge rates. In general, this result may be associated with the much more intensive borohydride hydrolysis as well as lower hydrogen absorprion/desorption capability of the composite electrodeposited electrodes.

Conclusions for the reaction mechanism on both types of electrodes could be done by comparison of estimated data for the decrease of total borohydride concentration in the progress of discharge with those recorded for the fuel utilized for anodic oxidation, the borohydride exhausted by hydrolysis, as well as the amount of hydrogen stored in the electrodes.

The proposed model will be further applied for investigation of other hydrogen-absorbing materials.

***Acknowledgements***. *The authors would like to thank National Science Fund of Bulgaria for the financial support through the Contract D01-386, Program "New Technologies in the Energetics".*

**References**

1. Amendola SC, Sharp-Goldman SL, Janjua MS, Spencer NC, Kelly MT, Petillo PJ, Binder M (2000) A safe, portable, hydrogen gas generator using aqueous borohydride solution and Ru catalyst. *Int. J. Hydrogen Energy* **25**, 969-975.
2. Bliznakov S, Mitov M, Petrov Y, Lefterova E, Vassilev S, Popov A (2004) Electrochemical properties of nanosized metal hydride alloys. In: *Nanoscience & Nanotechnology*, vol. 4, Balabanova E, Dragieva I (eds.), Heron Press, Sofia, pp.139-141.
3. Mitov M, Hristov G, Hristova E, Rashkov R, Arnaudova M, Zielonka A (2007) Electrocatalytic activity of electrodeposited cobalt-based multilayers for direct borohydride oxidation. *Environm.Chem.Lett.* (submitted).
4. Mitov M, Rashkov R, Atanassov N, Zielonka A (2007) Effects of Nickel Foam Dimensions on Catalytic Activity of Supported Co-Mn-B Nanocomposites for Hydrogen Generation from Stabilized Borohydride Solutions. *J.Mat.Sci.* **42(10)**, 3367-3372.
5. Nikbin D, McEntee J (2006) An evolving strategy on hydrogen storage. *Fuel Cell Rev.* **3(3)**, 19-22.
6. Petrov Y, Mitov M, Popov A (2005) Materials for Negative Electrodes for Direct Borohydride Fuel Cells. In: *Proceedings of the International Workshop "Portable and emergency energy sources - from materials to systems"*, Stoynov Z, Vladikova D (eds.), Centre of Excellence POEMES Serries, Sofia, P 8-1 – P 8-5.
7. Ponce de Leon C, Walsh FC, Rose A, Lakemana JB, Browning DJ, Reeve RW (2007) A direct borohydride - Acid peroxide fuel cell. *J. Power Sources* **164(2)**, 441-448.

First Regional Symposium on Electrochemistry of South-East Europe, Rovinj, Croatia, May 4-8, 2008.

P-1-012

# ELECTROCHEMICAL PREPARATION OF CONDUCTIVE DIAMOND POWDER – BASED COMPOSITE ELECTROCATALYSTS FOR ENERGY CONVERSION APPLICATIONS

**N. Spătaru[1], M. Marcu[1], A. Banu[2], T. Spătaru[1]**

[1]*Institute of Physical Chemistry of The Romanian Academy, Bucharest, Romania.*
[2]*University "Politehnica", Bucharest, Romania, E-mail: nspataru@icf.ro*

Due to its unique electrochemical features, boron-doped diamond (BDD) is an excellent substrate for the deposition of metal or metal oxide electrocatalysts.[1-3] It was found that the use of conductive diamond as a substrate results in high-activity deposits, with excellent conductivity and negligible substrate effects. This allows the deposition of isolated particles, down to nanometer dimensions, or discontinuous films, thus maximizing the electrochemical utilization of the catalyst by ensuring good access to electrolyte ions and short ionic pathways within the electrocatalyst itself. Additional advantages of the use of BDD supports are the excellent stability of the electrochemical response and extreme robustness of the material, even under severe operating conditions.[4] With an electrically conductive support, it is advantageous to deposit the catalytic compound electrochemically, thereby ensuring that all of it is in direct electrical contact with the substrate. This is particularly important for high-area supports, in which it is possible for electroactive materials to be deposited yet not be in electrical contact.[5]
The present work is aimed at studying the possibility of using conductive diamond as a substrate for the electrochemical deposition of several electrocatalysts, with an eye toward electrochemical conversion devices applications. For the reasons already mentioned, i.e., maximization of the dispersion of the electrocatalyst and providing a robust, highly conductive matrix, we believe that the use of BDD powder as a support could result in minimizing the noble metal loading, and in improving the stability of electrochemical conversion systems. The cost for the currently used BDD powder is not sufficiently low for widespread utilization, but efforts are in progress to boron-dope more inexpensive nanodiamond particles.
Conductive diamond powder was used in this study as substrate for electro-chemical deposition of $Co_3O_4$, Pt, $TiO_2$ and $RuO_2$ particles and Fig. 1 shows SEM images of the composite materials thus obtained.
It was observed that the cobalt oxide deposit is preferably formed on the edges of the BDD crystals, whereas in the case of all the other investigated electrocatalysts the particles are uniformly distributed on the substrate surface. For example, the deposited Pt particles are rather uniform in size (5 to 15 nm), although they form particle clusters. These particles are significantly smaller than those in most of the works cited, excepting those in which nanoparticles were synthesized separately and then deposited. The latter, although it produces highly uniform nanoparticles, is more difficult to use when depositing on a particulate support material.

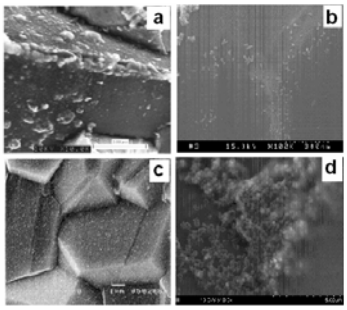


*Fig. 1 SEM images of the BDD powder surface after catalysts deposition: a) $Co_3O_4$; b) Pt; c) $TiO_2$; d) $RuO_2$.*

It was observed that the cobalt oxide deposit is preferably formed on the edges of the BDD crystals, whereas in the case of all the other investigated electrocatalysts the particles are uniformly distributed on the substrate surface. For example, the deposited Pt particles are rather uniform in size (5 to 15 nm), although they form particle clusters. These particles are significantly smaller than those in most of the works cited, excepting those in which nanoparticles were synthesized separately and then deposited. The latter, although it produces highly uniform nanoparticles, is more difficult to use when depositing on a particulate support material.

After depositing the electrocatalysts, the conductive diamond powder was used as electrode material for investigating electrochemical processes of practical interest (such as oxygen evolution and methanol oxidation) or for assessing their possible use in the field of supercapacitors and fuel cells. It was found that the materials thus obtained exhibit high electrocatalytic performances together with excellent stability of the electrochemical response and extreme robustness of the electrodes, even under severe functioning conditions. As an example, Fig. 2 illustrates the advantage of using BDD powder as a substrate for hydrous ruthenium oxide in view of supercapacitors applications.

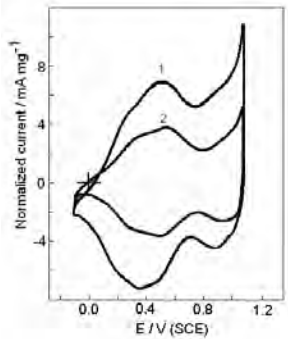


*Fig. 2 Cyclic voltammograms recorded for BDD powder (1) and BDD film (2) electrodes with the same total $RuO_2$ loading; electrolyte, 0.5 M $H_2SO_4$; sweep rate, 20 mV $s^{-1}$.*

Thus, it was observed that the same amount of $RuO_2$ resulted in a much higher reversible voltammetric charge when deposited on BDD powder, compared to the case when BDD films were used as substrates. By taking into account the average of the anodic and cathodic charges (integrated within the potential range 0.00 to 1.10 V), it appears that the specific charge of the $RuO_2$ is strongly enhanced by the use of the BDD powder support, i.e., from ca. 142 C $g^{-1}$ to ca. 288 C $g^{-1}$. Although

this is a rough estimation, these results are noteworthy, because they show that, in terms of specific charge, conductive diamond powder is a very suitable substrate for hydrous ruthenium oxide deposition. It should be noted also that in all the investigated cases the stability of the BBD powder –based electrode materials favorably compares with that available when using conventional carbon material as substrate.

**References:**

1. S. Ferro and A. De Battisti, *J. Phys. Chem. B*, **106**, 2249 (2002).
2. N. Spataru, C. Terashima, K. Tokuhiro, I. Sutanto, D.A. Tryk, S.M. Park, and A. Fujishima, *J. Electrochem. Soc*., **150**, E337 (2003).
3. A. Manivannan, N. Spataru, K. Arihara, and A. Fujishima, *Electrochem. Solid-State Lett*., **8**, C138 (2005).
4. Q.Y. Chen, M.C. Granger, T.E. Lister, and G.M. Swain, *J. Electrochem. Soc*., **144**, 3806 (1997).
5. J.W. Long, K.E. Swider, C.I. Merzbacher, and D.R. Rolinson, *Langmuir*, **15**, 780 (1999).

First Regional Symposium on Electrochemistry of South-East Europe, Rovinj, Croatia, May 4-8, 2008.

P-1-013

# THE EFFECT OF THE ADDITION OF WC POWDER TO Pt-BLACK ON THE METHANOL OXIDATION REACTION

**M.D. Obradović[1]*, B.M. Babić[2], V. V. Panić[1], S.Lj. Gojković[3]**

*[1]Institute of Chemistry, Technology and Metallurgy, University of Belgrade, Njegoševa 12, 11000 Belgrade, Serbia, E-mail: obradovic@ihtm.bg.ac.yu*
*[2]Vinča Institute of Nuclear Sciences, P. O. Box 522, 11001 Belgrade, Serbia*
*[3]Faculty of Technology and Metallurgy, University of Belgrade, Karnegijeva 4, 11120 Belgrade, Serbia*

According to literature, investigations of the methanol oxidation reaction (MOR) revealed that tungsten bronze doped with Pt, platinum-tungsten oxide, carbon supported platinum modified by $WO_y$ and high surface are tungsten oxide containing Pt centers have better electrocatalytic properties than Pt alone or even Pt-Ru alloy [1]. In addition, $PtWO_y/C$ electrocatalyst and Pt/C impregnated by phosphotungstic acid presented better CO tolerance in oxidation of $H_2$/CO mixtures, compared to unmodified Pt/C. Enhancement of MOR kinetics and CO tolerance have been related to the promotion of the electrochemical CO desorption by active tungsten hydrous oxide.

In this study, the electrocatalytic activity of a mixture of Pt-black powder (Alfa Aesar, BET surface area 24 – 29 $m^2g^{-1}$) and WC powder, provided by Woksal, Užice, has been investigated and compared to Pt-black alone. They were applied to a glassy carbon substrate (rotating disk electrode, 5 mm diameter) in the form of a thin-film. Pt black powder was suspended in high purity water, while WC and the mixture of WC and Pt black were suspended in 2-propanol. In all cases, 50 μL of the Nafion® solution (5 wt. %, 1100 E.W., Aldrich) was added per 1 $cm^3$ of the suspension. The concentration of the suspensions of single WC and Pt was 50 $mgcm^{-3}$ and 2.7 $mgcm^{-3}$, respectively. The suspension of WC + Pt powder contained 41.2 mg $cm^{-3}$ WC and 8.5 $mgcm^{-3}$ Pt. After 1 h of agitation in an ultrasonic bath, 5 μL of the suspension was placed on the glassy carbon electrode and left to dry over night. The ratio of Pt black and WC powder in the catalyst layer was chosen to simulate a composition of a supported Pt nanocatalyst.

A standard glass cells was used with a Pt wire as the counter electrode and a saturated calomel electrode (SCE) as the reference electrode. All the potentials reported here are expressed on the scale of the reversible hydrogen electrode (RHE). The supporting electrolyte of 0.1 M $H_2SO_4$ was prepared with high purity water and deaerated by the bubbling of $N_2$. MOR was investigated in unstirred electrolyte containing 0.1 M $CH_3OH$. The experiments were conducted at 298 ± 0.5 K. A Pine RDE4 potentiostat and Philips PM 8143 X – Y recorder were employed. Cyclic voltammograms of WC, Pt black and the mixture of Pt black and WC powder in 0.1 M $H_2SO_4$ are given in Fig. 1.

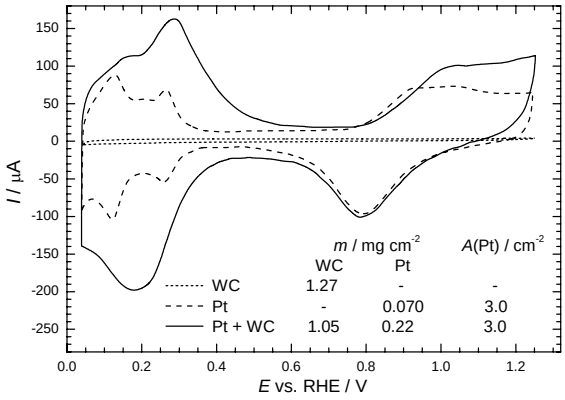


*Fig. 1. Steady-state cyclic voltammograms of thin layers of WC, Pt and Pt + WC mixture in deaerated 0.1 M $H_2SO_4$ recorded at 20 mV $s^{-1}$.*

At the potentials more negative than ~0.5 V, the voltammetric charge of the mixed WC + Pt layer is much higher than that for Pt alone. The pair of peaks at 0.18 V / 0.28 V cannot be ascribed to the hydrogen adsorption/desorption on Pt, because their potentials are shifted. On the other hand, the charge under the cathodic peaks at ~0.8 V, which are due to the reduction of Pt oxide, are the same for Pt alone and for WC + Pt mixture, although the amount of Pt is three times higher in the mixed catalyst layer. Thus, we concluded that Pt sites are partially covered by a hydrous tungsten oxide and that the coverage is about 2/3. This oxide is prone to the intercalation of hydrogen [2], so the cathodic peak at 0.18 V corresponds to the intercalation and the anodic peak at 0.30 V corresponds to the deinter-calation of hydrogen. The intercalation/deintercalation of hydrogen was also observed in the hydrous tungsten oxide formed at WC layer, but the addition of Pt significantly promoted this reaction, probably because of the spillover of hydrogen atoms adsorbed on bare Pt sites.

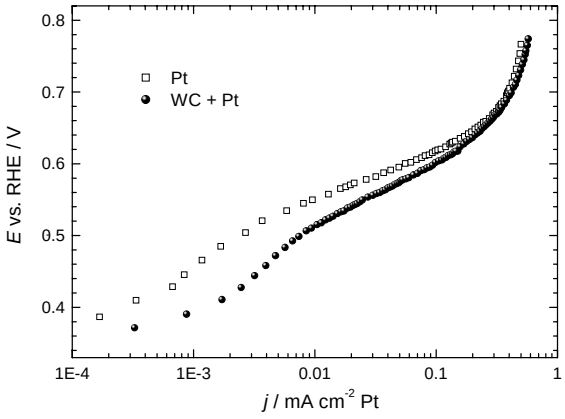


*Fig. 2. MOR on thin layers of Pt and WC + Pt in deaerated 0.1 M $H_2SO_4$ + 0.1 M $CH_3OH$. Tafel plots recorded at 1 mV $s^{-1}$ in the first scan.*

Tafel plots of MOR on the thin layers of Pt and WC + Pt mixture of the same composition as in the experiments in Fig. 1 are given in Fig. 2. The current densities were calculated with respect to the surface area of bare Pt, which was estimated from the reduction charge of Pt oxide. The results show that the onset potential for MOR is about 50 mV less positive in the presence of WC. In the potential range 0.4 to 0.5 V the enhancement factor of 3 is observed, while at more positive potentials the influence of WC reduces.

Higher MOR rate on the mixed WC + Pt catalyst layer was attributed to the modification of Pt atoms by the hydrous tungsten oxide. The $H_xWO_3$ species attached to Pt sites can help to regain free Pt sites, which are necessary for the reaction, in the several ways. Hydrogen atoms from Pt sites can be transferred to $H_xWO_3$ by spillover mechanism and intercalated in it. Another possibility is that CO adsorbed

on Pt sites is oxidatively removed through the surface reaction with OH from $H_xWO_3$, which is known as bifunctional mechanism. An alternative mechanism of the $CO_{ads}$ removal from Pt in the presence of a base metal is a proton-shift model, in which cleavage of W-O-Pt bonds creates Pt-OH sites. Having in mind that oxidation of $H_{ads}$ on Pt is very fast reaction and that oxidation of $CO_{ads}$ is considered as the rate determining step on single Pt catalyst as well as on various Pt-M catalysts, it can be assumed that promotion of Pt by WC (actually $H_xWO_3$) is through either bifunctional mechanism or the proton-shift model.

The results presented suggest that Pt nanoparticles supported on WC can be a promising electrocatalyst, because such a support should modify Pt by the tungsten species, which enhances its activity for MOR. Also, further investigation are needed to tune Pt:WC ratio, i.e. the coverage of Pt by the hydrous tungsten oxide, in order to attain higher activity of the catalyst.

**Reference:**

1. E.J. McLeod, V.I. Birss, *Electrochim. Acta*, **51** (2005) 684.
2. H. Chhina, S. Campbell, O. Kesler, *J. Power Sources*, **164** (2007) 431.

First Regional Symposium on Electrochemistry of South-East Europe, Rovinj, Croatia, May 4-8, 2008.

P-1-014

# DEVELOPMENT OF QUANTITATIVE ELECTROSPRAY IONIZATION MASS SPECTROMETRY ANALYSIS FOR METHANOL OXIDATION PRODUCTS

**M. Chojak, Z. Jusys, J.R. Behm**

*Institute of Surface Chemistry and Catalysis, Ulm University, D-89069-Ulm, Germany*
malgorzata.chojak@uni-ulm.de

Because of their ability to operate also at low temperatures (room temperature to about 50°C), Direct Methanol Fuel Cells (DMFC) could be used for powering, e.g., cellular phones and laptop computers. Important for low temperature operation is not only a high catalyst activity, but also to exclude the formation of incomplete oxidation products, in particular that of toxic formaldehyde. This requires a detailed understanding of the methanol oxidation process [1,2] and the resulting product distribution ($CO_2$, HCHO and HCOOH), which was shown to sensitively depend on methanol concentration, temperature, catalyst loading and flow rate [3,4].

The application of differential electrochemical mass spectrometry (DEMS) with on-line gaseous (volatile) product detection [3,5], which can be used for product identification and quantification, is often limited by the too low volatility of the products or the overlap of ion fragments with those of other reactant/product species, which hinders or even excludes their detection by electron impact mass spectrometry (EI-MS). To overcome these limitations, electrospray ionization mass spectrometry (ESI-MS) [5] may be used. In this technique, the liquid analyte is directly injected into the MS via a steel capillary kept at high voltage. Carboxylic acids are easily detectable by ESI-MS, while carbonylic compounds (aldehydes and ketones) are harder to ionize. Severe complications for the application of ESI analysis in electrocatalytic reactions arise from the high concentration of supporting electrolyte (mineral acid), which not only affects the ionization probability of small amounts of organic molecules, but also leads to intolerable corrosion of the device.

In the present contribution, we present first results on the development of this analytical technique for product analysis in fuel cell related electrocatalytic reactions. Specifically, we report on the ex-situ analysis of the product distribution during methanol oxidation. Formaldehyde was detected via derivatization with 2,4-dinitrophenylohydrazine, which forms a hydrazone that is easily ionized by ESI. The effect of formic acid and sulfuric acid as well as methanol on the detection limit will be illustrated. Quantitative formic acid detection with the ESI-MS will be demonstrated, and the impact of the methanol background, the presence of hydrazone and mineral acid will be discussed. The sulfuric acid concentration was significantly reduced by ion exchange techniques.

These results demonstrate the general suitability of ESI-MS for application in electrocatalytic studies. Its on-line application, however, still needs to be developed.

## References:

[1] V.S. Bagotzky, Y.B. Vassiliev, O.A. Khazova, *J. Electroanal. Chem.*, **81** (1977) 229
[2] T. Iwasita, *Electrochim. Acta*, **47** (2002) 3663
[3] Z. Jusys, J. Kaiser, R.J. Behm, *Langmuir*, **19** (2003) 6759

[4] H. Wang, T.Löffer, H. Baltruschat, *J. Appl. Electrochem.*, **31** (2001) 759
[4] Z. Jusys, R.J. Behm, *J. Phys. Chem. B*, **105** (2001) 10874
[5] S. Gaskell, *J. Mass Spectr.*, **32** (1997) 677

First Regional Symposium on Electrochemistry of South-East Europe, Rovinj, Croatia, May 4-8, 2008.

P-1-015

# ELECTROOXIDATION OF FORMIC ACID ON UNMODIFIED AND Bi MODIFIED $Pt_2Ru_3$ NANOCATALYST

**A.V. Tripković[a], S.Lj. Gojković[b], K.Đ. Popović[a], J.D. Lović[a], A. Kowal[c]**

*[a]ICTM-Institute of Electrochemistry, University of Belgrade, Njegoševa 12, P.O.Box 473, 11000 Belgrade, Serbia, E-mail: jlovic@tmf.bg.ac.yu*
*[b]Faculty of Technology and Metallurgy, University of Belgrade, Karnegijeva 4, P.O.Box 3503, 11000 Belgrade, Serbia*
*[c]Institute of Catalysis and Surface Chemistry, Polish Academy of Sciences, Krakow, Niezapominajek 8, 30-239, Poland*

Formic acid oxidation was investigated on nanosized $Pt_2Ru_3$ and on Bi modified $Pt_2Ru_3$ particles supported on glassy carbon in sulfuric acid media. The aim of this work was to estimate in what extent modifiers such as Ru and Bi can improve the activity and stability of Pt electrocatalyst.

Basic voltammograms of unmodified and Bi modified $Pt_2Ru_3$ electrodes are given in Fig. 1(a) and they can be divided into two regions: hydrogen adsorption/desorption (-0.25 V up to 0.0 V) and adsorption/desorption of oxygen containing species and Ru-oxides formation at more positive potentials. $Pt_2Ru_3$ catalyst was modified by immersion in the solution containing $Bi_2O_3$ [1]. The charge for desorption of hydrogen is approximately 10% less on modified $Pt_2Ru_3$ surface due to Bi adsorption assuming that Bi adsorbs only on Pt atoms [2].

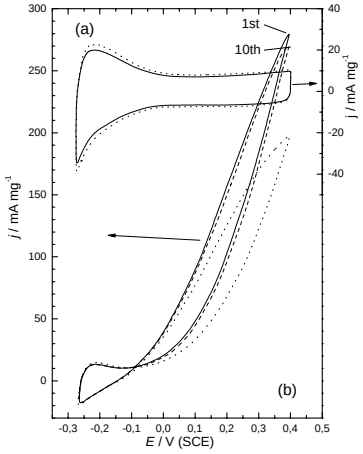


*Fig. 1.* ***(a)*** *Basic voltammograms of unmodified (dotted line) and Bi modified $Pt_2Ru_3$/C electrode (solid line).* ***(b)*** *Potentiodynamic curves for the HCOOH oxidation (first and steady-state sweep) on Bi modified(solid and dash line) and unmodified(dotted line) $Pt_2Ru_3$/C electrode in 0.1 M $H_2SO_4$ solution. Scan rate: 50 mV $s^{-1}$.*

Potentiodynamic curves for HCOOH oxidation on both $Pt_2Ru_3$ electrodes were presented in Fig 1(b). Irreversibly adsorbed Bi prevents the poisoning of the surface since the difference between first and tenth scan in negligible. Comparing the steady-state activities of modified and unmodified $Pt_2Ru_3$ electrodes it can be observed that Bi adlayer shift the onset potential negatively and increase the reaction rate of HCOOH oxidation for ca. 50%.

Catalytic action of Bi on HCOOH oxidation is derived from minimizing of surface poisoning by $CO_{ad}$ species. In that sense the oxidation of preadsorbed CO was studied on unmodified and Bi modified $Pt_2Ru_3$ electrodes (Fig. 2). Charge under the peak for Bi modified surface is 24% lower compared to unmodified surface. Since CO does not adsorbed on Bi [3], this difference indicates that irreversibly adsorbed Bi hinders the adsorption of CO on Pt as a consequence of electronic and/or ensemble effects.

Figure 3 presents Tafel plots for unmodified and Bi modified $Pt_2Ru_3$ electrodes , as well as on unmodified and Bi modified supported Pt nanocatalyst. When Bi is adsorbed on Pt atoms, either on pure Pt or on $Pt_2Ru_3$ surface, the onset potential of HCOOH oxidation is shifted negatively for about 50 mV. The currents at Bi modified $Pt_2Ru_3$ electrode are approximately double of those on unmodified surface, while the effect of Bi is much more expressed on Pt nanocatalyst (ca. factor 7). This is understandable, because the coverage by $CO_{ad}$ on $Pt_2Ru_3$ surface is already diminished by the presence of Ru.

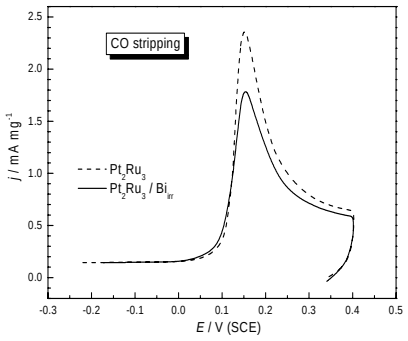


*Fig.2. CO stripping voltammograms on $Pt_2Ru_3$/C and Bi modified $Pt_2Ru_3$/C electrode (first positive going sweeps) in 0.1 M $H_2SO_4$ solution. Scan rate 1 mV $s^{-1}$.*

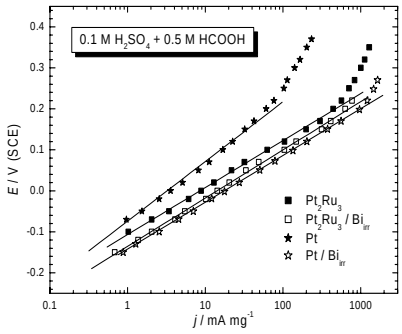


*Fig.3. Tafel plots for oxidation of 0.5 M HCOOH in 0.1 M $H_2SO_4$ solution on unmodified and Bi modified $Pt_2Ru_3$/C and Pt/C electrodes. Scan rate 1 mV $s^{-1}$.*

Both Ru and Bi enhance the HCOOH oxidation rate by diminishing $CO_{ad}$ coverage, but probably through different mechanisms. Ru acts through bifunctional mechanism, i.e. OH species adsorbed on Ru oxidizes $CO_{ad}$ from Pt sites, while Bi hinders the adsorption of CO on Pt sites via electronic and/or ensemble effects. The simultaneous presence of both modifiers leads to improvement in activity and especially stability of the electrocatalyst. A systematic study of ternary Pt-Ru-Bi electrocatalyst should be carried out to find an optimum composition with the minimum poisoning effect.

**References:**

[1] J. Clavilier, A. J.M. Feliu, A. Aldaz, *J. Electroanal. Chem.*, **243** (1988) 419.
[2] A.V. Tripković, S.Lj. Gojković, K. Đ. Popović, J.D. Lović, A. Kowal, *Electrochim. Acta.*, (2007).
[3] M.T. Paffett, C.T. Campbell, R.G. Windham, B.E. Koel, *Surf. Sci.*, **207** (1989) 274.

First Regional Symposium on Electrochemistry of South-East Europe, Rovinj, Croatia, May 4-8, 2008.

P-1-016

# FORMIC ACID ELECTROOXIDATION ON $Pt_4Mo$ ALLOY

**S.Lj. Gojković[1], A.V. Tripković[2], R.M. Stevanović[2], N.V. Krstajić[1]**

*[1]Faculty of Technology and Metallurgy, University of Belgrade, Karnegijeva 4, P.O.Box 3503, 11000 Belgrade, Serbia, E-mail: sgojkovic@tmf.bg.ac.yu*
*[2]ICTM-Institute of Electrochemistry, University of Belgrade, Njegoševa 12, P.O.Box 473, 11000 Belgrade, Serbia*

Platinum is the most active material for the adsorption of HCOOH, but as it is readily poisoned by $CO_{ads}$, its practical application requires modification of the surface by some foreign metal atoms. Significant increase of the HCOOH oxidation rate was found with Pt-Pb,[1] Pt-Bi,[2,3] Pt-Sn,[4] and Pt-Pd[5] systems. The action of different foreign metal atoms is commonly explained by bifunctional mechanism[4], third-body and the electronic effects[2].

To date, electrocatalysts based on Pt and Mo or its oxide have been investigated with respect to oxidation of CO and alcohols, but only occasionally for oxidation of HCOOH. In this work, we examined HCOOH oxidation on well defined $Pt_4Mo$ alloy[6] and correlated the reaction rate to the electrochemical pretreatment of the $Pt_4Mo$ surface.

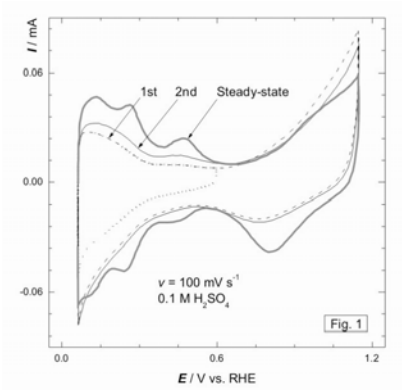


Cyclic voltammograms of $Pt_4Mo$ electrode, in quiescent solution of 0.1 M $H_2SO_4$, are presented in Fig.1. A profile with weak signs of hydrogen adsorption/desorption is obtained when the potential is cycled up to 0.6 V. When the positive potential limit is set to 1.15 V, an anodic peak with the maximum at about 0.47 V appears together with its cathodic counterpart. At the same time, the peaks for hydrogen adsorption/desorption on Pt emerge. That may be explained by partial dissolution of Mo or more likely by the Pt surface cleaning at positive potentials. Since basically the same voltammogram is obtained when the electrode is transferred into the fresh electrolyte, it appears that Mo is not completely leached from the surface.

Anodic peak at 0.47 V can be ascribed to the oxidation of a Mo-oxide to a higher oxidation state. Dos Anjos et al.[7], who observed the same Mo-oxide redox couple on Pt-Mo alloys, assumed that Mo oxo species generated in the solution re-adsorbe

at the Pt surface at $E < 0.4$ V. However, as the increase of the redox peaks is not followed by the decrease in hydrogen adsorption/desorption peaks, it seems that they re-adsorbe on Mo-oxide sites. Gradual increase of the redox peaks, and the fact that they disappear if the electrode rotation is initiated, suggest that a loosely bound hydrated Mo-oxide is growing on Mo-sites. In the stirred electrolyte, the amount of hydrous Mo-oxide is low, if any, but Mo is still present, probably in some form of more compact surface oxide.

Oxidation of HCOOH was investigated on Pt and $Pt_4Mo$ surfaces pre-conditioned by the potential cycling up to 1.15 V (c*f.* Fig. 1) on the stationary ($\omega = 0$ rpm) and on the rotating electrode ($\omega = 1000$ rpm). Tafel plots of Fig.2a show that $Pt_4Mo$ surface, pre-conditioned $\omega = 0$ rpm, is much more active than pure Pt. At the 0.4 V the enhancement factor is 40. The rotated $Pt_4Mo$ electrode performs similarly to pure Pt at low potentials. However, at >0.7 V it reaches the activity of $Pt_4Mo$ pre-conditioned $\omega = 0$ rpm. Since all the current densities are given per Pt surface area, the increase in the reaction rate is the consequence of the hydrous Mo-oxide presence nearby the Pt sites at which the reaction takes place.

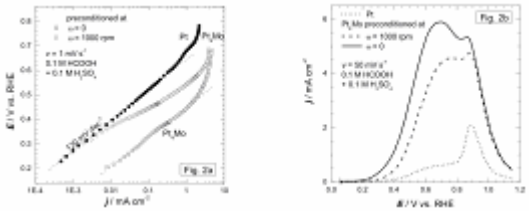

The insight in the amount of the poisoning species on the electrode surface can be obtained from potentiodynamic curves of Fig. 2b. Voltammogram for the pure Pt suggests that the HCOOH oxidation at low potentials proceeds through the direct path, with formation of $CO_{ads}$ in parallel. Increasing $CO_{ads}$ coverage reduces Pt surface available for the direct path and the current density reaches the plateau at about 0.55 V. Subsequent oxidative removals of $CO_{ads}$, is manifested as the current peak at 0.8 V. However, with $Pt_4Mo$ electrodes at low potentials the current densities are much higher than those on pure Pt. Oxidation of $CO_{ads}$ is displayed at the descending part of the curve. This indicates significantly less poisoned $Pt_4Mo$ surfaces compared to that of pure Pt, resulting in the enhanced rate of the direct path.

Cyclic voltammetry did not show significant difference of Pt surface area with two types of Mo-oxide, and the difference of the HCOOH oxidation rate on two $Pt_4Mo$ surfaces is too large to be explained by geometric restriction i.e. the third body effect. Since the presence of hydrated Mo-oxide was found to be essential for the enhancement of the HCOOH reaction rate, the bifunctional mechanism seems to be more plausible, meaning that HCOOH adsorption proceeds on Pt sites producing $CO_{ads}$, possibly formate and some other active intermediate, while neighboring hydrous Mo-oxide facilitates oxidation of $CO_{ads}$. However, recalling that in the presence of Mo-oxide $CO_{ads}$ is not completely absent (Fig. 2b), it can be disputed that the enhancement in activity by more than one order of magnitude is caused only by the reduced $CO_{ads}$ coverage, It can be also possible that hydrous Mo-

oxide, besides the suppressing $CO_{ads}$ coverage, enhances intrinsic rate of the direct oxidation path, as it was proposed earlier for the influence of Pd,[5] Pb,[1] and Bi[8].

## References

(1) Xia, X.; Iwasita, T. *J. Electrochem. Soc.* **1993**, *140*, 2559-2565.
(2) Casado-Rivera, E.; Gál, Z.; Angelo, A. C. D., Lind, C.; DiSalvo, F. J.; Abruña, H. D. *Chem. Phys. Chem*. **2003**, *4*, 193-199.
(3) Tripković, A. V.; Popović, K. Đ.; Stevanović, R. M.; Socha, R.; Kowal, A.; *Electrochem. Commun*. **2006**, *8*, 1492-1498.
(4) Chetty, R.; Scott, K. *J. New Mat. Electrochem. Systems* **2007,** *10*, 135-142.
(5) Rice, C.; Masel, R.I.; Wieckowski, A. *J. Power Sources* **2003,** *115*, 229.
(6) Jaksić, J. M.; Vračar, Lj.; Neophytides, S. G.; Zafeiratos, S.; Papakonstantinou, G.; Krstajić, N. V.; Jaksić, M. M. *Surf. Sci.* **2005,** *598*, 156-173.
(7) Dos Anjos, D. M.; Kokoh, K. B.; Leger, J. M.; de Andrade, A. R.; Olivi P.; Tremiliosi-Filho, G. *J. Appl. Electrochem.* **2006,** *36*, 1391-1397.
(8) Oana, M.; Hoffmann, R.; Abruna, H. D.; DiSalvo, F. J. *Surf. Sci*. **2005**, *574*, 1-16.

First Regional Symposium on Electrochemistry of South-East Europe, Rovinj, Croatia, May 4-8, 2008.

P-1-017

# ELECTROCHEMICAL OXIDATION OF FORMIC ACID ON PtBi ALLOY

**A.V. Tripković[a], K.Đ. Popović[a], R.M. Stevanović[a], A. Kowal[b]**

[a]*ICTM-Institute of Electrochemistry, University of Belgrade, Njegoševa 12, P.O.Box 473, 11001 Belgrade, Serbia, E-mail: ksenija@tmf.bg.ac.yu*
[b]*Institute of Catalysis and Surface Chemistry, Polish Academy of Sciences, Krakow, Niezapominajek 8, 30-239, Poland*

Platinum, the most studied catalyst for electrochemical oxidation of HCOOH, is very susceptible to poisoning species, which significantly reduces its catalytic performance at low potentials. In order to improve its activity by minimizing the poisoning effects, Pt was modified by submonolayer to monolayer amounts of foreign metal adatoms [1], or by alloying with other metals [2]. Intermetallic PtBi was proposed as a powerful catalyst for formic acid oxidation [3]. The origin of its catalytic activity was related to electronic effects enhancing the affinity of PtBi for HCOOH adsorption and producing surface oxides at low potentials, as well as to geometric effects reducing the affinity for CO poisoning.

In this work, formic acid oxidation in acid solution was examined on a PtBi alloy in order to elucidate its extremely large catalytic effect relative to that of polycrystalline Pt.

The PtBi electrode was characterized by X-ray photoelectron spectroscopy (XPS). Three chemical states of Bi, i.e. PtBi or Bi(0), $Bi_2O_3$ and BiO(OH) were found. The results presented lead to a model in which the PtBi alloy is covered by a layer of $Bi_2O_3$ and the very top of this layer contains BiO(OH) species [4].

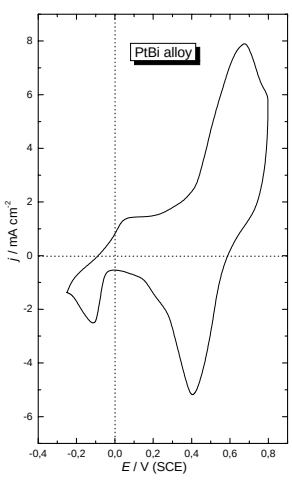


*Fig. 1. Cyclic voltammograms for PtBi electrodes in 0.1 M $H_2SO_4$. $\nu$ = 50 mV $s^{-1}$; T = 295 K.*

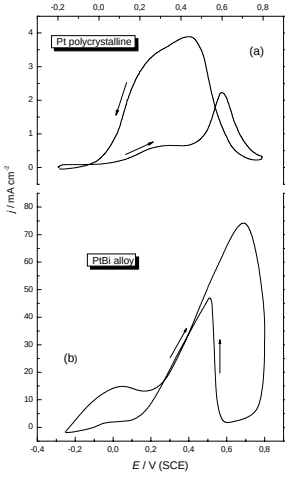


*Fig. 2. Cyclic voltammograms for the oxidation of 0.125 M HCOOH on Pt and on PtBi electrodes in 0.1 M $H_2SO_4$. $\nu$ = 50 mV $s^{-1}$; T = 295 K*

The voltammogram of PtBi alloy is presented in Fig. 1. In the potential range up to 0.05 V the electrode activity and the processes involved are determined by behavior of the pure Bi. In that sense, the cathodic peak at $E$ ~ -0.15 V, as well as the wave at $E$ ~ 0.05 V can be correlated to the reduction/oxidation of Bi species [4]. Extensive oxide formation/reduction is represented by the anodic peak at $E$ ~ 0.65 V and cathodic peak at $E$ ~ 0.4 V. Dissolution of Bi, i.e. leaching from the alloy matrix, proceeds all along anodic potential scan. All processes, i.e. deposition/dissolution of Bi as well as those of oxide formation/reduction are mass transport controlled.

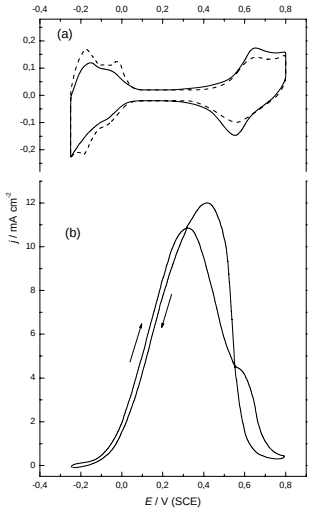


*Fig. 3. Cyclic voltammograms (a) for pure Pt (– – –) and Bi modified Pt (——) electrode and (b) for the oxidation of 0.125 M HCOOH on Bi modified Pt electrode in 0.1 M $H_2SO_4$. $\nu = 50$ mV $s^{-1}$; $T = 295$ K.*

Cyclic voltammograms for the oxidation of formic acid on Pt and PtBi alloy electrodes are given in Fig. 2. The most important data resulting from a comparison of these two voltammograms is the enormous electrocatalytic activity of PtBi in respect to Pt.

In order to find the origine of high activity of PtBi alloy after recording the voltammogram for PtBi (Fig. 1), the PtBi electrode was replaced with Pt. The voltammogram displayed in Fig. 3 is typical for formic acid oxidation on a Bi modified Pt surface [5], indicating that dissolved Bi by leaching can be adsorbed on Pt sites as an UPD layer. It clearly suggests that formic acid oxidation on the PtBi alloy occurs on Bi modified Pt sites on the PtBi surface, i.e.that UPD phenomena of Bi on Pt is the cause of a enormous activity of PtBi alloy.

Tafel plots for Pt, Bi modified Pt and PtBi electrodes are given in Fig. 4. They confirm the results obtained in transient measurements. Relative to the Pt electrode, rotated PtBi alloy has a significantly enhanced performance in terms of the onset potential and the current density. The onset potential on PtBi is shifted by 0.25 V towards less positive potentials and the current densities are higher by more than two orders of magnitude.

The exceptional activity of PtBi electrode is caused dominantely by UPD phenomena of Bi on Pt (electrochemically detected), although some contribution of a bifunctional action, enabled by the presence of hydroxylated Bi species (detected by XPS), should be taken into account.

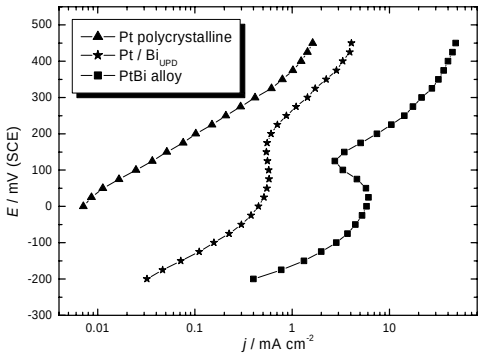


*Fig. 4. Tafel plots for the oxidation of 0.125 M HCOOH in 0.1 M $H_2SO_4$ on Pt, Bi modified Pt and PtB electrodes. $\nu$ = 1 mV $s^{-1}$; T = 295 K.*

**References:**

[1] R. Adžić, A.V. Tripković, N. Marković, *J. Electroanal. Chem.*, **150** (1983) 79.
[2] N.M. Marković, P.N. Ross Jr., Surface Sci. Reports, **45** (2002) 117.
[3] E. Casado-Rivera, Z, Gal, A.C.D. Angelo, C. Lind, F.J. DiSalvo, H.D. Abruna, *Chem.Phys.Chem*., **4** (2003) 193.
[4] A.V. Tripković, K.Đ. Popović, R.M. Stevanović, R. Socha, A. Kowal, *Electrochem., Comm.*, **8** (2006) 1492.
[5] S.A. Campbell, R. Parsons, *J. Chem. Soc., Faraday Trans*., **88** (1992) 833.

First Regional Symposium on Electrochemistry of South-East Europe, Rovinj, Croatia, May 4-8, 2008.

P-1-018

# THE EFFECT OF A TITANIUM OXIDE INTERMEDIARY LAYER ON THE ELECTROCHEMICAL BEHAVIOR OF A PLATINUM – CONDUCTIVE DIAMOND COMPOSITE MATERIAL

**M. Marcu[1], T. Spătaru[1], L. Georgescu[2], N. Spătaru[1]**

*[1]Institute of Physical Chemistry of The Romanian Academy, Bucharest, Romania*
*[2]University "Politehnica", Bucharest, Romania, E-mail: m_marcu2000@yahoo.com*

The observation that specific titanium – platinum interaction enhances the electrocatalytic efficiency triggered very active research, devoted to the investigation of the electrochemical behavior of Ti – Pt composite films synthesized in various ways.[1-6] It was found that $Pt/TiO_2$ layers involving isolated Pt particles encapsulated within titanium oxide enable only moderate catalytic activity, whereas platinum particles deposited directly on the $TiO_2$ substrate give much better results. For example, in the case of anodic oxidation of methanol, the enhancement of the activity is induced by photogenerated holes produced by the UV irradiation of the titanium oxide. It is therefore likely that the use of a $Pt/TiO_2$ composite electrocatalyst will allow better efficiency for methanol electrochemical oxidation. Furthermore, it was recently shown that the use of titanium oxide as support for platinum deposition ensures strong substrate – catalyst bonds, resulting in a significant improvement of the stability of the platinum deposit.[3]

The present work was devoted to the study of the effect of a titanium oxide intermediary layer on the catalytic properties of a composite material obtained by electrochemical deposition of Pt particles on a boron-doped diamond (BDD) substrate. Electrochemical deposition of $TiO_2$ on the conductive diamond surface was performed from a 50 mM $TiCl_3$ solution (pH 2) at a deposition potential of 0.6 V *vs.* SCE. The oxide loading was controlled by adjusting the deposition charge and the extent of the surface coverage was assessed by cyclic voltammetry in the presence of $Ru(bpy)_3Cl_2$. In order to scrutinize the photoelectrocatalytic behavior of the $TiO_2$/BDD system we carried out a simple ethanol oxidation reaction under illumination. We have found that the photogenerated charge carriers are efficiently utilized in this hybrid system: the holes generated in the $TiO_2$ oxidize the ethanol while the electrons pumped to the conduction band are injected into the diamond substrate.

The surface of the titanium oxide deposited on the BDD substrate was further modified by electrochemical deposition of platinum particles and Fig. 1 shows a SEM image of the composite material thus obtained.

In order to assess the electrocatalytic activity of the $Pt/TiO_2$/BDD structures for methanol oxidation, cyclic voltammetric experiments were performed in acid media and the results are illustrated in Fig. 2.

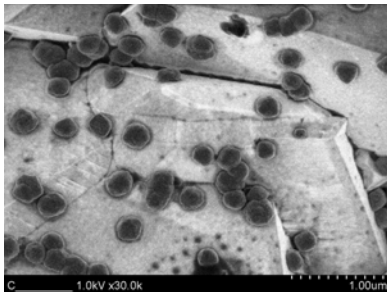


*Fig. 1. SEM image of the composite material obtained by electrochemical deposition of platinum on a BDD substrate covered with titanium oxide.*

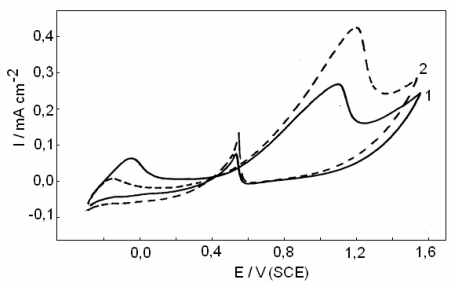


*Fig. 2.*
*Cyclic voltammograms recorded in 0.5 M $H_2SO_4$ + 1 M $CH_3OH$ at Pt/$TiO_2$/BDD electrodes in dark (1) and under UV irradiation (2). Scan rate, 20 $mVs^{-1}$; Pt loading 76.4 $\mu g\ cm^{-2}$.*

It can be observed that, although the shape of the voltammograms is affected by the ohmic drop induced by the presence of the $TiO_2$ intermediary layer, the UV irradiation results in an increase of *ca*. 45 % of the methanol oxidation current. Steady-state polarization measurements were also carried out and it was observed that, at the time scale of these experiments, the increase of the current under illumination leads to a more important fouling of the Pt/$TiO_2$/BDD electrodes compared to the Pt/BDD ones. A possible explanation for this behavior is provided by assuming that higher methanol oxidation current results in a higher amount of adsorbed carbon oxide that could block to some extent the active sites from the platinum surface. Nevertheless, it is worthy to note that the presence of the $TiO_2$ intermediary layer allows obtaining a photoelectrocatalytic activity for methanol oxidation of about 5.23 A / g of platinum.

**Reference:**

1. B.C. Beard and P.N. Ross, *J. Electrochem. Soc*., **133**, 1839 (1986).
2. S.V. Mentus, *Electrochim. Acta*, **50**, 3609 (2005).
3. K.W. Park, S.B. Han and J.M. Lee, *Electrochem. Commun*,. **9** 1578 (2007).
4. B.E. Hayden, D.V. Malevich and D. Pletchen, *Electrochem. Commnu*., **3**, 395 (2001).
5. S. Gan, Y. Liang, D.R. Baer, M.R. Slevers, G.S. Herman and C.H.F. Peden, *J. Phys. Chem. B*, **105**, 2412 (2001).
6. H. Song, X. Qiu, X. Li, F. Li, W. Zhu and L. Chen, *J. Power Sources*, **170**, 50 (2007).

First Regional Symposium on Electrochemistry of South-East Europe, Rovinj, Croatia, May 4-8, 2008.

P-1-019

# ELECTROCATALYTIC ACTIVITY OF A COMPOSITE MATERIAL OBTAINED BY ELECTROCHEMICAL DEPOSITION OF PLATINUM ON CONDUCTIVE DIAMOND

**T. Spătaru[1], M. Marcu[1], A. Banu[2], N. Spătaru[1]**

[1]*Institute of Physical Chemistry of The Romanian Academy, Bucharest, Romania.*
[2]*University "Politehnica", Bucharest, Romania, tspataru@icf.ro*

A problem of intense interest in current research on high-efficiency fuel cells is how to minimize the loadings of electrocatalytic noble metals (mainly platinum or Pt-based alloys) while maintaining high electrocatalytic activity. A related problem is how to maintain high activity over the projected lifetime of the cell. The principal way to attack both problems is to deposit such metals as small particles on a high surface area support material (mainly carbon black) so that a large number of reaction sites can be provided in a small volume. Most conventional carbon blacks can undergo irreversible oxidation at non-negligible rates, particularly at the rather positive potentials common for the oxygen. When carbon particles undergo prolonged oxidation, the electrode structure can become less electrically conductive and can even lose mechanical integrity. The metal electrocatalyst particles can also be released from the surface and then can become mobile, which can lead to loss of electrical contact as well as agglomeration.

Conductive boron-doped diamond (BDD) has been proposed as a replacement for graphitic carbons in fuel cells due to its significantly greater chemical and electrochemical stability, however, little work has been reported thus far for conductive diamond powders.[1,2] The expected advantages of BDD particles compared to carbon blacks include not only the avoidance of electrode stability problems, but also perhaps enhanced performance and stability with decreased amounts of precious metals, due to the ability to purposefully modify the surface with robust, covalently linked complexing moieties for precious metals.

The present work was aimed at studying the possibility of using BDD powder as a substrate for platinum deposition, with an eye to fuel cell applications.

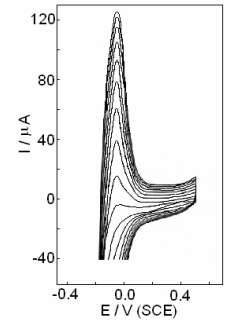


*Fig. 2. Cyclic voltammograms recorded in 0.5 M $H_2SO_4$ during platinum reduction at electrodes coated with Pt/BDD powder; scan rate, 20 mV $s^{-1}$*

The platinum catalysts supported on conductive diamond powder and on graphite powder (Pt/BDD and Pt/C, respectively) were prepared by a method similar to that described in the literature for the preparation of Pt/C.[3] The powders thus obtained

were used as electrode materials, and platinum was then electrochemically reduced. Figure 1 illustrates the voltammetric behavior of the coated type Pt/BDD powder electrode during the first ten cycles. It can be observed that, for consecutive scans, the potential of the onset of the hydrogen evolution gradually shifts towards higher values, while the height of the anodic peak, for the oxidation of both gaseous and adsorbed hydrogen, increases. This is clear indication of the continuous increase of the amount of deposited platinum.

In order to assess the electrocatalytic activity of the electrodes, cyclic voltammetric measurements were performed in a 0.5 M $H_2SO_4$ deaerated solution within the –0.2 to 1.0 V potential range, in the presence of 1 M $CH_3OH$. It was interesting to note that the two types of electrodes (Pt/BDD and Pt/C) exhibited almost the same activity for $CH_3OH$ oxidation (as estimated from the height of the peak obtained during the positive-going potential scan), although the active surface area of the catalyst was *ca*.1.6 times higher in the case of the graphite powder support. In order to put into better perspective the advantages of using conductive diamond powder as a catalyst support for practical fuel cell applications, porous gas-diffusion-type electrodes were fabricated by pressing a small amount of either Pt/BDD or Pt/C (previously made into a paste with Teflon suspension and Nafion solution) between two small sheets of Nafion membrane, together with a thin gold wire to ensure electrical contact. This assembly was suspended on the surface of the electrolyte and was used for electrochemical measurements in a floating configuration. Floating electrodes prepared with both Pt/BDD powder and Pt/graphite powder were used for steady-state measurements in 0.5 M $H_2SO_4$ deaerated solution in the presence of 1 M methanol. Under steady-state conditions, at the same potential, the current for $CH_3OH$ oxidation was higher for the Pt/graphite electrode than for the Pt/BDD powder electrode.

Figure 2 shows Tafel plots for $CH_3OH$ oxidation, typical of the behavior observed for the two types of electrodes. It was found that the Tafel slope measured for the Pt/BDD powder floating electrode (~65 mV decade$^{-1}$) was lower than that for the Pt/graphite powder counterpart (~80 Mv decade$^{-1}$). Thus, the slope for methanol oxidation was slightly improved by the use of the BDD powder support (*ca*. 18%).

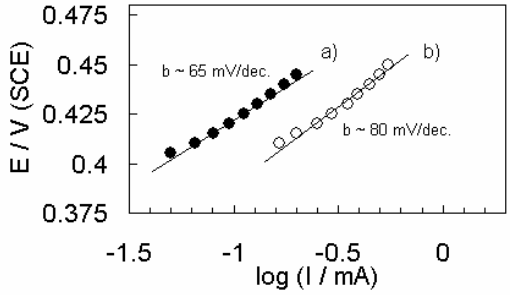


*Fig. 6. Steady-state polarization results obtained in 0.5 M $H_2SO_4$ + 1 M $CH_3OH$ for (a) Pt/BDD and (b) Pt/C porous gas-diffusion floating electrodes.*

The activity of Pt/BDD and Pt/graphite porous electrodes for methanol oxidation was also checked by long-term electrolysis measurements, performed in a 0.5 M $H_2SO_4$ + 1 M $CH_3OH$ solution, at an applied potential of 0.45 V. It was observed that, for short-time electrolysis (*ca*. 75 min), the decrease of the current was slower for the Pt/graphite porous electrode, again, probably due to its higher active

surface area and dispersion of the platinum particles. However, after *ca*. 4 hours of continuous polarization, the oxidation current at the Pt/BDD electrodes reached ~10% of its initial value, while that for the Pt/graphite decreased to ~5%. This is an indication that, during methanol oxidation in acidic media, the platinum electrocatalyst on diamond powder is slightly less sensitive to deactivation, e.g., via CO poisoning, compared to platinum on graphite.

**Reference:**

1. J. Wang and G. M. Swain, *Electrochem. Solid-State Lett.*, **5**, E4 (2002).
2. G. R. Salazar-Banda, K. I. B. Eguiluz and L. A. Avaca, *Electrochem. Commun.*, **9**, 59 (2007).
3. B. Yang, Q. Lu, Y. Wang, L. Zhuang, J. Lu, P. Liu, J. Wang and R. Wang, *Chem. Mater*., **15**, 3552 (2003).

First Regional Symposium on Electrochemistry of South-East Europe, Rovinj, Croatia, May 4-8, 2008.

P-1-020

# ELECTROCHEMICAL BEHAVIOR OF PALLADIUM NANOPARTICLES AND NANOWIRES DEPOSITED ONTO CARBON SURFACES

**V.C. Diculescu*, A.M. Chiorcea Paquim, O. Corduneanu, A.M. Oliveira-Brett**

*Departamento de Química, Faculdade de Ciências e Tecnologia, Universidade de Coimbra, 3004-535, Coimbra, Portugal, *victorcd@ipn.pt*

The behaviour of palladium nanostructures deposited onto a glassy carbon surface depend on the pH of the electrolyte buffer solution. Nanoparticles and nanowires of palladium metal were electrochemically deposited onto carbon surfaces and were investigated using cyclic voltammetry, impedance spectroscopy and atomic force microscopy.

In acid or mild acid solutions at applied negative potentials, hydrogen can be adsorbed on the palladium surface or absorbed into the palladium lattice. By controlling the applied negative potential different quantities of hydrogen can be incorporated, and this process is followed by analyzing the oxidation peak of hydrogen, Fig. 1. It has been shown that the formation of a palladium oxide pre-monolayer film begins at a negative potential. This phenomenon is strongly dependent on the size and morphological characteristics of Pd(0) nanostructures existent on the surface of the electrode, relevant for palladium electrocatalysis [1].

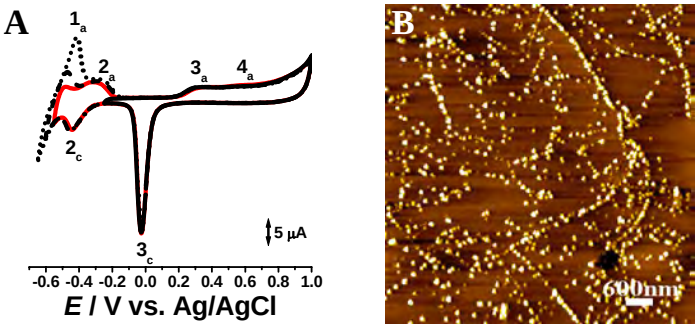


*Figure 1. (A) CVs of Pd(0) nanoparticles on the GCE surface in pH 7.0 0.1 M phosphate buffer between a positive potential limit of + 1.00 V and a variable negative potentials limit. (B) AFM topographical images in air of Pd(0) nanoparticles deposited onto HOPG, between -0.5 V and +0.9 V; Scan rate* $\nu = 100\ mV\ s^{-1}$.

At high positive potentials, the Pd(0) on the electrode surface undergoes oxidation leading to the formation of a mixed oxide layer that may also contain nucleation points for additional Pd metal growth, increasing the electrode surface coverage. Atomic force microscopy (AFM) showed that nanoparticles were formed by overpotential deposition (OPD) whereas using underpotential deposition (UPD) nanowires were preferentially electrodeposited on surface defects on the HOPG surface.

1. Diculescu, V.C.; Chiorcea-Paquim, A.M.; Corduneanu, O.; Oliveira Brett, A.M. *J. Solid State Electrochem.* **2007**, 11, 887-898.

First Regional Symposium on Electrochemistry of South-East Europe, Rovinj, Croatia, May 4-8, 2008.

P-1-021

# SUPPORT EFFECT IN Pt CATALYSTS ON CARBON MATERIALS

**S. Stevanović[a], V.M. Jovanović[a], M. Mitrić[b], B. Kaluđerović[b]**

*[a]University of Belgrade, ICTM – Institute of Electrochemistry, P.O.Box 473, 11000 Belgrade*
*[b]Vinča Institute of Nuclear Sciences,P.O.Box 522, 11001 Belgrade, Serbia*

Owing to its physico-chemical features carbon is, in a variety of forms, extensively used as an electrode material in different electrochemical systems. Very often it is applied as a catalyst support. One of the most intensively studied is platinum catalyst supported on high area carbon. Electrocatalytic activity of these catalysts for methanol oxidation in acidic solutions, as well as effects influencing their performance are discussed in number of papers[1-6] because of a possible application in a fuel cell. It was noticed that the nature of high area carbon support affected structure of platinum deposits and thus their activity[1-4]. Yet, particle size, distribution and loading of platinum have been in focus of the research and appeared to have a significant role in the electrocatalysis[1-6]. Using platinum electrochemically deposited on glassy carbon (GC) as a model system, we showed that proper activation of the support could lead to the enhancement of the catalyst activity for methanol oxidation more than ten times in comparison with polished GC[7] as well as that morphology of the support could have large impact on the structure of Pt catalyst particles and thus thair activity[8]. In this work we focused our studies on these influences of the support on Pt chemically deposited on grinded different carbon fibers and on carbon black for comparison.

Cellulose or polysulphonated fibers (with different pore size and distribution) $HF_C$ or $HF_S$ respectively, as carbon precursors were pyrolized to 1000$^o$C in inert atmosphere and grinded to the particles of approximately same size. Platinum was chemically deposited on non-activated or activated fibers. Activation was performed chemicaly using $Na_2HPO_4$ solution before carbonization proces. Grinded fibers were washed in destilled water. On this way, different functional groups were formed as well as thair dirrerent fraction on the surface of the material leading to its different morphology.

Platinum was deposited on all substrates applying modified $NaBH_4$ assisted ethylen glycol procedure[9]. The procedure was finalized with the addition of HCl to assist deposition of Pt nanoparticles on the support. The obtained catalyst was dried over night at 120$^o$C.

On this way catalysts with 14 wt % were prapared. All of the catalysts as well as supports were characterized by microscopic techniques, X-ray diffraction and cyclic voltammetry. The activity of the catalysts was tested for the oxidation of methanol and formic acid. The results were compared with those obtained for commercial E-tek catalyst with the simmilar Pt content.

The catalysts were applied to the disk electrode in a form of a thin layer. The layer was prepared by attaching ultrasonically re-dispersed catalyst suspension in triply pyrodistilled water onto the glassy carbon, resulting in a constant metal loading of ~ 20

μg Pt/cm$^{-2}$. After drying, the deposited catalyst layer was covered with ~ 20 μl of diluted aqueous Nafion solution and dried again.

The results obtained showed the impact of the support properties on the properties of the Pt catalyst. Pt deposited on carbon black has particle diameter between 2.5 and 3.5 nm and has approximately 2 times higher activity for formic acis oxidation in comparison with comercial catalyst. Properties of the catalysts supported on the carbon fibers dippend on the precursor. Smaller particles, better dispersion and higher activity ehxibite Pt deposited on polysulphonated fibers. Fig. 1 shows cyclic voltammograms of these catalysts in 0.5 M $H_2SO_4$.

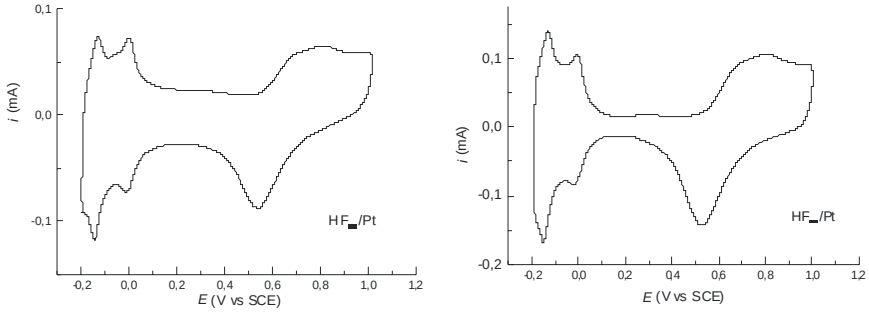


*Fig. 1.: Cyclic voltammograms of Pt deposited on non-activated carbonized cellulose and polysulphonated hollow fibers in 0.5 M $H_2SO_4$ (sweep rate 50 mV/s)*

Activation of the fibers influences Pt dispersion, particle size and activity but depende on the precursor as well as on the conditions applied.

**References:**

1. T. Frelink, W. Visscher, J.A.R. van Veen, *J. Electroanal. Chem.* **328** (1995) 65
2. A. Stoyanova, V. Naidenov, K. Pertov, I. Nikolov, T. Vitanov, E. Budevski, *J. Appl. Electrochem.* **29** (1999) 1197
3. S.Lj. Gojkovic, T.R. Vidakovic, *Electrochim. Acta* **47** (2001) 633
4. P.A. Attwood, B.D. McNicol, R.T. Short, *J. Appl. Electrochem.* **10** (1980) 213
5. M. Watanabe, S. Saegusa, P. Stonehart, *J. Electroanal. Chem.* **271** (1989) 213
6. O.V. Cherstiouk, P.A. Simonov, E.R. Savinova, *Electrochim. Acta* **48** (2003) 3851
7. V.M. Jovanović, S. Terzić, A. V. Tripković, K. Đ. Popović, J. D. Lović, *Electroceh.Comm.*, **6** (2004) 1254-1258.
8. D. Tripković, S. Stevanović, A. Tripković, A. Kowal, V.M. Jovanović, *J.Electrochem. Society* (submitted)
9. P. Kim, J.B.Joo, W.Kim, J.Kim, I.K.Song and J.Yi, *J.Power Sources* **160** (2006) 987

First Regional Symposium on Electrochemistry of South-East Europe, Rovinj, Croatia, May 4-8, 2008.

P-1-022

# SURFACE AREA DETERMINATION OF PLATINUM DEPOSITED ON ACTIVATED CARBON SUBSTRATE

**S. Stevanović, R.M. Stevanović, V.V. Panić, A.B. Dekanski, V.M. Jovanović**

*University of Belgrade, ICTM – Institute of Electrochemistry, Njegoševa 12, P.O.Box 473, 11000 Belgrade, Serbia, E-mail: vlad@tmf.bg.ac.yu*

Activation of carbon substrate prior to deposition of Pt catalyst enhances activity of the catalyst in oxidation of small organic molecules[1-7]. Applying glassy carbon (GC) as a model support, we showed that it's activation by anodic polarization in sulfuric acid could enhance activity of electrochemically deposited Pt depending on the reaction even for more than 10 times[6,7]. Cyclic voltammetry of Pt deposited on oxidized GC i.e. of $GC_{OX}$/Pt electrode revealed features of both Pt and oxidized GC[6]. However, increased double layer charge of activated GC support i.e. background currents and roughness can mask characteristic peaks of Pt. This can make the determination of the real surface area of the Pt catalyst from hydrogen adsorption/desorption coulometry difficult or even impossible. Real Pt surface area can be determined from the CO UPD charge[4,8] or from the Cu UPD charge which Green and Kucernak[9,10] used for measuring the surface area of highly dispersed Pt or Pr-Ru catalysts. We proposed another method[6,7]. The real surface area of platinum deposited on oxidized GC was estimated from the difference between electrode voltammetric charges prior to and after deposition of Pt catalyst: $\Delta Q = Q_{GCox/Pt} - Q_{GCox}$. The charges were determined by cyclic voltammetry in the region of H adsorption and desorption (from –0.2 V to 0.15 V vs SCE) and corrected for a double layer charging of 12 % for polycrystalline Pt.

In this work, we present our results on comparison of surface area of Pt deposited on mechanically or electrochemically treated GC support determined by 3 different methods: hydrogen adsorption/desorption coulometry, difference in charge and Cu UPD coulometry in 0.5 M $H_2SO_4$ solution.

First we tested our approach and compared it with other two methods using thin film of Pt black applied on polished or oxidized GC (at 2 V vs SCE during 95 s in 0.5 M $H_2SO_4$). The results are presented in the Table. Difference in the calculated area of less than ~ 20 % confirms the applicability of our approach. Than we deposited Pt by potential step method (from – 0.2 V to 0.1 V after 5 s) from 0.5 M $H_2SO_4$ + 6 mM $H_2PtCl_6$ on polished or oxidized GC (at 2 V vs SCE during 95 s in 0.5 M $H_2SO_4$) and calculated surface areas using all three methods. The results obtained are also given in the Table. Although again the difference was acceptable it happened that in some repeated experiments the area calculated from Cu UPD (1 mM $CuSO_4$) was much smaller both in the case of GC/Pt and $GC_{OX}$/Pt. This discrepancy was related with the increased difference in peak heights between strongly and weakly bonded hydrogen ($h_w/h_s$).

| electrode | $A_{Pt}$ ($cm^2$) – $H_{ads/des}$ | $A_{Pt}$ ($cm^2$) – $\Delta Q$ | $A_{Pt}$ ($cm^2$) – Cu UPD |
|---|---|---|---|
| $GC/Pt_{black}$ | 0.63 | 0.64 | 0.67 |
| $GC_{OX}/Pt_{black}$ | | 0.42 | 0.53 |
| GC/Pt | 0.55 | 0.52 | 0.49 |
| $GC_{OX}/Pt$ | | 0.45 | 0.56 |

The ratio of peak heights for weakly and strongly bonded hydrogen in the region of hydrogen adsorption/desorption should reflect a change in structural properties of Pt catalyst[2,3]. In order to elucidate this relation of Cu UPD and $h_w/h_s$ ratio we continued our examinations using Pt polycrystalline electrode. The ratio between strongly and weakly bonded hydrogen we changed by treating the electrode with abrading materials ($Al_2O_3$ suspensions and fine emery paper) of different grain size (***d*** from 0.05 μm to 46 μm) and cycling the potential between – 0.2 V and 1.2 V at 100 mV/s in 0.5 M $H_2SO_4$ solution. The results are given in the Fig.

Two interesting features were observed. Although the roughness should increase and thus Pt surface area due to increase of size of abrading particles, the area exhibits maximum if calculated from hydrogen coulometry but remains almost unchanged if calculated from Cu UPD. Also the increase in weakly bonded hydrogen as expected reflects in increase of area calculated from hydrogen coulometry but has practically no effect on Cu UPD.

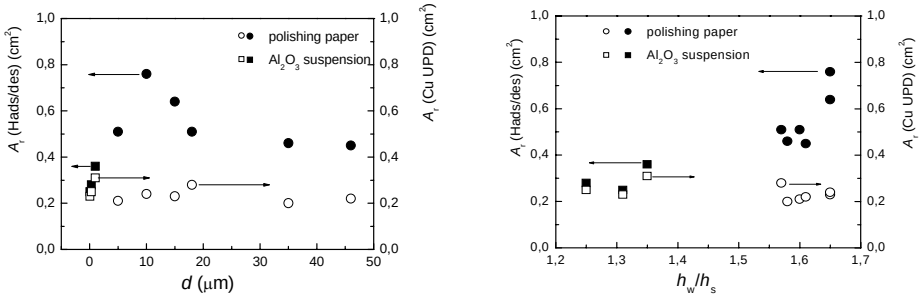


It may be concluded that the real surface area of Pt deposited on oxidized GC can be determined from the difference between electrode voltammetric charges, prior to and after the deposition of Pt catalyst. Determination from the Cu UPD charge is of a limited relevance, since the charge is here found to be almost independent on the surface roughness and structure of the Pt grains (reflected in $h_w/h_s$ ratio). Scortichini also reported about limited applicability of Cu UPD charge for determination of real surface area of Pt.[11]

**References:**

1. P. A. Attwood, B. D. McNicol, R. T. Short, *J. Appl. Electrochem*., 10 (1980) 213.
2. T. Frelink, W. Visscher, J. A. R. van Veen, *J. Electroanal. Chem*., **328** (1995) 65.
3. A. Stoyanova, V. Naidenov, K. Pertov, I. Nikolov, T. Vitanov, E. Budevski, *J. Appl. Electrochem*., **29** (1999) 1197.
4. F. Gloaguen, J. M. Leger, C. Lamy, *J. Appl. Electrochem*., 27 (1997) 1052.

5. Y. Takasu, T. Iwazaki, W. Sugimoto, Y. Murakami, *Electrochem Comm.* **2** (2000) 671.
6. V.M.Jovanović, S. Terzić, A. V. Tripković, K. Đ. Popović, J. D. Lović, *Electrochem.Comm*., **6** (2004) 1254.
7. V.M.Jovanović, D. Tripković, A. Tripković, A. Kowal and J. Stoch, *Electrochem. Comm.*, **7**, 1039 (2005).
8. O. V. Cherstiouk, P. A. Simonov , E. R. Savinova, *Electrochim. Acta*, **48** (2003) 3851.
9. C.L.Green and A.Kucernak, *J.Phys.Chem.B* **106** (2002) 1036
10. C.L.Green and A.Kucernak, *J.Phys.Chem.B* **106** (2002) 11446
11. C.L.Scortichini and C.N.Reilly, *J.Catalysis* **79** (1983) 138

First Regional Symposium on Electrochemistry of South-East Europe, Rovinj, Croatia, May 4-8, 2008.

P-1-023

# A THIN-FILM ROTATING ELECTRODE STUDY: OXYGEN REDUCTION ON CARBON CATALYSTS

**Z. Grubač[1], M. Metikoš–Huković[2], Z. Čeralinac[3]**

*[1]Department of General and Inorganic Chemistry, Faculty of Chemistry and Technology, University of Split, Teslina 10/V, 21000 Split, Croatia*
*[2]Department of Electrochemistry, Faculty of Chemical Engineering and Technology, University of Zagreb, Savska 16, PO Box 177, 10000 Zagreb, Croatia, mmetik@marie.fkit.hr*
*[3]Department for Materials and Technology, Končar Electrical Engineering Institute, Fallerovo šetalište 22, Croatia*

For the anodic oxidation of hydrogen as well as the catodic reduction of oxygen a commonly used electrocatalyst in low-temperature polymer electrolyte fuel cells is platinum supported on high-surface-area substrates. Of major interest is to develop new or modified catalyst with improved activity for fuel cell applications. The explicit method for comparing the electrocatalytic activity of an alternative high-surface-area catalyst under fuel cell working conditions is to produce a membrane electrode assembly and to measure the catalytic activity in a single cell configuration.

In this work, the electrode kinetics of oxygen reduction reaction was studied using thin-film rotating disk electrode (RDE) technique in 0.1 M $HClO_4$ solution in temperature range from 20°C to 60°C. The limiting factor of diffusion resistance through the Nafion film was also investigated in the function of temperature. The method involves attaching the catalyst particles to a glassy carbon RDE *via* a sub-micrometer thick Nafion film. So prepared thin-film RDE avoid or reduces the problems with the mass-transport resistances and/or incomplete wetting of the electrode structure and enables direct extracting of kinetic current densities using the unmodified mass-transport correlations for simple RDE. This allows the direct extrapolation of RDE data on the performance of polymer electrolyte membrane (PEM) fuel cell electrodes. As catalysts, the high surface area Vulcan XC72 carbon supported mono- and bimetallic catalysts (Pt, PtSn, PtRu) were used. A comparative investigation under the same conditions was carried out on the Pt-catalyst, which was used as a model-system.

First Regional Symposium on Electrochemistry of South-East Europe, Rovinj, Croatia, May 4-8, 2008.

P-1-024

# COPPER NANOSTRUCTURED ELECTRODES FOR CARBON DIOXIDE REDUCTION

**M. Jitaru, O. Gabriel, R. Jitaru**
*Babes-Bolyai University, Faculty of Chemistry&Chemical Engineering, Associated Francophon Laboratory 11, Arany Janos street, 400028 Cluj-Napoca, Romania*
*E-mail: mjitaru@chem.ubbcluj.ro*

The electrocatalytic activity of nanostructured copper particles towards oxygen reduction is interesting due to the possible application in electrocatalysis and fuel cell. On the other hand, the electrocatalytic activity for carbon dioxide reduction of metals, including copper is well known. On the other hand, nanostructured metals exhibit different and usually more efficient activity.
In this work we present the preparation and characterization of copper growing a 3D array of copper nanorods onto a copper coin by deposition through an alumina membrane that is later dissolved. By this, active material surface contacts is increased, as it can been clearly seen from Figure 1.
This work is divided into three main parts:

- elaboration of the nanostructured Cu support;
- electrochemical characterization of the nanostructured Cu electrodes;
- preliminary assays of $Cu_{nano}$ for carbon dioxide electroreduction.

The copper nanostructures were obtained by deposition through an alumina membrane (AAO) that is later dissolved. The diameter of the copper nanorods deposited on Cu is about 150 nanometres, which is in good agreement with the AAO membrane pore size used in the electrolysis process. The nanorods were found to be vertically aligned and no collapsing was observed with the height deposited, which was around 2 μm, Figure 2.

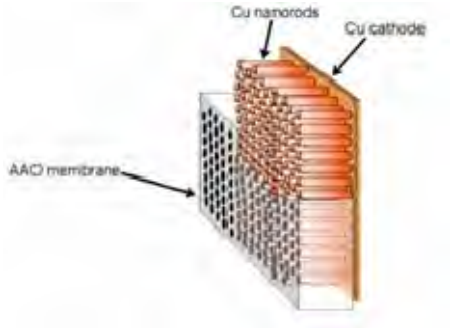


*Fig.1. Image of Cu nanorods*

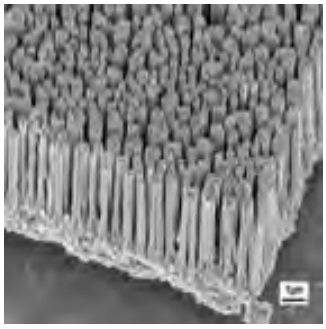

*Fig.2. SEM of obtained Cunano*

Electrochemical characterisation of nanostructure $Cu_{nano}$ electrodes was performed with a BAS100W computer aided potentiostat, equipped with a three-electrode system (WE- nanostructured Cu rods; CE-Pt wire and RE-standard calomel electrode).

The most common reactionsduring the electroreduction of carbon dioxide are as follows*:

$CO_2 + H^+ + 2e^- \rightarrow HCOO^-$ $E^0 = - 0.61V$ (1)

$CO_2 + 2H^+ + 2e^- \rightarrow CO + H_2O$ $E^0 = - 0.53\ V$ (2)

$CO_2 + 6H^+ + 6e^- \rightarrow CH_3OH + H_2O$ $E^0 = - 0.38\ V$ (3)

$CO_2 + 8H^+ + 8e^- \rightarrow CH_4 + 2H_2O$ $E^0 = - 0.24\ V$ (4)

$2CO_2 + 2e^- \rightarrow (COO^-)_2$ (5)

$(COO^-)_2 + 3H^+ + 2e^- \rightarrow {}^-O_2C - CH(OH)_2$

$\downarrow$

$^-O_2C - CHO + H_2O$ (6)

* (at pH 7 in aqueous solution versus NHE, $25^0$C, 1 atmosphere for the gases, and 1 M for the other solutes).

On $Cu_{nano}$ the main reduction compounds are $CH_4$ , $H_2$ and formic acid, Figure 3.

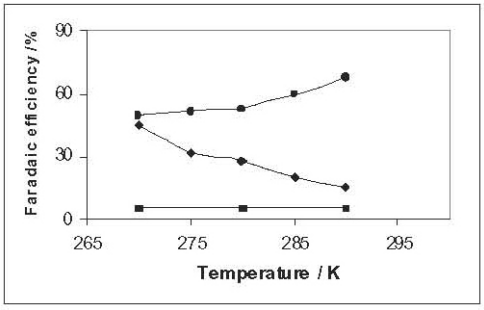


*Fig. 3. Faradaic efficiencies for the products formation on Cu electrodes in bicarbonate solution at - 2.0 V, depending on temperature.* (●) *H ;* (◆) *CH ;* (■) *HCOOH .*

The main competitive reactions (7-11) involve electrosorbed species with hydrogen atom participation. Thus, in the electrochemical reduction of $CO_2$ in water, hydrogen formation competes with the $CO_2$ reduction reaction. Therefore, the suppression of hydrogen formation is very important because the applied energy is wasted on hydrogen evolution instead of being used for the reduction of $CO_2$.

$H^+ + e^- \longrightarrow H_{ad}$ (7)

$CO_2 + H_{ad} \longrightarrow HCOO_{ad}$ (8)

$HCOO_{ad} + H_{ad} \longrightarrow HCOOH$ (9)

$HCOO_{ad} + CH_3OH \longrightarrow CH_3COOH + OH_{ad}$ (10)

$OH_{ad} + H_{ad} \longrightarrow H_2O$ (11)

Further work is in progress to study the electrocatalytic parameters influencing the selectivity of $Cu_{nano}$ electrodes for $CH_4$ preparation and the electrode reaction kinetic.

***Acknowledgements***

*This work has been supported by Romanian CEEX –MATNANTECH No.68/2006*

First Regional Symposium on Electrochemistry of South-East Europe, Rovinj, Croatia, May 4-8, 2008.

P-1-025

# PREPARATION OF POLYANILINE/RU-OXIDE COMPOSITE FOR ELECTROCHEMICAL SUPERCAPACITORS

**M. Kraljić Roković[1], Z. Mandić[1], V. Horvat-Radošević[2], K. Kvastek[2]**

*[1]Faculty of Chemical Engineering and Technology, P. O. Box 177, 10000 Zagreb, Croatia, mkralj@marie.fkit.hr*
*[2]Rudjer Bošković Institute, Bijenička c. 54, 10000 Zagreb, Croatia*

It has already been found that owing to high specific capacitance, high reversibility, wide potential range and very good cycleability, hydrous Ru-oxide is one of the best materials for electrochemical supercapacitors [1]. However, electrochemical reactions giving rise to its high pseudocapacitance are limited to a rather thin surface layer of deposited film. It is therefore of high importance to improve utilization of Ru material and achieve higher gravimetric energy and power densities. Among various strategies for preparation of hydrous Ru-oxide electrode with enhanced capacitance, formation of different composite materials has already been attempted in the literature [2-4]. Such composites are synthesized in order to combine beneficial properties of hydrous Ru-oxide with advantages of other materials such as high surface area. Due to the extremely high surface area and charge storage capability, conducting polymers are already found as promising candidates for formation of composite with Ru-oxide.

In this work, different methods of polyaniline (PANI)/Ru-oxide composite preparation at glassy carbon (GC) electrodes are reported. Nafion$^{TM}$ was introduced as a template for PANI growth and for improving mechanical properties of electrodes. The results are compared with PANI/Ru-oxide composite prepared at Pt electrodes without the Nafion$^{TM}$. The electrochemical behaviour of prepared composites were characterized in $H_2SO_4$ acid solution by cyclic voltammetry and electrochemical impedance spectroscopy techniques. Two different procedures (Methods A and B) for preparation of PANI/Ru-oxide composites are developed and described as follows:

**Method A** (four-step procedure): i) Nafion layer was casted onto GC electrode and left overnight for evaporation of solvent; ii) PANI matrix was formed potentiodynamically within Nafion$^{TM}$ matrix from aniline/$H_2SO_4$ solution at defined scan rate and different number of cycles; iii) Ru was electrodeposited onto PANI matrix by the potential square wave method from $RuCl_3$/HCl electrolyte solution; iv) deposited Ru was oxidised to hydrous Ru-oxide in $H_2SO_4$ solution by cycling the potential within strongly defined potential limits and scan rate.

**Method B:** (two-step procedure): i) Suspension of Nafion and Ru-oxide was casted onto GC electrode and left overnight for evaporation of solvent. ii) PANI films were formed within the pores of Nafion/Ru-oxide as in Method A.

Cyclic voltammograms of Pt/PANI and Pt/PANI/Ru-oxide electrodes are in 0.5 mol $dm^{-3}$ $H_2SO_4$ solution at scan rate 50 mV $s^{-1}$ are shown in Fig. 1. Cyclic voltammograms of GC/Nafion/PANI and GC/Nafion/PANI/Ru-oxide electrodes

prepared by Methods A and B in the same solution and scan rate are shown in Figs. 2 and 3, respectively.

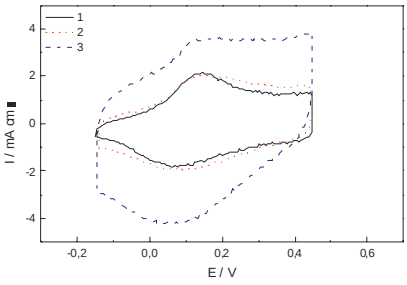


*Fig.1 Cyclic voltammograms of **1:** Pt/PANI, **2**: Pt/PANI/Ru-oxide (smaller amount of electrodeposited Ru), **3:** Pt/PANI/Ru-oxide (higher amount of electrodeposited Ru).*

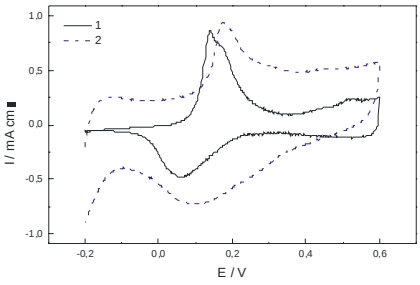


*Fig. 2. Cyclic voltammograms of **1:** GC/Nafion/PANI and **2: GC**/Nafion/PANI/Ru-oxide prepared by **method A.***

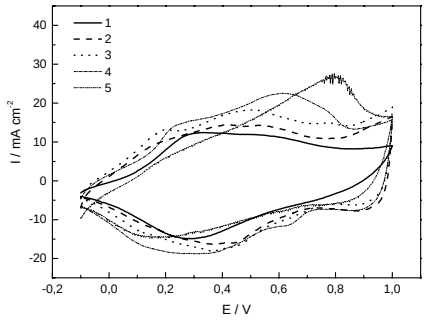


*Fig. 3. Cyclic voltammograms of **1:** GC/Nafion/Ru-oxide, **2:** GC/Nafion/Ru-oxide/PANI1, **3:** GC/Nafion/Ru-oxide/PANI2, **4:** GC/Nafion/Ru-oxide/PANI3, **5:** GC/Nafion/Ru-oxide/PANI4 prepared by **method B**.*

The results demonstrate that both methods lead to the overall increase of specific charges of composite electrodes. This is particularly prominent for the composite prepared by the Method A where additionally, a widening of the voltage range of capacitive response is observed (Figs.1-2). Increase of the overall charge is observed also for the composite prepared by the Method B, except for thicker PANI4 deposits, where irreversible damages to the electrodes are observed through deformation of volatammograms (Fig.3). Further experimental investigations related to varying the amounts of Ru-oxide and PANI and other details of preparation procedures are currently in a progress.

**References:**

[1]. B. E. Conway, *Electrochemical Supercapacitors. Scientific Fundamentals and Technological Applications*, Kluwer Acad./Plenum Publ., New York. 1999.

[2] M. Min, K. Machida, J.H. Jang, K. Naoi, *Journal of the Electrochemical Society* **153** (2006) A334-A338.

[3] H. Kim, J.-H. Kim, K.-B. Kim, *Electrochemical and Solid-State Letters* **8** (2005) A369-A372.

[4] H. Kim, B. N. Popov, *J. Power Sources* **104** (2002) 52-61.

First Regional Symposium on Electrochemistry of South-East Europe, Rovinj, Croatia, May 4-8, 2008.

P-1-026

# INFLUENCE OF NATURE AND DOPANT CONTENT ON ELECTROCHEMICAL BEHAVIOUR OF SPINELS $LiMe_XMn_{2-X}O_4$ (Me=Cr, Co) AS CATHODIC MATERIALS FOR Li-ION BATTERIES

**A.V. Churikov, E.I. Khachibaya*, V.O. Sycheva, I.A. Ivanischeva, A.V. Ivanischev, R.A. Imnadze*, T.V. Paikidze***

*Saratov State University, 83 Astrakhanskaya street, 410012 Saratov, Russia*
**Institute of Inorganic Chemistry and Electrochemistry, 11 Mindely street, Tbilisi, Georgia, E-mail: churikovav@info.sgu.ru*

Existence of reversible lithium intercalation/deintercalation reactions in $LiMn_2O_4$ allows to consider it as promising cathode materials for rechargeable lithium batteries. However, Li-Mn-O system is characterized by poor cyclability and low initial discharge capacity. The substitution of Mn atoms by $Cr^{3+}$ or $Co^{2+}$ into the site is accompanied by an oxidation of $Mn^{3+}$ to $Mn^{4+}$ resulting in an increase in the average valency of the manganese ions, and hence a suppression of the Jahn-Teller distortion, which is one of possible sources of capacity fading in the spinel material $LiMn_2O_4$.

Electrode materials were obtained by melt-impregnation method. Electrochemical testing of such electrodes were carried out by applying cycle voltamperometry at a scan rate of 0.1 $mV \cdot s^{-1}$ on cycling in the 3.5 – 4.5 V voltage window versus $Li/Li^+$. Including, the electrochemical reversibility can be evaluated by such measurements (Fig. 1a.). The discharge capacity/cycle number dependencies represents on Fig. 1b. Apparently, $LiMn_{1.95}Cr_{0.05}O_4$-spinel demonstrates high initial discharge capacity and relative cycling stability. This compound possess the best Mn:Cr proportion. In contrast, the same ratio of Mn:Co = 1.95:0.05 results in the structural instability of spinel. So, electrochemical properties of substituted spinels depend also on nature of dopant. More covalent Mn-O bond makes the spinel structure more resistant to destructive expansion (insertion of Li) and contraction (extraction of Li) observed in $LiMn_2O_4$ electrodes. The covalence of the Mn-O bond of Cr-substituted electrode materials is greater than that for Co-doped spinel. Hence, the introduction of small quantity of dopant ions (Cr) leads to some degree of local stability in the structure of $LiMn_2O_4$ which results in the increased discharge capacity and enhanced cycling performance.

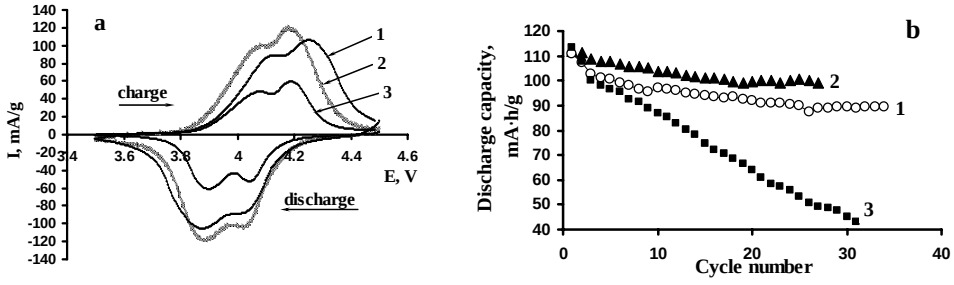


*Fig. 1. Cycle voltammograms (**a**) and discharge capacity as a function of cycle number (**b**) for: **1**– $LiMn_2O_4$; **2**– $LiMn_{1.95}Cr_{0.05}O_4$; **3** – $LiMn_{1.95}Co_{0.05}O_4$. Scan rate: 0.1 $mV \cdot s^{-1}$.*

First Regional Symposium on Electrochemistry of South-East Europe, Rovinj, Croatia, May 4-8, 2008.

P-1-027

# ELECTROCHEMICAL REACTIONS OF $V_2O_5$ IN AQUEOUS SOLUTIONS

**S. Mentus, I. Stojković*, I. Pašti, N. Cvijetićanin**

*Belgrade University Faculty of Physical Chemistry, Studentski trg 12 Belgrade, Serbia*
*ivana@ffh.bg.ac.yu

Electrochemical intercalation is a recent field of research, related primarily to the development of Li-ion batteries. Batteries with non-aqueous electrolytes are commonly used in practice, however, several types of ones using aqueous electrolytes were also proposed [1]. Vanadates are well known electrode materials and vanadium pentoxide was used as a material for electroche-mical capacitors [2]. Intercalation of alkali ions into $V_2O_5$ was investigated in non-aqueous solutions with potential application as alkali ion storage material or as electrochromic devices [3]. In the here presented contribution, intercalation behavior of $V_2O_5$ in aqueous solutions was demonstrated on the basis of cyclic voltammetry (CV) and galvano-static cycling. X-ray diffractometry and SEM were used for material characterization.

Electrodes were prepared by mixing commercial $V_2O_5$ powder (60 wt.%), carbon black (30 wt.%) and PVdF binder (10 wt.%, used as a 2% solution in N-methyl-2-pyrrolidone). A part of $V_2O_5$ was previously treated with $H_2O_2$ according to ref.[4], in order to obtain nanoparticles. Mixture was pasted on glassy carbon stick and then dried under vacuum at 140°C for 12 hours. Saturated

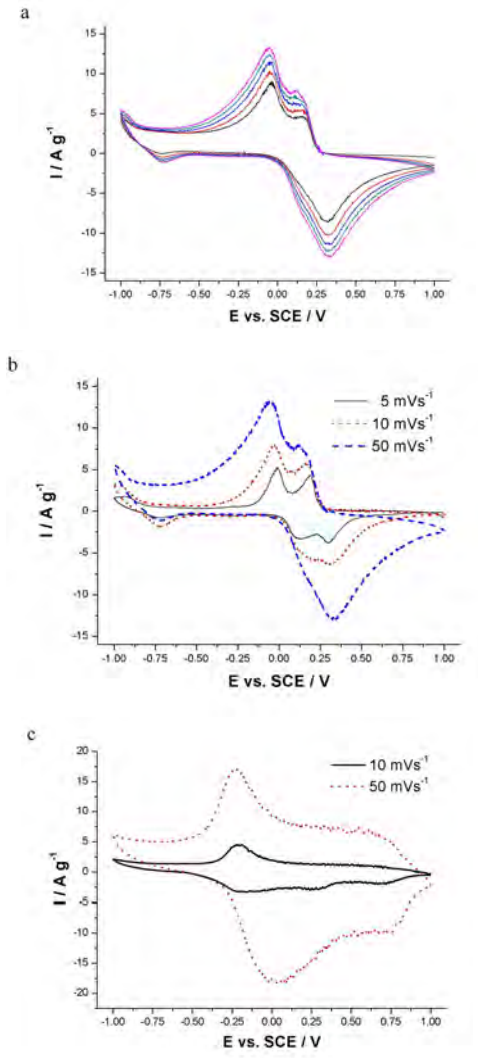


*Figure 1. First five CV curves for $V_2O_5$ in saturated $LiNO_3$ at scan rate 50 $mVs^{-1}$, current is increasing in every cycle (a), CV curves of $V_2O_5$ at three different scan rates (b), CV curves of $V_2O_5$ treated with $H_2O_2$ at two different scan rates*

aqueous $LiNO_3$ and $Mg(NO_3)_2$ solutions have been used as electrolytes.

CV curves in saturated $LiNO_3$ are shown in Fig. 1a. Two pairs of redox peaks were observed, indicating that the reduction of $V_2O_5$ (accompanied by intercalation) is two-step process.

It was found that current increased during first few cycles and then reached a steady value giving completely repeatable CV curves. Current peaks are clearly visible and well separated at lower scan rates. CV curves of $V_2O_5$ treated with $H_2O_2$ in saturated $LiNO_3$ (Fig. 1c) solution indicated a considerably enlarged faradaic capacity as well as a very good repeatability.

Cyclic voltammograms recor-ded in saturated $Mg(NO_3)_2$ indicate the redox reactions commercial $V_2O_5$ (Fig. 2a to 2b) too. Current peaks are located at lower potentials with respect to the one of in Li-salt solution. Similar to Li-salt solution, initial current growth during first few cycles was recorded, finishing with repeata-ble steady values.

For commercial $V_2O_5$ in Li-salt solution, average faradaic capacity of around 63 $mAhg^{-1}$ was determined, while $V_2O_5$ treated with $H_2O_2$ displayed faradaic capacity of roughly 100 $mAhg^{-1}$. For Mg-salt solution, faradaic capacity of origi-nal $V_2O_5$ was 30 $mAhg^{-1}$, while for $H_2O_2$ treated $V_2O_5$ the correspond-ding value was 120 $mAhg^{-1}$.

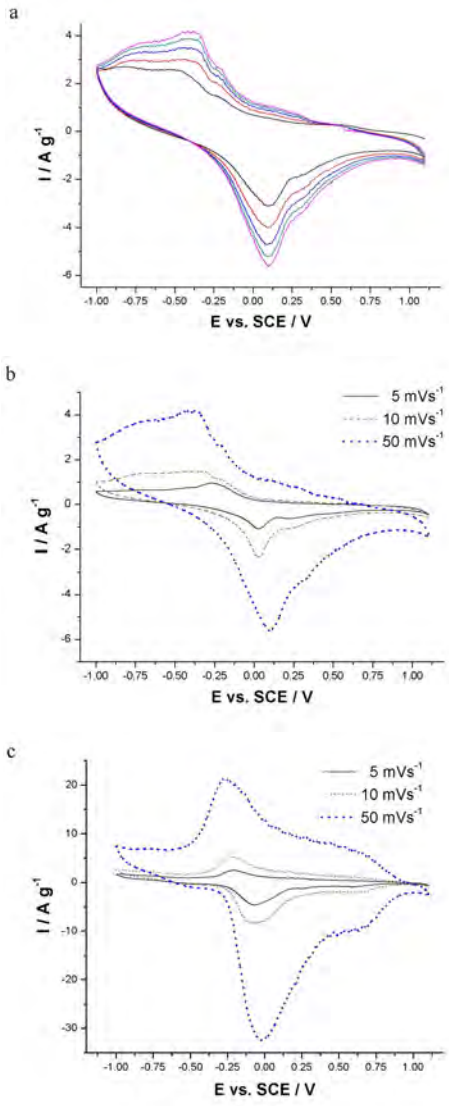


*Figure 2. CV curves for $V_2O_5$ in saturated $Mg(NO_3)_2$; First five CV's with commercial $V_2O_5$ at a scan rate 50 $mVs^{-1}$- current increasing in every cycle (a); commercial $V_2O_5$, rising scan rates (b); $H_2O_2$ treated $V_2O_5$ , rising scan rates (c)*

These preliminary results revealed interesting electrochemical properties of $V_2O_5$ in aqueous solutions. Future investigations can be guided in two possible directions: either toward detailed analysis of mechanism of ion intercalation, or toward the improvement of materials to become applicable in Li and Mg cells.

**References:**

1. Wang H., Zeng Y., Huang K., Liu S., Chen L., *Electrochimica Acta* **52** (2007) 5102–5107.
2. Lao Z.J., Konstantinov K., Tournaire Y., Ng S.H., Wang G.X., Liu H.K., *Journal of Power Sources* **162** (2006) 1451–1454
3. Donsanti F., Kostourou K., Decker F., Ibris N., Salvi A. M., Liberatore M., Thissen A., Jaegerman W., Lincot D., *Surf. Interface Anal.* **38** (2006) 815–818
4. Alonso B., Livage J., *Journal of Solid State Chemistry* **148** (1999) 16-19

First Regional Symposium on Electrochemistry of South-East Europe, Rovinj, Croatia, May 4-8, 2008.

P-1-028

# ELECTROCHEMICAL OBTAINING OF $Ni(OH)_2$ FROM SULFATE SOLUTION BY FLOWING SLIT DIAPHRAGM ELECTROLYZER

**V.L. Kovalenko, V.A Kotok*, V.V. Malishev**

*Department of technical electrochemistry, Ukrainian State University of Chemical Engineering 8, Gagarin Avenue, Dnepropetrovsk, Ukraine, 49005*
*E-mail: Valeriy_e-ch@ukr.net*

## Introduction

Alkaline secondary cells are widely used in different mobile devises, in cars with electric or hybrid engine, etc. $Ni(OH)_2$ is used as an active substance of positive electrode in Ni-Cd, Ni-Fe, Ni-MH secondary cell. Its characteristics depend on nickel hydroxide properties [1]. Industrial method for $Ni(OH)_2$ production is periodic chemical. The aims of the present work are the development of electrochemical method for $Ni(OH)_2$ obtaining and investigation of the influence of obtaining condition to properties of nickel hydroxide.

## Experimental

Electrochemical method of $Ni(OH)_2$ obtaining was developed. It bases on electrolysis of nickel sulphate solution, which was pumped through cathode space of slit diaphragm electrolyzer. Alkaline solution was pumped through anode space. Reaction took place in the cathode space:

Surface $2H_2O + 2e = H_2 + 2OH^-$;

Volume $Ni^{2+} + 2OH^- = Ni(OH)_2$.

Obtaining of $Ni(OH)_2$ was carried out under different current density (from 4 to 15.7 $A/dm^2$). Under all obtaining condition nickel hydroxide is formed only in stream and it move out from electrolyzer. After that hydroxide was filtered by vacuum pump. All samples were treated corresponding to scheme: primary drying, milling and sifting, rinsing, filtered and secondary drying.

*Table 1. Samples of nickel hydroxide*

| Sample | A | B | C | D | E | F | G | H* |
|---|---|---|---|---|---|---|---|---|
| Current density, $A/dm^2$ | 4 | 6 | 8 | 10 | 12 | 14 | 15.7 | - |

* - Industrial sample, Co containing (“BOHEMIA”). Used as reference sample.

Properties of all samples have been investigated by following methods: HR SEM, XRD patterns, termogravimetric analysis, cyclic voltammogram (active mass - 74% $Ni(OH)_2$, 16% C, 10% PTFE, solution – 4.5M KOH), galvanostatic charge-discharge cycle (active mass - 74% $Ni(OH)_2$, 16% C, 10% PTFE, solution – 4.5M KOH).

XRD patterns (fig. 1) show that reference sample H consist of high enough crystallinity β-$Ni(OH)_2$. Sample F also consist of β-$Ni(OH)_2$, but the first peak, corresponding to crystal plane [001], is weakly showed. Therefore, the size of crystal in this direction is small, and form of crystal is a thin plate. Crystallinity of other samples (A, B, C, D, E, G) increases when current density increases too. But

XRD patterns of this sample have not only peaks of β-$Ni(OH)_2$, but peak of α-$Ni(OH)_2$ (2θ=13-16˚). So the suggestion may be proposed: these samples have structure like layered double hydroxide (LDH [2])– layers of β-phase and layers of α-like phase. α-Like phase of $Ni(OH)_2$ may be stabilized by $SO_4^{2-}$, because there is an excess of nickel sulphate near hydroxide particles during precipitating in the electrolyzer.

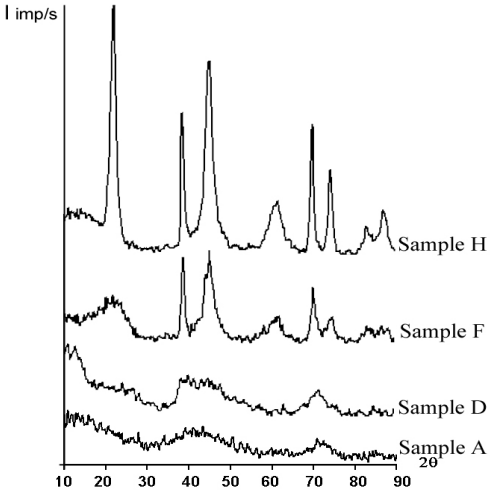


*Fig. 1. X-ray patterns of samples $Ni(OH)_2$.*

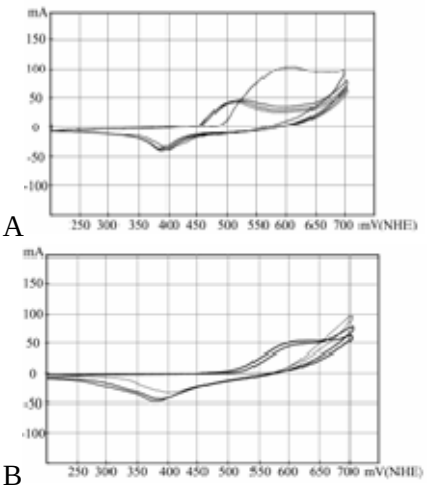


*Fig. 2. Cyclic voltammograms of $Ni(OH)_2$: A – sample D, B – sample H (1 mV/s).*

This suggestion confirms the results of HR SEM (elements' analysis) and qualitative chemical analysis: there aren't free $SO_4^{2-}$ ions in these samples, but there are $SO_4^{2-}$ ions in general. For investigation of electrochemical properties cyclic voltammograms have been observed. The results showed, that samples with LDH-like structure get up to maximum capacity quicker (fig. 2A), than the sample H (fig. 2B). One of the most important characteristic of $Ni(OH)_2$ is specific capacity, measured in galvanoststic condition. Values of these parameters are showed in the Table 2 (charge 1/18 C (with 20% overcharge), discharge 1/5 C, cadmium counter electrode, 4.5 M KOH as electrolyte).

*Table 2. Galvanostatic specific capacity of nickel hydroxide samples*

| Sample | A | B | C | D | E | F | G | H |
|---|---|---|---|---|---|---|---|---|
| C, mA·h/g | 159 | 182.1 | 193.6 | 216.8 | 211 | 167.6 | 190.7 | - |
| **C, mA·h/g | - | - | - | 240 | 260.1 | - | - | 185*** |

** - With addition of Co activator (5 % Co relative to Ni); *** - Industrial sample H primary contains Co.

The best results are shown for samples D and E, which have medium crystallinity and LDH-like structure. The specific capacity of these hydroxides is more than the specific capacity of industrial sample H.

**Conclusions**

1) Uninterrupted electrochemical method for nickel hydroxide obtaining has been developed.
2) Properties of $Ni(OH)_2$, obtained under different current densities, have been investigated. The best results have been receipted for samples D and E (i=10 and 12 $A/dm^2$): specific capacity 240-260 mAh/g with Co activator addition.
3) Electrochemically obtaining samples of nickel hydroxide have the same structure as layered double hydroxides.

**References:**

1. J.Chen, D.H. Bradhurst, S.X. Dou, H.K. Liu, *J. of Electrochem Soc.*, **146** (10), 1999, 3606-3612.
2. M. Rajamathi, P. V. Kamath and R. Seshadri, *J. of Materials Chemistry*. **10**, 2000, 503-506.

First Regional Symposium on Electrochemistry of South-East Europe, Rovinj, Croatia, May 4-8, 2008.

P-1-029

# THE STABILITY OF ALUMINIUM-SUBSTITUTED ALPHA-NICKEL HYDROXIDE

**V.A. Kotok*, N.D. Koshel, V.L. Kovalenko, A.A. Grechanuk**

*Department of technical electrochemistry, Ukrainian State University of Chemical Engineering 8, Gagarin Avenue, Dnepropetrovsk, Ukraine, 49005,*
*E-mail: Valeriy_e-ch@ukr.net*

## Introduction

The nickel hydroxide is used as an active substance of positive electrode in Ni-MH, Ni-Cd, Ni-Fe accumulators. It is well known that the nickel hydroxide exist in alpha and beta forms. The alpha form of nickel hydroxide has greater mass utility and average discharge potential in comparison with beta form. However, pure α-$Ni(OH)_2$ is not stable. To increase stability of α-$Ni(OH)_2$ nickel cations are partially substituted by some other ions: $Al^{3+}$, $Zn^{2+}$, $Fe^{3+}$, $Co^{3+}$[1], $Cr^{3+}$, $Mn^{2+}$[2]. In presence of these cations compounds precipitated from nickel solutions are isostructural with alpha nickel hydroxide and are named layered double hydroxides (LDHs). These compounds have high electrochemical activity but on the other hand they decompose in alkaline solution. This process is known as ageing [3]. The aim of the present work is to determine aluminium-substituted α -$Ni(OH)_2$ stability.

## Experimental

The alpha form of nickel hydroxide was obtained by addition of $NiSO_4$ and $Al_2(SO_4)_3$ solution ($Ni^{2+}$ to $Al^{3+}$ ratio 4:1) to NaOH and $Na_2CO_3$ solution under constant stirring [1]. Then precipitate was washed from free alkaline, dried under 60˚C and sieved through grid with cell size 70μM. The X-ray pattern in Co-Kα radiation of precipitated powder is shown in Figure1. It shows presence only alpha nickel hydroxide.

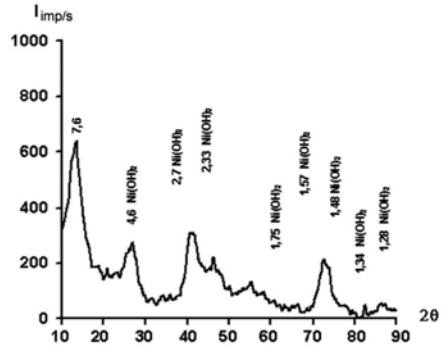


*Fig.1 The X-ray pattern of α-$Ni(OH)_2$.*

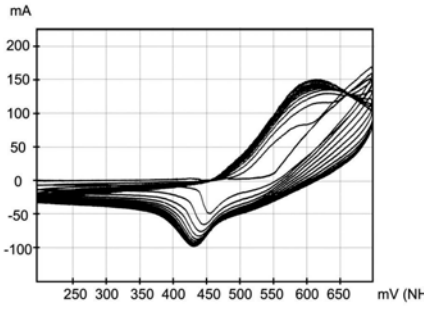


*Fig 2. The cycle voltammogram of electrode (5mV/s).*

The galvanostatic cycling of electrodes with 81% α-$Ni(OH)_2$, 16% graphite and 3% of PTFE (polytetrofluoroethylene) in 6M KOH solution under 0.2C discharge rate showed

the average mass utility of 103% and 144% (in activators presence: Co(OH)2 in electrode, LiOH in electrolyte). After third - fifth cycles took place gradual loss in specific capacity was observed. The cycle voltammogram of non-cycled electrode (90% α-$Ni(OH)_2$, 10% of PTFE) in 6 M KOH is shown in Figure 2. After ageing 1 day in 6 M KOH the electrode cycling showed changes in cycle voltammogram shapes – Figure3.These changes can be explained by ageing process.

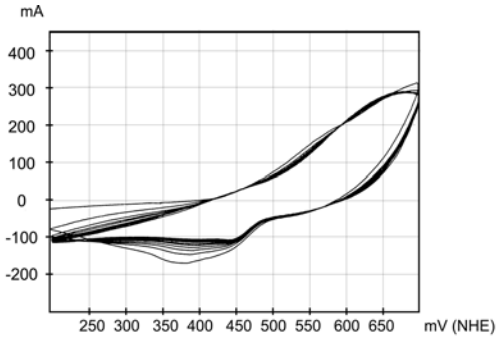


*Fig.3 The cycle voltammogram of electrode aged for 1 day in 6M KOH (5mV/s).*

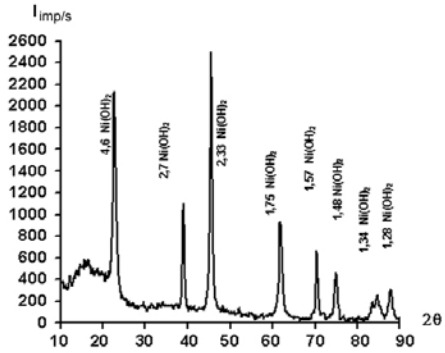


*Fig.4. The X-ray pattern of powder α-$Ni(OH)_2$ boiled in 6M KOH.*

For better understanding of ageing influence the powder of α-$Ni(OH)_2$ was boiled in 6M KOH solution. The cycle voltammogram of this powder showed a small anodic and cathodic current peak. The reason of that can lie in α –structure destroying (see Fig.4 and Fig.1) and self-poisoning by aluminum ions. However, the electrode contained α-$Ni(OH)_2$ and boiled in 6 M KOH solution showed cycle voltammogram similar to that of non-boiled electrode.

First-day ageing voltammogram (Fig. 5) of that electrode indicates in insignificant changes by comparison with non-boiled electrode voltammogram (Fig.2). The following voltamograms of boiled electrode under ageing process in alkaline solution showed gradual current peaks shifts out of a center.

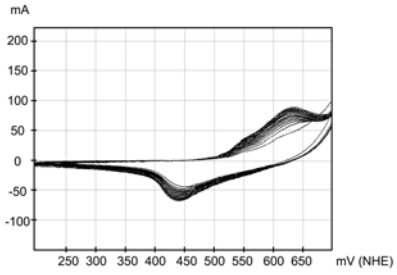


*Fig.5.The cycle voltammogram of boiled electrode aged for 1 day in 6M KOH (5mV/s).*

**Conclusions**

It is shown that the α-$Ni(OH)_2$ is unstable in alkaline medium and under elevated temperature α-phase stability decreases strongly.

The rate of ageing depends on conditions of the process.

**References**

1. B. Liu, X.Y. Wang, H.T. Yuan, Y.S. Zhang, D.Y. Song and Z.X. Zhou, *J. of Appl. Electrochem.* **29** (1999) 855.
2. R. S. Jayashree and P. Vishnu Kamath. *J. of Power Sources*., **107** (2002), 120.
3. R.S. Jayashree and P. Vishnu Kamath. *J. of Appl. Electrochem.* **31** (2001) 1315.

First Regional Symposium on Electrochemistry of South-East Europe, Rovinj, Croatia, May 4-8, 2008.

P-1-030

# IN-SITU GRAZING INCIDENCE X-RAY DIFFRACTION STUDY OF THE ELECTROCHEMICAL REACTION ON LEAD ELECTRODES IN VARIOUS ELECTROLYTES

**A. Gavrilović[1], P. Angerer[1], R. Mann[1], S. Stoimaier[1], G.E. Nauer[1,2]**

*[1]ECHEM Kompetenzzentrum für angewandte Elektrochemie GmbH, Viktor-Kaplan-Strasse 2, A-2700 Wiener Neustadt, a.gavrilovic@echem.at*
*[2]University of Vienna, Faculty of Chemistry, Währinger Strasse 42, A-1090 Wien, Austria*

In this study we present the formation of the crystalline phases anglesite ($PbSO_4$) and lead dioxide ($PbO_2$) during the anodic oxidation of pure lead in various electrolytes (1 molar sulphuric acid $H_2SO_4$, and a mixture of 0.687 mol $H_2SO_4$ and 0.25 mol $NaHSO_4$ filled up to 1 litre with distilled water). The change of the phase composition during the electrochemical reaction was observed by non-destructive in-situ grazing incidence angle X-ray diffraction (GIXD) method (figure 1). The electric potential and the electric current was also detected during the measurement series.

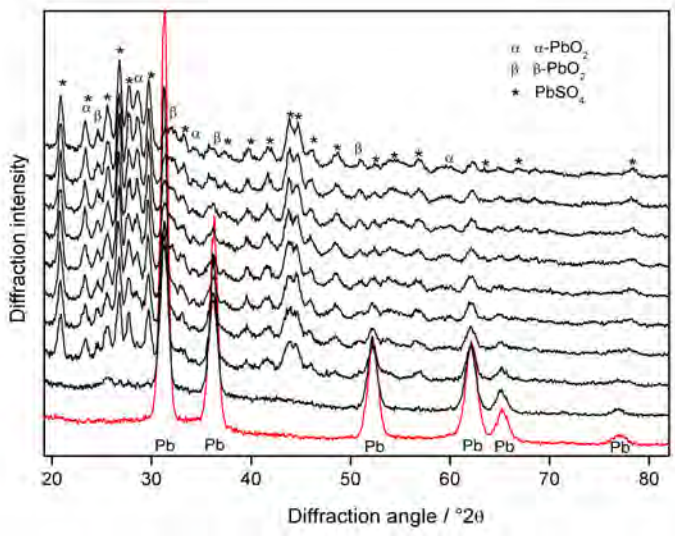


*Figure 1. Results of XRD measurements during electrochemical reaction*

During the oxidation process the intensity of the sulphate pattern increases continuously while the intensity of the lead substrate peaks decreases. A quantification of the phase content by Rietveld refinement has been attempted; however the observed values are strongly influenced by the layered structure of the sample and by the different absorption coefficients of the phases. The results are corresponding only the composition of the sample region penetrated by the radiation.

*The work was supported within the K plus programme by the Austrian Research Promotion Agency and the government of Lower Austria.*

First Regional Symposium on Electrochemistry of South-East Europe, Rovinj, Croatia, May 4-8, 2008.

P-1-031

# ELECTROPHORETIC DEPOSITION OF GLASS POWDER FOR PASSIVATION OF HIGH VOLATAGE ELECTRONIC DEVICES

**G.M. Nikolić[1], R.S. Nikolić[2]**

*[1]Department of Chemistry, Faculty of Medicine, University of Niš, Bulevar dr Zorana Đinđića 81, 18000 Niš, Serbia*
*[2]Faculty of Sciences and Mathematics, University of Niš, Višegradska 33, 18000 Niš, Serbia, E-mail: ruzicanf@yahoo.com*

Dielectric films have numerous applications in the manufacturing process of electronic devices, one of the most important being the surface passivation [1]. Fused glass powder films proved to be very good passivating material for high voltage devices due to their good mechanical, chemical, and electrical properties [2, 3].

Among the various deposition techniques used for glass deposition, electrophoretic deposition seems to be especially suitable because good particle adhesion prior to sintering is obtained and good process control is possible [4]. Current understanding of electrophoretic deposition of dielectric materials also allows for good control of the influence of specific deposition parameters on the quality of deposits [5].

In this paper we investigated the influence of electrophoretic deposition parameters of glass powder on the quality of fused glass films. Glass deposition was performed on silicon wafer surfaces covered with thermally grown $SiO_2$ and opened p-n junctions in deep grooves since such structure is characteristic for some high voltage diodes and transistors. Two types of glass, one of the lead-borosilicate (LBS) and the other of the zinc-borosilicate (ZBS) type, both obtained from comercial sources, have been investigated. Home made apparatus for electrophoretic deposition was used.

Isopropyl alcohol was used for the preparation of glass suspension (20 g/L) to which small amount of 25% aqueous ammonia (0.75 mL/L) was added. Glass suspension was ultrasonically aggitated for 10 min and then leaved 5 min without aggitation. Carefully decanted suspension was used for electrophoretic deposition. Deposition was carried on silicon wafer as cathode with platinum grid counterelectrode with the fixed distance of 2 cm. Various deposition times (from 1 to 3 min) and deposition potentials (from 60 to 200 V) were tried in order to obtain good filling of grooves with minimal deposition of glass on the masking $SiO_2$ layer. Deposited glass was sintered for 30 min at 700°C in diffusion furances under the atmosphere of $N_2/O_2$ (1:1) or pure $N_2$. Controlled pushing and pulling of wafers was performed in order to minimize mechanical stress on the silicon-glass interface during the heatig and cooling of wafers.

Visual inspection of wafer surface after sintering of deposited glass revealed that the best deposition results were obtained with the deposition time of 2 min and deposition potential of 100 V. However, even under the best deposition conditions it was not possible to avoid some galss deposition on the masking $SiO_2$ layer. The

glass deposited over the $SiO_2$ may cause problems in the subsequent steps of device fabrication (eg. problems with photoresist adhesion during the contact formation). These problems could be elliminated to the good extent by the treatment of sintered wafers with 70% perchloric acid which could eliminate the great deal of glass particles from the $SiO_2$ layer. The treatment with perchloric acid is more effective in the case of ZBS glass. Also the ZBS glass suspensions were more stable than LBS glass suspensions allowing for better reproductivity of electrophoretic deposition.

Detailed electrical characterization of fabricated structures was not performed because no high purity conditions were maintained during all the glass deposition steps, but some of fabricated devices were of good quality.

Our results clearly demonstrate that electrophoretic deposition could be a technique of choice for glass deposition during teh passivation of high voltage electronic devices.

**References:**

[1.] W.A. Pliskin, *J. Vac. Sci. Technol.* **1977**, *14*, 1064.
[2.] P.B. Parchinskii, S.I. Vlasov, U.T. Turgunov, *Inorg. Mater.* **2002**, *38*, 750.
[3.] P.B. Parchinskii, S.I. Vlasov, A.A. Nasirov, *Semiconductors* **2004**, *38*, 1345.
[4.] M. Shimbo, K. Tanzawa, M. Miyakawa, T. Emoto, *J. Electrochem. Soc.* **1985**, *132*, 393.
[5.] Zhitomirsky I., *Adv. Colloid Interfac.* **2002**, *97*, 279.

First Regional Symposium on Electrochemistry of South-East Europe, Rovinj, Croatia, May 4-8, 2008.

P-1-032

# ELECTRODEPOSITION OF NANOSTRUCTURED FERROMAGNETIC POWDERS

**L. Rafailović[1], H.P. Karnthaler[1], P.F. Rogl[2], T. Trišović[3]**

*[1]Physics of Nanostructured Materials, Faculty of Physics, University of Vienna, Boltzmanngasse 5, 1090 Vienna, Austria, lidija.rafailovic@univie.ac.at*
*[2]Institute of Physical Chemistry, Faculty of Chemistry, University of Vienna, Währinger Straße 42, 1090 Vienna, Austria*
*[3]Institute of Technical Science of Serbian Academy of Science and Arts, K. Mihailova 35/4, 11000 Belgrade, Serbia*

The morphology and microstructure of electrodeposited ferromagnetic nickel, iron and cobalt powders were investigated.
The microstructure and morphology of the powders depend on both deposition current density and bath composition. It is shown by analysis with X-ray diffraction and SEM methods that composition, phase, structure, shape and size of the electrochemically obtained particles of nickel, iron and cobalt alloy powders strongly depend on current density. The increase of current density decreases the grain size of electrodeposited powders.
The powders were electrodeposited at the constant current regime at high current densities (specifically selected for each system). Simultaneously hydrogen evolution occurred during powder deposition (on the Ti cathode) since the surface of the deposited alloy powder acts as a catalyst for hydrogen evolution. The total current density of electrodeposition can be as high as 1 $Acm^{-2}$ depending on the system.

First Regional Symposium on Electrochemistry of South-East Europe, Rovinj, Croatia, May 4-8, 2008.

P-1-033

# ELECTROCHEMICAL SYNTHESIS OF BRUSHITE COATINGS ON TITANIUM

**M. S. Đošić[1], V. B. Mišković-Stanković[2]*, B. M. Jokić[2], J. Stojanović[1]**

*[1] Institute for Technology of Nuclear and Other Mineral Raw Materials, Franse d'Epere 86, 11000 Belgrade, Serbia,*
*[2] Faculty of Technology and Metallurgy, University of Belgrade, Karnegijeva 4, P.O.Box 3503, 11120 Belgrade, Serbia, *E-mail address: vesna@tmf.bg.ac.yu*

Calcium phosphates exist in different forms exhibiting different crystal structures.[1,2] Calcium hydroxyapatite, $Ca_{10}(PO_4)_6(OH)_2$, is known as a bioactive ceramics due to chemical similarity to the calcium phosphate minerals present in the biological hard tissue.[3,4] Metal have been used in various forms as implants and prostheses. An improve of biocompatibility of metal implants includes the surface modification by inorganic mineral coatings.[5] Brushite, $CaHPO_4 \cdot 2H_2O$, is a phase of calcium phosphate that is relatively soluble in simulated body fluid. In such environment, it can dissolve and possible provide increased levels of calcium and phosphate ions near tissue-implant interface.[6] For that reason, brushite is used as precursor for HA formation during biomimetic process. In this work, brushite coatings were electrochemically deposited at titanium electrode. The influence of current density and deposition time on the mass and morphology of brushite coatings on titanium were studied.

For electrochemical synthesis of brushite coatings, the titanium plate was used as the cathode, two Pt plates as counter electrodes and SCE as the reference electrode. Brushite coatings on titanium were electrochemically deposited from homogeneous solution of $Ca(NO_3)_2$ and $NH_4H_2PO_4$ at different values of constant current densities between 3.0 and 9.0 mA $cm^{-2}$, for various deposition times of 5 to 30 min and pH value of 4.0. The electrochemically deposited brushite coatings were dried at room temperature for 24 h before weighing. The phase composition and structure of brushite coatings were determined by X-ray diffraction (XRD) and the microstructure was examined by scanning electron microscopy (SEM).

The mass of the brushite coating, *m*, as a function of deposition time, *t*, for different current densities is shown in Fig. 1. The increase in deposition time, for all applied current densities, increases the brushite coating mass. The maximum values for coating mass can be observed for deposition time of 30 min. XRD patterns of coatings obtained for deposition time of 30 min at current densities of 3.0 and 9.0 mA $cm^{-2}$ are shown in Fig. 2a and 2b, respectively. The only crystalline phase in all samples was brushite. According to the peaks intensity, it could be observed that coating electrodeposited at 9.0 mA $cm^{-2}$ consists of smaller crystallites in respects to the peak intensity for coating electrodeposited at 3.0 mA $cm^{-2}$.

Morphological analysis of SEM micrographs (Fig. 3) suggests that brushite coatings surfaces have plate-like structure. At lower applied current density (Fig. 3a), the hydrogen bubbles formed at the electrode during the electrochemical synthesis, remain for some period at the surface, causing the electrochemical synthesis occurs around the bubbles, which leads to formation of volcano-like sites. Increase in current density to 9 mA $cm^{-2}$

increases the rate of hydrogen evolution but also enables $H_2$ bubbles to leave the substrate easily, which results in formation of coating without volcanoes places.

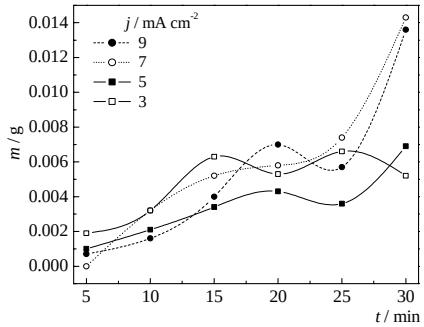


*Fig. 1. Dependence of the brushite coating mass on deposition time for different current densities*

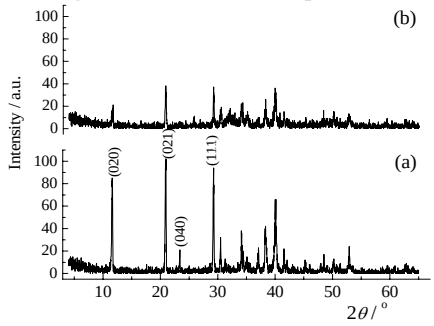


*Fig. 2. XRD pattern of brushite coatings obtained for 30 min at current densities of (a) 3 mA cm$^{-2}$ and (b) 9 mA cm$^{-2}$*

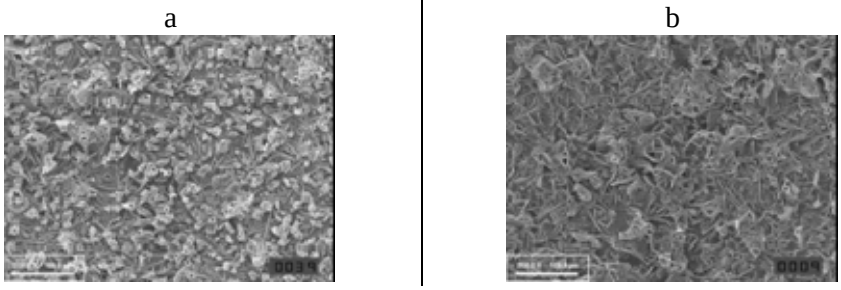


*Fig. 3. SEM micrographs of brushite coatings electrodeposited at (a) j = 3 mA cm$^{-2}$ and (b) j = 9 mA cm$^{-2}$*

It can be concluded that applied current density significantly influences the brushite coating mass, crystallite domain size and morphology. The phase composition of coatings was determined by XRD and the only detected crystalline phase in all samples was brushite. Increase in current density decreases the crystallite domain size of brushite coating. SEM analysis of electrochemically deposited brushite coatings shows that coating morphology depends on the applied current density. The coatings have plate-like structure with volcano-like places. Increase in applied current density decreases the volcano-like places on the brushite coatings surfaces. The influence of deposition time on the mass of brushite coatings on titanium shows that the coatings of maximum thickness can be obtained for 30 min at all applied current densities.

## References

1. G. R. Sivakumar, E. K. Girija, S. N. Kalkura, C. Subramanian, *Cryst. Res. Technol.* **33** (1998) 197.
2. M. H. Prado Da Silva, J. H. C. Lima, G. A. Soares, C. N. Elias, M. C. De Andrade, S. M. Best, I. R. Gibson, *Surf. Coat. Techn.* **137** (2001) 270.
3. R. H. Doremus, *J. Mater. Sci.* **27** (1992) 285.
4. J. S. Chen, H. Y. Juang, M. H. Hon, *J. Mater. Sci. Mater. Med.* **9** (1998) 297.
5. J. E. Ellingsen, P. Thomsen, S. P. Lyngstadaas, *Periodontology 2000* **41** (2006) 136.
6. M. Kumar, J. Xie, K. Chittur, C. Riley, *Biomaterials* **20** (1999) 1389.

First Regional Symposium on Electrochemistry of South-East Europe, Rovinj, Croatia, May 4-8, 2008.

P-1-034

# STUDY BY EIS OF THE GROWTH OF NANOSTRUCTURED $Cu_2O$ THIN FILMS PREPARED BY ELECTRODEPOSITION

**S. Bijani[1], M. Gabás[1], L. Martínez[1], J. Morales[2], L. Sánchez[2], E. Dalchiele[3] J.R. Ramos-Barrado[1]**

*[1]Departamento de Física Aplicada. Laboratorio de Materiales y Superficie (Unit associated to CSIC). Universidad de Málaga. España, barrado@uma.es*
*[2]Departamento de Química Inorgánica. Universidad de Córdoba. España.*
*[3]Instituto de Física. Universidad de la República. Montevideo, Uruguay*

Oxides of 3d transition metals (Fe, Co, Ni and Cu) have recently been proposed as potential candidates for use as negative electrodes in Li-ion batteries [1–5]. Copper oxides are especially attractive in lithium cells because of their good performance [6]; also, they are non-toxic, abundant and hence inexpensive. In particular, CuO and $Cu_2O$ films were shown to exhibit a good electrochemical response in lithium cells [7, 8]. Recently, we have reported about the reactivity of $Cu_2O$ thin films with lithium [9, 10]. These films were prepared using the electrodeposition technique, which provides advantages such as the possibility of using low synthesis temperature, low cost and a high purity in the product yield. $Cu_2O$ electrodeposition was accomplished by using a conventional three-electrode single-compartment electrochemical cell. $Cu_2O$ films were electrodeposited in the potentiostatic mode on titanium substrates (plates 1 $cm^2$ in surface area) that were previously polished with emery paper, rinsed with deionized water, immersed in 24% HF for 20 s, and rinsed with water. A platinum sheet was used as counter-electrode and saturated calomel electrode (SCE) as reference electrode. $Cu_2O$ was electrodeposited by reduction of an alkaline aqueous solution of cupric lactate according to the reaction $2Cu^{2+} + 2e^- + 2OH^- \rightarrow Cu_2O + H_2O$, which was previously reported by Zhou and Switzer [11]. The electrolytic bath contained copper (II) sulphate (0.4 M), and 3 M lactic acid as chelating agent; its pH was adjusted to 9 with sodium hydroxide. The bath temperature was 30°C. Variable applied potentials were tested with a view to obtain $Cu_2O$ films of diverse microstructure and morphology. Deposits were air-dried at 100°C for further characterization. Purity of electrodeposited films is guaranteed by XRD and XPS analysis.

In this communication, we report unpublished EIS results for films with different deposition times using two applied potentials of -575 mV and -150 mV. The measures were carried out using an Autolab potentiostat with a frequency range between 0.01 Hz and 10 kHz with a potential of 20 mV. The results were analyzed by the equivalent circuit method by a complex non linear fitting [12]. The spectra were fitted to three different circuits:

| Circuit 1 | Circuit 2 | Circuit 3 |
|---|---|---|
| 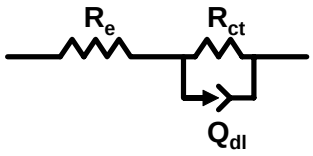 | 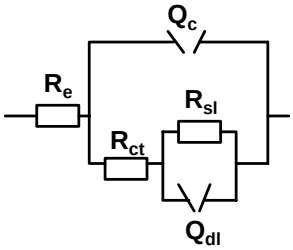 | 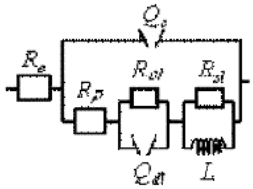 |



where $R_e$ is electrolyte resistance, $R_p$ the porous resistance, $Q_c$ is a CPE corresponding to the deposited material, $R_{ct}$ the charge transfer resistence, $Q_{dl}$ is a generalized double layer, $R_{sl}$ the resistance of the surface layer and L is a pseudo-inductance.

For the films obtained at -575 mV, the circuit 1 represents the behaviour of films with deposition times of 0 and 0.5 minutes, the circuit 2 fits to data corresponding to films with deposition time of 1 minute and the circuit 3 explains the behaviour of the films obtained at deposition times ranging from 5 to 30 minutes. Spectra of the films obtained at -150 mV present some differences respect to the films growth at -575 mV. For that potential, films deposited at times from 0 to 10 minutes follow circuit 1 behaviour, while data corresponding to deposition times from 30 to 60 minutes fit with circuit 1.

This different behavior may be attributed to the different morphology of the samples growth at -575 mV and-150 mV. The first ones show a cauliflower pattern and in the films growth at -150 mV well-faceted crystalline particles can be

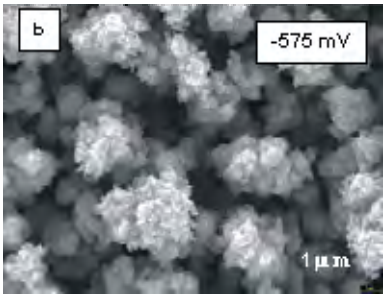


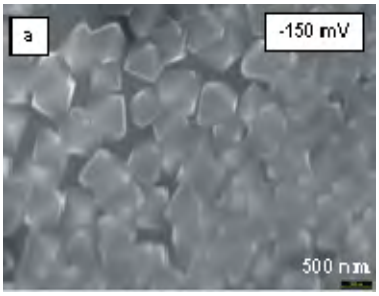


*Fig. 1. a) Film obtained at -150 mV; b) Film obtained at -575 mV*

## References

[1] P. Poizot, S. Laruelle, S. Grugeon, L. Dupont, J.M. Tarascon, *Nature* **407** (2000) 496.
[2] G.X. Wang, Y. Chen, K. Konstantinov, M. Lindsay, H.K. Liu, S.X. Dou, *J. Power Sources* **109** (2002) 142.
[3] F. Badway, I. Plitz, S. Grugeon, S. Laruelle, M. Dollé, A.S. Gozdz, J.M. Tarascon, *Electrochem. Solid State Lett.* **4** (2002) A115.
[4] D. Larcher, M. Masquelier, C.D. Bonnin, Y. Chabre, V. Masson, J.B. Leriche, J.M. Tarascon, *J. Electrochem. Soc.* **150** (2003) A133.
[5] M.N. Obrovac, R.A. Dunlap, R.J. Sanderson, J.R. Dahn, *J. Electrochem. Soc.* **148** (2001) A576.

[6] S. Grugeon, S. Laruelle, S.R. Herrera-Urbina, L. Dupont, P. Poizot, J.M. Tarascon, *J. Electrochem. Soc.* **148** (2001) A285.
[7] J. Morales, L. Sánchez, F. Martín, M. Sánchez, J.R. Ramos-Barrado, *Electrochim. Acta* **49** (2004) 4589.
[8] Y.H. Lee, I.C. Leu, S.T. Chang, C.L. Liao, K.Z. Fung, *Electrochim. Acta* **50** (2004) 553.
[9] J. Morales, L. Sánchez, S. Bijani, L. Martínez, M. Gabás, J.R. Ramos-Barrado, *Electrochem. Solid State Lett.* **8(3)** (2005) A159.
[10] S. Bijani, M. Gabás, L. Martínez, J.R. Ramos-Barrado, J. Morales L. Sánchez, *Thin Solid Films* **515** (2007) 5505.
[11] Y. Zhou, J.A. Switzer, *Scr. Mater.* **38** (1998) 1731.
[12] J.R. MacDonald, CNLLS program.

First Regional Symposium on Electrochemistry of South-East Europe, Rovinj, Croatia, May 4-8, 2008.

P-1-035

# STUDY OF ELECTRODE PROCESSES DURING ELECTRODEPOSITION OF COPPER USING IONIC LIQUIDS BASED ON CHOLINE CHLORIDE

**A.M. Popescu[1], V. Constantin[1], A. Cojocaru[2], M. Olteanu[1], T. Visan[2]**

*[1]Romanian Academy, „Ilie Murgulescu" Institute of Physical Chemistry, Splaiul Independentei 202, Bucharest-006021, Romania, popescuamj@yahoo.com*
*[2] University POLITEHNICA of Bucharest, Department of Applied Physical Chemistry and Electrochemistry, Calea Grivitei 132, 010737-Bucharest, Romania*

Recently, ionic liquids have become of interest in many fields of chemistry because of their unique properties. For instance, water free, low melting point and completely ionic media seem to be perfect candidates for obtaining new metallic coatings (elementary metals, alloys) with desirable characteristics.

The paper presents the electrochemical studies (cyclic voltammetry, electrochemical impedance spectroscopy) on the electrode processes during copper electrodeposition using ionic liquids as electrolytic media. We mention that this deposition procedure represents an alternative for the classical copper electrodeposition techniques which are used presently in industry and pollute the environment. Supplementary, this new proposed method of copper deposition is an ecological one because the ionic liquids are recyclable, non-volatile and non-toxic.

It was found previously that choline chloride (hydroxy-ethyl-trimethyl ammonium salt) forms an ionic liquid with urea and some added hydrated metal salts and this electrolyte is air and moisture stable [1-3]. In our experiments we have prepared a series of ionic liquids by mixing choline chloride – urea systems with CuCl and $CuCl_2$ salts in various concentrations. Cyclic voltammetry and electrochemical impedance spectroscopy investigations were conducted at various temperatures (from room temperature to $80^0$C) in choline chloride – urea systems with either separated single salts or with both CuCl and $CuCl_2$ (generally in 0.05-0.5M concentration range). All mixtures were freshly prepared with p.a. reagents.

We investigated both cathodic and anodic processes of $Cu^+$ and $Cu^{2+}$ ions at different sweep rates on these new electrolytic systems based on choline chloride. The electrochemical characterization of univalent and divalent copper ions behaviour during cathodic polarization was carried out also by recording potentiodynamic and potentiostatic curves. The electrochemical impedance spectroscopy investigations consisted in recording Nyquist and Bode spectra by polarizing the working electrode at various cathodic potentials. Voltammetric measurements were performed supplementary for determining the electrochemical window for the above ionic liquids. The cyclic voltammetry was selected as experimental technique for this study because observation of the electrochemical reactions can be made rapidly over a wide potential range.

In our experiments a computer driven Zahner IM 6e potentiostat was used. The conventional three-electrode cell contains a stationary working electrode as a Pt foil ($0.5cm^2$) or a Cu disk ($0.2cm^2$), a platinum gauze as auxiliary electrode and a

reference electrode which may be even a quasi-reference electrode (generally silver wire). The compatibility and stability of ionic liquid medium using various reference electrodes was thus studied, together with the influence of temperature on electrical conductivity of electrolyte.
We demonstrated by this study an alternative to the classical copper electrodeposition. Because they can be now made on a commercial scale, ionic liquids are the key to new green technology in the electroplating industry, environmentally friendly. The described electrodeposition process may be also used for recycling the wastes containing copper compounds that exist in metallurgical industry of non-ferrous metals.

***Acknowledgement:*** *The financial support within the PNCD-2, CNMP Romanian Programme-Grant nr.3094/2007 is gratefully acknowledged.*

References

[1] A.P. Abbot, G. Capper, D.L. Davies, H. Munro, R. Rasheed, V. Tambyrajah, in *"Ionic liquids as green Solvents: Progress and Prospects"*, R.D. Rogers, K.R. Seddon Editors, *ACS Symposium Series*, 2003 p. 439.
[2] L.Anicăi, M.Dutu, P.Prioteasa, T.Vişan, A comparative study of Ni-W alloys electrodeposition from aqueous electrolytes and ionic liquids, paper presented at *57-th Annual Conf. of Int.Soc.Electrochemistry (ISE)*, Edinbourgh 2006, Book of abstracts, p. S5-P-130
[3] L.Anicai, M.Dutu, A.Pertache, T.Visan, Electrodeposition of nickel from ionic liquids based on choline chloride, *Corrosion and Corrosion Protection Journal* (Cluj-Napoca, Romania) **2(4)** 2007, 10-17.

First Regional Symposium on Electrochemistry of South-East Europe, Rovinj, Croatia, May 4-8, 2008.

P-1-036

# POTENTIODYNAMIC AND GALVANOSTATIC STUDY OF COPPER AND ZINC DEPOSITION FROM SULPHATE ELECTROLYTES

**G. Hogjaoglu, I. Ivanov**

*Institute of Physical Chemistry "Acad. R. Kaishew", Bulgarian Academy of Sciences*
*Acad. G. Bonchev Str., bl.11, 1113 Sofia, Bulgaria, E-mail: gyunver@ipc.bas.bg*

By means potentiodynamic and galvanostatic methods the simultaneous Cu and Zn deposition from sulphate electrolytes, containing 50 g $dm^{-3}$ $Zn^{2+}$ and different concentrations of $Cu^{2+}$ is studied. It is obtained that at potentials more positive than -1.6 V vs SSE only pure Cu deposits when $Cu^{2+}$ concentration is 1 or 5 g $dm^{-3}$. At $Cu^{2+}$ concentration 10 g $dm^{-3}$ (in the absence) and at 1, 5 and 10 g $dm^{-3}$ (in the presence) of 130 g $dm^{-3}$ $H_2SO_4$ pure Cu deposition takes place in whole potential area studied (from -0.6 to -1.8 V vs SSE) . Pure Cu deposits at current densities from 0.5 to 5.0 A $dm^{-2}$ in the presence of sulphuric acide. In the presence of the organic additive hydroxyethylated butyne-2-diol-1.4 (Ferasine) more dense, smooth and fine-grained Cu coatings are obtained.

First Regional Symposium on Electrochemistry of South-East Europe, Rovinj, Croatia, May 4-8, 2008.

P-1-037

# SOME ASPECTS REGARDING TIN AND NICKEL ELECTRODEPOSITION FROM CHOLINE CLORIDE BASED IONIC LIQUIDS

**A. Petica[1], L. Anicai[2], A. Florea[2], T. Visan[3]**

[1] *INCDIE ICPE-Advanced Research, Splaiul Unirii 313, sector 3, Bucharest, Romania*
[2]*Div.of Ecological Technologies Development, PETROMSERVICE SA, Calea Grivitei 8-10, 010772, Bucharest, Romania*
[2]*Department of Physical Chemistry and Applied Electrochemistry, POLITEHNICA University of Bucharest, Calea Grivitei 132, 010737, Bucharest, Romania*
*E-mail: aura_p25@yahoo.com; lanicai@itcnet.ro*

In the last years there has been proved that an ionic medium with interesting perspectives in metals electrodeposition is that based on choline chloride (2-hydroxi-ethyl-trimethyl ammonium) mixed with urea ($NH_2C{=}ONH_2$). The room temperature ionic liquid is resulted due to the hydrogen bonds formed between the ammonium quaternary salt and amide. These kinds of electrolytes present a larger potential window as compared with aqueous ones, usually between 3-6 V and during the electrolysis no gaseous are produced, so that their use in galvanotechnical applications should be very attractive. Additionally such ionic liquids involving choline chloride proved also to be environmentally friendly, so that they belong to the so-called „green chemistry“[1,2,3]. Abbott et al.[4] have investigated in detail the possibility of formation of various ionic liquids usually characterized by a freezing point of maximum 100$^o$C, preferably around 60$^o$C.

In the field of metals electrodeposition involving ionic liquids there are still missing aspects regarding the modalities to obtain metallic coatings with controlled, suitable morphology and physical characteristics that are correlated also with fundamental aspects that are not yet fully elucidated. Additional information in this field may significantly contribute to the extension of the practical applications of these systems.

With this in view, the present paper deals with some preliminary experimental results regarding the electrodeposition of Sn and Ni from some choline chloride based ionic liquids. Some aspects regarding synthesis and characterization of the formed ionic liquid are also discussed.

To investigate the synthesis of the desired ionic liquids various chemical reagents have been involved, respectively: choline chloride ($C_5H_{14}NOCl$), urea ($CH_4N_2O$),nickel chloride ($NiCl_2$ x $6H_2O$), tin chloride ($SnCl_2$ x $2H_2O$), malonic acid ($C_3H_4O_4$).

Some physical properties of the obtained ionic liquids have been determined, including: melting and freezing temperature, consistency, color, their stability in time. The dependence of their electrical conductivity against temperature has also investigated, using a conductometer with conductometer probe WTW type 340i model, the cell constant being K=0,469 cm$^{-1}$.

To investigate the electrochemical behaviour, cyclic voltammogrames have been recorded at a sweep rate of 20 mV/s, using a Pt working electrode (S = 0.19625 $cm^2$) in the case of Sn based ionic liquids and a stainless steel one (S = 2 $cm^2$) in the case of Ni based ones against Ag wire as quasi-reference electrode and a Pt, Ni or graphite counterelectrode. To evaluate the characteristics of Sn and Ni electrochemical coatings involving the syntethized choline chloride based ionic liquids there has been performed electrolysis at a constant current using a metallic substrate of copper. The obtained electrodeposits have been characterized from appearance, adherence and layer thickness (deposition rate) view points.

According to the experimental results it has been found out that:

- in the case of Ni based systems, from cyclic voltammetry recordings for a temperature domain between 30-80$^oC$ the presence of redox couple Ni/Ni(II) has been evidenced and cathodic limiting currents of 10-15 mA/ $cm^2$ were determined;
- the use of ionic liquids containing 1-7% Ni as $NiCl_2 \cdot 6H_2O$ *in* choline chloride – malonic acid (2:1 masic ratio) led to adherent, uniform Ni deposits, for a temperature range of 30-60$^oC$;
- from conductivity – temperature recordings an activation energy of the above mentioned system, of about 29 KJ/mol has been determined in accordance with other literature data [5];
- a suitable electrochemical behaviour has been evidenced in the case of choline chloride-urea-$SnCl_2$ (1:2:0.5 molar ratio), materialized by high cathodic limiting currents , of about 800 mA /$cm^2$ and good quality deposits, as shown in Figure 1.

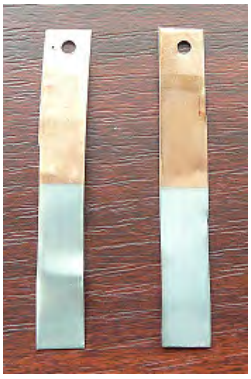

*Figure 1. Sn deposit onto Cu substrate from choline chloride based ionic liquids containing Sn $Cl_2$*

***Acknowledgements:*** *Part of this work was supported by the Romanian Ministry of Education and Research, PNCDI II Program, under Research Contract No.11-036/1-2007.*

## References

1. Abbott, G.Capper, D.L.Davies, H.L.Munro, R.K.Rasheed, V.Tambyrajah, *Ionic liquids as green solvents: progress and prospects*, în: R.D.Rogers, K.R.Seddom, Eds.,ACS Symposium Series, 2003, p.439.
2. F.Endres, *Ionic Liquids. Solvents for the Electrodeposition of Metals and Semiconductors*, CHEMPHYSCHEM 2002, no. 3, p. 144-154
3. A.P. Abbott, G.Capper, K.J. McKenzie, K.S. Ryder, *Electrochim.Acta*, **51(21)** (2006) 4420.
4. A.P.Abbott, D.L.Davies, G.Capper, R.K.Rasheed, V.Tambyrajah, US Patent 2004/0097755.
5. A. P. Abbott, D.Boothby, G. Capper, D. L. Davies, R.K.Rasheed, .*J.Am.Chem.Soc.*, **126** (2004), 9142.

First Regional Symposium on Electrochemistry of South-East Europe, Rovinj, Croatia, May 4-8, 2008.

P-1-038

# ELECTRODEPOSITION OF BISMUTH ONTO GLASSY CARBON AND GRAPHITE ELECTRODES FROM NITRATE SOLUTIONS

**N. Vladislavić, S. Brinić**

*Faculty of chemistry and technology, Teslina 10/V, 21000 Split, Croatia, nives@ktf-split.hr*

Glassy carbon (GC) exhibits a rather high chemical inertness and a rather low oxidation rate which, together with very small pore sizes and a small gas and liquid permeability, makes it a convenient inert electrode. It is known that the activity of the glassy carbon electrodes depends on the properties of the glassy carbon examined, the temperature and thermal treatment as well as the mechanical and electrochemical pretreatment of the sample. For preparing and activating the glassy carbon electrode surface different pretreatments have been widely discussed, like mechanical treatment, laser treatment, irradiation of glassy carbon with ultrasound, electrochemical treatment, etc. [1]

In this work the kinetics and mechanism of cathodic electrodeposition of bismuth on glassy carbon (GC) and carbon electrodes were studied using cyclic voltammetry and chronoamperometry. As electrolyte the deaerated nitrate solutions $c(HNO_3)$ = 0.5 mol $dm^{-3}$ with different concentrations of $Bi^{3+}$ (concentration range from 20 mM to 0.5 mM) ion were used. Experiments were performed on AUTOLAB PGSTAT 302N, controlled by PC in standard three-electrode cell with platinum electrode as counter electrode and saturated calomel electrode (SCE) as reference electrode at the temperature 25°C.

The electrochemical activation of electrodes was performed by continuously cycling in deaerated 0.5 M $HNO_3$ solution in the potential range between the hydrogen and oxygen evolution.

Cyclic voltammograms of GC electrode in 0.5 M $HNO_3$ solution with the presence of $Bi^{3+}$ ion showed a couple of well defined cathodic and anodic peaks and a crossover between the cathodic and anodic branches. The presence of the crossover is diagnostic for the formation of bismuth nuclei on the GC electrodes. The potentials of the cathodic deposition and the anodic dissolution of bismuth depend on concentration of $Bi^{3+}$ ion in the electrolyte.

The initial stage of bismuth electrodeposition was studied using potentiostatic pulse technique. The potentiostatic pulses were performed from the potential 290 mV to the various formation potentials in the range of bismuth nucleation and growth. The shape of the obtained transients is typical for the nucleation and growth of deposits on a conducting surface. As the transient potential ($E_t$) shifts to the cathodic side, the current maximum ($j_m$) increases, while the corresponding time maximum ($t_m$) decreases. The potentiostatic transients were normalized according to the current maximum and time maximum values and compared wit the theoretical curves for two and three dimensional nucleation and growth under diffusion control. Through the applications of relations which hold true for such a nucleation model the following parameters were determined: the cathodic

nucleation potential ($E_{CN}$), the rate of nucleation ($AN_{\infty}$), the diffusion coefficient ($D$) and the density of growing sites ($N_s$). The results obtained at different carbon electrodes were discussed.

**References:**

1. A. Dekanski, J. Stevanović, R. Stevanović, B. Ž. Nikolić and V. M. Jovanović, *Carbon* (2001) 1195.
2. M. Yang and Z. Hu**,** *Journal of Electroanalytical Chemistry*, 583 (2005).
3. B. Scharifker, G. Hills, *Electrochim, Acta*, **7** (1983) 879.
4. Z. Grubač and M. Metikoš-Huković, *Thin Solid Films*, **413** (2002) 248.

First Regional Symposium on Electrochemistry of South-East Europe, Rovinj, Croatia, May 4-8, 2008.

P-1-039

# EFFECT OF EXPERIMENTAL CONDITIONS ON COMPOSITION OF THE ELECTRODEPOSITED Ni-P COATINGS

**O. Dolgikh, N.V. Sotskaya**

*Voronezh State University, Voronezh, Russia, dov@niif.vsu.ru*

Nickel-phosphorous alloys are widely used in industry because of their useful mechanical, chemical and magnetic properties. Their wide spread utilization depends on ability of production of coatings with prescribed composition and, consequently, with defined properties. So, it is important to develop the simple way to control the deposition process.

It is well known that composition of electrodeposited alloys depends on experimental conditions, namely on bath components ratio, cathodic current density and temperature.

Ni-P coatings were deposited from electrolytes which compositions are listed in Table 1. Bath **I** is one of commonly used electrolytes for Ni-P deposition. Baths **II** and **III** allow us to investigate the influence of glycine concentration and of organic compound addition on the process characteristics.

*Table 1. Composition of baths for Ni-P deposition (pH 5.5)*

| Component | Concentration, mol·L$^{-1}$ | | |
|---|---|---|---|
| | **I** | **II** | **III** |
| $NiCl_2 \cdot 6H_2O$ | 0.08 | 0.08 | 0.08 |
| $NaH_2PO_2 \cdot H_2O$ | 0.24 | 0.24 | 0.24 |
| $NH_2CH_2COOH$ | 0.20 | 2.00 | 0.20 |
| $CH_3COONa \cdot 3H_2O$ | 0.12 | 0.12 | 0.12 |
| Organic additive | — | — | $1 \cdot 10^{-6}$ |

Ni-P coatings were deposited from one of stated electrolytes in potentiostatic mode. Dependencies of their composition on deposition potential are shown on Fig.1 along with hydrogen current efficiency. It can be seen that both Ni content and hydrogen current efficiency increase with rising of cathodic potential. This fact can indicate that these two reactions are coupled with each other.

In order to describe obtained dependencies for Ni-P alloys composition we use semi-empirical equation obtained with the assumption that both alloy component deposits under control of charge transfer step:

$$\lg \frac{\langle \mathrm{Ni} \rangle}{\langle \mathrm{P} \rangle} = A + B \lg i_k \,. \qquad (1)$$

Treatment of obtained data in the criterion coordinates corresponding to Eq. 1 yields linear dependencies with high correlation coefficient (Fig. 2). Fracture on these lines answer the potential at which change of mechanism of component deposition takes place.

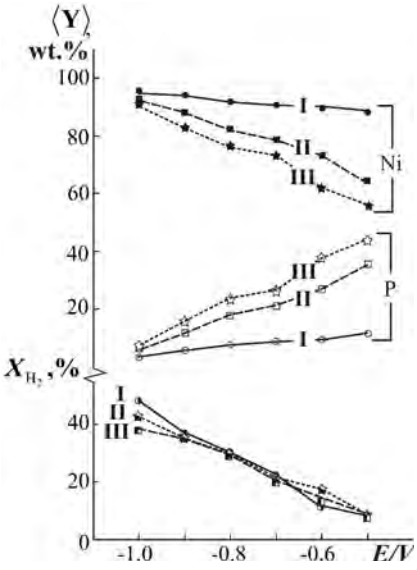


*Fig. 1 Dependencies of Ni and P Content in Ni-P alloys deposed from baths (I – III) and hydrogen current efficiency on deposition potential*

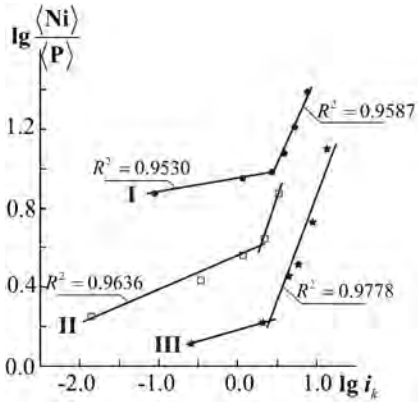


*Fig. 2 Dependencies of component ratio in Ni-P alloys electrodeposited from different electroytes on cathodic current densities*

Good agreement of experimental data with calculated according to Eq.1 enable to use this equation for choosing of conditions for deposition of Ni-P coatings with prescribed composition. This method together with knowledge of main peculiarities of influence of different factors (such as glycine concentration, addition of organic compound etc.) opens up possibilities of alloy composition control.

First Regional Symposium on Electrochemistry of South-East Europe, Rovinj, Croatia, May 4-8, 2008.

P-1-040

# STUDY OF ELECTRODEPOSITION ON Ni-Co ALLOYS

**P. Popa[1], G. Cârâc[1], P. Cojocaru[2],T. Lampke[3]**

[1]*Department of Chemistry, University "Dunarea de Jos", Domneasca Street 47, 800008 Galati, Romania; popapaula2000@yahoo.com*
[2]*Politecnico di Milano, Chemistry Materials and Chemical Engineering "Giulio Natta", Piazza Leonardo da Vinci 32, 20133 Milano,Italy,*
[3]*Chemnitz University of Technology, Nanoma-Center for Nanostructured Materials and Analytics, Reichenhainer Strasse 70, 09126 Chemnitz, Germany*

Treatments application on the surface is a very used method to improve the new materials properties. Advanced composite materials have superior properties compared with a single metal or alloys. This paper presents results obtained for Ni-Co alloys by electrodeposition on glassy carbon and copper electrodes. Electrodeposits of Ni and Co were obtained by cyclic voltammetry on vitreous carbon electrodes in dilute chloride baths. These coatings were analysed by cronoamperometry and cyclicvoltammetry in acidic medium, scanning electron microscopy (SEM), EDX and dot-mapping techniques in relation to the final potential and the concentrations of metal ions in the bath.

The paper describes the results of electrochemical investigations of Ni–Co deposition from a sodium citrate ($C_6H_5Na_3O_7 \cdot 2H_2O$) 0.2 M bath in the presence of boric acid and two additives. The individual deposition of nickel was shown to be partly inhibited by the adsorption of sodium citrate ions at low polarization; such inhibition was not observed for cobalt. The introduction of saccharin at 0.5-0.7 g/L, with a wetting agent seems to hinder sodium citrate adsorption and Ni deposition departs at less cathodic potentials.

The effects of temperature and pH of the plating baths as well as the potential range and cycle number of cyclic voltammetry on the composition and morphology of Ni-Co deposits were systematically investigated.

Composition of the electrolyte, i.e. the ratio of $Ni^{2+}/Co^{2+}$ concentration is found to influence both, the phase structure and the morphology of Ni-Co alloy powders. It is shown that the current density practically does not influence the morphology of Ni-Co alloy powders as well as alloy powder composition. At the highest ratio of the $Ni^{2+}/Co^{2+}$ ions typical spongy particles were obtained. With the decrease of the Ni-Co ions ratio agglomerates of the size of about 100 μm, composed of a large number of fern-like dendrites on their surface were obtained. At the lowest Ni-Co concentration ratio, among more dendritic particles, agglomerates typical for pure Co powder deposition were detected.

The electrolyte used for nickel deposition were presented the composition: $NiCl_2 \cdot 6H_2O$ 0.1M, sodium citrate 0.2M and another electrolyte with $CoCl_2$ 0.1M, at the pH 4.0. Many factors during of electrodeposition processes are contributed to obtaining of qualitative coatings

The electrochemical aspects of coatings were studied by cronoamperometry, cronopotentiometry and cyclicvoltametry measurements in order to have a better understanding of the structure coatings. In presence of saccharine, as an organic additive, the reduction potential value is more negative. The saccharine causing a reduction process inhibits. Ni-Co electrodeposition processes.
The structure of layers depends on the deposition potential and electrodeposition time also.

**Reference**

1. M. Schlesinger, M. Paunovic, *Modern Electroplating*, Fourth Edition, New York, 2000, 667
2. A. N. Correia and S. A. S. Machado**,** *Electrochimica Acta***, 45(11)** 2000, 1733-1740
3. Goldbach S., de Kermadec R., Lapicque F., *Journal of Applied Electrochemistry*, **30(3)**, 2000, 277-284

First Regional Symposium on Electrochemistry of South-East Europe, Rovinj, Croatia, May 4-8, 2008.

P-1-041

# ELECTROCHEMICAL DEPOSITION AND CHARACTERIZATION OF THE Ni-Mo-O SYSTEM POWDERS

**U. Lačnjevac[1], B.M. Jović[1], V.D. Jović[1], M.G. Pavlović[2]**

[1]*Institute for Multidisciplinary Research, 11030 Belgrade, P.O.Box 33, Serbia,*
[2]*Institute of Electrochemistry ICTM, 11000 Belgrade, Njegoševa 12, Serbia*
*E-mail: vladajovic@ibiss.bg.ac.yu*

Electrodeposition of Ni-Mo-O alloy powders from ammonium chloride supporting electrolytes of different Ni/Mo ions concentration ratios was investigated by polarization measurements. Three different electrolytes were used for the investigations: 0.1 M $NiCl_2$ + 1 M $NH_4Cl$ + 0.7 M $NH_4OH$ + *x* M $Na_2MoO_4$, with *x* being 0.05 M, 0.1 M and 0.3 M respectively. In such a way the Ni/Mo ions concentration ratio was 1/0.5, 1/1 and 1/3(pH 9). All powders for microstructure, composition and phase composition analysis were electrodeposited at the limiting current density (position of the inflection point B on the polarization diagrams, see Fig. 1). The polarization curves recorded in different electrolytes are shown in Fig. 1 (Ni/Mo ratio is marked for each curve). As can be seen polarization curves characterized by two inflection points, of a similar shape, were obtained. The first inflection point (A) reflects the beginning of the alloy deposition, while the second one (B) corresponds to the moment when the deposition process is controlled by the rate of hydrogen bubble formation, actually the potential at which the diffusion limiting current of alloy deposition is reached (as explained in our previous papers [1,2]). The potential of the beginning of alloy deposition (A) becomes more negative with the increase of molybdate ions concentration, as it could be expected since the potential of the Mo deposition is much more negative than that of Ni. At the same time a co-deposition of Mo-oxide could only take place in the presence of Ni (induced co-deposition [3]). It should also be mentioned that the current efficiency for alloy deposition in all cases is very low, about 5 %.

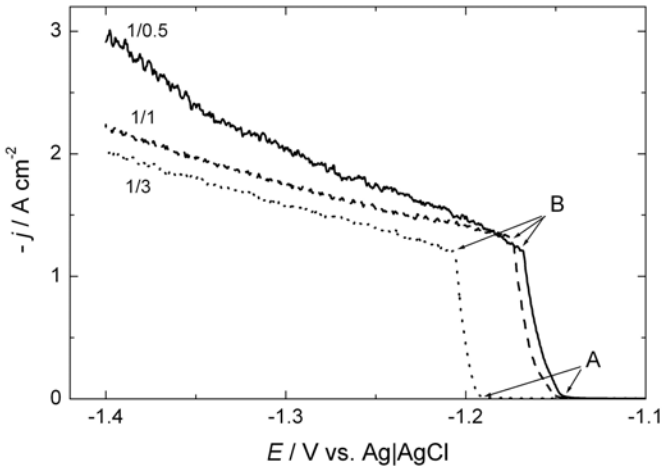


*Fig. 1. Polarization diagrams for Ni-Mo-O powders electrodeposition.*

*The morphology of the as-deposited powders*

The morphology of powder particles electrodeposited onto glassy carbon electrode from electrolytes with different Ni/Mo ratios is mainly characterized with cauliflower type particles of rounded edges and the presence of cracks.

*The XRD analysis of as-deposited and recrystallized powder*

The phase composition analysis of the powders was performed using XRD. In the case of as-deposited powders no peaks were detected on the diffractograms (except one halo observed near $2\theta$ = 44º, see Fig. 2 – quasy-amorph.). It seems that, as in the case of compact deposits [4,5], the crystallites were extremely small, i.e. of the order of nanometers and the powders were quasi-amorphous. Annealing (recrystallization) was performed in $N_2$ atmosphere at 600 $^0$C for 2 h. XRD analysis for sample deposited at Ni/Mo ratio 1/3, shown in Fig. 2 (recryst.), revealed structural transformation and formation of $NiMoO_4$ phase (▼), indicaing that it is possible to obtain single phase powder of the system Ni-Mo-O by electrodeposition.

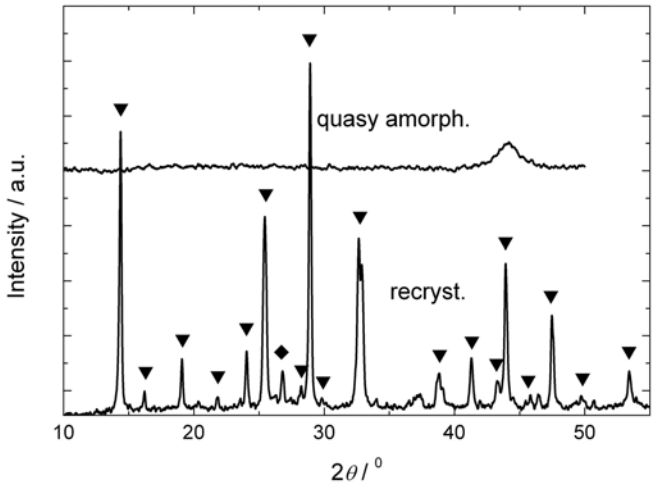


*Fig. 2. Diffractograms of as-deposited (quasy amorph.) and recrystallized (recryst.) powder electrodeposited from the electrolyte with Ni/Mo ratio 1/3.*

**References:**

[1] V.D. Jović, B.M. Jović, M.G. Pavlović, *Electrochim. Acta* **51** (2006) 5468.
[2] V.D. Jović, B.M. Jović, V. Maksimović, M.G. Pavlović, *Electrochim. Acta* **52** (2007) 4254.
[3] A. Brenner, *Electrodeposition of Alloys*, Vol. II, New York, Academic Press Inc. 1963.
[4] E. Chassaing, N. Portal, A.F. Levy, G. Wang, *J. Appl. Electrochem.* **34** (2004) 1085.
[5] M. Donten, H. Celsiulis, Z. Stojek, *Electrochim. Acta* **50** (2005) 1405.

First Regional Symposium on Electrochemistry of South-East Europe, Rovinj, Croatia, May 4-8, 2008.

P-1-042

# MODELLING OF THE VICKERS MICROHARDNESS OF THE ELECTROCHEMICAL $Ni_{100-x}P_x$ THIN LAYERS

**H. Medouer[1], S. Messaadi[1], L. Bennour[1], A.J. Tosser[2]**

*[1]L.E.P.C.M, Département de Physique, Faculté des Sciences, Université de Batna A^vn chahid Med El hadi Boukhlouf, 05000 Algérie. messaadi_saci@yahoo.fr*
*[2]L.P.L.I. , 1 Bld Arago, 57078 Université de Metz cedex 03, France*

The microhardness is one of the most important and often studied material caracteristics. The Vickers mercrohardness of thin electrochemical Ni-P layers can be increased signifanctly by adding saccharine in the solution using the Bückle's model.

## Electrochemical theory

The electrochemical layers of Ni-P can be deposited on the chemical Ni-P layers of the same nature, by using the components (see table 1), as they were mentionned in literature [1].

*Tab. 1: Chemical composition of the baths.*

| Solution | 1/4 - 3/4 | 1/2 - 1/2 | 3/4 - 1/4 |
|---|---|---|---|
| Sodium Hypophosphite: $NaPH_2O_2$ | $125cm^3$ | $250cm^3$ | $375cm^3$ |
| Nickel acétate: $C_4H_6NiO_4, 4H_2O$) | $375cm^3$ | $250cm^3$ | $125cm^3$ |
| Sodium acétate: $C_2H_3NaO_2, 3H_2O$) | $500cm^3$ | $250cm^3$ | $250cm^3$ |
| Palladium Chloride: $PdCl_2$ (0.5g/l) | $10cm^3$ | $10cm^3$ | $10cm^3$ |

The Palladium chloride ($PdCl_2$), plays the catalyst role while the sodium acetate ($C_2H_3NaO_2$) reduces the PH variations in the solution. The effect of the $PdCl_2$ was studied for three volumes (10, 15 an 20 $cm^3$). The chemical layers of good quality are obtained when using 10 $cm^3$ of $PdCl_2$, their thcknesses could reach 1400 A°, while the time needed for depositing these layers is nearly 30 minutes.
Brenner and Riddel [2], was the first to propose an electrochemical theory for Ni-P alloys, the potential of the sample during the electrodeposition is about 0.9 V in the acid solution in contrast to saturated calomel electrode that should be significantly negative in order to have the cathodic reduction done. The reactional mechanism, in the acid solution is described by the following equations:

$$H_2PO_2^- + H_2O \leftrightarrow H_2PO_3 + 2H^+ + 2e \qquad E_0=0.506\ V$$

$$Ni^{++} + 2e \leftrightarrow Ni\ E_0= -0.250\ V \text{ and } H_2PO_2^- + e \leftrightarrow P + 2OH^-\ E_0= -2.05\ V$$

The electrodeposition of thin Ni-P layers requires the following conditions:

- The chemical layers substrate must have homogeneous and cleaned surface,
- The thickness of chemical layers substrate must be above 1100A°,
- The potential between the electrodes must be greater than 25 mV,
- The electrode current density is equal 250 $mA/cm^2$.

**Bückle's model**

To evaluate the influence of the substrate that has a hardness $H_s$, upon the resistance to penetrating into the film with intrinsic hardness $H_f$, Buckle [3] assumes the zone in between the penetrating in the film, has a serial of (K-1) layers that have the same thickness equal to h, where h is the depth of penetration. All models involve partitionning of the contributions to hardness of the substrate $H_s$ and the film $H_f$ in some manner. In the most general approach proposed by Bückle [3], the composite hardness Hc of the film/substrate system is given by:

$$H_c = H_s + a°(H_f - H_s) \text{ , where } a° + b° = 1$$

a° is a coefficient, supposed to depend on the film thickness. The theoretical curves obtained in the framework of the Bûckle's model are given in figure (1). These results exhibit the similar behaviour of that given by Baleva et al [4] related the iron-silicon.

The Vickers microhardness of the electrochemical Ni-P alloys has been examined for the thicknesees equal to 20 µm, using two different substrates (copper and chemical Ni-P), where the current density is around J=15 mA/cm$^2$ and phosphorus percentage equal to 12%. The obtained results are given in table 2.

| Substrate | copper | chemical Ni-P |
|---|---|---|
| Substrate microhardness | 152(Hv) | insufficient thickness |
| Electrochemical Ni-P microhardness | 841(Hv) | 901 (Hv) |

*Tab.2: Microhardness of the electrochemical Ni-P alloys.*

The Vickers microhardness increases by adding saccharine up to 3grams in the electrochemical solution (see figure 2).

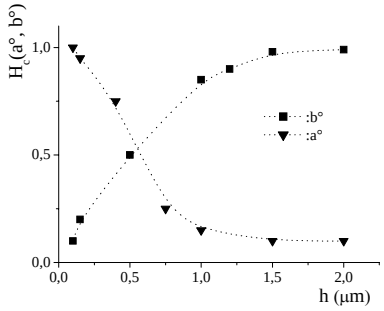


*Fig. 1: Variations of Hc= f(h) in the framework of the Bückle's model.*

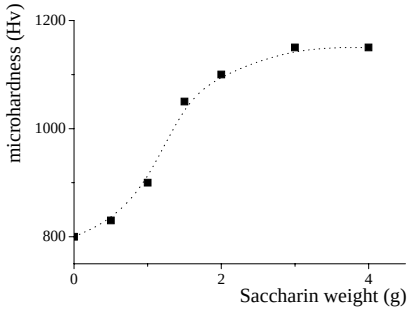


*Fig. 2: Variations of the microhardness of Ni-P with saccharin's weight.*

**Conclusion**

To conclude, we can outline two main points:

- The electrochemical layers of Ni-P have a microhardness which varies between 600 Hv and 800 Hv. This microhardness coul reach 1150 Hv in the case of adding saccharin.

- The values of the electrochemical microhardness can be interpreted by the Bückle's model.

**References:**

[1] S. Messaadi, Thesis of Doctorat, University of Nancy France (1987).
[2] A. Brener and G. E. Riddel, *J. of Res. NBS* (1946)), **37**,1.
[3] H. Bückle, *The science of hardness Testing and its research Applications, American socity of metals*, Metals park, OH, 1973, p. 453.
[4] M. Baleva, V. Drakchieva, E. Gorana, E. P. Trifonova, *Mat. Sci. and Ingen.* **B78** (2000), 131-134.

First Regional Symposium on Electrochemistry of South-East Europe, Rovinj, Croatia, May 4-8, 2008.

P-1-043

# EIS STUDY OF THE ELECTROCHEMICAL BEHAVIOUR OF FILMS OF $Nb_2O_5$ IN A $LiClO_4$ ACETONITRILE SOLUTION OBTAINED BY SPRAY PYROLISIS ON ITO

**R. Romero[1], E. Dalchiele[2], F. Martin[1], D. Dietmar[1], L. Martinez[1], M. Gabás[1], J.R. Ramos-Barrado[1]**

*[1]Departameto de Fisica Aplicada y Ingeniería Química Laboratorio de Materiales y Superficie (Unit associated at CSIC). Universidad de Málaga. España. barrado@uma.es*
*[2]Instituto de Física. Universidad de la Republica, Montevideo Uruguay*

$Nb_2O_5$ is a high band gap (3.3 eV) dielectric material ($10 < \varepsilon < 100$). It has a high index of refraction (2.2–2.6). In the form of thin films, it has been used as an electrochromic coating on glass due to the changing of transmission in the UV/visible/IR range from 85% to less than 20% by reversible insertion of $H^+$ or $Li^+$ ions into the crystal lattice,[1–4] as a porous coating in electrochemical solar cells, [5] as a support or ionic interchanger in catalysis as well as electrode material in electrocatalysis,[6] and as porous layers in oxygen gas sensors.[7]
Thin films of $Nb_2O_5$ (niobium oxide) were obtained by spray pyrolysis. The films were deposited onto indium tin oxide (ITO) coated glass substrates from a $10^{-2}$ M $NbCl_5$ precursor solution at 300ºC temperature. The structural properties of the $Nb_2O_5$ thin films depend on the post-annealing temperature because as-deposited films are amorphous (500 ºC during 2 hours in air atmosphere). The chemical composition of the films was studied by XPS with a PHI 5700 instrument. A standard x-ray source (15 kV, 300 W, Mg $K_\alpha$(1253.6 eV)) was used. The niobium oxide films present a tissue-like morphology, i.e $Nb_2O_5$ fibers woven to a dense but highly porous net with a $Nb_2O_5$ fiber diameter of about 250 nm and pores, in a three-dimensional net, of the micrometer size. The effect of the substrate temperature and the post annealing implies an increase in the size of the pores and a decrease in the fiber diameters as well as the substrate temperature increases, that it has its origin in a reduction of the deposition rate with the increase of the substrate temperature. A more detailed description was showed in previous paper [8]. Only the samples deposited at 300º C and post annealing present a crystalline structure with a TT-$Nb_2O_5$ phase.

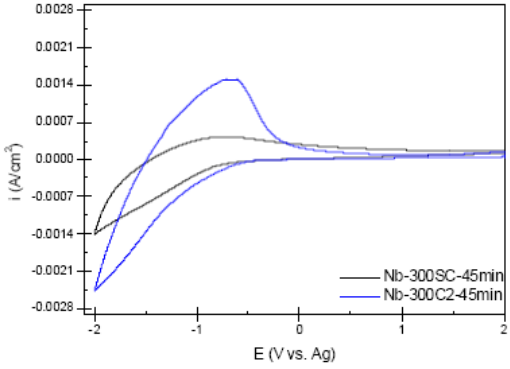


*Fig. 1. Voltamogram of the films as deposited (Nb-300SC-45 min) and with a post annealing during 2 hours at 500 ºC in air atmosphere (Nb-300C2-45min).*

The electrochemical measurements were carried out by using an Autolab with PGSTAT30 potentiostat and a conventional three electrode cell. The cell was previously purged with dry $N_2$ gas. The counter electrode was a platinum foil and the reference electrode was a silver wire. The electrolyte was a 0.1 M solution of $LiClO_4$ dissolved in acetonitrile.

The impedance spectroscopy was carried out for different potential in the cathodic path (lithium insertion) from -0.55 V to -1.75 V (vs. Ag) and in the anodic path (lithium extraction) from -1.75 V to +0.05 V (vs. Ag). The frequency range was between 50 mHz and 10 kHz and an applied potential of 20 mV.

The EI spectra of the samples deposited at 300 ºC and post annealing in the cathodic path can be fitting to a Randles circuit composed by a CPE (Qc) in parallel combination of a serial association of a resistance, (Rct, charge transfer resistance) and a finite length Warburg element with short circuit boundary condition. The charge transfer resistance increase slowly with the applied potential; however, the resistance associated with the Warburg element decrease slowly with the applied potential. The behavior of the sample without annealing can not be fitted to the same circuit model because the Warburg element is, now, an infinite length Warburg element; moreover, the charge transfer resistance decreases with the applied potential.

In the anodic path, the EI spectra of the samples deposited at 300 ºC and post annealing can be modeled by a modified Randles circuit composed by infinite length Warburg element for the voltages between -1.75 V and -1.15 V (vs. Ag). Continuing with the anodic path, a circuit equivalent compose for parallel association of a CPE and a resistance (Rct) fitted the obtained EIS spectra for the voltages between -0.85 V and +0.05 V (vs. Ag); in this circuit, the Rct resistance is the charge transfer resistance and the CPS represents the double layer capacitance but with some dispersion (n parameter about 0.6). The Rct increases with the applied potential.

These behaviors are very similar to describe for the $Nb_2O_5$ prepared by other methods. The increase of Rct in the cathodic path is due to saturation in the $Li^+$ when the potential is increasing and the increase of Rct in the anodic path may be due to a decrease of the exchange current intensity by the exhaustion of the $Li^+$ ions.

## References

[1] C.G. Granqvist, *Handbook of Inorganic Electrochromic Materials*, Elservier, Amsterdam, 1995.
[2] A. Pawlicka, M. Atik, M.A. Aegerter, *Thin Solid Films* **301** (1997) 236
[3] C.O. Avellaneda, A. Pawlicka, *Journal of Materials Science* **33** (1998) 2181.
[4] A.V. Rosario, E.C. Pereira, *Solar Energy Material and Solar Cells* **71** (2002) 41.
[5] D. Filho, D.W Franco, P.P.A. Filho, L.O. Alves, *Journal of Materials Science*, **33** (1998) 2607.
[6] C.A. Pessoa, Y. Gushikem, J*ournal of Electroanalytical Chemistry* **477** (1999) 158.
[7] D. Rosenfeld, P.E. Schmid, S. Széles, F. Lévy, V. Demarne, A. Grisel, *Sensors and Actuators B: Chemical* **37** (1996) 83.
[8] R. Romero, J.R. Ramos-Barrado, F. Martin, D. Leinen, *Surf. Interfase Anal.* **36** (2004) 888.

First Regional Symposium on Electrochemistry of South-East Europe, Rovinj, Croatia, May 4-8, 2008.

P-1-044

# ELECTROCHROMISM IN ANODIC $Nb_2O_5$ FILMS

**L. Skatkov[1], V. Gomozov[2], I. Stepanova[2]**

*[1]PCB "Argo", 4/23 Shaul ha-Melekh str., 84797 Beer Sheva, Israel*
*[2]National Technical University "KhPI", 21 Frunze str., 61002 Kharkov, Ukraine*
*E-mail: sf_lskatkov@bezeqint.net*

Over a long period of time, up to now, our researchers conducted a number of researches dealing with electrochrome effect (EChE) in certain transition-metal oxides, primarily in $Nb_2O_5$ anode oxide films (AOF).
The research principal results of the research are as follows:
Along with study of $Nb_2O_5$ polycrystalline films whose electrochromism has been established already in [1], we were the first to obtain amorphous AOF of niobium pentoxide [2,3] that show pronounced electrochrome effect, i.e. retain high contrast during numerous "coloring-discoloration" cycles.
In practical terms, amorphous AOF are of particular interest as they are free from degradation typical for a crystalline structure.
We have patented [4] a technique for preparation of amorphous anode electrochrome films on niobium, comprising a totally ingenious electrolyte composition and anode oxidation mode.
We have stated the EChE mechanism both in polycrystalline and in amorphous AOF of $Nb_2O_5$ [5], and then proved experimentally.
Besides, we have developed the pulsed electrochemical polarization conditions for already known electrochrome structures (not only on niobium), which permit to raise coloring voltage, and consequently, electrochrome process rate, still preserving the predominance of hydrogen injection into oxide over gas discharge [ 6,7 ].

## References

1. L.S. Palatnik, Yu.I. Maluk, V,V. Belozerov, *DAN SSSR*, 1974, **215(5)**, 182.
2. Maluk Yu.I., Skatkov L.I.., *Pis'ma v ZTF*, 1987, **13(8)**, 504.
3. L. Skatkov, V. Gomozov, *CONCIM 2003* Book of Abstract (Bonn, Germany, 2002). – p.109.
4. Patent Russia #1379345.
5. Bayrachny B.I., Gomozov V.P., Liashok L.V., Skatkov L.I., *Phys.Stat.Sol(a)*, 1989. – **115,** 207.
6. Skatkov L.I., *Rus. Z. Prikl. Chimii*, 1997, **70(4)**, 685.
7. L. Skatkov, V. Gomozov, Proc.ACEC 2005 (China, 2005), p.2P47.

First Regional Symposium on Electrochemistry of South-East Europe, Rovinj, Croatia, May 4-8, 2008.

P-1-045

# DEVELOPMENT OF CHALCOGENIDE THIN FILM SENSORS FOR GAS DETECTION

**K. Kolev[1], B. Monchev[1], C. Popov[2], P. Petkov[3], T. Petkova[1]**

*[1]Institute of Electrochemistry and Energy Systems, BAS, 113 Sofia, Bulgaria*
*[2]University of Kassel (I M A), 34109 Kassel, Germany*
*[3]University of Chemical Technology& Metallurgy, 1756 Sofia, Bulgaria*

Sensors for gas tracking are interesting for many domestic, environmental and industrial applications. Different types of gas sensing devices are already in use basing upon different principles of operation, e.g. optical sensors, electrochemical, mechanical etc.
Chalcogenide thin film gas sensor have the advantage of opportunity to integrate the sensing unit together with the readout electronics and the analysis circuits onto one integrated circuit, this allows low production costs. Their long lifetime, low power consumption and high sensitivity are also outstanding.
Relatively new method of gas sensing and monitoring is the method of micromechanical cantilever-based chemical sensors. The mechanism of the gas sensing is related to the sorption of the gas molecules onto the sensitive layer and reflects on the effective mass of the cantilever/coating structure. The changes in the effective mass are registered by shift in the resonance frequency. The performance of the cantilever-based chemical sensors depends not only on their mechanical characteristics – geometrical dimensions, spring constant, and resonance frequency – but also on the physical and chemical properties of the sensitive layer. In this respect development of new materials as sensitive layered materials is an important task in ever increased requirements in the environment monitoring and fight with the environmental pollution.
A new all solid-state chemical sensor has been developed on the basis of chalcogenide glass-sensitive materials Ge(As)-S-AgI by means of the vacuum thermal evaporation (VTE). The composition, structure and thickness of the deposited sensitive layer have been investigated by means of Electron Dispersive X-ray Analysis (EDAX) and Scanning Electron Microscopy (SEM). The topography of the film has been examined by Atomic Force Microscopy (AFM). The combination of chalcogenide glass-sensitive materials with the method of thin-film layer deposition (VTE technique) allows developing sensing materials with a wide spectrum of predefined properties in the thin film state, giving opportunity for the development of miniaturized thin film sensors. Such sensors can be utilized in multisensor systems for the multicomponent analysis of complex media.
The films have been coated on cantilever-based gas sensors and studied upon exposure to water, acetone, and ethanol vapours. The results reveal that the sensor acted like a resonance microbalance, showing highest sensitivity towards the analyte with the highest molecular weight, i.e. towards acetone. Modification of the surface of the sensitive layer after the exposure to ammonia is associated with chemisorption of the analyte molecules on it and results in increase sensitivity towards water due to the chemisorbed $NH_3$ molecules.

First Regional Symposium on Electrochemistry of South-East Europe, Rovinj, Croatia, May 4-8, 2008.

P-1-046

# PHOTOCURRENT AND IMPEDANCE SPECTROSCOPY STUDIES ON ELECTRODEPOSITED POLYPYRROLE

**V. Figà**

*Dipartimento di Ingegneria Chimica dei Processi e dei Materiali – Università di Palermo*
*Viale delle Scienze – 90128 Palermo (Italia), viviana_fg@yahoo.it*

An investigation on the solid state properties of tensiostatically electrodeposited polypyrrole was carried out by the synergetic use of three techniques: Photocurrent Spectroscopy (PCS), Differential Admittance Measurements (DA) and Electrochemical Impedance Spectroscopy (EIS).
PCS is a non-destructive optical technique based on the analysis of the electrochemical response (photocurrent or photopotential) of the electrode/electrolyte interface, under irradiation with photons of suitable energy. It can provide informations on the energetic of the junction (flat band potential determination, conduction and valernce bands location). EIS allows to model the electrochemical behaviour of the sistem polypyrrole/electrolyte by means of an equivalent electrical circuit. DA measurements allow to get informations on the polypyrrole electrodeposited in the investigated conditions.
From PCS studies, as we expected, just a cathodic photocurrent was recorded, indicating a p-type semiconductor behaviour. The value of the optical band gap is in agreement with literature [1].
The negative slope of the Mott-Schottky plots confirms the p-type semiconductor behaviour. Capacitance vs applied voltage plots, at different frequencies, show a strong dependence of the capacitance from both voltage and frequency. It suggests that the polypyrrole film electrodeposited in our conditions is an amorphous semiconductor.
From the best fitting results, the polypyrrole film can be represented by a constant phase element (CPE) in parallel with a resistance and a Warburg element in series. The power coefficient of the constant phase element is $0.84<n<1$ so the CPE represents a distorted capacitance, due to the surface roughness or non-uniformly distributed properties of the irregular electrode surface. The Warburg element regards the diffusion phenomena inside or outside the polymer film.

[1] Y. Yang, Z.G. Lin, *Synthetic Metals*, **64** (1994) 43-48

First Regional Symposium on Electrochemistry of South-East Europe, Rovinj, Croatia, May 4-8, 2008.

P-1-047

# EXPERIMENTAL ARTEFACTS IN IMPEDANCE SPECTRA MEASURED WITH THREE-ELECTRODE CELL. POLYANILINE FILM MODIFIED Pt-WORKING ELECTRODE CASE

**V. Horvat-Radošević, K. Kvastek**

*Ruđer Bošković Institute, Bijenička c. 54, 10000 Zagreb, Croatia, vhorvat@irb.hr*

Distortions of high frequency parts of impedance spectra of either (very) low or (very) high working electrode (WE) impedance ($Z_{WE}$) measured using a three-electrode cell could be ascribed to parasitic impedances generated by instrumentation, wirings and particularly to a physical body of the cell. For conducting polyaniline (PANI) modified Pt WE in acidic electrolyte solutions, parasitic impedances were found to appear in a form of capacitive/inductive impedances that are strongly dependent on a type of the reference electrode (RE) and its position *vs*. WE [1,2]. It has also been shown that application of transformation formula that converts three-electrode cell into two-terminal whole set-up electrical equivalent circuit (EEC) [3] could successfully be applied for quantitative evaluations of experimental artefacts. The whole set-up EEC is shown in Fig. 1, where $Z_x$ is the WE branch comprising $Z_{WE}$ and solution resistance ($R_s$) between surface of WE and end of RE, while $C^*$, $L^*$ and $R^*$ stand for total parasitic stray capacity, parasitic inductivity and parallel sum of the RE and counter electrode (CE), respectively.

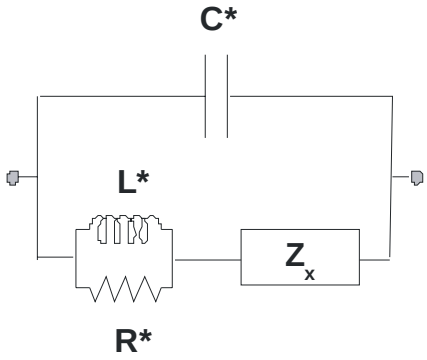


Fig. 1

Here, contributions of experimental artifacts in impedance spectra are quantitatively determined in conditions of increasing $Z_{WE}$ insured by the potential step initiated conducting to insulating transition of PANI films. Impedance spectra are measured in a three electrode cell with conventional RE (SCE) equipped with a HL capillary. Bode plots and high frequency parts of complex impedance plane are for ~0.2 μm thin PANI film modified Pt electrode at potentials of conducting to insulating transition in 0.05 mol $dm^{-3}$ $H_2SO_4$, shown in Fig. 2, where shaded areas denote the frequency region of interference between $Z_x$ and parasitic stray impedances.

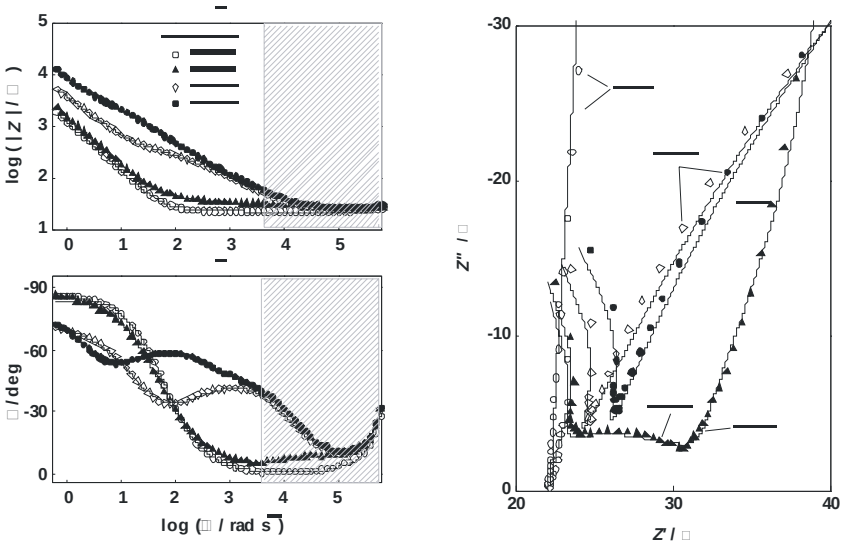


Fig. 2

Differences between measured impedances and $Z_x$ calculated by use of the whole set-up EEC in Fig. 1 is shown in Fig. 3, where strong influence of stray impedances on the values of parameters describing $Z_x$ is indicated.

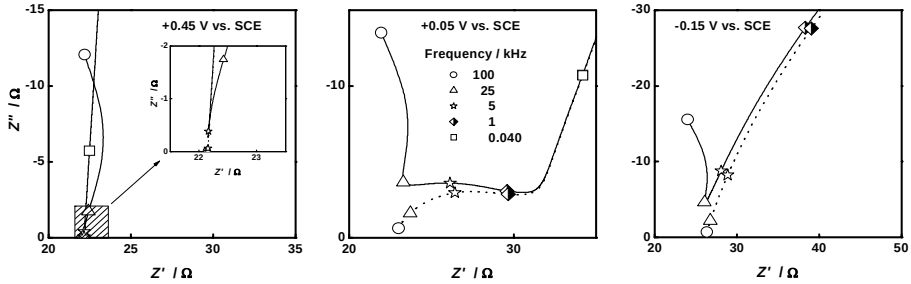


Fig. 3

Comparison between the values of model parameters for fits of the whole set-up EEC in Fig. 1 determined for the whole available frequency region between $1x10^5$ and 0.01 Hz and these calculated for $Z_x$ over restricted frequency region between $1x10^4$ and 0.01 Hz are, together with relative standard deviations (*sd*) for each mean parameter value, listed in Table 1. $Z_{WE}$ is in both cases modeled as impedance of the PANI film ($Z_F$) in parallel with impedance of underlying parts of Pt substrate ($Z_c$) [4], while transfer functions for $Z_F$ and $Z_c$ are given in the heading row of Table 1. Generally higher $Z_{WE}$'s (higher $Z_f$ and higher $Z_c$) have always been determined by the second modeling procedure, where underestimated values of $R_s$ are the main source of errors for other parameter values estimated by usual CNLS routine.

*Table 1*

| Parasitic stray impedance parameters | | | | | $Z_c(i\omega) = Q_d^{-1}(i\omega)^{-\alpha}$ | | $Z_f(i\omega) = R_f + \{[R_{TL-1}(i\omega\tau_1)^{1/2}\coth(i\omega\tau_1)^{p1}]^{-1} + [R_{TL-2}(i\omega\tau_2)^{1/2}\coth(i\omega\tau_2)^{p2}]^{-1}\}^{-1}$ | | | | | |
|---|---|---|---|---|---|---|---|---|---|---|---|---|
| E / V | $10^8 C^*$/ F | $10^5 L^*$/ H | $R^*$ / Ω | $R_s$/ Ω | $10^5 Q_d$/ $\Omega^{-1} s^{\alpha}$ | α | $R_f$/ Ω | $R_{TL-1}$/ Ω | $10^3 \tau_1$ / s | $R_{TL-2}$/ Ω | $10^3 \tau_2$ / s | $10^4 C_f$/ F |
| +0.45 | [a]5.95<br>-- | [a]1.90<br>-- | 500<br>-- | [sa]22.1<br>[sa]21.8 | -- | -- | -- | [c]0.13<br>[c]1.00 | [c]0.08<br>[c]0.60 | -- | -- | 6.1<br>6.0 |
| +0.05 | [a]6.10<br>-- | [a]2.12<br>-- | 500<br>-- | [a]22.8 [a]<br>19.7 | [c]2.00<br>[c]1.84 | [a]0.85<br>[a]0.79 | [b]6.73<br>[b]9.62 | [c]11.1<br>[c]11.9 | [c]2.8 [c]<br>3.1 | [c]102<br>[c]106 | [c]26 [c]<br>27 | 5.1<br>5.1 |
| -0.05 | [a]5.86<br>-- | [a]2.26<br>-- | 500<br>-- | [a]24.0 [a]<br>22.1 | [b]4.18<br>[b]6.23 | [a]0.78<br>[f]0.73 | [b]163<br>[b]231 | [b]447<br>[b]345 | [b]65 [b]<br>44 | -- | -- | 1.4<br>1.3 |

[s] $R_s + R_f$ ; [f] fixed values; *sd* : [a] ≤ 2 %, [b] 2-10 %, [c] > 10 %.
$p_1$ and $p_2$ = 0.42-0.48.

*This work is supported by the MSES (Republic of Croatia) under the Project 098-0982904-2905.*

References:

[1] V. Horvat-Radošević, K. Kvastek, *Electrochim. Acta*, **52** (2007) 5377.
[2] V. Horvat-Radošević, K. Kvastek, *J. Electroanal. Chem.*, **613** (2008) 139.
[3] S. Fletcher, *Electrochem. Commun.*, **3** (2001) 692.
[4] G. G. Láng, M. Ujvári, T. A. Rokob, G. Inzelt, *Electrochim. Acta*, **51** (2006) 1680.

First Regional Symposium on Electrochemistry of South-East Europe, Rovinj, Croatia, May 4-8, 2008.

P-1-048

# STUDY OF $(GeS_{1,2})_{100-x}(AgI)_x$ GLASSES BY IMPEDANCE SPECTROSCOPY

**B. Monchev[1], T. Petkova[1], I. Kanasirski[2], P. Petkov[2]**

[1]*Institute of Electrochemistry and Energy Systems, BAS, 1113 Sofia, Bulgaria*
[2]*University of Chemical Technology & Metallurgy, 1756 Sofia, Bulgaria*

The conductivity of semiconducting glasses is known to be frequency dependent which, as expected is due to conduction in localized state. Measurements of ac conductivity is therefore a powerful experimental method to obtain information about the existence and the location of these states. The ac conductivity, $\sigma ac(\omega)$, of amorphous chalcogenide semiconductors is usually expressed as

$$\sigma ac(\omega) = \sigma T - \sigma dc = A\omega s \qquad (1)$$

where $\omega$ is the angular frequency, $A$ is a constant (s) is the frequency exponent, and $\sigma T$ is the total conductivity including the frequency dependent conductivity measured under ac field and $\sigma dc$ is the dc conductivity. This equation is valid for several low mobility amorphous and even crystalline materials [1].

The correlated barrier hopping (CBH) model proposed by Elliott [2] has been applied to the chalcogenide glassy semiconductors. The CBH model is the most acceptable model used to describe the ac conductivity behavior of amorphous semiconductors. In this model correlated barrier hopping of bipolarons (i.e. two electrons hopping between charged defects $D^+$ and $D^-$) has been proposed to interpret the frequency dependence of conductivity in chalcogenide glasses as given in Eq. (1). The theory has explained many low temperature features, particularly the dependence of the A and s parameters on temperature. However, it does not explain the high temperature behavior so well, in the low frequency range. Singh and Shimakawa [3] suggested that $D^\circ$ states are produced by thermal excitation of $D^+$ and /or $D^-$ states, and that single polaron hopping (i.e. one electron hopping between $D^\circ$ and $D^+$ or $D^-$) contributes at high temperature. Generally the electrical properties of glasses depends on the chemical composition and the structural features.

This study has two objectives; the first was to study the conduction mechanism of our Ge–S-AgI glassy system, and consequently determine the related parameters such as the frequency exponent ($s$) the frequency dependence of the dielectric constant $\varepsilon$, and the ac activation energy $W$m; and the second was to clarify the concept of constraint theory and surface floppy modes for the systems under investigation.

$(GeS_{1,2})_{100-x}(AgI)_x$ ($0 \le x \le 20$ at.%) ionic conductor glasses, prepared by a melt-quenching method, are investigated by impedance spectroscopy in the frequency range 1 Hz–2 MHz at different temperatures $T$ from room temperature to 393 K. The conductivity of the glasses $\sigma$ was obtained as a function of the silver concentration and the temperature.

From the real part of this parameter, the d.c. conductivity (frequency independent component) is also calculated showing an Arrhenius-type dependence on temperature. The pre-exponential factor in this dependence indicates that the electrical conduction takes place by hopping between localized states in the gap. This theoretical model also explains the rise in conductivity when the silver content is increased.

The frequency dependent component of a.c. conductivity fits adequately well to the Debye model. This fact implies that ionic conductivity is much lower than electronic conductivity in these materials, and the dielectric relaxation process shown has been explained in terms of the hopping model described for d.c. electrical conduction.

The experimental results indicate that dielectric constant (real permittivity), dielectric loss and loss angle έ, ε'' and tan δ, increase with increasing temperature. The complex impedance (Z) was measured over the same temperature and frequency ranges. All samples gave a semicircle arc. This indicates that each composition can be described only by one bulk resistance $R_b$ and one capacity $C_b$, both parallels combined. The center below the real axis indicates the relaxation behavior of the system.

**References:**

[1] N.Mott, E.Davis, in *Electron Processes in Non-Crystalline Materials*, Clarendon Press, Oxford, 1979.

[2] S.Elliott, in *Physics of Amorphous Materials*, Longman, NY, 1990.

[3] J.Singh, K.Shimakawa, in *Advances in Amorphous Semiconductors*, Taylor&Francis, NY, 2003.

First Regional Symposium on Electrochemistry of South-East Europe, Rovinj, Croatia, May 4-8, 2008.

P-1-049

# SUPRAMOLECULAR NANOSTRUCTURED ASSEMBLIES OF HEMIN INTO A POLYMER MATRIX FOR $H_2O_2$ ELECTROCATALYSIS

**G.L. Turdean, I.C. Popescu**

*„Babes-Bolyai“ University, Physical Chemistry Department, 400028 Cluj-Napoca, Romania, gturdean@chem.ubbcluj.ro*

The study of molecules and their self organised structures is a multidisciplinary challenge to develop new materials with unique and addressable properties. The creation of supramolecular nanostructures on electrode surface bears unique potential to explore new surface phenomena and to tailor localised functions such as electron transport, molecular recognition or pathways of interfacial reactions.

Hemin (iron protoporphyrin IX) is the active center of the family of heme-proteins, such as b-type cytochromes, peroxidase, myoglobin and hemoglobin. Also, hemin exhibits mimetic peroxidase activity and therefore, its study as catalyst into the detection of $H_2O_2$ becomes an atractive area of research in the field of bioanalytical chemistry, clinical chemistry and environmental science [1].

Electropolymerisation is a powerfull tool for development of new electrode materials. Among advantages of this technique one should point out that the electropolymerisation provides a simplicity of targeting for selective modification of electrode s

urface. In addition, the electropolymerised films usually possess some distinctive properties which are not peculiar to the corresponding monomers.

A comparative study of different monomers (resorcinol, cathecol and hydroquinone [2]) as matrix for nanostructured hemin assembly on the graphite electrode surface by electrochemical measurements was carried out. Thus, cyclic voltammetry provided a quantitative evaluation of the influence of the immobilization matrix on the hemin electrocatalytic activity for $H_2O_2$ detection.

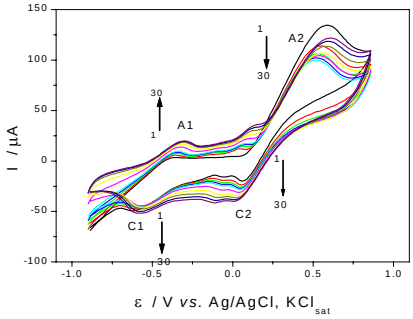


*Cyclic voltammetry of the 5 mM hemin in 5 mM TRIS buffer(pH 8.6) containing 5 mM catechol. Experimental conditions: scan rate, 100 mV/s; 30 cycles; starting potential, -0.9 V vs. Ag/AgCl, $KCl_{sat}$.*

*The authors gratefully acknowledge for financial supports of CNCSIS Romania grants: A 34-1529-2007 and A-51-1319-2007.*

1. G.L. Turdean, I. C. Popescu, A. Curulli, G. Palleschi, *Electrochim. Acta*, **2006**, 51, *6435-6441*.
2. J. K. Park, P. H. Tran, J. K. T. Chao, R. Ghodadra, R. Rangarajan, N. V. Thakor, *Biosens. Bioelectron.*, **1998**, 13, *1187-1195*.

First Regional Symposium on Electrochemistry of South-East Europe, Rovinj, Croatia, May 4-8, 2008.

P-1-050

# NANOSTRUCTURED ORGANIC FILMS ON GOLD: ELECTROCHEMICALLY ASSISTED SELF-ASSEMBLY

**Ž. Petrović, M. Metikoš–Huković***

*Department of Electrochemistry, Faculty of Chemical Engineering and Technology, University of Zagreb, 10000 Zagreb, P.O. Box 177, Croatia, *mmetik@fkit.hr*

The organization of organic molecules into thin films through self-assembly provides a facile method of preparing surfaces with a well-defined composition, structure and thickness. These films potentially enable to tailor and to optimize the surface properties for a variety of technological applications as well as for fundamental studies of surface phenomena.

In the present work nanostructured films of 1-dodecanethiol onto the polycrystalline gold surface were prepared by the potential assisted self-assembly. Contact angle goniometry, surface-enhanced Raman spectroscopy, cyclic voltammetry, and impedance spectroscopy were used to investigate the monolayer properties in aqueous electrolytes. The closely packed and well ordered monolayers are stable over a wide potential range in aqueous electrolytes. Their dielectric barrier properties were evaluated by performing electrochemical measurements without and in the presence of a redox couple. The obtained results have shown that the monolayer of 1-dodecanethiol is essentially free of pinhole defects, and the electron transfer reaction takes place through tunnelling mechanism at collapsed sites in the monolayer.

*Keywords:* Gold, Nanostructured dodecanethiol films, Dielectric properties, Electron transfer reaction.

First Regional Symposium on Electrochemistry of South-East Europe, Rovinj, Croatia, May 4-8, 2008.

P-1-051

# COLLAGEN COATINGS BY ELECTROLYSIS INDUCED SELF ASSEMBLY ONTO ALUMINOSILICATE SURFACE

**F. Bănică[1], S. Cavalu[1], V. Simon[2]**

*[1]University of Oradea, Faculty of Medicine and Pharmacy, N. Jiga Street, No 29, Pharmacy Departament, Oradea, Romania, E-mail: fbanica@uoradea.ro*
*[2]Babes-Bolyai University, Faculty of Physics, Kogalniceanu 1, Cluj-Napoca, Romania*

Aluminosilicate microspheres containing rare earth ions (yttrium or dysprosium) and iron are suitable biomaterials for in situ irradiation of deep cancer. The composites with radioactivable and magnetic properties could be obtained by development of magnetic phases in aluminosilicate materials with rare earth ions prepared by sol-gel method.
Functionalized surfaces of microspheres are performed by electrolytic deposition of type I collagen in order to prepare an uniform coating. This technique operates at physiological conditions and can mediate collagen self-assembly and mineralization at the same time.
Electrolytic deposition was carried out in the three-electrod electrochemistry system controlled by a potentiostat TraceLab 50.
ATR-FTIR spectrometry was then carried out to confirm the presence of the collagen coating. Structural information related to the adsorbed collagen layer is obtained by analysis of the conformationally sensitive amide I absorption band (1660 $cm^{-1}$) using deconvolution technique. The results are interpreted in terms of biocompatibility taking into account the nature of the rare earth ion (Y or Dy) and the iron concentration in samples.

First Regional Symposium on Electrochemistry of South-East Europe, Rovinj, Croatia, May 4-8, 2008.

P-1-052

# ELECTROCHEMICAL AND SPECTROSCOPIC CHARACTERIZATION OF PRUSSIAN BLUE-MODIFIED TITANATE NANOTUBES

**D. Iveković[1], A. Gajović[2,3], M. Ceh[3], B. Pihlar[4]**

[1]*Faculty of Food Technology and Biotechnology, University of Zagreb, Zagreb, Croatia;*
*divekov@pbf.hr*
[2]*Rudjer Boskovic Institute, Zagreb, Croatia;*
[3]*Jozef Stefan Institute, Ljubljana, Slovenia;*
[4]*Faculty of Chemistry and Chemical Technology, University of Ljubljana, Ljubljana, Slovenia*

During the last few years, hydrothermally prepared titanate nanotubes have attracted a lot of attention due to unique combination of physical and chemical properties they possess. High aspect ratio and high surface area of titanate nanotubes, combined with their ion-exchange and intercalation properties, semiconductor behavior, and photocatalytic activity make them promising substrate for applications in the field of heterogeneous catalysis, photocatalysis, electrocatalysis, energy storage, and chemical sensors. Although the exact crystal structure of titanate nanotubes has not been determined yet, it is known that the walls of titanate nanotubes consist of several layers of scrolled or concentric titanate nanosheets, with an interlayer spacing of about 0.7–0.8 nm. The interlayer space is occupied by water molecules and alkali metal cations (usually $Na^+$) that can be easily exchanged with $H^+$ ions and transition metal ions.

In this work the ion-exchange properties of titanate nanotubes were exploited to obtain titanate nanotubes modified with iron(III) hexacyanoferrate(II) (Prussian Blue, PB) nanoparticles. Morphological and structural characterization of PB-modified titanate nanotubes was performed by transmission electron microscopy (TEM), energy dispersive X-ray spectroscopy, UV-VIS reflectance spectroscopy, and Fourier transform infrared spectroscopy. Electrochemical and electrocatalytic properties of samples were examined by cyclic voltammetry and hydrodynamic voltammetry at rotating disc electrode.

Titanate nanotubes have been prepared by hydrothermal treatment of anatase $TiO_2$ powder with 30% (w/w) aqueous NaOH solution at 115 °C. To obtain PB-modified titanate nanotubes, raw nanotubes were first converted to the H-form by treating them with 0.1 M HCl. In the next step, interlayer $H^+$ ions were exchanged with ferrous ions, and finally, PB was deposited on the surface of titanate nanotubes by soaking the Fe-modified nanotubes in solution containing ferricyanide ions. In order to obtain titanate nanotubes with higher PB loading, deposition cycle was repeated up to three times.

TEM analysis of modified nanotubes revealed that large number of homogenously distributed PB nanoparticles (ca. 5-20 nm in diameter) was formed on the surface of titanate nanotubes (Fig. 1). By increasing the number of deposition cycles from 1 to 3, the iron content in samples increased from 1.6 to 5.0 %. On cyclic

voltammograms of PB-modified titanate nanotubes a pair of voltammetric peaks appears in the potential range between 0 and 0.3 V (*vs.* Ag|AgCl|3.5M KCl) corresponding to the reduction/oxidation of high spin iron centers in the crystal lattice of PB (Fig. 2.a). PB-modified titanate nanotubes exhibit exceptionally high catalytic activity toward the electrochemical reduction of hydrogen peroxide. In the presence of hydrogen peroxide the onset of cathodic current corresponding to the reduction of $H_2O_2$ was observed at potentials as high as 0.4 V (Fig. 2.b). Such a high catalytic activity of PB-modified titanate nanotubes, in combination with their other properties (e.g. high density of surface –OH groups available for further modifications), makes them a promising material for application in electrochemical sensors for hydrogen peroxide, or biosensors based on amperometric detection of hydrogen peroxide produced in enzymatic reaction with analyte.

*Figure 1. TEM micrograph of PB-modified titanate nanotubes.*

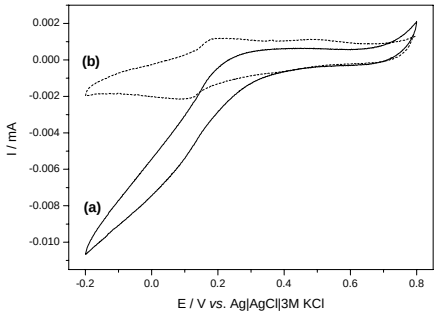


*Figure 2. Cyclic voltammograms recorded at graphite paste electrode containing 2.5% PB-modified titanate nanotubes in (a) 5 mM $H_2O_2$ and (b) supporting electrolyte only (0.1 M KCl / 1 mM HCl)*

First Regional Symposium on Electrochemistry of South-East Europe, Rovinj, Croatia, May 4-8, 2008.

P-1-053

# NEW FUNCTIONALIZED POLYOXOMETALLATES (POMs) FOR MOLECULAR MEMORY DEVICES

**N. Joo[1], G. Delapierre[1], G. Bidan[2], A. Proust[3], R. Thouvenot[3], P. Gouzerh[3]**

*[1]CEA-Leti Minatec, Department of Biology and Healthcare, Grenoble,*
*nicoleta.joo@cea.fr*
*[2]CEA Grenoble, DRFMC/SCIB/RICC;*
*[3]Laboratoire de Chimie Inorganique et Matériaux Moléculaires UMR CNRS 7071,*
*Pierre and Marie Curie University*

The field of molecular electronics is driven by the prospect that devices relying on the bulk properties of semiconductors will fail to retain their characteristics properties as sizes reach nanoscale dimensions.[1] The attachment of redox molecules to diverse surfaces including metals (e.g., Au), semiconductors (e.g., Si, SnO2, TiO2), and insulators (e.g., SiO2) is essential for studies in the field of molecular electronics (Figure 1). Achieving successful device properties requires strategies that afford (1) uniform surface coverage, (2) a regular mode of attachment, and (3) homogenous organization of the electroactive molecules. Towards this goal, we are engaged in a program aimed at constructing devices that use the properties of polyoxometallates to store information. In our general approach, a redox-active molecule attached to an electroactive surface serves as the active storage medium, and information is stored in the discrete redox states of the molecules.

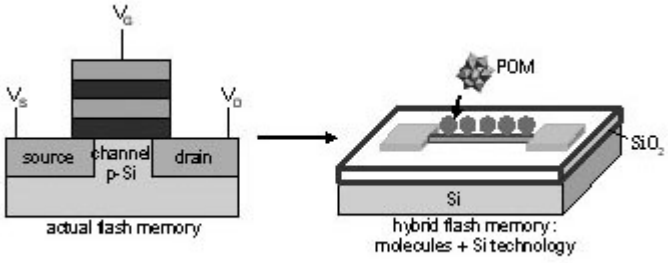


*Figure 1: Integration of POMs in a flash memory device*

We have already shown that polyoxometallates (POMs) are especially interesting since they can be reduced several times (Figure 2) and the reduced products are stable. In a first step, to integrate these molecules into such devices, we are currently developing grafting procedures of POMs on silicon substrates. In this poster, we will present the electrochemical properties of these molecules in solution and grafted on Si-H surfaces.

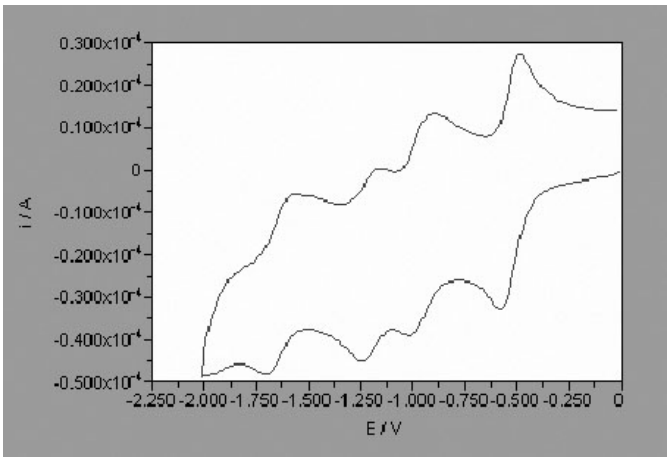


*Figure 2: Representative cyclic voltammograms of the POMs in solution, [POM]=1×10$^{-3}$ M/MeCN/ 10$^{-1}$ M $Bu_4NBF_4$. The scan rate is 100 mV s$^{-1}$.*

(1) Meindl, J.D.; Chen, Q.; Davis, J.A. *Science* **2001**, *293*, 2044-2049

First Regional Symposium on Electrochemistry of South-East Europe, Rovinj, Croatia, May 4-8, 2008.

P-1-054

# ACIDE CHARACTERISTIC OF FULLERENOL $C_{60}(OH)_{24}$ IN WATER

**A. Đorđević[1], Đ. Vastag[1], I. Ičević[1], V. Bogdanović[2]**

[1]*Faculty of Science, Department of Chemistry, Trg Dositeja Obradovica 3, 21000 Novi Sad, Serbia*
[2]*Institute of Oncology, Department of Experimental Oncology, Sremska Kamenica, Serbia, dvadj@ih.ns.ac.yu*

Fullerenes are the third pure crystal form of carbon in addition to diamond and graphite. Fullerenes consist of a spherical ($C_{60}$), ellipsoid ($C_{70}$), or cylindrical (carbon nanotubes) carbon atoms. $C_{60}$ molecule possesses geometry of truncated icosahedrons fulerene-60-$I_h$. Since the discovery of fullerenes, various biological activities for fullerene derivatives have been found: antiviral and antibacterial properties, antioxidative and neuroprotective activities, cell signalling and apoptosis. Some compounds have potential to develop as anticancer drugs and diagnostic agents[1]. Polyxydroxylated fullerenes, fullerenol $C_{60}$ $(OH)_{24}$ have been recently recognized as exogenous redox balance modulators, capable to exert anti-oxidative effects in both in vitro and in vivo systems[2]. Thus, the antioxidative activity of fullerenols is their most exploited property in medicinal chemistry. Our recently published results showed: the in vivo radioprotective efficiency of fullerenol in irradiated rats, as well as its nitric oxide (NO) – quenching activity in both in vivo and in vitro systems[3-5], might be a potential cardioprotector in doxorubicin-treated[6]. Fullerenol $C_{60}(OH)_{24}$ (Figure 1) was synthesized and characterized by Đorđević et al, from polybromine derivative $C_{60}Br_{24}$, which was synthesized in reaction of $C_{60}$ in $Br_2$ with $FeBr_3$ as catalyst [7].

In this study, a part of research, which is conducted with the aim to detect the connection between the biological activity and the chemical mechanism of fullerenol activity, is presented. Mastering such dependence can significantly influence the increase of the biological activity of fullerenol.In this study, the acido-alkaline properties of fullerenol in water solutions, as well as its coordinating abilities in presence of chosen metal ions, are presented. With the aim of achieving this, pH values of water solutions of fullerenol in different concentrations ($4.4\ 10^{-3}$ mol/dm$^3$, $4.4\ 10^{-4}$ mol/dm$^3$, $4.4\ 10^{-5}$ mol/dm$^3$, $4.4\ 10^{-6}$ mol/dm$^3$, $4.4\ 10^{-7}$ mol/dm$^3$) at room temperature, are presented. Based on the results of measuring, the degree of fullerenol dissociation was specified.

The structure of fullerenol signals to its possibility to behave as a polydentant ligand in biological systems, capable of attaching of metal ions. With the aim to learn its coordinating abilities, a preliminary monitoring of fullerenol with $Cu^{2+}$- ion was conducted through spectrophotometric method. In further work, it is planned to investigate the influence of metal ions concentration and fullerenol, as an influence of pH value of the solutions on the stability of synthesised complex compounds. The research is of a particular importance for

investigating the biological mechanisms of fullerenol when compared to some of the microelements.

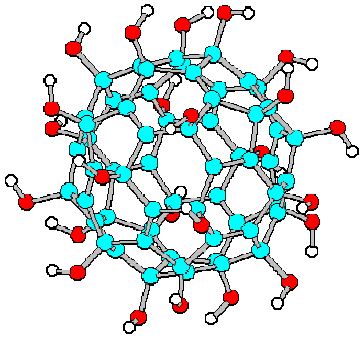

*Fig. 1. Fullerenol $C_{60}(OH)_{24}$*

References:

1. Bosi S, Da Ros T, Spalluto G, Prato M. *Eur J Med Chem*; **38**:913-923 (2003)
2. Djordjevic, A., Bogdanovic, G. and Dobric, *S. J.BUON*; **11**:391-404(2006)
3. Trajkovic, S., Dobric, S., Jacevic, V., Dragojevic-Simic, V., Milovanovic, Z. and Djordjevic, A. *Colloids Surf. B: Biointerfaces* ; **58**:39-43 (2007),
4. V. Bogdanović, K. Stankov, I. Ičević, D. Žikić, A. Nikolić, S. Šolajić, A. Djordjevic, G. Bogdanović, *J. Radiation Research*, in press
5. Mirkov, S.M., Djordjevic, A.N., Andric, N.L., Andric, S.A., Kostic, T.S., Bogdanovic, G.M., Vojinovic-Miloradov, M.B. and Kovacevic, R.Z. *Nitric Oxide*; **11**: 201–207 (2004)
6. R. Injac, M.Perse, M. Boskovic, V.Djordjevic-Milic, A.Djordjevic, A. Hvala, A. Cerar, B. Strukelj, *Technology in Cancer Research Treatment*; **7**: (2008)
7. A. Djordjevic, M.Vojinović-Miloradov, N.Petranović, A.Devečerski, D.Lazar, B. Ribar, *Fullerenes Sciences & Technology* **6**:689-694 (1998)

First Regional Symposium on Electrochemistry of South-East Europe, Rovinj, Croatia, May 4-8, 2008.

P-1-055

# VOLUMETRIC PROPERTIES OF AQUEOUS MIXED-ELECTROLYTE SYSTEMS WITH ALKALI CHLORIDES AT 298.15 K

**F. Sirbu[1], O. Iulian[2], C. Stoicescu[1]**

[1]*"Ilie Murgulescu" Institute of Physical Chemistry of Roumanian Academy, 202 Splaiul Independentei , 060021 Bucharest, Roumania, E-mail: sflorinela@yahoo.com*
[2]*University "Politehnica", Dept. Applied Physical Chemistry and Electrochemistry, 1 Polizu, 011061 Bucharest, Roumania*

The thermodynamic properties of aqueous electrolyte solutions have been studied in literature because their importance in biological, geological and industrial applications as well as in the scientific field. Generally, theoretical and practical approaches for volumetric property calculations are usually limited to dilute and moderate solutions and require complicated numerical calculation.

The Young and Patwardhan - Kumar methods are the methods which can predict, over the entire concentration range, the density and other volumetric properties of mixed aqueous electrolyte solutions from single electrolyte solutions[1] at the same ionic strength as that of mixed solutions. The predictive methods of Young (eq.1) and Patwardhan and Kumar (eq.2), without any empirical constants, were tested against available experimental data for aqueous $H_2O$ - NaCl - KCl and $H_2O$ – KCl - $CaCl_2$ electrolyte solutions at 298,15 K temperature. The mean apparent molar volume ($V_\Phi^*$) was calculated from experimental density and discussed for both systems (eq.3).

$$d = \sum_J \frac{m_J}{\sum_J m_J} d_J \qquad (1)$$

$$d = \frac{\sum_J \psi_J}{\sum_J \left( \frac{\psi_J}{d_J^0} \right)} \qquad (2)$$

$$V_\phi^* = \frac{1000 \cdot (d_0 - d)}{\sum_J m_J \cdot d \cdot d_0} + \frac{\sum_J m_J \cdot M_J}{\sum_J m_J \cdot d} \qquad (3)$$

The notations and terms used in eqs. 1, 2, 3 are the same as in the original papers[2,3,4].

Some results of density prediction with both methods ($\sigma^Y$, $\sigma^{PK}$) for $H_2O$ - NaCl - KCl system at different ionic strength values and different molar ratio $n_{NaCl}/n_{KCl}$ at T=298.15 K are given in Table 1. The obtained predictive accuracy for density at moderate and high concentrations for $H_2O$ – NaCl - KCl and $H_2O$ - $CaCl_2$ - KCl systems lies between 0.004 - 0.489 % and 0.0047 - 2.3% for Young method, repectively, and between 0.001 - 0.178%, and 0.001 - 0.80% for Kumar-Patwardan method, respectively. The Patwardan-Kumar method gives better results than Young methods for the studied systems. This model, without any empirical constants, can be use along with well-know thermodynamic equations to predict density for aqueous mixed-electrolyte solutions from single electrolyte solutions.

*Table 1. Standard deviations for density prediction with Young (Y) and Partwardhan-Kumar (P-K) methods for $H_2O$ -KCl-$CaCl_2$ system, at different molar ratio $n_{KCl}/n_{CaCl2}$ and different ionic strength at 298.15K(some exemples)*

| $n_{KCl}/n_{CaCl2}$=3,0138 | | | $n_{KCl}/n_{CaCl2}$=1,0000 | | | $n_{KCl}/n_{CaCl2}$=1/2,9930 | | |
|---|---|---|---|---|---|---|---|---|
| I, mol $Kg^{-1}$ | $10^2\sigma^Y$, % | $10^2\sigma^{PK}$,% | I, mol $Kg^{-1}$ | $10^2\sigma^Y$, % | $10^2\sigma^{PK}$, % | I, mol $Kg^{-1}$ | $10^2\sigma^Y$, % | $10^2\sigma^{PK}$, % |
| 0.0064 | -4.7 | -4.4 | 0.0260 | -7.8 | -5.7 | 0.0177 | -7.4 | -5.5 |
| 1.1096 | 36.7 | 1.5 | 2.4578 | 141.1 | 3.2 | 5.9114 | 260.1 | 8.8 |
| 2.6761 | 67.0 | 5.5 | 4.8226 | 186.5 | 10.9 | 9.8270 | 102.7 | 48.5 |
| 3.1064 | 71.9 | 6.7 | 6.0194 | 176.5 | 21.9 | 10.7055 | -33.9 | 66.0 |
| 4.9082 | 68.6 | 22.3 | 7.0106 | 168.5 | 19.6 | 11.8886 | 72.8 | 90.9 |

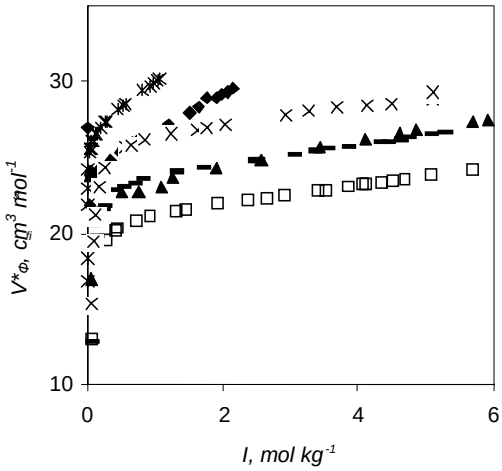


***Fig.1**. Mean apparent molar volume versus ionic strength at 298.15 K for $H_2O$ – KCl - $CaCl_2$ system at: ▲- $n_{KCl}/n_{CaCl2}$ = 1/2.9930, ◆- $n_{KCl}/n_{CaCl2}$=1,000, - $n_{KCl}/n_{CaCl2}$=3.0138; and $H_2O$-NaCl-KCl system at: ×-$n_{NaCl}/n_{KCl}$=0.33456, ▬ - $n_{NaCl}/n_{KCl}$ =1.001, □ - $n_{NaCl}/n_{KCl}$=2.9867*

The mean apparent molar volumes for both systems are calculated and presented in Fig.1. For both systems, the mean apparent molar volume increases with with the ionic strenght of mixture, generally, more evident for $H_2O$ - KCl - $CaCl_2$ system. The mean apparent molar volume values for $H_2O$ - Cl - $CaCl_2$ system arre greater then for $H_2O$ – NaCl - KCl.system.

## References

1. ICT, vol.3, in: DIPPR® Project 801 - Full Version, 2005, Thermophys. Prop. Lab., Dept. Chem. Eng., Brigham Young Univ., Provo, Utah, pag. 95-104
2. T. F. Young, M. B Smith-*J. Phys. Chem.*, **1954**, *58*, 716
3. O. Iulian, F.Sîrbu-*Rev. Roum. Chim.*, **2005**, *50*, 1027
4. Y. F Hu, S. S. Fan-*Fluid Phase Equilib.*, **2001**, *187-188*, 403
5. V. S Patwardhan, A. Kumar-*AIChEJ*, **1986**, *32*, 1419, 1429
6. A Kumar, V. P Mohandas, et al.-*J. Sol. Chem.*, **2004**, *33*, 995
7. H. L Zhang, S. J Han-*J. Chem. Eng. Data*, **1996**, *41*, 516, 42, **1997**, 526

First Regional Symposium on Electrochemistry of South-East Europe, Rovinj, Croatia, May 4-8, 2008.

P-1-056

# KINETIC MODELLING OF THE CRYSTAL VIOLET MINERALIZATION IN WATER BY THE ELECTRO- FENTON PROCESS

**I. Siminiceanu[1], C.I. Alexandru[1], E. Brillas[2]**

*[1]Universitatea Tehnica " Gh. Asachi" Iasi, Facultatea de Inginerie Chimica, Bd. Mangeron 71, Iasi 700050, Romania.*
*[2]University of Barcelona, Faculty of Chemistry, Barcelona 08028, Spain*
*E-mail: isiminic@ch.tuiasi.ro*

The mineralization of acidic aqueous solutions with 0.166 to 1.333 mM Crystal Violet (CV) in 50 mM $Na_2SO_4$ as background electrolyte has been studied by the electro- Fenton method, where the oxidizing hydroxyl radicals were produced from the Fenton reaction between added ferrous ions and hydrogen peroxide generated at a oxygen- diffusion cathode. The influence of a new operating factor on the mineralization degree has been investigated: anode material (platinum versus boron doped diamond).

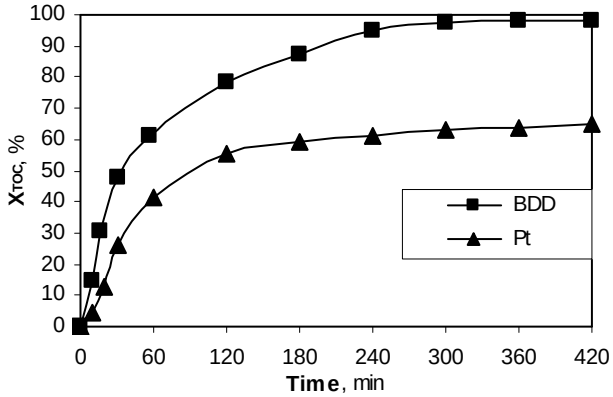


*Fig.1. Influence of the anode material at: 308 K, pH 3, 300 mA, 1mM Fe (II), 50 ppm initial TOC.*

The other five factors (pH, Fe (II) dose, current intensity, temperature, and initial concentration of CV) have been kept constant at the optimal values found in a previous work [1]. The kinetic curves have been correlated through a new kinetic model including two pseudo- first order rate constants.The complex mineralization mechanisms includes several consecutive and parallel reactions. Their exact identification is not of primary importance from a practical point of view. The mechanisms can be compacted in the simple scheme from figure 2, which could be named *general lumped kinetic model (GLKM).*

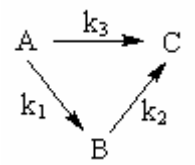


*Fig. 2. The general lumped kinetic model of Crystal Violet (A) degradation to mineral products (C).*

where: A = CV; B = intermediates (from the leuco dye to formic acid , in the detailed mechanisms); C = final mineral products ($CO_2$, $H_2O$, $NO_3^-$, $Cl^-$); $k_1$, $k_2$, $k_3$ = first order rate constants.

When $k_3 << k_1$ and $k_2$ (as suggested by the actual reaction pathways, where is no direct conversion of CV into final mineral products) the GLKM becomes a consecutive reaction model:

$$\frac{C_A + C_B}{C_A^0} = \frac{TOC}{TOC^0} = \frac{k_1}{k_1 - k_2} e^{-k_2 \tau} - \frac{k_2}{k_1 - k_2} e^{-k_1 \tau} \qquad (1)$$

The constants from the equation (1) can be obtained using the experimental data from figure 1. The results have been generalized under the form:

$$Y = a\,x + b \qquad (2)$$

where: $Y = \ln (TOC^0/ TOC)$; $a = (k_1 - k_2)$; $b = \ln \frac{k_1}{k_2}$

*Table 1.The experimental constants of the equation (13)*

| Anode | BDD | Pt |
|---|---|---|
| a | 0.51 | 0.49 |
| b | 0.0108 | 0.0040 |
| $k_1 x\, 10^2$, $min^{-1}$ | 2.740 | 1.020 |
| $k_2 x\, 10^2$, $min^{-1}$ | 1.660 | 0.616 |

The only value in the literature is that of $k_1$ found by Sahoo et al.[2] for the decolourization of CV by the UV/$TiO_2$ method. They found $k_1 = 3.33 x\, 10^{-2}$ $min^{-1}$. The value found in this work for BDD anode was of the same order of magnitude ($2.74 x\, 10^{-2}$ $min^{-1}$). The data from table 1 show that the rate of CV disappearance is 1.65 times faster than the subsequent steps of mineralization for both anode materials, and that for both steps (decolourization, and mineralization) the rate is 2.694 times higher using BDD instead of Pt anode.

1. Siminiceanu I., Alexandru C.I., Brillas E., (2006), Study of Crystal Violet mineralization in water by the electro- Fenton method, *Revista de Chimie*, **57,** 1082- 1085.
2. Sahoo C., Gupta A.K., Pal A., (2005), Photocatalytic degradation of Crystal Violet on silver ion doped $TiO_2$, *Dyes and Pigments*, **66,** 189- 196.

First Regional Symposium on Electrochemistry of South-East Europe, Rovinj, Croatia, May 4-8, 2008.

P-1-057

# BIOCHEMICAL STUDY OF SACCHAROMYCES CEREVISIAE YEAST AS A MICROREACTOR FOR BIOFUEL CELLS

**Y. Hubenova[1], M. Mitov[2,3]**

*[1]Department of Biochemistry and Microbiology, "Paisii Hilendarski" University, Plovdiv, Bulgaria, jolinahubenova@yahoo.com*
*[2]Department of Chemistry, South-West University "Neofit Rilsky", Blagoevgrad, Bulgaria*
*[3]Institute of Electrochemistry and Energy Systems – Bulgarian Academy of Sciences, Sofia, Bulgaria*

Combining the biotechnological principles with those of electrochemistry we are looking for new ways for sustainable energy production. Biochemical fuel cells are a perspective approach for overcoming both the dramatically increasing energy demands and the irreversible environmental pollution caused by the use of nonrenewable carbon-based fuel resources. In addition, biofuel cells potentially offer solutions to the trend towards miniaturization and portability of computing, communications as well as implantable electrically operated devices.

The aim of this study is a verification of possibilities for introducing budding yeast cells as a microreactor into biochemical fuel cells. The investigation includes optimization of conditions for high efficiency utilization of *in vivo* produced electrons within the main biochemical pathways, which naturally cover the energy needs of the living cells. We traced out the three stages of cellular respiration - glycolysis, citric acid cycle and oxidative phosphorylation in eukaryotic cells, aspiring to shuttle the electrons between the biological system and the fuel cell anode by using appropriate mediators. To realize that, the biofuel cell/medium elements will be modulated in such manner that the mediator could capture the electrons from the biological electron transport chains and transfer them subsequently through the double mitochondrial membrane, cytosol and outer membrane of intact cells and finally, to the electrode.

In this *ab initio* study, the log-phase of growth during *Saccharomyces cerevisiae* yeast cell cycle was examined under aerobic as well as anaerobic conditions. Different amounts of yeast were cultivated in suspension media containing carbohydrates and phosphate buffer pH 7. The assimilation levels of monosaccharide glucose and disaccharide sucrose in the yeast medium were quantified by 3,5-dinitrosalicilic acid (DNS) colorimetric method. In parallel, the quantity of the inorganic phosphate converted into organic one in the progress of cell cycle was analyzed by means of Molybdenum blue phosphorous method. The time limit, during which enough adenosine 5'-triphosphate (ATP) amount had been synthesized without inhibiting effect for the glycolysis regulation enzymes, was determined. Thereby, we proved indirectly the stage of further running of processes involved in Krebs cycle and the transfer of electrons (of importance for the fuel cell application) by the electron-carriers nicotine-amideadenine-dinucleotide (NAD) and flavine-adenine-dinucleotide (FAD) into respiratory chains.

The results from quantitative analyses are summarized in Table 1:

*Table 1 Quantitative determination of glucose and inorganic phosphate by DNS and Molybdenum blue phosphorous methods during yeast cultivation.*

| Yeast suspension | 0.1 g/ml yeast + 250 mM glucose/ 67 mM phosphate buffer, pH 7 | | | | 0.1 g/ml yeast + 250 mM sucrose/ 67 mM phosphate buffer, pH 7 | | | |
|---|---|---|---|---|---|---|---|---|
| Conditions | aerobic | | anaerobic | | aerobic | | anaerobic | |
| Incubation time (at 30°C), minutes | Conc. glucose mM | Conc. $PO_4^{3-}$ mM | Conc. glucose mM | Conc. $PO_4^{3-}$ mM | Conc. glucose mM | Conc. $PO_4^{3-}$ mM | Conc. glucose mM | Conc. $PO_4^{3-}$ mM |
| 20 | 11 | 48 | 9 | 20 | 40 | 20 | 39 | 21 |
| 30 | 9 | 20 | 8 | 19 | 40 | 16 | 34 | 15 |
| 40 | 5 | 19 | 7 | 19 | 40 | 16 | 32 | 15 |

Under aerobic conditions, the oxidation of glucose in the examined yeast strain runs more intensively than the further pyruvate transmutation in citric acid cycle and oxidative phosphorylation. In a contrast, the glycolysis and the processes of formation of ATP obviously take place with similar rates even at the first 20 minutes under anaerobic conditions.

The sucrose hydrolysis and participation of fructose in the cell catabolism intensify cellular respiration under both aerobic and anaerobic conditions.

Electrochemical experiments for verification of obtained in this study results in regards to application of yeast as a microreactor in biofuel cell are in a progress.

**References:**

1. Bennetto HP, Delaney GM, Mason JR, Roller SD, Stirling JL, Thurston CF (1985) The sucrose fuel cell: efficient biomass conversion using a microbial catalyst. *Biotechnol. Lett.* **7**:699-705.
2. Bennetto HP (1990) Electricity generation by microorganisms. *Biotechnology Education* **1(4)**:163-168.
3. Bullen RA, Arnot TC, Lakeman JB, Walsh FC (2006) Biofuel cells and their development. *Biosens Bioelectron.* **21(11)**:2015-2045.
4. Gascon S, Lampen JO (1968) Purification of the internal invertase of the yeast. *J. Biol. Chem.* **243**:1567-1572.
5. Hartwell LH, Mortimer RK, Culotti J, Culotti M (1973) Genetic Control of the Cell Division Cycle in Yeast: Genetic Analysis of cdc Mutants. *Genetics* **74(2)**:267-286.
6. Kilkenny BC, Hinshelwood C (1951) The Utilization of Carbon Sources by Certain Yeast Strains. *Proc. R. Soc. Lond. B Biol. Sci.* **138**(892):375-385.
7. Liberatore PA, Cintra 10e—Enhanced Sensitivity from 600–1,200 nm, Analysis of Phosphorus to Sub-ppb Levels. GBC Scientific Application Notes—UV-Visible, 35-40.
8. Palmore GTR, Whitesides GM (1994) Microbial and Enzymatic Biofuel Cells. In: *Enzymatic Conversion of Biomass for Fuels Production, Himmel ME, Baker JO, Overend RP* (eds) ACS Symposium Series № 566, American Chemical Society, Washington DC, pp.271–290.
9. Prasad D, Arun S, Murugesan M, Padmanaban S, Satyanarayanan RS, Berchmans S, Yegnaraman V (2007) Direct electron transfer with yeast cells and construction of a mediatorless microbial fuel cell. *Biosens Bioelectron.* **22(11)**:2604-2610.

First Regional Symposium on Electrochemistry of South-East Europe, Rovinj, Croatia, May 4-8, 2008.

P-1-058

# STUDY OF THE REDOX BEHAVIOR OF COLCHICINE USING ON-LINE ELECTROCHEMISTRY – ELECTROSPRAY IONIZATION MASS SPECTROMETRY

**E. Bodoki[1], A. Bota[2], R. Săndulescu[1]**

*[1]Analytical Chemistry Department, University of Medicine and Pharmacy "Iuliu Haţieganu",E-mail: bodokie@umfcluj.ro*
*[2]Inorganic Chemistry Department, University of Medicine and Pharmacy "Iuliu Haţieganu",13, Emil Isac St., 400023, Cluj-Napoca, Romania*

On-line electrochemistry / electrospray ionization mass spectrometry (EC/ESI-MS) was performed using a special microflow electrolytic cell with a graphite felt - glassy carbon working electrode, formerly described by Arakawa and al [1]. This technique was applied in order to elucidate the still unclear electrochemical oxidation and reduction pathway of colchicine monitoring the intermediates and products resulted in these processes. Effects of electrolytic potentials on ion intensities of product ions were examined in aqueous and non-aqueous (acetonitrile, dimethylformamide) solutions at different pHs and electrolytes. The formation of neutral, radicalic or dimer electrochemical products of colchicine could be followed, being distinguished from hydrogen bonded complexes by MS/MS experiments. The importance of reaction media in the stability of intermediates is also discussed.
Electrochemical reaction mechanisms are speculated based on the obtained MS data and on former knowledge of colchicine's redox behavior.

***Acknowledgements:*** *The authors are grateful for the financial support given by research grants CNCSIS TD 469/2006 and CEEX 6/2005.*

[1] R. Arakawa, M. Yamaguchi, H. Hotta, T. Osakai, T. Kimoto, *J Am Soc Mass Spectrom* 2004, **15**, 1228-1236

First Regional Symposium on Electrochemistry of South-East Europe, Rovinj, Croatia, May 4-8, 2008.

P-1-059

# SPECTROELECTROCHEMICAL STUDY OF THE REDOX BEHAVIOUR OF SOME 5-SUBSTITUTED 2-ALKYLIDENE-4-OXOTHIAZOLIDINE DERIVATIVES

**I. Cekić-Lasković[1,3], D. Minić[1,3], R. Marković[2,3], E. Volanschi[4]**

[1]*Faculty of Physical Chemistry, University of Belgrade, Serbia*
[2]*Faculty of Chemistry, University of Belgrade, Serbia, isidora@fh.bg.ac.yu*
[3]*Institute of Chemistry, Technology and Metallurgy, Belgrade, Serbia*
[4]*Faculty of Chemistry, University of Bucharest, Romania*

The aim of this work is research on electrochemical activity of selected new stereodefined *push-pull*[1] 2-alkylidene-4-oxothiazolidines **(1)**, differing in side chain substituents in aprotic media (0,1 M TBAHFP in MeCN or DMSO) by cyclic voltammetry coupled with spectral EPR and UV-vis-absorption techniques. Characterization of these compounds has been previously done by $^{1}$H NMR and $^{13}$C NMR, IR, UV and MS spectroscopy and X-ray structural analysis [2,3].

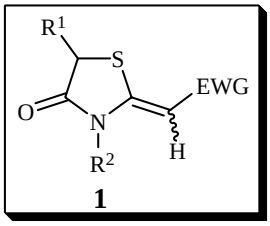


**1**

EWG = COPh, CONHPh, CN
$R^1$ = Me, $CH_2COOEt$: $R^2$ = Me

**(1)**

The results outline the influence of the electron withdrawing group and the substituent at C(5)-position of the thiazolidine ring[4], on the electrochemical reduction and oxidation processes.

Correlations between the electronic structure of 2-alkylidene-4-oxothiazolidines and the reactivity of the intermediate species involved are also discussed.

Corroboration of electrochemical and spectral results allows to propose a possible reaction pathway in electrochemical redox processes of selected 2-alkylidene-4-oxothiazolidine derivatives.

## References

1. R. G. Giles, N. J. Lewis, J. K. Quick, M. J. Sasse, M. W. J. Urquhart, *Tetrahedron*, **56**, (2000), 4531.
2. R. Marković, M. Baranac, Z. Džambaski, M. Stojanović, P.J. Steel, *Tetrahedron* **59** (2003) 7803.
3. R. Marković, M. Baranac, N. Juranić, S. Macura, I. Cekić, D. Minić, *J. Molecular Structure*, **800** (2006) 85.
4. D. M. Minić, I. Cekić, F. T. Pastor, V. Jovanović, R. Marković, *Russian J. of Physical Chemistry A*, **81(9)** (2007) 1458.

First Regional Symposium on Electrochemistry of South-East Europe, Rovinj, Croatia, May 4-8, 2008.

P-1-060

# STRUCTURE-ELECTROCHEMICAL PROPERTIES CORRELATIONS FOR BIS-(10*H* PHENOTHIAZIN-3-YL)-METHANE DERIVATIVES

**D. Gligor[1], C. Cristea[2], G. Cormos[3], L.M: Mureşan[1], I.C. Popescu[1]**

[1]*Department of Physical Chemistry, Babes-Bolyai University, 400028 Cluj-Napoca, ROMANIA*
[2]*Department of Organic ChemistryBabes-Bolyai University, 400028 Cluj-Napoca, ROMANIA*
[3]*L. Blaga" University, Faculty of Medicine, Sibiu, ROMANIA*
ddicu@chem.ubbcluj.ro

In last years, the electrochemical characterization of phenothiazine derivatives has retained the attention of many researchers. These compounds were studied either dissolved in solution [1,2] or adsorbed on an electrode surface [3,4]. The main advantage of investigations carried out on adsorbed systems is the use of small quantities of substance. As a consequence of adsorption, modified electrodes can be obtained, with interesting properties, recommending them as efficient electrocatalysts, selective and sensitive transducers for sensors/biosensors, etc.
In this context, continuing our preoccupation in this domain [3,4], the electrochemical behavior of five new phenothiazine derivatives, based on bis-(10*H*-phenothiazin-3-yl)-methane moiety was studied. The electrochemical parameters (peak potential, current potential, heterogeneous electron transfer rate constant, $k_s$) corresponding to the voltammetric response of compounds (bis-(10*H*-phenothiazin-3-yl)-methane (**I**), *bis*-(10-ethyl-3-phenothiazinyl)-methane (**II**), 10*H*-phenothiazin-3-yl)-phenyl-methane derivatives, where R = H, *meta*-$NO_2$ or *para*- $NO_2$ (**III**-**V**)), adsorbed on graphite electrodes, were estimated from cyclic voltammetric measurements performed at different potential scan rates. The observed differences were assigned to the influence of substituents on the bis-(10*H* phenothiazin-3-yl)-methane moiety redox behavior.

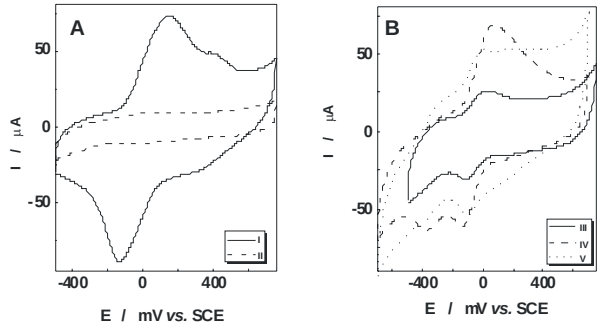


*Figure 1. Cyclic voltammograms of compounds **I-V** adsorbed on graphite electrodes. Experimental conditions: potential scan rate, 50 mV $s^{-1}$; supporting electrolyte, 0.1 M phosphate buffer, pH 7.*

References

[1] G Cauquis *et al.*, *Bull. Soc. Chim. France*, **1977,** 295-302.
[2] M. Jitaru, C. Cristea, I. A. Silberg, *Rev. Roum. Chim.*, *44*, **1999**, 865-868.
[3] D. Dicu *et al.*, *Electrochim. Acta*, *45*, **2000**, 3951-3957.
[4] D. Gligor *et al.*, *Rev. Roum. Chim.*, *48*, **2003**, 463-470.

First Regional Symposium on Electrochemistry of South-East Europe, Rovinj, Croatia, May 4-8, 2008.

P-1-061

# ADSORPTION OF PRIMARY AMINO-ACIDS ANIONS ON PLATINUM

**A. Vvedenskii, E. Bobrinskaya, T. Kartashova, A. Gorschkova, D. Boyarkin**

*Voronezh State University, Russia, 394006. Voronezh, Universitetskaya pl.1*
*E-mail: alvved@chem.vsu.ru*

Electrochemical conversion of amino-acids, undoubtedly, should go through a stage of adsorption and to be the extremely sensitive to their charging condition determined by a correlation between pH of medium and isoelectric point. Frequently adsorption of ionic forms of amino-acids is accompanied them dissociation with formation of atomic hydrogen or larger molecular fragments.

The research task is the establishment principles of adsorption of the relatives on structure primary amino- acids: glycine (Gly) and a α-alanine (α-Ala) on a platinum electrode in 0,1M solution NaOH where the submitted amino-acids are mainly as anions.

For the decision of a task in view we, at the first stage, to give a theoretical analysis of process one and multicentered substitutive adsorption of surface-active substance from the water medium within the framework of the basic phenomenological models act of adsorption in view effects of dissociation and dimerization of adsorbate; the generalized isotherms of adsorption are constructed, the description of kinetic of process adsorption accumulation is lead.

At the second stage the opportunity dissociative chemical adsorption on platinum anion forms $Gly^-$ and $\alpha\text{-}Ala^-$ with removal atomic of hydrogen is experimentally determined; it is designed quasi-equilibrium degree of covering of surface Pt electrode ($\Theta_L$) and $\Theta_L(t)$ ; the type of equilibrium and kinetic isotherms of adsorption of both amino-acids is established. To research of adsorption $Gly^-$ and $\alpha\text{-}Ala^-$ applied methods of electrooxidation in adsorption layer, no-current chronopotentiometry and complex of potentiostatic cathodic-anodic pulses. Calculations lead in the assumption, that adsorption $Gly^-$ and $\alpha\text{-}Ala^-$ on Pt submits modified quasi-logarithmic to an isotherm in the form:

$$e^{f\Theta_L}\,[\Theta_L/(1-\Theta_L)] = K_a(0)[X_L/(1-X_L)],$$

and kinetic of this process it is described by expression of the generalized kinetic isotherm one-centered adsorptions:

$$d\Theta_L/dt = \vec{K}_a(a_L/a_{H_2O})(1-\Theta_L)\exp[-\alpha\psi(\Theta_L)].$$

Here $K_a(0)$ and $\vec{K}_a$ - a thermodynamic constant of balance and a formal-kinetic constant of speed of adsorption accordingly, and $\psi(\Theta_L) = f\cdot\Theta_L$.

It is established, that chemical adsorption $Gly^-$ and $\alpha\text{-}Ala^-$ on platinum it is not accompanied removal of H, however character of their adsorption varies with potential: so at $E_{ads}$ = -0,22 V occurs full dissociation of adsorbate on fragments,

larger, than H, whereas at $E_{ads}$ = 0,04B adsorption is undissociated. On a slope of the received isotherms values of a standard constant of balance $ln\ K_a^o(0)$ and a constant of speed $ln\vec{K}_a$, free Gibbs energy $\Delta G_a^o(0)$ of dissociative adsorptions, and also the factor of power heterogeneity of a surface *f* are designed. The obtained values appeared (table) are high enough, testifying about appreciable chemical adsorption interaction of anion $Gly^-$ and $\alpha$-$Ala^-$ with surface Pt.

*Table. Some parameters adsorptions of $Gly^-$(numerator) and $\alpha$-$Ala^-$ (denominator) on Pt at 298 K*

| $E_{ads}$, V | $ln\ K_a(0)$ | $\Delta G_a^0(0)$ kJ*mol$^{-1}$ | *f* | $ln\vec{K}_a$ ($\vec{K}_a$,$s^{-1}$) |
|---|---|---|---|---|
| -0,22 | 25±1,5<br>23,3±1,4 | -61,9±3,7<br>-57,6±3,5 | -61,9±3,7<br>-57,6±3,5 | 5,0±0,2<br>1,3±0,08 |

Corresponding of adsorption parameters especially describing kinetic adsorptions, for $\alpha$-$Ala^-$ are appreciablly lower, than for $Gly^-$. It is possible, that it is connected to increase in length of a lateral radical and, as consequence, occurrence additional steric difficulties. By size *f*, in researched processes essential distinction in binding energy $Gly^-$ - and ($\alpha$-$Ala^-$) - Pt on different part of a surface is observed.

First Regional Symposium on Electrochemistry of South-East Europe, Rovinj, Croatia, May 4-8, 2008.

P-1-062

# ANODIC OXIDATION OF GLYCINE AND α-ALANINE ON PLATINUM

**A. Vvedenskii, E. Bobrinskaya, T. Kartashova, T. Krastschenko**

*Voronezh State University, 394006. Voronezh, University pl.1*
*E-mail: alvved@chem.vsu.ru*

The research problem: to establish the kinetic scheme and nature of a limiting stage of process of anodic oxidation of anions elementary amino carbons acids on platinum.

The measurements were carried out by means of linear voltammetry and coulometry, and also modulated on potential reflective in situ IR-spectroscopy with Fourier-transformation.

It is established that the anodic oxidation of α-alanine anion on Pt electrode proceeds in the double- layer potential range and is characterized by two maxima of current, whereas electrochemical transformation of glycine proceeds in the potential range of oxygen adsorption, that meets only one maximum of current.

We have carried out the theoretical analysis of one-electronic anodic Red, Ox - process (not being diffusion-limiting) complicated largely by nondissociative adsorption of Red- or Ox-form. It was shown, that if the stage of ionization is kinetically irreversible, then the basic parameters of voltammograms are connected by criterion ratio; $d \lg i_F^m / d \lg v = 1$; $dE^m/dlgv$ = 0.118 V and $dE^m/dlgi_F^m$ =0.118 V , where $i_F^m$ - density of faraday current of reaction in the peak of $i_F$ -E dependence at $E^m$, and v - sweep rate of potential. Essentially, that this ratio is valid for adsorption isotherm of any type (the latter is usually unknown apriori). The nature of adsorbate can be established from the character of concentration dependence of a peak current: in the case of Red dominant adsorption $d \lg i_F^m / d \lg \tilde{N}_{Red} > 0$. At quasi-equilibrium current of anodic Red,Ox - reaction $dE^m/dlgv$ = 0.059V, and the influence of $C_{Red}$ on $i_F^m$ is absent.

The preliminary researches have shown that the obtained diagnostic criteria can be applied to study the kinetics of electrooxidation of glycine and α-alanine. Adsorption of these aminoacids on platinum is nondissociative, and current density in the anodic peak and its location do not depend on rotation number of Pt-electrode.

The current efficiency of electrooxidation process of both aminoacids is designed. It has appeared to be rather close to 100% as was the case with glycine and α-alanine. However these result are valid only for a "soft" mode of oxidation, proceeding with participation of four electrons and accompanied by formation $CO_2$, $NH_3$ and $HCOO^-$, as is assumed in the literature. For specification the nature of other products of glycine and α-alanine electrooxidation in alkaline medium in-situ IR-spectra of reflection were obtained on smooth Pt-electrode in a wide range of potentials. It has appeared, that besides the submitted above products of anodic oxidation, some others can be formed, particularly, $CN^-$, CO and particles of uncertain structure $CH_x$ (x=1 ÷ 3). The application of diagnostic criteria of linear

voltammetry for processing of experimental data has shown, that $i_F^m - v$ dependences are linear, and the average value of parameter $dlgi_F^m/dlgv$ is close to unit, that proves the kinetic process of electrooxidation with the participation of adsorption stages. We have assumed that the stage of first electron transfer limits the electrooxidation of both anions. It result from the practically complete coincidence of theoretical and experimentally received linear $E^m$, lgv – dependences slopes. The second diagnostic criterion of irreversibility of charge transfer stage is also carried out: the experimental dependences $E^m$ - $\lg i_F^m$ are linear in a wide range of aminoacids concentration. Their slopes not bad coincide with theoretical 0.118V, within the limits of an error of experience, reflecting the slowed down stage of ionization with n=1 and β=0.5. It is significant that, with growth of aminoacids concentration the value of $i_F^m$ increases in a wide enough interval of scan rates. Average, in v interval, value of parameter $dlg\, i_F^m/dlgc_{AK^-}$ equal to 0.28 ± 0.08 ($Gly^-$) and 0.27 ± 0.08 ($-Ala^-$), hence dominant adsorption form is anion glycine or α-alanine, and their oxidation is kinetically irreversible. The values of adsorption equilibrium constant $K_a(0)$ and charge of formation of $Gly^-$ and $-Ala^-$ adsorption monolayer $q_{mon}$ are determined. The average value of these parameters are as follows: $lnK_a$ (0) $Gly^-$ = 10.48 ± 0.40; $lnK_a$ (0) $Ala^-$ = 9.71 ± 0.34 and $q_{mon}$ ($Gly^-$) = 0.460 mC/cm$^2$; $q_{mon}$ ($Ala^-$) = 0.285 mC/cm$^2$. It is necessary to note, that the charge $q_{mon}$ for both aminoacids anions is close to values $q_{mon}$ (H) = 0.210 mC/cm$^2$ and $q_{mon}$ (O) = 0.420 mC/cm$^2$. In our opinion, that can indirectly point to the one-centered character of anions glycine and α-alanine adsorption on platinum accompanied, most possibly, with the replacement of one water molecule.

The set of the received results makes it possible to assume the general scheme of electrooxidation process of glycine and α-alanine:

$$^-OOC\text{-}CHR\text{-}NH_2 \rightarrow \left(^-OOC\text{-}CHR\text{-}NH_2\right)_{(ads)} \quad (1)$$

$$\left(^-OOC\text{-}CHR\text{-}NH_2\right)_{(ads)} \xrightarrow{\lim} (CHR\text{-}NH_2)_{(ads)} + CO_2 + \bar{e} \quad (2)$$

$$(CHR\text{-}NH_2)_{(ads)} + 4OH^- \rightarrow \ldots \rightarrow NH_3 + 2H_2O + HCOO^- + 3\bar{e} \quad (3)$$

First Regional Symposium on Electrochemistry of South-East Europe, Rovinj, Croatia, May 4-8, 2008.

P-1-063

# PROBING POLYMER ADSORPTION BY CELL ADHESION AT AN ELECTRIFIED AQUEOUS INTERFACE

**A. Hozić Zimmermann, V. Svetličić**

*Ruđer Bošković Institute, Bijenička 54, 10000 Zagreb, Croatia, ahozic@irb.hr*

Unicellular marine algae *Dunaliella tertiolecta* (cell diameter 6-9 μm) can be characterized through their adhesion at mercury electrode that results in well-defined adhesion signals at millisecond time scale, both at dropping[1] and static[2] mercury electrodes. It was previously shown that the frequency of adhesion signals depends on biopolymer surface concentration.[3] For the given cell density frequency of cell adhesion decreases with the increase in surface coverage of dextran molecules. In this study, we want to show that the existence and the extent of polymer adsorption at the charged mercury electrode/electrolyte interface can be probed by cell adhesion.

Nonpolar dextran and negatively charged dextran sulfate sodium salt, both of average molecular weight 500 000, were used as models of dissolved biopolymers. Dextrans are known for their specific adsorption (displacement of water molecules and ions) at mercury electrode/aqueous solution interface in a range of positive but also negative surface charges.[4] Adsorption of dextran molecules is fast and controlled by mass transport from the solution. The competition between polymer adsorption and cell adhesion was studied at the positively ($\sigma_{Hg}$ = +3.8 μC cm$^{-2}$) and negatively ($\sigma_{Hg}$ = -6.5 μC cm$^{-2}$) charged static mercury drop electrode/0.1M NaCl solution interface using electrochemical technique – chronoamperometry.

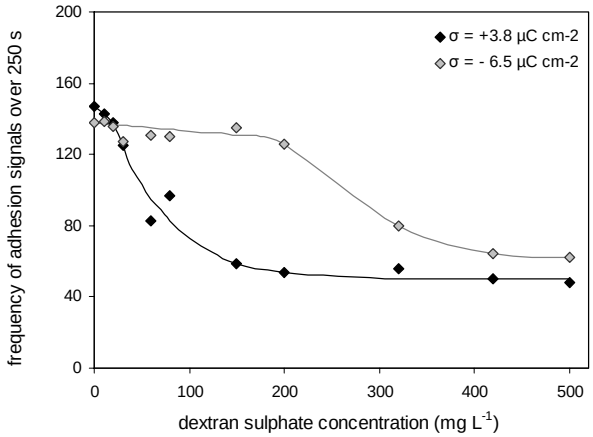


*Dependance of frequency of adhesion signals of* Dunaliella tertiolecta *cells on dextran sulfate concentration at positively and negatively charged static mercury drop electrode. Cell density 7.5 × 10$^7$ L$^{-1}$.*

As expected, the frequency of cell adhesion signals decreases significantly at positively and negatively charged mercury electrode upon the addition of nonpolar dextran. In contrast, the frequency of adhesion signals of *Dunaliella tertiolecta* cells decreases significantly with the addition of dextran sulfate only at the positively charged mercury electrode/electrolyte interface. Obtained results provide clear evidence for the electrostatic repulsion between dextran sulfate molecules and negatively charged mercury electrode since the frequency of adhesion signals is not affected by the addition of dextran sulfate up to the concentration of 150 mg $L^{-1}$.

**References:**

1. V. Svetličić, N. Ivošević, S. Kovač, V. Žutić: *Langmuir* **16** (2000) 8217-8220.
2. V. Svetličić, A. Hozić: *Electrophoresis* **23** (2002) 2080-2086.
3. S. Kovač, V. Svetličić, V. Žutić: *Colloids and Surfaces A* **149** (1999) 481-489.
4. B. Malfoy, J.A. Reynaud: *Anal. Biochem.* **84** (1988) 1-11.

First Regional Symposium on Electrochemistry of South-East Europe, Rovinj, Croatia, May 4-8, 2008.

P-1-064

# NADOx – HRP - Os-REDOX HYDROGEL MODIFIED GRAPHITE ELECTRODES FOR AMPEROMETRIC DETECTION OF NADH

**L.M. Mureşan[1,2]*, M. Nistor[2], E. Csöregi[2], I.C. Popescu[1]**

*[1]Department of Physical Chemistry, "Babeş-Bolyai" University, 400028-Cluj-Napoca, Romania*
*[2]Department of Analytical Chemistry, Lund University, 22100-Lund, Sweden*
**E-mail: lamur@chem.ubbcluj.ro*

Nicotinamide adenine dinucleotide oxidase (**NADOx**), extracted from *Thermus thermophilus*, has been previously used in mono- [1] or bienzyme biosensors [2] for the amperometric detection of NADH. For the first approach, Prussian Blue used as mediator for $H_2O_2$ detection induces biosensor instability, while the use of a dissolved mediator (hydroxymethyl ferrocene) represents a major drawback for the second approach.

This work is presenting another possible way for determination of NADH by a sensitive and highly selective amperometric biosensor, using a new detection scheme where **NADOx** is working in tandem with horseradish peroxidase (**HRP**), and $Os^{II}$-redox hydrogel (**RH**) was used to electrically connect **HRP** to graphite electrode [3]. Two designs were considered for the biosensor construction: (i) *the first one*, [**NADOx-HRP**], exploits the direct electron transfer between **HRP** and the graphite electrode [4]; (ii) in order to increase the efficiency of the connection between **HRP** and the electrode, *the second design*, [**NADOx-HRP-RH**], used Os(II)-redox hydrogel. The whole enzyme matrix was cross-linked with poly(ethylenglycol) diglycidyl ether. Calibration curves (see figure below) for both biosensors were recorded in a single line flow injection setup. The sensitivity for **NADOx-HRP-RH**, 30.2 nA $\mu M^{-1}$ $cm^{-2}$, was higher than that corresponding to a similar one symbolized as glassy carbon/**NADOx-HRP-RH-BSA-GA**, 20.5 nA $\mu M^{-1}$ $cm^{-2}$ [3]. (BSA stands for bovine serum albumin and GA for glutaraldehyde).

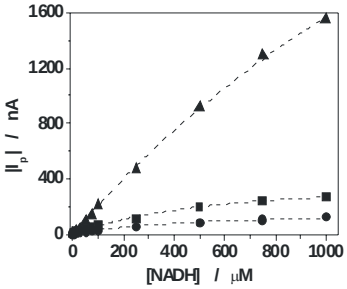


**Figure.** *Calibration curves for NADH recorded at bare graphite (■); **NADOx-HRP** (●), and **NADOx-HRP-RP** (▲). $|I_p|$ stands for the absolute value of the peak current. Experimental conditions: supporting electrolyte, 0.1 M phosphate buffer containing 0.1 M KCl (pH 7.2); applied potential, -50 mV vs. Ag/AgCl, $KCl_{0.1M}$; flow rate, 0.5 ml $min^{-1}$; dispersion coefficient, ~2.*

## References

1. Radoi A. *et al*., *Sens. Actuat.* **B 121** (2007) 501-506.
2. Serban S., El Murr N., *Electrochim. Acta* **51** (2006) 5143–5149.
3. Liu Z. *et al*., *Biosens. Bioelectron.* **14** (1999) 631–638.
4. Lindgren A. *et al*., *Electrochem. Comm*. **1** (1999) 171-175.

First Regional Symposium on Electrochemistry of South-East Europe, Rovinj, Croatia, May 4-8, 2008.

P-1-065

# URINARY OXALATE DETERMINATION BY FLOW INJECTION ANALYSIS USING BIENZYMATIC BIOSENSOR IN BIAMPEROMETRIC MEASUREMENT MODE

**S. Milardović*, I. Kereković, M. Nodilo**

*Department of General and Inorganic Chemistry, Faculty of Chemical Engineering and Technology, University of Zagreb, Marulićev trg 19, HR-10000 Zagreb, Croatia*
*E-mail: stjepan.milardovic@fkit.hr*

Calcium oxalate is the main component of urinary tract stones. Basically, oxalate is a product of protein metabolism and becomes toxic at high concentration due to production of insoluble complex salts with divalent cations (mainly calcium). Determination of oxalates in urine is important for diagnosis of many diseases and mostly indicates the presence of kidney stones. A biosensor for determination of oxalate concentration in urine has been developed by immobilisation of oxalate oxidase and peroxidase on the surface of an interdigitated gold electrode. Enzyme immobilisation was performed using BSA and glutaraldehyde. Oxalate oxidase enzyme immobilised on the surface of an interdigitated electrode converts oxalate to carbon dioxide and hydrogen peroxide according to equation 1.

$$(COOH)_2 + O_2 \xrightarrow{\text{oxalate oxidase}} 2CO_2 + H_2O_2 \qquad (1)$$

Coimmobilised peroxidase catalyses the reaction between hexacyanoferrate(II) and hydrogen peroxide as indicated by equation 2. Hexacyanoferate(II) was a component of the buffer carrier solution.

$$H_2O_2 + 2\left[Fe(CN)_6\right]^{4-} + 2H^+ \xrightarrow{\text{peroksidase}} 2H_2O + 2\left[Fe(CN)_6\right]^{3-} \qquad (2)$$

The produced hexacyanoferate(III) is then reduced at the interdigitated electrode as denoted by equation 3.

$$\left[Fe(CN)_6\right]^{3-} + e^- \rightarrow \left[Fe(CN)_6\right]^{4-} \qquad (3)$$

Biamperometric current is proportional to hexacyanoferrate(III) concentration and thus also to oxalate concentration. Biamperometric measurements were made in flow conditions both in aqueous oxalate solutions (tested concentration range between 25 μM to 10 mM) and in urine samples (tested measuring range between 1 to 100 μM). Optimal working conditions were examined for flow-injection analysis, and good correlation was achieved between added oxalate quantity and the one measured by biosensor in urine matrix ($R^2 = 0.9983$). The influence of some interferences (ascorbic acid, uric acid, paracetamol, acetylsalicylic acid) was also studied.

First Regional Symposium on Electrochemistry of South-East Europe, Rovinj, Croatia, May 4-8, 2008.

P-1-066

# POLYPYRROLE, ITS APPLICATION IN THE DELIVERY OF DOPAMINE

**G.M. Hendy, C.B. Breslin**

*Department of Chemistry, NUI Maynooth, Co.Kildare, Ireland.*
gillian_hendy@yahoo.co.uk

In recent years there has been considerable interest in the development of new and efficient drug delivery systems, particularly with the growth of sophisticated drugs that are based on DNA and proteins[1,2]. Currently, there are several materials under consideration in drug delivery, for example dendrimers[3], nanoparticles[4] and hydrogels[5]. Conducting polymers are also receiving much attention in biomedical research due to their light weight, good biocompatibility and ability to function at body temperature. In particular, conducting polymers exhibit a reversible electrochemical response.

In this paper, a conducting polymer, polypyrrole is considered as a drug delivery system. Polypyrrole can be reversibly switched between an electronically conducting and insulating state. This change in the net charge of the polymer requires ions to flow into or out of the film allowing the polymer to bind and expel ions in response to an applied potential. Here, we show that polypyrrole can be used to control the delivery of a well known cathecolamine, dopamine. Dopamine was selected as a model cationic drug as it has a protonated amine and can be used to represent a large class of pharmaceutically important compounds. This concept of controlled delivery is based on the well-known redox chemistry of polypyrrole; a change in the net charge on the polypyrrole film during its reduction or oxidation requires ions to flow into or out of the film. This, in turn, allows the polypyrrole film to bind and expel ions in response to electrical signals.

Polypyrrole was first synthesized electrochemically and then the dopamine was incorporated on reduction of the polypyrrole film in an appropriate solution of the cations. The cationic dopants were then released on oxidation of the polymer and the release profiles were monitored using UV-visible spectrophotometry.

## References

1. T.M. Allen and P.R. Cullis, *Science*, **303**, 1818 (2004).
2. K.E. Uhrich, *Chem. Rev*., **99**, 3181 (1999).
3. Yang, H.H and Kao, W.Y.J. *J. Biomat. Sci. Polym. Ed*., **2006**. 17, 3.
4. Wartlick, H.; Michaelis,K.; Balthasar, S.; Strebhardt, K.; Kreuter, J. and Langer,K. *J. Drug Targeting*, **2004**, 12, 461.
5. Serizawa, T.; Matsukuma, D. and Akashi, M. *Langmuir*, **2005**, 21, 7739.

First Regional Symposium on Electrochemistry of South-East Europe, Rovinj, Croatia, May 4-8, 2008.

P-1-067

# A SUPRAMOLECULAR APPROACH TO THE DETECTION OF DOPAMINE USING CYCLODEXTRIN MODIFIED POLYPYRROLE

**C.C. Harley, A.D. Rooney, C.B. Breslin**

*Department of Chemistry, National University of Ireland Maynooth, Maynooth, Co. Kildare, Ireland, claire.c.harley@nuim.ie*

Dopamine (DA) plays an important role in the body as a neurotransmitter (NTM) and a deficiency in this NTM has been related to serious neurological disorders such as Parkinson and Alzheimer diseases. As a result, there is continuing interest in the development of fast, sensitive and selective methods for the detection of DA. In particular there has been much interest in electrochemical methods because DA is electrochemically active and these methods are inexpensive and easy to employ. However, the determination of DA is complicated by the coexistence of many interfering compounds with ascorbic acid (AA) being of particular significance.

AA is the most problematic because it is oxidized at similar potentials to DA and AA is present in concentrations that are several hundred times higher than DA in the living organism. Furthermore, the oxidized dopamine product, dopamine-quinone, can be chemically reduced by AA to DA, which can be reoxidised at the electrode surface. One way of overcoming these problems is to form modified electrodes and several strategies for modifying the electrode surface have been developed[1-3].

In this paper, we show that polypyrrole doped with an anionic cyclodextrin can be used as a highly selective and sensitive DA sensor. Cyclodextrins exhibit conical structures with a hydrophobic internal cavity and a hydrophilic exterior. Their well-known ability to form supramolecular complexes with suitable organic and inorganic, neutral and ionic substances has resulted in the design of selective electrodes[4-5].

The DA was detected at the modified electrodes using a range of electrochemical techniques giving peak currents at approximately 500 mV (SCE) and 300 mV (SCE) respectively. However, the modified electrodes were unable to detect AA, even at a relatively high concentration of 0.001 mol $dm^{-3}$ to give a highly selective sensor for the detection of dopamine.

**References:**

1. S. Alpat, S.K. Alpat and A. Telefoncu, *Analytical and Bioanalytical Chemistry*, **383**, 695-700 (2005)
2. J.B. Raoof, R. Ojani and S. Rashid-Nadimi, *Electrochimica Acta*, **50**, 4694-4698 (2005)
3. A. Liu, M. Wei, I. Honma and H. Zhou, *Advanced Functional Materials*, **16**, 371-376 (2006)
4. N. Izaoumen, D. Bouchta, H. Zejli, M. El Kaoutit, A.M. Stalcup, K.R. Temsamani, *Talanta*, **66**, 111-117 (2005)
5. U.E. Majewska, K. Chmurski, K. Biesiada, A.R. Olszyna, R. Bilewicz, *Electroanalysis*, **18**, 1463-1470 (2006)

First Regional Symposium on Electrochemistry of South-East Europe, Rovinj, Croatia, May 4-8, 2008.

P-1-068

# ELECTROSYNTHESIS AND ELECTROCHEMICAL CHARACTERIZATION OF PHENAZINE POLYMERS FOR APPLICATION IN BIOSENSORS

**M.M. Barsan, E.M. Pinto, C.M.A. Brett***

*Departamento de Química, Universidade de Coimbra, 3004-535, Coimbra, Portugal*
*brett@ci.uc.pt

Electropolymerization is a powerful tool in the development of modified electrodes, and when the monomer is itself redox-active, conductive films with high electrical conductivity can be easily prepared. Phenazine dyes are such a kind of monomer (see Fig. 1). A comparative investigation of the electrosynthesis and electrochemical properties of three different electroactive phenazine polymers, made from the phenazine dye neutral red, and two phenothiazine dyes, methylene green and methylene blue was performed on carbon film electrodes [1].

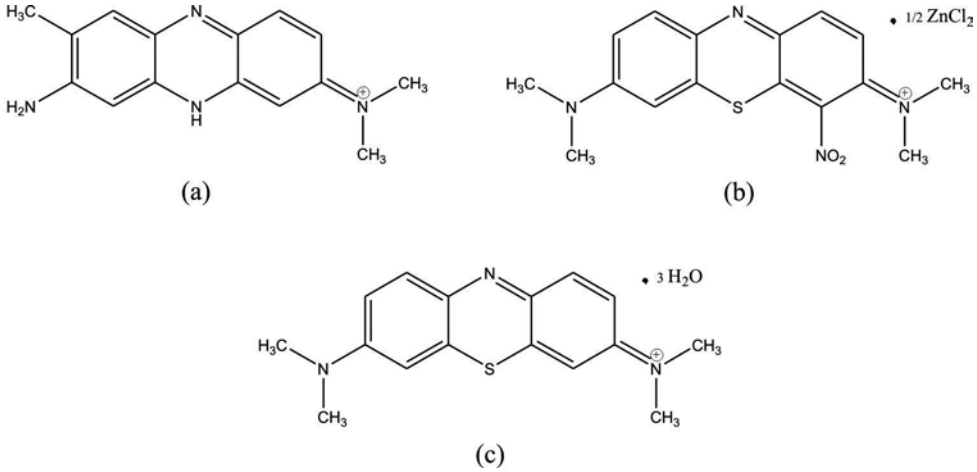


*Fig. 1. Chemical structures of phenazine monomers: (a) neutral red, (b) methylene green zinc chloride double salt and (c) methylene blue trihydrate.*

Polymerization conditions for all three polymer films were optimized. Formation of the radical cations was observed at different potentials and the chemical structures of the monomers influence the electropolymerization process. Of the three polymers, poly(neutral red) is shown to have the best adhesion at carbon film electrodes.

The influence of the electrolyte composition and pH on film growth and on the electrochemical properties was investigated. The formal potential varied with pH, decreasing linearly with increase in pH, in the range from 1 to 7, for all three polymers. Cyclic voltammetry showed that the diffusion of counter ions in solution is the rate-determining step of the overall redox process. Different electrolyte cations influence the electrochemical properties of the modified electrodes, the dimensions of the hydrated cation having most influence on the

current and charge passed. The modified electrodes were also characterized by electrochemical impedance spectroscopy. The interfacial characteristics of the two phenothiazine polymers were similar and oxygen dependent, but different to those of poly(neutral red), which were not significantly influenced by the oxygen. Perspectives for use in electrochemical biosensors are discussed.

**References:**

[1] M.M. Barsan, E.M. Pinto, C.M.A. Brett, *Electrochim. Acta*, in press.

First Regional Symposium on Electrochemistry of South-East Europe, Rovinj, Croatia, May 4-8, 2008.

P-1-069

# ELECTROCHEMICAL STUDY OF PHOSPHOLIPID MONOLAYER-MODEL LIPIDS INTERFACIAL INTERACTIONS

**B. Gašparović[1]*, S. Frka[1], Z. Kozarac[1], A. Nelson[2]**

*[1]Ruđer Bošković Institute, Center for Marine and Environmental Research, POB 180, HR-10002 Zagreb, Croatia, E-mail: gaspar@irb.hr*
*[2]Centre for Self Organising Molecular Systems, School of Chemistry, University of Leeds, LS2 9JT Leeds, UK*

Electrochemical impedance spectroscopy, *ac* voltammetry and fractal analysis were used to characterise interaction of model water insoluble compounds of increasing polarity with phospholipid monolayer. The mercury drop electrode uncoated and coated with a monolayer of dioleoyl phosphatidylcholine (DOPC) was used as a basis for investigation. The compounds studied in order of increasing polarity were: nonadecane, stearic acid, cholesterol and cardiolipin. From the electrochemical response, it is observed that both the molecular structure and polarity of the investigated compounds have a role in their interaction with the uncoated and DOPC coated electrode. In the fractal analysis the degree of fractal dimension *D* imparted to the DOPC layer is related to the degree of apolarity of the additive model compound (Fig. 1).

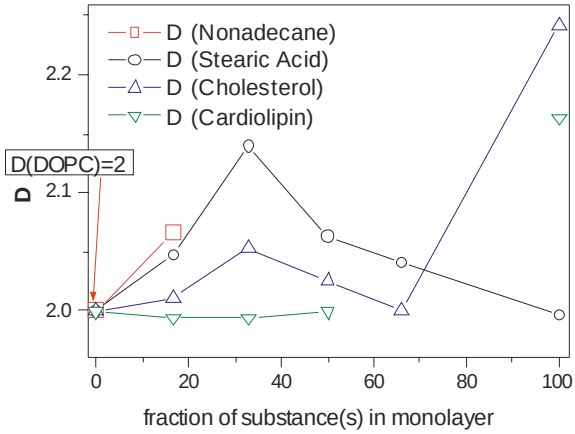


*Fig. 1. Fractal dimension (D) determined for increasing weight fraction of model lipid substance in DOPC monolayer for **(a)** nonadecane (□), stearic acid (○), cholesterol (△), and cardiolipin (▽).*

First Regional Symposium on Electrochemistry of South-East Europe, Rovinj, Croatia, May 4-8, 2008.

P-1-071

# DETECTION OF INFLUENZA VIRUS A BY USING IMPEDANCE BIOSENSORS

**B. Meric[1], L. Fojt[2], M. Ozsoz[1], V. Vetterl[2]**

*Ege University, Faculty of Pharmacy, Analytical Chemistry Department, 35100, Izmir, Turkey*
*[2]Institute of Biohysics,v.v.i.,Academy of Sciences of the Czech Republic, 61265 Brno, Czech Republic*

Influenza virus which belongs to the family of orthomyxoviruses is a major cause of respiratory infection in both adults and children. Different types of influenza viruses exist like A, B and C with antigenic differences of the nuclear and matrix proteins of the virus. Both A and B types cause epidemic diseases of human. The classical methods for the diagnosis of influenza virus like viral culture, immunofluorescence staining (IFA), enzyme immunoassays (EIA), DNA microarrays etc. are slow and expensive.

The impedance biosensor is described as a technique for the determination of influenza type A virus. 28-mer oligodeoxynucleotide (ODN) related to the section of the human genome for "Influenza aviensis " served as the capture probes (AM-245), the complementary ODN was target. A sensitive method for the detection of ODN hybridization is electrochemical impedance spectroscopy (EIS). The Nyquist plot (dependence of the imaginary part Z´´ of complex impedance on the real part Z´) of the impedance of the electrode double layer in the solutions of hexacyanoferrate $K_4[Fe(CN)_6]$ measured at the potential of + 0.24V, where faradayic current is observed. In supporting electrolyte without hexacyanoferrate there is no faradayic current and only capacitance response is observed which can be described by a constant phase element. In the solution of hexacyanoferrate the observed response can be described by a Randles circuit with a small charge transfer resistance (small radius of the semicircle observed at high frequencies, straight line with a slope close to $45^0$ at low frequencies). Single stranded ODN adsorbed at the electrode prevents the access of the the redox couple ($[Fe(CN)6]^{3-}$/$[Fe(CN)6]^{4-}$) to the electrode surface and the charge transfer resistance increases. This results in the increase of the radius of the Nyquist plot semicircle. The hybridization of target ODN to the surface attached probe ODN leads to a higher coverage of the electrode by the adsorbed ODN molecules an to the increase of the negative charge of the surface by negatively charged phosphates of the double helical ODN. This prevents the access of the anions ($[Fe(CN)6]^{3-}$/$[Fe(CN)6]^{4-}$) to the electrode resulting in a further increase of the charge transfer resistance and larger radius of the Nyquist plot semicircle.

*Acknowledgement: This work was supported by the grant project No. 1MO528*

"Centre for Dental and Craniofacial Research" of the Ministry of Education, Youth and Physical Training of the Czech Republic, by the project No. 202/08/1688 of the Grant Agency of the Czech Republic and by the project KAN200040651 of the Grant Agency of the Academy of Sciences of the Czech Republic.

First Regional Symposium on Electrochemistry of South-East Europe, Rovinj, Croatia, May 4-8, 2008.

P-1-072

# ELECTROCHEMICAL DETECTION OF DNA DAMAGE CAUSED BY HEAVY METAL IONS

**S.C.B. Oliveira, A.M. Oliveira-Brett**

*Departamento de Química, Faculdade de Ciências e Tecnologia, Universidade de Coimbra, 3004-535 Coimbra, Portugal, oliveirascb@ci.uc.pt*

Heavy metal ions, lead, cadmium and nickel, are well known carcinogens with natural different origins and their direct mode of action is still not fully understood. A dsDNA electrochemical biosensor, employing differential pulse voltammetry, was used for the *in situ* evaluation of $Pb^{2+}$, $Cd^{2+}$ and $Ni^{2+}$ interaction with dsDNA [1].

The study of the interaction of DNA with the heavy metal ions of Pb, Cd and Ni, using a multilayer dsDNA biosensor, helped to clarify the mechanism by which these metals bind to dsDNA and their possible mutagenic properties. The modifications caused to DNA integrity were electrochemically recognized as changes in the oxidation peaks of guanosine and adenosine bases.

Using modified electrodes with homopolynucleotides of guanine and adenine, it has been proved that the interaction between $Pb^{2+}$ and DNA causes oxidative damage and preferentially takes place at adenine-containing segments, with the formation of 2,8-dihydroxyadenine, the oxidation product of adenine residues and a biomarker of DNA oxidative damage. The $Pb^{2+}$ bound to dsDNA can still undergo oxidation. These results enable a better understanding of the molecular mechanism involved in $Pb^{2+}$-induced neoplasia.

The interaction of $Cd^{2+}$ and $Ni^{2+}$ with dsDNA caused no oxidative damage, and the results indicated that these heavy metal ions affect the double helix structure of dsDNA, causing conformational changes and opening the way to initiation of the action of other oxidative agents.

The results confirm that $Pb^{2+}$, $Cd^{2+}$ and $Ni^{2+}$ all bind to dsDNA, and that this interaction leads to different modifications in the dsDNA structure. The different interaction of $Pb^{2+}$ with dsDNA, leading to oxidative damage, compared with $Ni^{2+}$ and $Cd^{2+}$, which only caused conformation structural changes, was shown. The sensitivity of the multilayer dsDNA electrochemical biosensor offers the possibility to follow the interaction of metal ions with DNA under different conditions.

**References:**

1. S.C.B. Oliveira, O. Corduneanu, A.M. Oliveira-Brett, *In situ* evaluation of heavy metal-DNA interactions using an electrochemical DNA biosensor, *Bioelectrochemistry* **72** (2008) 53-58.

First Regional Symposium on Electrochemistry of South-East Europe, Rovinj, Croatia, May 4-8, 2008.

P-1-073

# MEASUREMENT OF BINDING CONSTANTS OF ANTIBODY IN DIFFERENT ELECTROCHEMICAL CONDITIONS

**M. Vasjari[a], V.M. Mirsky[b],**

[a]*Faculty of Natural Sciences, University of Tirana , Albania*
[b]*Institute of Analytical Chemistry, Chemo- and Biosensors, University of Regensburg, Germany.*

## Introduction

It is well known that a gold piece being in contact with an electrolyte has properties of the redox electrode: the potential difference between metal and electrolyte is defined by concentrations of electrochemically active substances in the electrolyte. Taking into account that many biological molecules and many biologically active molecules are redox active and most biological samples have redox-active impurities, this effect can cause poor reproducible electrochemical conditions during bioaffinity analysis. In this work we demonstrated that the potential of the gold layer has influence on the binding constant of antigen-antibody interaction.

## Materials and methods

Glass slides covered with a gold film of about 50 nm thick with Cr-adhesive layer (2 nm thick) were immersed into 1 mM ethanolic solution of 16-mercaptohexadecanoic acid and incubated there for at least 5 h to prepare the alkilthiol monolayer.

An opened cylindrical Teflon cell (8 mm in diameter) was attached to the gold surface of the glass slide. Ag/AgCl electrode with salt bridge was used as a reference electrode. The gold layer was electrically wired. Potential difference between the reference electrode and gold layer was controlled by the voltage source. The measurements were performed 32 ±0.2°C.

Bovine serum albumin (BSA, Sigma) and monoclonal anti-BSA (Sigma) was chosen as an example of the receptor-analyte pair. Antigen (BSA) immobilization solution was prepared in 140mM solution of NaCl containing an optimal addition of EDC (1-ethyl-3-(3-dimethylaminopropyl)-carbodimide) (pH=5). The standard solutions of Imunoglobuline were prepared in phosphate buffered solutions.

## Results and discussion

An influence of anti-BSA on electrical potential of thin gold layer coated by self-assembled monolayer of 16-mercaptohexadecanoic acid with immobilized BSA note that additions of the protein in concentrations which are typical for bioanalytical applications, lead to changes of the electrode potential for over 100 mV.

To understand possible influence of such potential variations of the gold layer on bioaffinity analysis, measurements of binding constants at different potential values of the gold electrode were performed. SPR was used as a detection technique. The measurements were performed at the electrode potentials of -600 mV, 0 mV and +600 mV (vs. Ag/AgCl) at pH 5 and 8. The calculated values of the binding constants are shown in the Figure. The binding constant at pH 5 were found to be about 2 - 4

times higher than at pH 8. Potential increase for 1200 mV increases the binding constant about 2.1 – 3.2 times. However, in both cases an increase of the binding constants was observed.

The effect of the electrical potential has a direct influence on the structure of binding sites. This is confirmed indirectly by changes of SPR signal of the receptor layer due to changes of the electrode potential. Taking into account typical potential fluctuations during bioaffinity analysis, the error in the determination binding constant is within 30%. In the devices without temperature stabilization it will be masked errors caused by temperature fluctuations. Also for many applications an error of 30% is ignorable. However, this is a systematic error, and it should be taken into account in precise quantitative measurements.

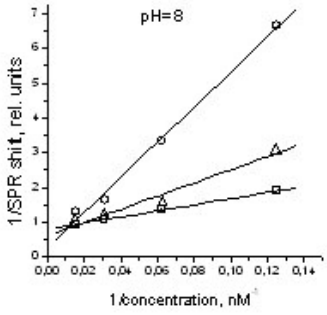


*Fig. 1. Linearization of sensor response in doubble reciprocal coordinates obtainedin pH = 8, defined electrode potential -0.6V (empty circles), 0.0V (triangel), +0,6V (filled circles)*

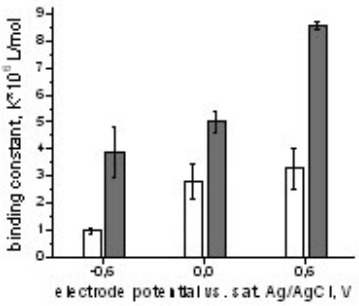


*Fig. 2. Binding constants of BSA-IGg system under defined potential conditions:* *pH = 8* *pH = 5*

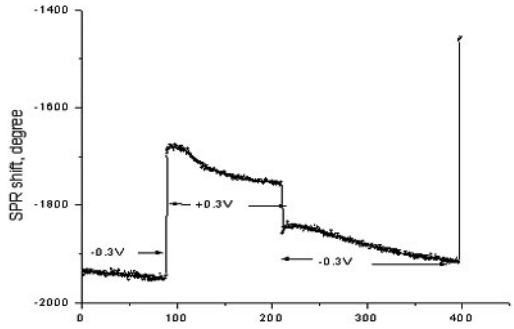


*Fig. 3. The shift of resonance angel due to the potential applied to the surface receptor layer in constant concentration of IGg(4mM)*

First Regional Symposium on Electrochemistry of South-East Europe, Rovinj, Croatia, May 4-8, 2008.

P-2-074

# CURRENT COMPONENTS IN DIFFERENTIAL PULSE POLAROGRAPHY

**M. Zelić, M. Lovrić, D. Jadreško**

*Center for Marine and Environmental Research, Ruđer Bošković Institute, POB 180, 10002 Zagreb, Croatia, zelic@irb.hr*

In voltammetry, results obtained by any differential technique could be presented in the form of a net signal or its components (or both). The latter approach is routinely applied in square wave voltammetry, not only for experimentally obtained current-potential curves, but also for presentation of simulated peaks [1]. It gives a quick insight into the origin of the net signal and makes possible recognition of reversible and irreversible electrode processes. In differential pulse polarography (DPP), however, similar approach is not used, although such a possibility exists in GPES program for obtaining and treatment of experimental data [2]. DPP net signal, recorded in a model system, together with its "forward" and "backward" currents is given in Fig. 1. Somewhat extreme conditions were applied in order to make the former component more pronounced.

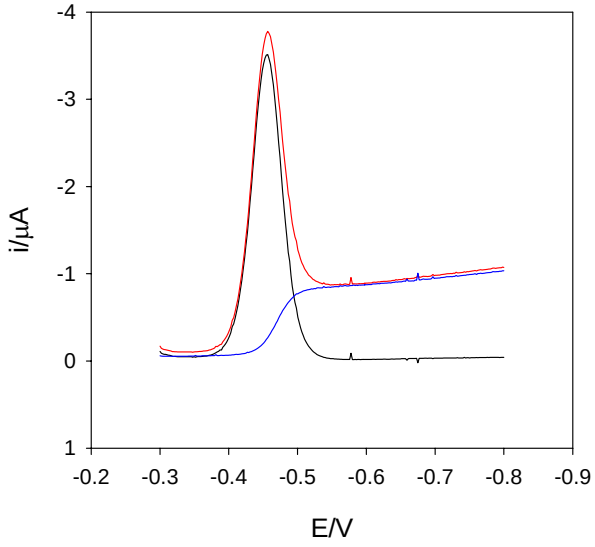


*Fig. 1. Differential pulse net polarogram (1) together with its forward (2) and backward (3) currents obtained from 0.1 mmol/L $Cd^{2+}$ in 4 mol/L $NaClO_4$ at pH 2. Interval time: 0.5 s; pulse duration: 5 ms; pulse height: 25 mV.*

Its dependence on potential is a wave with highly expressed maximum whereas for the "backward" currents it is a simple S-shaped curve. From inspection of the well known excitation signal in DPP, it follows that "backward" component is nothing else but a DC wave. With the "forward" component the situation is not so simple because it does not correspond to any individual voltammetric technique and therefore its interpretation

should be defined. The whole approach is also applicable to differential pulse voltammetry (DPV), i.e. results obtained on a single mercury drop, but in such a case current components, are peaks instead of waves (Fig. 2).
In order to test the possible applications of current components in DPP (or DPV) as diagnostic tools, several well defined systems, previously studied in our laboratory, were treated in such a way, i.e. new polarograms/voltammograms were recorded (for reversible and irreversible reductions, with and without adsorption) under different conditions and special attention was paid to their "forward" and "backward" currents.

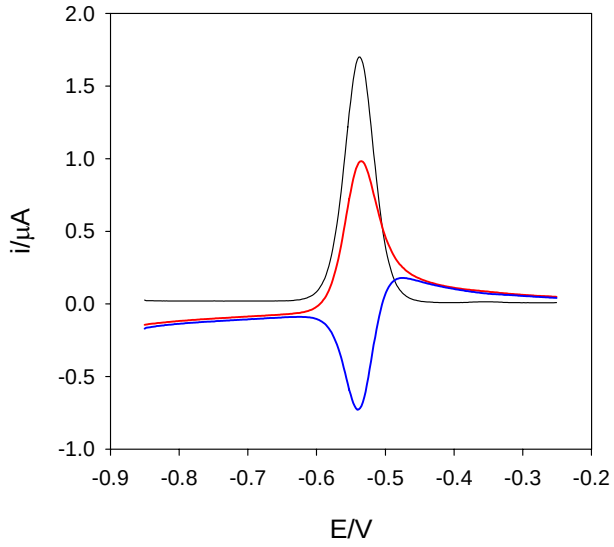


*Fig. 2. DPV stripping voltammogram (1) together with its forward (2) and backward (3) currents obtained from 2 µmol/L $Cd^{2+}$ in 2 mol/L $NaClO_4$ at pH 2. Interval time: 0.1 s; pulse duration: 50 ms; deposition time: 60 s.*

It follows that DPP (or DPV), mainly known for its high sensitivity, could be a powerful diagnostic tool when its components are taken into consideration. As the response(s) of other voltammetric technique(s) are "hidden" within it, application of DPP/DPV can save the time during analysis of an unknown system. The whole approach is applicable even at trace concentrations, i.e. to the experimental results obtained by cathodic or anodic stripping voltammetry. Finally, presentation of experimental results in the form of a net signal together with its components could be useful in teaching and understanding of different electrode processes

**References:**

1. V. Mirčeski, Š. Komorsky-Lovrić, M. Lovrić, *Square Wave Voltammetry*, Springer, Berlin 2007.
2. Modular Electrochemical Instruments, *Eco Chemie B.V.*, Utrecht 2001.

First Regional Symposium on Electrochemistry of South-East Europe, Rovinj, Croatia, May 4-8, 2008.

P-2-075

# SQUARE WAVE VOLTAMMETRY OF SURFACE-ACTIVE, ELECTROINACTIVE COMPOUNDS

**D. Jadreško, M. Zelić, M. Lovrić**

*Department for Marine and Environmental Research,*
*"Ruđer Bošković" Institite, P.O. Box 180, 10002 Zagreb. Croatia*

Square wave voltammetry (SWV) is generally considered as being insensitive to capacitive currents, which is true if it is compared to alternating current voltammetry, but less so if the comparison is made to pulse and differential pulse voltammetry. In fact, the sensitivity of SWV to capacitive current depends on the frequency of signal. It is well known that in the base current a broad peak appears at about -0.6 V vs SCE, which is caused by the reorientation of water molecules on the working electrode surface. Also, adsorption and desorption peaks of berberine and canadine, condensed on the mercury electrode surface, were observed and these tensametric peaks were comparable in magnitude to the faradaic peak of berberine reduction. In this communication a basic theory of square wave voltammetry of surface-active, electroinactive compounds is developed. It is shown that in tensametry SWV appears as useful alternative to phase selective *ac* polarography.

First Regional Symposium on Electrochemistry of South-East Europe, Rovinj, Croatia, May 4-8, 2008.

P-2-076

# DETERMINATION OF CATIONIC SURFACTANTS IN PHARMACEUTICAL DISINFECTANTS USING A NEW, HIGHLY SENSITIVE POTENTIOMETRIC SENSOR

**D. Madunić-Čačić[1], M. Sak-Bosnar[2], O. Galović[2], N. Sakač[2], R. Matešić-Puač[2], Z. Grabarić[3]**

[1]*Saponia, Chemical, Pharmaceutical and Foodstuff Industry, M.Gupca 2, Osijek, Croatia*
[2]*Department of Chemistry, Josip Juraj Strossmayer University of Osijek, F. Kuhača 20, Osijek, Croatia, E- mail: msbosnar@kemija.unios.hr*
[3]*Faculty of Food Technology and Biotechnology, University of Zagreb, Pierottijeva 6, Zagreb, Croatia*

Cationic surfactants are widely used in industrial and commercial formulations, including disinfectants, textile softeners, cosmetics and pharmaceuticals. The development of sensor procedures for determination of cationic surfactants is of great practical interest [1], where potentiometric titrations using surfactant-selective electrodes have found wide application [2-4].

A new sensitive potentiometric surfactant sensor was prepared based on a highly lipophilic 1,3-didecyl-2-methyl-imidazolium (DMI) cation and a tetraphenylborate (TPB) antagonist ion. This compound was used as a sensing material and incorporated into the plasticized PVC-membrane. The sensor responded fast and showed a Nernstian response for all the investigated cationic surfactants: 59.8 mV/decade for cetylpyridinium chloride (CPC), 58.6 mV/decade for hexadecyltrimethylammonium bromide (CTAB), and 56.8 mV/decade for Hyamine.

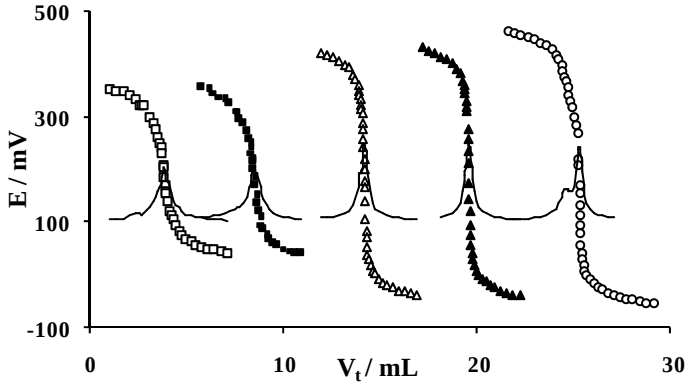


*Titration curves and their corresponding first derivatives of several technical grade cationic surfactants using DMI-TPB surfactant sensor and sodium TPB as titrant*
□ = *triethanolamine di-esterquat methosulfate (TDM),*
■ = *dihydrogenated tallowethyl hydroxyethylammonium methosulfate (DTHM),*
Δ = *alkyldimethylbenzylammonium chloride (ADBAC),*
▲ = *alkyldimethylbenzylammonium bromide (ADBAB),*
○ = *didecyldimethylammonium chloride (DDAC).*

The cationic surfactant ($CS^+$ = analyte determined) reacts during titration with the anionic surfactant ($AS^-$ = titrant), accompanied by formation of a water insoluble (1:1) ion-pair $CS^+AS^-$ (ion-exchange or ion-pair complex), which dissociates as follows:

$$CS^+ AS^- \leftrightarrow CS^+ + AS^-$$

The sensor served as an end-point detector in ion-pair surfactant potentiometric titrations using sodium tetraphenylborate as titrant, and displayed satisfactory analytical performances within a pH range of two to eleven. The influence of the ethoxylated alcohols (EONS), a widely used class of nonionic surfactants on the shape of titration curves was negligible if the mass ratio of EONS:CS was not greater than five. The selectivity coefficients were determined by fitting the Nikolskii-Eisenman equation to the experimental data obtained by the mixed solution method. The sensor exhibited excellent selectivity performances for CPC over all organic and inorganic cations investigated.
Several commercial disinfectant products containing various cationic surfactants were potentiometrically titrated using the new DMI-TPB sensor as an indicator.

*Results of potentiometric titrations of six disinfectant products using sodium TPB ($c = 5 \times 10^{-3}$ mol/L) as titrant and DMI-TPB surfactant sensor as an indicator, in comparison with the results obtained with commercial sensor.*

| PRODUCT | CATIONIC SURFACTANT CONTENT* | | | |
|---|---|---|---|---|
| | DMI-TPB sensor | | Commercial sensor | |
| | found (%) | RSD (%) | found (%) | RSD (%) |
| Mouthwash A | 0.0554 | 0.99 | 0.0536 | 1.02 |
| Mouthwash B | 0.0584 | 0.94 | 0.0564 | 0.97 |
| Disinfectant for food industry | 4.3360 | 0.96 | 4.3690 | 0.89 |
| Disinfectant for hospital use A | 5.0230 | 0.34 | 5.0040 | 0.12 |
| | found (mol/L) | RSD (%) | found (mol/L) | RSD (%) |
| Disinfectant for hospital use B | 0.1510 | 0.23 | 0.1505 | 0.19 |
| Disinfectant for hospital use C | 0.00373 | 0.79 | 0.00351 | 0.73 |

* average of 5 determinations

The results, compared to those obtained using a commercial surfactant electrode exhibited satisfactory mutual agreement. The resulting potentiometric titration curves from all the investigations revealed analytically usable inflexions, enabling reliable equivalence point detection using the first derivative method.

**References:**

[1] T. Masadome, T. Takahashi, *Anal. Lett.*, **40** (2007) 441-448.
[2] K. Vytras, J. Kalous, J. Symersky, *Anal. Chim. Acta* **177** (1985) 219-223.
[3] R. Matesic-Puac, M. Sak-Bosnar, M. Bilic, B.S. Grabaric, *Electroanalysis* **16** (2004) 843-851.
[4] T. Kimbeni Malongo, B. Blankert, O. Kambu, K. Amighi, J. Nsangu, J.-M. Kauffmann, *J. Pharm. Biomed. Anal.*, **41** (2006) 70-76.

First Regional Symposium on Electrochemistry of South-East Europe, Rovinj, Croatia, May 4-8, 2008.

P-2-077

# DETERMINATION OF THE CATIONIC SURFACTANTS IN HAIR CONDITIONERS AND LAUNDRY SOFTENERS

**M. Šarić, A. Stanisavljev, M. Tadić**

*Institute of Public Health, Belgrade, Bulevar Despota Stefana 54a, Serbia*
marija.saric@zdravlje.org.yu

Cationic surfactants are used in hair conditioners and laundry softeners as anti-static agents. They make fabrics and hair less prone to static electricity buildup by making them soft and slightly conductive. In our laboratory, we control the content of cationic surfactants in products before they are released for free sale.

The purpose of this work is to illustrate the difference between the results obtained by two different methods:

1. Extraction with 96% ethanol, where cationic surfactants are being extracted and inorganic compounds stay unsolved. Approximately 10g of sample is weighted with accuracy ±0,01g, dissolved in ethanol, and boiled for 1 hour with reflux condensator. Thereafter, the ethanol extract is filtrated and evaporated and dried out to constant weight.
   The content of the cationic surfactants, expressed as a percentage by mass, is calculated using the equation:

   %cat.surf. = p × 100 / m
   p = weight of the dried residue (g);
   m = sample weight (g)

2. Potentiometric titration with anionic surfactant sodium dodecylsulfate by potentiometric titrator Metrohm 794 Basic Titrino, equipped with Metrohm 802 stirrer. Processing software Metrodata Vezuv 3.0 PC has been used.
   Cationic surfactant present in the sample, expressed as a percentage by mass, is calculated related to the specific cationic surfactant that has been specified on the product declaration or specification.
   Metrodata Vezuv software calculates the percent of cationic surfactant by the following equation:

   %cat.surf. = EP1 × 0.005 × 100 × C36 × Mw / (m × 1000)
   EP1 - volume of the titrant in endpoint (ml)
   0.005 - theoretical concentration of titrant (mol/l)
   100 - for 100g of sample
   C36 - titer of titrant
   Mw - cationic surfactant molecular weight (g/mol)
   m - sample weight (g)
   1000 - correction factor for mmol

Since October 1, 2007, when potentiometric method was established, until nowadays, about 50 different samples of hair conditioners and laundry softeners were analyzed in our lab. The content of cationic surfactant was between 0.5% and 3% in hair conditioners, and between 5% and 20% in laundry softeners, depending on the sample. Reproducibility and precision were determined from 10 measurements of the same sample, with RSD(%)=1.34 (with the upper limit of satisfaction 2.8%), while the systematic error of the method was 0.0076 (with the upper limit of satisfaction 0.01). Reproducibility and precision for ethanol extraction method were determined from 10 measurements of the same sample, with RSD(%)=5.31. During the implementation of potentiometric method, we have analyzed samples by both methods for a while. Comparing the results obtained with these methods, we have concluded that results for the content of cationic surfactants obtained by ethanol extraction method were 10 times higher in hair masks, 2-3 times higher in hair balsams, and 16-23% higher in laundry softeners, than the content of cationic surfactants obtained by potentiometric method. These results showed that the ethanol extraction method is non-selective and that more other organic compounds such as emollients, emulsifiers, thickening agents, polymers, and eventually present nonionic surfactants can be extracted by ethanol. By potentiometric titration only the specific cationic surfactant that is present in the sample is determined. In addition, procedure for potentiometric titration is simpler, more accurate and more reliable.

First Regional Symposium on Electrochemistry of South-East Europe, Rovinj, Croatia, May 4-8, 2008.

P-2-078

# NEW CONTRIBUTION FOR CHARACTERISATION OF THE CARBON PASTE ELECTRODES

**T. Mikysek[1], I. Švancara[1], K. Vytřas[1], J. Ludvík[2], K. Kalcher[3]**

[1]*Department of Analytical Chemistry, Faculty of Chemical Technology, University of Pardubice, nám.Čs.legií 565, CZ-53210 Pardubice, Czech Republic; Tomas.Mikysek@upce.cz*
[2]*J. Heyrovsky Institute of Physical Chemistry, Academy of Sciences of the Czech Republic, CZ-18223 Prague, Czech Republic;*
[3]*Institute of Analytical Chemistry, Karl-Franzens University Graz, A-8020 Graz, Austria*

This contribution includes an overview of achievements and prospects of some characterisation of the carbon paste electrodes (CPE). Several general guidelines are pointed out and illustrated by experimental results. Carbon pastes (i.e. intimate mixtures of carbon powder and a hydrophobic liquid binder) are widely used in electroanalytical chemistry and bioelectrochemistry for preparing electrochemical sensors with a more or less degree of alteration by suitable additives (such as catalysts, biocatalysts, metal-ion binding reagents [1,2,3]). Their heterogeneous character, the specific influence of the liquid binder and the variability of the used electrode material shows a necessity to characterise it. Since the first CPE was developed about fifty years ago many papers dealing with some kind of characterisation were published [4]. There is still space to continue and add some more specific information thereby clarify the way of conductivity of the carbon paste from physico-chemical point of view or specify some advanced parameters from kinetic reactions taking place at electrode surface. The first case is based on resistivity measurements of CPE containing different ratios of carbon powder, binder and also deals with theory of close packing of spherical particles. Experiments agree well with theory and show that conductivity of the carbon paste is assured by direct touch of carbon particles (until now the mechanism was not clear yet). The electrochemical study of CPEs was performed with cyclic voltammetry (with linear change of potential) with a $Fe^{2+}/Fe^{3+}$ reversible redox system. The measurements pointed out different behaviour at carbon paste, where this system tends to be quasi-reversible and becomes even more irreversible with increasing amount of binder. For such a description of reversibility measure proposed parameter "$\chi$" could be used [4]. Another parameter to characterise CPE could be the effective area calculated from the Randles-Sevcik equation. All performed experiments could be helpful for some interpretation of the behaviour of carbon paste electrodes as well as with their preparation.

***Acknowledgements:*** *Financial grants from the Ministry of Education, Youth, and Sports of the Czech Republic (projects MSM0021627502 and LC 06035) are gratefully acknowledged as well as financial support from CEEPUS exchange programm: CII-CZ-012-01-0708.*

## References

1. Švancara, K. Vytřas, J. Barek, J. Zima, *Crit. Rev. Anal. Chem.*, **31** (2001) 311.
2. K. Kalcher, J.M. Kaufmann, J.Wang, I. Švancara, K. Vytřas, C. Neuhold, Z. Yang: *Electroanalysis*, **7** (1995) 5.
3. L.Gorton, *Electroanalysis*, **7** (1995) 23.
4. K. Kalcher, I. Švancara, R. Metelka, K. Vytřas, A. Walcarius, in: *The Encyclopedia of Sensors*, Vol. 4 (C.A. Grimes, E.C. Dickey, M.V. Pishko, eds.), pp. 283-430. American Scientific Publishers, Stevenson Ranch, 2006.

First Regional Symposium on Electrochemistry of South-East Europe, Rovinj, Croatia, May 4-8, 2008.

P-2-079

# VOLTAMMETRIC DETERMINATION OF COLLAGEN AT A MODIFIED CARBON PASTE ELECTRODE

**S. Cavalu, F. Bănică, T. Jurca, E. Marian, D. Bănică**

*University of Oradea, Faculty of Medicine and Pharmacy, N. Jiga Street, No 29, Pharmacy Departament, Oradea, Romania, E-mail: fbanica@uoradea.ro*

Functional composite films made from collagen are reported in this paper. The collagen has been deposited on the surface of to sundries aluminosilicate microspheres containing rare earth ions (yttrium or dysprosium) and iron by maintaining them in collagen solution at 37 degrees C, for 48 hours.
The collagen solution has been dosed from the residual solution using electrochemical techniques using a potentiostat TraceLab 50.
Collagen in functional composite films have much highear rates of electron transfer than collagen in solutions on carbon paste electrodes. Cyclic voltammograms all give a pair of well-defined and qausi-reversible peaks, corresponding to redox couple of collagen. Differential pulse voltammograms also show the same formal potential ($E^{0'}$) values of collagen under identical conditions. The $E^{0'}$ value for collagen is found to be pH dependent.

First Regional Symposium on Electrochemistry of South-East Europe, Rovinj, Croatia, May 4-8, 2008.

P-2-080

# SELECTIVE DETERMINATION OF ACETAMINOPHEN IN SIMPLE AND MIXTURE AQUEOUS SOLUTIONS USING A BORON-DOPED DIAMOND ELECTRODE

**C. Cofan[1], C. Radovan[2], D. Cinghita[2]**

*[1]University of Medicine and Pharmacy" Victor Babes", Piata E. Murgu Nr. 2, 300041, Timisoara (Romania)*
*[2]West University of Timisoara, Str. Pestalozzi Nr. 16, 300115, Timisoara (Romania)*
*E-mail: cofancodruta@umft.ro*

Acetaminophen, paracetamol (AC) or N – acetyl – *p* – aminophenol is a widely used antipyretic and analgesic drug. Unlike aspirin, it is known to cause liver and kidney damage. However, the association with ascorbic acid in pharmaceutical formulations sustains its use by the antioxidant protective effect of the latter.

A large number of analytical methods for the determination of acetaminophen in pharmaceutical formulations and presence of several complementary components have been reported, but electrochemical alternatives still remain an open problem in basis and in application. The goal of our work consists in the selective determination of acetaminophen in simple and mixture aqueous solutions containing ascorbic acid with the concomitant test of various supporting aqueous media and using a boron-doped diamond electrode. Unmodified boron-doped diamond electrode (BDDE) is a relatively new and very useful material for anodic determination of a large series of analytes. Due to the high oxygen overpotential, it plays practically a similar role for anodic process as mercury electrode does for cathodic ones, exhibiting a very large electrochemical window, high chemical and mechanical stability of its surface in aggressive conditions and low background current.

We report the selective detection and determination of AC in presence of AA at a BDDE by cyclic voltammetry (CV) and differential pulse voltammetry (DPV), using 0.1M sodium sulfate pH 7, 0.1M phosphate buffer pH 7, and Britton-Robinson pH 1.96 as supporting electrolytes. The first aspect of this investigation was devoted to clarify the fundamental aspect of the distinct potential disposal for AC and AA current peaks, in accord with an original hypothesis regarding the role of adjacent pH change at electrode surface, anodic free or restricted acidification, sustained by our CV and DPV data and previous reference data from literature.

The final aim of the work consisted in defining the optimum electroanalytical conditions, obtaining the calibration plots for AC, and the selective determination of AC contents with adequate amperometric correction in presence of AA into a pharmaceutical product by DPV and standard additions.

## References

1. M. C. Granger, J. Xu, J. W. Strojek, G. M. Swain, *Anal. Chim. Acta* **397** (1999) 145-161.
2. C. Radovan, F. Manea, *Electroanalysis* **19** (2007) 91-95.
3. J. J. Van Benschoten, J. Y. Lewis, W. R. Heineman, D. A. Roston, P. T. Kissinger, *J. Chem. Ed.* **60** (1983) 772-776.
4. Navarro I, Gonzalez-Arjona D, Roldan E, Rueda M, *J. Pharm. Biomed. Anal.* **6** (1988) 969-976.

First Regional Symposium on Electrochemistry of South-East Europe, Rovinj, Croatia, May 4-8, 2008.

P-2-081

# ANODIC ASSESSMENT OF THIOACETAMIDE IN AQUEOUS SOLUTIONS

**D. Cinghita[1], C. Radovan[1], F. Manea[2], I. Vlaicu[3], C. Cofan[4], D. Dascalu[1], A. Ciorba[1]**

*[1]West University of Timisoara, Str. Pestalozzi Nr. 16, 300115, Timisoara (Romania)*
*[2] "Politehnica" University of Timisoara, Piata Victoriei Nr. 2 , 30006 Timisoara, Romania*
*[3]R. A. AQUATIM, Str. Gh. Lazar, Nr.11A, 300081, Timişoara (Romania)*
*[4]University of Medicine and Pharmacy" Victor Babes", Piata E. Murgu, Nr. 2, 300041, Timisoara (Romania) E-mail: dancinghita@yaoo.com*

Thioacetamide, a largely used sulfur-containing compound as substitute of hydrogen sulfide in the laboratory practice and as thioamidic substance in various technical applications, which has well-known carcinogenic properties, can be present in air and waters. Thus, the detection of thioacetamide in real time has become more and more important.

Beside the classical precipitation or potentiometric methods, the electrochemical potentiodynamic variants, for example the use of mercury electrode and cathodic stripping voltammetry, cathodic stripping voltammetry at silver electrode or pulsed amperometric detection at platinum or gold electrodes, are old alternatives which involve several complications specific for metallic electrode in presence of thioamidic compounds. The carbon based electrode materials and especially doped diamond electrode offer frequently the adequate conditions for their use as unmodified or modified anodic sensors.

The boron-doped diamond (BDD) is considered an important material for electroanalysis, since it has several electrochemical valuable properties such as a wide potential window in aqueous solution, a low background current and a high stability. These characteristics make it significantly superior to other commonly used electrode materials.

The electrochemical behaviour of thioacetamide (TA) has been investigated at a BDDE and glassy carbon electrode (GC) in unbuffered 0.1 M $Na_2SO_4$ supporting electrolyte and buffer solutions.

The voltammetric and chronoamperometric data obtained using glassy carbon (GC) and boron-doped diamond regarding anodic oxidation of TA showed the marked current peaks in a well delimited potential range. The useful anodic amperometric signals for electroanalytical purposes were sustained by the linearity of the calibration plots of current peaks vs. concentration. The high correlation parameters, the sensitivities, RSD and LOD suggested a potential applicability of both electrodes for electroanalytical purpose, but low fouling effects and stability recommend the BDDE as sensor.

The electrochemical assessment of TA using as sensor unmodified GC electrode and especially BDDE can be regarded as an accessible and attractive option in the electrochemical investigation and determination of this toxic sulfur-containing compound from waste or tap waters.

## References

1. M. A. Constantinou, S. E. Theocharis, E. Mikros, *Tox. Appl. Pharm.*, **218** (2007) 11.
2. A. Zaleska, P. Gorska, J. W. Sobczak, J. Hupka, *Appl. Cat. B Environ.*, **76** (2007) 1.
3. T. Z. Polta, D. C. Johnson, *J. Electroanal. Chem.* **209** (1986) 159.
4. Yu. V. Pleskov, *Russ. J. Electrochem.*, **38** (2002) 1275.

First Regional Symposium on Electrochemistry of South-East Europe, Rovinj, Croatia, May 4-8, 2008.

P-2-082

# CHRONOPOTENTIOMETRIC DETERMINATION OF α-TOCOPHEROL IN PHARMACEUTICAL PREPARATIONS

**J. Švarc-Gajić, Z. Suturović, N. Marjanović, S. Kravić, Z. Stojanović**

*Faculty of Technology, Department for Applied and Engineering Chemistry, Bul. Cara Lazara 1, 21 000 Novi Sad, Serbia, jaroslava@tehnol.ns.ac.yu*

Vitamin E is a fat-soluble vitamin that exists in eight different forms. Each form has its own biological activity, which is the measure of potency or functional use in the body [1]. Alpha-tocopherol (α-tocopherol) is the name of the most active form of vitamin E in humans. It is also a powerful biological antioxidant [2-3].
Vitamin E protects the cells from the free radical activity and it is shown to play an important role in immune function, in DNA repair, and other metabolic processes [2-3].
Determination of vitamin E in various foodstuffs and pharmaceutical product is most often performed by high performance liquid chromatography with eather fluorescence or UV detection [4-6]. The analysis can also be performed by gas chromatography after derivatisation [7]. In this work the method for chronopotentiometric analysis [8] was developed for the determination of α-tocopherol in different pharmaceutical formulations. Among the electroanalytical techniques, the application of differential voltammetry [8] or square wave voltammetry [9] for tocopherol determination has previously been reported.
All analyses were performed using the house-made stripping analyser for potentiometric and chronopotentiometric stripping analysis. Glassy carbon electrode (d = 3 mm) was used as a working electrode, while 3.5 mol/l Ag/AgCl electrode was used as the reference and platinum wire (l = 7 mm, d = 0.07 mm) was auxiliary electrode. After each analysis it was necessary to clean the surface first with acetone, and then with triply-distilled water.
All chemicals used were of analytical reagent grade. Triply distilled water was used for all dilutions. A 1 g/l and 10.5 g/l stock solution of α-tocopherol was made by dissolving it in ethanol. The standard solutions were kept in the refrigerator in the dark bottles.
Five commercially available pharmaceutical products (1-5) of vitamin E were available. Three were in the form of tablets and the other two in the form of capsules. Two of them were from a foreign producer (4 and 5). Since the vitamin E in the commercial product is in the form of tocopheryl-acetate, due to the higher stability, the sample preparation step involved the alkaline hydrolysis step. The samples were pulverized and homogenized with 3 mol/l KOH. After the hydrolysis step, the samples were transferred in the volumetric flask with the mixture of ethanol:toluene (1:1). Sulphuric acid was added to the concentration of 0.2 mol/l. In the prepared samples the concentration was calculated applying the calibration curve method. Calibration curve was defined in the matrix of blank.

Experimental parameters were defined in the matrix of prepared sample, while the sensitivity limit was defined in the matrix of blank.

Linearity was examined in the wide concentration range in the prepared solution of the sample 1, applying the oxidation current of 9.1 μA and starting potential of 0.3 V. Due to the polynomial increase of tocopherol transition time (τ) with the concentration, it is recommended to define the calibration curve for a narrow concentration range or to linearise it by representing the dependence of the square root of the transition time of the concentration. Very good linearity can be observed in this case: $\tau^{1/2} = 3.76 + 0.06C_m$, r = 0.9999 (100 – 360 mg/l); $\tau^{1/2} = 6.34 + 0.16C_m$, r = 0.9988 (20 - 65 mg/l).

Influence of the oxidation current was investigated in the range from 3.6 μA to 11.2 μA in the prepared solution of the sample 1. Transition time of tocopherol showed exponentional decay with greater currents applyied.

Repeatability was calculated as a result of seven concequtive analyses performed in the matrix of sample 2, applying the oxidation time of 9.1 μA and starting potential of 0.3 V. Coefficient of variation was 2.4%.

Detection limit was determined in the matrix of the blank applying the oxidation current of 3.6 μA. Limit of detection was 12 mg/l with the reproducibility of 4.03%, expressed as a coefficient of variation of the seven consequtive analysis of different solutions.

The samples were analysed in five probes, applying the oxidation currents of 9.1 μA. Analysis was performed starting at the potential of 0.3 V and ending with the potential of 0.9 V. Determined and corrected (to tocopheryl-acetate) mean values, certified contents, and the results of recovery assay are shown in the table 1.

*Table 1. The content of tocopheryl-acetate.*

| Sample | Certified (mg/tablet (capsule) | Determined (mg/tablet (capsule) | RSD (%) | Recovery (%) |
|---|---|---|---|---|
| 1 | 10 | 9.05 | 1.5 | 91.6 |
| 2 | 100 | 70.54 | 2.4 | 92.6 |
| 3 | 150 | 149.00 | 0.7 | 92.0 |
| 4 | 100 | 29.6 | 3.0 | 89.3 |
| 5 | 645.5 (400 I.U.) | 212 | 2.0 | 92.3 |

In this work the method for the determination of α-tocopherol in pharmaceutical preparations by means of chronopotentiometry was developed. In most of the samples determined contents were lower comparing with the certified contents. Good results of recovery assay confirmed the correctness of the sample preparation procedure as well as the correctness of the defined technique. It can be assumed that the technique can be succesfully applied for the tocopherol determination in other pharmaceutical products as well.

## References

1. Traber MG and Packer L. Vitamin E: Beyond antioxidant function. *Am. J. Clin. Nutr.* **62**, 1995:1501S-1509S.
2. Traber MG. Vitamin E. In: Shils ME, Olson JA, Shike M, Ross AC, ed. *Modern Nutrition in Health and Disease*. 10th ed. Baltimore: Williams & Wilkins, 1999:347-362.
3. Farrell P and Roberts R. Vitamin E. In: Shils M, Olson JA, and Shike M, ed. *Modern Nutrition in Health and Disease*. 8th ed. Philadelphia, PA: Lea and Febiger, 1994:326-341.
4. Quingping L, Scheller K K and Schaefer DM. A technical Note: Simplified Procedure for Vitamin E Determination in Beef Muscle. *J. Anim. Sci*. **74**, 1996: 2406-2410.
5. Ubaldi A, Serventi P and Delbono G. Determination of Vitamine E Levels in Aged Cheeses. *Ann. Fac. Medic. Vet. Di Parma*, **26**, 2006: 137-144.
6. Gimeno E, Castellote AI, Lamuela-Raventos RM, de la Torre MC, Lopez-Sabater MC Rapid determination of vitamin E in vegetable oils by reversed-phase high-performance liquid chromatography. *J. Chromat.* **881**, 2000: 251-254.
7. Hartman KT. A simplified gas liquid chromatographic determination for vitamin E in vegetable oils. *J. Am. Oil Chem. Soc.* **54**, 1977: 421-423.
8. Suturović ZJ and Marjanović NJ. Chronopotentiometric Study of Tocopherols in Vegetable Oils. *Electroanalysis*, **3**, 1999: 207-209.
9. Mikheeva EV and Anisimova LS. Voltammetric determination of vitamin E (α-Tocopherol acetate) in multicomponent vitaminized mixtures. *J. Anal. Chem.* **62**, 2007: 373-376.
10. Clough AE. The determination of tocopherols in vegetable oils by square-wave voltammetry. *J. Am. Oil Chem. Soc.* **69**, 1992: 456-460.

First Regional Symposium on Electrochemistry of South-East Europe, Rovinj, Croatia, May 4-8, 2008.

P-2-083

# ELECTROCHEMICAL BEHAVIOR OF NEW MODIFIED ELECTRODES WITH CLAYS FOR THE DETECTION OF PHARMACEUTICAL COMPOUNDS

**C. Cristea[1], F. Lapadus[1], A. Marian[2], I.O. Marian[2], R. Săndulescu[1]**

*[1]University of Medicine and Pharmacy « Iuliu Hatieganu », Faculty of Pharmacy, Department of Analytical Chemistry, 4 Pasteur 400 349 Cluj-Napoca, Romania,*
*ccristea@umfcluj.ro*
*[2]Babes Bolyai University, Faculty of Chemistry and Chemical Engineering, 11 Arany Janos Street, 400 021, Cluj-Napoca, Romania*

The development of new electrodes applied in the pharmaceutical analysis or in the detection of pollutants became one of our main interests.
Our geographical area is reach in different types of clays. Chemical composition studies as well as difractometry, IR and X ray studies established the properties of several clays originated from the north part of our country. The electrochemical behavior of the electrodes modified with thin films of clays was tested in the presence of some pharmaceutical compounds as ascorbic acid, acid acetylsalicylic and acetaminophen.
Acetaminophen is widely used as analgesic antipyretic drug having actions similar to aspirin. It is a suitable alternative for the patients who are sensitive to aspirin and safe up to therapeutic doses [1]. The large scale therapeutic use of that drug generated the need for the development of rapid and reliable methods for the determination of acetaminophen. Current methods for the analysis of acetaminophen include spectrophotometric, chromatographic and electrochemical approaches. The use of nanoporous magnetic nanoparticles for the construction of amperometric HRP immobilized biosensor was done with a good linearity range [2].
The development of composite electrodes for biosensors construction based on HRP and clays (bentonite) film for acetaminophen detection is described. The enzyme immobilization is performed by retention in a polyetilenimine and clay porous gel film, technique that offers a good entrapping and in the mean times a "protective" environment for the biocomponent.

***Acknowledgements:*** *Financial supports of the Romanian Minister of Education and Research (grant MATNANTECH CEEX 6/2005) and of CNCSIS (AT 180/2006) are appreciated.*

**References:**

1. V. Sima, C. Cristea, F. Lapadus, I.O.Marian, Ana Marian, R.Săndulescu, *Journal of Pharmaceutical and Biomed. Analysis*, submitted
2. D. Yu, O. Dominguez Renedo, B. Blankert, V. Sima, R. Sandulescu, J. Arcos, J.-M. Kauffmman, *Electroanalysis* **18**(17) (2006) 1637-1642

First Regional Symposium on Electrochemistry of South-East Europe, Rovinj, Croatia, May 4-8, 2008.

P-2-084

# ELECTROCHEMICAL AND SPECTRAL STUDY OF THE REDOX BEHAVIOR AND CARDIOTOXICITY OF ANTICANCER DRUGS WITH ANTHRAQUINONE STRUCTURE: QUINIZARIN

**A. Latus, E. Volanschi**

*Department of Physical Chemistry, University of BucharestBlvd Elisabeta 4-12, Bucharest, RO-030018 ROMANIA, E-mail: volae@gw-chimie.math.unibuc.ro*

1,4-dihydroxyanthraquinone (quinizarin, $AH_2$) is the simplest molecule, which represents the structure of the specific chromophore for some biological and pharmaceutical compounds; it is the main part in the chemical structure of daunorubicine, doxorubicine, and mitoxantrone [1].

The generally accepted mechanism for the cardiotoxicity of the anthracyclines implies the mono or bielectronic reduction of the drug, with the appearance of reactive reduction intermediates, radical species which may mediate electron transfer to molecular oxygen, with formation of superoxide anion radicals, responsible for cellular damage and cardiotoxicity [2].

The present paper investigates the behavior in reduction and oxidation processes of quinizarin in aprotic neutral and basic media by coupled electrochemical and spectral techniques (in-situ techniques), including absorption spectroscopy, in order to identify the intermediate species and to propose a reaction mechanism. The influence of electrogenerated bases (EGB) was investigated by comparison with the spectroelectrochemistry in presence of added tetrabutylammonium hydroxide (TBOH). The proposed reaction sequences are supported by Digisim 3.03 simulations.

Semiempirical MO-calculations were performed to determine the electronic structural features implied in reduction and oxidation processes and to analyze the energetics of the electron transfer (ET) from different reduction intermediates to molecular oxygen.

The results show that the reduction potential of quinizarin is more positive than that of mitoxantrone (-0.4V *vs.* -0.7V) what means that quinizarin can be involved in reductive activation by reductases, being implicated in the formation of free radicals, and therefore a higher cardiotoxicity is to be expected.

Analysis of the energetics of the ET reactions to molecular oxygen based on gas-phase PM3 semiempirical calculations, indicates that the reductive activation of molecular oxygen to the superoxide anion is not energetically favorable from the anion radical of quinizarin and mitoxantrone, but is favorable from the dianion of both compounds. For diquinone (resulting compounds after bielectronic oxidation of quinizarin or mitoxantrone), the electron transfer from the dianion of diquinone derived from quinizarin is more favorable than that of mitoxantrone, suggesting that the reduced intermadiates of diquinone could play an important role in the redox cycling of these compounds [3].

## References:

1. D. Jancura, S. Sanchez-Cortes, E. Kocisova, A. Tinti, P. Miskovsky, A. Bertoluzza, *Biospectroscopy* **1**, 1995, 265
2. J. Mayer, R. Krasiukianis, *Radiat. Phys. Chem*. **37**, 1991, 273—278
3. M. Enache, C. Bendic, E. Volanschi, *Bioelectrochemistry*, 2007, in press

First Regional Symposium on Electrochemistry of South-East Europe, Rovinj, Croatia, May 4-8, 2008.

P-2-085

# INTERACTION OF ANTICANCER DRUG MITOXANTRONE WITH ANIONIC SURFACTANT SODIUM DODECYL SULFATE (SDS) ANALYZED BY ELECTROCHEMICAL AND SPECTRAL METHODS

**M. Enache[1], I. Serbanescu[2], D. Bulcu[2], E. Volanschi[2]**

*[1]"I. Murgulescu" Institute of Physical Chemistry, Romanian Academy, Splaiul Independentei 202, Bucharest 060021, Romania*
*[2]Department of Physical Chemistry, University of Bucharest, Blvd. Elisabeta 4-12, Bucharest 030018, Romania E-mail: menache@icf.ro*

Mitoxantrone (1,4-dihydroxy-5,8-bis (2-((2-hydroxyethyl) amino)- ethylamino)-9,10-anthracenedione is a synthetic anticancer drug which shows significant clinical activity, combined with a lower cardiotoxicity (1). It has a planar anthraquinone ring intercalating between DNA base pairs, the positively charged nitrogen-containing side chains interacting with the negatively charged phosphate backbone of DNA (2).

The molecular mechanism of action of mitoxantrone is complex, involving free radical generation with consequent induction of DNA damage or lipid peroxidation (3), initiation of DNA damage via inhibition of topoisomerase II (4). The molecular basis of the cardiotoxicity was previously investigated, using coupled electrochemical, spectral and semiempirical MO calculations (5).

Taking into account the importance of micellar systems (surfactant aggregates) in the pharmaceutical field as possible drug delivery systems, the aim of the present paper is to investigate the interaction of mitoxantrone with an anionic surfactant, sodium lauryl sulfate, by electrochemical (cyclic and linear voltammetry with stationary and rotating disc electrode, RDE) and spectral (UV-VIS absorption) methods, in order to evidence the drug species involved and to elucidate the nature of the interactions in premicellar and micellar range of concentrations.

Cyclic voltammetry and spectral results indicate two processes: process I in premicellar range, assigned to the electrostatic interaction between the drug's positive charge and the surfactant's negative charge; and process II in micellar range when the surfactant micelles are formed and the drug is encapsulated in the micelles in monomer form. Using non-linear fitting of the experimental data, values of the binding constant, K and the stoechiometry of the interaction were determined.

References:

1. F.E. Durr, S*emin. Oncol.*, **11**, 3-19, 1987
2. L.S. Rosenberg, M.J. Carblin, T.R. Krugh, *Biochemistry*, **25**, 1002-1008, 1986
3. G.R. Fisher, L.H. Patterson, *Cancer Chemother. Pharmacol.*, **30**, 451-458, 1992
4. G. Boos, H. Stopper, *Toxicol. Lett.*, **116**, 7-16, 2000
5. M. Enache, C. Bendic, E. Volanschi, *Bioelectrochemistry*, 2007, in press

First Regional Symposium on Electrochemistry of South-East Europe, Rovinj, Croatia, May 4-8, 2008.

P-2-086

# A STUDY OF THE ELECTROCHEMICAL ACTIVITY OF SOME MACROLIDE ANTIBIOTICS ON A GOLD ELECTRODE IN A NEUTRAL ELECTROLYTE

**M.L. Avramov Ivić[1], S.D. Petrović[2,3], D.Ž. Mijin[2]**

[1]*ICTM - Institute of Electrochemistry, University of Belgrade, Njegoševa 12, Belgrade, Serbia*
[2]*Faculty of Technology and Metallurgy, University of Belgrade, Karnegijeva 4, Belgrade, Serbia*
[3]*Hemofarm Group, Pharmaceutical and Chemical Industry, Vršac, Serbia*
*E-mail: milka@tmf.bg.ac.yu*

Macrolide antibiotics are active on both gram-positive and, to a lesser extent on gram-negative microorganisms. They exert their antimicrobial action by binding to the bacterial 50S ribosomal subunit and inhibiting ribosomal assembly and protein synthesis. Erythromycin is a natural compound metabolized by a strain of *Streptomyces erythreus*. As a broad-spectrum antibiotic it has proved invaluable for the treatment of bacterial infections in patients with β-lactam hypersensitivity. From this parent macrolide, several derivatives have been synthesized. Beckmann rearrangement of the 9-oxime followed by reduction and methylation gives azithromycin which shows good activity against gram-negative bacteria, including *Haemophilus influenzae*. If the 6-hydroxy group is methylated, clarithromycin is obtained, which has an improved pharmacokinetic profile compared to the parent molecule.

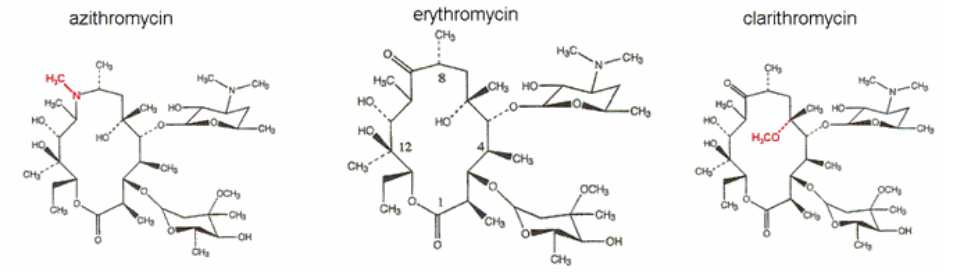


*Figure 1. Macrolide antibiotics*

Azithromycin has a methylated nitrogen atom at position number nine on the macrolide lactone ring, and clarithromycin has a methyloxyl substitution at position number six of the macrolide ring.

Azithromycin and clarithromycin present several clinical advantages over erythromycin, including better oral bioavailability, enhanced spectrum activity, higher tissue concentrations, and improved tolerability. Clarithromycin is widely used for the eradication of *Helicobacter pylori* which causes gastritis and gastric ulcers. Oral clarithromycin is used in combination with amoxicilin and lansoprazole or omeprazole (triple therapy) for the treatment of *Helicobacter pylori* infections and duodenal ulcers. Quantitative methods using high

performance liquid chromatography (HPLC) procedures for the analysis of azithromycin and clarithromycin have been widely applied. Electrochemical methods for macrolide antibiotics determination are promising being the cheaper and faster{1,2}.

The aim of the present study is to present electrochemical behavior and qualitative and quantitative determination of azithromycin at a gold electrode and to present good catalytical surface of gold electrode for the activation of clarithromicin and erithromycin with the study of its structural changes using FTIR analysis of the bulk electrolyte. It is shown that differencies in molecule structure of macrolide antibiotics strongly affect their electrochemical behavior.

**References:**

B. Nigović, B. Šimunić, *J. Pharm. Biomed. Anal.* **32** (2003) 197.

1. M.L. Avramov Ivić, S.D. Petrović, V.Vonmoos, D.Ž. Mijin, P.M. Živković, K.M. Drljević, *Electrochem. Commun.* **9** (2007) 1643.

First Regional Symposium on Electrochemistry of South-East Europe, Rovinj, Croatia, May 4-8, 2008.

P-2-087

# ELECTROCHEMICAL AND SPETROPHOTOMETRIC INVESTIGATION OF ANTIOXIDANTS IN DARK FRUIT JUICES

**L. Valek[1], J. Piljac Žegarac[2], S. Martinez[1], A. Belščak[2]**

*[1]Department of electrochemistry, Faculty of Chemical Engineering and Technology, Savska c.16/I, P.O. Box 177, 10 000 Zagreb, Croatia, lvalek@fkit.hr*
*[2]Department of molecular biology, Institute 'Ruđer Bošković', Bijenička c. 54, P.O. Box 180, 10000 Zagreb, Croatia*

It has been proven that a diet rich in fruits and vegetables containing various classes of polyphenols decreases the risk of premature mortality from major clinical conditions, including cancer and heart disease. Dark fruit products such as juice have been shown to contain up to 10-fold higher concentration of polyphenols than light-colored juices. The purpose of this study was to characterize the antioxidants present in six dark fruit juices commercially available on the Croatian market (black currant, blueberry, cranberry, pomegranate, strawberry and cherry) and to examine the redox behavior of standards (trolox and gallic acid) and polyphenols in juices. The electrochemical behaviour of juices diluted in acetate buffer (pH 3) was investigated using cyclic voltammetry on glassy carbon electrode.

Electrochemical parameters describing the oxidation and reverse reduction process of phenolics were extracted from cyclic voltammograms of juices diluted 50x recorded up to 950 mV. The first anodic peak appearing at approximately 130 mV was attributed to oxidation of ene-diol of ascorbic acid. The major anodic peak present around 440 mV was attributed to powerful low formal potential phenolics (phenolic acids, flavanols, catechin monomers, proanthocyanidins, flavones, flavanones) characterized by an *ortho*-dihydroxy-phenol group. Oxidation process resulted in formation of a stabile quinone which can be reduced in the reverse scan, appearing as a cathodic peak around 350 mV. The third anodic peak detected at potentials higher than 600 mV was ascribed to oxidation of the monophenol group (p-coumaric acid, ferulic acid, malvidin anthocyanins, and t-resveratrol) or the meta-diphenols on the A-ring of flavanoids. Electrochemical parameters derived from cyclic voltammograms of 100x diluted juices recorded to 600 mV, were used to perform the diagnostic tests of oxidation/reduction reaction of phenolics in juice.

Cyclic voltammetry and potentiometric titration were employed to elucidate antioxidant capacity and ascorbic acid content, respectively, of tested juices. The results were compared with those obtained using spectrophotometric Brand-Williams assay (DPPH) and Folin-Ciocalteu assay (FC). The influence of 29-day refrigerated storage on total phenol content and antioxidant capacity was also evaluated.

First Regional Symposium on Electrochemistry of South-East Europe, Rovinj, Croatia, May 4-8, 2008.

P-2-088

# ELECTROANALYTICAL OXIDATION OF *P*-COUMARIC ACID

**P. Janeiro[1], I. Novak[1,2], M. Šeruga[2] A.M. Oliveira-Brett[1]***

*[1]Departamento de Química, Faculdade de Ciências e Tecnologia, Universidade de Coimbra, 3004-535 Coimbra, Portugal, *E-mail: brett@ci.uc.pt*
*[2]Department of Applied Chemistry and Ecology, Faculty of Food Technology, University of J.J. Strossmayer, Osijek, Croatia.*

Polyphenols are a diverse group of secondary plant metabolites naturally present in plants. The two main subclasses of polyphenols are the flavonoids and the non-flavonoids (i.e. phenolic acids, stilbens and others).
Hydroxycinnamic (HCA) and hydroxybenzoic acids (HBA) belong to the phenolic acids group. The HCAs are among the widely distributed phenylpropanoids in the plant kingdom, with fruits, vegetables, beverages, and cereal being abundant dietary sources. The interest in HCAs is also related to their pharmacological, anti-mutagenic and anti-carcinogenic activity. These biological effects are related to radical scavenging (antioxidant) properties of such compounds. In wines, hydroxycinamic acids can affect the colour, astringency, biterness, oxidation level and clarity of the beverage.
The *p*-coumaric acid can be electrochemically oxidized due to the hydroxyl group attached to the aromatic ring. The mechanism of the electrochemical oxidation of *p*-coumaric acid on a glassy carbon electrode was investigated using cyclic, differential pulse and square wave voltammetry at different pHs. The oxidation of *p*-coumaric acid is irreversible over the whole pH range. After successive scans the *p*-coumaric acid oxidation product deposits on the electrode surface forming a polymeric film that undergoes reversible oxidation at a lower potential than *p*-coumaric acid. This polymeric film increases in thickness with the number of scans, covering the electrode surface and impeding the diffusion of *p*-coumaric acid and its oxidation on the electrode surface. The oxidation of *p*-coumaric acid is pH dependent up until values close to the $pK_a$. For pHs higher than $pK_a$, the *p*-coumaric acid oxidation process is pH independent.
The electroanalytical determination of *p*-coumaric acid in pH 8.7 0.2 M ammonium buffer was performed and a detection limit, LOD = 82.6 nM, and limit of quantification, LOQ = 250 nM, were obtained.

First Regional Symposium on Electrochemistry of South-East Europe, Rovinj, Croatia, May 4-8, 2008.

P-2-089

# A NOVEL CYCLODEXTRIN MODIFIED POLYPYRROLE SENSOR FOR BENZYL VIOLOGEN: INVESTIGATIONS INTO ITS SUPRAMOLECULAR CHEMISTRY

**V. Annibaldi, C.B. Breslin, D.A. Rooney**

*Department of Chemistry, National University of Ireland Maynooth*
valeria.annibaldi@nuim.ie

Cyclodextrins are natural occurring cyclic oligosaccharides, which have a rigid torus shape, with an inner hydrophobic cavity and an outer hydrophilic one [1]. They possess a remarkable ability to form inclusion complexes with host molecules and have found applications in the pharmaceutical, cosmetic, food and separation industry [2,3].

Sulfated β-cyclodextrin, in particular, shows a high solubility in water and an anionic behaviour in aqueous solution so it can be electrochemically incorporated in a polymer matrix during an oxidative process. This method is simple, fast and cheap.

In this work sulfated β-cyclodextrin has been permanently incorporated within a polypyrrole matrix during electropolymerization and the system has been widely characterized.

The sensor obtained has been used to detect benzyl viologen, which is a versatile redox system with a different electroactivity from polypyrrole, avoiding interference of the respective electrical signals[4]. Moreover, its structure is similar to a variety of pollutants so it represents a good molecular model to point out a new strategy in pollution remediation.

The interaction between the benzyl viologen and the modified polypyrrole involves a very high adsorption component. By simple cyclic voltammetry the detection limit is 0.4 mM. Detection properties have been compared with a corresponding polymer doped with a large non-macrocyclic anion such as sodium dodecylsulfate, which is permanently included within the polypyrrole matrix but it cannot form inclusion complexes. Results show higher sensitivity for the sensor composed of polypyrrole doped with sulfated β-cyclodextrin.

Further investigations are required in order to verify the entrapment of the benzyl viologen inside the sulfated β-cyclodextrin cavity. In this case the sensor would be able not only to detect viologen but also to remove it from solutions.

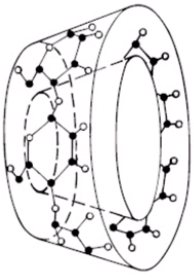

*Fig.1 β-cyclodextrin*

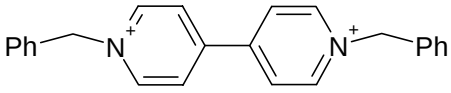


*Fig.2 benzyl viologen*

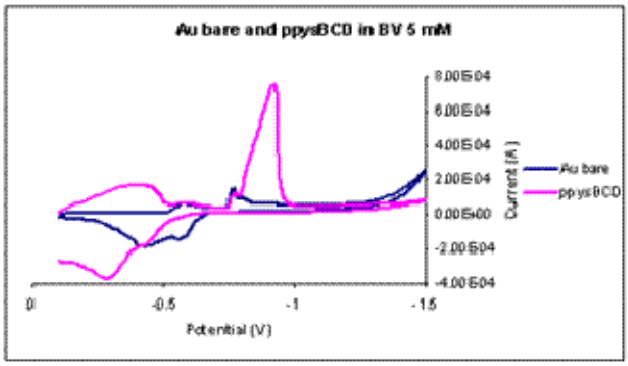


*Fig.3 cycly voltammetry of the sulfated β-cyclodextrin doped polypyrrole in a 5 mM solution of benzyl viologen*

## References:

1. J. Szetjli; *"Introduction and general overview of cyclodextrin chemistry"; Chem Rev;* 1998, **98**,1743-53.
2. M.E. Davis, M.E. Brewster; "Cyclodextrin-based pharmaceutics: past, present and future"; *Nature Reviews Drug Discovery*, 2004, **3**, 1023-35.
3. D.W. Armstrong, T.G. Ward; "Separation of drug stereoisomers by the formation of β-Cyclodextrin inclusion complexes"; *Science*; 1986, **232**, 1132-35.
4. E.E. Engelman and D. H. Evans; "Investigation of the nature of electrodeposited neutral viologens formed by reduction of the dications"; *J. Electroanal. Chem.*, 1993, **349**, 141-58.

First Regional Symposium on Electrochemistry of South-East Europe, Rovinj, Croatia, May 4-8, 2008.

P-2-090

# ELECTROCHEMICAL STUDY OF MAJOR AND TRACE METAL INTERACTIONS WITH CONCENTRATED MARINE DISSOLVED ORGANIC MATTER

**Y. Louis[1], C. Garnier[2], V. Lenoble[1], D. Omanović[3], S. Mounier[1] I. Pižeta[3]**

*[1]Laboratoire PROTEE, Université du Sud Toulon - Var – BP 20132, 83957 La Garde, France*
*[2]Groupe de Physico Toxico Chimie des Systèmes Naturels, Institut des Sciences Moléculaires (ISM - UMR CNRS 5255), Université Bordeaux I, 33405 Talence, France*
*[3]Center for Marine and Environmental Research, Ruđer Bošković Institute, P.O. Box 180, 10002 Zagreb, Croatia, E-mail: omanovic@irb.hr*

Complexing affinities of a concentrated marine dissolved organic matter (DOC content of 1.2 $mmol_C\ L^{-1}$) towards major and trace cations were studied by potentiometric and voltammetric titration techniques. A 2-steps protocol, involving nanofiltration and reverse osmosis, was applied for organic matter pre-concentration. A homewritten software, named PROSECE, was used for fitting of all experimental data in order to obtain complexation parameters. Four distinct classes of acidic sites with pKa of 3.6, 4.8, 8.6 and 12 were resolved according to potentiometric titration experiment. A total acidic sites density of 446.4 $meq/mol_C$ was estimated, with a majority of carboxylic-like sites (60% of the acidic sites).

Pseudopolarography of concentrated seawater sample with increasing concentration of copper ions identified three classes of copper complexes (1) labile – with reduction wave at ~ -0.2 V, (2) inert - with reduction wave at ~-1.4 V and (3) strong inert non-eletroactive (Figure 1). Simultaneous competition between copper, calcium and proton revealed the presence of two classes of binding sites forming inert complexes. These sites were of phenolic-like type with respective pKa of 8.6 and 8.2. The first class of binding sites was more specific to copper ($logK_{CuL}$ of 9.9 and $logK_{CaL}$ of 2.5), whereas stronger competition between copper and calcium occurred for the second class of sites ($logK_{CuL}$ of 6.9 and $logK_{CaL}$ of 5.5). The site density of second class was about six time higher than that of first class (10.25 $meq/mol_C$ compared to 1.72 $meq/mol_C$), which, in summary, is only small part of the total acidic site density.

The validity of sample preconcentration and data treatment was confirmed by very good accordance of the experimental titration data measured in non-concentrated seawater sample (DOC content of 0.09 $mmol_C\ L^{-1}$) with the data predicted by MINEQL simulation using complexing parameters obtained in the concentrated seawater sample. Furthermore, this comparison highlighted that the applied concentration protocol had negligible influence on organic matter properties when considering copper complexation.

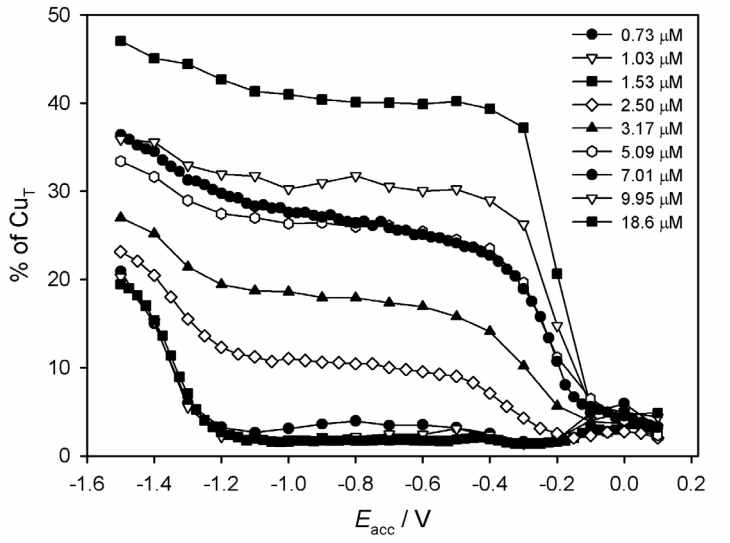


*Figure 1. Pseudopolarograms of copper obtained by DPASV for logarithmic additions on the concentrated sample (pH = 8.2) represented as the fraction of measured electro-active copper (compared to total added copper).*

**References:**

1. Garnier, C., Pižeta, I., Mounier, S., Benaïm, J.Y., Branica, M., 2004b. Influence of the type of titration and of data treatment methods on metal complexing parameters determination of single- and multi-ligand systems measured by stripping voltammetry. *Anal. Chim. Acta* **505**, 263-275.
2. Garnier, C., Mounier, S., Benaïm, J.Y., 2004c. Influence of dissolved organic carbon content on modelling natural organic matter acid-base properties. *Water Res.* **38**, 3685-3692.
3. Louis, Y., Cmuk, P., Omanović, D., Garnier, C., Lenoble, V., Mounier, S., Pižeta, I., 2008. Speciation of trace metals in natural waters: the influence of an adsorbed layer of natural organic matter (NOM) on voltammetric behaviour of copper. *Anal. Chim. Acta*. **606**, 37-44.
4. Luther III, G.W., Rozan,T.F., Witter, A., Lewis, B., 2001. Metal–organic complexation in the marine environment, *Geochem. Trans.* **2**, 65-74.
5. Lu, Y. and Allen, H.E., 2002. Characterization of copper complexation with natural dissolved organic matter (DOM)—link to acidic moieties of DOM and competition by Ca and Mg. *Water Res.* **36**, 5083-5101.
6. Tipping, E. and Hurley, M.A., 1992. A unifying model of cation binding by humic substances. *Geochim. Cosmochim. Acta* **56**, 3627-3641.

First Regional Symposium on Electrochemistry of South-East Europe, Rovinj, Croatia, May 4-8, 2008.

P-2-091

# EFFECTS OF INTERACTION OF HEAVY METALS IONS ON LAND AND PLANTS

**B. Blagojević, M. Vlajković, T. Golubović, B. Barjaktarov**

[1]*Faculty of Occupational Safety FZNR Nis, Serbia*
[2]*Sanitary Ecology Society SANEKO Belgrade, Serbia, www.saneko98.com; saneko98@yahoo.com*

Land is one of ther most important natural resourses, where, because of fertility, plants grow as the main source of the food for animals and man. Taking in consideration that land and plants are very dynamic creations, we see that their characteristics are influenced by many biotic and non-biotic aspects.
One of the non-biotic aspects which has recently been in focus of research and which is important for adoptation and phyisiological effects of polluting substances, is interaction of ions which relate to antagonism and sinergism.
In a case of polluting the land with heavy metals, where higher content of numerous heavy metals is present, it is very important to know their ion interaction, because their mutual influence is based on their physiological effect and on competition for uniting spots on land particles or on membrane surface of root cells. Antagonism of Calcium and Plumbum (Ca and Pb) is very important. If the two heavy metals find together on the nutritious surface and if the contains at least one of them is above the point of toxicity then we have the synergistic behavior (Cd i Zn).
Content of heavy metals in plants is dependent on their content in external environment, so increasing concentration of heavy metal ions in external environment icreases their adoptation, and therefore their concentration in plants increases too whereby we have antagonism and sinergism We believe that antagonism come up because of a differences in diameters, valences and electrical conductivity of ions.
Interaction of heavy metals ions we have study on medical plants and we notice that Nickel agitated translocation of Cadmium in to the flower of Matricariae Chamomilae. We use that for fitoexstrecting of cadmium from soil.

*Key words:* Concentration and interaction of ions of heavy metals, land, medical plants.

First Regional Symposium on Electrochemistry of South-East Europe, Rovinj, Croatia, May 4-8, 2008.

P-2-092

# INVESTIGATIONS OF BIOAVAILABILITY OF HEAVY METALS WITH ANODIC STRIPPING VOLTAMMETRY (DPASV)

**N. Đonlagić**

*Faculty of Natural sciences, University of Tuzla, Bosnia and Herzegovina*

Monitoring of contamination and bioavailability of heavy metals in natural waters and soil is of great importance from the ecological point, since these contaminants are bioaccumulative and can enter the food chains even in trace amounts.
Beside this, heavy metal's traces are present in agricultural cultivars and food, and for that reason monitoring of heavy metal's intake with approved and recommended analytical methods could present the regular practice. The application of highly sensitive electroanalytical technique, DPASV, enables regular monitoring of bioavailability of heavy metals, and for that reason , stripping techniques present reccommended alternative to the spectrometric methods.
On University of Tuzla (Department for physical chemistry and electrochemistry) research projects of fundamental and applicative character were realized within several doctoral and master theses . In past decade the folowing investigations were performed:

- Bioavailability of heavy metals (Pb,Cu,Cd,Zn) in natural waters (artificial hydro-accummulation Modrac and Pannonica; rivers of Tuzla canton)
- Influence of soil characterictics and fertilizers on intake of heavy metals (Pb,Cu,Cd,Zn) into agricultural cultivars and vegetables
- Monitoring of heavy metal's content in food stuffs

1. Monitoring of heavy metal's (Pb,Cu,Cd,Zn) content and bioavailability was performed with anodic stripping voltammetry(DPASV) during four year's seasons in artificial hydro-accummulation Modrac. Inorganic and organic metal speciation was investigated . Inorganic speciation was defined with respect to the chemical composition of water and with aid of thermodynamical method. Complexing capacities were determined for Cu and Pb , and in that way defined conditions of formation of inert complexes. The influence of pH and chemical composition of water on metal complex formation depended on the year's season, and can be predicted on the basis of DPASV measurements and appropriate thermodinamical program (CHEAQS, MINTEQ). Distribution of heavy metal's traces was investigated in bioindicators and in sediment of the representative locations.
2.The investigations of soil characterictics and different commercial fertilizers on heavy metal's intake into agricultural cultivars and vegetables on Spreca field in Tuzla canton, showed that there is strong correlation with soil characterictics and chemical composition of fertilizer with heavy metal intake. DPASV method was suitable and reproducible results were achieved.Coefficients of distribution of heavy metals were determined.The reoccommended procedures of sample treatment play important role and influence the reproducibility and accuracy.

3. Monitoring of heavy metals with DPASV in food stuffs and vegetables (flour, milk, oil, canned food) showed that there are elevated concentrations of $Pb^{2+}$ in some commercial samples. Thermal treatment of bio matrices prior to DPASV investigations was time consuming, but resulted with more reproducible results. Tolerable doses of intake were determined (PTWI-Provisional Tolerable Weekly Intake) in accordance with WHO recommendations.

It can be concluded that investigations of bioavailability of heavy metals with DPASV method, combined with necessary thermodinamical programs, present an appropriate methodology of environmental management of heavy metal accummulation and contamination, as well as for investigations of bio-geochemical dynamics of heavy metals.

**References:**

1 A. Teesier and D.R. Turner, «*Metal Speciation and Bioavailability in Aquatic Systems*»,1995, John Wiley and Sons, Chichester
2. T.M. Florence and K.J.Mann, *Anal.Chim.Acza*,1987, **200**, 305.
3. E. Omeragić, *MSc Thesis, University of Tuzla, 2005*
4. A. Odobašić, *PhD Thesis, University of Tuzla, 2005.*
5. H. Keran, *PhD Thesis , University of Tuzla, 2006*

First Regional Symposium on Electrochemistry of South-East Europe, Rovinj, Croatia, May 4-8, 2008.

P-2-093

# NEW MODIFIED POROUS SELECTIVE ELECTRODES FOR HEAVY METALS

**C. Cristea[1], B. Feier[1], R. Crisan[1], F. Geneste[2], R. Săndulescu[1]**

*[1]University of Medicine and Pharmacy « Iuliu Hatieganu », Faculty of Pharmacy, Department of Analytical Chemistry, 4 Pasteur 400 349 Cluj-Napoca, Romania, ccristea@umfcluj.ro*
*[2]Laboratoire d'Electrochimie et Organométalliques, Institut de Chimie, University of Rennes 1, Campus de Beaulieu, 35042 Rennes Cedex, France*

The modified graphite felt electrodes were used over 20 years in electrocatalysis or in electro synthesis. Our first approach using these kinds of electrodes was to prepare by an unconventional way new heterocycles having biological activity. Lately the covalent attachment of different catalyst on graphite-felt electrode was achieved.

The removal of heavy metals from diluted solutions is a research direction with application in environmental, drugs quality control and recovery of heavy metals, etc. The main idea of the research was to covalently attach a diamino derivative in order to trap the heavy metals ions.

Many divalent cations from heavy metals present a four coordinance and can be trapped with tetra dentate ligands having four hetero atoms (O, N, S). Previously, it has been published [1] the anodic grafting of amino derivatives onto graphite felt electrode *via* a radical coupling. According to the same procedure, several starting compounds having two terminal amino groups un/protected have been grafted on graphite felt in order to trap heavy metal cations.

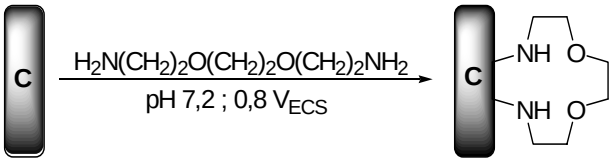


The voltamperometric analysis shows the grafting of several cations. Because of the equilibrium between the free cation in solution and the crypted cation, the result is different for each cation. It appears a higher selectivity for $Pb^{2+}$ ($1{,}6 \times 10^{-7}$). The presentation will show the modifying procedure, the kinetic studies and the results obtained for different cations. Optimization of the covalent attachment of the diamino compound (linear and cyclic forms) as well as the traping of different cations procedure was investigated.

The modified porous electrodes could be used several times by simply modifying the applied potential.

***Acknowledgments:*** *The authors thank CNCSIS (grant $A_T$ 180/2006) for the financial support.*

## Reference:

1. F. Geneste, C. Moinet, *New J. Chem*, **29**, 269-271, 2005.

First Regional Symposium on Electrochemistry of South-East Europe, Rovinj, Croatia, May 4-8, 2008.

P-2-094

# MODIFIED ELECTRODES FOR THE DETECTION OF MERCURY IONS

**G.O. Buica[1], E.M. Ungureanu[1], J.C. Moutet[2], C. Bucher[2], E. Saint-Aman[2], G. Royal[2]**

*[1]Faculty of Applied Chemistry and Material Science, University "Politehnica" of Bucharest, Splaiul Independentei 313, 060042, Romania, buica_george@yahoo.com*
*[2]Departement de Chimie Moleculaire, UMR CNRS 5630, Université Joseph Fourier, BP 53, 38041 Grenoble Cedex 9, France*

Heavy metal ions are commonly found in many industrial effluents. Most heavy metal ions are toxic or carcinogenic and hence present a threat to human health and to the environment. Even at very low concentrations in water [1-4], they are potentially dangerous to living beings, depending on the chemical form and exposure level [5]. Mercury is one of the most toxic substances and is known to bio-accumulate in the body of people with chronic exposure [2, 6]. Determinaton of trace levels of this element in the environment is a highly important, yet challenging analytical problem. To determin the environmentally toxic trace levels of mercury, highly sensitive and selective methods need to be developed.

Simple methods are highly required for rapid measurements of trace levels of mercury in environment. Electrochemical detection offers several advantages, including remarkable sensitivity, inherent minaturization and portability, independence of optical path lengh or sample turbidity, low cost and high compatibility with advanced micromachining technologies [7].

Stripping voltammetry is the most sensitive electrochemical method for determination of trace metals. The method is based on the preconcentration and stripping of an analyte in a sample solution [8, 9]. Stripping analysis using a chemically modified electrode (CME) has higher selectivity due to the selective binding of specific metal ions. When the experimental conditions are optimized, CME exhibit nearly no interference with other species present in the sample.

The complexing properties of some poly(pyrrole-EDTA like) coated electrodes towards Hg(II) cations using the open circuit chemical preconcentration-anodic stripping technique will be presented. The monomers $\mathbf{L_1}$ and $\mathbf{L_2}$ were used to produce the CME by electropolymerization

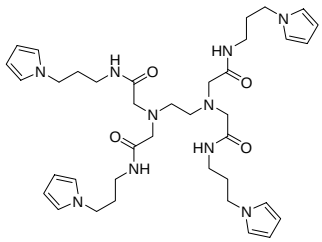

**$L_1$**

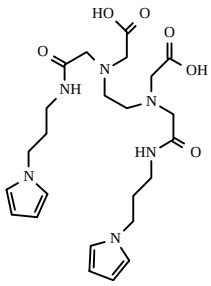

**$L_2$**

We will demonstrate that selectivity of the molecular electrode materials can be subtly modulated upon playing on the complexation parameters such as pH, reduction potential, concentration and accumulation time. The polymer films modified electrodes obtained by electropolymerization of **$L_1$** and **$L_2$** turned out to be selective towards Hg(II) ions and particulary insensitive to the presence of Cd(II) and Pb(II).

The use of imprinted polymer-coated electrodes prepared by electropolymerization of metal complexes of **$L_1$** allowed to significantly improve the detection limit of Hg(II) ($5\times10^{-10}$ M).

***Acknowledgments:*** *Financial support from CNCSIS CH-41-07-11 and 41-07-13 is gratefully acknowledged.*

**References:**

[1] Kadirvelu, K.; Faur-Brasquet, C.; Cloirec, P. L. *Langmuir* **2000**, *16*, 8404-8409.
[2] Descalzo, A. B.; Martı´nez-Ma´n˜ ez, R.; Radeglia, R.; Rurack, K.; Soto, J. *J. Am. Chem. Soc.* **2003**, *125*, 3418-3419.
[3] Xiao, B.; Thomas, K. M. *Langmuir* **2005**, *21*, 3892-3902.
[4] Deng, S.; Bai, R. B.; Chen, J. P. *Langmuir* **2003**, *19*, 5058-5064.
[5] J. P. Vernet, Impact of Heavy Metals on the Environment, Elsevier, New York 1992.
[6] Liu, C. Q.; Huang, Y. Q.; Naismith, N.; Economy J. *Environ. Sci. Technol.* **2003**, *37*, 4216-4268.
[7] T.A. Bendikov, J. Kim, T.C. Harmon, Sens. Actuators B 106 (2005) 512.
[8] Vydra, F.; Stulik, K.; Julakova, E. *Electrochemical Stripping Analysis*; Horwood: Chichester, U.K., 1976.
[9] Wang, J. *Stripping Analysis: Instrumentation and Application*; Verlag Chemie: Deerfield Beach, FL, 1985.

First Regional Symposium on Electrochemistry of South-East Europe, Rovinj, Croatia, May 4-8, 2008

P-2-095

# POTENTIOMETRIC STRIPPING ANALYSIS OF CADMIUM IN WATER

**B. M. Kaličanin[1], A. Stojčevski[2]**

*[1]University of Niš,Faculty of Medicine, Department of Pharmacy,*
*Bulevar dr Zorana Đinđica 81, 18000 Niš, Serbia; E-mail: bkalicanin@yahoo.com*
*[2]XIII High School, Lješka 47, 11000 Belgrade, Serbia*

Cadmium is considered as one of the most dangerous occupational and environmental poisons (1). Cadmium is more mobile in aquatic environments than most other heavy metals (e.g., lead). Cadmium in soils may leach into water. Cadmium-containing soil particles may also be entrained into the air or eroded into water, resulting dispersion of cadmium into these media (2). Cadmium concentration in water is inversely related to the pH and the concentration of organic material in the water (2).

Human exposure to cadmium can result from consumption of food, drinking water, or incidental ingestion of soil or dust contaminated with cadmium; from inhalation of cadmium- containing particles from ambient air; from inhalation of cigarette smoke, which contains cadmium taken up by tobacco; or from working in an occupation involving exposure to cadmium fumes and dust (3).

The basis of cadmium toxicity is its negative influence on enzymatic systems of cells, owing to substitution of other metal ions (mainly $Zn^{2+}$ and $Cu^{2+}$) in metalloenzymes and its very strong affinity to biological structures containing –SH groups (4). Excessive Cd exposure may give rise to renal, pulmonary, hepatic, skeletal, reproductive effects and cancer. The mayor effects of this metal poisoning are experienced in the lungs, kidneys and bones (5). Briefly, it is seen that this metal can dangerously affect human health even at ultra trace concentrations.

The determination of cadmium in natural waters is increasingly growing due to the knowledge its extremely toxicity for human even at very low levels.

The aim of the paper is to define the method for determining the cadmium in the natural water samples by applying the potentiometric stripping analysis (PSA) with oxygen as an oxidant (6).

All the analyses were performed by using commercially available computerized stripping analyzer M1 (Faculty of Technology, Novi Sad and Elektrouniverzal, Leskovac, Serbia) (7).

In order to optimize the PSA determination of cadmium the effect of mercury time electrodeposition, the electrolysis potential, and the solution stirring rate of the cadmium analytic signal was investigated. After the optimization of the determination conditions, both the linearity and the reproducibility of the analytical signal were defined.

On the basis of the above examinations the method for determining the cadmium in the various natural water samples was by the potentiometric stripping analysis (PSA) with oxygen as an oxidizer was defined. Defined method considering

samples analysis (sea, river, mineral and tap water) on the thin-layered mercury electrode with the electrodeposed mercury depth of 130 nm on the glassy carbon as inert support formed at the constant current of 50 μA, at the electrodeposition time of 240 s; at the electrolysis potential of -1.067 V against Ag/AgCl, KCl (3.5 mol/L) electrode, during 900 s and the stirring rate rapidity of 4000r.p.m.
Cadmium concentrations in natural water samples were obtained in the range of 0.12-0.36 μg/L for tap water, 0.15/0.21μg/L for mineral water, 1.25-3.52 μg/L for river and 6.67-13.25 μg/L for sea water.

**References:**

1. K.B. Jacobson, J.E. Turner, *Toxicology* **16** (1980) 1.
2. U.S. Environmental Protection Agency, *Office of Water Regulations and Standards*. EPA-0440/4-85-023.1985a.
3. S.J. Stohs, D. Bagchi, M. Bagchi, *Inhal. Toxicol.* **9** (1997) 867.
4. F. Bronner, *Neurotoxicology* **13** (1992) 775.
5. A.C. Davis, P. Wu, X. Zhang, X. Hou, B.T. Jones, *Appl. Spectrosc. Rev*. **41** (2006) 35.
6. D. Jagner. *Analyst* **107** (1982) 593.
7. B.M. Kaličanin, R. Nikolić, N. Marjanović N (2004) *Anal. Chim. Acta* **525** (2004) 111.

First Regional Symposium on Electrochemistry of South-East Europe, Rovinj, Croatia, May 4-8, 2008.

P-2-096

# INVESTIGATION OF THE ELECTROCHEMICAL REDUCTION OF PERCHLORATE IONS ON RHODIUM

**M. Ujvári[1], G.G. Láng[1,*], N.S. Sas[1], S. Vesztergom[1], G. Horányi[2]**

*[1]Eötvös Loránd University, Institute of Chemistry, Department of Physical Chemistry H-1117 Budapest, Pázmány P. s. 1/A*

*[2]Research Institute of Materials and Environmental Chemistry, Chemical Research Center, Hungarian Academy of Sciences, H-1525 Budapest, *langgyg@chem.elte.hu*

Current interest in the chemistry of perchlorate is primarily due to its presence as a contaminant in groundwater and drinking water. The presence of perchlorate in the environment is a potential health concern because perchlorate can hinder proper functioning of the thyroid gland [1,2]. Chemical and electrochemical reactions that lead to the reduction of perchlorate are of great interest to those seeking economical and efficient methods e.g. for the remediation of contaminated groundwater.

Perchlorate reduction in aqueous solution is strongly favored thermodynamically. The standard potential of the electrode reaction for the eight-electron reduction

$$ClO_4^- + 8e^- + 8H^+ = Cl^- + 4H_2O$$

of perchlorate to chloride is $E_r^\circ$ = 1.388 V, but the kinetics of the reduction reactions indicate the rate of this process is inhibited. This is why in the electrochemical literature it's very often assumed, that perchlorate ions are stable in aqueous solutions so their reactions can be neglected during electrochemical investigations. However, it has been found that in the presence of some metals (Co, Zn, Al, Fe) a considerable amount of $ClO_4^-$ is decomposed even at room temperature [2,3]. On the other hand perchlorate ions can be electrochemically reduced at several other metals e.g. Pt, Rh, etc. [2]. Analogous to the reduction of perchlorate in homogeneous solution, the reduction of perchlorate at an electrode (or any surface) must involve oxygen atom transfer. Applying the considerations outlined in the literature to the case of the Rh electrode it should be assumed that the adsorption of perchlorate ion is an elementary step in the overall reduction.

In the present work, the electrochemical reduction of perchlorate ions on rhodium was investigated in a series of experiments (voltammetry, chronoamperometry, impedance spectroscopy), performed at different electrode potentials and different temperatures. Cyclic voltammograms obtained for a Rh rotating disc in contact with perchloric acid solutions differs considerably from curves recorded at stagnant electrodes. In case of stationary electrodes the distortion of the anodic peak gradually disappears during subsequent potential cycles, i.e. the negative current during the positive sweep is continuously decreasing over the consecutive scans. In contrast to this, in case of rotating disc electrodes the shape of the voltammogram does not change after the second or third cycle, and a negative current can be always observed during the positive sweep. It means that the desorption rate of $Cl^-$ ions generated during the reduction process is significantly influenced by the hydrodynamic conditions, probably through desorption/diffusion coupling. This conception is supported by the results of chronoamperometric

measurements carried out at different temperatures. During these experiments the current was recorded as a function of time at constant electrode potentials and at different electrode rotation rates. Well-defined stationary currents were observed in all cases. The values of the stationary currents depend on the rotating rate of the RDE, the electrode potential and the temperature. The impedance of the electrode were measured at different rotating rates of the RDE and at different electrode potentials. The impedance measurements were started as soon as stationary conditions were reached (e.g. about 20 min after changing the rotation rate of the RDE). The impedance spectra are very similar to what is expected qualitatively for the case of a single charge transfer step coupled with diffusion [4]. It means that the assumption, that the $ClO_4^- \rightarrow ClO_3^-$ transformation is the rate determining step is a relevant and acceptable interpretation of the phenomena observed. Experiments with $ClO_3^-$ ions strongly support this hypothesis.

On the basis of the experimental results a new mechanism for the electrocatalytic reduction of perchlorate ions has been proposed. According to this reaction scheme, after a potential step from a potential at which the adsorption of $ClO_4^-$ does not occur, the reduction process is starting with the adsorption of perchlorate ions at free active sites on the metal surface. The decomposition reaction can be written as:

$$ClO_4^-(\text{ads}) \rightarrow \text{ intermediates } \rightarrow Cl^-(\text{ads})$$

After the production of a certain amount of $Cl^-$ ions, practically all active sites are occupied by $Cl^-$ or $ClO_4^-$ ions, and a well defined stationary state with constant current is established. For the stationary state the following reaction scheme can be suggested:

$$ClO_4^-(0) + Cl^-(\text{ads}) = ClO_4^-(\text{ads}) + Cl^-(0) \qquad \text{(S1)}$$

$$ClO_4^-(\text{ads}) + 2H^+ + 2e^- \rightarrow ClO_3^-(\text{ads}) + H_2O \quad \text{(slow)} \qquad \text{(S2)}$$

$$ClO_3^-(\text{ads}) \rightarrow \text{ intermediates } \rightarrow Cl^-(\text{ads}) \quad \text{(very fast)} \qquad \text{(S3)}$$

$$Cl^-(0) = Cl^-(\text{sol}), \qquad \text{(S4)}$$

"(ads)" denotes here that the species is adsorbed on an active site, while "(0)" refers to components in the solution phase in the immediate vicinity of the electrode surface (see e.g. [5]). It is also assumed that the whole process starting from perchlorate ion occurs on the surface and the role of desorption of intermediates can be neglected.

On the basis of the kinetic model an expression has been derived for the impedance of the electrode, which fits the experimental data fairly well.

*Financial support by the Hungarian Scientific Research Fund (OTKA K045888, OTKA K67994) is gratefully acknowledged.*

**References:**

[1]*Perchlorate in the Environment*, ed. by E.T. Urbansky, Kluwer Academic Publ. (2001).
[2] G.G. Láng, G. Horányi: *J. Electroanal. Chem.* 552 (2003) 197.
[3] G.G. Láng, G. Inzelt, A. Vrabecz, G. Horányi: *J. Electroanal. Chem.* 582 (2005) 249.
[4] G. Láng, L. Péter, *ACH-Models in Chem.* 131 (1994) 137.
[5] L. Kiss, '*Kinetics of Electrochemical Metal Dissolution*' (Studies in Physical and Theoretical Chemistry, Vol. 47) Elsevier, Amsterdam, 1988.

First Regional Symposium on Electrochemistry of South-East Europe, Rovinj, Croatia, May 4-8, 2008.

P-2-097

# THE INFLUENCE OF PLASTICIZER ON THE ANALYTICAL PERFORMANCE OF A PORPHYRIN BASED NICKEL-SELECTIVE ELECTRODE

**D. Vlascici[1], O. Spiridon Bizerea[1], E. Făgădar-Cosma[2]**

*[1]West University of Timisoara, Faculty of Chemistry – Biology – Geography, Inorganic Chemistry Department, Str. Pestalozzi 16, 300115 - Timisoara, Romania,*
*E-mail: danavlascici@yahoo.com*
*[2]Institute of Chemistry Timisoara of Romanian Academy, Bd. M. Viteazul 24 300223-Timisoara, Romania*

In the last years, a lot of metalloporphyrin based ion-selective electrodes for the potentiometric determination of different anions have been developed. In all of the cases, the electrodes showed a selectivity pattern different from the Hofmeister sequence as a result of the specific interaction of metalloporphyrins with the analyzed anions [1]. An important characteristic of the porphyrins is that they are forming 1:1 complexes with almost all metals [2]. The above mentioned complexes with transition metal ions are very stable. This is the reason why, we have investigated an unmetalated porphyrine as ionophore in cation-selective electrodes.

As ionophore we have used *meso*-tetraphenylporphyrin ($H_2TPP$) which was synthesized in accordance with previously published procedures [3]. The potentiometric response characteristics (slope and selectivity) of nickel-selective electrodes based on $H_2TPP$ in o-nitrophenyloctylether (*o*-NPOE), dioctyl phtalate (DOP) and dioctyl sebacate(DOS) plasticized poly(vinyl chloride) membranes are compared. All the membranes contain a lipophilic anionic derivative (sodium tetraphenylborate) as additive. The results are presented towards a lot of mono- and di-valent cations. Potentiometric selectivity coefficients were determined according to the separate solution method [4] by using the experimental EMF values obtained for 0.1 M solutions of the test cations and a theoretical slope of 29.6 mV/pNi for the primary cation. The electrodes exhibited linear response with a near-Nernstian slope toward nickel ions and a good selectivity.

The determination of nickel is important due to its toxic nature. He may be presented in various effluents and is present in low concentrations in red meat, chocolate, unsaturated oils, milk and milk products. The nickel toxicity conducts to different diseases such as: pneumonitis, dermatitis, asthma and others [5]. For all these reasons, the nickel ion must be precisely determined and one of the possible methods for this may be the potentiometric determination using ion-selective electrodes.

**References:**

[1] Egorov V.V., Rakhman'ko E.M., Rat'ko A.A. (2002). Metalloporphyrin-based anion-selective electrodes with unusual selectivity, *J. Anal. Chem*. **57(1)**, 46-53
[2] Biesaga M., Pyrzynska K., Trojanowicz M. (2000). Porphyrins in analytical chemistry. A review. *Talanta*.**51**, 209-224

[3] Adler A.D., Longo F.R., Goldmacher J., Assour J., Korsakoff L. (1967). A simplified synthesis for meso-tetraphenylporphine. *J. Org. Chem.* **32**, 476-487.

[4] Guilbault G.G., Durst R.A., Frant M.S., Freiser H., Hansen E.H., Light T.S., Pungor E., Rechnitz G., Rice N.M., Rohm T.J., Simon W., Thomas J.D.R.. (1976). IUPAC recommendations for nomenclature of ion-selective electrodes. *Pure Appl. Chem*. 48, p. 127–132.

[5] Gupta V.K., Jain A.K., Singh L.P., Khurana U. (1997). Porphyrins as carrier in PVC membrane potentiometric sensors for nickel (II). *Anal. Chim. Acta*. **355,** 33-41

First Regional Symposium on Electrochemistry of South-East Europe, Rovinj, Croatia, May 4-8, 2008.

P-2-098

# A POLYANILINE-SKELETON NICKEL ELECTRODE FOR THE POTENTIOMETRIC DETECTION OF NITRATE AND NITRITE

**N. Plesu[1], A. Kellenberger[2], N. Vaszilcsin[2]**

[1]*Romanian Academy-Institute of Chemistry, Bd.Mihai Viteazul 24, Timisoara, Romania, plesu_nicole@yahoo.com*

[2]*University "Politehnica" of Timisoara, Piata Victoriei 2, 300006 Timisoara, Romania*

The nitrate and nitrite determination presents importance to pollution control. Nitrate and nitrite usually exists in industrial wastewaters, polluted groundwater and radioactive solutions. The nitrate is a non-toxic compound; it can be reduced to nitrite, which is a precursor in the formation of nitrosamines, compounds with potential carcinogenic effect. The clasic methods for nitrate determination are based on spectroscopic, chromatographic, and electrochemical detection [1-3].

The aim of this study was to investigate the sensing properties of a modified electrode obtained by the electrochemical depositon of polyaniline from aqueous acid solutions on a rough substrate of skeleton nickel. For the deposition of PANI an unconventional substrate was selected, namely skeleton nickel [4]. This kind of substrate improves the adherence of the polyaniline film but doesn't affect the sensing properties of the modified electrode, thus, the potentiometric response is the same as in case of conventional substrates.

PANI was deposited from an aqueous solution of 0.027 mol $L^{-1}$ aniline in 1 mol $L^{-1}$ sulfuric acid, by sweeping the potential between -0.2 V/SCE and 1.2 V/SCE, at 100 mV $s^{-1}$ scan rate for 10 cycles. Afterwards the anodic potential limit was lowered to 1.0 V/SCE to avoid the oxidative degradation reactions of the polymer chain and the potential cycling was continued for 10 more cycles.

The cyclic voltammograms given in Figure 1 show the appearance of an anodic peak A at 0.2 V/SCE in the first cycle attributed to the oxidation of the nickel substrate.

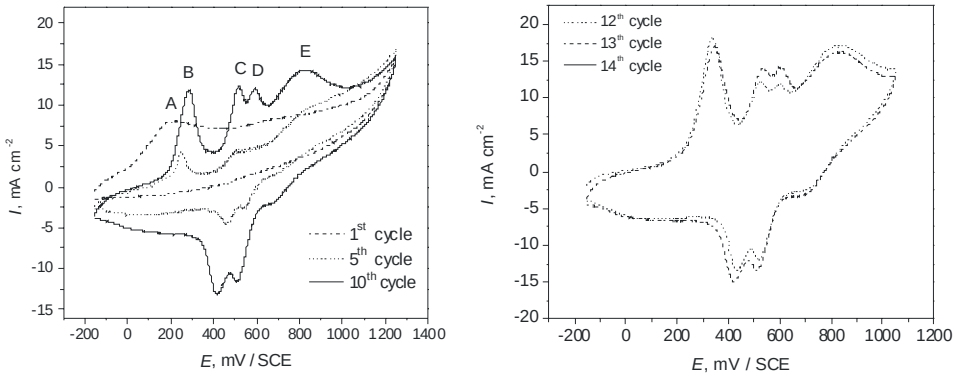


*Figure 1. Cyclic voltamogramms for the electrochemical polymerization of aniline on skeleton nickel electrode, 1 mol $L^{-1}$ $H_2SO_4$ + 0.027 mol $L^{-1}$ aniline solution, scan rate 100 mV $s^{-1}$, potential range a) −0.2 ÷ 1.2 V/SCE, b) −0.2 ÷ 1.0 V/SCE.*

The polyaniline film growth starts after the passivation of the nickel substrate and four oxidation peaks (B, C, D, and E) appear in cyclic voltamogramms, associated with different steps of the electrochemical polymerization mechanism.
The potentiometric response of the skeleton Ni-PANI electrode was measured for nitrate and nitrite anions. Before the measurements the modified electrode was conditioned for 24 hours in a $10^{-5}$ mol $L^{-1}$ solution of the corresponding anion to achieve the anion exchange equilibrium. During this step the sulfate dopant anions are exchanged with nitrate or nitrite anions.
The calibration curves given in Figures 2 a and b were obtained in $NaNO_3$ and $NaNO_2$ solution with different concentrations, ranging from $10^{-1}$ to $10^{-5}$ mol $L^{-1}$.

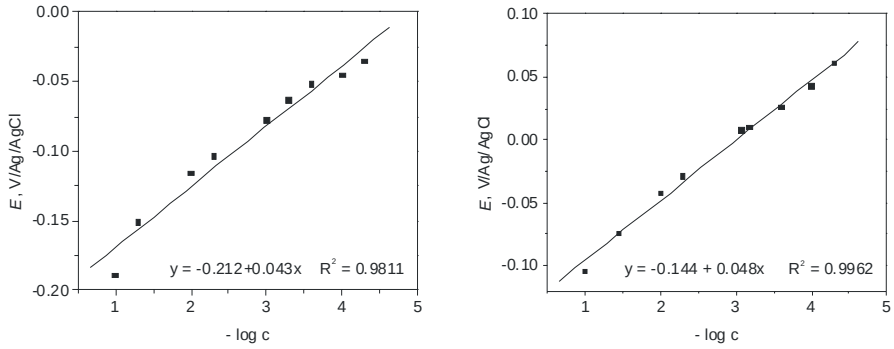


*Figure 2. Potentiometric calibration curves for a) nitrate and b) nitrite*

The modified electrode behaves as a second order electrode and gives a Nernstian potentiometric response in the studied concentration range.The slope of the calibration curves approaches the theoretical value of 0.059 V decade$^{-1}$ for each anion. The detection range was $5 \cdot 10^{-5}$ mol $L^{-1}$ for both nitrate and nitrite anions. The selectivity coefficient $K_{NO_3^- - NO_2^-}$ of the modified electrode for $NO_3^-$ anions, with respect to $NO_2^-$ interfering ions evaluated by the separate solution method. The value of the calculated selectivity coefficient is equal to 0.44. The good selectivity coefficient of the PANI-skeleton nickel electrode combined with the rapid response and stability in time, ease of preparation and insolubility of PANI in organic solvents make the electrode attractive.

**References:**

1. D. Tsikas, F. M. Gutzki, S. Rossa, H. Bauer, C. Neumann, K. Dockendorff, J. Sandmann, J. C. Frölich, *Anal. Biochem.*, 1997, **244**, 208-220.
2. R. J. Davenport, D. C. Johnson, *Anal. Chem.*, 1973, **45**, 1979-1980.
3. Y. Kitamaki, J.-Y. Jin, T.Takeuchi, *J.Cromatography A*, 2003, **1003**, 197-202.
4. N. Plesu, A. Kellenberger, N. Vaszilcsin, I. Manoviciu, *Chem.Bull.Politehnica Univ.(Timisoara)*, 2000, **45(59),** 198-207.

First Regional Symposium on Electrochemistry of South-East Europe, Rovinj, Croatia, May 4-8, 2008.

P-2-099

# AN APPLICATION OF SILVER NANOPARTICLES IN ENVIRONMENTAL CHEMISTRY: SENSING OF NITRATES

**C.M. Fox, C.B. Breslin, A.D. Rooney**

*Department of Chemistry, National University of Ireland Maynooth, Co. Kildare, Ireland.* catherine.m.fox@nuim.ie

Nitrogen containing compounds, while essential minerals for all life, can pose an environmental risk when they become concentrated in our rivers, lakes and drinking water. Consequently, in this era where the protection of the environment is of major concern, monitoring nitrate concentration has become a high priority. So sensors that are reliable, cheap and capable of continuous monitoring have become the focus of intense research in the field of environmental technologies.

Electrochemical sensors offer many of the criteria listed above. Such sensors allow the measurement of many inorganic and organic pollutants in the field rather than in the laboratory. They are inherently sensitive and selective towards electroactive species such as nitrate, are fast and accurate, compact, portable and inexpensive. Nanotechnology is a rapidly growing area in chemistry and the features of nanoparticles have the potential to greatly enhance the effectiveness of an electrochemical sensor, for example increased surface area and increased catalytic activity. Furthermore electrochemistry can be used to synthesis these nanoparticles directly on to the surface of an electrode.

In this paper, we show how to simply prepare silver nanoparticles via various electrochemical methods. First, colloidal silver was formed potentiostatically under the protection of the stabilising agent, poly(N-vinylpyrrolidone)[1]. Like most methods for synthesising nanoparticles electrochemically, these are prepared by chemical reduction of the metal salt, in this case silver nitrate ($AgNO_3$). The stabilising agent immediately coats the particles and therefore prevents agglomeration. These particles were analysed-using UV-Visible spectroscopy, which is a very accurate and simple tool to measure the size of the nanoparticles. Silver nanoparticles show a strong absorption band at approximately 420 nm.

Next we show how silver is directly deposited on a glassy carbon electrode via a potentiostatic single-pulse technique[2]. Again it involves the reduction of the metal salt, this time at the electrode surface, for only a few seconds. The longer the deposition time the larger the particles. We investigated the modified electrodes sensitivity to nitrate using cyclic voltammetry. The electrochemical reduction of nitrate shows two signals, with peak potentials at approximately –1.3 V and –1.6 V. A detection limit of $5x10^{-5}$ M $KNO_3$ was reached.

**References:**

1. B. Yin, H. Ma, S. Wang and S. Chen, *J. Phys. Chem. B*, **107**, (2003), 8898-8904
2. A. A. Isse, S. Gottarddello, C. Maccoto and A. Gennaro, *Electro. Comm.*, **8**, (2006), 1707-1712

First Regional Symposium on Electrochemistry of South-East Europe, Rovinj, Croatia, May 4-8, 2008.

P-2-100

# METAL OXIDE GRAPHITE COMPOSITE ELECTRODES: APPLICATION TO NITRITE SENSING

**B. Šljukić[a], C.E. Banks[b], R.G. Compton[c]**

*[a]Faculty of Physical Chemistry, University of Belgrade, Studentski trg 12, 11000 Belgrade, Serbia, biljka@ffh.bg.ac.yu*
*[b]Now at School of Biology, Chemistry and Health ScienceManchester Metropolitan University, Chester St., Manchester, M1 5GDUK*
*[c]Physical and Theoretical Chemistry Laboratory, University of Oxford, South Parks Road, Oxford, OX1 3QZ, UK*

The concerns over a significant increase in the accumulation of toxic substances in the environment due to human activities have lead to a development of amperometric sensors for environmental monitoring. The most commonly used amperometric electrodes are made of carbon based materials. However, these typically suffer from slow electron transfer rates resulting in high overpotentials required for oxidation / reduction of different compounds. Recently, special attention has been given to chemically modified carbon electrodes and carbon composite electrodes to improve the electrocatalytic activity for the determination of different analytes.

In the present contribution a wet impregnation procedure was developed for modification of carbon powder with different metal oxides, namely copper, manganese and lead oxide. The carbon powder separately modified with each of the metal (Cu, Mn or Pb) oxides was characterized using electrochemical and spectroscopic techniques. Novel composite metal oxide modified carbon powder epoxy electrodes were developed for electrocatalytic sensing of nitrites as model analyte.

The modification of carbon powder with metal (Cu, Mn or Pb) oxide was carried out by a wet impregnation procedure. First, carbon powder was impregnated with metal nitrate by stirring carbon powder (1 g) in concentrated aqueous solution of a metal nitrate (25 $cm^3$) at room temperature for 1 hour. The metal nitrate – carbon powder composite was exposed to temperature of 823 K in the case of Cu and Pb and to 793 K in case of Mn resulting in metal oxide modified carbon powder.

The working electrodes were made of a composite of metal oxide modified carbon powder and epoxy resin. For the fabrication of the composite electrode, epoxy resin was blended with a mixture of metal oxide modified carbon powder (10 weight %) and unmodified carbon powder (90 weight %), with powder to resin ratio of 1:3. The resulting paste was mixed in an ultrasonic bath for 30 min and then placed in a glass tube of 6 mm inner diameter up to 6 mm depth. The electrical contact was completed using a copper wire inserted into the tube up to 3 mm depth. The electrodes were subsequently dried at 40˚C for 60 hr. For comparison purposes, carbon powder epoxy composite electrode was prepared by the same procedure.

Preliminary studies were performed for potential electrocatalytical detection of nitrites, Figure 1. Cyclic voltammogram of BPPG electrode abrasively modified with copper

oxide modified carbon powder in nitrite solution showed a well-defined nitrite oxidation peak at *ca.* + 0.987 V *vs.* SCE. In contrast, no peak was observed in the absence of nitrite. The peak corresponding to the oxidation of nitrite at the bare BPPG electrode appears at *ca.* + 1.158 V *vs.* SCE, 171 mV more positive potential than the one obtained for modified BPPG electrode, also being of smaller intensity.

Next, the copper oxide carbon powder epoxy composite electrodes were applied to the detection of nitrite in aqueous solutions. CVs of CuO-CP-E composite electrode were run in nitrite solution in 1 mM $HClO_4$ + 1M $NaClO_4$. The oxidation peak could be observed at *ca.* + 1.1 V *vs.* SCE. Subsequently, the blank solution was spiked with 100 μM additions of sodium nitrite. The proposed method allowed the detection of nitrite with a detection limit (based on 3 sigma) of 0.6 μM.

The potential application of lead (IV) oxide modified carbon powder epoxy composite electrode for sensing of nitrite ions was also studied. A well-defined peak of nitrite oxidation at PbO-CP-E electrode could be seen at *ca.* + 1.0 V *vs.* SCE. The limit of detection for nitrite ions using $PbO_2$-CP-E composite electrode was evaluated and found to be 0.9 μM. When CVs of the manganese dioxide modified carbon powder epoxy composite electrode were initially run in nitrite solution a distinct peak could be observed at *ca.* + 0.95 V *vs.* SCE. The peak current values showed a strong linear correlation with nitrite concentration with a limit of detection for nitrite of 1.2 μM.

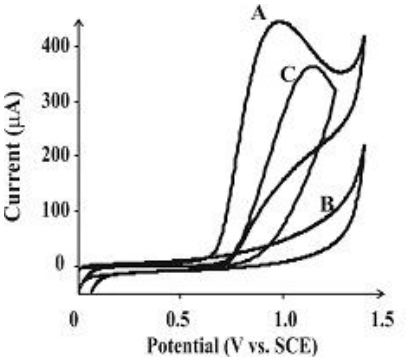


*Figure 1. Comparison of CVs of BPPG electrode abrasively modified with copper oxide modified carbon powder in 1 mM $HClO_4$ + 1 M $NaClO_4$ (A) and in 10 mM $NaNO_2$ solution (B) at a scan rate of 50 $mVs^{-1}$. CV of bare BPPG electrode in 10 mM nitrite solution is included (C)*

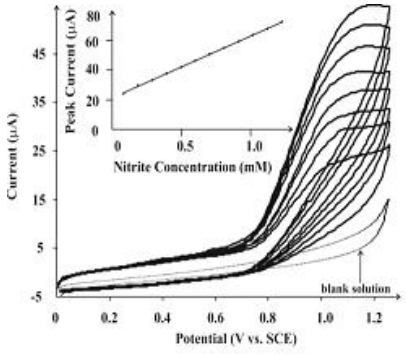


*Figure 2. Cyclic voltammograms for the oxidation of nitrite ions at CuO-CP-E composite electrode in 1 mM $HClO_4$ + 1 M $NaClO_4$ solution increasing the nitrite ion concentration at a scan rate of 50 $mVs^{-1}$*

Note that these detection limits are comparable or lower than detection limits obtained with other electrochemical methods [1-3] indicating that the composite electrode can potentially be used for monitoring of the concentration of nitrites in water.

For application of the composite electrodes for the detection of nitrite ions in real samples it is necessary to recognize the possible interference of species being present in complex media. However, the detection of nitrite on metal oxide composite electrode was examined in presence of a range of potential

environmental interferents, namely cyanide and ascorbic acid and was unaffected by the presence of up to 1 mM concentrations of these three species. The results obtained for the detection of nitrite, together with composite electrodes having flexible design and low cost offers the potential application of composite electrodes in biosensors.

**References:**

1. J. Davis, R. G. Compton, *Anal. Chim. Acta* 2000, **404**, 241.
2. A. Abbaspour, M. A. Mehrgardi, *Talanta* 2005, **67**, 579.
3. J.-L. Chang, J.-M. Zen, *Electroanalysis* 2006, **18**, 941.

First Regional Symposium on Electrochemistry of South-East Europe, Rovinj, Croatia, May 4-8, 2008.

P-2-101

# VOLTAMMETRY OF COPPER OXIDE MICROPARTICLES IMMOBILIZED ON DIATOMITE SURFACE

**Š. Komorsky-Lovrić[1], L. Marinić-Pajc[2], N. Tadej[3], A.J.M. Horvat[4], J. Petran[2]**

*[1]"Ruđer Bošković" Institute, Center for Marine and Environmental Research, Zagreb, Croatia*
*[2]INA - Department of Development and Research, Zagreb, Croatia*
*[3]Faculty of Mining, Geology and Petroleum Engineering, University of Zagreb, Department of Mineralogy, Petrology and Mineral Resources, Zagreb, Croatia*
*[4]Faculty of Chemical Engineering and Technology University of Zagreb, Department of Analytical Chemistry, Zagreb, Croatia*

Copper oxide microparticles immobilized on diatomite surface were prepared by coating diatomite from solution of copper (II) salts under room condition followed by thermal transformatin or sintering at two different temperatures (900 $^{o}$C and 1100 $^{o}$C).
The purpose of these investigations was to develop a method for detection and identification of copper on modified diatomite. Characterisation of copper-modified diatomite was performed by abrasive stripping voltametry and compared with X-ray diffraction results on powdered samples (XRD) and scanning electron microscopy (SEM).
Abrasive stripping voltammetry is a technique in which microcrystals of water-insoluble compounds are mechanically immobilized on the surface of graphite electrode and immersed into an aqueous electrolyte to be studied by the voltammetric methods. It is used to analyse the chemical composition of solids and the redox state of electroactive ions in their structure. Metal identification is possible by the classical scheme of anodic stripping voltammetry: a cathodic potential is first applied to the sample-modified electrode, and a further anodic scan yields stripping oxidation peaks characteristic of metals existing in the sample. Additionally, cathodic scan can provide reduction peaks able to characterize higher oxidation states of metallic species in the microparticle, while the lower oxidation states can be detected by the anodic scans. Electrode reactions of microcrystals include transfer of anions between the aqueous phase and the solid phase. So, voltammetric responses are sensitive to the choice of aqueous supporting electrolyte.
XRD results obtained at different sintering temperatures reveal formation of mixtures of phases with tenorite (CuO) and cuprite (Cu2O) structures. Microstructure of the coppermodified diatomite changes on varying of sintering temperature as can be seen by SEM, rising of sintering temperature gains agglomeration.

First Regional Symposium on Electrochemistry of South-East Europe, Rovinj, Croatia, May 4-8, 2008.

P-2-102

# HUMIC POLYELECTROLYTE COMPLEXING CAPACITY DETERMINATION BY ION-SELECTIVE ELECTRODE POTENTIOMETRY

**T. Anđelković[1], J. Perović[1], R. Nikolić[1], M. Purenović[1], D. Anđelković[2], A. Bojić[1]**

*[1]Faculty of Sciences and Mathematics, University of Niš, Višegradska 33, 18000 Niš, Serbia, E-mail: ruzicanf@yahoo.com*

*[2]Water Work Association "Naissus", Kneginje Ljubice 1/1, 18000 Niš, Serbia*

The role humic acid (HA) play in a range of environmental issues is wide and various, due to theirs presence in water and soil as weel. The most important processes are: soil and water acidification, nutrient control, weathering, soil formation, soil structure, mobility and distribution of heavy metals, radioactive waste disposal, pesticides, xenobiotics, ecosystem buffering, etc. In almost all of those issues, cation binding is recognised to be an important factor.

In order to investigate the influence of carboxyl groups in cation-humic interactions, carboxyl groups were selectively blocked by esterification with the methanol-thionyl chloride procedure suggested by Schnitzer and Skinner (1966) and Hosangadi and Dave (1996), while influence of phenol groups was determined with acetylated humic derivative obtained by acetylation with acetic anhydride and $H_2SO_4$. Selective blocking of the functional groups was confirmed by FT-IR spectra of underivatized, esterified HA (EHA) and acetylated HA (AHA).

HA was obtained following the procedure suggested by the International Humic Substances Society (IHSS) from a well-humified organic horizon of old beech-forest soil (10 cm depth), in autumn 2003, using standard grinding equipment.

Ion-selective electrode (ISE) for cadmium was used to measure Cd complexation. The ISE experimental technique has been shown to be a reliable for measuring Cd concentrations in the range $10^{-7}$ to $10^{-2}$ M Cd in a complex organic matrix. Complexometric titrations were made with two Hach sension3 pH/ion-meters; one of them was used for pH measurements and the other was used with an ion selective electrode (ISE-Metrohm, 6.0502.110) for Cd(II) against an double junction Ag/AgCl reference electrode (Metrohm, 6.0726.100). For pH monitoring a Hach gel-filled combination glass electrode (51935-00) was used. Throughout the titrations a $N_2$ gas was initially bubbled through the solution and then a constant atmosphere was maintained above the solution which was thermostat in a water bath at 25.0 ± 0.1ºC. The pH of the solution was adjusted to 6.50 ± 0.05, by addition of minute amounts of diluted KOH or $HNO_3$. Titrations were performed with 40.00 ml of humic acid suspension, titrated with $5.19 \cdot 10^{-4}$ M $Cd^{2+}$ in ionic medium of 0.1M $KNO_3$.

Total acidity [$Ba(OH)_2$ method] and carboxylic acidity [$Ca(OAc)_2$ method] were determined according to Schnitzer and Gupta (1965), while phenolic acidity was determined by difference between total and carboxylic acidity.

The Scatchard plot for underivatized HA is curvelinear, as it was expected due to a range of binding sites with different binding energies on the humic macro-molecule. Also, a variety of electrostatic and conformational changes influencing the binding strength of functional groups contribute to the curvelinearity. For both HA derivatives, a range of binding sites with different binding energies can be ascribed, which is in agreement with literature data.

The total concentration of cation binding sites was 0.982 mmol $g^{-1}$ for HA, 0.424 mmol $g^{-1}$ for EHA, and 0.354 mmol $g^{-1}$ for AHA (Table), which indicates that 59.8% of humic acid metal binding sites can be attributed to carboxyl groups. This result obtained by the Scatchard plot is confirmed by the barium hydroxide and calcium acetate methods for total and carboxylic acidity determination. Thus, according to the obtained values of total acidity for HA and EHA (Table), 58.1% of humic acid proton binding sites can also be attributed to the carboxyl groups. Considering that the same percentage of COOH groups is involved in cadmium and in proton binding, our findings suggest that there is correlation between complexing capacities and carboxyl acidity in humic acid. Due to this correlation one can predict Cd-complexation capacity of HA on the base of COOH group content. Besides results obtained by comparison between underivatized and esterified humic acid, the observation is confirmed by calcium acetate determination of carboxyl acidity, when it is determined that carboxyl content of HA is 2.80 mmol $g^{-1}$ (60% of total acidity). Obtained values are consistent with view that roughly 50% of humic acidity is due to carboxyl moieties.

*Table. Conditional stability constants (K), complexing capacities ($C_C$), phenol (PA), carboxyl (CA) and total acidities (TA) for the underivatized and derivatized humic acids at 25 ± 0.1°C, pH = 6.50 ± 0.05 and ionic medium of 0.1M $KNO_3$ obtained according to Scatchard plots (obtained results from triplicated experiments)*

| | log K | $C_C$ (mmol $g^{-1}$) | PA | CA | TA |
|---|---|---|---|---|---|
| **HA** | 3.57 | 0.982 | 1.88 | 2.80 | 4.68 |
| **EHA** | 3.41 | 0.424 | 1.76 | 0.20 | 1.96 |
| **AHA** | 3.38 | 0.354 | 0.60 | 1.12 | 1.72 |

In conclusion, cadmium used in this study, showed a tendency to preferably associate with unmodified HA, due to higher content of carboxyl groups available for cadmium interaction. The differences in the total concentration of binding sites and conditional stability constants were directly related to availability of carboxylic groups for interaction with ions, indicating their importance in complexation. Acetylation decreased TA value due to transformation of ionizable groups to methyl ethers.

**References:**

1. E. Tipping, *Cation binding by humic substances*, Cambridge University Press, Cambridge, 2002.
2. G. Abate, J.C. Masini, *J. Braz. Chem. Soc.* 2001, **12**, 109.
3. A.S. Mathuthu, J.H. Ephraim, *Talanta* 1995, **42**, 1803.
4. D. Sparks, J. Bartels, J. Bigham (eds.) *Methods of Soil Analysis. Part 3. Chemical Methods*. Soil Science Society of America, Madison WI, 1996,USA.
5. B.D. Hosangadi, R.H. Dave *Tetrahedron Letterrs* 1996, **37**, 6375.
6. M. Schnitzer, S.I.M. Skinner *Soil Science* 1966, **6**, 361.
7. M. Schnitzer, U.C. Gupta, *Soil Sci. Soc. Proc.* 1965, **27**, 274.

First Regional Symposium on Electrochemistry of South-East Europe, Rovinj, Croatia, May 4-8, 2008.

P-2-103

# AZODYES ELECTROCHEMICAL OXIDATION ON MODIFIED NANOSTRUCTURED ELECTRODES

**M. Toma, R. Jitaru, M. Jitaru**

*Babes-Bolyai University, Faculty of Chemistry&Chemical Engineering, Associated Francophon Laboratory 11, Arany Janos street, 400028 Cluj-Napoca, Romania*
mjitaru@chem.ubbcluj.ro

Dyes are common pollutants in a large variety of industrial wastewaters, and the treatment of these wastes by electrocoagulation (EC) has been extensively studied in the literature. The electrocoagulation process is very effective in removing organic pollutants including dyestuff wastewater and allows for the reduction of sludge generation.

The purposes of this study were:

- To investigate the effects of the operating parameters, such as current density, electrolyte concentration, dyestuff concentration, pH of solution, on decolorization by continuous electrocoagulation;
- To obtain information about the dye removal efficiencies and reaction rate constants;
- Finally, the behaviors of decolorization according to dyestuff types were also examined.
-

Initially, a simple electrochemical cell was prepared with an anode and a cathode. Then the effect of each variable was studied separately using synthetic wastewater in a batch mode. The efficiency of the method tested was determined by measurement of color removal and reduction of Chemical Oxygen Demand (COD).

For dye solutions with COD of approximately 40 ppm and dye concentrations less than 150 ppm, high color removal (93%) was obtained when the pH ranged from 7 to 9, time of electrolysis was approximately 5 min, current density was 80-100 $A/m^2$, the temperature 280- 300 K. During the EC process under these conditions, the COD decreased was 75- 85%, depending on conditions.

First Regional Symposium on Electrochemistry of South-East Europe, Rovinj, Croatia, May 4-8, 2008.

P-2-104

# CHRONOPOTENTIOMETRIC STRIPPING METHOD IN THE ANALYSIS OF POLYMERIC ORGANIC MATERIAL IN SEAWATER

**S. Strmečki, M. Plavšić, B. Ćosović**

*RuđerBošković Institute Zagreb, Croatia, E-mail: strmecki@irb.hr*

Polymeric material, mainly polysaccharides (PS), represents the main fraction of phytoplankton organic exudates. Organic matter from seawater samples and from diatom culture *Skeletonema costatum* was electrochemically characterized. Emphasis was on the determination of N-containing polymeric organic material (N-PM) as well as surface active substances (SAS) and cooper complexing capacity (CuCC). Concentration of N-PM was expressed with respect to model protein - human serum albumin (HSA) which calibration plot is a straight line (Fig. 1.), and concentration of SAS with respect to nonionic detergent - Triton-X-100 (T-X-100) which calibration plot is an adsorption isotherm. HSA contains 15.7 % of nitrogen.

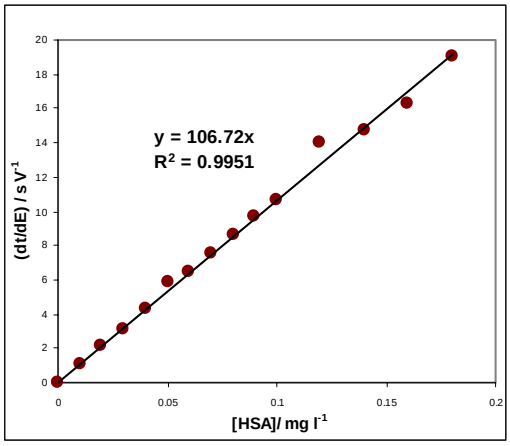


*Fig.1. Calibration plot of human serum albumin. Conditions in potentiometric analysis: deposition potential, $E_d$ = -0,6 V, time of deposition, $t_d$ = 60 s, constant stripping current, I = -1 μA.*

Measurements were performed with a μ-Autolab Analyzer (EcoChemie, Utrecht, The Netherlands) connected with a 663 VA Stand multimode system (Metrohm, Herisau, Switzerland). Static mercury drop electrode (SMDE) had the role of a working electrode, Ag/AgCl(3 M KCl) was a reference electrode and glassy carbon an auxiliary electrode.

N-PM have been determined using chronopotentiometric stripping analysis (CPSA) with a constant current stripping step [Tomschik et al., 1998], SAS using

phase sensitive a.c. voltammetry [Ćosović and Vojvodić, 1998] and CuCC using differential pulse anodic stripping voltammetry (DPASV) [Plavšić et al., 2003].
CPS signal is a result of a "presodium" catalysis of electroreduction of hydrogen ions. Nitrogen has an important role in this process; it carries hydrogen ions from bulk solution to the surface of mercury drop where they get reduced to form hydrogen, and peak "H" appears [Heyrovsky, 2006]. It is situated at a quite negative potential ($E_p$ = -1.70 to -1.80 V) while S-containing PM has "H" peak at $E_p$ ~ -1.50 V [Ciglenečki et al., 2003].

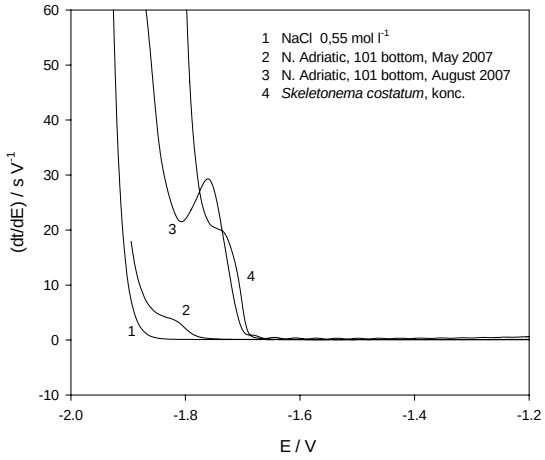


*Fig.2. CPS signals of analyzed solutions. The same conditions as in Fig. 1.*

N-PM from seawater samples and diatom culture give well define catalytic peaks (Fig. 2). In seawater sampled in May 2007, 6.10 μg $L^{-1}$ N-PM equivalent to HSA was found, while for the sample in August 2007 it was 161 μg $L^{-1}$. In S*keleonema costatum* culture medium the amount of N-PM was 63.7 μg $L^{-1}$.
The results show that a sensitive and fast CPS method can be usefully applied for the determination and characterization of different types of organic polymeric material in the seawater.

**References:**

1. Tomschik, M., Havran, L., Fojta, M., and Paleček, E., Constant current chronopotentiometric stripping analysis of bioactive peptides at mercury and carbon electrodes, *Electroanalysis* **10**, 1998, 403–409.
2. Ćosović. B., Vojvodić, V., Voltammetric analysis of surface active substances in natural seawater, *Electroanalysis* **10**, (6), 1998, 429-434
3. Plavšić, M., Electroanalytical techniques applied for studying the interaction of organic matter and particles with metal ions in natural waters, *Analytical Letters*, **36(1)**, 2003, 143-157
4. Heyrovsky, M., Research Topic-Catalysis of Hydrogen Evolution on Mercury Electrodes, *Croat. Chem. Acta*, **79** (2006) 1-4
5. Ciglenečki, I., Plavšić, M., Vojvodić, V., Ćosović, B., Pepi, M., Baldi, F., Mucopolysaccharides transformation by sulfide in diatom cultures and natural mucilage, *Marine Ecology Progress Series*, **263**, 2003, 17-23

First Regional Symposium on Electrochemistry of South-East Europe, Rovinj, Croatia, May 4-8, 2008.

P-2-105

# ELECTROCHEMICAL APROACH OF TIME DEPENDING REDOX TRANSFORMATION OF NATURAL ALIMENTARY DYES

**M. Jitaru, R. Jitaru, M. Toma**

*Babes-Bolyai University, Faculty of Chemistry&Chemical Engineering, Associated Francophone Laboratory 11, Arany Janos street, 400028 Cluj-Napoca, Romania*
*E-mail: mjitaru@chem.ubbcluj.ro*

All food dyes are carefully regulated in order to guarantee the food safety.
In theory, the natural or synthetic food dyes are likely to be oxidized or reduced. This behavior can be used either with the quantitative determination or with the destruction of azo bond by electrochemical way, by using like clean reagents the electrons, the ions hydroxyl and the protons. In addition, the dyes are subjected to the oxydo-reducing action of the enzymes and the transformations following the changes of pH.
In the continuity of our work in this field [1, 2] in this work was followed by cyclic voltammetry, using BAS100W electrochemical system and Autolab PGSTAT 12, the influence of the various electrochemical factors (nature of the material electrocatalytic, potential of electrode and density of the current) and of the chemical factors (composition of the medium pH, concentration), on the chronovoltamperometric answer of the natural food dyes obtained by the extraction.
The electrochemical behavior of the dyes was also followed under conditions similar to the human organism with an aim of establishing their electrochemical stability with pH, in the stomach and in the presence of physiological NaCl solution, like electrolyte.
During the cathodic sweeping of the potential the majority of the dyes, present one well defined reduction wave, strongly depending on pH, located in the field of -(200-920) mV, Fig.1.

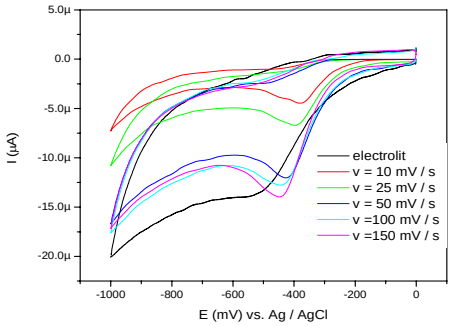


*Fig.1. CVs for electroreduction of cyanidine extracted from Aronia Melanocarpa*
*WE : CV ; RE: Ag/AgCl, AE : Pt*
*$C_{cyanidine}$ = 1.5 ×$10^{-3}$M ; electrolyte: 40 % EtOH + 60 % ascorbic acid*

With the positive potentials the current of oxidation of the grouping - N=N- and so proportional to the concentration, Fig.2
As notices general the processes of transfer of electrons of the natural dyes take place easier in the case of the natural dyes.

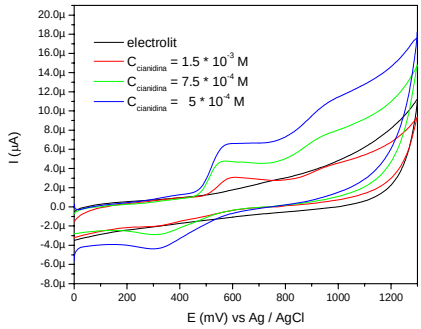


*Fig.2. CVs for electro-oxidation of cyanidine extracted from Aronia Melanocarpa*
*WE : CV ; RE: Ag/AgCl, AE : Pt*
*$C_{cianidină}$ = 1.5 ×$10^{-3}$M ; electrolyte: 40 % EtOH + 60 % ascorbic acid*

The voltamperometric data were used from analytical point of view and, on the other hand to establish the influence of the mentioned factors on the speed of degradation and stability of the dye either by electrochemical reduction (discoloration), or by oxidation (total mineralization).

**References:**

[1] Mihaela Lang, Elsa Weiss, Karine Groenen-Serrano, Andre Savall et Maria Jitaru *Cahier ELCONDES*, Ed. Casa Cartii de Stiinta, Cluj-Napoca, ISBN 973-686-712-9. 2005**,** 47-52.
[2] Marian Stan, Mihaela Lang, A.Savall, Karine-Groenen Serano, Elsa Weiss and Maria Jitaru *Studia Universitatis Babes-Bolyai Chemia*, 2006, **50(1)**.

First Regional Symposium on Electrochemistry of South-East Europe, Rovinj, Croatia, May 4-8, 2008.

P-2-106

# A NEW HIGHLY SENSITIVE POTENTIOMETRIC SENSOR FOR LOW LEVELS OF ANIONIC SURFACTANTS IN EFFLUENTS

**M. Sak-Bosnar[1]*, D. Madunić-Čačić[2], M. Kovačević[1], B.S. Grabarić[3]**

*[1]Department of Chemistry, Josip Juraj Strossmayer University of Osijek, F. Kuhača 20, HR-31000 Osijek, Croatia, E- mail: msbosnar@kemija.unios.hr*
*[2]Saponia, Chemical, Pharmaceutical and Foodstuff Industry, M.Gupca 2, HR-31000 Osijek, Croatia*
*[3]Faculty of Food Technology and Biotechnology, University of Zagreb, Pierottijeva 6, HR-10000 Zagreb, Croatia*

Anionic surfactants are widely used in numerous household and industrial product formulations, and in washing and industrial wastewater they can affect environmental water quality and organism. The use of surfactant sensitive sensors for the potentiometric determination of low concentrations of anionic surfactants has been described in several papers [1-3].

A new highly sensitive surfactant-selective liquid membrane electrode based on 1,3-didecyl-2-methyl-imidazolium-tetraphenylborate (DMI-TPB) ion-exchange complex as a sensing material has been prepared [4]. In the investigations described DMI-TPB sensor was tested for determination of anionic surfactants in effluents.

The sensor responded fast and exhibited a Nernstian response. Its main application was indication of the end-point in ion-pair surfactant potentiometric titrations. DMI-TPB sensor exhibits excellent selectivity performances for DS over almost all organic and inorganic anions investigated. The organic and inorganic anions commonly used in surfactant based industrial and household formulations, do not interfere in anionic surfactant potentiometric determination. The mixed solution method [5] has been used for measurement of selectivity coefficients.

Response characteristics of DMI-TPB based liquid membrane selective to the anionic surfactants given together with ± 95 % confidence limits.

| PARAMETERS | ANIONIC SURFACTANTS | |
|---|---|---|
| | DODECYLSULFATE | DODECYLBENZEN SULFONATE |
| Slope / (mV/decade) | 59.3 ± 0.6 | 57.8 ± 0.6 |
| Correlation coefficient (r) | 0.9993 | 0.9994 |
| Detection limit (mol/L) | $3.2 \times 10^{-7}$ | $6.0 \times 10^{-7}$ |
| Useful conc. range (mol/L) | $4 \times 10^{-7}$ - $5 \times 10^{-3}$ | $8 \times 10^{-7}$ - $6 \times 10^{-4}$ |

The titration curves obtained with $5 \times 10^{-4}$ mol/L titrant give very sharp inflexions (potential change at the equivalence point of approx. 190 mV), whereas those obtained using $1 \times 10^{-4}$ mol/L exhibit less pronounced, but still usable potential breaks. 1,3-didecyl-2-methylimidazolium chloride (DMIC) was used as standard cationic titrant.

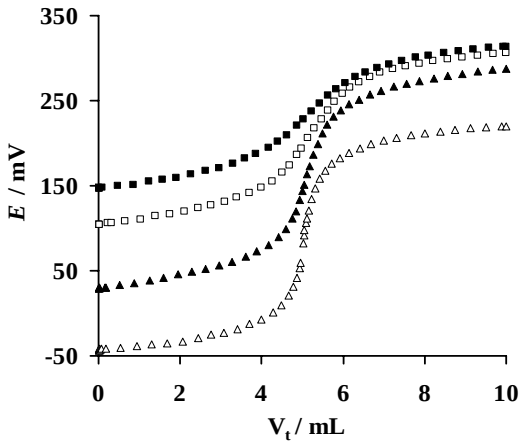


*Potentiometric titration of sodium dodecylsulfate solution with DMIC of several different concentration using DMI TPB surfactant electrode as indicator (■ $5x10^{-4}$ mol/L, □ $1x10^{-3}$ mol/L, ▲ $2x10^{-3}$ mol/L, Δ $4x10^{-3}$ mol/L).*

The sensor is used for titration of diluted industrial detergent products without pretreatment, except for those containing complexed surfactant mixture, where pH adjustment was needed. It was used for the monitoring of anionic surfactants in industrial wastewaters too, without pretreatment, except filtration when necessary. The equivalence points of slightly distorted titration curves or those with poorer and noisy inflexions can be calculated using multiple point parabola fit. The results obtained agree satisfactory with standard extraction-spectrophotometric MBAS (Methylene Blue Active Substance) method [6] for low concentration of anionic surfactants in effluents and surface waters. The average lifetime of the membrane was at least six months, depending on the nature of the analytes.

**References:**

[1] M. Gerlache, Z. Sentürk, J. C. Vire and J. M. Kauffmann, *Anal. Chim. Acta* **349**, (1997) 59-65

[2] S. Martinez-Barrachina, J. Alonso, L. Matia, R. Prats and M. del Valle, *Anal. Chem*. **71**, (1999) 3684-3691

[3] M. Sak-Bosnar, R. Matesic-Puac, D. Madunic-Cacic and Z. Grabaric, *Tenside Surf. Det.* **43**, (2006) 82-87

[4] D. Madunic-Cacic, M. Sak-Bosnar, R. Matesic-Puac, Z. Grabaric, *Sensor Lett*. **6** (2008) 1-8

[5] S. H. Hoke, A. G. Collins and C. A. Reynolds, *Anal. Chem.* **51** (1979) 859-862

[6] Water quality - Determination of surfactants - Part 1: *Determination of anionic surfactants by measurement of the methylene blue index (MBAS)*, **ISO 7875-1**, International Standardization Organization, Geneva, Switzerland 1996

First Regional Symposium on Electrochemistry of South-East Europe, Rovinj, Croatia, May 4-8, 2008.

P-2-107

# REMOVAL OF NITROPHENOLS FROM WASTEWATER BY ELECTROCHEMICAL WAY

**M. Tertis, M. Jitaru**

*Babes-Bolyai University, Faculty of Chemistry&Chemical Engineering, Associated Francophon Laboratory 11, Arany Janos street, 400028 Cluj-Napoca, Romania*
*mjitaru@chem.ubbcluj.ro*

The electrochemical reductions of nitrophenols were studied in aprotic solvents, such as DMF, and DMSO, but they have mainly been studied in protic solvents.
Even in so-called "aprotic" solvents, the radical anion of 4-NP is unstable, due to the acidic nature of the parent molecule, giving rise to a self protonation reaction, which is a very rapid step.
The electrochemical reduction of 4-nitrophenol (4-NP), Fig.1 and 2,6-dinitrophenol (2,6-DNP) in different conditions (0.2N $H_2SO_4$ and 0.1 M NaCl aqueous solution) were studied in this work. In the case of 4-NP the cathodic materials were nickel and graphite, and the electrochemical reduction processes were performed in two different reactors (two compartment reactor type filter-press, and undivided electrochemical reactor, both with electrolyte recirculation). In the case of 2,6-DNP the cathode was made from graphite using two compartment reactor with electrolyte recirculation. The experimental processes were pursued by different methods: cyclic voltammetry (BAS100), and spectrophotometry in UV-Visible (Unicam Helyos B and DR/2000 HACH); $\lambda_{max}$ = 318 nm for 4-nitrophenol and $\lambda_{max}$ = 440 nm for 2,6-DNP.

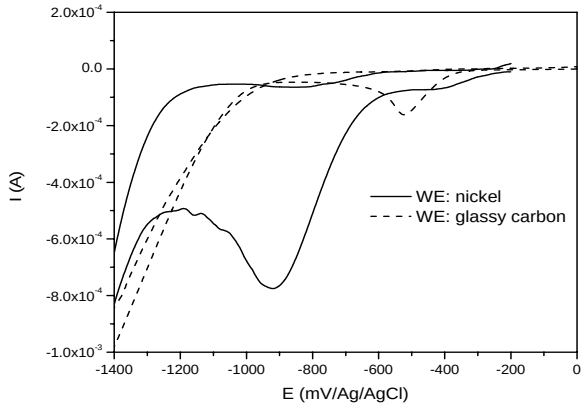


*Fig.1. Cyclic voltammograms for a ($10^{-2}$ M) 4-NP solution in 0.2N $H_2SO_4$ WE: GC and Ni; RE: Ag/AgCl,KCl; CE: Pt; v : 50mV $s^{-1}$; s: 100 µA $V^{-1}$.*

The reduction potential strongly depends on pH, both for 4-NP and 2,6-DNP. The first peak potential, $Ep_1$ for 2,6-DNP, shows two linear regions with different slopes, corresponding to an acid behavior specific to nitrophenols values (pKa = 4-5) [14]. The first peak height reaches the maximum value in acidic media.

The variation of the peak intensity and the peak potential with the scan rate was studied. An approximately linear relationship was found between the reduction peak intensity of p-NP and the first peak intensity for 2,6-DNP, both corresponding to the reduction of one nitro group, to the corresponding hydroxyle amines, and the square root of the scan rate. The peak potentials were found to move slightly more negative when

The absorbance of 2,6-DNP solution, Fig.2, diminishes with approximately 75% in the first 15 minutes, comparative tot he initial value, (theoretical calculated time is 20 minutes) and the discouloration is continuing (99% after 100 minutes).

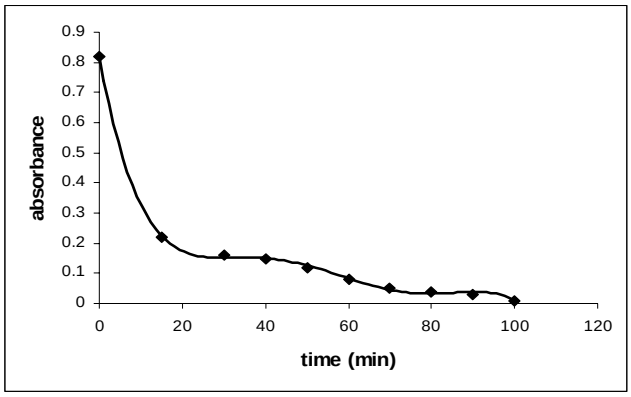


*Fig.2. Spectrophotometric control of electrochemical reduction process for $4.5 \times 10^{-5}$M 2,6-DNP in (0.1N) NaCl, on graphite cathode (experimental set-up C). $\lambda_{max}$ = 440 nm; log Є = 3.58.*

The summarized average results (two determinations for every case) are presented in Table1.

*Table 1. Synoptic presentation of experimental determinations.*

| Experimental set-up | Treated nitrophenol | Cathodic material | Initial concentration (mol $l^{-1}$) | Flow rate of recirculation (ml $min^{-1}$) | Nitrophenol removal (%) |
|---|---|---|---|---|---|
| A | 4-NP | nickel | $10^{-3}$ | 3.3 | 94.2 |
| B | 4-NP | graphite | $10^{-2}$ | $1.2 \times 10^{3}$ | 90.6 |
| C | 2,6-DNP | graphite | $4.5 \times 10^{-5}$ | $1.4 \times 10^{3}$ | 99.0 |
| | 2,6-DNP | nickel | $4.5 \times 10^{-5}$ | $1.4 \times 10^{3}$ | 98.8 |

The experimental determinations demonstrated practically 65-99% removal yield for the both nitro derivatives, depending on the experimental conditions. The best result have been obtained, in the case of 4-NP, in undivided electrochemical reactor with graphite electrode (90% of 4-NP removal), and in the case of 2,6-DNP the final removal was of 99% in two compartment reactor with graphite cathode.

***Acknowledgements:*** *This work has been supported by Romanian CEEX – MATNANTECH No.68/2006*

First Regional Symposium on Electrochemistry of South-East Europe, Rovinj, Croatia, May 4-8, 2008.

P-2-108

# THE ELECTROPHORETIC COATING ON CARBON STEEL FOR ELIMINATION OF CREVICE CORROSION

**A. Lame (Galo)[1], M. Hysenagolli (Saraçi)[2]**

[1]*Department of Chemistry, Faculty of Natural Sciences University of Tirana, Albania, Laboratory of corrosion, E-mail: alketalame@yahoo.com*
[2]*Department of Chemistry, Faculty of Natural Sciences University of Tirana, Albania, Laboratory of corrosion (Diploma student), E-mail: marselasaraci@yahoo.com*

This article presents the way we can coat a material, such as carbon steel. Before this method was used, there have been many problems with crevice corrosion especially when we did experiments using potenciostatic and electrochemical noise methods. Therefore, in our case, electrophoretic coating is used to avoid crevice corrosion. The experiments are carried out using carbon steel 45, and all the coating material is deposited on the surface of the metal. This deposit protects the metal from corrosion and the layer that is formed is opaque. Electrophoretic coating is used not only for protection against corrosion but it has some other benefits as well, such as high resistance, which means that the electrophoretic process assures a long lasting. Furthermore, among other benefits we would mention; its suitability for external usage even in adverse environments, it has high efficiency, which implies that the production efficiency of electrophoretic equipment is much higher than the electroplating equipment and finally, by using this method we can protect precious metals without causing any damage to their appearance.

*Keywords:* electrophoretic coating, crevice corrosion.

First Regional Symposium on Electrochemistry of South-East Europe, Rovinj, Croatia, May 4-8, 2008.

P-2-109

# THE INHIBITION CORROSION OF CARBON STEEL IN HYDROCHLORIC ACID BY USING N-ACETYL P-AMINOBENZENE SULFONAMIDE

**A. Patru Samide[1,*], I. Bibicu[2], E. Turcanu[1], M. Preda[1]**

[1]*University of Craiova, Faculty of Chemistry, Calea Bucuresti 107i, CP 200585, Craiova, Romania, samide_adriana@yahoo.com*
[2]*National Institute of Materials Physics,077125 Magurele, Bucharest, Romania*

Treatments with organic compounds have been proposed in order to improve anticorrosion protection. A large number of aliphatic and aromatic compounds containing nitrogen, oxygen and sulphur atoms are found to cause a distinct decrease in corrosion rates of steel in hydrochloric acid [1-4]. The present study aims to determine the role of new inhibitor N-acetyl *p*-aminobenzene sulfonamide (APAS) in improving the protection film in case of generalized corrosion of carbon steel in hydrochloric acid.The corrosion and inhibition behavior of carbon steel in 2 M HCl in the presence of N-acetyl *p*-aminobenzene sulfonamide (APAS) was investigated using weight loss measurements and electrochemical measurements. The morphology of carbon steel surface was investigated by using scanning electron microscopy(SEM) and Mössbauer spectrometry. The percentage inhibition efficiency (P) of APAS for carbon steel were determined in HCl 2M solution in the presence of some variable concentrations of inhibitor: 0.1 mM; 0.2 mM; 0.3 mM; 0.4 mM.
The values of inhibition efficiency increase with APAS concentration reaching a maximum value of 76.5 % at 0.4 mM, from electrochemistry measurements (P/EM), nearly equal than the value obtained from loss weight data, 74.2% (P/W).Figure 1 is as example.

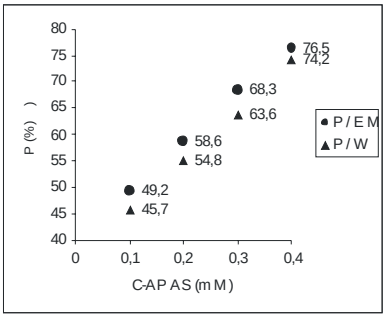


*Figure 1. Variation percentage protection efficiency obtained by loss weight(P/W) and percentage protection efficiency obtained by electrochemical measurements(P/EM) with the concentration of APAS for the carbon steel in 2M HCl, at room temperature*

Mössbauer spectroscopy shows in the case of the corroded samples in a solution of 2M HCl containing of APAS that the process of corrosion is considerable slowed and a superficial compound of $Fe^{3+}$ without a magnetic arrangement is formed. By estimating its relative area, this compound has a smaller thickness than the layer formed in the corrosion process without inhibitor. The Mössbauer parameters of

superficial compound found on corroded sample in solution without inhibitor show the presence of $Fe^{3+}$ species and are similar to those shown by amorphous $Fe^{3+}$ oxyhydroxides, superparamagnetic α-FeOOH and/or γ-FeOOH, β-FeOOH, β-FeOOH and γ-FeOOH and Fe $(OH)_3$. At this stage it is expected that the main product of corrosion is a non-stoichiometric amorphous $Fe^{3+}$ oxyhydroxide, consisting of a mixture of α, β and γ-FeOOH. The Mössbauer parameters of the compound found for the corroded sample in the solution with inhibitor do not differ significantly from the precedents parameters. We consider that the APAS inhibitor acts as an incipient "rust transformer" and favors the formation of a "superficial closed layer". The inhibitor transforms some constituents of rust into corrosion inhibiting oxide phases.

The morphology of carbon steel surface after corrosion in 2 M HCl solution, and in HCl solutions containing different concentrations of APAS was examined with an electronic microscope VEGA TESCAN (Figure 2). Figure 2 shows the evidence of formation a protective film on the surface of carbon steel. It can be concluded that the inhibitor molecules are adsorbed on the carbon steel surface.

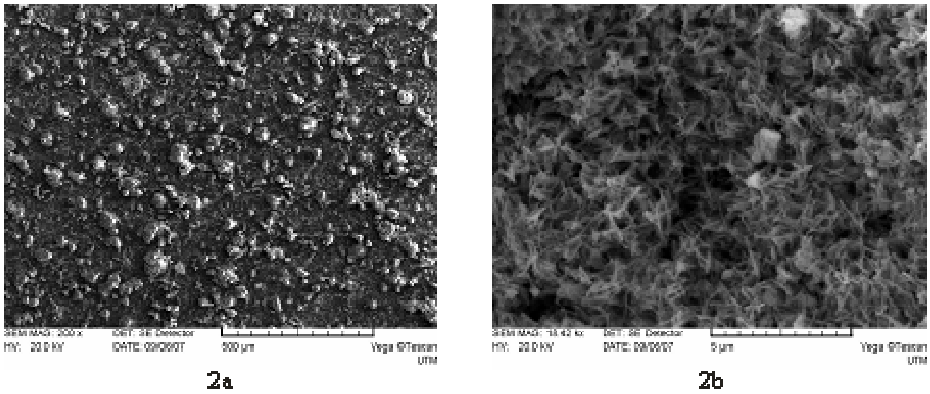

2a 2b

*Figure 2. Scanning electron micrograph of the carbon steel surface treated in: (2a) 2M HCl solution; (2b) 2M HCl/0.4 mM APAS*

*The authors thank for the financial support of the CNCSIS/Grant-Program 592 and 751/2007 competition*

**References:**

[1]. L. Larabi, Y. Harck, M. Traisnel, A. Mansri, *J. Appl. Electrochem.* **34** (2004) 833
[2]. A. Samide, I. Bibicu, M. S. Rogalski, M. Preda, *Corr. Sci.* **47** (2005) 1119
[3]. A. Samide, I. Bibicu, M. S. Rogalski, M. Preda, *Rev. Chim.* **54** (2003) 927
[4]. E. S. Ferreira, F. C. Giacomelli, A. Spinelli, *Mat. Chem.Phys.* **83** (2004)136

First Regional Symposium on Electrochemistry of South-East Europe, Rovinj, Croatia, May 4-8, 2008.

P-2-110

# "SWEET" OR $CO_2$ CORROSION STUDY BY SEM (EDAX) TECHNIQUE

**A. Llabani, Z. Gaçe, M. Prifti**

*University of Tirana, Faculty of Natural Sciences, Department of Chemistry;*
*E-mail albertallabani@yahoo.com*

"Sweet" or $CO_2$ corrosion of carbon steel pipelines steel remains a problem of great practical and economical concern for the oil and gas industry. Steps in $CO_2$ corrosion process are four:

1. Formation of reactants (chemical species in the bulk)
2. Transportation of reactants (bulk to surfaces)
3. Electrochemical reactions at the surface
4. Transportation of products (surface to bulk)

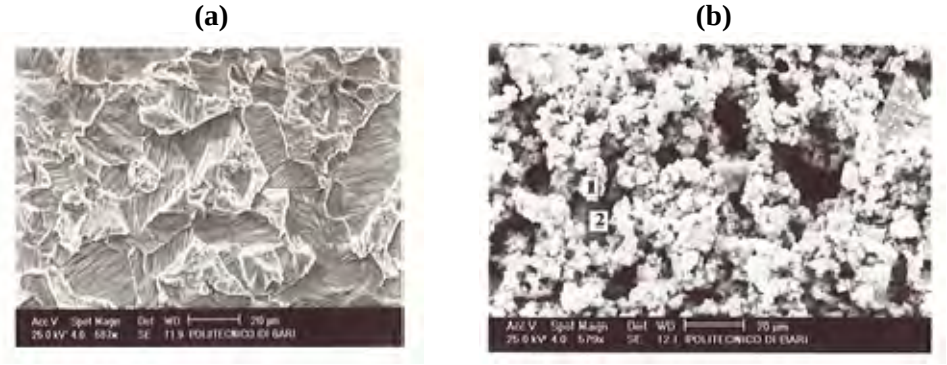


*Fig. 1: SEM images of the coupon after 240 hours under flowing conditions (900rpm) at temperature 25°C after exposure: (a) in brine solutions, (b) in $CO_2$ saturated brine solutions.*

The combined effect of flow and dissolved gases, such as hydrogen sulphide ($H_2S$) and carbon dioxide ($CO_2$), is very important in oil and gas industry [1], [2]. $CO_2$ corrosion of carbon steel has been the subject of a number of excellent studies [3], [4]. The objectives of this research were to identify the effect of $CO_2$ in a brine stirring solution on the corrosion morphology of carbon steel. A carbon steel was tested in brine solution, saturated with $CO_2$ (sweet environment) at 25°C, pH = 5.3 and with high speed stirring (900 rpm) to ensure turbulent flow conditions. Scanning electron microscope SEM (EDAX) method was used to analyse corrosion products and to study surface morphology. The mild steel used for the experiments has the following composition in wt. %: C 0,24, Si 0,20, S 0,50, P 0,014, Mn 0,02, Ni 0,06, Cr 0,01, Mo 0,02, Cu 0,03, W 0,01, Ti 0,02. Specimens were in the form of coupons having dimensions of 40mm x 30mm x 3mm. The test duration was fixed at 10 days. The corrosion specimens were fully immersed in the natural brine solutions. Three specimens were run

simultaneously for weight loss measurements. The decreasing of the pH value from 7.74 (before bubbling $CO_2$) to 5.3 (after bubbling $CO_2$) is also a reason for the high value of corrosion rate of carbon steel in $CO_2$ saturated brine solutions. Thus it can be seen from Figures 1 (b) that this carbon steel after exposure in $CO_2$ saturated brine solution exhibit uniform corrosion and is not sensitive to pitting corrosion. Research has shown that $CO_2$ increases the corrosion rate of carbon steel from 0,12837 mm/y to 0.31801 mm/y. In $CO_2$ saturated brine solutions, $CO_2$ is the dominant corrosive species in the system. Under the test conditions of our study, the de Waard and Milliams Nomogramm for Prediction of Steel Corrosion in $CO_2$ Systems [5], predicts a corrosion rate which is in good agreement with the corrosion rate obtained for $CO_2$ saturated brine solution. Examination of a sample of the deposit on the surfaces of the coupon under a scanning electron microscope with EDAX analysis facilities showed it to be iron based with significant levels of oxygen, chloride; calcium and carbon also being present. The absence of the sulphide ions on the surface of the steel is also confirmed by the results of EDAX analysis. These results suggest that in $CO_2$ saturated brine solutions, $CO_2$ is the dominant species in the system. The test solution in this case can be considered as being a sweet one. Based on the experimental results the following conclusions can be drawn:

The experimental results by weight loss method in this study are in good agreement with the predicted value using De. Ward and Milliams Nomogramm for prediction of steel corrosion in $CO_2$ Systems.

The corrosion morphology of carbon steel in $CO_2$ saturated brine solutions (sweet system), under the test conditions in this study, is uniform.

**References:**

1. Llabani A, Gace Z.; Chemical Inhibition of Flow Induced Localized Corrosion (FILC) in $CO_2$/$H_2S$ Containing Media in Oil and Gas Industry, *XI Balkan Mineral Processing Congress*, Albania, 2005, 399-406.
2. Llabani A, Gace Z.; Corrosion of Carbon Steel in Brine Solution of Crude Oil; (13-P-517), *EUROCORR 2004*; 12-16 September, (2004), Nice, France.
3. Gray Tremaine L.G.S.; Effect of pH and temperature on the Mechanism of carbon steel corrosion by Aqueous carbon Dioxide, *CORROSION 90*, paper no. 40 Houston, TX, NACE, International, (1990).
4. De Waard et al, Influence of liquid flow velocity in $CO_2$ corrosion of carbon steel, *Corrosion* , **95**, 128/1 – 128/15, (1995).
5. de Waard C., Lotz U., and Milliams D.E, Predictive Model for $CO_2$ Corrosion Engineering in Wet Natural Gas Pipelines, *Corrosion*, **47(12)**, (1991) 976.

First Regional Symposium on Electrochemistry of South-East Europe, Rovinj, Croatia, May 4-8, 2008.

P-2-111

# EFFECT OF HEXAMETHYLPARAROSANILINE CHLORIDE (CRYSTAL VIOLET DYE) ON MILD STEEL CORROSION IN ACIDIC MEDIA

**E.E. Oguzie[1], V.O. Njoku[2]**

[1]*Electrochemistry and Materials Science Research Laboratory, Department of Chemistry, Federal University of Technology Owerri, PMB 1526, Owerri. Nigeria*
[2]*Department of Chemistry, Imo State University, PMB 2000, Owerri. Nigeria,*
*E-mail: viconjoku@yahoo.com*

The corrosion inhibition of mild steel in 0.5 M $H_2SO_4$ and 1 M HCl by hexa_methylpararosaniline chloride (HMPC) was investigated using the gravimetric technique in the temperature range 303 – 333K. The results indicate that HPMC inhibited the corrosion reaction in both acid media at all temperatures and inhibition efficiency increased with HMPC concentration. The inhibiting action is attributed to general adsorption of protonated and molecular HPMC species on the corroding metal surface. Adsorption followed a modified Langmuir isotherm and the Temkin isotherm, with very high negative values of the free energy of adsorption ($\Delta G°_{ads}$). An increase in temperature reduced the inhibition efficiency of HPMC in 0.5 M $H_2SO_4$ but increased efficiency in 1 M HCl. Activation parameters such as activation energy ($E_a$), activation enthalpy ($\Delta H^*$) and activation entropy ($\Delta S^*$) as well as the adsorption heat ($Q_{ads}$) were evaluated from the effect of temperature on corrosion and inhibition processes.

*Keywords:* Adsorption, inhibition efficiency, Arrhenius equation, Eyring equation, kinetic-thermodynamic model.

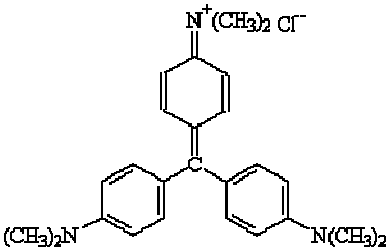


*Molecular structure of HMPC*

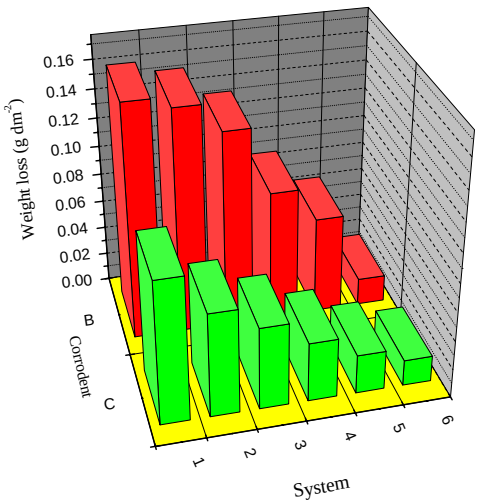


*Effect of different concentrations of HPMC on the corrosion of mild steel in (B) 0.5 M $H_2SO_4$ and (C) 1 M HCl; [1 = Blank; 2 = 0.0001, 3 = 0.001, 4 = 0.01, 5 = 0.1, 6 = 1.0 mM]*

First Regional Symposium on Electrochemistry of South-East Europe, Rovinj, Croatia, May 4-8, 2008.

P-2-112

# PLANT EXTRACTS AS ENVIRONMENTALLY FRIENDLY INHIBITORS FOR THE ACID CORROSION OF MILD STEEL

**E.E. Oguzie[1], V.O. Njoku[2]**

*[1]Electrochemistry and Materials Science Research Laboratory, Department of Chemistry, Federal University of Technology, PMB 1526, Owerri, Nigeria, E-mail: oguziemeka@yahoo.com*
*[2]Department of Chemistry, Imo State University, PMB 2000, Owerri. Nigeria*

Corrosion inhibition of mild steel in 2 M HCl and 1 M $H_2SO_4$ by extracts of selected plants was investigated using a gasometric technique at temperatures of 30 and 60°C. The studied plants materials include leaf extracts *Occimum viridis (OV), Telferia occidentalis (TO), Azadirachta indica (AI)* and *Hibiscus sabdariffa (HS)* as well as extracts from the seeds of *Garcinia kola (GK)*. The results indicate that all the extracts inhibited the corrosion process in both acid media by virtue of adsorption and inhibition efficiency increased with concentration. Synergistic effects increased the inhibition efficiency in the presence of halide additives. Inhibition mechanisms were deduced from the temperature dependence of the inhibition efficiency as well as from assessment of kinetic and activation parameters that govern the processes. Comparative analysis of the inhibitor adsorption behaviour in 2 M HCl and 1 M $H_2SO_4$ as well as the effects of temperature and halide additives suggest that both protonated and molecular species could be responsible for the inhibiting action of the extracts.

*Keywords:* Mild steel; Acid corrosion; Plant extract: Inhibition: Halide ions: Synergism.

*Table 1. Major chemical constituents of the studied plants*

| Plant | Major constituent |
|---|---|
| ***Occimum viridis*** | Mono and triterpenoids, ascorbic acid, carotenoids, aromatic oils |
| ***Azadirachta indica*** | Tannins, triterpenoids |
| ***Hibiscus sabdariffa*** | Ascorbic and amino acids, flavonoids, β-carotene |
| ***Telferia occidentalis*** | Amino acids, flavonoids |
| ***Garcinia kola*** | Primary and secondary amines, flavonoids, unsaturated fatty acids |

First Regional Symposium on Electrochemistry of South-East Europe, Rovinj, Croatia, May 4-8, 2008.

P-2-113

# ANTICORROSIVE PERFORMANCE OF POLYPYRROLE / ZINC-MOLIBDATE COATINGS ON STEEL ELECTRODE

**C. Pirvu[1], M. Mindroiu[1], P. Drob[1]**

*[1]Faculty of Applied Chemistry and Materials Science University Politehnica Bucharest, c_pirvu@chim.upb.ro*
*[2]Institute of Physical Chemistry "Ilie Murgulescu"*

## Aim

The morphology, electrochemical features and anticorosive performances of polypyrrole / zinc-molibdate surfaces on steel electrode were characterized.

## Experimental

The electrochemical measurements were performed with a potentiostatic / galvanostatic assembly Zahner of three electrodes: a working electrode, a platinum counter-electrode and a reference electrode (Ag/AgCl). The corrosion studies were conducted in 3% NaCl testing solution. Open circuit potential, cyclic voltammetry and electrochemical impedance measurements were used to monitor the layer performance during immersion in NaCl testing solution.
In order to improve the anticorrosive properties of polypirrole films the zinc-coated steel surfaces was pre-treated with cerum and molybdenum salts. The results are presented by comparation with chromium passivated surfaces in order to avoid using of chromium (VI) for corrosion prevention of zinc-coated surfaces.
A single-step electropolymerization of pyrrole on zinc-coated steel electrodes was investigated under several techniques (potentiodynamic, galvanostatic and potentiostatic modes) in tartrate aqueous medium.
The corrosion behaviour of zinc-molibdate steel electrode, electrochemical modified by polypyrrole films were estimated by open circuit potential, DC polarization and electrochemical impedance spectroscopy in 3% NaCl aggressive solution.
The electrodeposited conducting polymers were characterized for their morphology, and microstructure by electrochemical atomic force microscopy (EC-AFM).

## Conclusions

The obtained results show that the polypyrrole / zinc-molibdate coatings on steel electrode present good anticorrosive abilities by modifying of corrosion potential and reduction of corrosion current.

***Acknowledgements:*** *This paper was supported by the National Romanian CEEX program in the frame of the project ECOMATICA No. 216/2006. The authors gratefully acknowledge their financial support.*

First Regional Symposium on Electrochemistry of South-East Europe, Rovinj, Croatia, May 4-8, 2008.

P-2-115

# CORROSION POTENTIAL OF 304L STAINLESS STEEL IN THE NEUTRAL SULPHATE SOLUTION

**J.P. Popić[1], B.V. Jegdić[2], D.M. Dražić[1]**

*[1]IHTM - Department of Electrochemistry, Njegoševa 12, Belgrade, Serbia*
*E-mail: popicj@eunet.yu*
*[2]Institute GOŠA, Milana Rakića 35, Belgrade, Serbia*

The potentiodinamyc testings of electrochemical behavior of the 304L stainless steel in the deaerated neutral sulfate solution have shown existence of two corrosion potentials. Forming of these two corrosion potentials are result proceeding two different reaction mechanisms of hydrogen evaluation on the stainless steel.
These experiments were performed on the 304L austenitic stainless steel (0.03% C + 18.9% Cr + 9.22% Ni), in the deaerated solution 0.1 M $Na_2SO_4$, pH 6. Polarisations of steel electrode were conducted in the region of potential from 0.1 to 1.6 V and oposite, from 1.6 to 0.1 V, in the continuity. Polarisations were performed with scan rate from 0.4 to 2 mV $s^{-1}$ at the different rate electrode rotations (900 to 3600 rpm).

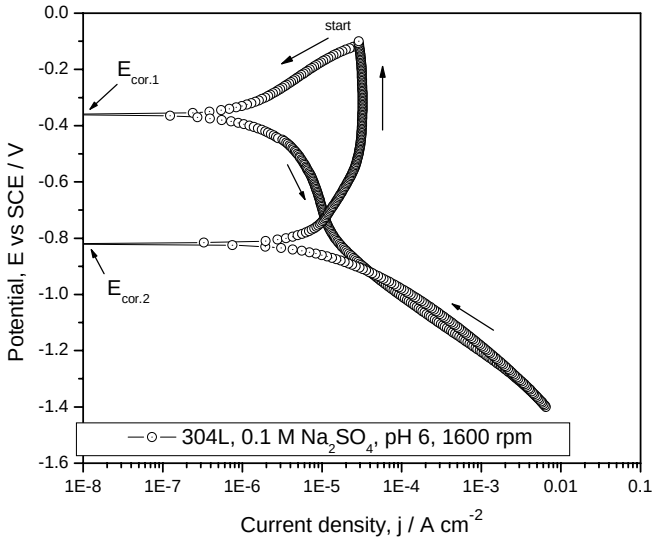


*Figure 1. Anodic and cathodic polarisation curves of the stainless steel in 0.1 M $Na_2SO_4$, pH 6, v=2 mV $s^{-1}$, w=1600 rpm.*

Figure 1. shows anodic and cathodic polarisation curves of the stainless steel in sulfate solution. Corrosion potential $E_{cor.1}$ which establishes spontaneously after introduction of steel electrode in solution, takes place as mixed potential of anodic process of dissolution steel through the passive layer and cathodic process of evaluation hydrogen on passive layer. During the time, anodic process inhibits, while cathodic process remains unaffected. As a result, corrosion potential, $E_{cor.1}$, becomes more positive.

The current density of hydrogen evaluation reaction (after cathodic polarisation of steel from $E_{cor.1}$), obtained border value, which spread to the potential at ~ -0.9 V. In this region, neither rate cathodic process is diffuse controled, nor the significant change occurs by decreasing potential scan rate. It is obvious (Fig. 2) that the current density stabilizes on the value ~ 3 μA $cm^{-2}$, by holding potential at -0.6 V. Hydrogen evaluation rate increases by polarisation steel to more negative potentials than -0.9 V and obtain Tafel strain line with slope ~ -0.17 V $dec^{-1}$.

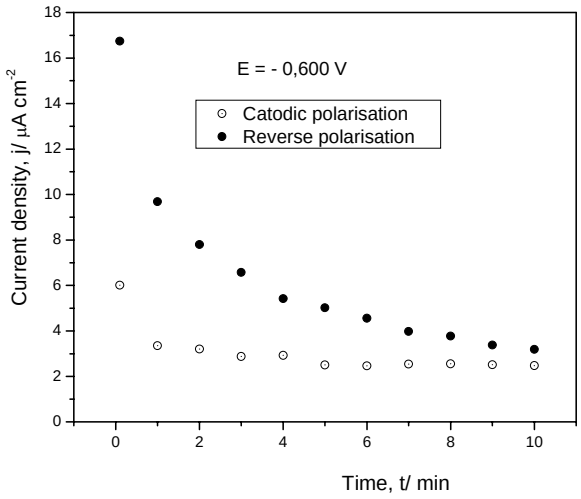


*Figure 2. Change of current density of the stainless steel at potential -0.6 V. Solution 0.1 M $Na_2SO_4$, pH 6, w=1600 rpm.*

These results lead to the conclusion that in the region of potentials more negative than -0.9V, hydrogen evaluation is activation controled, and performed with the mechanism of direct discharge of water molecules. In the region of potential at $E_{cor.1}$ to -0.9 V hydrogen evaluation process begins to flow with the discharges of the $H^+$ ions. These $H^+$ are the result of dissociation of water molecules catalised by the oxide layer present on the steel surface.

During the oposite polarisation, other corrosion potential $E_{cor.2}$ establishes on the steel, which has more negative value for ~0.45 V according to $E_{cor.1}$. During the anodic polarisation of steel (from the corrosion potential $E_{cor.2}$ to -0.1V), anodic current density obtained border value. The border anodic current density increases when previous cathodic polarisation reaches higher negative potentials, or holds the potential of steel in cathodic region. Holding electrode potential on value -0.6V (Figure 2), the anodic current density exponentially decreased by the time and reaches the value around 3 μA$cm^{-2}$. This behavior of steel is in accordance to earlier obtained results in the acidic solutions[1], and it is the result of flowing electrochemical process of anodic oxidations of absorbed hydrogen in the passive steel.

These results lead to the conclusion that the corrosion potential $E_{cor.2}$ establishes as mixed potential by cathodic process hydrogen evaluation with mechanism of direct discharging of water molecules and anodic process hydrogen oxidation which is absorbed in the passive steel. Corrosion potential $E_{cor.1}$ on steel establishes when all absorbed hydrogen is oxided,

**Reference:**

1. B.V. Jegdić, D.M. Dražić, J.P. Popić, *J. Serb. Chem. Soc.*, **71(5)**, 2007., 543

First Regional Symposium on Electrochemistry of South-East Europe, Rovinj, Croatia, May 4-8, 2008.

P-2-116

# ELECTROCHEMICAL STUDY OF AISI 316L STEEL AFTER WELDING

**S. Kožuh[1]*, M. Gojić[1], T. Sorić[2]**

*[1]Faculty of Metallurgy, University of Zagreb, Aleja narodnih heroja 3, 44103 Sisak, Croatia,*
**E-mail: kozuh@simet.hr*
*[2]INA d.d., Šubićeva 29, 10000 Zagreb, Croatia*

The results of electrochemical corrosion testing of plates made from AISI 316L austenitic stainless steel, with a thickness of 15 mm, are presented. Before welding the plate surfaces were thoroughly cleaned and brushed. The welding of V-joints was carried out with the Böhler FOX SAS 4-A electrodes. After welding, specimens of the base and weld metals were cut into samples (ϕ5 mm) for electrochemical measurements.

Electrochemical measurements were performed at room temperature using a conventional three-electrode cell with a platinum counter electrode. The potentials were recorded with respect to a Ag/AgCl reference electrode. A rotating (1500 rpm) disc electrode prepared from the AISI 316L base and weld metals was used as a working electrode. Each specimen was wet-grounded to a 800 and 900 grit surface and then polished with $Al_2O_3$ (0.5 μm alumina). Finally, the working electrode was ultrasonically cleaned in ethanol and dried.

The subject of investigation was the corrosion behavior of the base and weld metals as dependent on a protective passive film formed on the steel surface following exposure to 3.5 % NaCl (pH=5.0). Before the experiment the solution was deaerated with nitrogen for 600 s to keep the system free of dissolved oxygen. The time for reaching the stabilized open circuit potential was 900 s. The corrosion properties of the base and weld metals were examined by means of cyclic polarization and electrochemical impedance spectroscopy methods. Before each measurement the working electrode was cathodically polarized at –1.0 $V_{Ag/AgCl}$ for 300 s. Cyclic polarization was performed in the potential range from –1.0 to +2.0 $V_{Ag/AgCl}$ at different scan rates (10, 50, and 100 $mVs^{-1}$). Impedance measurements were carried out in the range of potential where hydrogen evolution reaction exists and in the passive region (from –0.2 to +0.5 $V_{Ag/AgCl}$).

Pitting corrosion is considered to be of a great practical interest in structure engineering [1]. The cyclic polarization curves clearly showed the pitting corrosion resistance of the weld metal to be a bit superior to that of the base metal (Figure 1). The pitting potential ($E_{pit}$) of the weld metal was more positive (0.586 V) than of the base metal (0.472 V), but repassivation potentials ($E_{rp}$) were the same. The corrosion resistance of alloys is known to depend also on the individual material capability for repassivation. Pitting is prevented only if $E_{rp}>E_{pit}$, and from cyclic polarization curves it was evident that $E_{rp}<E_{pit}$ (Figure 1). The changes in the polarization curves as a result of increasing scan rate were insignificant for base metal only. The active to passive transition takes place at the critical current equal to the current of passivity. A relatively wide plateau of the potential-independent current indicated that passivity was present over a broad potential region (from –0.2 to +0.5 $V_{Ag/AgCl}$).

The impedance plots (Figure 2a) measured at –1.0 $V_{Ag/AgCl}$ showed a capacitive loop with relatively low values of charge transfer resistance. Such behavior was attributed to the hydrogen evolution reaction. In the potential region between –0.2 and +0.5 $V_{Ag/AgCl}$ the impedance plots were characterized by the passive region (Figure 2b). The Nyquist plots showed a higher charge transfer resistance for the weld metal than for the base metal suggesting an enhanced thickness of the passive film on the weld metal surface. Better corrosion properties of the weld metal could also be accounted for by higher molybdenum and chromium contents [2, 3].

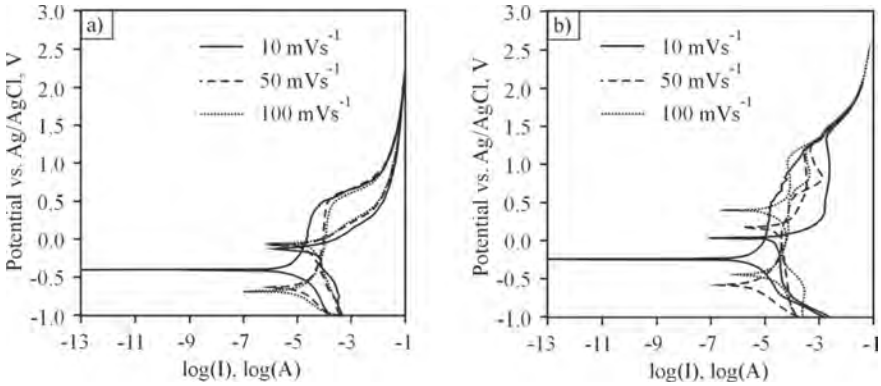


*Figure 1. Cyclic polarization curves of AISI 316L base (a) and weld (b) metals in 3.5% NaCl solution in the potential range from –1.0 $V_{Ag/AgCl}$ to +2.0 $V_{Ag/AgCl}$ at different scan rates*

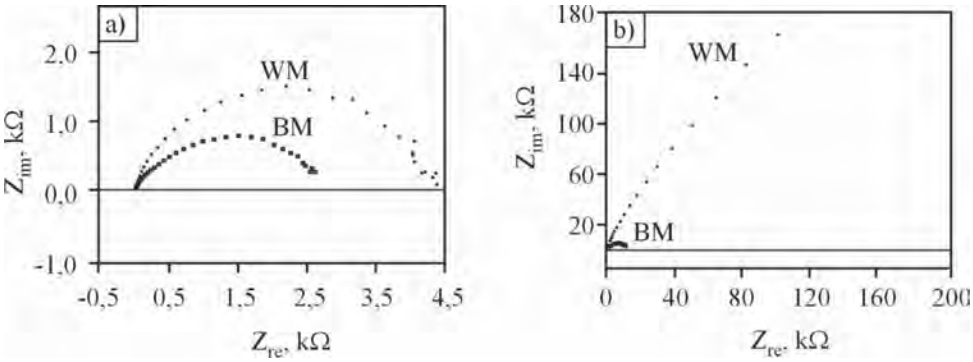


*Figure 2. Nyquist impedance diagrams of AISI 316L base and weld metals in 3.5 % NaCl solution at –1.0 $V_{Ag/AgCl}$ (a) and at 0.0 $V_{Ag/AgCl}$ (b)*

**References:**

1. Gooch, T. G., *Welding Research* **75** (1996) 5, 135s-154s.
2. Hashimoto, K., Asami, K., Kawashima, A., Habazaki, H., Akiyama, E., *Corrosion Science* **49** (2007) 1, 42-52.
3. Bastidas, J. M., Torres, C. L., Cano, E., Polo, J. L., *Corrosion Science* **44** (2002) 3, 625-633.

First Regional Symposium on Electrochemistry of South-East Europe, Rovinj, Croatia, May 4-8, 2008.

P-2-117

# ELECTROCHEMICAL CORROSION BEHAVIOR OF AN ANTIBACTERIAL STAINLESS STEEL

**Y. Liu[1], J. Li[2], E.E. Oguzie[3], Y. Li[2], D. Chen[1], K. Yang[1], F. Wang[2]**

*[1]Center for Engineering Materials, Institute of Metal Research (IMR), Chinese Academy of Sciences (CAS), 72 Wenhua Rd., Shenyang 110016, China*
*[2]State Key Laboratory for Corrosion and Protection (SKLCP), Institute of Metal Research (IMR), Chinese Academy of Sciences (CAS), 62 Wencui Rd., Shenyang 110015, China*
*[3]Electrochemistry and Materials Science Research Laboratory, Department of Chemistry, Federal University of Technology Owerri, PMB 1526, Owerri. Nigeria*
*E-mail: oguziemeka@yahoo.com*

A new antibacterial stainless steel (ASS) with martenstic microstructure has been recently developed as a new functional material having broad-spectrum antibacterial properties. The electrochemical behavior in 0.05 mol/L NaCl was assessed - using linear polarization, electrochemical impedance spectroscopy (EIS), and Mott-Schottky analysis. A contrasting stainless steel (SS) containing no copper was also studied as a control to determine the copper effect. The ASS exhibited higher corrosion susceptibility in the chloride medium; with a more negative (active) corrosion potential, higher anodic current density and lower charge transfer resistance. This is attributable to the occurrence of copper-catalyzed interfacial reactions. 3-D presentation of EIS data was employed in analyzing electrochemical corrosion processes as well as probing complex interfacial processes.

*Keywords:* Antibacterial stainless steel (ASS); Linear polarization; Electrochemical impedance spectroscopy (EIS)

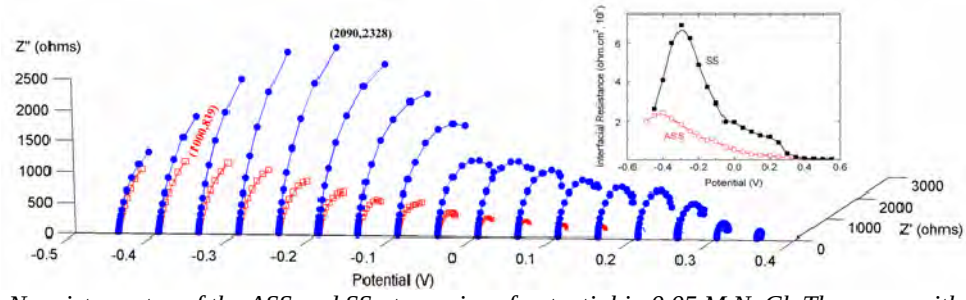


*Nyquist spectra of the ASS and SS at a series of potential in 0.05 M NaCl. The curve with the solid (empty) square is of the ASS (SS) sample. The inset shows the interfacial resistance which is obtained by fitting the data based on an equivalent circuit $R_s(QR)$.*

First Regional Symposium on Electrochemistry of South-East Europe, Rovinj, Croatia, May 4-8, 2008.

P-2-118

# INHIBITION PROPERTIES OF TRITON-X-100 ON FERRITIC STAINLESS STEEL IN SULPHURIC ACID AT INCREASING TEMPERATURE

**R. Fuchs-Godec**

*Faculty of Chemistry and Chemical Engineering, University of Maribor, Smetanova 17, 2000 Maribor, Slovenia, E-mail: fuchs@uni-mb.si*

Corrosion problems have received a considerable amount of attention because of their attack on materials especially in high aggressive media. It is well known that surfactants can drastically change the interfacial properties and hence are used in many industrial processes such as emulsification, cosmetics, drug delivery, chemical mechanical polishing, enhanced oil recovery, and also as corrosion inhibitors [1,2]. The adsorption of surfactants on the metal surface is influenced by a number of factors [3]. The increasing temperature is one of these influential factors being responsible for the improving or worsening of the inhibition efficiency of the chosen surfactant. The objective of the present work was to study the effect of a non-ionic surfactant TRITON-X-100 as inhibitor of processes on stainless steel (SS), type X4Cr13. The inhibition of this SS in aqueous solutions of 1 mol $L^{-1}$ $H_2SO_4$ was studied using the potentiodynamic polarization method whose were performed at five temperatures ranging from 25 to 45 °C. Thermodynamic parameters such as adsorption heat, adsorption entropy and adsorption free energy were obtained from experimental data of the temperature studies of the inhibition process in the absence and presence of inhibitor in the temperature range mentioned above.

We applied the conventional three-electrode configuration to conduct the potentiodynamic studies. All the potentials were measured against the saturated calomel electrode (SCE) and the counter electrode was made from Pt. The surface coverage $\theta$ was calculated via the kinetic parameters measured in corrosion processes as well as the polarization resistance $R_p$, and the corrosion current density $i_{corr}$. We found that the TRITON-X-100 inhibitor behaviour in the selected temperatures range can be fitted to the Flory-Huggins adsorption isotherm [4], which has a form as follows:

$$\log\left[\frac{\theta}{c_{inh}}\right] = \log(xK) + x\log[1-\theta] \qquad (1)$$

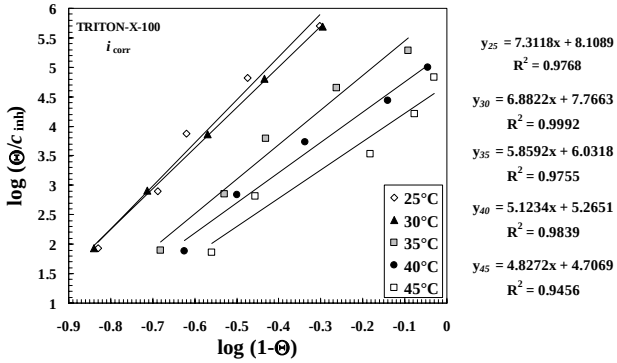


*Fig.1: Flory-Huggins adsorption isotherm for TRITON-X-100 on SS type X4Cr13 in 1.0 M $H_2SO_4$ obtained from the corrosion current density ($i_{corr}$).*

According to the Flory-Huggins model, plots of log[$\theta$/C] versus log[1 − $\theta$] give straight lines of slope ($x$) and intercept log($xK$) as showing in Fig.1. The data indicate that the values of $x$ changed from 7.3 to 4.8 with increasing temperature. This suggests that one molecule of adsorbed TRITON-X-100 on the metal surface replaces more than 7 water molecules at 25°C and reduced to less than 5 at 45°C.

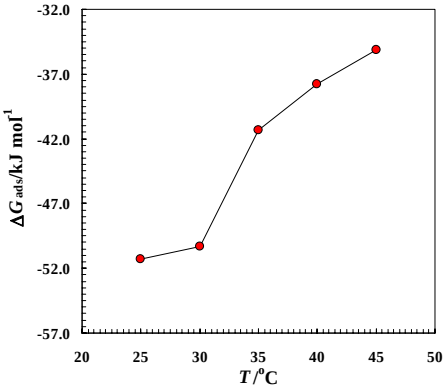


*Fig .2: The free energy of adsorption $\Delta G_{ads}$ for TRITON-X-100 in 1.0 M $H_2SO_4$ investigated in the the range of temperatures 25–45 ℃.*

All values of $\Delta G_{ads}$ are negative (Fig.2), suggesting therefore the spontaneity of the adsorption process. With increasing temperature $\Delta G_{ads}$ increases. One possible explanation of this effect is that the adsorption gets unfavourable with increasing temperature as the result of desorption of inhibitor from the steel surface. Another is that the dynamics of the anodic process at higher temperatures is more destructive. Such behaviour reduces the possibility of adsorption of organic molecules on the metal surface.

Good inhibition efficiency of TRITON-X-100 on SS type X4Cr13 in 1.0 M $H_2SO_4$ was limited to temperatures below 35°C or at the surfactant concentration higher than $c$ = 0.001 mol $L^{-1}$ (Fig.3).

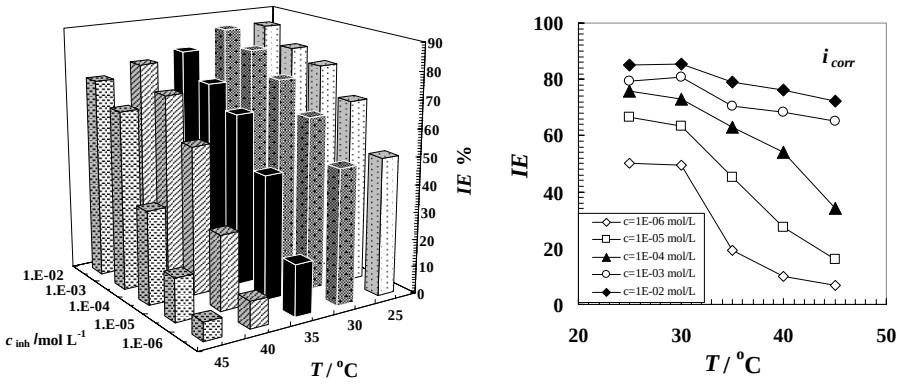


*Fig. 3: The corrosion inhibition efficiency (IE = θ × 100) for TRITON-X-100 in 1.0 M $H_2SO_4$ (obtained from $i_{corr}$) investigated in the range of temperatures 25–45 °C.*

## References:

1. M. Bouklah, B. Hammouti, M. Lagrenée and F. Bentiss, *Corr. Sci.*, **48** (2006) 2831.
2. M. A. Migahed, Mater. *Chem. &Phys*., **93** (2005) 48.
3. S. Paria, K. C. Khilar, Adv. *Colloid & Interface Science*, **110** (2004) 75.
4. R. Fuchs-Godec, *Electrochim. Acta*, **52** (2007) 4974.

First Regional Symposium on Electrochemistry of South-East Europe, Rovinj, Croatia, May 4-8, 2008.

P-2-119

# CORROSION RESISTANCE OF NANOSTRUCTURED HYBRID SOL-GEL COATINGS

**R. Raicheff[1], G. Chernev[2], V. Zaprianova[2], D. Ivanova[2], B.Samuneva[2], P. Djambazki[2]**

*[1]1nstitute of Electrochemistry and Energy Systems –Bulgarian Academy of Sciences, Sofia 1113, Bulgaria, E-mail: raicheff@bas.bg*
*[2]University of Chemical Technology and Metallurgy, Sofia 1756, Bulgaria*

The improved mechanical and corrosion resistance is one of most substantial demand for high performance coating systems. The inorganic-organic hybrid materials offer various opportunities to combine the desirable properties of polymers (elasticity, toughness) with those of inorganic solids (hardness, chemical and thermal resistance). In this respect, the sol-gel method provides an appropriate route for preparation of hybrid coating materials with universal properties that can be easily applied to most metallic substrates. The obtained coatings may have an improved adhesion to the metal surface as well high abrasion and corrosion resistance. The aim of the present work is to produce inorganic-organic nanostructured sol-gel coatings and to study their structure and corrosion resistance.

The silica hybrid coating materials were synthesized by sol-gel technology at room temperature using three types of silicon precursors – methyltriethoxysilane (MTES), ethyltrimethoxysilane (ETMS) or vinyltrimetoxysilane (VTMS) as well as methyl-methcrylate (MMA) as an organic material in different proportions (5-20 wt.%). The coatings were deposited on mill steel substrates by dipping at controlled rate of 15 cm/min. The obtained transparent homogeneous layers (thickness 5-8 μm) were dried for 24 hours at room temperature and thermally treated at various tempertures (50 - 200 $^{o}$C) in air atmosphere.

The structure and surface morphology of the hybrids and the obtained coatings were studied by means of FT-IR, XRD, BET-Analysis, EDS, SEM and AFM methods. The potential sweep technique (Princeton Corrosion Measurement System, PAR 263A potentiostat with Soft Corr III package) was applied for electrochemical corrosion measurements and characterization of corrosion resistance of the coatings. As model corrosive environment 0,5M $Na_2O_4$ solution at 25 $^{o}$C was used.

The X-ray diffraction analysis showed that all hybrids obtained have basically an amorphous structure but the type of the XRD patterns indicates that some processes of ordering have also taken place. The FT-IR spectra proved the presence of strong chemical bonds (such as Si-O-C, Si-C, etc.) between inorganic and organic parts in all hybrid coatings. The presence of a chemical bond of the ETMS-based hybrid coating with iron from the substrate is also established, which is in accordance to the good adhesion and protective properties of this type of coating. The data from BET analysis showed that the surface area of the coatings is in the range of 90 to 310 $m^2/g$ and it decreases with increase of the content of the organic part (MMA).

The surface morphology of the hybrid coatings was studied by AFM. As seen in the AFM micrographs and the height distribution profiles of surface roughness of typical samples with different precursors (cf. Fig.1), a heterogeneous surface structure with well defined nanounits is observed in all cases. The average size of the nanoparticles is from 5 to15 nm.

The surface topography and structure of nanobuilding blocks in each coating however are different and depend on the chemical composition of the hybrid material. It was established that the surface roughness decreases with increase of the quantity of the organic component in all hybrids studied.

The electrochemical measurements illustrate the good protective properties and corrosion resistance of all hybrid coatings (Figs. 2). The coatings affect both partial corrosion reactions (anodic metal dissolution and cathodic oxygen reduction), but it decreases more strongly the anodic reaction and leads to a considerable decrease (more than an order of magnitude) of the corrosion rate of the steel substrate. It also established that the protective ability of the coatings with all precursors enhances considerably with increase of the portion of the organic compound in the hybrid material. The temperature of thermal treatment of the coatings affects the corrosion resistance of the coatings, obviously due to additional densification of the hybrid structure, but the effect is rather mild. The results of the present study suggest possible applications of the obtained silica hybrid materials as transparent coatings with good adhesion and good protective properties.

***Acknowledgements:*** *The financial support of the Bulgarian NSF under contract №VU-TN-102 is gratefully acknowledged.*

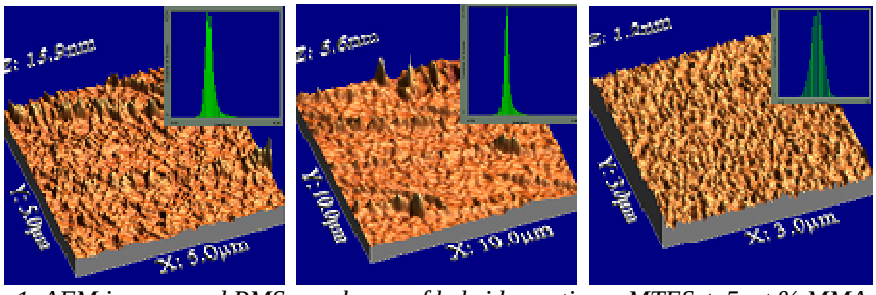

*Fig.1. AFM images and RMS roughness of hybrids coatings: MTES + 5 wt.% MMA (a); ETMS + 5 wt.% MMA (b); VTMS + 5 wt.% MMA (c)*

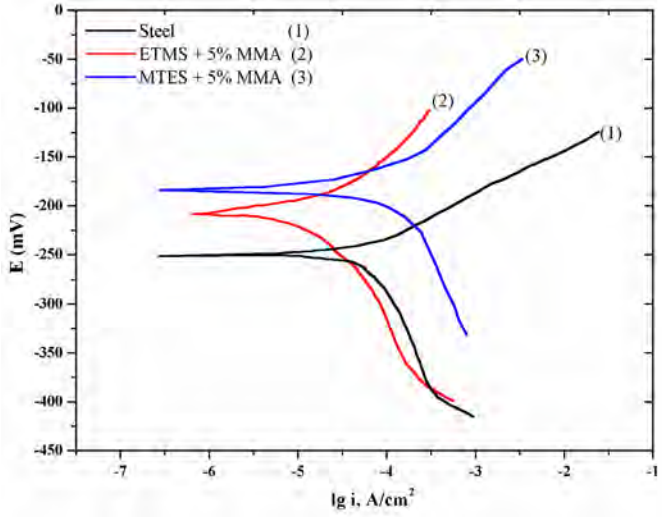


*Fig.2. Potentiodynamic polarization curves of steel substrate (1) and steel with coatings containing: ETMS + 5 wt.% MMA (2); MTES + 5 wt.% MMA (3), dried at 25$^0$C*

First Regional Symposium on Electrochemistry of South-East Europe, Rovinj, Croatia, May 4-8, 2008.

P-2-120

# THE STUDIES OF PASSIVE FILMS FORMED ON 316L STAINLESS STEEL SURFACES FOR ORTHOPEDIC IMPLANT APPLICATIONS BY USING MÖSSBAUER SPECTROSCOPY

**I. Bibicu[1], A. Patru Samide[2,]*, A. Ciuciu[2], M. Preda[2]**

[1] *National Institute of Materials Physics str. Atomistilor nr. 105 bis, Magurele-Bucharest,Romania*
[2]*University of Craiova, Faculty of Chemistry, calea Bucuresti 107i, Craiova, Romania*
samide_adriana@yahoo.com

Metals and alloys are widely used as biomedical materials and indispensable in the medical field. The most important property of biomaterials is safety. Therefore, corrosion resistant materials such as stainless steel are employed. Metals ions released into human bodies do not always damages the bodies. The partner for combination with metals ion is very important. Every molecule has chance to combine with the ion. Reactions between the surface of metallic materials and living tissues are the initial events when the materials are implanted in human body. Tissue compatibility is governed by the reactions in the initial stage. In this regard, the surface properties of materials are important [1-3]. In this study the surface behaviour of 316L stainless steel in the lipid solution (in vivo) is discussed comparatively with the surface of the same 316L stainless steel implanted in a femur for 1 year (in vivo). The surfaces of 316L stainless in vitro and in vivo were studied by Mössbauer spectroscopy. Measurements were performed at room temperature in the transmission (TMS) and conversion electron spectroscopy (CEMS) [4] using a conventional constant-acceleration spectrometer with a $^{57}$Co-Rh source. In the $^{57}$Fe Mössbauer spectroscopy the penetration depth maximum of conversion electron is of the order of 250 nm. The CEMS measurements were conducted with a high degree of accuracy, ensuring the same geometry of the detection space and same gas flow rate for all the samples. The parameters of the Mössbauer spectra were calculated using a computer-fitting program, which assumed a Lorentzian line shape. The isomer shifts were referred to α-Fe. All spectra (TMS and CEMS) show a central broad line, typical for austenitic stainless steels.

We will present and discuss the CEMS spectra. We used for them 3 variants for data fit: single line, doublet and two lines. The best fitting of the spectrum measured for reference (uncorroded) surface sample was obtained for single line The parameters of this line were following: position –0,11 mm/s; width 0,41 mm/s; effect 12.5%.

The best fitting of the CEMS spectra obtained for corroded sample in lipid solution. (Figure 1) gives also a single line with identical parameters within experimental errors except the effect, comparatively with reference sample. This means that the surface was, practically, insignificant changed during corrosion process. Mössbauer measurements do not point out micro-structural changes on surface in the investigated samples. The effect decrease proves the presence of a superficial layer on corroded samples. The Mössbauer spectroscopy confirms, thus, the uniformity, compactness and stability of the superficial passive films and the corrosion resistance of our stainless steel in the tested conditions.

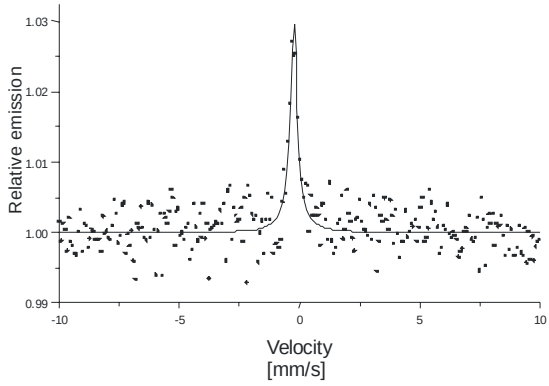


*Figure 1. Conversion electron Mössbauer spectra of of 316L stainless steel corroded in lipid solution (• data; — fit)*

In Figure 2 is shown the CEMS spectrum of the implanted samples. In this case the best fit was obtained for a doublet. The relative areas of the two lines are: 27% and 73%. It is clear that during implantation a change in the superficial microstructure took place and a corrosion process was presently. Another difference between the reference sample and implanted sample consists in a decrease of the intensity line for implanted sample. This proved the presence of a thin superficial layer formed during implantation process. We believe that surface layer consist mainly of oxidic species. A slight improvement of the goodness of the fit, within the experimental errors, was obtained for implanted sample by using a sextet line near 2 lines. This fact suggests a possible apparition of a ferrite phase on surface.

*The authors thank for the financial support of the CNCSIS/Grant-Program, 592/2007 competition*

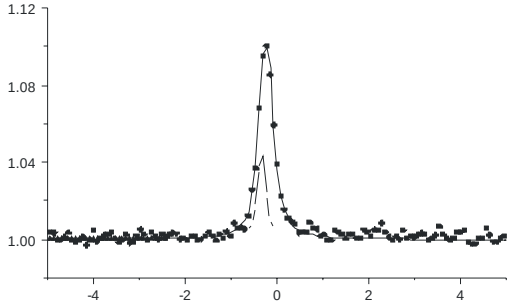


*Figure2. Conversion electron Mössbauer spectrum of the surface after 1 year implant in the femur (• data; ── fit; —▲— line 1; —▼— line 2).*

**References:**

[1] B.Tutunaru, A. Patru Samide, I. Bibicu, M. Preda, *JOAM* **11**, (2007) 3400
[2] T. Hanawa, *Corrosion Engineering*, **49** (2000) 687.
[3] T. Hanawa, S*cience and Technology of Advanced Materials*, **3** (2002) 289.
[4] I. Bibicu, M.S. Rogalski, G. Nicolescu, *Meas. Sci. Technol*. **7** (1996) 113.

First Regional Symposium on Electrochemistry of South-East Europe, Rovinj, Croatia, May 4-8, 2008.

P-2-121

# CORROSION BEHAVIOUR OF BLACK LAYERS ONTO ALUMINUM INVOLVING ALTERNATIVE CURRENT ELECTROLYSIS

**L. Anicai, A. Florea**

*Div.of Ecological Technologies Development, PETROMSERVICE SA,*
*Calea Grivitei 8-10, 010772, Bucharest, Romania, lanicai@itcnet.ro*

Electrochemically produced black thin films on various metallic substrates are widely used for an efficient conversion of solar energy in thermal energy. A major goal to reduce the costs and improve the thermal performance is to get surfaces with high solar absorptance ($\alpha$) and low thermal emittance ($\varepsilon$). Also, the formed black layers should be characterized by good stability when they are exposed to environmental conditions including aggressive atmosphere, both from color maintaining and corrosion resistance view points. Aluminum and its alloys are the most attractive metallic substrates, due to their lightness and high strength to weight ratio, associated with excellent thermal and electrical conductance, good reflectivity and low working cost

The paper presents some experimental results dealing with electrochemical synthesis and corrosion behavior of various black layers types onto Al substrates, suitable to be used as selective absorber coatings in the case of thermal energy production from solar energy, involving a.c. electrochemical coloring of aluminum anodic oxides using $AgNO_3/H_2SO_4$, $NiSO_4$ based solutions.

The obtained black layers are characterized by a good throwing power, homogeneity, smoothness and adherence, as shown by SEM and AFM investigations. Also, they present a good solar absorption and low values of infrared emittance.

To evaluate the resistance of black coating layers against corrosion, several accelerated corrosion tests have been performed, respectively: (i) continuous immersion in 0.5M NaCl for 408 hours with intermediary visual examinations and recording of corrosion potential; (ii) salt mist test for 336 h with intermediary visual examinations (ii) potentiodynamic polarization curves in 0.5M NaCl; (iii) impedance spectra in 0.5M NaCl at open circuit potential using a Zahner IM6e potentiostatic equipment.

According to the obtained results, the black layers formed using a.c.electrolysis involving $NiSO_4$ based electrolytes exhibited corrosion currents of around 1-2 $\mu A/cm^2$ as compared with values of 8-10 $\mu A/cm^2$.

The EIS spectra showed the same evolution, materialized by polarization resistances for the initial moment of immersion of about 300 k$\Omega$ in the case of Al/Ni a.c. systems and around 26 k$\Omega$ for Al/Ag a.c. ones. When immersion period increased, the film resistance decreased correspondingly, so that after 408 hours of conditioning values of about 10-12 k$\Omega$ for Al/Ni a.c. systems have been determined; in the case of Al/Ag a.c. systems, after 144 hours of immersion the black color was degraded and polarization resistances diminished towards 4 - 5 k$\Omega$.

The corrosion performances are discussed taking into account the applied preparation procedures.

First Regional Symposium on Electrochemistry of South-East Europe, Rovinj, Croatia, May 4-8, 2008.

P-2-122

# THE INFLUENCE OF ALUMINIUM SURFACE MODIFICATION ON THE CORROSION STABILITY OF POLYESTER COATING

**J.B. Bajat[1,*], V.B. Mišković-Stanković[1], S. Vještica[1], J.P. Popić[2], D.M. Dražić[2]**

*[1]Faculty of Technology and Metallurgy, Karnegijeva 4, Belgrade, Serbia,*
*[2]ICTM - IEC, Njegoševa 12, Belgrade, Serbia, jela@tmf.bg.ac.yu*

The influence of the aluminium substrate modification on the corrosion stability of a protective system based on polyester coating was investigated. The aluminium surface was modified by silane film, anodizing (with and without siling) and by phosphating.

The protective properties of these coatings were investigated by different methods: electrochemical impedance spectroscopy (EIS), adhesion pull-off measurements and by NMP test, i.e. determining the N-methyl pyrolidone retention time (NMPRT).

By fitting of EIS experimental data the values of pore resistance were determined and are plotted as function of time of exposure to 3 % NaCl in Fig. 1.

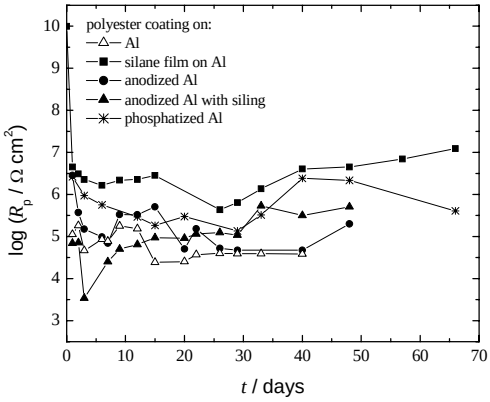


*Fig. 1. Time dependence of pore resistance, $R_p$, for polyester coatings on aluminium and modified aluminium, during exposure to 3% NaCl.*

The general trend of the decrease in pore resistance with time [1-3] is observed for all samples. Initially, during the first few days for all samples, the pore resistance decreases as a consequence of the water uptake [4,5]. The saturation period follows when the values of pore resistance remain almost constant over a longer period of time indicating the maintenance of good protective properties of the polyester coating [6]. The highest values of $R_p$ for poyester coating on aluminium modified by silane film indicate the highest corrosion stability of this protective system.

Both the dry and wet adhesion of polyester coatings on aluminium and modified aluminium were measured by the standard pull-off method. The dry adhesion was

not possible to measure by this method, since there was always cohesive failure for all protective systems. However, the highest NMPRT, indicating the highest adhesion, was obtained for polyester coating on aluminium modified by silane coating.

The changes in pull-off adhesion strength with time of immersion in 3 % NaCl solution, for different protective systems, are shown in Fig. 2. The adhesion of polyester coating on aluminium modified by silane film is not shown in Fig. 2 as in all examined cases we were not able to measure the pull-off strength on this substrate, since the failure was always cohesive, indicating the excellant adhesion of polyester coating on aluminium modified by silane film.

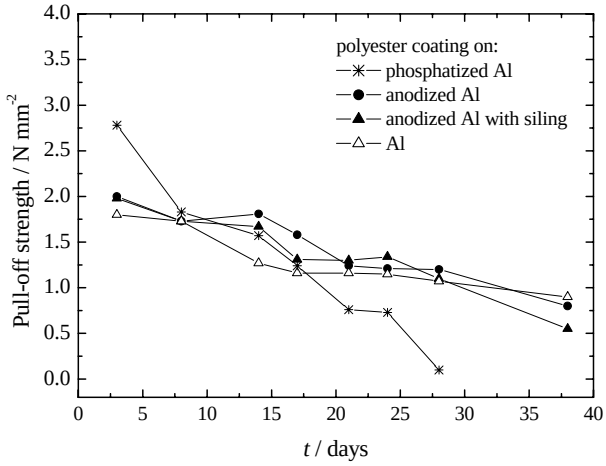


*Fig. 2. The pull-off strength for polyester coatings on aluminium and modified aluminium, during exposure to 3% NaCl.*

The general trend of the initial decrease in adhesion strength is observed for all other samples. The highest pull-off adhesion strength was observed for the initial time of exposure to 3 % NaCl for polyester coating on phosphatized aluminium but, as can be seen from Fig. 2, values of wet adhesion for this protective system sharply drop during immersion in NaCl solution.

Based on these results it could be concluded that silane film is favorable in forming strong bonds with polyester coating.

It was also shown that for protective systems investigated in this work EIS results correlate well with adhesion measurements obtained both with a pull-off and NMP test.

**References:**

[1] F.Deflorian, L.Fedrizzi, S.Rossi, P.L.Bonora, *Electrochim.Acta* **44** (1999) 4243.
[2] U.Rammelt, G.Reinhard, *Prog.Org.Coat.* **21** (1992) 205.
[3] J.B.Bajat, V.B.Mišković-Stanković, *Prog. Org. Coat.* **49** (2004) 183.
[4] J.B.Bajat, M.D.Maksimović, V.B.Mišković-Stanković, S. Zec, *J.Appl.Electrochem.* **31** (2001) 335.
[5] F.Deflorian, V.B.Mišković-Stanković, P.L.Bonora, L.Fedrizzi, *Corros.Sci.* **50** (1994) 438.
[6] D.M.Dražić, V.B.Mišković-Stanković, *Prog.Org.Coat.* **18** (1990) 253.

First Regional Symposium on Electrochemistry of South-East Europe, Rovinj, Croatia, May 4-8, 2008.

P-2-123

# VINYLTRIETHOXYSILANE COATINGS ON ALUMINUM

**Ž.S. Jovanović, V.B. Mišković-Stanković, J.B. Bajat**

*Faculty of Technology and Metallurgy, University of Belgrade, P.O. Box 3503, Karnegijeva 4, 11120 Belgrade, Serbia, E-mail: vesna@tmf.bg.ac.yu*

Trialkoxysilanes (silanes) are hybrid organic-inorganic compounds with general formula $X_3Si(CH_2)_nY$, where X is an alkoxy group (ethoxy-, methoxy-) and Y is an organofunctional group (vinyl-, mercapto-, amino-). Silanes are bonded to metal surface via silanol groups, SiOH, formed by hydrolysis of X-groups, and to organic film via Y-group. The silane layers deposited on aluminum alloys provide both, adhesion promotion and corrosion protection.[1,2]

The vinyltriethoxysilane coatings (VTES), $CH_2=CHSi(OC_2H_5)_3$, on aluminum were deposited on the metal surface previously degreased by alkaline solution at 65-75 °C, rinsed with deionised (DI) water and air dried. Silane solutions were prepared by silane disolving in ethanole/DI water mixture. The silane/DI water/ethanole ratio was 2/6.5/91.5 v/v for 2 vol. % and 5/5/90 v/v for 5 vol. % silane solution. The solutions were stirred for 1 h and then aged in ambient conditions for 2 days before use. The coatings were deposited at different values of deposition time (30 s, 10 min) and curing time at 100 °C (10 min, 30 min).

The corrosion behavior of aluminum pretreated with VTES films was investigated during exposure to 3 wt. % NaCl solution using potential–time measurements, electrochemical impedance spectroscopy (EIS), gravimetric liquid sorption measurements and adhesion measurements.

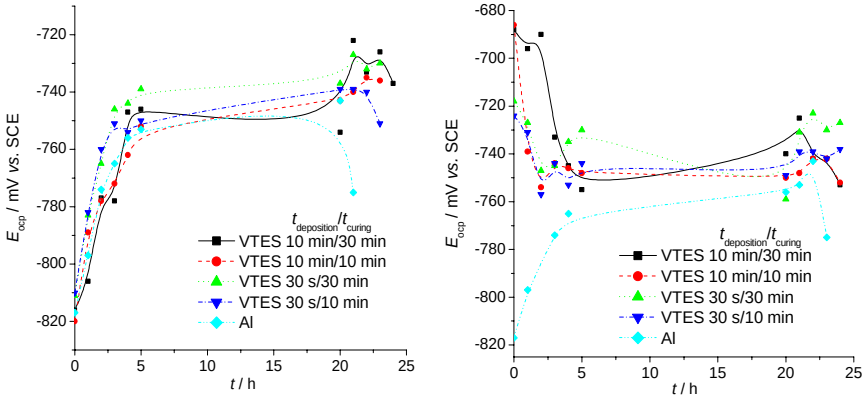


*Fig. 1. Time dependences of open circuit potential, $E_{ocp}$, in 3 wt. % NaCl for aluminum and VTES coatings deposited from (a) 2 vol. % and (b) 5 vol. % solution*

Time dependences of the open circuit potential, $E_{ocp}$, during exposure to 3 wt. % NaCl for silane-treated and bare aluminum samples are plotted in Fig. 1. VTES films deposited from 2 vol. % solution (Fig. 1a) behaved similarly to an oxide film, while VTES films deposited from the 5 vol. % solution (Fig. 1b) exhibited the characteristic

behavior of barrier polymer films. Deposition time and curing time have no influence on the $E_{ocp}$ values of the silane films.

By fitting of experimental data obtained by EIS measurements with equivalent electrical circuit with one time constant, the values of the coating pore resistance, $R_p$, were obtained (Fig. 2). Time dependences of coating pore resistance, $R_p$, for VTES films deposited from both 2 vol. % (Fig. 2a) and 5 vol. % silane solutions (Fig. 2b) show the behavior of barrier polymer films.[3,4] Based on EIS and potential-time measurements, it can be concluded that VTES films deposited from 5 vol. % solution have greater corrosion stability, while the effect of deposition time and curing time was not observed.

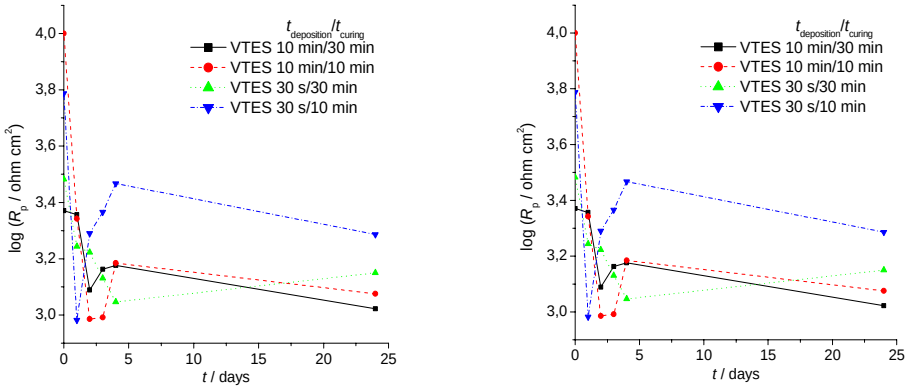


(a) (b)

*Fig. 2. Time dependences of the coating pore resistance, $R_p$, in 3 wt. % NaCl for VTES coatings deposited from (a) 2 vol. % and (b) 5 vol. % solution*

Gravimetric liquid sorption measurements did not show any change in mass of silane-treated samples with time of immersion in 3 wt. % NaCl. Hence, the water uptake in the micropores of the polymer net was not observed, indicating the high hydrophobicity of the VTES films.

The adhesion of VTES films on aluminum was determined by NMP test[5] and pull-off test of adhesion. The obtained results indicate an excellent adhesion at the aluminum/silane interface, and can be explained by interfacial layer consisting of SiOSi and SiOAl bonds, which provide highly cross-linked network of siloxane bonds and consequently high hydrophobicity of the silane films. These results are in accordance with sorption measurements.

**References:**

1. D. Zhu, W.J. van Ooij, *Electrochim. Acta* **49** (2004) 1113.
2. W. Trabelsi, L. Dhouibi, E. Triki, M.F. Montemor, *Surf.Coat. Technol.* **192** (2005) 284.
3. V.B. Mišković-Stanković, D.M. Dražić, M.J. Teodorović, *Corros. Sci.* **37** (1995) 241.
4. V.B. Mišković-Stanković, D.M. Dražić, Z. Kačarević-Popović, *Cor. Sci.* **38** (1996) 1513.
5. W.J. van Ooij, R.A. Edwards, A. Sabata, J. Zappia, *J.Adhesion Sci.Technol.* **7** (1993) 897.

First Regional Symposium on Electrochemistry of South-East Europe, Rovinj, Croatia, May 4-8, 2008.

P-2-124

# CORROSION PROTECTION OF Al-0.8Mg ALLOY BY GENTISIC ACID IN CHLORIDE SOLUTION

**L. Vrsalović, M. Kliškić, J. Radošević**

*Department of Electrochemistry and Protection of Materials, Faculty of Chemistry and Technology, University of Split, Teslina 10/V, 21000 Split, Croatia, E-mail: ladislav@ktf-split.hr*

This study examined the possibility of corrosion inhibition of the Al-0.8Mg alloy in NaCl solution by means of gentisic acid. Measurements were performed on a rotating disc electrode in a quiescent solution and at different electrode rotation rates and electrolyte temperatures. The basic solution was 0.5 mol $dm^{-3}$ NaCl solution to which gentisic acid was added in concentrations of $1\times10^{-3}$, $5\times10^{-4}$, $1\times10^{-4}$, $5\times10^{-5}$ and $1\times10^{-5}$ mol $dm^{-3}$. Gentisic acid belongs to the group of phenolic acids, substances that naturally occur in fruit, vegetables, nuts, seeds, flowers and some herb beverages [1,2]. Its presence has been established in the acidic fraction of aqueous extract of Rosemary leaves. This phenolic acid shows good antioxidant and also antibacterial activity [2,3]. Investigations with other phenolic acids have shown that these compounds can be used as corrosion inhibitors [4,5].

Measurements were carried out in the electrochemical glass cell with a platinum counter electrode and a saturated calomel electrode in contact with working electrode via Luggin capillary. The potentiodynamic polarization measurements were performed in potential range of -0.2 V to +0.15 V from the corrosion potential, with the scanning rate of 0.2 mV $s^{-1}$. The polarization resistance, $R_p$, was determined from the slope of polarization curves obtained by measurements in the potential range from -10 mV to +10 mV from the corrosion potential at the scanning rate of 0.2 mV $s^{-1}$.

The results obtained indicate that increase in electrode rotation rate and electrolyte temperature leads to a stronger corrosion attack on the alloy examined. The addition of gentisic acid inhibits corrosion of the Al-0.8Mg alloy, and the inhibition efficiency increases with increasing inhibitor concentration but decreases with increasing electrode rotation rate and electrolyte temperature.

Figure 1 shows the potentiodinamic polarization curves for the Al-0.8Mg alloy in a 0.5 mol $dm^{-3}$ NaCl solution without and in the presence of different concentrations of gentisic acid.

The investigated compound acts as a cathodic-type inhibitor and the inhibition is ascribed to the adsorption of the inhibitor onto the electrode surface. The adsorptive behaviour of gentisic acid follows the Freundlich adsorption isotherm (Figure 2).

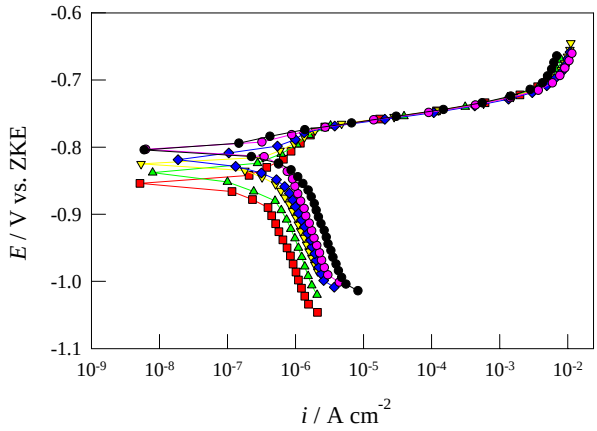


*Fig. 1. Potentiodynamic polarization curves for the Al-0.8Mg alloy in quiescent NaCl solution without (●) and in the presence of gentisic acid in the concentration of $1\times10^{-5}$ mol dm$^{-3}$ (●), $5\times10^{-5}$ mol dm$^{-3}$ (♦), $1\times10^{-4}$ mol dm$^{-3}$ (▼), $5\times10^{-4}$ mol dm$^{-3}$ (▲) and $1\times10^{-3}$ mol dm$^{-3}$ (■).*

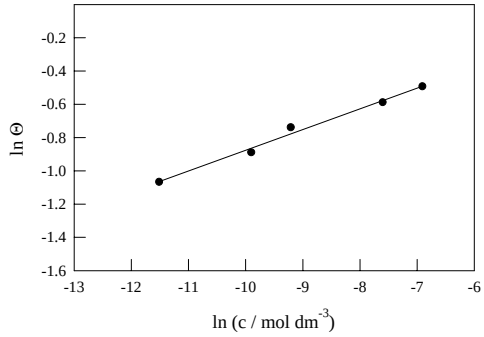


*Fig. 2. Adsorption isotherm of gentisic acid.*

The value determined for standard free energy of adsorption indicates physical adsorption of this phenolic acid on the electrode surface.

**References:**

[1] G. Zgorka and K. Glowniak: *J. Pharm. Biomed. Anal.* **26** (2001) 79.
[2] J. Pokorny, N. Yanishlieva and M. Gordon, in: *Antioxidans in food*, Woodhead Publishing Limited, Cambridge England, 2001.
[3] M.A. Fernandez, M.D. Garcia and M.T. Saenz: *J. Ethnopharmacol.* **53** (1996) 11.
[4] J. Radošević, M. Kliškić, A. Višekruna, *Kem. Ind.* **50** (2001) 537.
[5] L. Vrsalović, M. Kliškić, J. Radošević and S. Gudić: *J. Appl. Electrochem.* **37** (2007) 325.

First Regional Symposium on Electrochemistry of South-East Europe, Rovinj, Croatia, May 4-8, 2008.

P-2-125

# ELECTROCHEMICAL AND SHG INVESTIGATIONS ON THE ANODIC DISSOLUTION OF COPPER COMPOSITE FILMS

**R. Lange[1], D. Thiemig[1], F. Bogani[2], E. Tondo[2], B. Bozzini[2], A. Bund[1]**

*[1]Dresden University of Technology, Physical Chemistry, D-01062 Dresden, Germany*
*[2]INFM—Dipartimento di Ingegneria dell'Innovazione, Università di Lecce, I-73100 Lecce, Italy, E-mail: ronny.lange@chemie.tu-dresden.de*

The incorporation of inert particles during metal electrodeposition has reached scientific and technological interests for decades [1-3]. Recently, electrocodeposition has been industrially implemented to produce abrasion and corrosion resistant coatings, e.g. for automotive applications [4]. However, up to date the mechanism of particle codeposition as well as the improvement of the chemical, electrical and mechanical film properties has not been fully understood. In order to gain detailed information on the corrosion resistance of the composite films, we decided to study the anodic dissolution behaviour by electrochemical as well as optical techniques.

In the present paper we systematically investigate the anodic dissolution behaviour of pure Cu, Cu-$Al_2O_3$ and Cu-$TiO_2$ composite films deposited on to a platinum rotating disk electrode. These films have been deposited from acidic copper sulphate electrolytes containing 0 to 10 g $l^{-1}$ of $Al_2O_3$ (Ø 13nm) and $TiO_2$ nanoparticles (Ø 21nm), respectively. The anodic dissolution of the films was analyzed in the plating electrolyte, i.e. a mixed sulphate-chloride solution, as well as in an acidic chloride solution by means of potentiodynamic measurements. As a result of the particle incorporation, the copper dissolution in both electrolytes was significantly altered compared to the pure copper layer. Since the anodic dissolution of copper in acidic solutions chloride and sulphate solutions occurs in several stages where different adsorbed interfacial species are generated [5], further details were achieved by applying optical second harmonic generation (SHG) during electrochemical experiments. Finally, distinct variations in the SHG-signal were found, which can be explained by changes in the oxidation rate and/or in the coverage of adsorbates.

**References:**

[1] P.M. Vereecken, I. Shao, P.C. Searson, *J. Electrochem. Soc.* **147** (2000) 2572.
[2] J.L. Stojak, J. Fransaer, J.B. Talbot, *Review of Electrocodeposition*, in: R.C. Alkire, Kolb, D.M. (Eds.), Adv. Electrochem. Sci. Eng., Wiley-VCH Verlag, Weinheim, 2002.
[3] A. Hovestad, L.J.J. Janssen, *J. Appl. Electrochem.* **25** (1995) 519.
[4] J.-P. Celis, J. Fransaer, *Galvanotechnik* **88** (1997) 2229.
[5] J.B. Matos, L.P. Pereira, S.M.L. Agostinho, O.E. Barcia, G.G.O. Cordeiro, E. D'Elia, *J. Electroanal. Chem.* **570** (2004) 91–94.

First Regional Symposium on Electrochemistry of South-East Europe, Rovinj, Croatia, May 4-8, 2008.

P-2-126

# COPPER BASE ALLOYS CORROSION BEHAVIOR IN CIRCULATED MEDIUM

**A. Bărbulescu[1], D.C. Toncu[1]**

*Ovidius University of Constanța, Romania, alinadumitriu@yahoo.com*

Corrosion is among the main causes of metal degradation, which consists of both superficial and structural change. It causes economic and industrial loss and must be prevented mainly by choosing the right metal or alloy for the given conditions. In order to overcome the effects of corrosion, it is necessary to study and control the phenomenon.

The paper makes an analysis of copper base alloys, especially brass and bronze used in ship construction, establishing their different corrosion strength. The experiments were carried out under water and sea water, in a circulated medium. The purpose was to compare these results with the ones obtained with the same alloys, in the same medium, but in the presence of cavitation.

First Regional Symposium on Electrochemistry of South-East Europe, Rovinj, Croatia, May 4-8, 2008.

P-2-127

# SPECTROELECTROCHEMICAL INVESTIGATION OF COPPER-ALLOYS FOR APPLICATION IN THE MARINE ENVIRONMENT

**I. Škugor[1], Z. Grubač[1], M. Metikoš–Huković [2]**

[1]*Department of General and Inorganic Chemistry, Faculty of Chemistry and Technology, University of Split, Teslina 10/V, 21000 Split, Croatia*
[2]*Department of Electrochemistry, Faculty of Chemical Engineering and Technology, University of Zagreb, Savska 16, PO Box 177, 10000 Zagreb, Croatia, mmetik@marie.fkit.hr*

Copper-based alloys, such as the copper nickels, aluminum bronzes and nickel aluminum bronzes, have an extensive range of marine application. However, in spite of their excellent corrosion resistance, in some instances, corrosion has been observed due to water contamination, higher velocity and/or disturbed flows, even at low Reynolds numbers. To overcome the corrosion problem various methods of protection have been investigated and proposed. For example, benzotriazole has become one of the most effective inhibitors for Cu and Cu-Ni alloys in many electrolyte solutions [1,2]. An excellent corrosion protective ability of self-assembled monolayers of alkanethiol [3,4] and some complexing agents [5] on Cu and Cu-Ni alloy surfaces has been demonstrated.
The aim of the present study was to investigate the influence of sodium-diethyl-dithiocarbamate and N-vinylcarbazole selfassembled films on the corrosion resistance of Cu and Cu-10 Ni alloy in simulated seawater at various impingement velocities by means of *dc* and *ac* electrochemical methods. The surface films were characterized using infrared spectroscopy and X-ray diffraction methods.

**References:**

1. M. Metikoš-Huković, R. Babić, A. Marinović, *J. Electrochem. Soc.* **145** (1988) 4045.
2. R. Babić, M. Metikoš-Huković, M. Lončar, *Electrochim. Acta* **44** (1999) 2413.
3. M. Metikoš-Huković, R. Babić, Ž. Petrović, D. Posavec, *J. Electrochem. Soc.* **154** (2007) C138.
4. Ž. Petrović, M. Metikoš-Huković, R. Babić, *Prog. Org. Coat.* **61** (2008) 1.
5. S. Martinez, M. Metikoš-Huković, *J. Appl. Electrochem.* **36** (2006) 1311.

First Regional Symposium on Electrochemistry of South-East Europe, Rovinj, Croatia, May 4-8, 2008.

P-2-128

# BENZOTRIAZOLE INFLUENCE ON COPPER PITTING CORROSION IN ALKALINE-NITRATE SOLUTIONS

**E.A. Skrypnikova, S.A. Kaluzhina, A.S. Moiseenko**

*Voronezh State University 394006 University Sq. 1, Voronezh, Russia,*
*kaluzhina@vmail.ru*

Inhibitive action of azoles against copper general corrosion in neutral and acidic mediums was widely presented at modern literature. Significantly little attention were paid to azoles protective action applying to copper pitting corrosion (PC), which is one of the most dangerous types of corrosion and usually develops in waters with different pH values and anion composition. At present work it was made an attempt to estimate benzotriazole (BTAH) influence on copper PC in alkaline mediums with $NO_3^-$ - ions additive.

The experiments were carried out on stationary copper electrode (Cu 99,99%) at 0.01M NaOH+0.01M $NaNO_3$+XM BTAH ($X=10^{-7}\div10^{-1}$M) solutions. Cyclic and inversion voltammetry, chronoamperometry, microscopy were used for receiving a detailed kinetic characteristics of investigated electrochemical process and for estimation of interface Me/electrolyte state. All experiments were performed under room temperature in naturally aerated solutions.

The obtained results has shown that in background 0.01M NaOH+0.01M $NaNO_3$ solution copper undergoes PC. It is supported by 1) anodic current hysteresis loop revealing at cyclic voltammogramm (CVA); 2) the results of chronoamperometric investigations, according to which the potential PC $E_{PC}$=0.600 V and the induction period $\tau_{ind}$=72 s. The electrochemical data is confirmed by the results of microscopic observation: after experiment metal surface was covered by loose transparent - blue layer with numerous small pittings under it (Fig.1a).

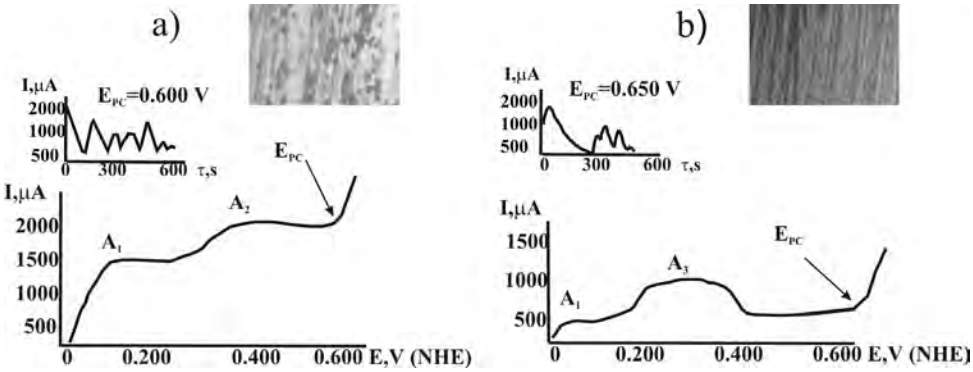


*Fig.1 Anodic polarization curve of copper, chronoamperogramm under $E_{PC}$ and microphoto of local damage at copper surface in a)0,01M NaOH+0,01M $NaNO_3$ and b)0.01M NaOH+0.01M $NaNO_3$+$1\times10^{-5}$ BTAH M, where $A_1$-Cu/$Cu_2O$, $A_2$- $Cu_2O$/CuO*

Addition of BTAH in the concentration range $1\times10^{-7}\div1\times10^{-5}$M causes decrease of anodic peaks height (Fig.1b). The inhibitor additive stabilizes the system

($E_{PC}$ shifts to positive values region up to 0.650 V, $\tau_{ind}$ increases up to 320 s (under C(BTAH)=1×10$^{-5}$M) and pittings amount decreases). According to the results of microscopic observation pittings depth and amount decrease under BTAH concentration growth. The efficiency of BTAH as PC inhibitor [3] was determined with using coefficient Z, which in the investigated system was calculated according to the following equation:

$$Z = \frac{\left(1/\tau_{ind}\right)_0 - \left(1/\tau_{ind}\right)_{inh}}{\left(1/\tau_{ind}\right)_0} \times 100\%$$

where $\left(1/\tau_{ind}\right)_0$ and $\left(1/\tau_{ind}\right)_{inh}$ - PC rate in background solution and in the solution with inhibitor addition respectively. In the researched system Z increases under inhibitor concentration growth from 71 % (at 1×10$^{-7}$M) up to 77 % (at 1×10$^{-5}$M). Further BTAH concentration increase causes copper PC amplification: $E_{PC}$ shifts to more negative values region (to 0.550 V under C(BTAH)=10$^{-2}$M). After experiment copper surface is covered by numerous pittings. BTAH inhibitive effect decrease is observed (Z changes to 44% under C(BTAH)=1×10$^{-2}$M).

Earlier [1] it was found that at background electrolyte copper PC process mechanism takes place corresponds to D. Macdonald point defects model [2]. According to Yu. Kuznetsov theory, PC process can be presented as a reaction substitution of passivating oxygen containing particles of surface complex by aggressive anions with further hydrolysis of obtained compound [4].

$[Me(OH)_m]^{z1-m} + L\ NO_3^- \rightarrow [Me(OH)_{m-L}(NO_3)_L]^{z2-m} + L\ (OH)^- + (z_1-z_2)\bar{e}$ stage 1

$[Me(OH)_{m-L}(NO_3)_L]^{z2-m} \rightarrow L\ NO_3^- + Me^{z3} + (m-L)OH^- + (z_2-z_3)\bar{e}$ stage 2

But if aggressive ($NO_3^-$) and inhibitor ($BTA^-$) ions are in the electrolyte, the last as more powerful nucleophile predominantly adsorbs at the most electrophile, or the most dangerous for PC sites of passive film and blocks them:

$[Me(OH)_m]^{z1-m} + L\ BTA^- \rightarrow [Me(OH)_{m-L}\ BTA]^{z4-m} + L\ OH^- + (z_1-z_4)\bar{e}$ stage 3

Under inhibitor concentration growth BTAH blocks all less reactionary capable surface centers. Copper PC on them can be slowed down on so many that its rate becomes commensurable with replacement of inhibitor anions by activators rate:

$[Me(OH)_{n-k}\ BTA]_s^{z4-n} + k\ NO_3^- \rightarrow [Me(OH)_{n-k}(NO_3)_k]_s^{z2-n} + k\ BTA^- + (z_4-z_1)\ \bar{e}$ stage 4

And under some critical BTAH concentration copper PC mechanism changes from (1-2) to (4).

According to obtained data benzotriazole has shown inhibitive properties at investigated system from C=1×10$^{-7}$ to C=1×10$^{-5}$M. Further inhibitor concentration increase up to 1×10$^{-2}$ M causes copper PC amplification.

**References:**

1. Kaluzhina S.A., Kobanenko I.V. *Protection of metals* **37** 266 (2001) (Russian).
2. Macdonald D. *Electrochem Soc.Proceedings*, **25** 141 (2000).
3. Rosenfeld J.L. *The Inhibitors of Corrosion* p.317 (1982) (Russian).
4. Kuznetsov Yu. I. *Sbornik dokladov NIFCHI Karpova L.Y.* **1** 161 (2000) (Russian).

First Regional Symposium on Electrochemistry of South-East Europe, Rovinj, Croatia, May 4-8, 2008.

P-2-129

# THE CORROSION BEHAVIOUR OF BRASS AND ITS INHIBITION IN ACIDIC SOLUTIONS

**Z. Avramović[1], M. Antonijević[2]**

*[1]TiR, Copper Smelter and Electrolysis Plant, D.Vajfert 20, 19210 Bor, Serbia,*
*E-mail: zavramovic@ptt.yu*
*[2]University in Belgrade, Technical Faculty Bor, VJ 12, 19210 Bor, Serbia*

The corrosion behaviour of brass was studied in acid sulphate solution at pH-value 2 with additional chloride ions and five organic inhibitors namely: thiourea (TU), benzotriazole (BTA), ethylene diamine tetraacetic acid (EDTA), hydrazine sulphate (HS) and 2-butin-1,4 diole (DS-3) using potentiodynamic polarization techniques. Increase of a concentration of the $Cl^-$ ions, exept for value of $5 \cdot 10^{-2}$ moldm$^{-3}$, resulted in a significant increase of value for corrosion current densities. Polarization measurements showed that the organic compounds investigated are mixed type inhibitors, inhibiting the corrosion of brass by blocking the active sites of the metal surface.

Many authors [1-8] from this field have tested different methods and concluded that zinc dissolves mostly in the initial period of dezincation. Individual attack appears in a shortly-defined time period and penetrates through several monolayers at the surface of brass. Further separation of zinc within the same process is unlikely, since the process requires extra energy in order for atoms of zinc to difund through the solid phase and reach brass surface. As the result, copper also starts to turn into solution after some time, together with zinc, with comparably less speed, including the change of potential. Redeposition of copper immediately follows the dissolution of remaining zinc in the solution. In the light of this investigation and interpretation, the phenomenon of dezincation is initiated by selective dissolution of zinc and intensified by simultaneous dissolution of copper and zinc, followed by redeposition of copper. Simultaneous dissolution and redeposition of copper are mutually independent processes, but both processes cause the change of experimental conditions.

Brass is widely used in various industrial operations and the study of corrosion of brass and inhibition is subject of practical significance. BTA, thiourea, hydrazine-sulphate, DS-3 and EDTA, have been used as effective acid corrosion inhibitors [8-12]. Nagiub [10], Jinturkar [12] and Sayed [13], studying the effect of **BTA** on alpha-brass exposed to a nitrate solution concluded that the presence of BTA inhibited the dissolution of brass due to the formation of a copper oxide layer on the brass surface.

According to some research on protective effect of BTA inhibitor [14,15], it was established that copper oxide ($Cu_2O$) was the basis for forming Cu(I)-BTA film. The presence of oxide $Cu_2O$ facilitates the initial chemisorption of BTA inhibitor. According to other authors [16,17,18], film Cu(I)-BTA is formed on an 'empty surface' of copper or brass. While analysing the film formed on brass surface, the same authors found that the formed film on brass surface was in the form of Cu(I)BTA complex, which was oxidised to Cu(II)BTA. Two inhibiting mechanisms of BTA inhibitor can be found in literature [19-23]: adsorption of BTA inhibitor on copper surface and forming of polymer film that includes complex ions Cu(I) and $(Cu^+BTA^-)_n$.

As good inhibitor of non-ferrous metals and copper corrosion in acids (HCl, $H_2SO_4$, $HNO_3$) thiourea is used with inhibition degree from 65% to 98%, depending on inhibitor concentration [24]. Investigation interest was focused on establishing the influence of the above mentioned corrosion inhibitors on corrosion behaviour of cold-deformed brass samples in acid solution of sodium sulphate with addition of $Cu^{2+}$ and chloride ions.

Inhibitor **EDTA** (Ethylene Diamine Tetra-Acetate) has one of its uses in chemical cleaning of generators from copper residue in nuclear plants [25-27]. Considering that critical potential for dissolving copper in ammoniac solutions is in the area of -0.3÷0.2V, the role of EDTA inhibitor is to maintain the potential within the indicated area, so that copper residue would be removed from the generator of a nuclear plant, with the use of ammonia and hydrogen peroxide.Inhibitors **hydrazine-sulphate** and **DS-3** are the inhibitors of steel corrosion in solutions of sulphuric and hydrochloric acid, and the inhibitor of copper and copper alloys in nitric acid and alkaline solutions.

The results of studies show that only thiourea, in concentration of $10^{-2}$%, inhibit the corrosion of brass in chloride solutions. Inhibitor benzotriazole in concentration of $10^{-1}$% inhibit the corrosion of brass with inhibition efficiency more then 94%. The film improved significantly the protecting ability of brass surface to corrosion in chloride solutions. When the films were modified with benzotriazole the quality and corrosion protection of films improved rapidly.

**References:**

1. E. Stupnisek-Lisac, A. Loncaric-Bozic, *Corrosion* **54** (1998) 713
2. R. Gasparac, C.R.Martin, E. Stupnisek-Lisac, *J.Electrochem.Soc.* **147** (2000) 548
3. R. Ravichandran, N.Rajendran, *Applied Surface Science* **241** (2005) 449
4. R. Ravichandran, N.Rajendran, *Applied Surface Science* **239** (2005) 182
5. Torchio, S., Mazza, F., *Corrosion Science*, **26** (1986) 813
6. Gupta, P., Chaudhary, R.S., Namboodhiri, T.K.G., *Br.Corros. J.* **17** (1982) 136
7. Kabasakaloglu, M., Kiyak, T., Sendil, O., *Applied Surface Sience*, **193** (2002) 167
8. El-Mahdy, G.A., *Journal of Applied Electrochemistry*, **3** (2005) 347
9. Tromans, D., Silva, J.C., *Journal of Science and Engineering Corrosion*, **53** (1997) 16
10. Nagiub, A., Mansfeld, F., *Corrosion Science*, **43** (2001) 2147
11. Shukla,J ., Pitre, K.S., *Corrosion Rev*., **20** (2000) 217
12. Jinturkar, P., Guan, Y.C., Han, K.N., *Corrosion*, **54** (1998) 106
13. Sayed, S.M., Ashour, E.A., Ateya, B.G., *Corrosion Science* **36** (1994) 221
14. Tamil Selvi, S., Raman, V., Rajendran, N., *J.Appl.Electrochem.*, **33** (2003) 1175
15. Villamil, R.F.V., Cordeiro, G.G.O., *Materials Chemistry and Physics*, **78** (2002) 448
16. Youda, R., Nishihara, H., Aramaki, K., *Corrosion Science* **28** (1) (1988) 87
17. Zhang, D.Q., Gao, L.X., Zhou, G.D., *Applied Surface Science*, **225** (2004) 287
18. Babic, R., Metikos-Hukovic, M., Lonchar, M., *Electrochim.Acta.*, **44** (1999) 2413
19. Papanayotov, D., Deligianni, H., Alkire, R.C., *J.Electrochem.Soc.*, **145** (1998) 3016
20. Polo, J.L., Pinilla, P., Cano, E., Bastidas, J.M., *Corrosion*, **59**(5) (2003) 414
21. R. Walker, *Corrosion* **31** (1975) 97
22. D. Modestov, G.D. Zhou, H.H. Ge, B.H. Loo, *J.Electroanal.Chem.* **375** (1994) 293
23. D. Thomas, R.H. Sun, *J.Electrochem.Soc.* **138** (1991) 3235
24. Dinnappa, R.K., Mayanna, S.M., *Corrosion Science*, **27** (1987) 349
25. Sieradzki, K., Kim, J.S., *J.Electrochem Soc*., **134** (1987) 1635
26. Newman, R.C., Shahrabi, T., Corrosion Science, **28** (1988) 873
27. El-Rehim, S.S.A., Assaf, F.H., *Mat. Trans., JIM*, **36(6)** (1995) pp.770

First Regional Symposium on Electrochemistry of South-East Europe, Rovinj, Croatia, May 4-8, 2008.

P-2-130

# INFLUENCE OF TEMPERATURE ON CORROSION BEHAVIOUR OF ZINC IN WATER

**I. Juraga[1], V. Alar[1], V. Šimunović[1], I. Stojanović[1], F. Kapor[2]**

*[1]Faculty of Mechanical Engineering and Naval Architecture, Ivana Lučića 1, Zagreb, CROATIA*
*[2]Faculty of Mining Geology and Petroleum Engineering, Zagreb, CROATIA*
vesna.alar@fsb.hr

Zinc is one of the most important metals used in the prevention of corrosion. It offers galvanic protection to steel and other materials and it is resistant to corrosive atmosphere as well as to sea water and tap water influences. Hot-dip galvanized steel is most frequently used in building constructions, container manufacture, taps and pipe fittings in domestic and industrial water works. Zinc is resistant to corrosion in water only in a very narrow pH interval (from 6 to 11). The degradation of galvanized steel hot water pipes leads to the conclusion that zinc is not always anodic in its relationship to steel.
The corrosion potential $E_{cor}$ as well as the corrosion rate of galvanized steel in tap and distilled water at temperatures of 20, 30, 40, 50, 60, 70 and 80 $^{o}$C are determined using the electrochemical method of quasi-potentiostatic polarization, ie by recording polarization curves and by Tafel extrapolation.

First Regional Symposium on Electrochemistry of South-East Europe, Rovinj, Croatia, May 4-8, 2008.

P-2-131

# ELECTROCHEMICAL IMPEDANCE SPECTROSCOPY STUDY OF POLYPYRROLE COATED ZINC-CHROMATE/STEEL ELECTRODE

**M. Mindroiu[1], R. Vasilescu[2], C. Pirvu[1]**

[1]*Faculty of Applied Chemistry and Materials Science University Politehnica Bucharest,*
*mihaela_istratescu@yahoo.com*
[2]*Institute of Physical Chemistry "Ilie Murgulescu"*

## Aim

In this paper a characterization of environmentally friendly conversion treatments based on $Cr^{3+}$ for zinc surface will be reported in comparison with traditional based $Cr^{6+}$ pretreatments on different zinc layers protected by conducting polymer coatings.

## Experimental

The electrochemical measurements were made with a potentiostatic assembly Zahner of three electrodes: a working electrode, a platinum counter-electrode and a reference electrode (Ag/AgCl). The corrosion studies were conducted in 3% NaCl testing solution.

## Results and discussion

A very popular way to reduce the corrosion rate of zinc was the use of chemical conversion layers based on $Cr^{6+}$, able to increase the passivation tendency of the zinc. This procedure is quite effective also for improving the adhesion of organic coatings deposited on the zinc surface, but there is the important problem that the use of chromium salts is now restricted because of environmental protection legislation.

It is therefore very important to develop new zinc surface treatments environmentally friendly to improve the corrosion resistance of zinc and the adhesion with the final organic protective layer.

Polypyrrole film was prepared on zinc coated steel electrode by anodic electropolymerization from aqueous solution containing monomer and a tartrate supporting electrolyte. From the practical point of view the aqueous electrolytes were preferred.

The corrosion behaviour of zinc-coated steel electrodes electrochemical modified by PPy films were estimated by Tafel curve in 3% NaCl, aggressive solutions.

Also, the samples were studied using EIS measurements, and the data analysis was mainly based on the discussion of different parameters evolution of the equivalent electrical circuit model.

The EIS has proved to be an excellent technique to verify the properties of polymer coatings as insulating materials and follow their deterioration processes under specific experimental conditions.
This approach was found more useful, in order to compare the performance of different used materials.
The impedance data was obtained at free potential value, the frequency ranged from 100 mHz to 100 kHz, and the amplitude used was set at 10 mV.
The impedance spectra were analyzed using the ZView program. The Bode plots of EIS measurements and the proposed equivalent electrical circuit model, for both polypirrole coated and uncoated Zn/Steel, Zn-$Cr^{3+}$/Steel and Zn-$Cr^{6+}$/Steel are shown in fig. 1.

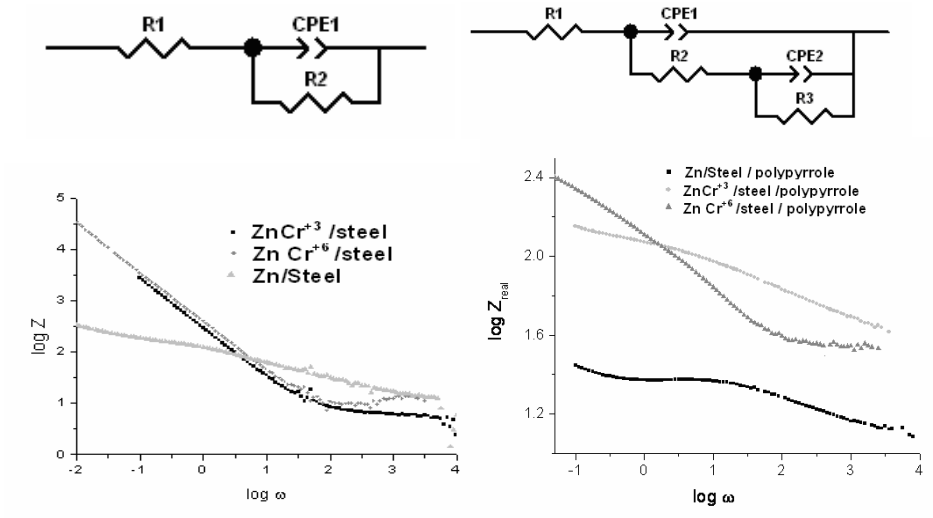


a) b)

*Fig. 1. Bode spectra for a) ZnCr/steel system and b) ZnCr/steel/polypyrrole*

**Conclusions**

The polypyrrole increase the corrosion resistance of polypyrrole/zinc-chromate/steel system.

***Acknowledgements:*** *This paper was supported by the National Romanian CEEX program in the frame of the project ECOMATICA No. 216/2006. The authors gratefully acknowledge their financial support.*

First Regional Symposium on Electrochemistry of South-East Europe, Rovinj, Croatia, May 4-8, 2008.

P-2-132

# ELECTROCHEMICAL BEHAVIOUR OF AMORPHOUS ELECTRODEPOSITED CHROMIUM COATINGS

**L. Sziráki[a], E. Kuzmann[b], K. Papp[c], M.R. El-Sharif[d], U. Chisholm[d]**

*[a]Eötvös L. University, Institute of Chemistry, Laboratory of Electrochemistry and Electroanalytical Chemistry, H-1117 Budapest, Pázmány P. S. 1/A, Hungary, sziraki@chem.elte.hu*
*[b]Laboratory of Nuclear Chemistry,HAS Central Research Institute for Chemistry, H-1117 Budapest, PázmányP. S. 1/A, Hungary.*
*[c]HAS Central Research Institute for Chemistry, H-1025 Budapest, Pusztaszeri u. 59, Hungary*
*[d]Glasgow Caledonian University, Glasgow G4 0BA, Scotland, United Kingdom*

The paper deals with the electrochemical characterization of the passive dissolution/corrosion behaviour of chromium coatings electroplated from bath of trivalent chromium complexed with glycine by using a high speed flow cell system developed by M. El-Sharif et al. [1]. The structure, morphology and elemental analysis of several chromium coatings deposited on copper substrates at various bath variables (bath temperatures 30- 60 $^{o}$C, current densities 0.3-1.8 A cm$^{-2}$, flow rate 0.2-1.4 m·s$^{-1}$) were investigated by XRD, SEM/EDS measurements. As a fine network of micro-cracks is inherently incorporated into the amorphous chromium-oxygen-carbon alloys, special care were taken to apply such electrochemical passivation conditions as to avoid the copper substrate attacks. Potentiodynamic polarization curves and impedance spectra were recorded after cathodic activation in de-aerated sulphuric acid solution. The corrosion potentials of Cr coatings after 1.5 h immersion time were established at about -0.3 V *vs* SCE. The evaluations of the impedance spectra measured at the corrosion potential, $E_{corr}$ was based on CNLLS fit to an equivalent circuit model of the corrosion kinetics.

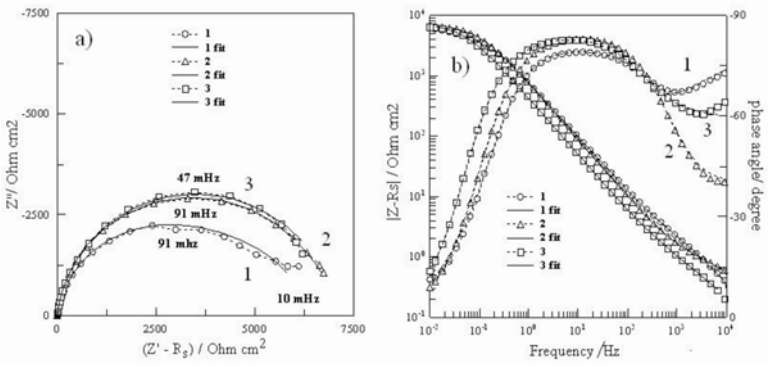


*Fig. 1. Impedance spectra obtained for the electrodeposited a- and pc-Cr samples in 0.5 M $H_2SO_4$ de-aerated with Ar gas. $E_{corr}$ after corrosion immersions:(1): (o) pc-Cr, -217 mV, 20 h; (2): (Δ)a-Cr electrodeposited at 30 $^{o}$C, -333 mV, 1.5h; (3): (□) a-Cr electrodeposited at 60 $^{o}$C, -331 mV, 1.5 h. The continuous lines are the fitted curves. (a) complex plane plot, (b) Bode plots.*

The change of the $R_{ct}$ of the overall corrosion process followed the tendency of the appearance of quality of the deposits and their corrosion products. The $R_{ct}$ values of amorphous chromium (*a*-Cr) deposit compared to those of a polycrystalline chromium (*p*-Cr) deposit self-passivated, revealed that the bright *a*-Cr deposit possesses similar and in some cases outperform the corrosion protection ability of the *pc*-Cr.

**References:**

[1] M. El-Sharif, C.U. Chisholm, *Trans IMF*, **75** (1997) 208., *Trans IMF*, **77** (1999) 139.

First Regional Symposium on Electrochemistry of South-East Europe, Rovinj, Croatia, May 4-8, 2008.

P-2-133

# ELECTROCHEMICAL BEHAVIOR OF A TWO BIOCOMPATIBLE MATERIALS

**A. Banu[1], M. Marcu[2]**

*[1]POLYTECHNICA University from Bucharest, Environmental Engineering and Corrosion Laboratory, IMST Faculty, a_banu_2000@yahoo.com*
*[2]Institute of Physical Chemistry "I.G. Murgulescu" Bucharest*

Because they're good biocompatibility and satisfactory hardness and ductility, good resistance to general and localized corrosion the chromium alloys are used as surgical implants or dental resistant materials. The corrosion resistance of chromium alloyed materials is due to the surface passive film formation. A lot of investigations have been carried out to define the electrochemical properties of passive films [1-2].
The alloy's behavior with respect to the passive (oxide) film formation is more complicated than that of pure metals because of the effect that the alloying elements exert on the films [3, 4].
The aim of the work is to study the influence of the alloying elements of two casting and cold worked alloys on the electrochemical characteristics, Open Circuit Potential (OCP), electrochemical polarization and tarnish behavior.

*Table 1. Chemical composition of casting alloys (% weight)*

| No. | Cr, % | Mo, % | Ni, % | Co, % |
|---|---|---|---|---|
| 1. | 18.17 | 4.95 | Base | - |
| 2. | 26.97 | 4.02 | - | Base |

The electrochemical experiments were carried out using a Gamry equipment, in a three electrode glass cell provided with a saturated $Hg/Hg_2Cl_2$//KCl, and a platinum electrode as reference and auxiliary electrodes respectively.
The electrochemical measurements were performed acording with ISO 10271/93; ASTM G5/94 using sintetic saliva [5] and potential range between –250mV and +250mV ) away and back, with a rate of 0,6V/h.The tarnish behavior was determined using stationary (for 168 hours, ISO 10271/93) and alternante immersion test according ISO 8891/98 respectvely ISO 3696 with immersion frequency of 10-15 sec/minut during 72 hours in sodium sulfide solution. The mass loss was measured by AAS.
After 168 hours of immersion time the loss of ions is presents in the table 2.

*Table 2. The ion's loss [μg cm$^{-2}$] after stationary immersion test*

| Nr crt | Alloy | Element | The loss, μg cm$^{-2}$ |
|---|---|---|---|
| 1 | NiCr | Ni | 77.85 |
| | | Cr | 4.234 |
| | | Mo | 4.402 |
| 2 | CoCr | Co | 0.314 |
| | | Cr | 0 |
| | | Mo | 0 |

The corrosion rate of the alloys after 168 of immersion time are presented in the Fig 1

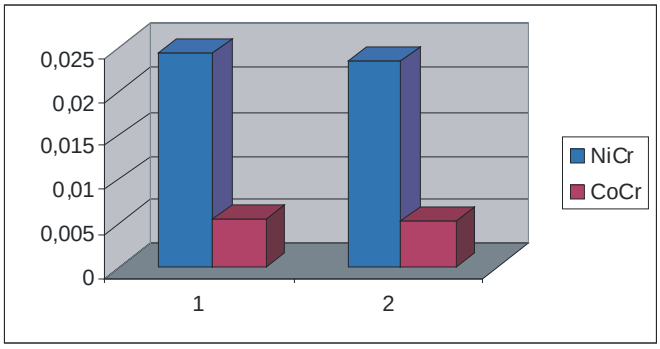


*1- g/m$^2$h*
*2- mm/an*

After 72 hours of alternante immersion time the sample's surface didn't present any staining or colour effect. The OCP and polarization curves show the better passivation behavior of CoCr alloy. The OCP and polarization curves show the better passivation behavior of CoCr alloy. After 168 hours the OCP of CrCo ally is about +180mV/sce since the OCP of NiCr alloy is +50 mV/sce with a depassivation tendency.

**References:**

1. I. Milosev, H.H. Strehblow, *J. Biomed. Mater. Res.*, **52** (2000)
2. I. Milosev, *J.Appl. Electrochem.*, **32** (2002) 311
3. J. Eimutis, et al, *J. Solid State Electrochem.*, **6** (2000) 302
4. P. H. Snegame, C. S. Fugivara, e.a, *J.Appl. Electrochem.*, 32 (2002) 1287
5. J.M.Meyer, J.N.Nally, Influence of Artificial salivas on the corrosion of dental alloys, *J. Dent. Res.*,**54**, 1975, IADR Nr.76

First Regional Symposium on Electrochemistry of South-East Europe, Rovinj, Croatia, May 4-8, 2008.

P-2-134

# CORRELATION BETWEEN THE ZIRCONIUM OXIDE FILMS AND NPS PRIMARY CIRCUIT CHEMISTRY

**M. Rãdulescu, I. Pîrvan**

*Institute for Nuclear Research POBox 78 115400 MIOVENI,1, Campului Street ROMANIA, E-mail: radulmi@yahoo.com*

It is known that the lifetime and the reliability in operation of zirconium alloys from a primary circuit of a CANDU PHWR Nuclear Power Station are often limited by the thickness and uniformity of the oxide from the waterside of these components.
Our experimental data were been obtained testing three following zirconium alloys: Zircaloy-2, Zircaloy-4 and Zr-2.5 % Nb autoclavized in some specific conditions to primary circuit, i.e. in aqueous solutions of several pHs at high temperature and pressure in the presence of different gases dissolved in the working environments and in solutions contaminated with $F^-$ (HF).
The obtained data have been used to represent the kinetic curves weight gain function of time. On the autoclavized samples were executed also some impedance measurements to determine the characteristics of zirconium oxides with the aim: to detect the failures in the films, to correlate the oxidation law of the respective zirconium alloys with the main characteristics of films obtained and to find some models of the interfaces zirconium oxide/ solution.
Based on the impedance (EIS) curves - Bode, Nyquist and phase angle – some correlations between the impedance spectra, oxidation kinetics and the protective/ no protective character of zirconium oxides and the physico-chemical characteristics of autoclavizing environment were established.

*Key words:* Nuclear Power Station (NPS), primary circuit chemistry, oxidation kinetics of zirconium alloys, EIS curves of zirconium oxides

First Regional Symposium on Electrochemistry of South-East Europe, Rovinj, Croatia, May 4-8, 2008.

P-2-135

# RAMAN SPECTRA OF ANODIZED VALVE METAL ELECTRODES

**I. Mickova, Lj. Arsov**

*Faculty of Technology and metallurgy, University "Ss Cyril and Methodius", Skopje, Macedonia E-mail: mickova@tmf.ukim.edu.mk*

The electrochemical anodization of valve metal electrodes from: Ti, Nb and Zr in various concentrations of $H_2SO_4$ and KOH electrolytes has been studies by in-situ Raman spectroscopy. For each electrolyte anodization was carried out at various fixed voltages and for each voltage the evaluation of Raman spectra was followed as a function of time. The critical voltage of film transformation from the amorphous to the crystalline state has been detected accurately. The spectra were measured in a cylindrical cell made of quartz and the 514.5 nm line of an argon ion laser operated at 300-400 mW was used as excitation. Spectra were recorded at room temperature using a Spex 1877 spectrograph in connection with a 512 diode multi-channel analyzer. The working electrodes were made from a massive cylindrical Ti, Nb, and Zr rods with diameter of 6 mm. Before each measurement the electrode surfaces were abraded using silicon carbide paper (1000 grade) and then gradually polished with diamond sprays of decreasing particle (1 μm) to yield a mirror finish. A spiral platinum wire was used as a counter electrode.
On fig. 1, 2 and 3 the Raman spectra are shown recorded for various voltages and time of anodization

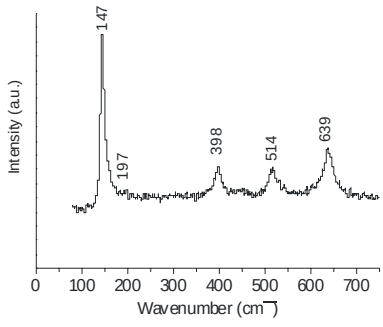


*Fig.1. Raman spectrum of Ti anodized at 120 V in 1 M $H_2SO_4$ for 30 s*

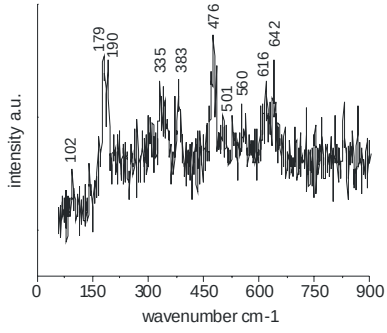


*Fig. 2. Raman spectrum of Zr anodized at 80 V in 2 M KOH for 2 s*

The appearance of active Raman bands due to the anodic oxide layers on the electrode is found to be a function of the voltage and time of anodization. For Ti in 1 M $H_2SO_4$ the first Raman bands appear at the voltage of 15 V and anodization time of 3 h. For higher anodic voltage, as in fig.1, the Raman spectrum develops within 30 s. Four strong bands are seen at: 147, 398, 514 and 639 $cm^{-1}$ and a weak band at 197 $cm^{-1}$, which corresponds to $TiO_2$ anatase mineral form.

The appearance of Raman bands of anodized Zr at 80 V in 2 M KOH for very short time, is shown on fig.2. At the same voltage for anodization time of 15 s, 13 strong peaks located on: 180, 190, 224, 308, 335, 348, 384, 476, 501, 538, 562, 614 and 641 $cm^{-1}$ and one weak band on 761 $cm^{-1}$ appear. All that bands are characteristic for $ZrO_2$ crystalline form.

The evaluation of Raman bands on Nb electrode in 1 M KOH at various voltages for anodization time of 30 s is shown on fig.3. For anodic voltage of 30 V two broad bands located at 234 and 702 $cm^{-1}$ appear, Fig.3. Increasing the voltage the bands rise in intensity and additional bands located on: 261, 308, 470, 485, 550, 606, 630, 660, 672, 892 and 992 $cm^{-1}$ appear. But on 92 V the Raman spectrum is changing. The band on 702 $cm^{-1}$ characteristics for $NbO_2$ is split into two new bands located on 630 and 660 $cm^{-1}$ tentatively assigned to the beginning of transformation of $NbO_2$ to the $Nb_2O_5$.

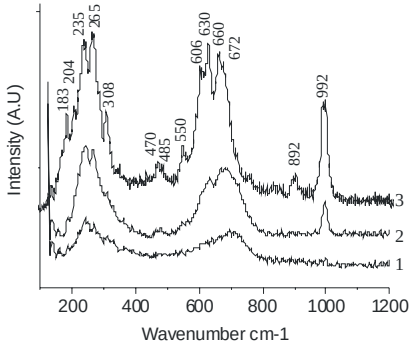


*Fig.3. Raman spectra of Nb anodized in 1 M KOH for 30 s at:1 – 30 V; 2 – 80 V; 3 – 92 V*

From Raman spectra measurements of 3 valve anodized metals the following conclusions can be drawn:

- For natural oxide films and up to 10 V, no Raman bands could be observed. For anodic voltage of 15 V the first active Raman bands for all three metals begin to appear. At low voltage, up to 10 V, the oxides formed are either hydrated or amorphous oxides. In literature data the transition from hydrated or amorphous oxides to crystalline is discussed in terms of the film breakdown. Some authors suggested that crystallization of anodic oxide films occurs in parallel with the breakdown [1]. Others observed crystallization of anodic films after breakdown [2]. Wood and Parsons have established a relation between the breakdown voltage and the electrolyte conductivity [3]. They concluded that the breakdown processes depends on the specific ion transport properties of formed layers. The present results have shown that the crystallinity develops in close relation with breakdown. During the anodic polarization, the current was oscilloscopically monitored showing small fluctuation at 15 V.

- The thickness of anodized Ti, Zr and Nb is nearly independent of the electrolyte concentration. Generally higher electrolyte concentrations lead to lower threshold voltages for transformation of amorphous to crystalline forms.

- In KOH electrolytes the transformation from amorphous to crystalline structure occurs abruptly. The breakdown process is more pronounced with increasing the concentration of KOH. In higher concentration of KOH solutions, during the anodic polarization at higher voltages, the visible spark were observed. Under these conditions a strong warming-up of the electrolyte is noticed. The breakdown process and evolution of crystallinity is a thermal effect resulting from local heating of the oxide film.

[1] J.Yakalom, J.Zahavi – *Electrochim. Acta*, **15**, 1429 (1970)
[2] J.Marchenoir, J.Loup, J.Masson – *Thin Solid Films* **66**, 357 (1980)
[3] G.Wood , C.Parsons – *Corr. Sci*., **7**, 284 (1967)

First Regional Symposium on Electrochemistry of South-East Europe, Rovinj, Croatia, May 4-8, 2008.

P-2-136

# PITTING CORROSION OF SILVER IN ALKALINE MEDIAS CONTAINING ANION-ACTIVATORS

**N. Lesnykh*, N. Tutukina, I. Marshakov**

*Voronezh State University, Universitetskaya pl. 1, 394006, Voronezh,Russia*
**E-mail: NNLesnykh@mail.ru*

## Introduction

The properties of silver and copper are likely, in particular copper in alkaline solutions are being exposed to the pitting corrosion but it is no description of pitting destroying on silver under anodic polarization and in the case of the free corrosion in the literature. Thus, it was interesting to investigate the anodic behavior of silver in alkaline solutions in the presence of the anions-activators.

## Experimental

Investigation was leaded on the silver electrode containing impurities about 0,01 at.%. The area of the working surface was equaled 0,25 $cm^2$. Solutions were prepared from the chemically pure reagents.

## Results and Discussion

On the base of the obtained experimental data it was made a supposition that the adsorption of hydroxyl ions occurs during the immersion of silver electrode into the alkaline solution, and the adsorption complexes are formed, also this process may be accompanied by the loss of the electron or its part. The composition of the superficial complex may be written as $AgOH_{ads}$. The interaction between the superficial silver atoms and hydroxyl ions is increasing with the anodic potential value rising. The electron structure of the adsorption complex is changing and occurring the formation of more difficult soluble complex $Ag(O\text{-}H)_{адс}$. Probable, these complexes are blocking active parts of the electrode surface and leads to the anodic passivity. Such complexes are well soluble and its dehydratation reduces to the formation of $Ag_2O$. Under potentials of peak $A_2$ the oxide $Ag_2O$ (or Ag) are oxidizing to the AgO, the passive state will be conditioned by the appearing of $[Ag(OH)_2]_{ads}$, which converted to the $[Ag(O\text{-}H)_2]_{ads}$.

Introducing of small amounts of sulphate ions into the alkaline solution leads to the acceleration of the anodic dissolution of silver. Probably because of competition adsorption of hydroxyl and sulphate ions more soluble mixed complexes are formed $[Ag(OH)(SO_4)]^{2-}_{ads}$, their dehydratation brings to the formation of $Ag_2O$. Passivation of silver behind the peak $A_1$ realizing by complex $[Ag(O\text{-}H)SO_4]^{2-}_{ads}$, and behind the peak $A_2$ by the complex $[Ag(O\text{-}H)SO_4)]^{-}_{ads}$, in these case silver is in the second degree of oxidation.

With the increasing of the sulphate-ions concentration the anodic activation of silver is observing. The new peak $K_3$ is appearing on the cyclic voltammogram (Fig. 1), which corresponds to the reducing of the $Ag_2SO_4$. It's important, that the activation take place on the separated areas of the electrode, when his main part was covered by the oxide. Joint existence of silver oxide and sulphate of silver

may be happening in the time of the decreasing of pH of solution which founding in the pore of sediment and than in the space of pitting. Local activation is occurring under the potentials between peaks $A_1$ and $A_2$.

So, local depassivation of silver in the present alkaline solution is observing under definite concentration of anion-activators and electrode potential, when the adsorption of anion-activators prevail over adsorption of hydroxyl ions, as the result soluble complexes are appearing. Depassivation occurs in the pores of oxide sediment from the silver oxide and carries local character.

Local depassivation of silver is observing in alkaline medias containing nitrate ions just as in alkaline solutions containing sulphate ions. However activation of metal is occurring not between the first and the second peaks of the anodic curve but after the second peak on the anodic branch. It indicates that the activating ability of nitrate-ions less than sulfate ions. Under these potentials besides the oxide AgO is occurring the falling out of sediment of $AgNO_3$ which confirmed by the appearing of the cathodic peak $K_3$ on the cyclic voltammogram.

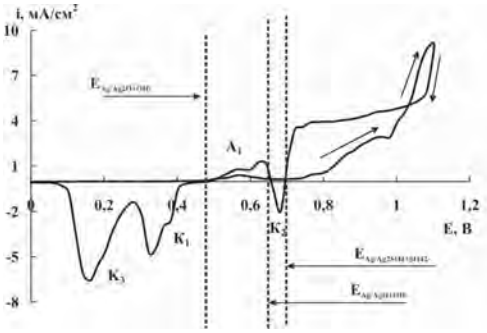


*Fig. 1. Cyclic voltammogram of Ag-electrode in 0.05 M NaOH + 0.5 M $Na_2SO_4$*

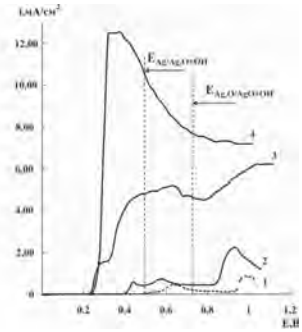

*Fig. 2. Anodic potentiodynamic curves of Ag-electrode in 0,01 M NaOH + x M NaCl, where x = 0(1); $5\times10^{-3}$ (2); $5\times10^{-2}$ (3); 0.,5 M (4)*

In chloride-alkaline solutions the picture is different. Introduction of chloride-ions into solution reduce to increasing current on the anodic branch of cyclogram (Fig. 2). The magnitudes of current in passive area also increase. New peak A', which corresponding to the formation of AgCl, also appears. The anodic-anionic activation of silver in acidic solutions containing $Cl^-$ ions is absent.

**Conclusion**

The anodic-anionic local activation and formation of pitting in alkaline solutions is observing just in the presence of sulphate- and nitrate-ions. Depassivation of silver occurs because of the nucleophilic substitution of hydroxyl-ions by the anion-activators in adsorption complexes. The stationary potentials of free corrosion of silver not achieve of the values of the potentials of local activation, that's why in such cases (in sulphate-alkaline and nitrate-alkaline solutions) the pitting defeats of silver can't be observed. However, in the presence of strong oxidizing or by the contact with the electropositive metals and with stray currents the potentials of local depassivation can be achieved and the pitting corrosion is appeared.

*The work is supported by RFBR project № 06-03-32274-a.*

First Regional Symposium on Electrochemistry of South-East Europe, Rovinj, Croatia, May 4-8, 2008.

P-2-137

# THE PARTIAL RATES OF PROCESSES OF ACTIVE ANODIC DISSOLUTION, OXIDE FORMATION AND IT'S CHEMICAL DISSOLUTION IN $Ag/Ag_2O/OH^-$ SYSTEM

**S. Grushevskaya*, A. Vvedenskii, D. Kudryashov**

*Voronezh State University, Department of Physical Chemistry,*
*Universitetskaya pl. 1, 394006 Voronezh, Russia*
**E-mail: sg@chem.vsu.ru*

The anodic dissolution of metals and alloys largely depends on the appearance of the film of insoluble products of the anodic reaction (oxides, first of all) at the surface. At the same time the kinetics of the anodic phase formation particularly at the initial stage is still insufficiently examined. To a great extent this is connected with a complicated calculation of partial rates of the processes simultaneously proceeding at the potentials of the oxide formation. The method of multicycle chronoammetry of the rotating ring disk electrode (*RRDE)* system makes it possible to obtain separately the partial currents of metal electrode ionization, anodic oxide formation and chemical oxide dissolution. The method is tested for $Ag|Ag_2O|OH^-(H_2O)$.

The faradaic current of the active dissolution and phase formation will be denoted by $I_a$ and $I_{ph}$. The silver oxide dissolution with the formation of hydroxyl complexes does not contribute to the overall polarization current of the electrode. However, it is convenient to measure the quantity of the oxide chemically dissolved per the unit of time in terms of current $I_c$. Hence the rates of partial reactions $i_a$, $i_{ph}$ and $i_c$ can be calculated by the normalization of the relevant currents to the electrode surface.

The aim of the work is to calculate $i_a$, $i_{ph}$ and $i_c$ for the process of the anodic dissolution of silver in an aqueous alkaline solution, using the multicycle chronoammetry of *RRDE*.

Let us consider that the current fixed on the silver disk electrode at potential$E_D$ = 0.48 – 0.53 V (s.h.e.) is a sum of independent currents $I_a$ and $I_{ph}$:

$$I_D(t) = I_a(t) + I_{ph}(t). \qquad (1)$$

The ring electrode is polarized at potential $E_R$ = -0.3 V of the reduction of soluble Ag(I) products. Hence the ring electrode current consists of the dissolution currents of the disk and oxide, as well as a background current $I_b$ (taking into account the efficiency coefficient N):

$$\frac{I_R(t)}{N} = I_a(t) + I_c(t) + I_b(t). \qquad (2)$$

Let us disrupt the polarization of the disk at the moment of time $t_D$. Then the relation (2) takes the form:

$$\frac{I_R(t > t_D)}{N} = I_c(t > t_D) + I_b(t > t_D), \qquad (3)$$

since $I_a$ almost instantaneously drops to zero. $I_b(t)$ is a certain value, hence one can determine $I_c$ at the moment of switching off the polarization of the disk. The next stages are the calculations of $I_a(t_D)$ by (2) and phase formation current $I_{ph}(t_D)$ by (1). If we increase $t_D$ gradually from one experiment to another, we will get the dependences of $I_a$, $I_{ph}$ and $I_c$ on time and establish the formal kinetics of the partial anodic processes.

In the range of low anodic potentials (0.48 ÷ 0.51 V) the process of active silver dissolution prevails; the phase formation current $i_{ph}$ rapidly drops. The oxide film is thin and the current efficiency of phaseformation is low. At higher potentials (0.52 ÷ 0.53 V) the active dissolution is practically excluded, the phase formation current prevails and noticeably exceeds the rate of the chemical oxide dissolution. The thickness of $Ag_2O$ film rapidly increases; and the net phase formation current is close to 100%.

*This work is supported by CRDF (RUXO-000010-VZ-06) and RFBR (06-03-32274-a).*

First Regional Symposium on Electrochemistry of South-East Europe, Rovinj, Croatia, May 4-8, 2008.

P-2-138

# THIN GOLD OXIDE SURFACE LAYER

**J. Katić, Ž. Petrović, M. Metikoš–Huković ***

*Department of Electrochemistry, Faculty of Chemical Engineering and Technology, University of Zagreb, Savska 16, P.O. Box 177, 10000 Zagreb, Croatia,*mmetik@fkit.hr*

The enhanced catalytic activity of Au nanoparticles has recently attracted particular attention of scientists in various disciplines such as surface chemistry and heterogeneous catalysis. It was suggested that the Au-oxide (Au(III)) is at the interface of metallic Au nanoparticles and oxide supports and the Au(III) species contribute to stabilize Au nanoparticles on the surface.
The formation of thin oxide films on gold coated quartz crystal electrode in 0.1 mol $dm^{-3}$ $NaClO_4$ solution at pH 5.45 have been investigated by means of nanogravimetry using an electrochemical quartz crystal nanobalance which provides a new dimension for such studies. Anodic oxide film nucleation, growth and reduction processes were also investigated using cyclic voltammetry and potentiostatic chronoamperometric techniques.
The oxide film nucleation kinetics was explained through a 3D nucleation mechanism with diffusion controlled growth and nucleation parameters were determined.
Characterization of the oxide layer and the structural composition of the gold surface were examined by X-ray photoelectron spectroscopy and observed XPS spectrum were characteristic for Au(III) species. In addition to XPS, photoelectrochemical method was also used to characterize the surface. Anodically formed oxide film on gold acted as n-type semiconductor.

*Key words:* Au oxide growth; Electrochemical quartz crystal nanobalance; Cyclic voltammetry, Chronoamperometry

First Regional Symposium on Electrochemistry of South-East Europe, Rovinj, Croatia, May 4-8, 2008.

P-2-139

# ANODIC SELECTIVE DISSOLUTION OF METAL ALLOYS: NON-STATIONARY DIFFUSION KINETICS

**O.A. Kozaderov*, A. Vvedenskii**

*Voronezh State University, Department of Physical Chemistry, Universitetskaya pl. 1, Voronezh, 394006, Russian Federation, *ok@chem.vsu.ru*

Charge transfer, decrystallisation, mass-transfer of ions in a solution and solid-phase interdiffusion of components on vacancy mechanism are limiting stages of the selective dissolution (SD) of a homogeneous alloy in the different time intervals. Non-stationary electrochemical methods (chronoampero-, chronopotentio- and chronovoltampe-rometry) are rather sensitive methods for the investigation of the solid-phase diffusion kinetics of SD. The form of the potentiostatic $I_A$,t-curve of the current recession, galvanostatic $\eta$,t-curve of the overpotential relaxation and potentiodynamic $I_A$,$\eta$(t)-dependence generally depends on the number of factors. It makes more difficult as revealing the solid-phase diffusion regime as correct determining the main parameters of the diffusion zone formed in an alloy (interdiffusivity and concentration of non-equilibrium vacancies).

Primary accumulation of one of the components of dissolving alloy in its surface layer as a result of the equilibrium solid-phase adsorption; roughness of an electrode surface; displacement of an interphase border alloy/solution; relaxation of the non-equilibrium vacancy subsystem of an alloy as a result of slowed down disappearance of super-equilibrium vacancies in the surface layer of an alloy are the main complicating factors of the selective dissolution proceeding in the solid-phase interdiffusion regime.

Detailed elaboration of each insufficiently explored factor is important not only for development of the theory of polycomponent metal phase's anodic dissolution but also for the solution of the practical problem of a protection of alloys from the selective corrosion.

During construction of theoretical model of chronogram formation the simultaneous account of all factors is superfluous. More simple approach used in the given work, consists in stage-by-stage introduction of this or that SD factor into theoretical consideration. It allows to establish borders of a time interval in which influence of this or that factor is significant, and to offer procedure of its account with accuracy necessary for practice.

The goal of this work is to establish the kinetic features of formation and parameters of solid-phase diffusion zones formed at anodic selective dissolution of homogeneous Ag-Au, Zn-Ag and Cu-Au alloys.

Researches are executed on polycrystalline silver, copper and alloys Ag-Au, Zn-Ag, Cu-Au. Solutions: 0.1 M $NaNO_3$ + 0.001 M $HNO_3$ + x M $AgNO_3$, $x = 10^{-4}$-$10^{-2}$ (anodic chronoamperometry and chronovoltamperometry of Ag-Au alloys); 1 M NaCl + 0.01 M HCl (anodic chronopotentiometry of Zn-Ag alloys); 0.1 M KCl + 0.01 M HCl (anodic chronopotentiometry of Cu-Au alloys) were pre-pared on bidistilled water using analytically-pure reagents, deaerated with argon.

It is theoretically shown that in first approximation action of the main complicating factors of SD is independent and comes to appearance of the corresponding additional multiplier in the basic equations by Cottrell, Sand and Randles-Ševcik which are the base of I,t-, E,t- and i,υ-measuring the main parameters of the diffusion zone in an alloy.

Results of the theoretical analisys are used in processing of the experimental data obtained by the different non-stationary electrochemical methods at studying of SD of Ag-Au, Zn-Ag and Cu-Au alloys.

It is established, that the account of equilibrium adsorption of components in surface layer of Ag-Au alloys with the volume atomic fraction $X_{Ag} \geq 0.65$ prior to the beginning SD results only in insignificant increase in diffusivity (interdiffusivity). At the same time the effect of displacement of interphase border at SD of such alloys is rather significant at determination of diffusion parameters, as against Zn-Ag alloys with $X_{Zn} \geq 0.25$ in which silver acts already as an electropositive component.

The presence of the borders of the time interval in which the role of an electrode surface roughness can be taken into account correctly in the simplest way is revealed: only in this interval it is necessary to use in calculations the true surface area instead of the geometrical one. The procedure of the step-by-step correction of a position of these borders using the experimental data is developed. It is found that very low diffusivities and interdiffusivities which are typical for SD of investigated alloys provide conditions when the current $I_A$ in the potentiostatic regime, transitive time $\tau_A$ in the galvanostatic regime and peak current Im in the potentiodynamic regime of SD of alloys are proportional to the roughness factor. On the contrary, in the case of diffusionally-controlled processes in a liquid phase with relatively high mobility of a diffusant the corresponding characteristic parameter of a non-stationary method is practically non-sensitive to the surface roughness.

It is established that at SD of Ag-Au alloys the concentration of non-equilibrium vacancies and the interdiffusivity depend exponentionally not only on $X_{Ag}$ but also on the anodic overpotential. Molar fraction of non-equilibrium vacancies galvanostatically generated in the surface layer of Zn-Ag and Cu-Au alloys is determined by the partial current of the Zn and Cu dissolution. It is the main reason of unfeasibleness of Sand criterion during the diffusionally-limited SD of a binary alloy.

The relaxation of non-equilibrium vacancy subsystem in Ag-Au alloys is found to proceed slowly enough that is why it is a principal reason of a curvature of chronoamperograms resulting to necessity of use of numerical processing I,t-curve for searching diffusion parameters. Sinks of vacancies in diffusion zone of Zn-Ag and Cu-Au alloys are ineffective too. The nature of the dominating sink of monovacancies in the investigated alloys is various: for system Zn-Ag assimilation of vacancies by the distributed defects is more probable, whereas in Ag-Au and Cu-Au alloys it is formation of bivacancies.

*The investigation is supported by the Grant of the President of the Russian Federation (proj. MK-1426.2007.3).*

First Regional Symposium on Electrochemistry of South-East Europe, Rovinj, Croatia, May 4-8, 2008.

P-2-140

# KINETICS OF SURFACE PHASE TRANSFORMATION OF GOLD ON Ag-Au ALLOYS DURING THE SELECTIVE DISSOLUTION

**O.A. Kozaderov*, O.V. Koroleva, A. Vvedenskii**

*Voronezh State University, Department of Physical Chemistry, Universitetskaya pl. 1, Voronezh, 394006, Russian Federation, *ok@chem.vsu.ru*

Selective dissolution (SD) of an electronegative component A from homogeneous alloy A-B at excess of critical potential $E_c$ and charge $q_{cp}$ is accompanied by sharp arising of true area of an electrode surface (i.e. infringement of its morphological stability) owing to passing nonequilibrium phase transformation (PT) of a stable electropositive component B in surface layer where it is in special energy-saturated state B*. Recrystallization of own phase $B^0$ during PT under schema $B^* \rightarrow B^0$ is accompanied by formation of a microporous structure which appearance can lower essentially corrosion and mechanical durability of A-B alloys. In spite of the fact that details of SD in overcritical ranges of the potentials, complicated with PT of the component B and development of a surface, till now are obscure, the first cause of originating PT is considered to be SD of a component A.

The purpose of the work is determination of kinetics of surface phase changes of gold with formation of own phase Au on an electrode in course of SD of Ag-Au alloys.

Researches are executed on polycrystal alloys of system Ag-Au ($X_{Ag}$=0.65÷0.95), and also on system Ag15Au doped with Ni, Ti, Si (on 0.5 at. %) in not stirred deaerated acidic nitrate solutions. Potentiostatic I,t-curves were registered at potentials $E = E_c + \Delta\eta_c$. Values of $E_c$ found in [1] by the graphical method of tangents under anodic polarizing curves were specified chronoamperometrically. Polarization time was chosen according to passing through system the electric charge twice exceeding value of $q_c$ found in [2]. In research of a role of surface-active organic additives the benzoic, caproic and valeric acids were used.

On chronoamperograms presented in logarithmic coordinates it is possible to find the linear fields adequate to diffusion control of SD (fig. 1). Only since some moment of a time $t = t_c$ the chronoamperogram becomes nonlinear. The deflection from linearity is more than the overpotential is higher. Assuming, that such nonlinearity is provided with originating and growth of a new phase of the gold, proceeding collaterally with SD, transient current of process of phase change $B^* \rightarrow B^0$ found as a difference between complete and diffusive (Cottrell) currents: $i_{PT}(t) = i_A(t) - \text{const}\cdot t^{-k}$. Kinetic features of new phase formation of gold have been revealed, analysing obtained transients within the framework of stochastic models of 2D-and 3D-nucleation rates. It was found that at large times the straightening is observed in $i_{PT}, t^{1/2}$-coordinates which are criterial for instantaneous nucleation in a 3D-diffusive rate (fig. 2). At small times two alternatives are equi-probable: instantaneous nucleation in a 3D-kinetic rate and continuous nucleation in a 3D-diffusive rate (fig. 2).

Dependence of PT-currents on the contents of gold in an alloy is not monotonic. Apparently, processes of PT are much more sensitive to weakly controlled local

concentration changes in the surface layer of a dissolving alloy, rather than to integrated changes of volumetric composition.

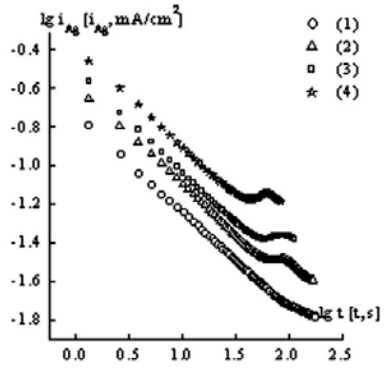


*Fig. 1. Chronoamperograms of Ag5Au alloy in 0.1 M $NaNO_3$ + 0.001 M $HNO_3$ + 0.001 M $AgNO_3$, obtained at $\Delta\eta_{cr}$ = 0 (1); 10 (2); 20 (3); 30 (4) mV*

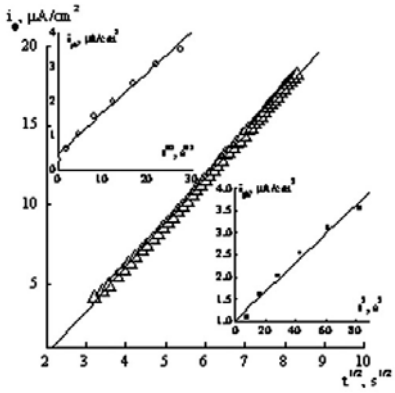


*Fig. 2. Chronoamperograms of the Au phase transformation process on the surface of Ag15Au alloy at $\Delta\eta_{cr}$=40 mV, presented in coordinates which are criterial for △ – 3D diffusion (instantaneous nucleation); ○ – 3D diffusion (continuous nucleation) and □ – 3D kinetic (instantaneous nucleation) rates.*

The value of a PT current sharply increases at arising of an overpotential, and parameter $t_c$, on the contrary, decreases in such conditions. These facts specify a determining role of selective dissolution of silver from alloy Ag-Au in kinetics of formation of own phase of gold in overcritical ranges of potentials. In fact dissolution of silver results in sharp augmentation of concentration of vacancies in surface layer of an alloy and, as consequence, ad-atoms of gold, capable to phase change after achievement of critical potential.

Addition of alloying constituents in alloy Ag15Au and introduction of surfactants in solution reduces currents of formation of a new phase of gold, however does not variate kinetics of PT process. Apparently, being adsorbed on more active places of a surface, organic acids reduce motility of surface atoms of gold, thus complicate their redistribution. In turn, alloying additions of nickel, titanium and silicon at potentials of dissolution of silver are oxidized, forming oxides which carry out a role of "stoppers" during phase change $B^* \rightarrow B^0$ in surface layer of a dissolving alloy.

*The investigation is supported by the Grant of the President of the Russian Federation (project MK-1426.2007.3).*

**References:**

1. Vvedenskii A.V., Kozaderov O.A., Koroleva O.V., *Korroziya: materialy, zaschita (Corrosion: materials, protection).* 2007. **3**, 7-14.
2. Vvedenskii A.V., Bobrinskaya E.V., Marshakov I.K., Storozhenko V.N., *Zaschita metallov (Protection of metals).* 1993, **29**(4), 561-567.

First Regional Symposium on Electrochemistry of South-East Europe, Rovinj, Croatia, May 4-8, 2008.

P-2-141

# ROLE OF GEOMETRICAL CONSTRUCTIVE ELEMENTS IN THE WORKING OF VERTICAL DIELECTROCHROMATOGRAPHIC CHAMBER

**V. Coman, Ş. Kreibik, M. Vlassa**

*«Babes-Bolyai» University, «Raluca Ripan» Institute for Research in Chemistry, 30 Fantanele Street, RO-400294 Cluj-Napoca, Romania, coman_virginia@yahoo.com*

The improvement of the separation process in classical thin layer chromatography (TLC) depends on some well-known physical parameters like working temperature, saturation degree of chromatographic chamber, inclination angle of chromatographic plate in the chamber, activating degree of thin layer plates, the type of adsorbent and of mobile phase respectively [1]. In the case of the application of a continuous electric field [2] or an transversal alternative electric field [3-5] on the TLC plate beside the TLC parameters shown above we must take into consideration some new appeared elements such as: *(i)* size and type of the applied electric field (continuous, alternative or of high frequency); *(ii)* geometry of the used electric field; *(iii)* dielectrical properties of porous medium and of mobile phase.

In our previous papers [3-5] we developed a new technique, named by us planar dielectrochromatography (PDEC). We mention that, like in electrophoretic chromatography [6], the application of a transversal external electric field does not create the Joule heating in the chromatographic system.

In the present paper, we extend our experiments using vertical planar dielectro-chromatographic (V-PDEC) chamber (**Figure 1**) [7]. We were preoccupied to understand the influence of armature shape and of their fasteners over the circulation of mobile phase vapours and on whole separation process also.

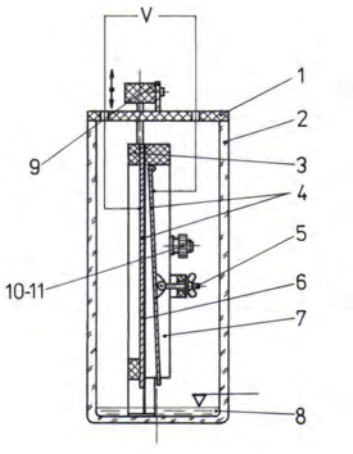


*Figure 1.*
*The constructive elements of V-PDEC chamber: lid (1), body of chamber (2), insulated body (3), armatures (4), screw (5), TLC plate (6), mobile frame (7), mobile phase (8), handle (9), screw and screw nut for fixing the mobile frame (10,11).*

By scraping the adsorbent, the TLC plate (6) was divided into two equal zones in order to perform simultaneously experiments with and without electric field. Armatures of different shapes (plane, lamellar, profilated etc.) manufactured by us were fixed in insulated bodies on mobile frames (7), outdistanced of TLC plate.
The experiments were achieved in the following conditions:

1. Without electric field.

1a. The assembly of armatures occupies a half part of TLC plate section.

1b. The free space from the TLC plate is occupied with an insulated padding body identical as dimensions with the armature assembly.

2. With transversal alternating electric field applied on armature assembly in conditions 1b.

It has been observed that the experimental results were different according to the conditions of movement of mobile phase vapours on the verticality of V-PDEC chamber. The obtained results were evaluated by the separation parameter Rx [5].

$$R_X = \frac{x_2}{x_1} = \frac{\text{Migration distance of compound in electric field}}{\text{Migration distance of compound without electric field}}$$

The results of our experiments achieved with lamellar armatures, in the 1.2 situation, in presence and absence of AC current using as solutes the lipophilic test dye mixture (Art. 9353, Merck) and as mobile phase (MP) toluene are given **Figure 2**.

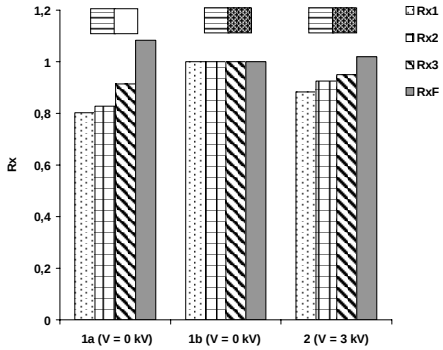


*Figure 2.*
*Rx values of lipophilic test dye mixture in different arrangement conditions:*
*1a, 1b - without AC current,*
*2 - with AC current.*
*Dyes:*
*1. Indophenol blue,*
*2. Sudan red G,*
*3. Dimethylaminoazobenzene.*
*F. Front of mobile phase*

One can notice that the chromatographic separation process in V-PDEC chamber is influenced by the circulation of mobile phase vapours.

## References:

1. E. Stahl, *THIN-LAYER CHROMATOGRAPHY*, Springer-Verlag, Berlin-Heidelberg-New York, 1969, p. 67.
2. J.K. Różyło and I. Malinowska, *Electroosmotically driven TLC*, Chapter 10 in: *PLANAR CHROMATOGRAPHY. A RETROSPECTIVE VIEW FOR THE THIRD MILLENNIUM*, Ed. Sz. Nyiredy, Springer, Budapest, 2001, p. 200-219.
3. Şt. Kreibik, V. Coman, C. Măruțoiu, Gh. Mihăilescu and S. Pruneanu, „Enhancement of Mobile Phase Velocity in TLC by Means of an External Alternating Electric Field" *J. Planar Chromatogr.*, **14** (2001) 335-359.

4. Şt. Kreibik, V. Surducan, V. Coman and C. Măruţoiu, „Horizontal Planar Dielectrochromatography. I. Preliminary Results", *J. Planar Chromatogr.*, **15** (2002) 425-428.
5. V. Coman and Şt. Kreibik, „Planar Dielectrochromatography. A Perspective Technique", *J. Planar Chromatogr*., **16** (2003) 338-346.
6. A.G. Howard and T. Shafik, „Thin-Layer Chromatography with Potential", *LC•GC Europe* (February 2000) 104-112.
7. V. Coman, Şt. Kreibik, M Filip and E. Bodoki, „New Approaches in Planar Dielectrochromatography Using the Vertical Chamber", International Conference *Modern Physical Chemistry for Advanced Materials*, 26-30 June 2007, Kharkov, Ukraine.

First Regional Symposium on Electrochemistry of South-East Europe, Rovinj, Croatia, May 4-8, 2008.

P-2-142

# ION TRANSFERS ACROSS CHOLESTEROL MODIFIED WATER|NITROBENZENE INTERFACE

**V. Mirčeski[1], F. Quentel[2], M. L'Her[2], F. Spasovski[1], M. Gaćina[1]**

*[1]Institute of Chemistry, Faculty of Natural Sciences and Mathematics, University „Ss Cyril and Methodius", PO Box 162, 1000 Skopje, Republic of Macedonia, valentine@iunona.pmf.ukim.edu.mk*
*[2]Laboratoire de Chimie Analytique, UMR-CNRS 6521, Université de Bretagne Occidentale, 6, avenue Victor Le Gorgeu, C.S. 93837, 29238 BREST Cedex 3, France*

Electrochemically driven ion transfer reactions of $ClO_4^-$, $NO_3^-$, $SCN^-$, and $K^+$ across a cholesterol modified water|nitrobenzene (W|NB) interface have been studied by means of square-wave and cyclic voltammetry at thin organic film modified electrodes. It has been found that cholesterol exhibits a profound accelerating effect toward the kinetics of $ClO_4^-$, $NO_3^-$, $SCN^-$ transfers, whereas a retarding kinetic effect was observed for $K^+$. Besides, the cholesterol layer alters significantly the mechanism of ion transfer, prompting adsorption of all studied ions as a consequence of specific interactions between cholesterol molecules and the transferring ion.

First Regional Symposium on Electrochemistry of South-East Europe, Rovinj, Croatia, May 4-8, 2008.

P-2-143

# PRINTING PLATES' POROUS STRUCTURE CHARACTERIZATION BY IMPEDANCE SPECTROSCOPY

**S. Mahović Poljaček[1], M. Gojo[1], D. Risović[2], K. Furić[2]**

*[1]Faculty of Graphic Arts, University of Zagreb, POB 225, HR-10000 Zagreb, Croatia*
*[2]Molecular Physics Laboratory, Ruder Boskovic Institute, POB 180, HR-10002 Zagreb, Croatia*

Size and quality of the grained microstructure, i.e. porous layer of the lithographic printing plate has most significant influence on the quality of the imprints and durability of the printing plates [1].
This structure is obtained by electrochemical processes of graining and anodic oxidation [2-5], resulting in formation of specific anodic layer on an aluminium foil which consists of a thin non-porous compact layer (barrier layer) and an outer extremely porous layer.
In this study we present the results of application of SEM and EIS in characterization of the changes in printing plates' oxide layer induced by processing in alkaline solutions of different processing age.
SEM micrographs of the investigated printing plate samples were obtained with JEOL JMS T300 scanning electron microscope, while the EIS measurements were performed in an unstirred and aerated 3.5% (w/w) $K_2SO_4$ solution at 25°C in a three-electrode electrochemical cell. EIS spectrum was measured over the frequency range from 10 mHz to 64 kHz under controlled potentionstatic conditions using using an EG&G Lock in Amplifier Type 5210 in combination with an EG&G Potentiostat/Galvanostat Type 263 A at an open circuit potential. Capacitance and resistance data were obtained by software PowerSine EIS Software Equivalent Circuit [6].
The results of the EIS measurements and analysis of equivalent circuits' capacitance and resistance behavior, as well as SEM micrographs of the investigated samples indicate that the surface structures of different types of lithographic printing plates and their change due to processing are different and type-related. Micro-structural characterization of nominally equivalent surfaces of the printing plates which can be used in the same reproduction process has shown totally different behavior and surface structure transformation during the alkaline processing. The observed changes also depend on the age of processing solution.
According to the results of the SEM micrographs analysis and corresponding EIS measurements on the aluminium oxide films it can be concluded that during the plate processing the observed surface structural changes are probably induced by two different mechanisms. The first one is the degradation and smoothening of the rough surface structure of the aluminium oxide layer and the second one is the chemical reaction of the aluminium oxide with alkaline solution during the chemical processing. The second mechanism is probably a consequence of the reaction of anhydrous aluminium oxide structure which adsorbs water from

alkaline solution resulting in a sealing process. Similar changes of the anodic films on aluminium have been reported previously [7, 8].
The equivalent circuit models corresponding to the anodized layer and to the anodized sealed layer were proposed and used in interpretation of experimental results. Thus it was demonstrated that the application of SEM and EIS methods in investigation of surface structural properties of aluminium printing plate provides new insight and enables tracking and characterization of processing induced structural changes that are of primary significance for the performance of the printing plates.

*This work was supported by Croatian Ministry of Science, Education and Sports grants: No.: 098-0982915-2899 "Organizational processes and optical interactions in condensed molecular systems"; No.: 128-1201785-2228 "Development of methods for printing plates' surface measurements"; No.: 098-0982904-2898 "Physics and applications nanostructures and bulk matter".*

**References:**

[1]. Th. Dimogerontakis, S. Van Gils, H. Ottevaere, H. Thienpont, H. Terryn, *Surface and Coatings Technology* **201** (2006) 918-926
[2]. O. Gobbetti, Electrochemical Graining of Aluminum or Aluminum Alloy Surfaces, *Patent No.: US 5,064,511*, 1991.
[3]. C.S. Lin, C.C. Chang, H.M. Fu, *Materials Chemistry and Physics* **68** (2001) 217–224
[4]. A. Nishino, Y. Masuda, H. Sawada, A. Uesugi, Process for Producing Aluminum Support for Lithographic Printing Plate, *Patent No.: US 6,682,645 B2*, 2004
[5]. T. Urano, K. Kohori, H. Okamoto, Photosensitive Lithographic Printing Plate and Method for making a Printing Plate, *Patent No.: US 6,689,537 B2*, 2004.
[6]. B.A. Boukamp, *Equvalent Circuit*, Users Manual, Second Revised Edition, University of Twente Enschede, Netherlands, 1989
[7]. J.J. Suay, E. Giménez, T. Rodríguez, K. Habbib, J.J. Saura, Characterization of anodized and sealed aluminium by EIS, *Corrosion Science* **45** (2003) 611–624
[8]. Zhao Xu-hui, Zuo Yu, Zhao Jing-mao, Xiong Jin-ping, Tang Yu-ming, A study on the self-sealing process of anodic films on aluminium by EIS, *Surface & Coating Technology* **200** (2006) 6864-6853

First Regional Symposium on Electrochemistry of South-East Europe, Rovinj, Croatia, May 4-8, 2008.

P-2-144

# STRUCTURAL MODIFICATION OF ZINC ELECTROPLATING BY ADDING PHENOL-RESIN DURING ELECTRODEPOSITION

**A.C. Ciubotariu[1,*], L. Benea[1], O. Mitoşeriu[2], P. Ponthiaux[3], F. Wenger[3]**

*[1]Dunarea de Jos, University of Galat , Competences Center Interfaces – Tribocorrosion and Electrochemical Systems (CC-ITES) *Alina.Ciubotariu@ugal.ro*
*[2]Dunarea de Jos, University of Galati, Metallurgy and Materials Science Faculty. 47 Domneasca Street, 80008 GALATI, Romania.*
*[3]Ecole Centrale Paris, Laboratoire Genie de Procedées Matériaux Grand Voie des Vignes, 92290 Chatenay Malabry, France.*

Metal composite materials have found application in many areas of daily life for quite some time. Often it is not realized that the application makes use of composite materials. These materials are produced in situ from the conventional production and processing of metals. For many researchers the term metal matrix composites is often equated with the term light metal matrix composites (MMCs). Substantial progress in the development of light metal matrix composites has been achieved in recent decades, so that they could be introduced into the most important applications. These innovative materials open up unlimited possibilities for modern materials science and development; the characteristics of MMCs can be designed into the material, custom-made, dependent on the application. From this potential, metal matrix composites fulfill all the desired conceptions of the designer.

Zinc metal has a number of characteristics that make it well suitable for use as a coating for protecting iron and steel products from corrosion. Its excellent corrosion resistance in most environments accounts for its successful use as a protective coating on a variety of products and in many exposure conditions.

The present work has the purpose of realization of composite coatings in zinc matrix by using PF resin type NOVOLAC with commercial name RESITAL 6358/1 (for the first time) synthesized by HÜTTENES - ALBERTUS Germany, in the electrodeposition process of zinc. It is necessary to note that by involving the particles of PF resin in a zinc matrix we can obtain materials with properties differing from those of the individual materials.

For electrodeposition we used an electrochemical cell. Zinc plate of 99.9% purity was used as anode. As cathod we used steel plate samples, which first were degreased with alkaline solution ($Na_2HPO_4 \cdot 12\ H_2O$ 50 – 60 g/L, $Na_2SiO_2 \cdot 5\ H_2O$ 25 – 30 g/L, liquid soap 2 – 3 g/L, temperature 80 – $90^0$C, time 10 min), and after treated with HCl 10% for 1-2 min and washing with distilled water.

The PF resin – zinc composite coatings was obtained from a suspension of PF resin particles (diameter < 0.056 mm and 0.056 mm< diameter < 0.1 mm) in aqueous zinc sulphate electrolyte

Phenol-Formaldehyde resin is a highly crosslinked thermosetting material that is produced by the poly-condensation of phenol and formaldehyde in the presence of either acidic or basic catalyst. An acid catalyst is usually used in preparing

NOVOLAC type of resin. A novolac resin is produced if the mole ratio of formaldehyde to phenol (F/P) is greater than one. This method produces relatively linear chains with molecular weights typically between 500 and 1000 g/mol.
Fig. 1 – 3 compare a pure zinc coating and PF resin – zinc composite coating obtained at 3 A/ $dm^2$ current density, 1h stirred at 1000 rpm witha concentration of PF resin particles of 10g/L and 25g/L (diameter < 0.056 mm).
The pure zinc coating (Fig. 1) has a rather regular surface, whereas the composite coatings surface has fine surface structure (Figs 2, 3). By increasing the PF resin concentration in the zinc electrolyte the surface structure of composite coating is changed more to finer crystallites (Fig. 3). The PF resin acts as reducing the crystals size of electrodeposited zinc during co-deposition.

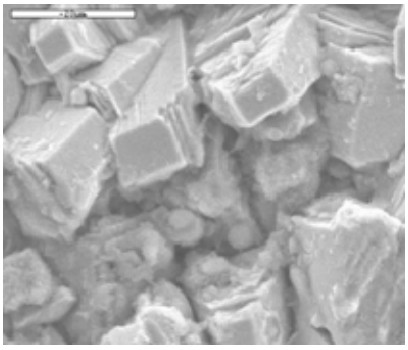

*Fig. 1: SEM surface morfology of pure zinc electroplating.*

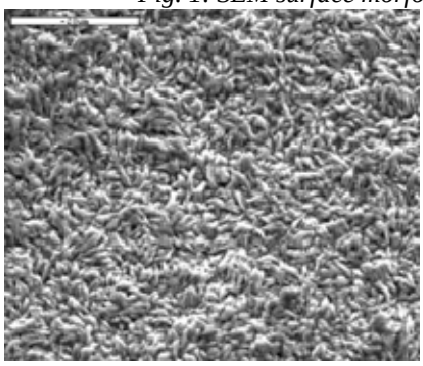

*Fig. 2. SEM surface morfology of PF resin – zinc composite coatings (10g/L PF resin)*

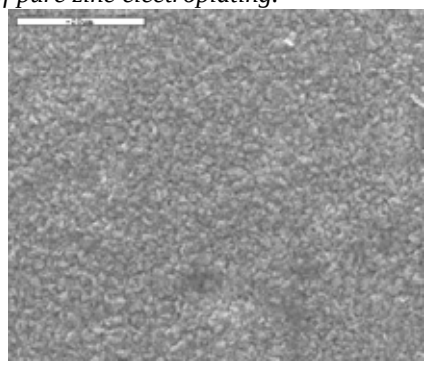

*Fig. 3: SEM surface morfology of PF resin – zinc composite coatings (25g/L PF resin)*

The PF resin could have an inhibition effect of zinc crystals growth and a catalytic effect in increasing nucleation sites.Our work proved that PF resin particles type NOVOLAC with commercial name RESITAL 6358/1 could be codeposited with zinc to obtain structured composite coatings.
The surface morphology of layers is different comparated with pure zinc coated. The surface of composite coating has a fine structure with smaller grain size compared with pure zinc coatings. We can say that by adding PF resin in sulphate zinc electrolyte for electrodeposition of zinc we obtain a very fine surface structure of composite coatings, considering as a method of obtaining nanocomposite coatings.

# AUTHOR INDEX



Click on the Page Number to reach an appropriate Abstract!

## Č



## Ć



## D



## Đ



## E



## F



## G



Click on the Page Number to reach an appropriate Abstract!

## H



## I



## J



## K



## L



Click on the Page Number to reach an appropriate Abstract!

## M



## N



## O



## P



Click on the Page Number to reach an appropriate Abstract!

## Q



## R



## S



Click on the Page Number to reach an appropriate Abstract!

## Š



## T



## U



## V



## W



## Y



## Z



## Ž



Click on the Page Number to reach an appropriate Abstract!